



PHD

## Methotrexate-protein conjugates as soluble drug delivery systems

Pape, Valerie Elizabeth

*Award date:*  
1990

*Awarding institution:*  
University of Bath

[Link to publication](#)

## Alternative formats

If you require this document in an alternative format, please contact:  
[openaccess@bath.ac.uk](mailto:openaccess@bath.ac.uk)

### General rights

Copyright and moral rights for the publications made accessible in the public portal are retained by the authors and/or other copyright owners and it is a condition of accessing publications that users recognise and abide by the legal requirements associated with these rights.

- Users may download and print one copy of any publication from the public portal for the purpose of private study or research.
- You may not further distribute the material or use it for any profit-making activity or commercial gain
- You may freely distribute the URL identifying the publication in the public portal ?

### Take down policy

If you believe that this document breaches copyright please contact us providing details, and we will remove access to the work immediately and investigate your claim.

**METHOTREXATE-PROTEIN CONJUGATES AS SOLUBLE DRUG  
DELIVERY SYSTEMS**

Submitted by Valerie Elizabeth Pape

for the degree of PhD

of the University of Bath

1990

**COPYRIGHT**

Attention is drawn to the fact that copyright of this thesis rests with its author. This copy of the thesis has been supplied on condition that anyone who consults it is understood to recognise that its copyright rests with the author, and that no quotation from the thesis and no information derived from it may be published without the prior written consent of the author.

This thesis may be made available for consultation within the University Library and may be photocopied or lent to other libraries for the purposes of consultation.

*Valerie E Pape*

UMI Number: U602183

All rights reserved

INFORMATION TO ALL USERS

The quality of this reproduction is dependent upon the quality of the copy submitted.

In the unlikely event that the author did not send a complete manuscript and there are missing pages, these will be noted. Also, if material had to be removed, a note will indicate the deletion.



UMI U602183

Published by ProQuest LLC 2014. Copyright in the Dissertation held by the Author.  
Microform Edition © ProQuest LLC.

All rights reserved. This work is protected against  
unauthorized copying under Title 17, United States Code.



ProQuest LLC  
789 East Eisenhower Parkway  
P.O. Box 1346  
Ann Arbor, MI 48106-1346

UNIVERSITY OF LATH LIBRARY		
23	- 9 SEP 1991	
PHD		

5054492.



## ABSTRACT

MTX has been covalently bound to proteins, to determine whether the macromolecular derivative could enhance its duration of action and reduce toxicity via changes in the pharmacokinetic parameters of the drug. MTX had a short terminal half-life at 102-117 minutes following IV injection in the rat and a large volume of distribution (1000 to 1600ml). BSA had a  $V_d$  of 26ml and  $t^{1/2}$  of 22 hours for the elimination phase. A series of conjugates, prepared between MTX and BSA with a range of loadings of MTX (3.4-13.6%w/w) were studied. Following IV injection they were all found to demonstrate a biexponential clearance from serum.  $t^{1/2}$  were at least ten fold greater than MTX and the  $V_d$  was reduced to a third. The BSA-MTX conjugates did not demonstrate the same pharmacokinetics as free protein. The beta phase  $t^{1/2}$  was found to increase with increased %w/w loading of MTX (range 17-33 hours) and there appeared to be a linear relationship ( $t^{1/2} = 1.312(\text{MTX \%w/w}) + 14.5$ ). There was a tendency for the  $V_d$  of the tissue compartment to increase with an increased loading of MTX (range 35 to 600ml). High strength conjugates (e.g. 11.55%w/w) were found to accumulate in the liver (70% in the first 15 minutes) and low strength conjugates appeared to exhibit a generalised non-specific uptake by most organs. The reason for the increased cellular uptake compared to BSA may be due to changes in the physical characteristics of the protein or due to a specific effect caused by the MTX, which has allowed the conjugate to enter cells via the folate transporter. In addition, FPLC analysis of the conjugates showed an increase in the amount of aggregated protein (up to 39% was present in an aggregated form) in the higher strength conjugates and this could explain, at least partly, the increased uptake by the liver. Other protein-MTX conjugates were studied. These included LA-MTX and RSA-MTX and these gave similar results in the rat to BSA-MTX.

Separate analysis of the drug and protein portions of the conjugate in the rat using  $^{125}\text{I}$ -BSA- $^3\text{H}$ -MTX (7.16%w/w) showed that the two isotopes had similar  $t^{1/2}$ . This suggests that the conjugate was not degraded during circulation. Following uptake by the liver, the  $^{125}\text{I}$ -BSA portion of the conjugate was degraded and transferred to the bile as iodotyrosine or  $^{125}\text{I}^-$  (65%) or oligopeptides with a molecular weight

below 1800, whereas  $^3\text{H}$  was selectively retained in the liver.  $^{125}\text{I}$  was excreted in the urine mainly as iodotyrosine or  $^{125}\text{I}^-$ .  $^3\text{H}$ -MTX was excreted at a slower rate than  $^{125}\text{I}$  (51% of injected  $^{125}\text{I}$  was excreted in the urine in 24 hours and 28.5% of  $^3\text{H}$ ).

The ability of the conjugates to extravasate was investigated *in vitro* using BAE-1 cells grown on filters. Free BSA was transported across the cell layer at a faster rate than BSA-MTX (4.54%w/w and 11.55%w/w). This could be because of the aggregated protein within the conjugates.

## ACKNOWLEDGEMENTS

I would like to thank my supervisors, Drs. Lidia Notarianni and Colin Pouton for their constant support and enthusiasm throughout the three years spent on this thesis. I would like to thank the technicians in the pharmacy department, particularly Gary Cooper and Lesley Moore for their assistance in some of the work described. I would like to thank Ciba Geigy Pharmaceuticals and in particular, Martin Mackay and Ian Hassan for allowing to me to work with them in the ADDR department at Horsham. I would like to thank Dr G. Black and Mr D Howes at Unilever Research and Mrs P.Wilmott at Glaxo, Ware for carrying out the whole body autoradiography. In addition, I would like to thank all members of the Department of Pharmacy at Bath for their friendship and advice over the years. I would like to thank William Moss for help with proof reading and typing. Finally, I would like to thank S.E.R.C for generous financial support and the University of Bath for providing research facilities.

## **ABBREVIATIONS**

<b>ALL</b>	<b>Acute lymphocytic leukaemia</b>
<b>AMN</b>	<b>Aminopterin</b>
<b>ASGP</b>	<b>Asialoglycoprotein</b>
<b>ATP</b>	<b>Adenosine triphosphate</b>
<b>BAE-1</b>	<b>Bovine aortic endothelium cell line</b>
<b>BSA</b>	<b>Bovine serum albumin</b>
<b>BSA-MTX</b>	<b>Bovine serum albumin-methotrexate conjugate</b>
<b>CA</b>	<b>Carbonic anhydrase</b>
<b>CEA</b>	<b>Chicken egg albumin</b>
<b>CHO</b>	<b>Chinese hamster ovary cell line</b>
<b>Cl</b>	<b>Clearance</b>
<b>CNS</b>	<b>Central nervous system</b>
<b>CPM</b>	<b>Counts per minute</b>
<b>CSF</b>	<b>Cerebrospinal fluid</b>
<b>CURL</b>	<b>Compartment of uncoupling of receptor and ligand</b>
<b>DHFR</b>	<b>Dihydrofolate reductase</b>
<b>DNP</b>	<b>2,4-Dinitrophenylalanine</b>
<b>DNR</b>	<b>Daunorubicin</b>
<b>DPM</b>	<b>Disintegrations per minute</b>
<b>ECDI</b>	<b>1-Ethyl-3-[3-(dimethylamino)propyl]carbodiimide</b>

ELISA	Enzyme-linked immunosorbent assay
FCS	Foetal calf serum
FTTC	Fluorescein isothiocyanate
FPLC	Fast protein liquid chromatography
FUDR	5-Fluorodeoxyuridine
G-BSA	Galactosamine-bovine serum albumin
GIT	Gastrointestinal tract
G-HPMA	Galactosamine-poly-N-(2-hydroxypropyl)methacrylamide
GPC	Gel permeation chromatography
HBGF	Heparin binding growth factor
HPLC	High performance liquid chromatography
HPMA	Poly-N-(2-hydroxypropyl)methacrylamide
HSA	Human serum albumin
IgG	Immunoglobulin G
IV	Intravenous
IP	Intraperitoneal
Kel	Elimination rate constant
LA	Lactalbumin
LA-MTX	Lactalbumin-methotrexate conjugate
LDL	Low density lipoprotein

mAb	Monoclonal antibody
M-BSA	Mannose-bovine serum albumin
MCR	Molar-conjugation ratio
MMC	Mitomycin C
MTX	Methotrexate
MTX(GLU) <sub>n</sub>	Polyglutamated methotrexate
MTX-PLL	Methotrexate-poly-L-lysine conjugate
7-OH-MTX	7-Hydroxymethotrexate
PBS	Phosphate buffer saline
PDL	Poly-D-lysine
PEG	Polyethyleneglycol
PLL	Poly-L-lysine
PVP	Polyvinylpyrrolidine
R <sup>2</sup>	Regression coefficient
RES	Reticuloendothelial system
RI	Refractive index
RSA	Rat serum albumin
RSA-MTX	Rat serum albumin-methotrexate conjugate
SC	Subcutaneous

**SDS-PAGE**     Sodium dodecyl sulphate polyacrylamide gel electrophoresis

**SEM**            Scanning electron microscope

**SEM**            Standard error of mean

**$t_{1/2}$**             Half life

**TCA**            Trichloroacetic acid

**TAA**            Tumour associated antigen

**TEM**            Transmission electron microscope

**V<sub>d</sub>**             Volume of distribution

**w/v**            Weight for volume

**w/w**            Weight for weight

## CONTENTS.

	Page
Abstract	i
Acknowledgements	iii
Abbreviations	iv
Contents	viii
Chapter 1: Introduction	
Chapter 2: Materials and Methods	33
Chapter 3: Kinetics of Methotrexate and Proteins in the Rat	66
Chapter 4: Analysis and Pharmacokinetics of Protein-MTX Conjugates in the Rat	114
Chapter 5: Visualisation and Body Distribution of the Conjugates	173
Chapter 6: Transport Experiments Using 2 Cell Lines <i>in vitro</i> ; Caco-2 and BAE-1 Cells. Uptake of BSA Conjugates by Macrophages <i>in vitro</i> .	209
Chapter 7: Conclusions	248
References:	257
Appendix 1: Calibration Curves and Reaction Mechanisms	A1
Appendix 2: Formulae and Procedures for Calculating Pharmacokinetics and statistics	A11
Appendix 3: Experimental Data for Chapters 3-6	A16



## **CHAPTER 1**

### **INTRODUCTION**

## **Rationale for Drug Targeting.**

Most drugs in current use have access to nearly all body compartments. Factors controlling drug distribution include the blood flow to a particular organ, protein binding of the drug in serum and in addition the inherent properties of the drug (e.g. hydrophobicity, electrical charge and molecular weight). Thus drugs can reach not only the site where they are pharmacologically active but also other organs where they can cause side effects. The majority of drug regimens would be improved if the access of the drug was restricted, in particular the targeting of anticancer and antiviral drugs would be a significant improvement due to the reduction in toxicity and an increase in efficacy. The work in this thesis has involved the covalent binding of methotrexate, a much used anticancer agent to large molecular weight carriers in the hope that an improvement in the delivery and distribution of the drug can be achieved.

This introduction will begin by describing some of the methods which can be exploited to achieve site specific drug delivery, which would occur due to improved distribution of the drug. It will then go on to describe methotrexate, the model drug used in this work, and some of the problems associated with its administration. The final section of the introduction will describe the scope of this project.

## 1.1 Site Specific Drug Delivery

Several factors may limit the use of a particular drug e.g. the drug may be prematurely metabolised or excreted before it has had time to reach its site of action, or it may be too hydrophilic to access its active site e.g. MTX cannot pass through the blood brain barrier. Conversely, the drug may have no problem reaching its target and likewise it can reach many other sites within the body causing side effects. These problems may be overcome by using a targeting agent to selectively deliver the drug to its site of pharmacological activity.

Site specific drug delivery has been described as achieving the maximum intrinsic activity of drugs by optimising their exclusive availability to their pharmacological receptor in a manner that affords protection both to the drug and body alike.<sup>(1)</sup>

Most approaches to drug targeting involve an interaction between a drug and a carrier, such that the normal distribution of the drug is altered and it no longer has free access throughout the body. Many systems have been exploited in research into site specific drug delivery and these may involve the use of a macromolecular carrier where the drug can be covalently bound e.g. monoclonal antibodies or particulate carriers where the drug is physically entrapped within its matrices. The distribution of drug-macromolecular complex will depend on the physicochemical characteristics of the carrier e.g. molecular weight, charge and hydrophobicity and these factors can be manipulated in order to achieve maximal benefit.<sup>(2)</sup>

There are many examples of particulate carriers eg. liposomes, albumin microspheres, erythrocyte ghosts. Since the work in this thesis has involved the use of a soluble carrier this section of the introduction will concentrate mainly on the soluble carriers which have been used in drug targeting.

A successful drug carrier should exhibit certain characteristics and these include;

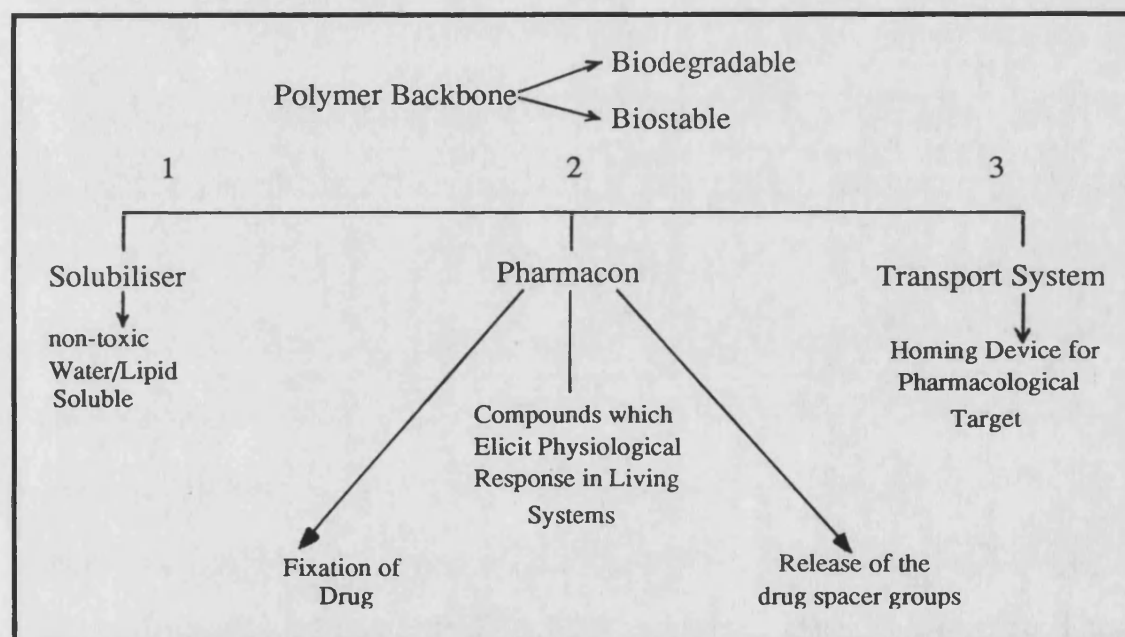
1. Protection of drug from metabolism and premature release.

2. Localisation of drug at its target site with subsequent release of the drug in active form.

3. It should not cause host toxicity or immunogenicity.

Figure 1.1 shows a model for a soluble drug-carrier conjugate. It is similar to that described by Ringsdorf.<sup>(3)</sup>

**Figure 1.1: A Diagrammatic Representation of the Requirements for a Soluble Drug-Carrier Conjugate.**



Drug delivery has been classified into 3 phases.<sup>(4)</sup> First order drug delivery involves distribution of drug-carrier complex to the capillary bed of the target site. Second order delivery should bring the complex to the intracellular fluid surrounding the target cells and third order delivery should result in the drugs presence within the cytoplasm of the target cells.

Another way of classifying the behaviour of a drug carrier complex is to describe the ability to actively or passively target the drug.<sup>(5)</sup> Active targeting involves the incorporation of a specific agent to deliver the drug e.g. a monoclonal antibody or a sugar residue (galactose receptors are found exclusively on hepatocytes).<sup>(6)</sup> Passive

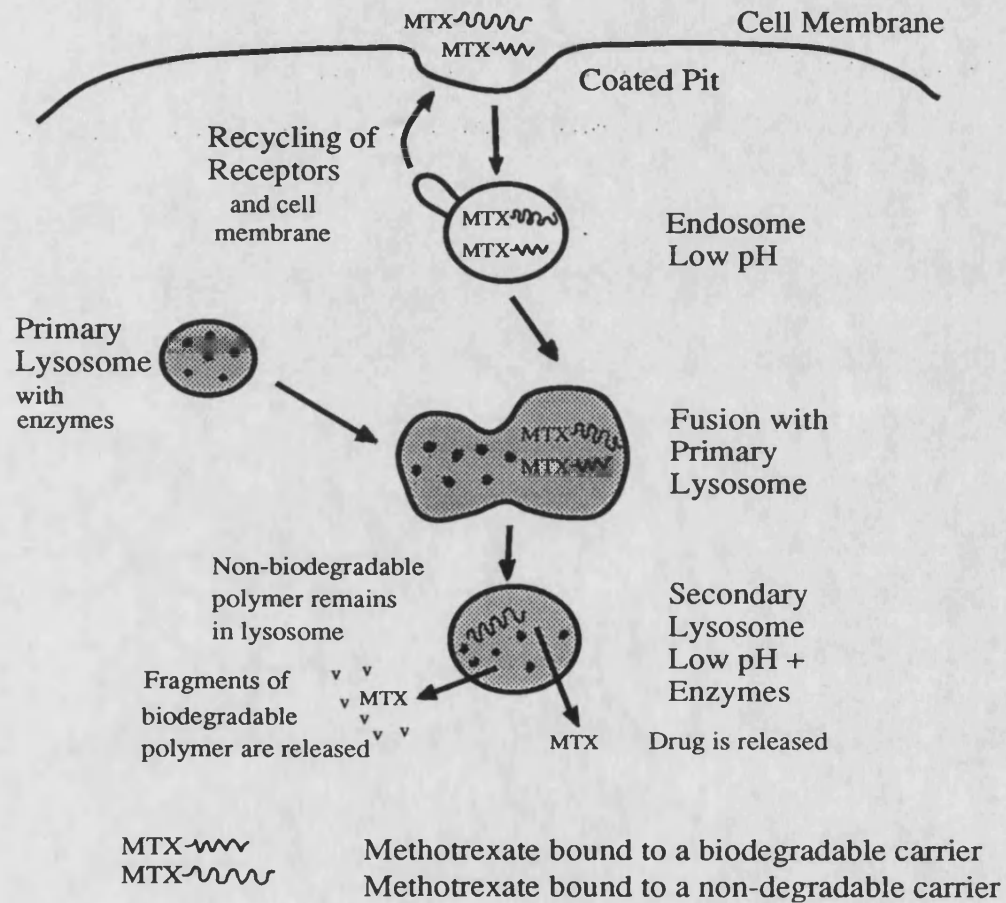
targeting relies on the inherent nature of the drug complex e.g. particulate and cellular carriers are taken up by cells of the RES.

A drug which is delivered to a cell, bound to a macromolecular carrier, cannot simply diffuse into the cell. It has to be taken up by pinocytosis. This is a ubiquitous process and individual cell types differ only slightly in the rate at which they pinocytose solutes.<sup>(7)</sup>

Figure 1.2 describes the process of pinocytosis. It can be of three types: Fluid phase (non-specific), adsorptive and receptor mediated. Adsorptive pinocytosis can account for the increased cellular uptake of hydrophobic or cationic macromolecules compared to non-charged hydrophilic molecules. Pinocytosis always occurs from the area of cell membrane known as a coated pit (except in endothelial cells).<sup>(7)</sup> The membrane captures fluid and solutes which are coated on or close to its surface. The vesicle formed then loses its clathrin coat and becomes known as an endosome or CURL (compartment of uncoupling of receptor and ligand). The endosome has a low pH, maintained by an active ATP powered proton pump. The endosome has two functions; to deliver ligand to the lysosome and to recycle membrane back to the cell surface. The receptor to which ligands are bound can be recycled as in the case of the LDL and asialoglycoprotein (ASGP) receptors<sup>(8)</sup> or the receptor can be transferred to the lysosome with the ligand e.g. Epidermal Growth Factor. In this situation, down regulation of the receptor occurs.

There are three routes out of the endosome. One leads to the lysosome and the proteolytic enzymes which it contains. The other two routes both lead to the cell surface; either the section of cell membrane from whence it came or, in polar cells e.g. the endothelia, to the opposite side of the cell (transcytosis). The lysosome contains approximately 50 different enzymes which can break down most biological molecules to their respective monomers.<sup>(7)</sup> The membrane of the lysosome is impermeable to macromolecules and to charged or hydrophilic molecules like sucrose. It also has a proton pump to maintain a low pH.

**Figure 1.2 The Route for Lysosomal Delivery.**



Most soluble drug-macromolecule conjugates are designed so that they are stable within the blood stream, and free drug is only liberated after internalisation of the conjugate into the cell, followed by lysosomal degradation. Before a drug-macromolecule conjugate can actually get to its target site, it must leave the blood stream. It would seem prudent at this stage, to discuss some of the aspects of the vascular compartment which should be considered and may be exploited in the design of a targetable form of a drug.

## **1.2 Physiology of Extravasation: The Endothelial Cell Barrier.**

The capillaries and other blood vessels constitute a barrier between plasma and interstitial fluid. This barrier consists of the blood endothelial interface, the endothelium, the basal lamina and the adventitia.<sup>(9)</sup>

Capillaries are the smallest blood vessels and form a barrier that is only one cell thick. The microvessels, which are the arterioles, capillaries and post-capillary venules,<sup>(10)</sup> are the vessels which are responsible for the exchange of solutes and gases. Capillaries can be divided into 3 groups; continuous capillaries are found in the myocardium and brain, fenestrated capillaries are usually found in organs whose functions demand a high rate of fluid exchange<sup>(11)</sup> such as the intestine, kidney and adrenal cortex and sinusoidal capillaries are found in organs of the RES e.g. liver and spleen.

Endothelial cells are coated on their luminal surface with an adsorbed layer of plasma proteins e.g. albumin, fibrin and heparin. Along with the glycocalyx this layer forms the blood endothelial interface. The coat continues into the plasmalemmal vesicles which open onto the luminal surface of the cells and into the transendothelial channels. It has a net negative charge due to the presence of acidic glycoproteins.<sup>(12)</sup>

The endothelial cells are squamous epithelia which are connected by intercellular junctions. The junctions are of two types i.e. tight (occluding) and gap junctions. Tight junctions are considered to seal the intercellular space thus preventing passage along this route.<sup>(9)</sup> Most endothelial cells are connected by tight junctions, but up to 30% of

the junctions found in venules have been found to exhibit gap junctions up to 6nm in diameter.<sup>(13)</sup>

Endothelial cells are metabolically active and they are differentiated to mediate and monitor bidirectional exchange of substances.<sup>(9)</sup> They demonstrate a large number of plasmalemmal vesicles with a diameter of 60-80nm. These can be open on either side of the cell and present within the cytoplasm. Fusion of these vesicles can occur, thus providing a transendothelial pathway. The density of vesicles within a cell is dependent on the organ within which it is found. The number found in brain capillaries is much lower than in other organs. The frequency of vesicles is also dependent on the type of microvessel in which they are found. Endothelial cells found in capillaries, particularly at the venular end, demonstrate the highest number.

In cell types other than the endothelium, the plasmalemmal vesicles would direct absorbed solutes to the lysosome. However in endothelial cells the process of transcytosis is favoured. Endothelial cells do contain lysosomes and it is other organelles within the cell which are responsible for delivery to them. Transcytosis of a macromolecule, be it an endogenous protein or an injected macromolecule, brings it into the interstitial fluid. From here it is returned to the blood stream via the lymphatics. The concentration of macromolecules in the interstitial fluid has been found to be the same as pre-nodal lymph in sub-cutaneous sites<sup>(14)</sup> and may be the same throughout the body.

Fenestrae are circular openings of approximately 70nm in diameter. They are found in visceral endothelial cells as already described. In all, apart from cells found in the glomerulus, the fenestrae have a diaphragm with exposed negative charges, which is made up of heparan sulphate proteoglycan.<sup>(15,16)</sup>

Coated pits (diameter 100-120nm) are found on both endothelial cell surfaces, but are more common on the luminal side. They are found in all cell types, particularly sinusoidal capillaries. The coat consists of clathrin. In continuous and fenestrated capillaries the coat has exposed anionic sites. In sinusoidal capillaries there are areas of

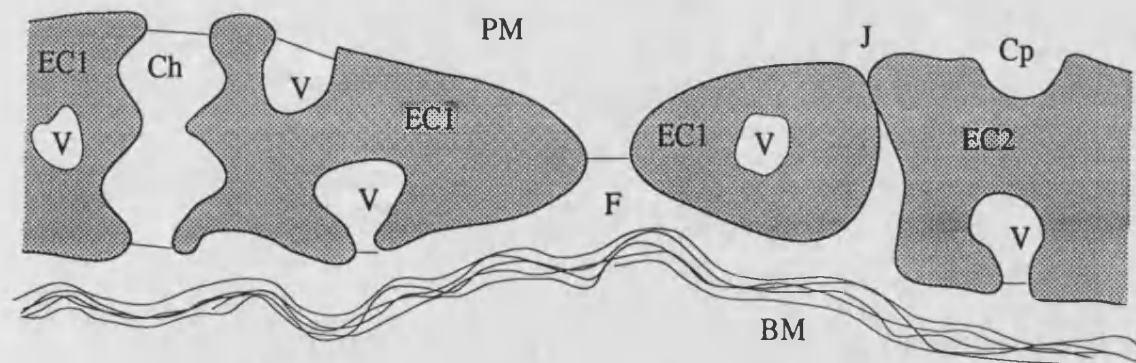


both anionic and cationic charge. Coated pits seem to be associated with the receptor mediated endocytosis of certain macromolecules e.g. LDL. The pits direct adsorbed material to the lysosome e.g. positively charged molecules. Solutes taken up by fluid phase endocytosis do not seem to be processed in this way.

Endothelial cells exhibit receptors for sugars, lectins,<sup>(17)</sup> insulin<sup>(18)</sup> and histamine. The histamine receptors are found on post capillary venules. Following occupancy of this receptor the endothelial cells contract<sup>(19)</sup> and this is an important factor in the inflammatory response.

The basal lamina forms a rest for endothelial cells. It is 5-8 nm thick and consists of components secreted by the endothelial cells themselves e.g. collagen types IV and V and fibronectin. The lamina appears as a continuous layer beneath continuous and fenestrated capillaries and is patchy beneath sinusoidal capillaries. The basal lamina has been demonstrated to form a negatively charged barrier.<sup>(20)</sup> Figure 1.3 shows the structure of a layer of the endothelial barrier.

**Figure 1.3 The Structure of the Endothelial Cell Layer.**



**KEY:**

BM = Basement Membrane, Ch = Channel, Cp = Coated Pit, EC1 = Endothelial Cell (1)  
EC2 = Endothelial Cell (2), F = Fenestra, J = Junction, PM = Plasma Membrane,  
V = Vesicle.

The capillary endothelial barrier has classically been described by physiologists as an impermeable layer that is perforated with 2 types of pores.<sup>(21)</sup> These are classified as large pores with a diameter of 50-70nm and a frequency of 1 pore/20 $\mu\text{m}^2$  and the small pores with a diameter of 6-9nm and a frequency of 10-15 pores/ $\mu\text{m}^2$ . This theory has arisen from theoretical considerations which resulted in the proposal of simple equations which equate solvent and solute flow across porous barriers. (Kedem and Katchalsky 1958 and 1963). In addition Patlak included a selectivity factor in his equation since he believed that all macromolecules would not be able to pass through the pores at the same rate.(Patlak 1963) This work has been reviewed by Taylor and Granger.<sup>(11)</sup>

Experimental work which has usually involved the simultaneous measurement of macromolecules in plasma and lymph has supported the two pore theory. However, investigations using the electron microscope have had difficulty in demonstrating them. The large pores may be explained by the plasmalemmal vesicles, channels or fenestrae. The small pores are more difficult to equate. They may be due to the gap junctions which are found in post-capillary junctions.<sup>(21)</sup>

### **1.2.1 Organ Selectivity in Transcapillary Exchange.**

The endothelium is involved in the sorting and gating of molecules.<sup>(9)</sup> It can sort molecules according to molecular size, charge, and chemical nature.

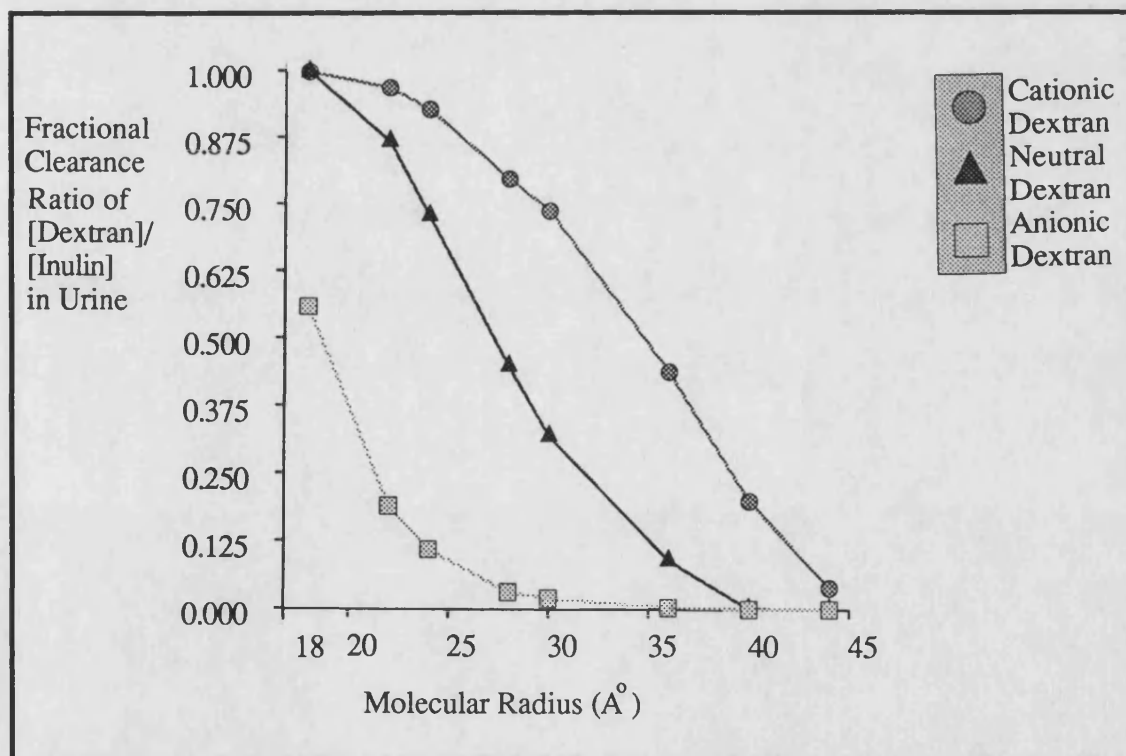
It has already been mentioned that organs can demonstrate one of 3 types of capillary (fenestrated, continuous and discontinuous). On top of this, each organ demonstrates its own inherent differences.

The continuous capillaries exhibit the greatest restriction to the passage of macromolecules. This type of capillary is the most widely distributed in the body. It appears that continuous capillaries situated in the lung are able to transport larger molecules than those found in sub-cutaneous and skeletal muscle. This data was determined by measuring the lymph to plasma ratios of endogenous proteins in these

organs.<sup>(11)</sup>

Of the fenestrated capillaries the kidney demonstrates the most obvious differences from the rest of its type. Its fenestrae are not covered by a diaphragm, yet it has a cut off molecular weight for transport of macromolecules at a much lower level than other capillaries of this type. Macromolecules with a radius of above 4.4nm are not transported from blood into the urine.<sup>(22)</sup> The reason for this size selectivity appears to lie with its considerably thicker basement membrane. This membrane also exhibits a negative charge. Bohrer<sup>(23)</sup> demonstrated that dextrans with a net positive charge were excreted more readily by the kidney than molecules of an equal size which are negatively charged or neutral up to a molecular radius of 4.3nm. Figure 1.4 taken from this reference<sup>(23)</sup> demonstrates this.

**Figure 1.4 Relationship between Fractional Solute Clearance and Molecular Radius in Rat Kidney for Neutral, Anionic and Cationic Dextrans.**



Several investigators have demonstrated, in the intestinal and lung capillaries, the increased transport of negatively charged molecules compared to equal sized positively charged.<sup>(24,25)</sup> Perry et al<sup>(24)</sup> believed that their results indicate that the plasmalemmal

vesicles exhibit a positive charge in the intestine but they had no evidence to substantiate this. Parker et al<sup>(25)</sup>, finding similar results in the lung, believed that this could be explained by cation exchange of the macromolecule with the small cations known to be found on the anionic sites of the plasmalemmal vesicles. Thus adsorbed cationic molecules were not transported. However the anionic molecules were able to move freely through the plasmalemmal vesicles.

### **1.2.2. Tumour Blood Vessels.**

An avascular tumour cannot grow to much more than 1 to 2 mm in size. At this size passive diffusion can no longer provide nutrients and remove waste products and for every new layer of cells that grow on the outside of the tumour a layer must die on the interior.<sup>(26,27)</sup>

If a tumour becomes vascularised then tumour cells grow in a cylindrical manner around the blood vessel.<sup>(28)</sup> Many tumours are able to promote angiogenesis (development of new blood vessels) by a process of sprouting from pre-existing vessels.<sup>(29)</sup> Inflammatory cells from the host may also be able to promote angiogenesis.

The first response to an angiogenic stimulus is the dissolution of the basement membrane surrounding a pre-existing post-capillary venule. Next the endothelial cells migrate out of the old vessel towards the tumour and this is accompanied by cell division. The next step is the formation of a three dimensional structure with a lumen. This can then differentiate into a capillary loop and then a mature vascular bed, the capillaries having a basement membrane.<sup>(30)</sup>

Several factors have been implicated in promoting angiogenesis.<sup>(26)</sup> Some like angiogenin, which is produced by the tumour<sup>(31,32)</sup>, can only induce one aspect of angiogenesis, in this case cell migration, while others can induce both mitogenesis<sup>(33,34)</sup> and angiogenesis<sup>(35)</sup> e.g. Heparin Binding Growth Factor (HBGF). The angiogenic properties of HBGF are enhanced by heparin.<sup>(36)</sup> There are also inhibitors of the angiogenic factors e.g. Angiogenin is blocked by placental ribonuclease inhibitor<sup>(37)</sup> and HBGF is inhibited by protamine and cortisone when it is administered with heparin<sup>(36)</sup> (cortisone alone has no effect).

It is hardly surprising, because of the way tumour blood vessels develop, that they are not like the blood vessels found in the host organ.<sup>(38)</sup> The differences can occur in the cellular composition of the vessel - the capillaries found in tumours are made up almost entirely of endothelial cells whereas normal capillaries will also contain pericytes. Pericytes appear to modulate the growth of endothelial cells<sup>(39)</sup>. Other differences are an increase in permeability and changes in vessel stability.

Most tumour capillaries are of a continuous type,<sup>(40)</sup> although it has been demonstrated that some tumours, particularly those found in liver, kidney or exocrine glands, can induce the angiogenesis of fenestrated or sinusoidal vessels.<sup>(41)</sup> The continuous endothelium found in tumours has been shown to be more leaky towards injected macromolecules (e.g. dextrans, IgG and fibrin) than normal vessels.<sup>(42,43)</sup> This leakiness was shown to be confined to the venules running along the periphery of tumours and at the tumour-host interface. However, immature vessels at the periphery and vessels within the tumour did not demonstrate the increased permeability.<sup>(42)</sup> It has been demonstrated that tumours actually release a factor which increases vascular permeability.<sup>(44-46)</sup>

Kinin generation also appears to be important in inducing increased vascular permeability in tumours<sup>(38)</sup>. Bradykinin and hydroxyprolyl<sup>3</sup>-bradykinin have been found in the ascitic fluid bathing human tumours.<sup>(47)</sup> When mice bearing ascitic tumours were given an IP injection of Soy-bean Trypsin inhibitor (an inhibitor of the production of kinins) the ascitic fluid production was suppressed.<sup>(38)</sup> Captopril and enalapril are potent inhibitors of the breakdown of kinins. This could be exploited to increase the vascular permeability in tumours to allow the entry of antibodies, while blood vessels in normal tissue are unaffected since they are not generating kinins.<sup>(48)</sup>

Tumour capillaries exhibit a reduced basement membrane which contains a higher concentration of hyaluronic acid and lower concentration of sulphated glycosaminoglycans.<sup>(49)</sup> This gives rise to an altered architecture which has been demonstrated to be more leaky.

Although tumours can induce endothelial cell migration, they cannot induce lymphatic invasion.<sup>(26,50)</sup> In addition the existing lymphatics within an organ can become obstructed by a tumour.<sup>(51)</sup> Thus the increased permeability of the capillaries leads to drainage of fluid and plasma proteins into the interstitial space and oedema results because the extra interstitial fluid cannot be channelled away. A rise in interstitial pressure occurs and this could also be due to the increase in tumour cell mass which has had to occur in a confined space.<sup>(26)</sup> One consequence of the increase in interstitial pressure is an occlusion of the blood vessels in the interior of the tumour with consequent ischaemia and tumour necrosis. There are two problems associated with the increased pressure; firstly it may facilitate the exit of tumour cells and secondary tumour development (metastasis). Secondly, because of the differential between high pressure in the interstitium and low pressure in the microvascular circulation, the delivery of exogenous drugs may be prevented and the entry of normal host defences barred.

### **1.3 Types of Carrier used in Drug Targeting.**

Soluble carriers have been classified into two groups;<sup>(52)</sup> either of natural origin e.g. proteins, carbohydrates like dextrans and DNA or of synthetic origin e.g. polyvinyl pyrrolidone (PVP), polylysine and poly-N-(2-hydroxypropyl) methacrylamide (HPMA). Some examples of these will be discussed below. They can also be categorised into their ability to be degraded *in vivo*. Polymers which are of natural origin are usually biodegradable and this is one advantage in using them. They also (apart from the polysaccharides) demonstrate little polydispersity. Synthetic polymers are not usually biodegradable unless they have been specifically synthesised to include biodegradable bonds<sup>(53)</sup> and because they are man made they are likely to be polydisperse. An advantage which synthetic polymers have over natural is that they are less likely to evoke an immunogenic response *in vivo*,<sup>(54)</sup> and they can be tailor made to requirements of molecular weight, charge and hydrophobicity.<sup>(55)</sup>

### 1.3.1 Synthetic Macromolecules as Carriers in Drug Targeting.

A great deal of research has centred around the use of HPMA copolymers as carriers for cytotoxic drugs. Seymour et al<sup>(56)</sup> demonstrated a size selective urine excretion of non-biodegradable HPMA copolymers. Copolymers with a molecular weight above 45 kD were not lost from the blood stream via the kidney, and only disappeared from the blood stream very slowly as they extravasated into the tissues. A size-dependent uptake of the copolymer by the liver was also demonstrated.

The aim of a drug targeting conjugate is to prevent loss of drug via the kidney and to limit cellular uptake to the process of pinocytosis.<sup>(57)</sup> Thus a carrier should have a molecular weight above 45 kD. However for a non-biodegradable carrier, this may present toxicity problems, as a molecule of this size cannot get out of the lysosome and would be retained for the life of the cell. Subr et al<sup>(53)</sup> tried to overcome this problem by linking sections of copolymer with peptide linkages. The resultant copolymer would not be excreted via the kidney until it had reached the lysosome of its target cell, and the copolymer bridges had been removed.

Replacing some of the hydroxypropyl groups, during synthesis of HPMA, with drug and targeting residues gives rise to a soluble drug-targeting conjugate.<sup>(58)</sup> Drugs that have been bound to HPMA include daunomycin,<sup>(59-61)</sup> puromycin,<sup>(59)</sup> adriamycin.<sup>(62,63)</sup> Each drug was successfully attached to the HPMA via a biodegradable peptidic spacer i.e. GLY-PHE-LEU-GLY-DRUG. This sequence was found to be stable in the blood stream but sensitive to lysosomal cysteine proteinases.<sup>(54)</sup> The conjugated form of these cytotoxic drugs was found not to distribute to the heart (site of major toxicity for this group of drugs and often the reason for prematurely stopping therapy) and this is an example of negative targeting.

Targeting groups have been applied to the HPMA-drug conjugates. These include antibodies e.g. anti-Thy 1.2<sup>(61,64)</sup> and sugar residues such as galactosamine<sup>(65,66)</sup> and fucosylamine.<sup>(60,62)</sup>

Another synthetic polymer which has been the subject of a great deal of research is poly-lysine.<sup>(67-69)</sup> Poly-lysine is a cationic molecule at physiological pH and it enters cells by the process of adsorptive pinocytosis.<sup>(70)</sup> It can be synthesised in a range of molecular weights and utilising either D-Lysine or L-Lysine. Polymers formed from L-lysine can be metabolised *in vivo* whereas poly-D-lysine (PDL) cannot be degraded in the body. Arnold et al,<sup>(67)</sup> using cultured HeLa cells and also Ehrlich Ascites Tumour Xenografts growing in mice demonstrated that poly-lysine is cytotoxic in its own right. This factor could be a disadvantage since quite small doses (LD<sub>50</sub> for 70KD poly-L-lysine (PLL) was 5 doses of 30mg) of the polymer were toxic to normal mice. The molecular weight of the polymer determines the degree of cytotoxicity; as molecular weight increases toxicity increases. The mechanism of this toxicity appears to be due to the cationic nature of the polymer since it causes cell aggregation and promotes the efflux of small molecules from the cell by creating openings in cell membranes.<sup>(71)</sup> There is a degree of selectivity in the poly-lysine toxicity since it has no effect on mice inoculated with L1210 leukaemia. Also, cancer cells generally exhibit an increased anionic charge which would make them more susceptible to poly-lysine.<sup>(67)</sup>

Ryser and Shen<sup>(70)</sup> conjugated MTX to poly-lysine and used the carrier complex to deliver MTX intracellularly to a MTX transport resistant CHO cell line. Galivan et al<sup>(72)</sup> also demonstrated cytotoxicity of a MTX-PLL conjugate in their MTX transport resistant H35 cell line. Unconjugated MTX was ineffective at the same concentration. The cytotoxicity of the MTX-PLL could be inhibited by leupeptin, a lysosomal enzyme inhibitor which prevents the liberation of pharmacologically active drug.

MTX directly conjugated to PDL has no cytotoxicity (apart from that due to the polymer) since free drug cannot be liberated from the conjugate. In order to make the conjugate cytotoxic, MTX had to be linked to the polymer via a biodegradable spacer. Ryser and Shen<sup>(70)</sup> demonstrated that a tripeptide spacer (GLY-GLY-GLY) was sufficient to allow liberation of active drug.

Other drugs have been successfully conjugated to poly-lysine to give conjugates with



cytotoxic activity. These include daunomycin and 6-aminonicotinamide.<sup>(67)</sup>

### 1.3.2 Dextrans

Dextran is a naturally occurring polysaccharide which can be obtained from *Leuconostoc mesenteroides*. It is highly water soluble, has been used for several years as a plasma expander so that its safety *in vivo* has been established, and it is available in a wide range of molecular weights ( $2 \times 10^3$  to  $10^6$ ).<sup>(2)</sup>

Drugs<sup>(73)</sup> and enzymes<sup>(74)</sup> have been successfully coupled to the hydroxyl groups of dextran. Takakura et al<sup>(75)</sup> have bound mitomycin C (MMC) to dextran using a 6-bromohexanoic acid spacer leading to a conjugate with an anionic charge. This spacer gave a bond which could be chemically hydrolysed under physiological conditions, thus allowing the gradual release of active drug. The half-life for the cleavage of the drug-spacer bond was 35 hours for a dextran with a molecular weight of 70kD. MMC is unstable within the environment of the lysosome, so it was inappropriate in this case to conjugate the drug to the dextran with a bond which could only be broken down enzymatically.<sup>(73)</sup> The dextran conjugate could be used as a reservoir of drug. The release was slow enough to allow the dextran to alter the distribution of MMC *in vivo*. One dose of the conjugate proved to be superior to free MMC at prolonging the life of mice inoculated with P388 leukaemia when administered via the same route as the tumour but 24 hours later.<sup>(73)</sup>

Cationic dextran conjugates have also been prepared by incorporating 6-amino caproic acid as the spacer.<sup>(76)</sup> These have enhanced antitumour activity *in vitro* compared to anionic conjugates.<sup>(77)</sup> However *in vivo* they have less antitumour activity because they are rapidly removed from the blood by the liver<sup>(78)</sup> and spleen.<sup>(76)</sup> In local injection cationic MMC-dextran conjugates proved to be superior to anionic conjugates since the cationic conjugate was retained at the injection site.

### 1.3.3 Proteins.

#### a) Monoclonal Antibodies

Monoclonal Antibodies (mAb) have been the object of a great deal of research in the drug-targeting field. They have already established themselves as valuable diagnostic agents for both primary and secondary tumour growths.<sup>(79,80)</sup> Most antibodies have little activity on the growth of the tumour themselves and so, for the treatment of cancer, drugs or toxins are bound to the mAb. Certain factors need to be considered to achieve a successful targeting complex.<sup>(81)</sup>

1. Is a specific antigen available for the tumour cell?
2. Does the mAb localise in the tumour *in vivo*?
3. Is the mAb suitable for drug linkage?
4. Does the toxicity or immunogenicity increase after drug is conjugated to the mAb?
5. Does the mAb still localise in the tumour after drug binding?

#### Problems Associated with the Use of mAb.

mAbs are usually produced in response to tumour associated antigens (TAA), which are commonly found on the surface of neoplastic cells. However they are not found exclusively on tumour cells; certain normal cells also demonstrate them, though at a much lower level.<sup>(82)</sup> These TAA may dissociate from the tumour and enter the blood stream. This would lead to neutralisation of some of the mAb before it had chance to reach and interact with the target cell.<sup>(81)</sup>

Another problem associated with the use of mAb to TAA is that some cells within a given tumour mass will not demonstrate a particular antigen. Kufe et al <sup>(83)</sup> demonstrated in their mammary carcinoma cell line, using the mAb B6.2 and B38.1, that cell binding was cell cycle specific with maximal binding occurring when a cell

was in the S-phase of cell growth. P. Horan Hand et al<sup>(84)</sup> demonstrated a patchwork of antibody binding in their mammary carcinoma cell line with 4 different mAb. If a single mAb drug conjugate was administered then all sensitive cells could be killed within a tumour cell mass, but cells which did not express the TAA would be unaffected. This problem could be overcome by administering two or more different mAb conjugates in the hope that each cell would be sensitive to at least one.<sup>(85)</sup>

M.V. Pimm in his recent review<sup>(81)</sup> has described many reports where only 0.005% of the mAb localised in human tumours, even after several days, although these may represent tumour to normal tissue ratios of up to 10:1. One of the problems associated with the use of mAb is their relatively large molecular weight (IgG=150kD) and thus they can only slowly get out of the blood stream. Although mAb are reactive to TAA, there are no receptors either for the antigen binding sites or the Fc portion on normal vascular endothelia.<sup>(86)</sup> Autoradiography of the tumour following administration of radiolabelled mAb showed the radioactivity to be confined to the periphery of the tumour mass.<sup>(87,88)</sup> As already described,<sup>(32)</sup> the vessels at the periphery of the tumour are more leaky than the vessels within the interior.

Several investigators have overcome the problem of size of the mAb by treating it with pepsin to yield either F(ab)<sub>2</sub> or Fab fragments. These should more readily leave the vasculature. However they exhibit a decreased binding potential to the TAA which results in a decrease in the amount of fragment localised in the tumour.<sup>(89)</sup>

Buchegger et al<sup>(90)</sup> demonstrated that their Fab fragment, although showing a lower absolute level in the tumour compared to intact IgG, did show a greater penetration into the tumour mass. In addition fragment which is not tumour bound may be cleared more rapidly avoiding systemic toxicity.<sup>(89)</sup>

One of the problems associated with binding drug to the mAb is that antigen binding ability may be reduced if the tertiary structure is altered or drug binds to the active site.<sup>(91)</sup> This loss of activity can be reduced if the active site is blocked reversibly before drug conjugation takes place.<sup>(92)</sup> Another way of preventing damage to the

antigen binding site is to conjugate large quantities of drug to a spacer and then bind the spacer to the mAb.<sup>(93,94)</sup> However, this has the disadvantage that the complex molecular weight is increased significantly, thus restricting extravasation still further.

The drug to be bound to the mAb must have a group which can participate in the reaction and the bond that is formed must be cleavable intracellularly so that the drug can be released from the conjugate. Garnett et al<sup>(95)</sup> showed convincing evidence that the 791T/36 mAb, after binding to its receptor, was internalised into endosomes or lysosomes. This would allow breakdown of the antibody and release of 'active' free drug.

Another system is the immunotoxin where a mAb has been covalently bound to a toxin e.g. ricin A chain,<sup>(96)</sup> diphtheria toxin and abrin.<sup>(97)</sup> The toxins are extremely poisonous. It has been estimated that only one ricin molecule is required to kill a cell. Thus, only one toxin molecule is required to be bound to a mAb and this may be useful in treating cancer cells which express only a low titre of antigen.<sup>(98)</sup> Because of the toxicity, stringent purification steps are required to remove traces of unconjugated toxin. Normal cells may also take up the immunotoxin by non-specific pinocytosis and this may lead to toxicity problems.

#### **b) Albumin.**

Chu and Whiteley<sup>(99)</sup> covalently bound MTX to BSA or mouse serum albumin using a carbodiimide coupling reaction. They tested these conjugates in mice with L1210 leukaemia and found that they were equally effective as free drug in prolonging the survival time when compared to untreated controls. However, when the conjugates were tested against L1210 cells *in vitro* they found that free MTX was approximately 100 times more active than the conjugated drug. These apparent differences could be due to the fact that MTX-albumin gave prolonged serum levels and decreased excretion in mice compared to the free drug thus giving the drug more time to reach the tumour cells *in vivo*. Indeed, measurement of drug levels in the extracellular fluid bathing the

tumour cells showed elevated levels of the conjugated drug at 24 hours.

The MTX-BSA conjugate was shown to enter cells by a method other than the folate transporter, since cellular uptake was not inhibited by folinic acid or at reduced temperature, as it was for free drug.<sup>(100)</sup> It was demonstrated that MTX was not liberated from the conjugate until it had been internalised.

IP injections of BSA-MTX were found to be superior to free MTX against Lewis Lung Carcinoma, both in reducing the size and number of metastatic nodules in the lung and in reducing the size of the SC implanted solid tumour.<sup>(101)</sup> The amount of drug in the tumour following administration of the MTX and MTX-BSA was found to be equivalent after 1 hour. However, after 8 and 24 hours the conjugate levels were double those of the free MTX. In another tumour model, Gardner Lymphosarcoma, MTX conjugated to HSA was found to be superior to the free drug in increasing life span.<sup>(102)</sup>

Other drugs have been linked to albumin. Daunorubicin (DNR) was linked to succinylated albumin using various peptide spacers.<sup>(103)</sup> In an *in vitro* experiment where the conjugated DNR was incubated in the presence of lysosomal enzymes it was shown that the spacer had to be at least three amino acids long (in this case Leu-Ala-Leu) to allow release of free drug. The activity of the conjugates *in vivo* against mice with L1210 leukaemia was also found to be dependent on the length of the peptide spacer. Conjugates with spacers of three or four amino acids in length were superior to free daunorubicin and produced long term survivors.

The conjugates between cytotoxic drugs and albumin described here have not incorporated a targeting agent. Where they have been successful in treating mice which have been infected with tumours cells, this is probably due to the fact that tumour cells have an increased metabolic rate compared to normal cells and as a result are more active in pinocytic uptake. In addition by prolonging the circulation half-life of the drug, it had more chance to reach its site of action.

### **c) Other Proteins.**

Chu and Whiteley<sup>(101)</sup> demonstrated that conjugates between chymotrypsinogen or non-specific IgG with MTX were equally effective in an IP-IP model at prolonging the life of mice with L1210 leukaemia as free MTX and MTX-BSA.

Conjugates have also been prepared between MTX and fibrinogen.<sup>(104,105)</sup> The rationale for using this protein is that it can be converted *in vivo* to fibrin. Fibrin is found deposited in solid tumours.<sup>(26)</sup> It is an insoluble protein which is formed by the action of thrombin on fibrinogen. The MTX-Fibrinogen conjugate can also be precipitated by the action of thrombin and so this conjugate may become deposited in the tumour following administration, thus acting as a slow release preparation. Dyr et al<sup>(104)</sup> found that the conjugate was inactive against HeLa cells *in vitro*. However, when proteolytic enzymes were added to the incubation media (e.g. trypsin), the conjugate was inhibitory towards cell growth. Freshly established tumour cell cultures are known to demonstrate high levels of fibrinolytic activity and so this conjugate may be effective in the clinical setting.

## **1.4 The Pharmacology of Methotrexate**

Methotrexate was chosen as the model anticancer drug for use in this thesis. It was chosen because it was readily available, a kind gift from Cyanamid UK, Gosport, Hants. It is a relatively non-toxic drug (compared to other cytotoxic drugs) and there is an antidote available. In addition it has a carboxylic acid group which can be used for linkage to proteins.

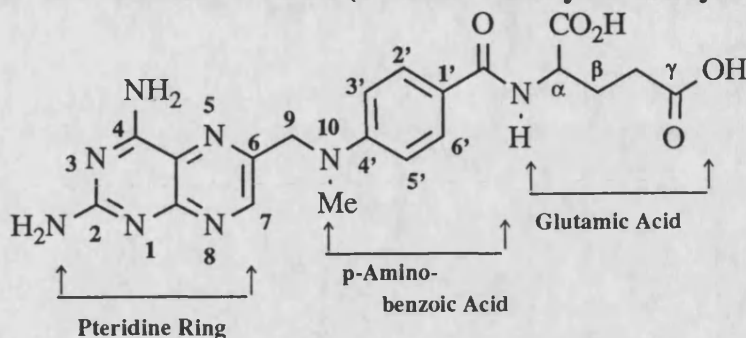
### **1.4.1 Biochemical Activity of MTX.**

Anticancer drugs can be conveniently divided into a series of groups e.g. alkylating agents, intercalating agents and antimetabolites. Most anticancer agents owe their activity to a non-selective inhibition of DNA synthesis.

MTX is an antimetabolite which means that it has a structural relationship to a natural

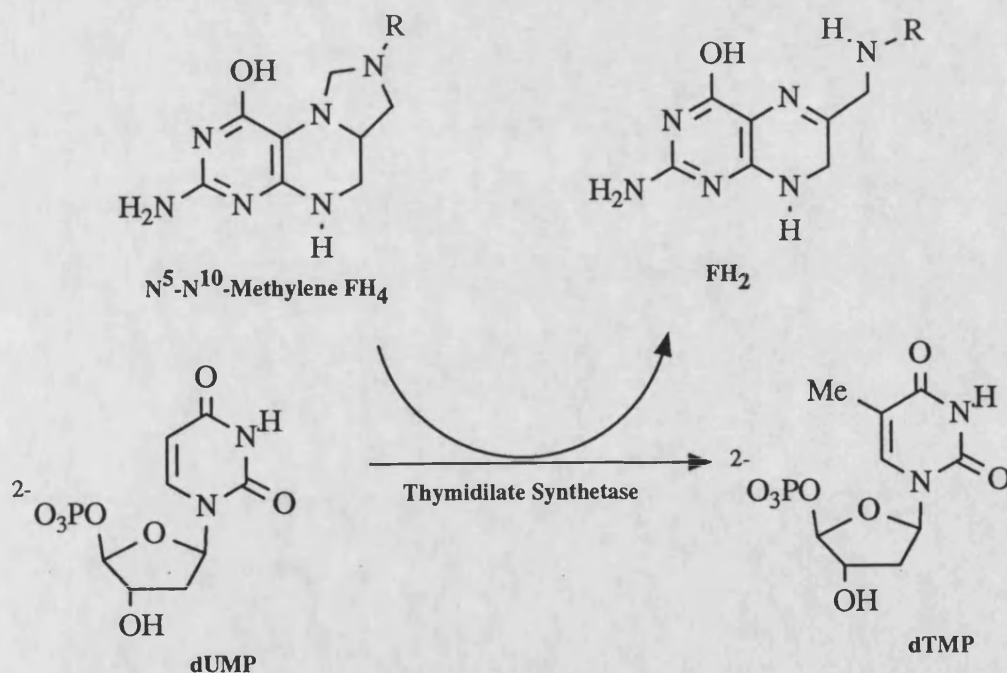
cellular metabolite and can thus bind to receptors to prevent the normal functioning of the cell. Figure 1.5 shows the structure of MTX. It is an analogue of folic acid.

**Figure 1.5 The structure of MTX (4-amino-4-deoxy-10-methyl-folic acid).**



The folate vitamins play an important role in reactions which involve a transfer of a one carbon unit. They are vital in the *de novo* production of thymidylic acid.<sup>(106)</sup> This is shown in figure 1.6.

**Figure 1.6 The role of the folate coenzymes in the production of thymidylic acid.**



The pathways in which the folate coenzymes function is depicted in figure 1.7. This figure is similar to those described by Jolivet<sup>(107)</sup> and Schweitzer<sup>(108)</sup> and includes the positions where MTX can block. As well as being necessary for the production of dTMP, the folates are also required for the production of purines and amino acids such

as methionine. Figure 1.7 shows that there are many forms of the folate coenzymes and that only the reduced forms are active. Dihydrofolate reductase is the enzyme which is responsible for replenishing the stocks of 'active' reduced folates. The primary site of MTX inhibition is thought to be the DHFR enzyme<sup>(109)</sup> where it is a competitive antagonist. The affinity for MTX at the active site of the enzyme has been calculated to be 20,000 times greater than dihydrofolate ( $\text{FH}_2$ ), its natural substrate.<sup>(110)</sup> The folates are polar molecules, which are ionised at physiological pH. In order to enter cells they use an active transport system. MTX utilises this same transporter to enter cells and has an equal affinity for it.<sup>(111)</sup> Thus it can also inhibit the entry of the coenzymes into cells.

Intra-cellular folates are subject to the actions of the enzyme pteroyl-polyglutamate synthetase.<sup>(112)</sup> This enzyme adds one or more glutamic acid residues to the gamma carboxylic acid group of the folates. The number of glutamates that are added is dependent on the extra-cellular folate concentration. At low folate levels the formation of longer chains is favoured. Intra-cellular folates found in the liver have an average chain length of 5 glutamates but chains of up to 8 amino acids long have been identified.<sup>(112)</sup> Polyglutamation of the folates appears to have a dual function. They act as a storable form of the coenzymes since they cannot readily diffuse out of the cell. They also appear to have greater affinity for some of the enzymes.<sup>(113)</sup>

MTX can also act as a substrate for pteroyl-polyglutamate synthetase. This is important since the addition of three or more glutamate residues leads to a slower rate of efflux than  $\text{MTX}(\text{GLU})_1$  and a selective retention in the cell following removal of extra-cellular drug. There is evidence that there is at least equal affinity for DHFR after polyglutamation<sup>(109)</sup>. Following addition of one or more extra glutamates it has been found that MTX has an increased affinity for thymidylate synthetase.<sup>(114)</sup> Thus it would appear that the presence of polyglutamate metabolite of MTX is an important factor in the cytotoxicity of the drug.



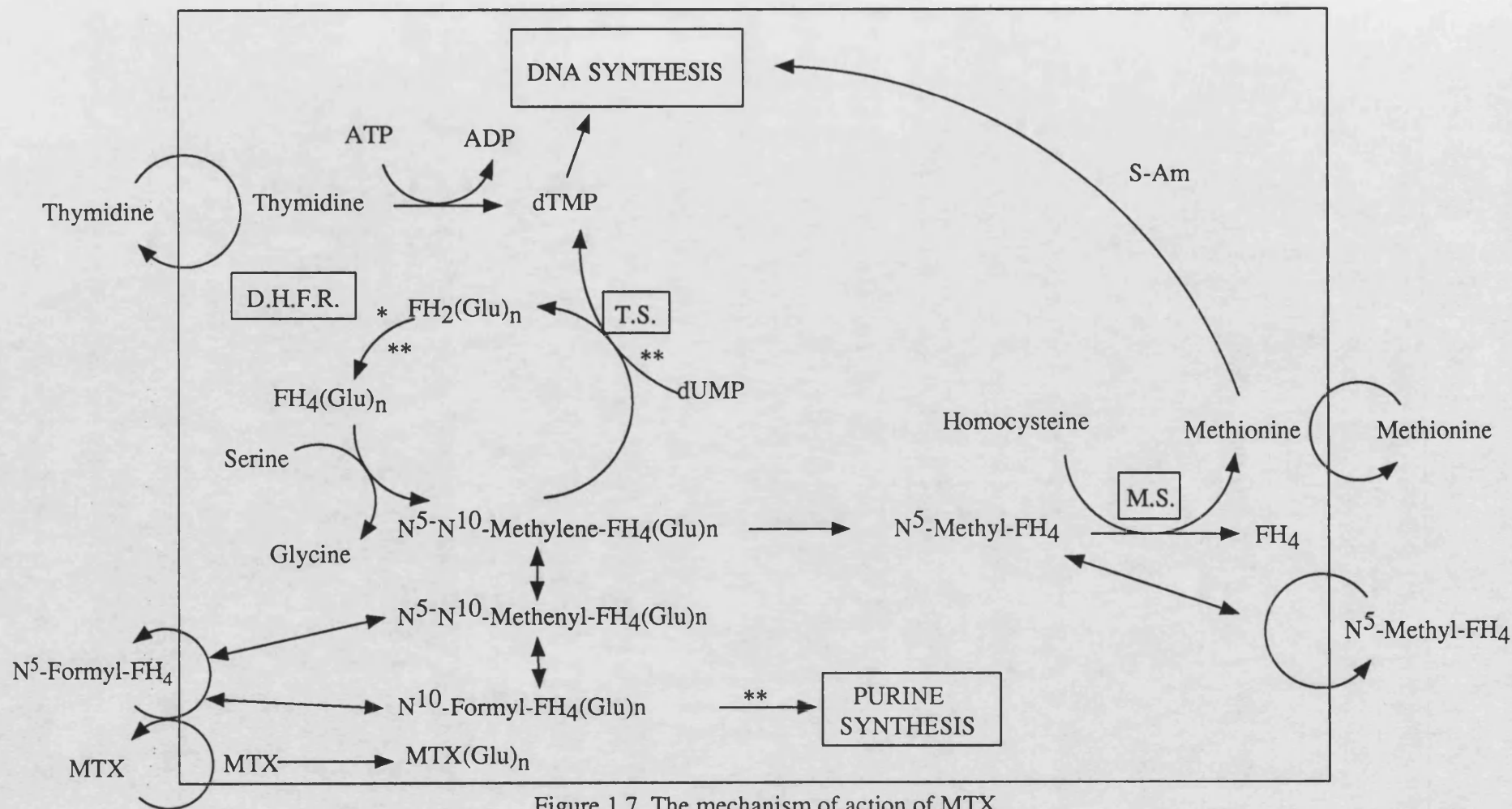


Figure 1.7. The mechanism of action of MTX

\* -MTX Block; \*\* -MTX(Glu)<sub>n</sub> Block

D.H.F.R.: Dihydrofolate Reductase, T.S.: Thymidylate Synthetase, FH<sub>4</sub>: Tetrahydrofolate

FH<sub>2</sub>: Dihydrofolate, S-Am: S-Adenosyl Methionine, Glu: Glutamyl, M.S.: Methionine Synthetase

The steps following appearance of MTX in the extracellular fluid are summarised below.<sup>(115)</sup>

1. Saturation of the folate transporter which brings MTX into the cytosol .
2. Saturation of the DHFR receptor and inactivation of the enzyme. This is the only enzyme which can convert the inactive dihydrofolate to the active form of the vitamin, tetrahydrofolate. The underlying rate of thymidylate synthesis determines the cytotoxicity of MTX.
3. Polyglutamation of non-DHFR bound MTX. The ability of a cell to add glutamic acid to MTX is another determinant of the cytotoxicity of the drug<sup>(116)</sup> since polyglutamates are retained in the cell long after monoglutamate levels fall. Certain cell types have poor pteroyl-polyglutamate synthetase activity (e.g. intestinal epithelia) and this may be the basis of a degree of selectivity.
4. Appearance of MTX(GLU)<sub>n</sub> in the non-exchangeable pool i.e. bound to enzymes such as DHFR and thymidylate synthetase.

#### 1.4.2 Clinical Uses of MTX.

MTX is the most widely used anti-metabolite in neoplastic diseases such as acute lymphocytic leukaemia (ALL), non-Hodgkins lymphoma, osteosarcoma, choriocarcinoma, head and neck cancer and breast cancer. It is often used in combination therapy with other drugs such as cytarabine or asparaginase where the combination can actually have synergistic activity. It is also used in diseases of an inflammatory nature.

It is administered at a very wide range of doses from 15-33,000 mg/m<sup>2</sup>.<sup>(117)</sup> It is one of the few anti-cancer drugs which has a natural antidote i.e. 5-formyl-tetrahydrofolate or folinic acid (Citrovorum factor). Doses of between 500-33,000mg/m<sup>2</sup> are followed by folinic acid rescue, at equimolar or up to 100 fold increased doses to that of MTX. The aim of folinic acid treatment is to time its arrival to normal cells before they have a requirement for dTMP synthesis. Cancerous cells however, because of their faster rate

of metabolism, should have already been affected by the drug. In normal cells folinic acid competes with MTX for the transporter, DHFR, Thymidylate Synthetase and pteroyl-polyglutamate synthetase. Folinic acid has a greater affinity for the latter enzyme and this may be the most important factor in the rescue.<sup>(118)</sup>

### 1.4.3 Cellular Resistance to MTX.

This is one of the greatest problems limiting the use of MTX. It can be natural or acquired after an initial response to the drug. Both of these take the same form.<sup>(108)</sup>

1. MTX is only active on cells which are in the S-phase. If a cell has a naturally slow rate of metabolism then it will be difficult to administer the MTX dose at the correct time.

2. Some cell lines *in vitro* have been demonstrated to show a decreased MTX affinity for the folate transporter. If this occurs *in vivo* then it could be overcome by the administration of large doses of MTX. Extra-cellular concentrations of above 20 $\mu$ M have been demonstrated to cause entry into the cell by a method other than the transporter.<sup>(107)</sup>

3. As mentioned previously, some cells only demonstrate low levels of the pteroyl-polyglutamate synthetase enzyme. This enzyme is important in maintaining high levels of folates and MTX in the cell after extra-cellular levels have dropped. It is thought to be important in the cytotoxicity of MTX.

4. Two factors giving rise to resistance have been demonstrated in the DHFR enzyme. It has been shown that the enzyme can change so that MTX has less affinity for it. A form of natural resistance may occur if the DHFR utilises NADH rather than the usual cofactor NADPH. MTX can form a ternary complex with DHFR and NADPH and this is very stable.<sup>(119)</sup> The MTX DHFR binary complex (which would result if NADH was the only available cofactor) has a much lower affinity.<sup>(120)</sup> In such a system MTX would still be inhibitory but significantly higher MTX concentrations would need to be achieved.

Gene amplification can also lead to increased levels of the enzyme.<sup>(121)</sup> Since MTX blocks DHFR it leads to an increase in intracellular  $FH_2$  levels. These are then available for competition with MTX for the enzyme.

#### **1.4.4 Side Effects of MTX Therapy.**

Like other anticancer drugs, these are due to the fact that MTX inhibits the growth of all rapidly dividing tissue. Thus nausea, vomiting, diarrhoea, myelotoxicity, bone marrow suppression and hair loss may all occur. MTX is a very well tolerated drug however, even when high dose therapy is employed, and the most common side effects seen are ulcerative stomatitis and diarrhoea.<sup>(107)</sup>

#### **1.4.5 Pharmacokinetics of MTX in Man.**

After an IV bolus of drug, three phases are seen. The first has a half-life of 2-8 minutes and is thought to be due to the distribution of drug. The second has a half-life of 0.9-2 hours and can be explained by excretion and metabolism. The third phase has a half life of 5.3-11 hours and is thought to be due to the gradual release of MTX from cells.<sup>(117)</sup> It has been demonstrated that high dose therapy leads to shorter half lives and smaller volumes of distribution.<sup>(117)</sup> Greatest tissue distribution occurs in highly vascularised organs such as kidney and liver. Lower levels are found in the gastro-intestinal tract and skeletal muscle.

Because MTX has limited lipid solubility it has difficulty getting into the brain.<sup>(107)</sup> It is usual to administer MTX directly into the CSF for diseases of the CNS. However it has been demonstrated that large doses of MTX (greater than  $5g/m^2$ ) will get into the brain at appropriate therapeutic concentrations ( $1 \times 10^{-6}M$  in CSF) in children with ALL.<sup>(122)</sup>

MTX is removed from the body predominantly unchanged by the kidney. However some metabolism of MTX does occur. MTX appears in the bile and is metabolised by intestinal flora to 4-amino-4-deoxy-10-methyl-pteroic acid (DAMPA). This metabolite is reabsorbed (only 1 or 2% of an injected dose is excreted in the faeces) and only has 1/200th the activity of MTX.<sup>(117)</sup> Another route of metabolism occurs in the liver.

Aldehyde oxidase metabolises MTX to 7-hydroxy-methotrexate (7-OH-MTX). This is actually less water soluble than MTX and can give rise to renal toxicity. Although at low doses of MTX this metabolite accounts for only 1-11% of the injected dose, at higher doses the 7-OH-MTX levels may exceed the MTX levels by up to 30 times.<sup>(111)</sup> At this concentration the effects of the metabolite may be more significant. 7-OH-MTX has a good affinity for the folate transporter, with a  $K_m$  approximately twice that of MTX, but it has only negligible blocking activity for DHFR (approximately 1/100th of MTX). Thus it can inhibit the cytotoxicity of MTX by blocking its entry into the cell. It is a good substrate for the folyl-polyglutamate synthetase enzyme and there is evidence to suggest that the glutamated form of 7-OH-MTX has a greater affinity for DHFR.<sup>(123)</sup> In practice the effects of the metabolite may have no action on the cytotoxicity of MTX since it is not produced until MTX has swamped the DHFR receptor.

#### **1.4.6 Problems associated with MTX therapy which would benefit from Drug Targeting.**

##### **1. Toxicity**

One of the major factors that limits the use of MTX, and all other anticancer drugs, is the problem of toxicity. Targeting by limiting drug access to its active site would reduce the side effects and have the added advantage that lower doses could be administered.

##### **2. Resistance**

Cancer cells have been demonstrated to acquire resistance to MTX. One mechanism for resistance is a reduced affinity of the folate transporter for MTX. Drug targeting would achieve cellular access of the drug by other means. Another way of overcoming this resistance could be by synthesis of a more lipophilic analogue of MTX which could gain access by simple diffusion into the cell and indeed research into a lipophilic analogue is in progress.<sup>(106)</sup>

### **3. Metabolism**

The 7-OH-MTX metabolite interferes with the action of native MTX. By preparing a conjugate of MTX which is not metabolisable until it reaches its active site this could be prevented.

### **4. Limited Access to Certain Sites.**

Because MTX is a relatively hydrophilic molecule its access into certain sites is inhibited e.g. the brain and poorly vascularised organs. Drug targeting usually exploits a site specific antigen to achieve access and for example this could be the transferrin receptor found on brain microvessels used to gain entry into the brain.

### **5. Short Half-life.**

MTX has a relatively short half-life. A targetable form of the drug could have the added advantage that it has a long circulation half-life and therefore more time to reach the site of action.

### **6. Large Volume of Distribution.**

MTX has a volume of distribution which is equivalent to 77% of the body mass. This could be reduced by conjugation of MTX to a large molecular weight carrier.

## **1.5 Objectives of this Thesis.**

A great deal of research has been carried out in the field of drug-targeting. This research has usually involved the interaction of a drug with a carrier molecule and subsequent testing of this complex on tumour cells *in vitro* and in tumour models *in vivo*. Although the conjugates are usually active in these experimental situations, when they have been tried in the clinical setting they have not always been successful<sup>(81)</sup>.

The aim of this project has been to form large molecular weight, soluble derivatives of methotrexate, a model anti-cancer drug. These conjugates have been administered *in*

*vivo*, using the rat as a model, to determine the distribution and pharmacokinetics. No targeting agent was applied to the conjugate initially, so that the distribution could be determined in normal healthy rats.

The initial studies described in the thesis involved the administration of drugs (methotrexate, digoxin and inulin) to the rat. Their purpose was to gain knowledge of the effects of molecular weight on transport of the drug from SC and IP sites into the blood stream. The molecular weight of methotrexate is 452D, digoxin is 781D and inulin is approximately 5000D. Also, since MTX had been selected as the model anti-cancer drug, it was important to determine the pharmacokinetics and distribution of the drug prior to its conjugation to soluble carriers.

The next series of experiments involved the administration of a number of proteins to the rat. These were mainly of bovine origin and were chosen to include a range of molecular weights from 14KD to 66KD, in the hope that some properties if not a suitable drug carrier could be identified. In order to detect the proteins in rat plasma they were either obtained in a radiolabelled form or were iodinated with  $^{125}\text{I}$ . After administration to the rat, it was anticipated that the proteins may be catabolised with the liberation of some "free"  $^{125}\text{I}$  as iodide. To evaluate what effect free iodide would have on the plasma levels determined for each protein, a study of the pharmacokinetics of  $^{125}\text{I}$ Na was conducted.

Since the proteins used were of bovine origin, they may lead to immune reactions in the rat. A number of experiments were performed in order to investigate whether BSA could precipitate an immune reaction in the rat.

Covalent conjugates were prepared comprising methotrexate linked to BSA, RSA or bovine LA. The pharmacokinetics and distribution of the  $^{125}\text{I}$  was determined after administration of a range of iodinated conjugates between proteins and MTX, including a range of loadings of MTX (%w/w) with each protein. The conjugates were administered by three routes; IV, IP and SC, since route of injection can be exploited to alter the distribution of a macro-molecular species. Following administration of the

conjugates into SC sites, absorption into the blood stream should occur via the lymphatics. Thus SC administration could be used where there is metastatic spread of the cancer within the lymphatic system. The rationale for employing IP administration was that, in theory this would bring drug directly into contact with the organs of the cavity and could be used to treat cancers such as ovarian cancer.

The next step was to try to target the carrier-drug complex. It was decided to use the galactose receptor present on hepatocytes as the targeting region.

The final section of this work investigated the distribution characteristics of the protein drug carriers *in vitro*. The system used was a model of the capillary and was used to determine the ability of the conjugates to extravasate.



**CHAPTER 2**

**MATERIALS AND METHODS**

## **2.1 Materials.**

### **2.1.1. Electron Microscopy reagents.**

All reagents used were of the appropriate grade and were obtained from BDH, Poole, Dorset. Embedding resin was from Taab, Reading, Berks. and Conductive Carbon Cement was from Biorad, Watford, Herts.

### **2.1.2 Gel Chromatography.**

Biogel P4 was obtained from Biorad. Sephadex G15 and blue dextran (relative molecular weight 2 million) were obtained from Sigma Chemical Company, Poole, Dorset. Sephadex G50 was from Pharmacia Ltd, Milton Keynes. PD10 columns and all other columns and associated equipment were obtained from Pharmacia.

### **2.1.3. HPLC.**

HPLC analysis was performed using 15cm, 4.5mm i.d., Apex ODS 5 $\mu$  column or 15cm, 4.5mm i.d., Hypersil ODS 5 $\mu$  columns both of which were obtained from LDC, Stone, Staffs. Mobile phase was passed through the column using an LDC Constametric model III pump and passed through an LDC spectromonitor III UV detector. Samples were injected onto the column using a 7132 rheodyne valve fitted with a 50 $\mu$ l loop. An LDC/Milton Roy integrator and plotter was used to calculate peak heights and areas. The FPLC analysis was performed using a 30cm, 10mm i.d., Superose 12 column (Pharmacia) attached to the pump as above: peaks were detected using a Gilson 113 variable UV detector and recorded using a Servogor 120 recorder.

All solvents were of the appropriate grade and were obtained from Fisons, Loughborough, Leics. Aminopterin was from Sigma. Sep-pak C18 cartridges were from Waters and PEG molecular weight standards were from Polyscience, Warrington, and Polymer Laboratories, Church Stretton, Shropshire.

#### 2.1.4. Proteins.

BSA-Galactosamide (1M protein:26M sugar), A5908 and BSA-p-aminophenyl- $\alpha$ -Mannopyranoside (1M protein:28M sugar), A4664 were from Sigma. BSA (A3294), RSA (A6272), CA (C7500) and LA (L6010) were obtained from Sigma. Peroxidase linked anti-rat IgG (A9037) was obtained from Sigma. Collagenase (C5138) and Protease E (P5147) were obtained from Sigma.

#### 2.1.5. Radioisotopes.

Isotope	Source	Specific activity
$^{14}\text{C}$ -Methylated-CEA (A6418)	Sigma	12.3 $\mu\text{Ci/mg}$
$^{125}\text{I}$ -HSA (IM17P)	Amersham	2.5 $\mu\text{Ci/mg}$
$^{14}\text{C}$ -Carboxy-Inulin (29,757-7)	Sigma	2.6 $\mu\text{Ci/mg}$
$^{125}\text{I}$ -Na (IMS.30)	Amersham	13.3mCi/ $\mu\text{g}$ iodine
Mannitol D-[1- $^{14}\text{C}$ ] (NEC 314)	NEN	0.29mCi/mg
$^3\text{H}$ -Methotrexate(TRK.224)	Amersham	61.1mCi/mg
PEG 900 [1,2- $^3\text{H}$ ] (NET 404)	NEN	6.75 $\mu\text{Ci/mg}$
$^{14}\text{C}$ -PEG 4000 (CFA 508)	Amersham	60 $\mu\text{Ci/mg}$

#### 2.1.6. Tissue Culture.

Gelatin (calf skin) was obtained from Sigma. PBS tablets were from Oxoid, Basingstoke, Hants. Synperonic OP10 was obtained from Cargo Fleet Chemical Company Ltd, Eaglescliffe, Stockton. All other reagents and media were obtained from Flow Laboratories, Irvine, Scotland. Tissue culture flasks were obtained from Flow Labs. Six-well and 24-well plates were from Costar, c/o Northumbria Biologicals Ltd, Cramlington, Northumbria. Millicell HA filter inserts were obtained from Millipore.

All other reagents used were of an analytical grade and were obtained from Sigma.

All biological samples were either analysed immediately or were stored in a freezer at -20°C until they were analysed.

#### **2.1.7 Buffer formulae.**

1. Phosphate buffer 0.02 M pH 6.8 for HPLC analysis of MTX;

24.5 ml 0.2 M  $\text{Na}_2\text{HPO}_4$ , 25.5 ml 0.2 M  $\text{NaH}_2\text{PO}_4$ , to 1000 ml with water

2. Phosphoric acid buffer for HPLC analysis of PEG;

1mM phosphoric acid + 5 ppm nitric acid

3. Phosphate buffered saline pH 7.4;

6.79 g  $\text{KH}_2\text{PO}_4$ , 34.5 g  $\text{Na}_2\text{HPO}_4$ , 22.97 g NaCl, to 5l with water

4. Calcium free buffer for hepatocyte separation;

8.3 g NaCl, 0.5 g KCl, 2.4 g Hepes, to 1000 ml with water, pH to 7.4

5. Collagenase buffer;

3.9 g NaCl, 0.5 g KCl, 0.7 g  $\text{CaCl}_2$ , 24 g Hepes, 100mg Collagenase, to 200 ml with double distilled water, pH to 7.6

## 2.2 Procedure for Radio-iodination of Proteins.

The method used was a modification of the chloramine T method described by McConahey and Dixon.<sup>(124)</sup>

All operations were carried out in an ice bath in a designated fume hood. 10 $\mu$ l of 100 $\mu$ M HCl was added to 10 $\mu$ l of  $^{125}$ I (1mCi). To this solution, 10mg of protein in 200 $\mu$ l of PBS (pH 7.4) was added with 100 $\mu$ g (in 10 $\mu$ l PBS) of Chloramine T. The reactants were left to stand for 10 minutes. To stop the reaction 250 $\mu$ g (in 20 $\mu$ l PBS) of sodium metabisulphite was added and 500 $\mu$ g of potassium iodide was used to solubilise any unreacted  $^{125}$ I. The reaction mechanism is given in appendix 1 (section A1.1).

2mg and 5mg quantities of proteins have also been iodinated using this method. All reactants (excluding  $^{125}$ I) were kept at the same ratio (to protein) as above.

The unbound  $^{125}$ I and other low molecular weight reactants were removed from iodinated protein using gel filtration. A 30cm long, 1.5cm i.d. column was packed with Sephadex G-15. The void volume was determined using blue dextran with a molecular weight of  $2 \times 10^6$  and was approximately 20ml. The solution containing iodinated protein and contaminants was passed down the column and 1ml fractions were collected, starting 2-3ml before the void volume was reached. The protein was collected in approximately 3ml at the void volume, the unreacted iodine was left on the column. The protein fractions were pooled and the volume made up to 5ml in PBS.

The apparent % unbound iodine activity in the protein fraction was determined by using trichloroacetic acid (TCA) to precipitate the protein. 20 $\mu$ l of solution was mixed with 20 $\mu$ l of 20% w/v TCA and allowed to stand for 15 minutes at room temperature. It was then centrifuged in an eppendorf microcentrifuge for 2 minutes at 6,600g and 20 $\mu$ l of supernatant was assayed for radioactivity. Since it was found that dialysing the protein solution against large quantities (approximately 20l over 48 hours) of PBS had little benefit in removing any of the 'unbound iodine' it was decided that if the apparent % unbound iodine activity accounted for greater than 5% of the total radioactivity, the

protein solution would be discarded.

$^{125}\text{I}$  activity was determined using an LKB-Wallac 1275 Minigamma Counter.

### 2.3 Preparation of Protein-MTX Conjugates.

Conjugates were prepared between MTX and BSA, RSA or bovine lactalbumin. The conjugates were injected into rats and the effect of protein conjugation on the pharmacokinetics of the drug was investigated. The use of BSA and lactalbumin gave information about the effects of molecular weight of the carrier on the distribution of the drug.

The reaction was carried out using the method described by Marriott.<sup>(125)</sup> The reaction involved the use of a carbodiimide coupling reagent. The carbodiimide reacted with the methotrexate via one of its carboxylic acid groups to give a reactive intermediate. This could then react with the albumin via one of the lysine residues and to a lesser extent histidine and arginine (see figure 2.1). The resultant conjugate has a covalent bond between the MTX and the albumin. By altering the amount of MTX and carbodiimide in the reaction mixture, conjugates with a range of loadings of drug could be produced. If the pH and temperature of the reaction were standardised then conjugates with a reproducible MCR could be synthesised.

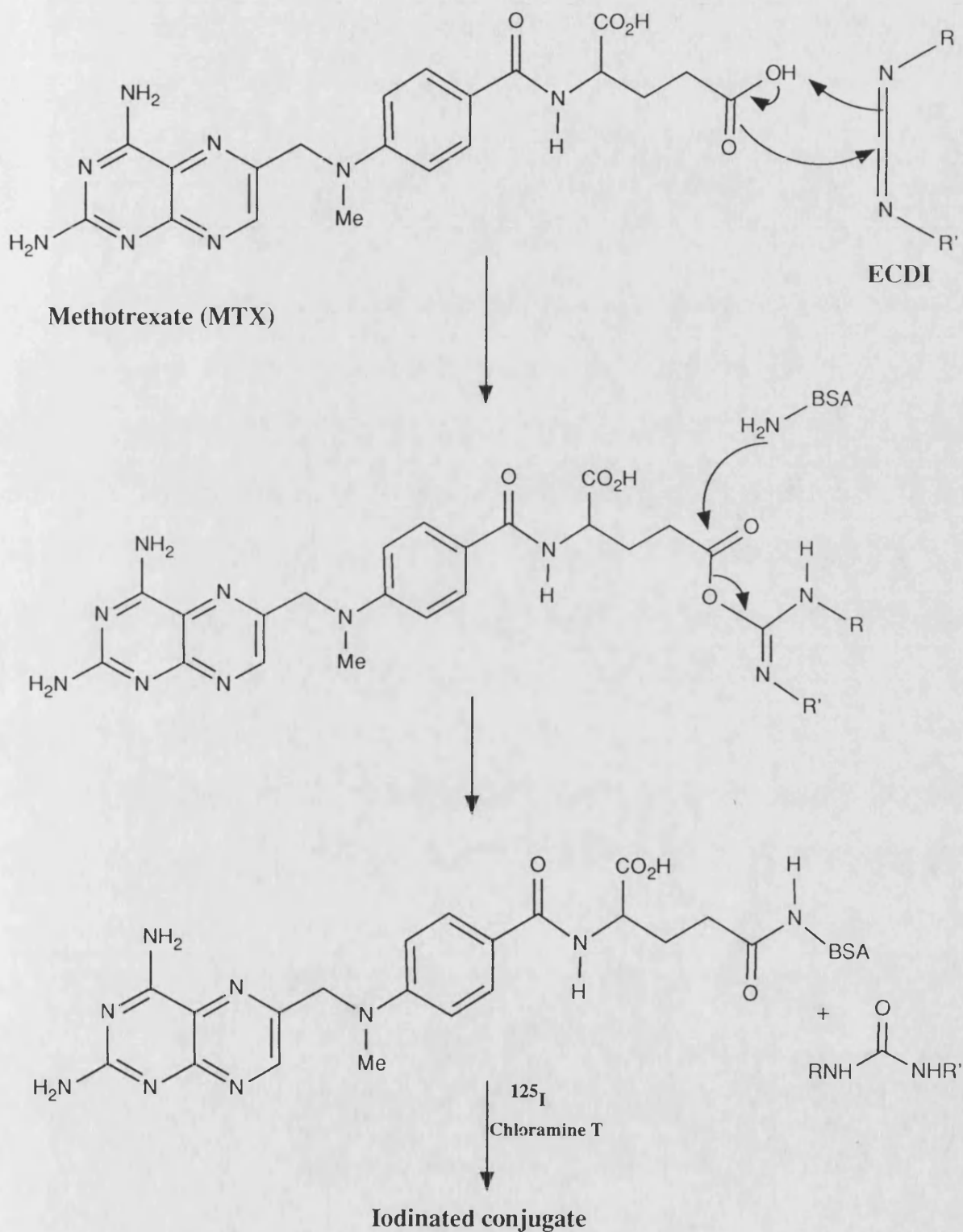
The carbodiimide used in the reaction was 1-Ethyl-3-[3(dimethylamino)propyl] carbodiimide hydrochloride (EDCI).

The reaction was carried out with the following molar ratio (using an albumin concentration of 150mg in 10.5ml):

Albumin:	MTX:	EDCI
1:	x:	x

Provided pH and temperature were constant the amount of MTX and EDCI in the reaction mixture determined the degree of MTX substitution in the conjugate. Figure 2.2 shows the molar ratio of methotrexate achieved in the conjugate versus the molar ratio of methotrexate (and EDCI) to albumin used in the reaction mixture. This figure is taken from the data in table 2.1.

Fig. 2.1. The Conjugation Reaction Between Methotrexate and Bovine Serum Albumin.



ECDI = 1-Ethyl-3-(3-dimethylaminopropyl)carbodiimide.

BSA = Bovine serum albumin.

Figure 2.2: MCR versus Concentration of MTX in Reaction Mixture.

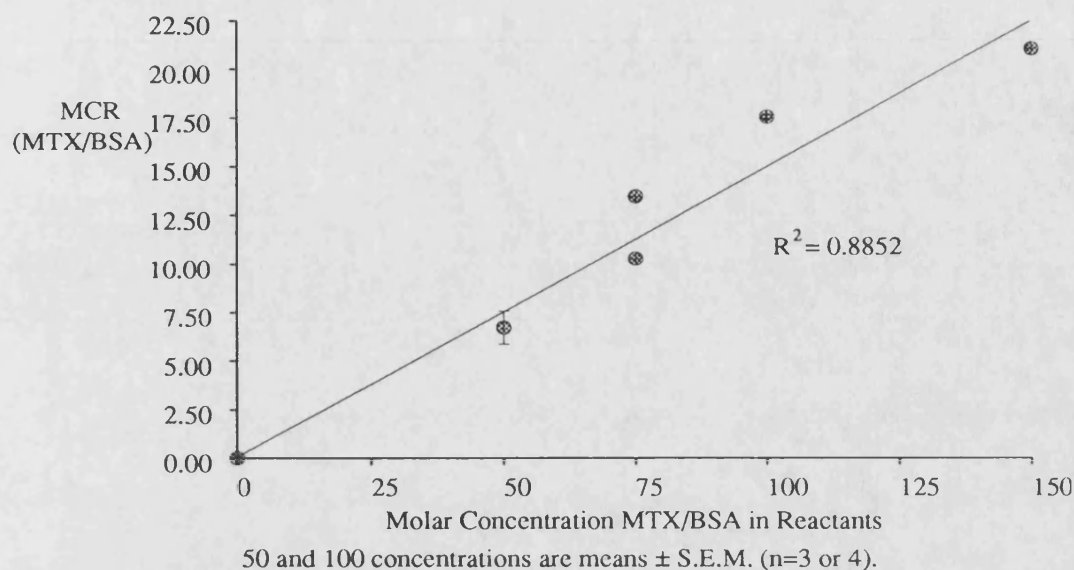


Table 2.1 shows the exact starting ratio of reactants and the resultant molarity and percent weight for weight loading of MTX in the conjugate produced. It also indicates the change in molecular weight of the conjugate compared to free BSA.

Table 2.1: Molarity and Total Molecular Weight of Each Conjugate Produced.

Amount of MTX in Reaction Mixture (M MTX: 1M Protein).	% w/w loading of MTX	Moles of MTX Bound to 1M of Protein.	Estimated Total Mol. Weight of Conjugate.
0	0	0	66296
50	3.4	4.62	68386
50	4.54	6.32	69153
50	5.1	7.15	69510
50	6.2	8.77	70259
75	7.16	10.26	70933
75	9.18	13.45	72376
100	11.55	17.36	74143
100	11.74	17.64	74269
100	11.76	17.65	74274
150	13.63	20.98	75779
150	13.64	21.00	75788



### 2.3.1 Synthesis of a Conjugate.

Conjugates were prepared at a range of %w/w loadings MTX as shown in Table 2.1. All conjugates were prepared using the same conditions, but to achieve a higher loading of MTX bound to the BSA more MTX and ECDI were added to the reaction mixture. As an example, the method of preparation for the 11.55% w/w conjugate is described below.

200mg of BSA was dissolved in 5ml of PBS (pH 7.4). To this solution 150mg of MTX in 3ml of PBS was added and then 57.8mg of ECDI in 2.5ml PBS. The reaction mixture was protected from light and the reaction took place at 4°C in the refrigerator. After 24 hours the reaction was stopped by passing the solution down a one metre long, 2.5 cm diameter Sephadex G50 column via a calibrated 10ml loop. The absorbance of the eluent was monitored at 306nm. The MTX bound to the protein eluted at the void volume whereas the free MTX and other low molecular weight products of the reaction were substantially retained. The mobile phase on the column was water so that the phosphate salts would be removed from the protein. The low ionic strength encouraged interaction with the Sephadex which was used to increase the retention time of the MTX while the conjugate remained unaffected.

The protein-methotrexate fraction was collected as soon as it started to elute (identified using a UV spectrophotometer set at 306nm) and made up to a known volume in water. One millilitre of this solution was diluted at least one in two with 0.1M NaOH and the UV absorbance at 375nm ( $\lambda_{\text{max}}$  of MTXNa<sub>2</sub>) was determined against a blank of 0.1M NaOH. The absorbance of the solution was used to determine the actual concentration of MTX present as protein conjugate, by using a calibration curve of absorbance of standard MTX solutions prepared in 0.1M NaOH at 375nm. (see appendix 1.2) The wavelength of 375nm was chosen because of the negligible absorbance of BSA at this wavelength. The MCR of the conjugate was calculated, assuming 100% recovery of protein from the column (i.e. a known amount of protein with a defined molecular weight was injected onto the column) and assuming all the MTX in the conjugate fraction was present in a covalently bound form.

The BSA-MTX conjugate was freeze dried using an Edwards Modulyo freeze drier over a 48 hour period.

### **2.3.2 Preparation of Conjugates using RSA and LA.**

Conjugates between MTX and RSA were produced in exactly the same manner as MTX-BSA. For LA the concentration of reactants was slightly different. For the same molar concentration of LA as for BSA, the actual number of molecules available to react would be the same but the number of amino acid residues would be approximately one fifth of that of BSA. (The molecular weight of BSA is 66,296 and LA is 14,200). It was decided that the number of amino acid residues present was more important than the number of molecules. Thus the mass of protein used (rather than the molar concentration) was the same as for BSA. An attempt was made to synthesise a conjugate between CA and MTX. However the lysine residues in CA must have been unavailable for reaction, since so little MTX actually reacted that it could only be identified using a UV scan and not using the UV assay at 375nm.

### **2.3.3 Analysis of the conjugates using FPLC.**

After freeze drying a solution of conjugate (500µg/ml in PBS) was prepared. 20µl was injected onto a Superose 12 FPLC column using PBS as mobile phase and the peaks obtained, detected using a Gilson UV detector at 280nm, were compared to that of native BSA. This would determine the degree of cross-linking of the protein that had occurred during the reaction with ECDI and MTX.

### **2.3.4 Analysis of the conjugates using a UV scan.**

Solutions of MTX (20µg/ml), BSA (100µg/ml) and BSA-MTX (100µg/ml) were prepared in 0.1M NaOH. A UV scan between 460nm and 180nm was obtained using a Perkin-Elmer lambda 3 scanning spectrophotometer. The scans for the free drug and the conjugates were compared.

### **2.3.5 Iodination of the conjugates.**

This was performed using the method described previously for native proteins (section 2.2). After separation of the iodinated conjugate from unbound iodine it was found that a slightly higher percentage of unbound activity remained in the protein fraction. This could be due to a non-specific and easily displaceable interaction with the methotrexate. If there was more than 12% TCA soluble  $^{125}\text{I}$  activity within the conjugate fraction then the batch was discarded.

### **2.3.6 Preparation of $^3\text{H}$ -MTX- $^{125}\text{I}$ -BSA.**

The conjugation reaction was performed as follows:

250 $\mu\text{Ci}$  of  $^3\text{H}$ -MTX (8.96 nmol or 4.09 $\mu\text{g}$ ) and 11.28mg of 'cold' MTX were reacted with 20mg of BSA and 4.34mg of ECDI in a total volume of 1.5ml. The reaction was carried out at 4°C. After 24 hours the reaction was stopped by passing the mixture down a PD10 column (Pharmacia). After separation on the column 100 $\mu\text{l}$  of the conjugate solution was diluted to 1ml with 0.1M NaOH and the absorbance at 375nm was determined. The remaining conjugate fraction was freeze dried and then radio-iodinated as previously described.

### **2.4 *In vivo* Work.**

Most of the animal experiments followed the same format. In order to prevent repetition, the salient points are stated below. Where they differed for a particular experiment, this is identified in the appropriate section.

Male Wistar rats (Bath University Strain) weighing between 230-250g were used. Animals were allowed free access to food and water throughout. They were fed on a Labsure (CRM) diet. Generally 24 rats were used in each experiment. These were divided into three groups of eight i.e. one for each route of administration IV, SC and IP. IV administration was performed into the tail vein with the rats under ether anaesthesia. For SC and IP dosage no anaesthesia was required. SC administered drugs

were delivered into the back of the neck region. Solutions for injection were prepared in sterile PBS (pH 7.4) or were filter sterilised before administration. Usually drugs were administered in a volume of 0.2ml of PBS for each route.

Blood samples (0.3-0.5ml) were taken from 2 animals in each group for each time point by cardiac puncture while the rat was under anaesthesia. If blood samples were taken in rapid succession then rats were anaesthetised with an IP injection of a mixture of 1 volume of Hypnorm (fluanisone 10mg/ml, fentanyl 0.315mg/ml) and 1 volume of midazolam (5mg/ml), 2 volumes water (800µl for a 250g rat). Otherwise samples were taken while the rat was under ether anaesthesia. A maximum of 4 blood samples were taken from each rat. Whole blood or plasma was analysed for drug content and from this pharmacokinetic parameters of the drug were determined. For surgical procedures (bile duct cannulation and liver perfusion) the rats were anaesthetised with hypnorm/midazolam.

When organ distribution was determined for a particular drug (radiolabelled only), the rat was first killed using CO<sub>2</sub> gas, and then the organs under investigation were removed by dissection, weighed, minced and a known weight was assayed for drug content. The organs selected were liver, spleen, heart, lung, kidney, stomach, small intestine and thyroid.

In most experiments, three rats from each group were kept singly in metabolic cages so that urine and faeces could be collected and the drug excretion could be determined. The total volume of urine excreted over the timed period was measured and a portion was assayed for drug activity. Total drug excreted in the urine could then be calculated. Faeces was collected for drugs labelled with <sup>125</sup>I only. The total quantity of faeces produced over the experiment was collected and the whole was assayed for drug content.

## 2.5 Administration of 'Drugs'.

### 2.5.1 Methotrexate

MTX was administered to rats at two dose levels - 2.5mg and 0.5mg per rat. Blood levels in plasma were determined by two methods. For the 2.5mg dose the levels could be determined using an HPLC assay. However, because of the limits of the assay, identification of the 0.5mg dose in plasma was performed using  $^3\text{H}$ -MTX. The 2.5mg dose was repeated using  $^3\text{H}$ -MTX to compare results obtained for both methods. A solution of  $\text{MTXNa}_2$  was prepared containing 2.5mg in 0.2ml. This was administered to rats by each of the three routes. Blood samples were collected at regular intervals over 4 hours.

#### HPLC Analysis.

The method used was a modification of that described by Nellie So et al.<sup>(126)</sup> Serum was diluted with milli Q water to give a concentration that would fall within the limits of the assay (0.1-1.0 $\mu\text{g/ml}$ ). All serum was diluted at least two times so that a "clean" chromatogram would be obtained. To each ml of diluted serum, 100 $\mu\text{l}$  of a 10 $\mu\text{g/ml}$  solution of aminopterin was added as internal standard. Aminopterin was chosen as internal standard since its retention time on the column did not interfere with that of MTX and also it absorbed at the chosen wavelength.

The serum was prepared for analysis using a Sep-pak C18 reverse phase column. Columns were pre-wetted with 10ml of methanol followed by 10ml of Milli-Q water. 0.4ml of diluted serum containing internal standard was passed down the column. Serum proteins were washed off the column with 5ml of water. MTX and aminopterin were eluted with 3ml of methanol. The methanol was evaporated at 45°C under a stream of nitrogen. The MTX and aminopterin were redissolved in 200 $\mu\text{l}$  of Milli-Q water. This procedure was carried out in duplicate for each sample of rat serum.

For the calibration curve standard solutions of MTX (50ng/ml to 1.0 $\mu\text{g/ml}$ ) were prepared in rat serum diluted to half strength with water. Aminopterin was added and

the samples treated in exactly the same way as for test serum.

HPLC was performed using the 15cm Apex ODS 5 $\mu$  column and using the system described in Materials. The UV detector was set at 306nm. The mobile phase used was 78% 0.02M Phosphate buffer (pH=6.8)/ 22% methanol and a flow rate of 0.8ml/minute.

Each sample was assayed in duplicate. Unknown and calibration samples were extracted and assayed simultaneously, so that a new calibration curve was prepared each day. Concentration of unknown samples was determined by the method of peak height ratios of MTX to aminopterin, and the calibration curve was linear over the range of 0.1-1.0 $\mu$ g/ml. Coefficient of variation for the 0.1 $\mu$ g/ml standard was 1.093% and for the 1.0 $\mu$ g/ml standard was 0.524%.

#### Determination of Rate of Excretion of Methotrexate.

Four rats were injected with 2.5mg of MTX into the tail vein. Rats were placed singly in metabolic cages. At 6.5, 24 and 48 hours after injection urine was collected, the volume was noted and the concentration of MTX in the urine determined using HPLC.

Urine was diluted 1 in 500 with Milli-Q water. To 1ml, 100 $\mu$ l of aminopterin 10 $\mu$ g/ml was added. The resultant solution was taken for HPLC as described above. Peak height ratios of MTX/aminopterin were determined in duplicate for each urine sample and the corresponding MTX concentration was determined from a calibration curve of Peak height ratios vs concentration of standard MTX solutions prepared in 1 in 500 diluted urine (obtained from a control rat) containing internal standard. This was linear over the range of 0.01 $\mu$ g/ml to 2.5 $\mu$ g/ml.

#### <sup>3</sup>H-Methotrexate

<sup>3</sup>H-Methotrexate was mixed with unlabelled drug to give a specific activity of 9.1  $\mu$ Ci/2.5mg or a total activity of 10 $\mu$ Ci/0.5mg in 0.2ml of sterile PBS. One of these solutions were injected by IV, SC or IP routes. Blood samples were taken every 15 minutes for 1 hour and then every 30 minutes up to 4 hours after injection. 100 $\mu$ l of

plasma was added to 5ml of Optiphase safe liquid scintillant (LKB) and the disintegrations per minute (DPM) determined in duplicate for each sample using an LKB-Wallac 1215 Rackbeta liquid scintillation counter, programmed to calculate DPM from measured CPM values. The plasma concentration of methotrexate for each sample was determined by assuming that DPM measured in plasma was equivalent to MTX concentration.

Urine excretion of radioactivity was also determined for three rats in each group after 6 hours and then daily for three days. Urine was assayed as for plasma and total methotrexate excreted over this period was determined.

### **2.5.2 Administration of Digoxin.**

Digoxin injection solution was prepared using the British Pharmacopoeia (BP) formula.<sup>(127)</sup> 1ml of this solution was diluted to 10ml with water to give a solution containing 2 µg/ml. This was filter-sterilised before administration. Rats were injected with a 250ng dose by each of the three routes. Digoxin given by IV injection was administered slowly to minimise cardiac toxicity. Blood samples were taken from 30 minutes up to 7 hours after injection.

Serum digoxin levels were measured using an enzyme linked immunosorbent assay (ELISA) obtained from Immunodiagnosics Boehringer Mannheim as per the kit instructions. The data sheet for this kit is shown in Appendix 1.6

### **2.5.3 Inulin.**

An injection solution of inulin was prepared so that it contained 1.6mg of total inulin with an activity of 4 µCi of <sup>14</sup>C-Inulin in 0.2ml. This was injected either sub-cutaneously or intra-peritoneally into male wistar rats. Blood samples were taken up to 10.7 hours after injection and plasma was assayed for <sup>14</sup>C content in the LKB scintillation counter programmed to calculate DPM from CPM.

#### 2.5.4 $^{125}\text{I}$ -Na.

A solution of  $^{125}\text{I}$ -Na obtained from Amersham was diluted in sterile PBS to give a final concentration of 0.654ng of iodine and an activity of 8.5  $\mu\text{Ci}$  in 0.2ml. The solution was injected IV into male wistar rats. Blood samples were taken regularly up to 48 hours after injection. In addition organ distribution was determined at 4, 7, 27 and 52 hours after injection. Urine was collected from 4 animals for up to 96 hours post injection.

#### 2.6 Administration of Proteins.

A number of proteins were chosen to give a range of molecular weights from 14kD to 66kD. These were either obtained in a radiolabelled form or were radio-iodinated with  $^{125}\text{I}$  so that detection in the rat was possible.

Table 2.2 lists the proteins that were injected, gives their approximate molecular weight. It also lists the specific activities as injected and whether the proteins were radioiodinated in the laboratory or whether they were obtained in a radiolabelled form.

**Table 2.2 Proteins injected into male wistar rats.**

Protein	Source	Molecular Weight	Specific Activity
LA	$^{125}\text{I}$ in laboratory	14,200	1.3 $\mu\text{Ci}/\text{mg}$
CA	$^{125}\text{I}$ in laboratory	29,000	3.3 $\mu\text{Ci}/\text{mg}$
CEA	Sigma ( $^{14}\text{C}$ )	45,000	2.6 $\mu\text{Ci}/\text{mg}$
HSA	Amersham ( $^{125}\text{I}$ )	67,000	2.5 $\mu\text{Ci}/\text{mg}$
BSA	$^{125}\text{I}$ in laboratory	66,296	2.3 $\mu\text{Ci}/\text{mg}$
RSA(5mg)	$^{125}\text{I}$ in laboratory	63,000	1.1 $\mu\text{Ci}/\text{mg}$
RSA(20mg)	$^{125}\text{I}$ in laboratory	63,000	0.85 $\mu\text{Ci}/\text{mg}$



### **2.6.1 $^{14}\text{C}$ -Chicken Egg Albumin.**

Rats were injected with 0.04mg of  $^{14}\text{C}$ -CEA (0.48 $\mu\text{Ci}$ ) in a solution which contained 20mg of cold CEA by the IV route only. Blood samples were removed at regular intervals over 24 hours and were collected in Li<sup>+</sup>Heparin tubes. 200 or 300 $\mu\text{l}$  plasma samples were added to 5ml of Optiphase safe and assayed for  $^{14}\text{C}$  content in the liquid scintillation counter. Urine was collected up to 144 hours after injection.

### **2.6.2 $^{125}\text{I}$ -HSA**

1ml of the Amersham solution was added to 4ml of a solution containing BSA (100mg/ml) in PBS. The resultant solution contained 16mg BSA and 0.8mg  $^{125}\text{I}$ -HSA (2 $\mu\text{Ci}$ ) in 0.2ml. Rats were injected with 200 $\mu\text{l}$  of this solution by each of the three routes. Blood samples were collected at regular intervals up to 149 hours post injection. Whole blood was analysed in the gamma counter.

### **2.6.3 Other proteins**

10mg samples of LA, CA, BSA or RSA were radioiodinated using the chloramine T method described in section 2.2. Each iodinated protein solution was then mixed with 140mg of unlabelled protein and the volume was made up to 6ml. Assuming 100% recovery of protein after the iodination and purification were complete, the resultant solution had a concentration of 5mg in 0.2ml. Rats were injected with 5mg of each of the proteins by each of the three routes. Blood samples were collected for up to 72 hours post injection for LA and for 96 hours post injection for the other proteins. For LA, CA and BSA serum was obtained by allowing the blood samples to stand for 2 hours at room temperature and then centrifuging in an eppendorf microcentrifuge for 1 minute at 6,600g and analysed for radioactivity. In addition, for RSA, whole blood as well as serum was analysed. Urine and faeces were collected daily for each protein. Organ distributions were also determined at regular intervals using 2 animals in each group at each time point at various times up to 96 hours after administration of the proteins.

In addition to the 5mg dose of RSA, a dose of 20mg was administered by the IV route. This was intended to indicate whether the quantity of protein given as an IV bolus actually affects its rate of elimination.

#### **2.6.4 20mg dose of RSA.**

Two milligrams of RSA were radio-iodinated using the chloramine T method described. The iodinated RSA in PBS was used to produce a solution containing 20mg of total RSA and an activity of 20  $\mu$ Ci in 0.3ml. 0.3ml was injected into male wistar rats by the IV route. Blood samples were collected over 96 hours and both whole blood and plasma were assayed for radioactivity. Urine was also collected over 96 hours.

### **2.7 Tests to determine the Antigenicity of BSA in the Rat.**

Three experiments were performed in order to determine whether BSA injected into rats led to an inflammatory response. These are described below.

#### **2.7.1 BSA.**

This experiment involved the administration of BSA to rats at various doses followed by a measurement of the total serum protein concentration.

##### **2.7.1a Measurement of Protein Levels in Serum.**

The method used to determine the protein concentration in rat serum was a modification of that described by Lowry.<sup>(128)</sup> The following solutions were prepared immediately prior to use.

Soln. A) 5% w/v  $\text{CuSO}_4 \cdot 5\text{H}_2\text{O}$

Soln. B) 10% w/v Sodium potassium tartrate

Soln. C) 2% w/v  $\text{Na}_2\text{CO}_3$  in 0.1M NaOH

Soln. D) 1 volume Folin-Ciocalteu reagent + 2 volumes water

Soln. E) 1 volume of (A) + 1 volume of (B) + 8 volumes water

Soln. F) 1ml of (E) + 50ml of (C)

Soln. G) Standard solutions of BSA in 0.9% NaCl ranging from 20-400µg/ml

0.4ml of the test solution was added to 4ml of solution (F). 0.4ml of solution (D) was added and immediately mixed in a vortex mixer. After a 30 minute incubation in the dark the absorbances (650nm) of the solutions were determined in a UV spectrophotometer against a reagent blank. The protein concentration of unknowns was determined from a calibration curve of absorbance versus standard BSA concentration. The calibration curve was linear over the range of 20-400µg/ml (see section A1.7). The coefficient of variation for the 20µg/ml standard was 3.58% and for the 400µg/ml standard was 1.17%. The solutions were all read in duplicate and a mean was taken.

### **2.7.1b Administration of BSA to the rats.**

15 male wistar rats weighing between 290 and 310g were divided into three groups. Group 1 were the control group and were not treated. Group 2 were injected with 300µl of 0.9% saline to determine whether the trauma of injection had led to an inflammatory response and group 3 were injected with 20mg of BSA in 300µl of 0.9% saline. Each rat had a 0.5ml blood sample removed by cardiac puncture after 2 hours, 4 hours and 7 hours. Serum was obtained, after allowing the samples to stand at room temperature for 2 hours in an eppendorf tube followed by spinning in a microcentrifuge at 6600g for 2 minutes. The serum was diluted to 1 in 500 with 0.9% saline to give a protein concentration that would fall within the range of the assay. Protein measurements for the diluted serum were obtained as described in section 2.7.1a.

In order to obtain a range of normal values for total protein serum concentration, a 0.5ml blood sample was obtained from 10 untreated male wistar rats and the serum treated as for those injected with BSA.

The experiment was repeated using doses of BSA of 40mg and 80mg.

### **2.7.2 Administration of Evan's Blue.**

Six male wistar rats weighing between 290 and 310g were injected via the tail vein with 1mg of Evan's Blue in 0.4ml of 0.9% saline. At the same time six weight matched rats were injected with 0.4ml of the same solution which contained in addition 20mg of BSA. 0.5ml blood samples were removed at timed intervals up to 28.5 hours after administration. Plasma was diluted to 1 in 10 with water and the absorbance was measured at 612nm against a blank of 1 in 10 diluted plasma. The concentration of Evans Blue was determined from a linear calibration curve of absorbance against concentration of dye in standard solutions (500ng/ml to 20µg/ml) prepared in 1 in 10 diluted plasma. (see appendix A1.8)

### **2.7.3 Blot test to determine Antigenicity of BSA in Rat serum *in vitro*.**

To a sheet of nitrocellulose paper (10cm by 10cm) (Sigma), 1µl samples of BSA at concentrations of 50, 100, 500, 750 and 1000µg/ml were applied. These were incubated on a shaking water bath, in a square 75ml Petri-dish containing 10ml of PBS (pH 7.4) with 0.05% Tween 20 and 100µl or 1ml of rat serum, for 1.5 hours. The samples were washed three times in buffer (20ml each) without serum. 10ml of PBS containing Tween 20 with 10µl of peroxidase linked anti-rat IgG was added and the sample was incubated for 1 hour. The samples were washed three times (20ml each) in PBS/0.05% Tween 20. 10ml of PBS was then added to the Petri-dish and to this 30mg of nickel chloride, 5mg of diaminobenzidine and 200µl of 30% hydrogen peroxide were added. If any rat IgG was present then a black spot on the nitrocellulose would develop at this stage.

### **2.8 Administration of <sup>125</sup>I-BSA-MTX to male wistar rats.**

Solutions of iodinated conjugates were prepared containing 5mg of BSA-MTX with between 5 and 10µCi of activity in 0.2ml of PBS. This was injected into rats by IV, IP or SC. Blood samples were taken at regular intervals for 96 hours. At timed intervals

over the experiment 2 animals in each group were killed and the organ  $^{125}\text{I}$  activity was determined. Three animals from each group were kept separately in metabolic cages and urine and faeces were collected. Pharmacokinetic parameters were calculated for each route of administration and each conjugate administered. The conjugates used in these experiments are those listed in table 2.1. In addition for the 11.55%w/w conjugate the bile duct was cannulated, 3 hours after administration of the conjugate in 2 rats. Bile was collected for a 20 minute period.

The RSA-MTX and LA-MTX conjugates were administered to male wistar rats as for BSA-MTX.

### **2.8.1 FPLC Analysis of Bile, Serum and Urine.**

Analysis of the molecular weight of the radioactive fraction present in bile after administration of the 11.55%w/w and for plasma and urine after administration of the 7.16%w/w conjugate was performed using the Superose 12 column already described (section 2.2.3). 1ml fractions of eluent were collected immediately after injection of the sample onto the column. Each fraction was analysed in the gamma counter.

### **2.8.2 $^{125}\text{I}$ -BSA- $^3\text{H}$ -MTX.**

0.86mg of the conjugate (20 $\mu\text{Ci}$   $^{125}\text{I}$  and 8.4 $\mu\text{Ci}$   $^3\text{H}$ ) was administered to 12 rats by the IV route. Plasma samples were obtained at regular intervals over 96 hours post administration. In addition urine was collected from 3 rats over 4 days. At 1, 6, 24, 48, 72 and 96 hours post administration 2 animals were killed and the liver, spleen, kidney, stomach, small intestine and thyroid were removed for conjugate analysis.

Each sample was analysed twice, first without any further preparation in the gamma counter and then using the LKB/Wallac 1219 liquid scintillation counter. Plasma and urine samples were analysed unchanged in both counters. Before organ samples could be analysed in the 1219 liquid scintillation counter they had to be solubilised and bleached. The LKB1219 counter was pre-programmed to read samples with a dual label of  $^3\text{H}$  and  $^{125}\text{I}$ , but before samples could be analysed 2 quench curves were prepared

one for each isotope. The DPM reading for  $^{125}\text{I}$  in each sample using the 1219 counter was compared to the CPM reading obtained from the gamma counter to ensure the results were similar and therefore acceptable.

Organ solubilisation was carried out as follows. 1ml of hyamine hydroxide in methanol was added to 200mg of tissue and the samples were left over night at 60°C. After solubilisation between 0.6-1.0ml of 30%  $\text{H}_2\text{O}_2$  was added until the sample was a pale yellow colour. The sample was warmed to remove excess  $\text{H}_2\text{O}_2$  and 15ml of Optiphase safe was added. The resultant alkaline solution was neutralised using 500-700 $\mu\text{l}$  of 1M acetic acid in toluene. The samples were left overnight before counting for  $^3\text{H}$  and  $^{125}\text{I}$ , to ensure that chemiluminescence had died down.

## **2.9 Targeting to the Liver.**

### **2.9.1 Administration of G-BSA and M-BSA.**

G-BSA and M-BSA were obtained from Sigma. The concentration of sugar residues was 26M and 28M sugar residue to 1M BSA respectively. 5mg of these were iodinated as described for native proteins (section 2.2) except that separation of the conjugate from the free iodine was performed using a Biogel P4 column since it was found that the sugar-protein conjugate bound very strongly to Sephadex gels. The Biogel column was prewashed with 5mg of M-BSA or G-BSA before the separation to avoid any loss of radio-iodinated protein.

A solution containing 200 $\mu\text{g}$  of iodinated protein in 0.2ml PBS was prepared and injected IV into 10 male wistar rats. 4 of the injected rats were first anaesthetised with a mixture of hypnorm and midazolam so that three blood samples could be taken from each, over 30 minutes. Ether anaesthetic would have been too slow for these rapid sampling times and also would have been particularly unpleasant for the rat. After 15 minutes and 30 minutes the rats were killed using  $\text{CO}_2$  gas and the organs dissected out and the  $^{125}\text{I}$  content analysed. The remaining six rats were anaesthetised with ether before three successive blood samples were taken. Two rats were killed as before at 1

hour, 3 hours and 5 hours after injection. As a comparison native BSA, LA, BSA-MTX (4.55%w/w) and BSA-MTX (11.55%w/w) were administered in a similar manner.

### **2.9.2 Whole body Autoradiography.**

Animals were dosed with the protein under investigation (BSA, BSA-MTX, G-BSA, M-BSA or LA) or MTX. For the  $^{125}\text{I}$ -proteins approximately 20-30 $\mu\text{Ci}$  of activity were injected and for  $^3\text{H}$ -MTX 250 $\mu\text{Ci}$  were administered. At the required time after injection; 15 minutes and six hours for the proteins and 5 minutes for MTX the rats were killed using  $\text{CO}_2$  gas. They were rapidly frozen using a mixture of petroleum ether 60/80 and dry ice. The rat was embedded in 1% polycell while still frozen and 100 $\mu\text{m}$  thick sections were taken using a chryomicrotome. The sections were exposed to hyperfilm and checked weekly until the required exposure was reached.

### **2.9.3 Liver Perfusion with Collagenase.**

The G-BSA and M-BSA were administered because of their ability to target to the liver. To determine which cell type they actually targetted to within the liver, the organ was separated into two cell types; the hepatocytes and the non-parenchymal cells. This process is described below.

Liver perfusion was performed via the mesenteric vessels according to the method of Seglen et al.<sup>(129)</sup> After anaesthetising the rat, the abdomen was opened and a cannula was inserted into the mesenteric artery. Approximately 100ml of calcium free buffer was perfused through the cannula into the circulation using a syringe. Blood and excess buffer was removed via a cannula in the vena cava. After removal of blood and calcium from the liver approximately 100ml of collagenase buffer was injected slowly (over about 10 minutes) into the circulation using a large syringe. During this time the liver swelled to approximately twice its size and small cracks could be seen within the structure of the liver. The liver was removed from the rat, washed in cold calcium-free buffer (see section 2.1.7) and placed on ice until the cells could be separated.

A liver cell suspension in calcium free buffer was obtained by gently teasing the liver

apart using forceps. Clumps of cells were removed by filtering the suspension through four layers of fine nylon mesh. The cells were separated using a centrifugation method. A suspension containing largely hepatocytes was obtained by centrifuging at 50g for 4 minutes. The hepatocytes which formed the pellet were washed three times, resuspended in 10ml and the cell count determined using a haemocytometer.

The supernatant from the original centrifugation contained a mixture of non-parenchymal cells and membrane vesicles which had formed due to the breakdown of hepatocytes. A suspension of non-parenchymal cells was obtained according to the method of van Berkel,<sup>(130)</sup> by incubating on ice for 1 hour in a buffer solution containing 0.25% protease E and 0.4% BSA. Hepatocytes are broken down by this enzyme whereas non-parenchymal cells remain largely unaffected. After incubation a pellet of non-parenchymal cells was obtained by centrifuging at 500g for 5 minutes. The pellet was washed twice and resuspended in 10ml of buffer and a cell count was determined in a haemocytometer.

G-BSA, M-BSA and MTX-BSA (11.55%w/w) were investigated. The solution under investigation was injected into the rat 10 minutes before the perfusion was carried out. After separation of the cells, 1ml of each suspension was assayed in the gamma counter for <sup>125</sup>I activity. Two different cell suspensions were obtained for each cell fraction for the same liver. The radioactivity in 1g of whole liver was also determined before the liver was teased apart. The concentration of conjugate in each cell type of the liver was determined for three rats.

### 2.10 Uptake of the Conjugates by Macrophages *in vitro*.

Each conjugate was analysed *in vitro* for its ability to be taken up by rat peritoneal macrophages. Resident peritoneal macrophages were obtained from rats which had previously been killed using CO<sub>2</sub>. 15ml of RPMI 1640 containing 50IU/ml penicillin and 50µg/ml streptomycin was injected into the peritoneal cavity. After gently massaging the abdomen to ensure mixing of the media with the organs a small slit was made through which media containing macrophages could be withdrawn using a plastic



pipette. If any media containing blood was withdrawn it was discarded. Media containing macrophages was pooled and centrifuged at 500g for 5 minutes. The cells were resuspended in 10ml of media which contained 10% v/v FCS and a cell count was determined using a haemocytometer.  $1 \times 10^6$  cells were seeded into each well of six well plates and incubated overnight in 4ml of media. Typically between ten or twenty million cells were obtained from each rat.

A solution containing 8µg/2ml of iodinated protein or conjugate in RPMI 1640 without FCS was prepared. Media was removed from the macrophages and replaced with 2ml of the media containing  $^{125}\text{I}$ - protein. At timed intervals over 1 hour the media was removed from three wells and the cells were washed 3 times in PBS which contained 0.02% sodium azide. The macrophages were left overnight at room temperature in 1ml of a solution containing 0.1% Synperonic OP10 in PBS. This solubilised the cells. Each well was washed with a further 1ml of this solution. The solubilised cells were assayed for  $^{125}\text{I}$  activity in the gamma counter. In addition 1ml of media was assayed for radioactivity and the percentage of unbound iodine activity was determined using a TCA precipitation. Each experiment was carried out at 37°C and at 0°C. The rationale for this was that at 0°C although the protein could bind to the receptor it would not be internalised and thus protein breakdown could be prevented.<sup>(131)</sup> The proteins that were investigated in this way included BSA, BSA-MTX (4.55% w/w), BSA-MTX (11.54% w/w), G-BSA (26M:1) and M-BSA (28M:1).

In order to check that the cells obtained from the rat peritoneal cavity were actually macrophages, they were prepared for identification using a scanning electron microscope. One million cells were seeded onto a sterile glass cover slip in a 24-well plate and incubated in RPMI 1640 with 10% FCS at 37°C overnight. Preparation for SEM was carried out exactly as for cells grown on filters (section 2.11.5).

### **2.11 Cell Culture Experiments using Caco-2 and BAE-1 Cell-lines.**

Two cell lines were under investigation; the Caco-2 cell line and the BAE-1 cell line. The Caco-2 cell experiments were performed in the Advanced Drug Delivery Unit at

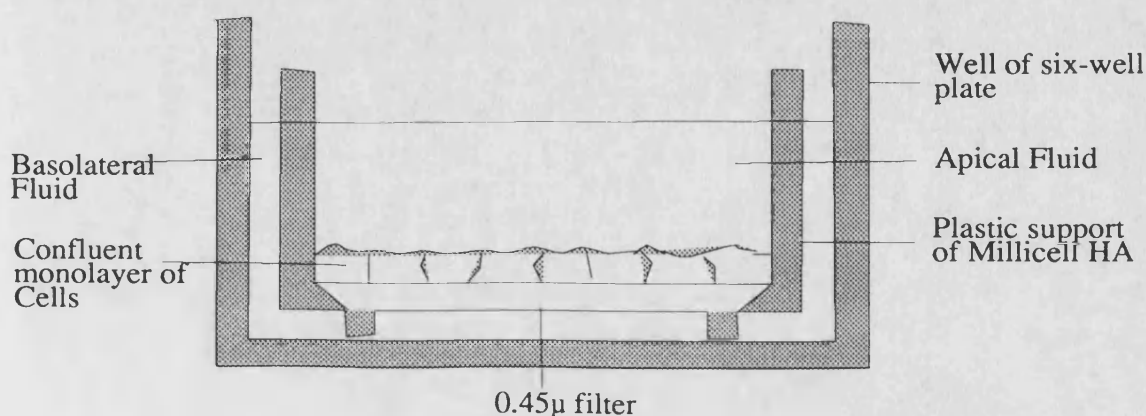
Ciba Geigy Pharmaceuticals, Horsham and utilised an established technique. For the BAE-1 cell line the experimental techniques had to be decided. Both cell types were grown under the same routine conditions.

### 2.11.1 Routine Cell-Culture.

Cells were routinely grown in DMEM buffered with 5% CO<sub>2</sub> gas in air and 2g of NaHCO<sub>3</sub>/litre and supplemented with 1% non-essential amino acids, 1% glutamine (200mM), 50IU/ml penicillin, 50µg/ml streptomycin and 10% Foetal Calf Serum in 150 cm<sup>2</sup> tissue culture flasks. The media was changed on alternate days and the cells were sub-cultured weekly. Three flasks were obtained from each confluent Caco-2 flask every week and between three and six flasks from each BAE-1 flask each week depending on experimental requirements. Sub-culture was performed using 0.25% trypsin and 0.2% EDTA for the Caco-2 cell line and using 0.25% trypsin and 0.02% EDTA for the BAE-1 cell line.

Filter culture was carried out as follows. Millicell HA filters (30mm diameter) were transferred to six well plates using sterile forceps. To prepare the filter for cell seeding, 2ml of culture media was pipetted inside each filter chamber and 3ml of media was pipetted directly into the well of the six-well plate. The plates were transferred to an air tight plastic container and placed in an incubator at 37°C. Humidity was maintained inside the container using water soaked tissue. This ensured adequate wetting of the filter, whilst the cells were prepared for seeding. Both Caco-2 and BAE-1 cells were seeded at a density of 2x10<sup>6</sup> cells in 2ml of media into the filter chamber. Figure 2.3 shows the apparatus used for filter culture.

**Figure 2.3 The Apparatus used for Culture of Cells on Filters.**



The high cell density was chosen so that cells would already be confluent after seeding and during the incubation time cells could differentiate. Experiments were performed 15 days after cell seeding for Caco-2 cells. For the BAE-1 cells an incubation time had to be ascertained by means of comparative experiments at timed intervals after cell seeding. During incubation the media was removed from both inside and outside the Millicell HA insert using a suction pump and replaced with new media on alternate days.

#### **2.11.2 Transport Experiments using cells grown on cellulose filters.**

Radiolabelled drug was used to allow easy identification in the basolateral fluid. Between 0.5 and 2  $\mu$ Ci of each drug was applied to the apical surface of the cell layer. Appearance of drug in the basolateral fluid was determined at timed intervals for three filters for each time point. At the same timed intervals electrical resistance measurements were taken for each cell coated filter. The uptake of the drug by the cells and the filter combined was determined at the same times by washing and then removing the filter using a scalpel and assaying for radioactivity.

#### **2.11.3 Caco-2 Filter Culture.**

The transport of mannitol, PEG 900 and PEG 4000 was investigated. PEGs are notoriously polydisperse polymers. Two HPLC systems were used to investigate the degree of polydispersity of the two molecular weights.

#### **HPLC using Reverse Phase C<sub>18</sub> Column.**

This method was a modification of that described by van der Wal<sup>(132)</sup> and was only suitable for polymers with a molecular weight below 1200 and thus the PEG 4000 was not investigated in this way. A 15cm hypersil ODS 5 micron column was attached to the system described in Materials. The detector was set at 190nm. An LDC/Milton Roy integrator and plotter was used to calculate peak heights and areas. The mobile phase used consisted of 20% acetonitrile (far UV grade) in phosphoric acid (see buffers 2.1.7). 100 $\mu$ l samples were injected onto the column and the PEG was separated into its

individual oligomers.

#### HPLC using GPC

This GPC assay separated PEGs according to their molecular weight. It could not identify the individual oligomers, but could be used to identify the mean molecular weight of a sample. Separation was performed using a TSK 3000 column with precolumn. The mobile phase was 0.1M LiBr containing 45ppm triton-X 100. Flow rate was 0.5ml/min. The PEGs were detected using their refractive index. For radiolabelled PEG samples, 0.25ml samples were collected after measurement of RI, 5ml of lumogel was added and their radioactivity was assayed in a Beckman liquid scintillation counter. A series of standard molecular weight PEGs were injected onto the column and the retention times were identified. A graph of log molecular weight against retention time gave a straight line for PEGs of 600 to 20,000D. (Appendix A1.9).

#### Transport of mannitol by Caco-2 cells grown on filters.

A solution of mannitol containing approximately 0.25 $\mu$ Ci/ml (4.9nmol/ml)  $^{14}$ C-Mannitol was prepared in media. 2ml of this solution was pipetted onto the apical surface of the cells (P97). 2ml of normal media was pipetted into the basolateral chamber of the cells. At timed intervals over 24 hours, apical and basolateral fluids were removed from three filters, centrifuged in an eppendorf microcentrifuge to remove cell debris and 1ml was added to 10ml of lumogel and assayed for  $^{14}$ C content.

After removal of the media, fresh normal media was added (5ml inside the insert and 3ml outside) and the resistance measurements taken using the WPI Evom. Filters and cells were washed three times in PBS azide, the filter was removed from the insert and assayed whole for  $^{14}$ C content in 10ml of lumogel.

#### PEG 900 Transport.

To a 15 day culture of Caco-2 cells (P87) grown on nitrocellulose filters approximately 2 $\mu$ Ci (295.9nmol) of  $^3$ H-PEG 900 in 2ml of media was applied to the apical surface.

Samples of 200µl of baso-lateral fluid were removed at timed intervals over 24 hours and were replaced with 200µl of fresh media. Cell/filter uptake and resistance measurements were determined as for mannitol.

#### PEG 4000 Transport.

A solution containing 2µCi/2ml (8.4nmol) in media was prepared. 2ml was applied to the apical surface of the cells (P97). There were 36 filters for the experiment and three filters were analysed for each time point. Cell/filter uptake and resistance measurements were taken as for mannitol experiment.

#### **2.11.4 BAE-1 Filter Culture.**

Caco-2 cell filter culture procedures had been established at Ciba Geigy. Electron microscopy techniques, electrical resistance measurements<sup>(133)</sup> and the transport of low molecular weight fluid phase markers had ascertained that the incubation period and the number of cells seeded had resulted in a confluent and differentiated cell monolayer at 15 days after cell seeding. Since the BAE-1 cell line had recently been obtained from the ECAC (Porton Down) these parameters had to be established before filter culture experiments could be performed.

Many references to endothelial cells used in transport experiments utilised a collagen/fibronectin<sup>(134)</sup> or gelatin<sup>(135)</sup> coated filter to allow the cells to adhere and form a confluent monolayer. Experiments were performed to ascertain whether coating the Millicell HA filter was necessary.

#### Gelatin coating the Millicell HA filter.

The method for gelatin coating filters was obtained from Millipore and is summarised below. A solution was prepared containing 5%w/v calf skin gelatin and 5%w/v sucrose in double distilled water by heating on a water bath. Aliquots were stored at -20°C and defrosted in a 37°C water bath as required. The millicell HA filter inserts were transferred to six-well plates and just enough of the gelatin solution was applied to the

filter to cover it. Excess gelatin was removed immediately using a suction pump. The gelatin coated filters were air dried under the laminar flow for approximately 15 minutes.

The six well plate was placed on ice and washed in sterile PBS for 10 minutes. The PBS was removed and 2ml of fixative was added. The fixative consisted of 25% v/v glutaraldehyde in PBS.

After 30 minutes the fixative was removed and the filter was washed 5 times in sterile PBS over a 20 minute period at room temperature. The fixative was quenched using a solution of glycine (0.76%w/v) in sterile PBS. After 30 minutes the glycine solution was removed and the filters were washed twice with sterile PBS. Finally the filters were washed three times in culture medium and were then ready for cell seeding as above.

The transport of  $^{125}\text{I}$ -HSA by BAE-1 cells grown on coated nitrocellulose filters was compared 3.75 days, 7 days and 10 days after cell seeding. In addition, the HSA transport for gelatin coated and non-coated filters was compared at 7 days after cell seeding. The permeation of HSA across gelatin-coated or non-coated filters which had not been seeded with cells was also determined.

#### Transport of HSA.

$2 \times 10^6$  BAE-1 cells were seeded onto each of 36 gelatin coated filters. At the same time cells were seeded onto 12 uncoated filters. After the required incubation time, 200 $\mu\text{g}$  of  $^{125}\text{I}$ -HSA (Amersham) was applied to the apical surface of 12 filters for each filter type and the appearance of the  $^{125}\text{I}$ -HSA in the basolateral fluid was measured at 8 time points over 24 hours after addition of the protein. The protein was applied in normal media. The HSA transport was analysed twice for each filter during the experiment. The first time the basolateral fluid was sampled, 200 $\mu\text{l}$  was removed and replaced with 200 $\mu\text{l}$  of fresh media. The second time all the fluid could be removed and analysed. A correction step was brought into the calculation to allow for the initial removal of HSA.

100µl or 1ml of media was analysed for  $^{125}\text{I}$  content in the mini gamma counter. 100µl was used to determine the amount of non-protein bound iodine within the sample by using TCA to precipitate the  $^{125}\text{I}$ -HSA. 100µl of 20%w/v TCA was added, incubated for 15 minutes, centrifuged in an eppendorf microcentrifuge and 100µl of supernatant was assayed for  $^{125}\text{I}$  activity. The total  $^{125}\text{I}$  activity in the basolateral fluid was corrected for that found to be present as non-protein bound activity.

The uptake of  $^{125}\text{I}$ -HSA by the filter and cells combined was estimated. After removal of experimental media the filters and cells were washed three times in cold PBS azide. The cell coated filter was removed from the plastic insert using a scalpel and assayed whole in the mini gamma counter. The permeability of the gelatin-coated and non-coated filter without cells for  $^{125}\text{I}$ -HSA was determined. Twelve filter inserts were transferred to six-well plates. Six were coated with gelatin. 4ml of media was pipetted inside the insert and 3ml was pipetted into the well. The plates were placed inside an air-tight plastic container and placed in an incubator over night to ensure adequate wetting of the filter. The experiment was performed as for the cell coated filters.

#### Cell and filter resistance measurements.

After completion of the experiment but before washing filters in PBS azide, the electrical resistance of the endothelial cell layer was determined on both the gelatinised filter and the non-gelatinised filter. The resistance of the filters without cells was also determined. 5ml of normal media was pipetted into the insert, 3ml was pipetted outside (into the well). Resistance was measured using the World Precision Instruments voltohmmeter. An alternating current of  $\pm 20 \mu\text{A}$  at 12.5 Hz was applied to the cell monolayer.  $\text{Ohms.cm}^2$  was calculated by first subtracting the resistance determined for a filter without cells ( $\text{ohms}_2$ ) from the resistance measured for the cell monolayer ( $\text{ohms}_1$ ) and then multiplying by the area of the filter.

$$\text{Ohms.cm}^2 = (\text{ohms}_1 - \text{ohms}_2) \times 4.2$$

#### BSA transport by BAE-1 cells grown on uncoated filters.

BSA was radio-iodinated with  $^{125}\text{I}$  as described under section 2.2 and a solution containing  $33\mu\text{g}/2\text{ml}$  was prepared. This solution was applied to 4, 7, and 10 day old cultures of BAE-1 cells (P29) grown on uncoated nitrocellulose filters. At timed intervals over 24 hours samples of basolateral fluids were removed from 3 filters at each time point. Resistance measurements and cell/filter uptake was determined as described previously. The percentage of TCA-precipitable  $^{125}\text{I}$  was also determined.

#### Transport of BSA and BSA conjugates.

The permeability of a monolayer of BAE-1 cells (P28-P32) grown on millicell HA filters for  $^{125}\text{I}$ -BSA,  $^{125}\text{I}$ -BSA-MTX (4.55 %w/w),  $^{125}\text{I}$ -BSA-MTX (11.54 %w/w), and  $^{125}\text{I}$ -LA was determined. Although the age of the cells on the filter did not appear to alter the rate of transport it was decided to use 7 day old cultures as a standard.  $9.23\mu\text{g}$  of iodinated protein or iodinated protein conjugate was applied to the apical surface of the cells and the basolateral compartment of the cells was sampled as before.

#### **2.11.5 Preparation of Cell Samples Grown on Nitrocellulose Filters for Electron Microscopy.**

Cells were seeded on to millicell HA filters ( $2 \times 10^6$  per filter) and media was changed every other day until confluence was reached (Caco-2 = 15 days and BAE-1 = 7 days). Filters were removed from the plastic holders using a scalpel and cut into quarters. Filters were fixed in 2.5% glutaraldehyde, 4% formaldehyde in 0.1M cacodylate buffer (pH 7.4) for 1 hour at room temperature. Cells were washed twice (5 minutes each) in cacodylate buffer, then fixed in 1% osmium tetroxide in cacodylate buffer for 1 hour. During this time the cells went brown. Next cells were washed twice (5 minutes each) in distilled water.

At this stage cells prepared for scanning electron microscopy (S.E.M.) were fixed in 1% tannic acid in cacodylate buffer for 0.5 hours. Cells both for transmission electron microscopy (T.E.M.) and S.E.M. were dried in graded ethanol as shown below:



% v/v Ethanol	Time (minutes)
0	2 x 5
30	2 x 10
50	2 x 10
70	2 x 10
100	3 x 10

Cells prepared for S.E.M were critical point dried from 100% ethanol and then a thin coat of gold was applied in an Edwards Sputter Coater S150B. Small sections of cell coated filter were glued onto 10mm x 10mm stubs (Jeol) using conductive carbon cement (Leit C) and examined using Jeol JSM 35C Scanning Electron Microscope.

Preparation of cells for T.E.M. was continued by embedding the filter quarters in 50% Taab embedding resin in 100% Ethanol and then rotating. Over the following 48 hours the resin was changed twice to 100% resin and rotation was continued. During this period the filters rolled up like swiss rolls. After 72 hours each quarter of filter was placed in a separate Taab Embedding mould (CO50) and the mould was topped up with resin. The moulds were placed in an oven at 50°C for 48-72 hours.

Sections were taken using a C. Reichert OM U3 microtome with a glass knife. 90nm sections were taken and placed on grids. The sections were stained in the dark with 2% uranyl acetate for 7 minutes, washed 4 times with distilled water and stained for 7 minutes with Reynolds Lead Citrate in a petri dish lined with filter paper soaked in 1M NaOH. The sections were washed 4 times in distilled water, dried and viewed in a Jeol 1200 Ex Transmission Electron Microscope.

In addition some slightly thicker sections were studied under the light microscope. The sections were dried on a glass slide on a hot plate and stained with 1% toluidine blue in 1% borax. The stain was washed off and the section was mounted in D.P.X. and viewed using a Zeiss Ultraphot microscope fitted with a 35mm camera.

### **CHAPTER 3:**

### **KINETICS OF METHOTREXATE AND PROTEINS IN THE RAT.**

All calibration curves used in the calculation of values in this chapter are shown in Appendix 1. The method of calculation of the pharmacokinetic parameters is shown in Appendix 2. All tables of data are listed in Appendix 3. These tables have the prefix A.

### 3.1 Pharmacokinetics of Methotrexate

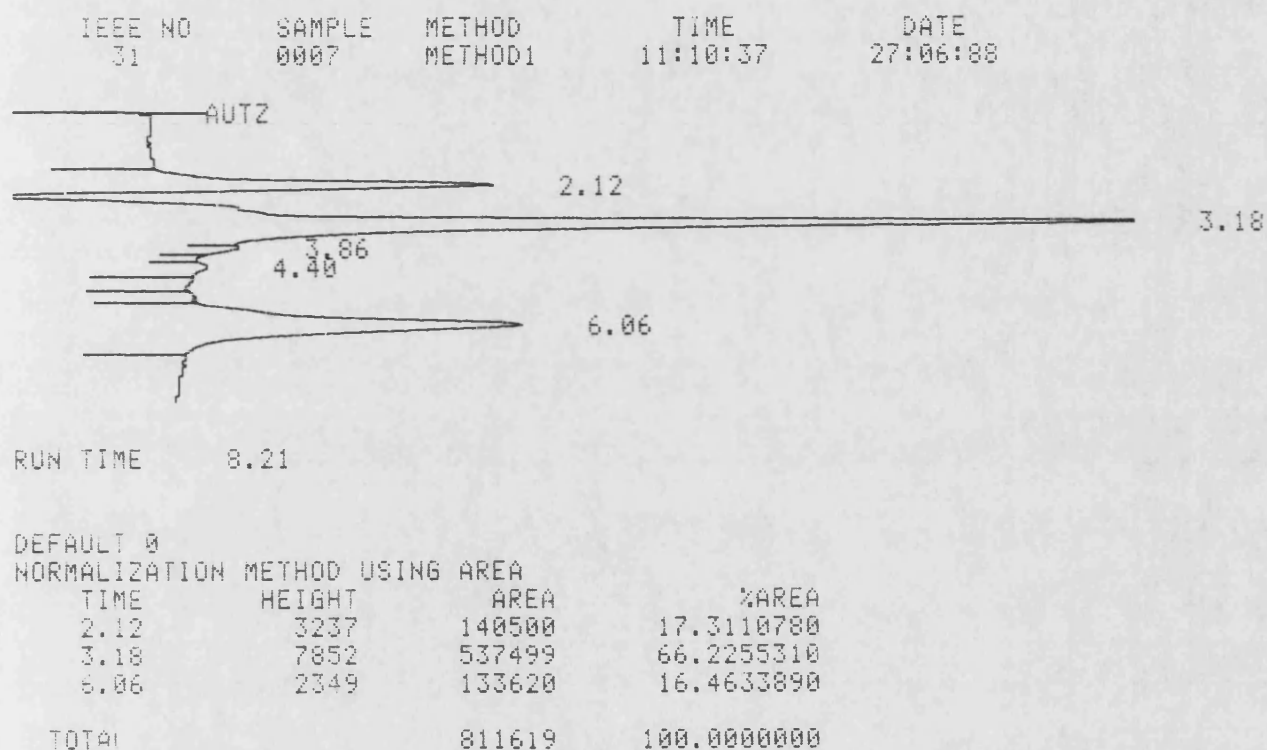
Methotrexate was chosen as the model drug for the work in this thesis. In later sections (see Chapter 4), experiments are described, in which the drug was bound to protein carriers, in order to change the pharmacokinetics of the drug. The pharmacokinetic parameters of 'free' MTX were calculated first.

Plasma concentrations of MTX were determined using two methods. (HPLC and using radiolabelled MTX). A dose of 2.5mg of MTXNa<sub>2</sub> was administered to rats by IV, IP and SC injection and the plasma concentration of the drug was determined using HPLC. A typical chromatogram obtained after injection of a rat plasma sample containing MTX, onto the column is shown in figure 3.1.1. This sample had been spiked with the internal standard, aminopterin. Table A3.1.1 gives the plasma levels determined by HPLC for rats dosed with 2.5mg of MTX. The plasma levels following administration of a 2.5mg dose to rats were also determined using <sup>3</sup>H-MTX, as described in section 2.5.1 in the methods. The plasma concentrations obtained are listed in table A3.1.2 for each of the routes.

<sup>3</sup>H-MTX was also administered at a total drug dose of 0.5mg/rat and plasma levels were determined as described above. These are shown in table A3.1.3.

Figure 3.1.2 is a plot of log concentration of <sup>3</sup>H-MTX in plasma against time for the 2.5mg dose, for each of the routes of administration. For the other doses of MTX the plot (not shown) was very similar. Figure 3.1.3 compares plasma concentrations attained after administration of a 2.5mg dose of MTXNa<sub>2</sub>, with HPLC detection and using <sup>3</sup>H-MTX. Figures 3.1.2 and 3.1.3 show that there was very little difference between plasma levels achieved for each route of administration and each dose. Each plot shows a biexponential clearance. Phase 1 was believed to be the distribution or

Figure 3.1.1: A typical chromatogram obtained after injection of a sample of plasma from a rat which had been injected with 2.5mg of MTXNa<sub>2</sub>. The plasma was extracted as described in the methods (2.5.1) and was spiked with AMN as internal standard.



The peak with a retention time of 3.18 minutes was due to AMN.

The peak with a retention time of 6.06 minutes was due to MTX.

Figure 3.1.2 Log Concentration of  $^3\text{H}$ -MTX after administration of 2.5mg total drug to male wistar rats by one of three routes. n=8 for each route. Each point represents data from one rat.

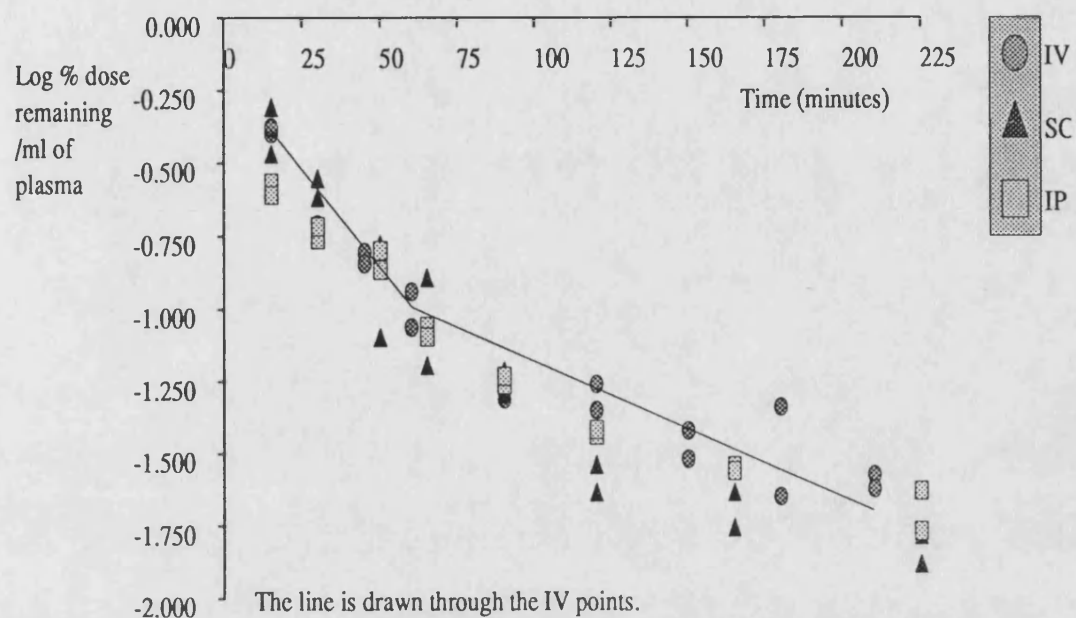
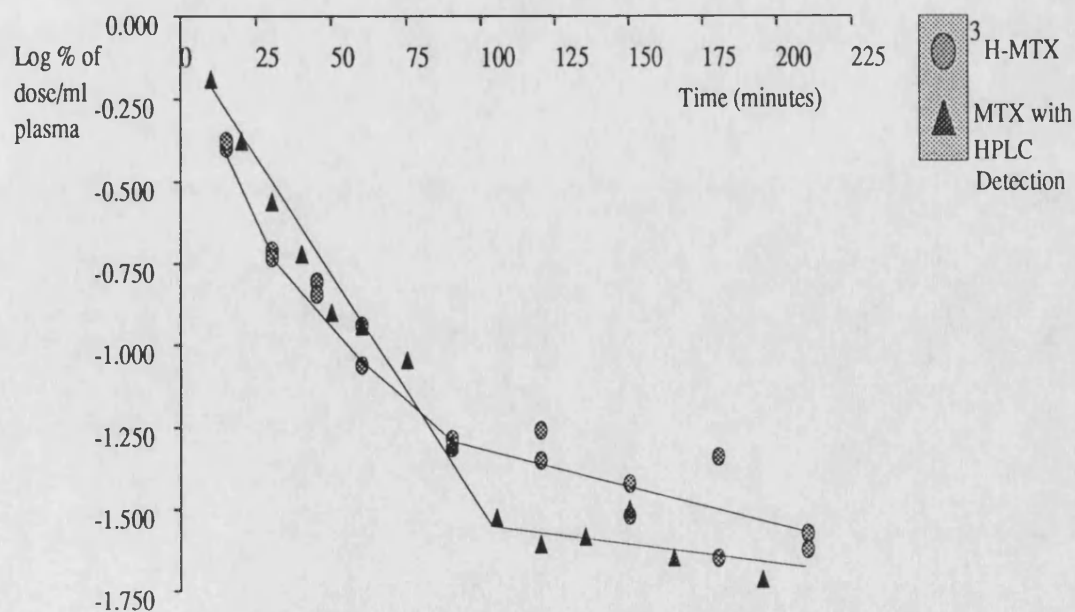


Figure 3.1.3: Log concentration of  $^3\text{H}$ -MTX and MTXNa (with HPLC detection) following IV administration to male wistar rats. 2.5mg of total drug was administered. (n=8 for each dose). Each point is a concentration determined from one rat.



alpha phase and phase 2 was believed to be the elimination or beta phase. Following SC and IP administration no initial absorption phase was seen, indicating that absorption was very rapid from these sites and probably occurred directly into the blood stream. Over the elimination phase the plot of log plasma concentration against time is linear and pharmacokinetic parameters could be calculated for each route of administration and for each dose of drug. These are shown in table 3.1. The pharmacokinetic parameters for the distribution phase were also calculated. The method for this calculation is described in appendix 2.

**Table 3.1 The pharmacokinetic parameters calculated for each dose of drug and for each route of administration.**

**1. IV Route for each dose.**

Dose	0.5mg <sup>3</sup> H-MTX	2.5mg <sup>3</sup> H-MTX	2.5mg MTX (HPLC)
<b>a) Alpha Phase</b>			
time span	15-80minutes	15-60minutes	10-90minutes
R <sup>2</sup>	0.9679	0.9091	0.9654
m* (min <sup>-1</sup> )	-0.0211±0.0014	-0.0206±0.0027	-0.0174±0.0015
c* (Log Co)	-0.0597±0.0695	-0.225 ±0.109	-0.137 ±0.067
n <sup>#</sup>	10	8	8
kel (min <sup>-1</sup> )	0.0485	0.0474	0.040
t <sup>1/2</sup> (min)	14.28	14.61	17.33
Vd (ml)	114.7	167.9	137.1
Cl (ml/min)	5.56	7.96	5.48
<b>b) Beta Phase</b>			
time span	120-240min	90-210min	90-195min
R <sup>2</sup>	0.9408	0.6463	0.6418
m* (min <sup>-1</sup> )	-0.00256±0.0002	-0.00262±0.001	-0.00294±0.001
c* (log Co)	-1.2083±0.034	-1.0394±0.11	-1.1603±0.078
n <sup>#</sup>	12	10	7
kel (min <sup>-1</sup> )	0.00589	0.00603	0.00677
t <sup>1/2</sup> (min)	117.5	115.0	102.4
Vd (ml)	1615	1094	1446
Cl (ml/min)	9.51	6.59	9.79

**Table 3.1: Continued (Pharmacokinetic Parameters for MTX).**

**2. IP Route for each dose.**

Dose	0.5mg <sup>3</sup> H-MTX	2.5mg <sup>3</sup> H-MTX	2.5mg MTX (HPLC)
<b><u>a) Alpha Phase.</u></b>			
time span	7-84minutes	15-90minutes	15-90minutes
R <sup>2</sup>	0.9036	0.9453	0.8277
m* (min <sup>-1</sup> )	-0.0115±0.0011	-0.0159±0.0013	-0.0173±0.0025
c* (log Co)	-0.4187±0.053	-0.4224±0.076	-0.158±0.0025
n <sup>#</sup>	12	10	12
kel (min <sup>-1</sup> )	0.0264	0.0367	0.0398
t <sup>1/2</sup> (min)	26.21	18.90	17.39
Vd (ml)	262.3	264.5	144.0
Cl (ml/min)	6.92	9.44	5.73
<b><u>b) Beta Phase</u></b>			
time span	107-240min	120-225min	105-180min
R <sup>2</sup>	0.7154	0.8780	0.8310
m* (min <sup>-1</sup> )	-0.00248±0.0004	-0.0026±0.0005	-0.00298±0.0005
c* (Log Co)	-0.9296±0.078	-1.1215±0.084	-1.1249±0.078
n <sup>#</sup>	14	6	8
kel (min <sup>-1</sup> )	0.00571	0.00592	0.00686
t <sup>1/2</sup> (min)	121.3	117	101
Vd (ml)	850.3	1323	1333
Cl (ml/min)	4.86	7.83	9.14

**Table 3.1: Continued (Pharmacokinetic Parameters for MTX).**

**2. IP Route for each dose.**

Dose	0.5mg <sup>3</sup> H-MTX	2.5mg <sup>3</sup> H-MTX	2.5mg MTX (HPLC)
------	--------------------------	--------------------------	------------------

**a) Alpha Phase.**

time span	7-84minutes	15-90minutes	15-90minutes
R <sup>2</sup>	0.9036	0.9453	0.8277
m* (min <sup>-1</sup> )	-0.0115±0.0011	-0.0159±0.0013	-0.0173±0.0025
c* (log Co)	-0.4187±0.053	-0.4224±0.076	-0.158±0.0025
n <sup>#</sup>	12	10	12
kel (min <sup>-1</sup> )	0.0264	0.0367	0.0398
t <sup>1/2</sup> (min)	26.21	18.90	17.39
Vd (ml)	262.3	264.5	144.0
Cl (ml/hr)	6.92	9.44	5.73

**b) Beta Phase**

time span	107-240min	120-225min	105-180min
R <sup>2</sup>	0.7154	0.8780	0.8310
m* (min <sup>-1</sup> )	-0.00248±0.0004	-0.0026±0.0005	-0.00298±0.0005
c* (Log Co)	-0.9296±0.078	-1.1215±0.084	-1.1249±0.078
n <sup>#</sup>	14	6	8
kel (min <sup>-1</sup> )	0.00571	0.00592	0.00686
t <sup>1/2</sup> (min)	121.3	117	101
Vd (ml)	850.3	1323	1333
Cl (ml/hr)	4.86	7.83	9.14



**Table 3.1 Continued (Pharmacokinetic Parameters for MTX).**

**3. SC Route for each dose.**

Dose	0.5mg <sup>3</sup> H-MTX	2.5mg <sup>3</sup> H-MTX	2.5mg MTX (HPLC)
<b><u>a) Alpha Phase.</u></b>			
time span	10-90minutes	15-90minutes	15-105minutes
R <sup>2</sup>	0.9102	0.8455	0.9760
m* (min <sup>-1</sup> )	-0.0121±0.001	-0.0158±0.002	-0.0171±0.0008
c* (Log Co)	-0.386±0.05	-0.243±0.135	0.0128±0.052
n <sup>#</sup>	16	10	14
kel (min <sup>-1</sup> )	0.0279	0.0365	0.0394
t <sup>1/2</sup> (min)	24.83	19.01	17.6
Vd (ml)	243.2	175.1	97.1
Cl (ml/min)	6.78	6.23	3.83
<b><u>b) Beta Phase.</u></b>			
time span	120-240min	120-225min	120-180min
R <sup>2</sup>	0.9302	0.7802	0.6022
m* (min <sup>-1</sup> )	-0.0024±0.0002	-0.0023±0.0006	-0.0030±0.0012
c* (log Co)	-1.1659±0.042	-1.3195±0.108	-1.2258±0.194
n <sup>#</sup>	10	6	6
kel (min <sup>-1</sup> )	0.00543	0.00592	0.00691
t <sup>1/2</sup> (min)	127.5	129	100.3
Vd (ml)	1465	2087	1682
Cl (ml/min)	7.95	12.35	11.62

Notes: \* Slopes or constants are quoted ± Standard Error.

# n= number of points used in the calculation.

Only two phases were seen in these experiments. In man it is known that MTX demonstrates a triexponential clearance.<sup>(117)</sup> It may be that the third phase began when the plasma concentrations were too low to be measured by this assay or the first phase had already occurred before plasma samples were taken.

There was little difference between the pharmacokinetic parameters calculated for each dose and the different routes of administration. MTX was shown to have a large volume of distribution (approximately 1.5l in a 250g rat). This volume is a hypothetical term which, in this case probably indicates that following its wide distribution, MTX was sequestered by a tissue or tissues. Upon entry of MTX into most cell types, it becomes bound to DHFR. Any remaining MTX is poly-glutamated. The poly-glutamated form of drug cannot readily leave the cell.<sup>(112)</sup> MTX also has a very short half-life (101 to 129 minutes for the beta phase). By binding the drug to a targeting agent both of these factors could be improved.

#### Urinary Excretion of MTX.

Table A3.1.4. shows the excretion of MTX in the urine with HPLC detection after administration by the IV route to male wistar rats. The HPLC assay was used only to determine the excretion of MTX itself and not any metabolites. After 48 hours approximately 89% of the MTX dose had been excreted unchanged in the urine. This is similar to the percentage excreted in man,<sup>(136)</sup> and to the results obtained by Chu and Whiteley<sup>(99)</sup> for <sup>3</sup>H-MTX excretion in the urine of mice.

Table A3.1.5 shows the urine excretion of <sup>3</sup>H- activity after administration of 2.5mg <sup>3</sup>H-MTX by each of the three routes. These results are shown graphically in Figure 3.1.4. Any metabolites of MTX as well as unchanged MTX were measured using this procedure. There was no significant difference in the amount of <sup>3</sup>H activity excreted for each of the three routes. Between 13 and 17 % of administered <sup>3</sup>H was excreted in the urine over 72 hours for each route of administration

A Student's t-test was performed on the IV data for urine excretion with HPLC

Figure 3.1.4:  
The urine excretion of  $^3\text{H}$  activity following administration of 2.5mg of  $^3\text{H}$ -MTX to rats by IV, IP and SC routes.

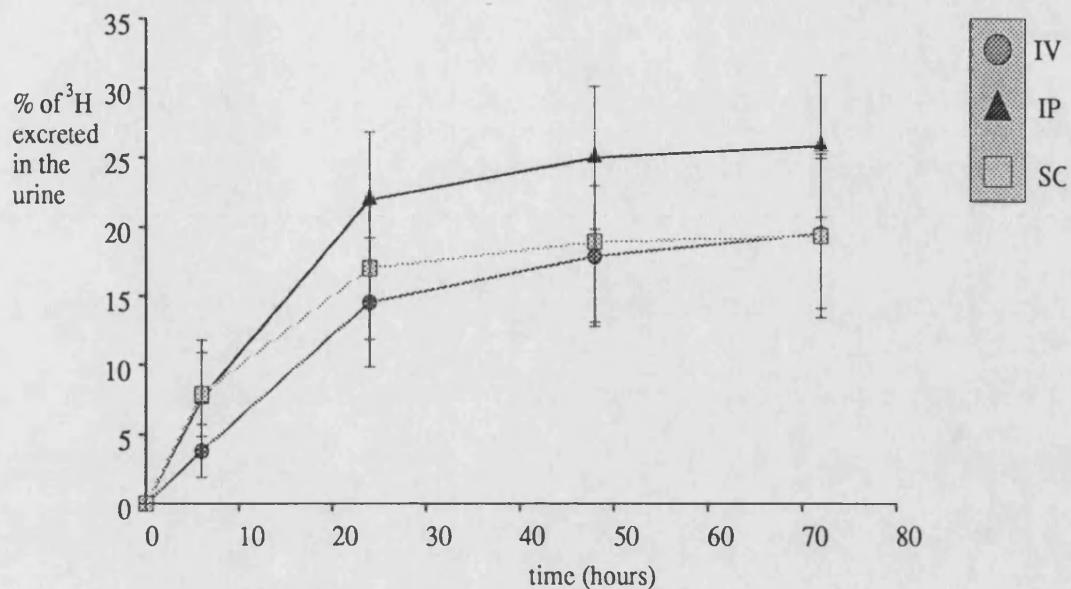
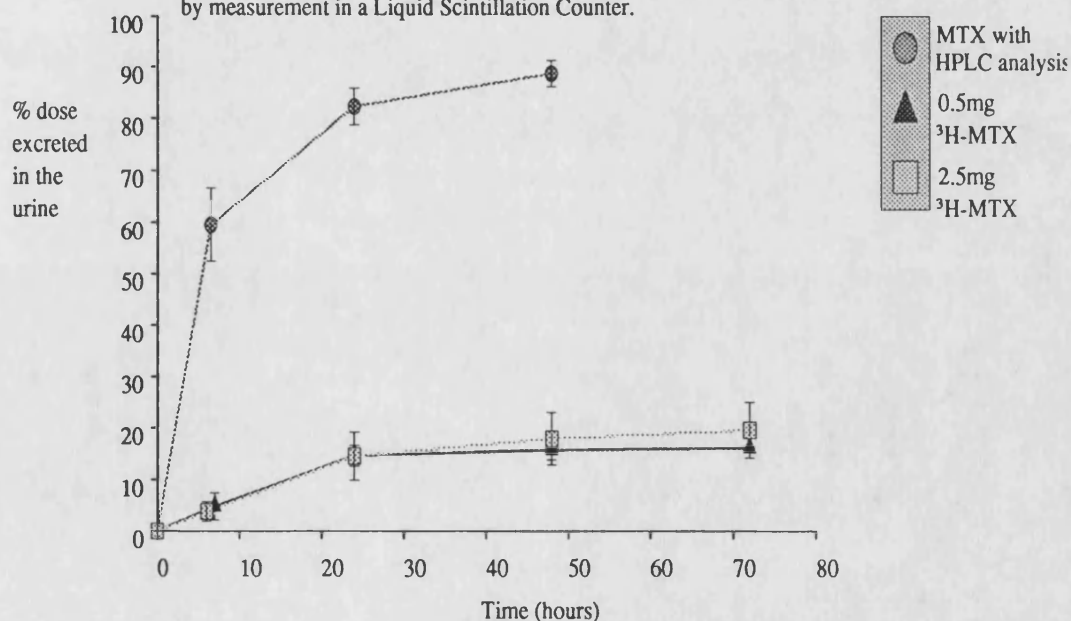


Figure 3.1.5:  
The Urine Excretion of  $\text{MTXNa}_2$  followed by HPLC analysis compared to the Urine Excretion of two doses of  $^3\text{H}$ -MTX (0.5mg and 2.5mg) followed by measurement in a Liquid Scintillation Counter.



detection and for  $^3\text{H}$ -MTX excretion at 24 hours and 48 hours after administration. At both time points the t values calculated were highly significantly different ( $p < 0.001$ ). Figure 3.1.5 compares the urine excretion for  $\text{MTXNa}_2$  and  $^3\text{H}$ -MTX (both 2.5mg and 500 $\mu\text{g}$  doses).

The urine excretion of  $^3\text{H}$  activity after administration of 0.5mg of  $^3\text{H}$ -MTX by each of the three routes (Table A3.1.6) was also determined. The cumulative % excreted was compared at each time point to the 2.5mg dose for each route by means of a non-paired t-test. All results were non-significant ( $p > 0.05$ ).

It is difficult to explain why less of the  $^3\text{H}$ -MTX was excreted than the  $\text{MTXNa}_2$ . Since the  $^3\text{H}$  activity excreted could actually be metabolites of MTX as well as drug, it was anticipated that the  $^3\text{H}$  activity excreted would overestimate the excretion of MTX. It may be that, following administration of  $^3\text{H}$ -MTX, the  $^3\text{H}$  exchanged with hydrogen molecules on endogenous compounds and thus was more slowly excreted. The  $^3\text{H}$ -MTX used was labelled on positions 3', 5' and 7. One of the metabolites of MTX is 7-OH-MTX. If this metabolite was formed in the rat, and it was excreted, then less  $^3\text{H}$  activity would be excreted per molecule of MTX. Since the calculated elimination half-lives and volumes of distribution were similar for both the  $^3\text{H}$ -MTX and the  $\text{MTXNa}_2$ , then it seems unlikely that part of the activity was retained *in vivo*.

### 3.2 Digoxin

Digoxin was administered to rats as a model drug with a larger molecular weight (781D) than MTX (452D) so that effects of molecular weight on rate of absorption from IP and SC sites could be identified. However it is difficult to directly compare the pharmacokinetics calculated for digoxin with those calculated for MTX because of the different nature of the 2 drugs. MTX is a polar molecule and digoxin is hydrophobic.

Table A3.2.1 lists the plasma levels determined for digoxin following administration of 250ng by each of the three routes. These results are shown graphically in Figure 3.2. Following administration by the SC route peak plasma levels were achieved

Figure 3.2

Serum Concentration (Log % dose/ml) after injecting male wistar rats with 250ng of Digoxin by one of three routes.

Levels were determined using an ELISA.

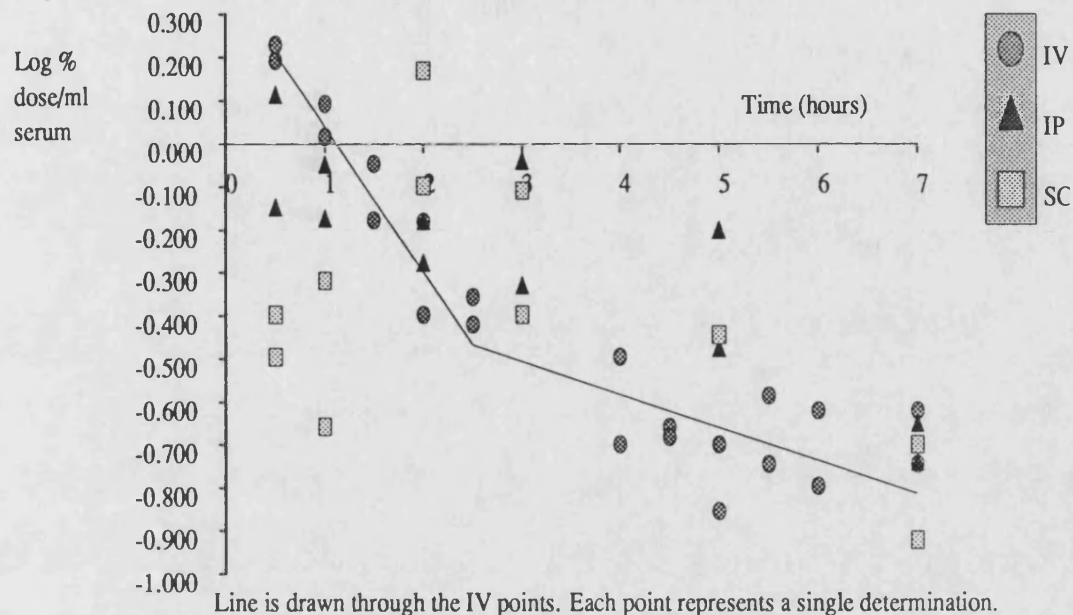
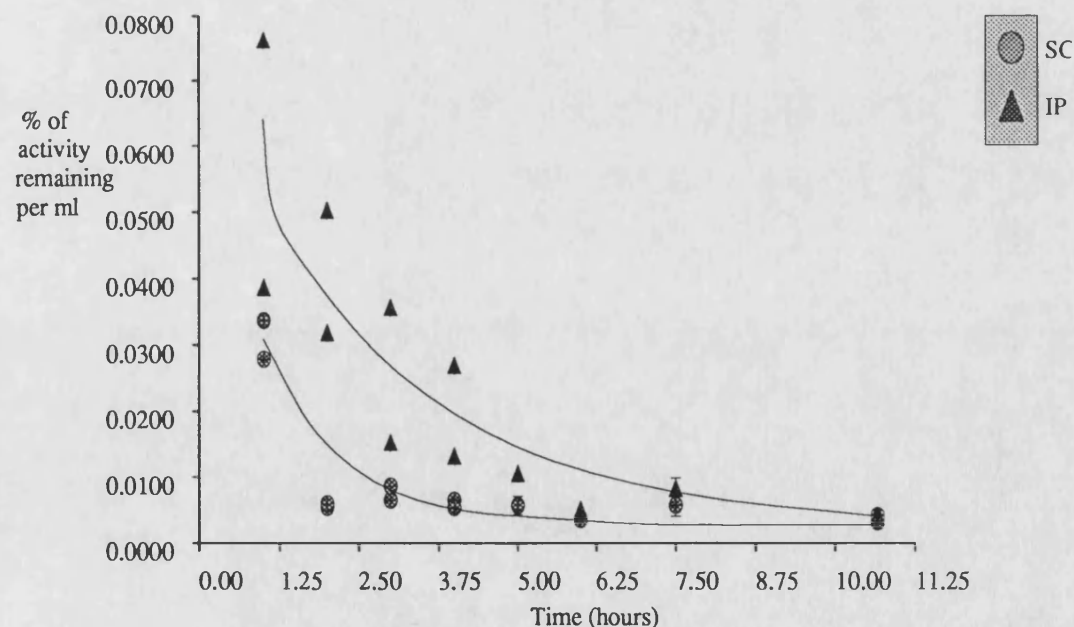


Figure 3.3: Plasma Concentration of  $^{14}\text{C}$  activity following administration of 1.6mg of  $^{14}\text{C}$ -Inulin to rats by SC and IP routes.



Points were determined from a single rat, except for 5 and 7.5 hours (n=3 or 4) IP and 7.5 and 10.66 hours SC (n=3). Bars are S.E.M.

approximately 2 hours after injection. Peak plasma levels were achieved within 30 minutes of IP injection. This indicates that absorption from SC sites occurred at a slower rate than from the peritoneal cavity, and in addition, absorption was slightly slower than for MTX. Following IV administration of 250ng of digoxin to rats, two phases were seen over the time period investigated. These were assumed to be due to an initial distribution (or alpha) phase followed by an elimination (or beta) phase. Table 3.2 lists the pharmacokinetic parameters calculated for digoxin for each of the routes. For IV dosed rats, parameters were calculated for alpha and beta phases and for SC and IP dosed rats, parameters were calculated for the beta phase only.

**Table 3.2 The Pharmacokinetic Parameters Calculated for Digoxin following IV, IP and SC administration of 250ng to rats.**

	IV (alpha)	IV (beta)	IP	SC
Time span	0.5-2.5hr	2.5-7	0.5-7	2.0-7
R <sup>2</sup>	0.7872	0.4195	0.8418	0.9250
m*	-0.636±0.12	-0.065±0.02	-0.092±0.016	-0.159±0.022
c*	0.478±0.185	-0.32±0.113	0.0064±0.06	0.307±0.10
n <sup>#</sup>	10	14	12	7
Kel (hr <sup>-1</sup> )	1.465	0.149	0.212	0.366
t <sup>1/2</sup> (hr)	0.473	4.651	3.269	1.893
Vd (ml)	33.27	209	123.6	49.32
Cl (ml/hr)	48.74	31.14	26.20	18.05

Notes: \* constants and slopes are quoted ± Standard Error.

# n= number of serum concentrations used in calculation.

The volume of distribution of digoxin calculated for the beta phase after IV injection was high representing the whole body of a rat. This was because of the hydrophobic

nature of digoxin. It rapidly leaves the blood stream and is deposited in muscle tissue and adipose.<sup>(137)</sup> The Vd calculated for the alpha and beta phases for each route of administration were found to be lower than for MTX. The  $t^{1/2}$  for elimination were slower following IV and IP injection than SC injection, which is difficult to explain.

### 3.3 Pharmacokinetics of Inulin

Inulin has a molecular weight of approximately 5000D. It was administered to rats in order to determine the pharmacokinetics and rate of absorption from IP and SC sites, of a drug larger than both MTX (452D) and digoxin (781D).

The plasma concentrations of SC and IP injected  $^{14}\text{C}$ -Inulin are shown in table A3.4.1. They are represented graphically in Figure 3.3 (page 76). Inulin was absorbed rapidly from IP and SC sites with peak plasma levels occurring within 1 hour of injection. Inulin has an average molecular weight of 5000 but this does not seem to restrict its absorption into the blood stream, probably because it is a highly polar molecule. Table 3.3 lists the pharmacokinetic data for inulin after IP and SC injection.

**Table 3.3 Pharmacokinetic Parameters for  $^{14}\text{C}$ -Inulin over the elimination phase.**

	IP	SC
Times used	1-10.7 hours	2-10.7 hours
R <sup>2</sup>	0.7787	0.3725
m*	-0.160±0.028	-0.0297±0.009
c*	-1.125±0.11	-2.13±0.059
n <sup>#</sup>	19	14
Kel (hr <sup>-1</sup> )	0.368	0.0685
$t^{1/2}$ (hr)	1.881	10.12
Vd (ml)	1333	13459
Cl (ml/hr)	491	922

Notes: \* slopes and constants are calculated ± Standard Error. # n= number of points used in the calculation.

There was a great deal of variation in the plasma levels of  $^{14}\text{C}$ -inulin achieved between different rats. This led to a very poor regression coefficient for the 'linear' section of the Log plasma concentration versus time plot for  $^{14}\text{C}$ -inulin. This large variation was probably due to differences in the renal clearance of the drug between rats. Inulin is used clinically to determine glomerular filtration rate in man.<sup>(138)</sup> It is rapidly removed from the circulation and is predominantly eliminated unchanged by the kidney by glomerular filtration, with no reabsorption occurring in the tubules.<sup>(139)</sup> This is demonstrated in Table 3.3 by the extremely large clearance (approximately 8-15 ml/minute). The half life of inulin in man following IV injection has been quoted as between 0.53 to 1.17 hours.<sup>(138)</sup> After IP injection the half life was found to be 1.9 hours and after SC it was found to be 10 hours. These apparent differences may be because the inulin was not completely absorbed from the injection sites (and SC absorption was slower than IP) and inulin was slowly being released into the blood stream during the elimination phase.

### **3.4 Pharmacokinetics of Proteins.**

All conjugates and most of the proteins (this section and chapter 4) were administered with an  $^{125}\text{I}$  label. Problems envisaged with this label were that any unconjugated iodine in the injection solution may interfere with the assay. Also, as the protein was broken down *in vivo*, it was anticipated that iodine or iodinated tyrosine would be released and again this may interfere with the assay. The  $^{125}\text{I}$  was injected so that the effects of any unconjugated iodine could be investigated.

#### **3.4.1 Pharmacokinetics of $^{125}\text{I}$ -Na**

$^{125}\text{I}$ -Na was administered to rats by the IV route. The serum concentration at various time points was determined and this data is listed in table A3.3.1. The results are shown graphically in Figure 3.4.1. The clearance of  $^{125}\text{I}$ -Na followed a biexponential model. Pharmacokinetic parameters were calculated for each phase and are listed in table 3.4.1.



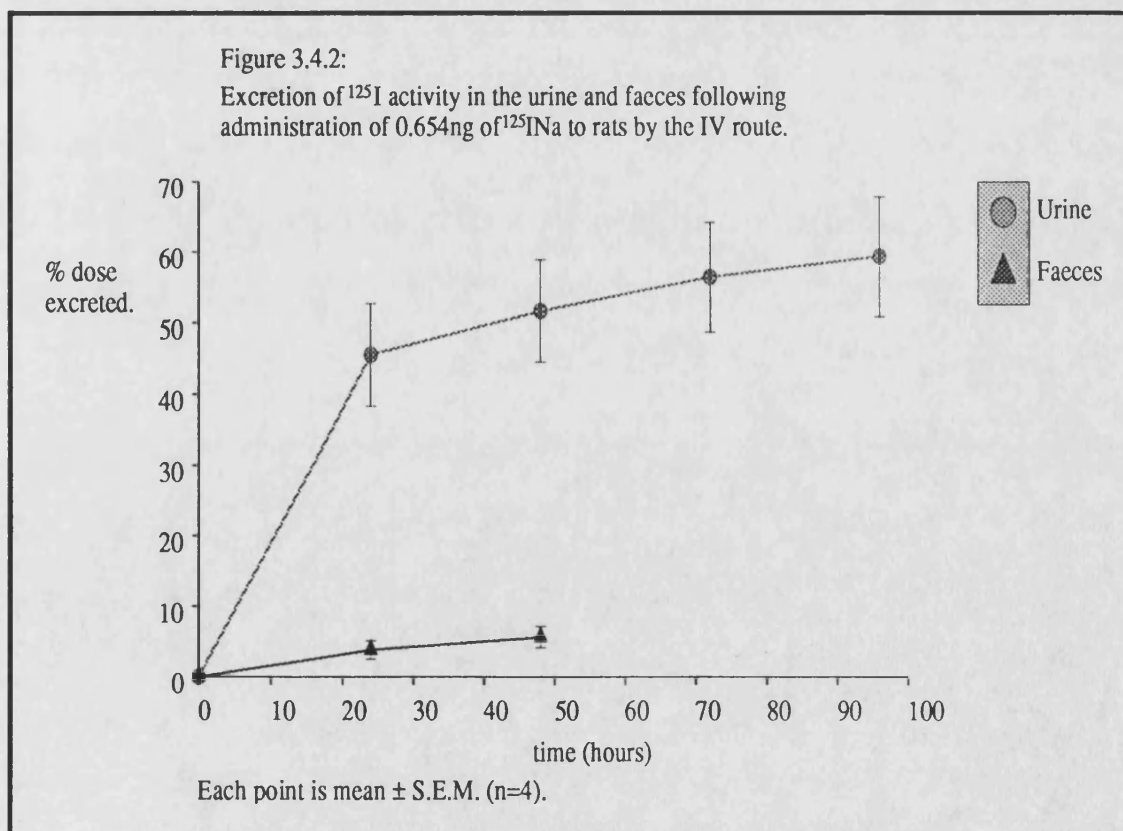
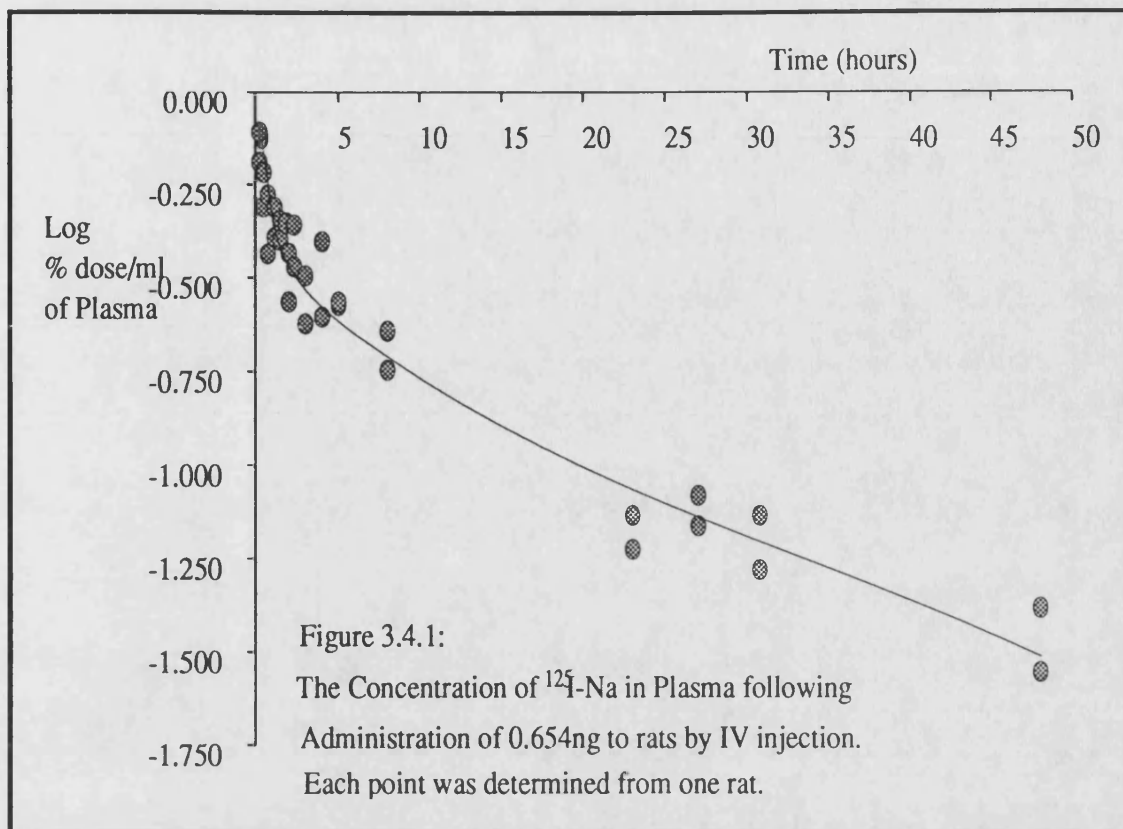


**Table 3.4.1: The pharmacokinetic parameters calculated for an IV dose of 0.654ng of  $^{125}\text{I}$ -Na administered to male wistar rats.**

	Alpha Phase	Beta Phase
Time span	15-150 minutes	3-48 hour
R <sup>2</sup>	0.7520	0.9157
m* (hr <sup>-1</sup> )	-0.359±0.062	-0.0222±0.002
c* (Log Co)	-0.415±0.086	-0.501±0.043
n <sup>#</sup>	16	16
Kel (hr <sup>-1</sup> )	0.826	0.0511
t <sup>1/2</sup> (hr)	0.838	13.55
Vd (ml)	260.0	316.9
Cl (ml/hr)	214.8	16.2

Notes:

\* Slopes and Constants are quoted ± Standard Error.

# n= Number of points used in the calculation.

The distribution half-life of  $^{125}\text{I}$ -Na was very rapid at approximately 50 minutes. The volume of distribution for the alpha phase was large and represents the total volume of the rat. Plasma clearance was also rapid for the distribution phase at approximately 3.6ml/minute. Three hours after administration (the start of the elimination phase) the plasma level had fallen to 0.32%/ml of the injected dose.

Table A3.3.2 and figure 3.4.2 show the urine excretion of  $^{125}\text{I}$  activity. Approximately 46% of the dose was excreted in the urine in the first 24 hours. Table A3.3.3 lists the amount of  $^{125}\text{I}$  activity that was excreted in the faeces. Only a small amount (5.6% in 48 hours) was excreted in the faeces.

Organ distribution in liver, kidney and thyroid was determined for the iodine (tabulated

in A3.3.4). These results are shown graphically in figure 3.4.3.  $^{125}\text{I}$  was sequestered into the thyroid but did not accumulate in the liver or kidney.

Because of the rapid clearance of the iodine from the plasma, the rapid uptake by the thyroid and lack of accumulation of the iodine in other organs, it was not anticipated that the small amount of unconjugated  $^{125}\text{I}$  that was injected (less than 10% in all experiments) would lead to errors in the  $^{125}\text{I}$  assay.

### 3.4.2 Lactalbumin (LA).

Lactalbumin is a milk protein with a molecular weight of 14.2kD. The LA used in this experiment was of bovine origin. Section 3.5 describes experiments which were performed, to investigate the possibility of bovine proteins causing an immune response in the rat. LA was administered as one of a range of proteins with different molecular weights, to determine the pharmacokinetic parameters and rates of transfer from IP and SC sites, as a function of molecular weight.

Table A3.5.1 lists the concentration of  $^{125}\text{I}$ -LA activity in rat serum. Figure 3.5.1 is a plot of Log serum concentration versus time for the  $^{125}\text{I}$  activity, for each of the three routes. Following IV administration this plot shows a biexponential clearance for LA. The first phase (alpha phase) was considered to be due to distribution throughout the serum and rapidly equilibrating tissues (central compartment). The second phase (beta phase) was due to elimination and distribution into a slowly equilibrating (tissue) compartment. Following IP injection absorption was rapid, with peak plasma levels being achieved within 1 hour of administration. Absorption from SC sites was also rapid. Again, peak plasma levels were achieved within 1 hour of injection. This rapid absorption phase implies that the protein was transferred straight into the blood stream from these extra-vascular sites, rather than requiring initial absorption into the lymph before it could pass into the blood stream. However it could also be explained by lymphatic absorption with the rate of transfer from lymph to blood being very rapid.

Following the initial absorption phase in IP and SC dosed rats, the serum concentration

Figure 3.4.3:

Percentage of  $^{125}\text{I}$  dose in Thyroid, Liver and Kidney following administration of 0.654ng of  $^{125}\text{I}$ Na to rats by the IV route.

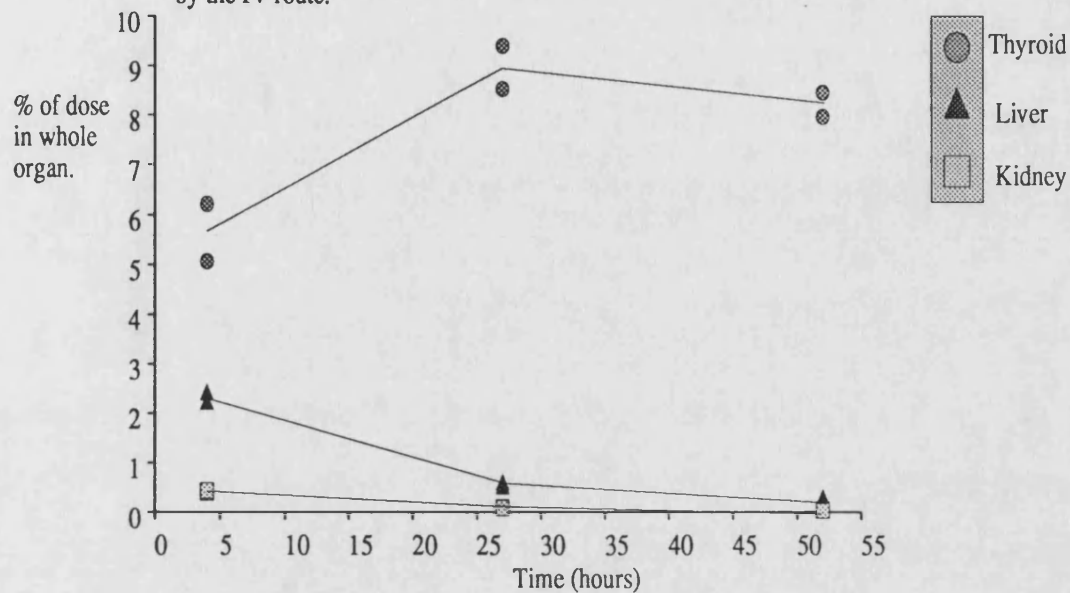
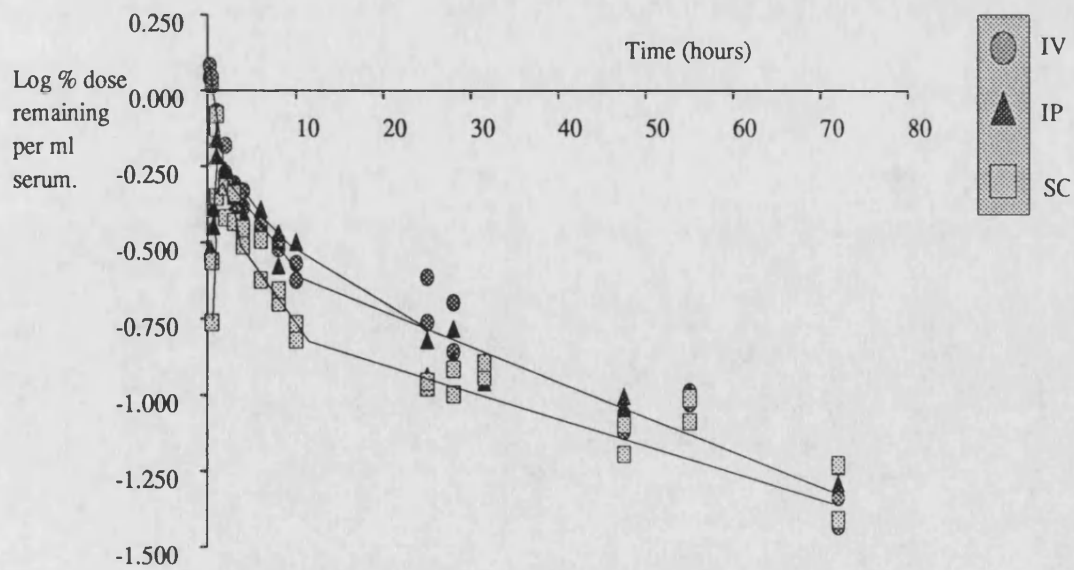


Figure 3.5.1:

Serum Concentration of  $^{125}\text{I}$  activity following administration of 5mg of  $^{125}\text{I}$ -Lactalbumin to rats by IV, IP and SC routes.



reached similar levels to IV and then began to fall at a similar rate. Table 3.5 lists the pharmacokinetic data calculated for  $^{125}\text{I}$ -LA injected into rats by each of the three routes.

**Table 3.5 The Pharmacokinetic Parameters Calculated for  $^{125}\text{I}$ -LA administered to rats by IV, IP and SC injection.**

	IV (alpha)	IV (beta)	IP (beta)	SC (beta)
Time span (hr)	0.25-3	3-72	4-72	10-72
R <sup>2</sup>	0.9407	0.9367	0.9026	0.8174
m*	-0.319±0.030	-0.0139±0.0008	-0.0123±0.0009	-0.0077±0.001
c*	-0.046±0.004	-0.374±0.028	-0.433±0.0344	-0.724±0.045
n <sup>#</sup>	10	22	20	14
Kel (hr <sup>-1</sup> )	0.735	0.032	0.028	0.0177
t <sup>1/2</sup> (hr)	0.943	21.6	24.5	39.08
Vd (ml)	111	236	271	530
Cl (ml/hr)	81.59	7.55	7.59	9.37

Notes: \* Slope and Constant are quoted ± Standard Error.

# n= number of points used in the calculation.

$^{125}\text{I}$ -LA injected IV or IP gave similar pharmacokinetic parameters during the beta phase. Following SC administration,  $^{125}\text{I}$ -LA was found to have a larger volume of distribution and slower elimination half life than that injected by the other routes, although serum levels did appear to be similar during this phase. The alpha half-life seen in IV dosed rats was rapid at less than 1 hour and the Vd represented about half the body weight of a rat.

Tables A3.5.2 and A3.5.3 list the urine and faecal excretion of  $^{125}\text{I}$  activity respectively.

Faecal excretion of the iodine was low with only between 6 and 8% of the injected dose being excreted in 72 hours. Urine excretion of  $^{125}\text{I}$  activity accounted for between 45 and 68% of the total dose in 72 hours (Figure 3.5.2). The urine excretion following IP and SC injection was very similar. However, after IV injection the rate of excretion was less than for the other two routes. Student's t-test was used to compare the amount excreted by IV dosed rats, at 24 and 72 hours, with the amount excreted by SC dosed rats and these were found to be highly significantly different at both time points ( $p < 0.001$  for 24 hours and  $p < 0.02$  for 72 hours).

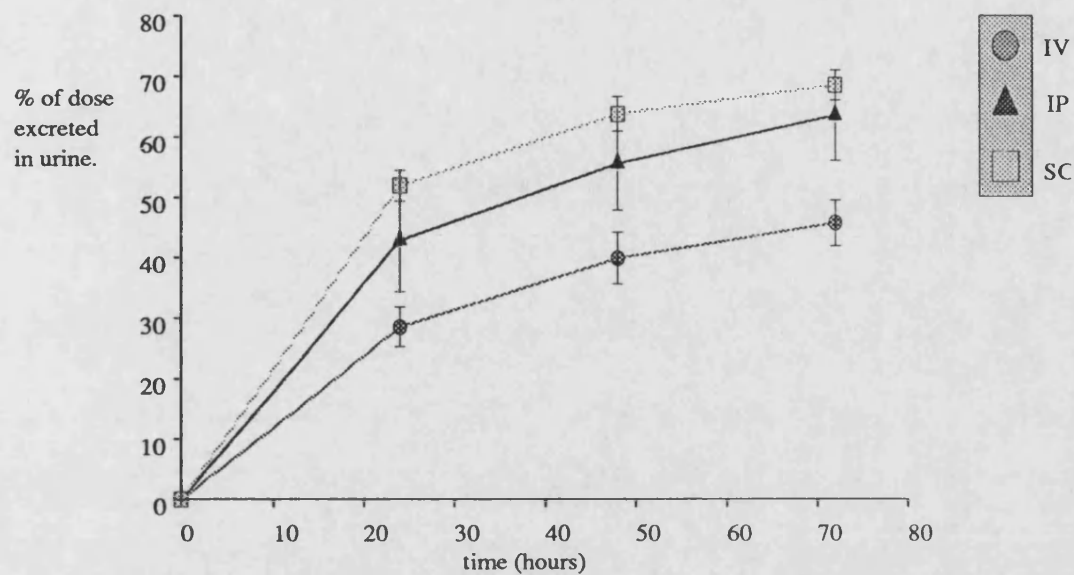
Seymour et al<sup>(56)</sup> demonstrated with HEMA copolymers that polymers up to a molecular weight of 45kD can be excreted in the urine. Thus LA has a molecular weight low enough to be excreted unchanged in the kidney and so urinary excretion would be expected to be rapid for this protein. It is possible that excretion after IP injection could be more rapid than after the other routes due to direct uptake by the kidney blood vessels, however this would not account for the increased excretion of SC dosed rats compared to IV. Thus it is possible that the IV dosed rats are showing falsely low urinary excretion.

Table A3.5.4 lists the organ distribution of  $^{125}\text{I}$  activity following administration of  $^{125}\text{I}$ -LA by each of the three routes. The organ distribution 28 hours after IV injection is shown in Figure 3.5.3. The results are expressed as a ratio, in this plot, of the  $^{125}\text{I}$  activity in the whole organ divided by the  $^{125}\text{I}$  activity in 1ml of whole blood. It was hoped that this transformation of the results would allow direct comparison of the organ distribution at different time points. For highly vascularised organs the percentage of activity in that organ would appear high even without tissue accumulation, if the activity in the blood remained high. Thus division by the activity present in 1ml of blood would compensate for this. If the organ, itself, had not taken up any of the  $^{125}\text{I}$  then the ratio obtained would be equivalent to the number of millilitres of blood present in that organ.

The ratio at other time points and for the other routes of injection for each of the organs

Figure 3.5.2:

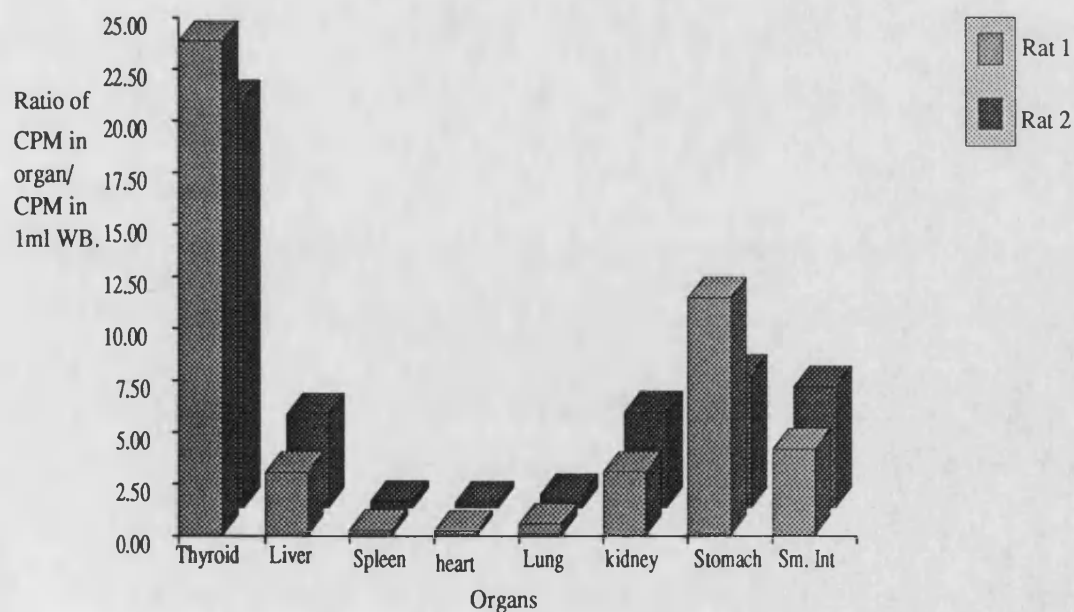
Percentage of  $^{125}\text{I}$  activity excreted in the urine following administration of  $^{125}\text{I}$ -LA to rats by IV, IP and SC routes.



Each point is a mean  $\pm$  S.E.M. (n=3).

Figure 3.5.3:

Organ Distribution of  $^{125}\text{I}$  activity following administration of 5mg of  $^{125}\text{I}$ -LA by IV injection. Determination was carried out at 28 hours after injection. Two rats were analysed.



was similar to that shown in Figure 3.5.3. At 28 hours after IV injection a small proportion of the  $^{125}\text{I}$ -LA had been broken down. This is shown by the high ratio in the thyroid (actual percentage was  $6.75 \pm 0.679$  for 6 rats). This breakdown would probably occur in the liver, although levels in the liver were not elevated compared to the other organs. Following breakdown, the  $^{125}\text{I}$  activity would have been transferred into the bile and then would appear in the gastro-intestinal tract and this may account for the high ratios in stomach and small intestine.

### **3.4.3 Carbonic Anhydrase (CA).**

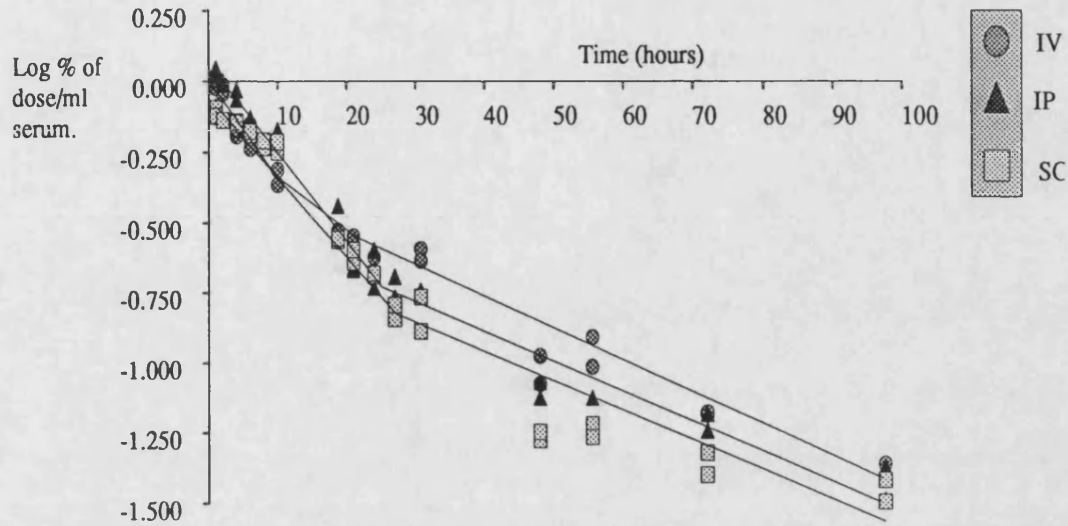
The carbonic anhydrase used in this experiment was of bovine origin. It has a molecular weight of 29kD and was administered as one of a range of proteins, as described previously, to investigate the effect of molecular weight on pharmacokinetics and rate of absorption from SC and IP sites. CA is a zinc metalloenzyme and it catalyses the conversion of carbonic acid to carbon dioxide and water.

$^{125}\text{I}$ -CA was administered to rats by each of the three routes. The serum levels calculated for the protein are shown in Table A3.6.1. A plot of Log concentration in serum versus time, for each of the three routes, is shown in Figure 3.6.1. This plot is very similar to that obtained for LA. Absorption from IP and SC sites appeared to be rapid, with peak plasma levels occurring within one hour of administration. Table 3.6 lists the pharmacokinetic parameters calculated for each route of administration. For IV dosed rats parameters for both the alpha and beta phases were calculated and for IP and SC dosed rats parameters were calculated only for the beta phase.



Figure: 3.6.1

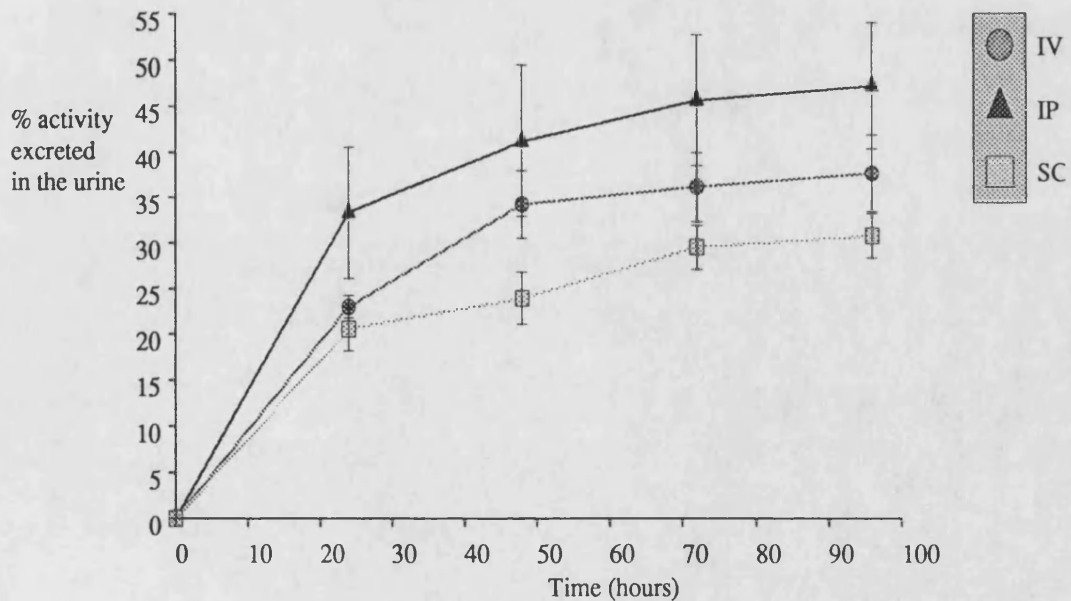
Serum concentration of  $^{125}\text{I}$  activity following administration of 5mg of  $^{125}\text{I}$ -CA to rats by IV, IP and SC injection .



Each point was determined from one rat. Eight rats were injected in each group.

Figure: 3.6.2

Urine Excretion of  $^{125}\text{I}$  activity following administration of 5mg of  $^{125}\text{I}$ -CA to male wistar rats by IV, IP and SC routes.



Each point is a mean  $\pm$  S.E.M. (n=3).

**Table 3.6 The Pharmacokinetic parameters calculated for  $^{125}\text{I}$ -CA injected by IV, IP and SC routes.**

	IV (alpha)	IV (beta)	IP (beta)	SC (beta)
Time Span (hr)	1-21	24-97.5	24-97.5	27-97.5
R <sup>2</sup>	0.9189	0.9238	0.8955	0.8099
m* (hr <sup>-1</sup> )	-0.0747±0.006	-0.0108±0.0009	-0.0105±0.001	-0.0094±0.001
c* (log Co)	-0.167±0.075	-0.379±0.059	-0.488±0.058	-0.644±0.087
n <sup>#</sup>	14	12	14	12
Kel (hr <sup>-1</sup> )	0.172	0.025	0.024	0.022
t <sup>1/2</sup> (hr)	4.03	27.7	28.7	32.1
Vd (ml)	147	240	307	440
Cl (ml/hr)	25.3	5.99	7.43	9.51

Notes: \* Slope and Constant are quoted ± Standard Error.

# n= number of points used in calculation.

The pharmacokinetic parameters calculated for IV and IP dosed rats were very similar over the beta phase. Like LA, rats dosed with  $^{125}\text{I}$ -CA by SC injection were found to have larger volumes of distribution than the other routes of administration and longer elimination half-lives. The distribution half-life calculated for IV dosed rats was longer than that calculated for LA. This may be due to a size selective restriction for transport from the blood stream, although the volumes of the central and tissue compartments were approximately the same.

Tables A3.6.2 and A3.6.3 list the percentage of  $^{125}\text{I}$  activity excreted in the urine and faeces of rats dosed with  $^{125}\text{I}$ -CA. Figure 3.6.2 is a plot of the percent  $^{125}\text{I}$  excreted in the urine versus time, for each of the routes. Between 29 and 46% of the  $^{125}\text{I}$  activity injected was excreted over 72 hours. This was less than for the LA dosed rats. A

Student's t-test was used to compare the % excretion of  $^{125}\text{I}$ -LA at 72 hours (over all routes) with excretion of  $^{125}\text{I}$ -CA at 72 hours. The t-value was calculated to be 4.068. This value has a probability of less than 0.001 with 16 degrees of freedom and thus the excretion of  $^{125}\text{I}$ -CA is highly significantly different from  $^{125}\text{I}$ -LA. Faeces excretion accounted for between 7 and 11 % of the  $^{125}\text{I}$  dose over 96 hours.

The organ distribution of  $^{125}\text{I}$  activity was determined 24 hours after IV and SC injection of  $^{125}\text{I}$ -CA. The calculated data is listed in table A3.6.4. Figure 3.6.3 compares the organ distribution of IV and SC dosed rats. The results are expressed as a ratio of the activity in the whole organ divided by the activity in 1ml of blood. There was little difference between the 2 routes. No organ seemed to selectively accumulate the  $^{125}\text{I}$ -CA. The slightly higher levels found in the gut may indicate that some of the protein had been broken down in the liver with release of  $^{125}\text{I}$  in to the bile. P. Goddard et al<sup>(140)</sup> measured the organ distribution of a copolymer of N-acylethylenimine (molecular weight 29,300 which is similar to CA) and they found that like CA, there was no accumulation in the organs investigated.

#### **3.4.4 Chicken Egg Albumin (CEA).**

Chicken egg albumin was obtained from Sigma and it was already labelled with a  $^{14}\text{C}$ -methyl group. CEA has a molecular weight of 45kD and was used as part of the range of proteins with increasing molecular weights.

The plasma concentrations determined following IV injection of  $^{14}\text{C}$ -CEA are shown in table A3.7.1. A graph of plasma concentration versus time is shown in figure 3.7.1. The plasma levels of  $^{14}\text{C}$  activity fell rapidly following IV injection. Over 24 hours two phases were seen. Although only 2 time points were used during the elimination phase, pharmacokinetic parameters were still calculated. Table 3.7 lists the pharmacokinetic parameters calculated for  $^{14}\text{C}$ -CEA after IV injection in rats.

Figure 3.6.3  
Organ Distribution of  $^{125}\text{I}$  activity, 24 hours after administration  
of 5mg of  $^{125}\text{I}$ -CA to rats by IV and SC routes.

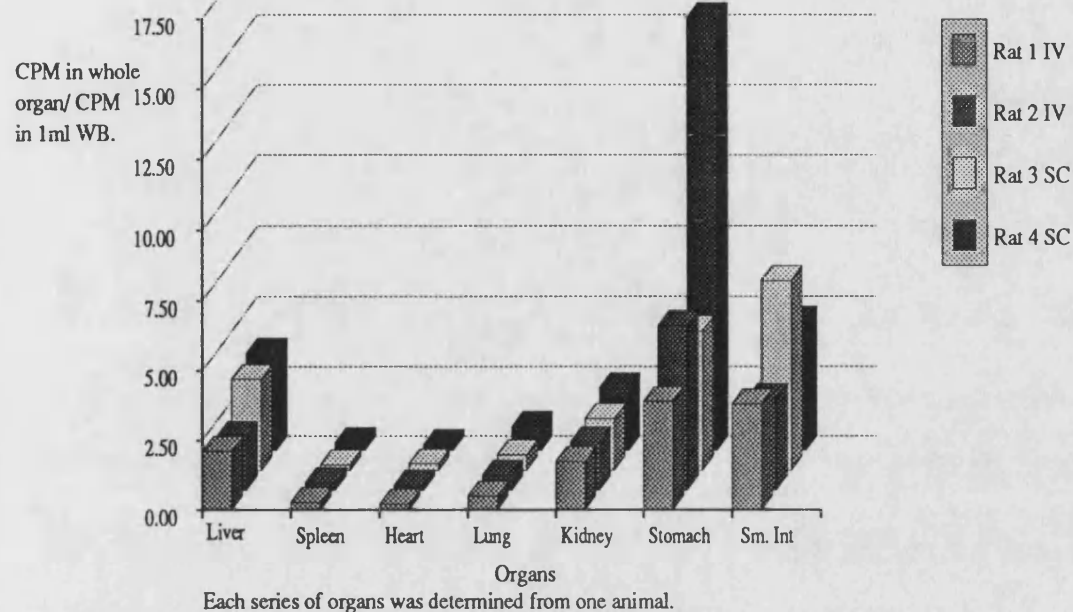
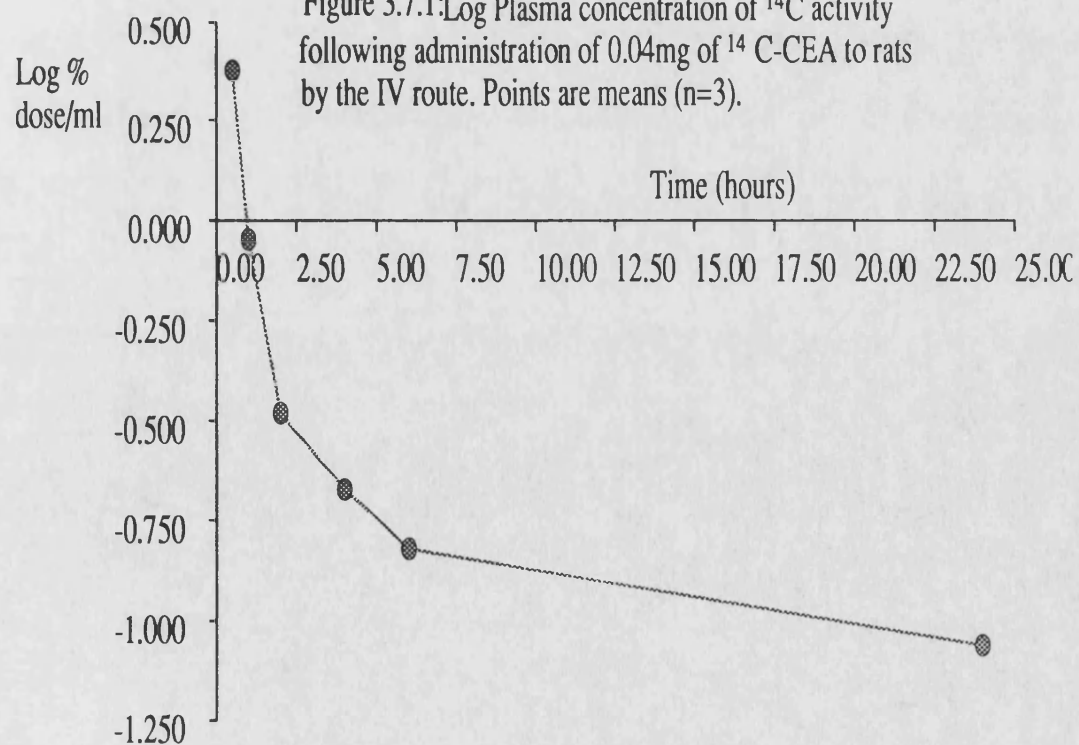


Figure 3.7.1: Log Plasma concentration of  $^{14}\text{C}$  activity  
following administration of 0.04mg of  $^{14}\text{C}$ -CEA to rats  
by the IV route. Points are means (n=3).



**Table 3.7: The Pharmacokinetic parameters calculated following IV administration of  $^{14}\text{C}$ -CEA to rats.**

	Alpha phase	Beta phase
Time span	0.5-6 hours	6-24 hours
R <sup>2</sup>	0.9400	0.6527
m* (hr <sup>-1</sup> )	-0.356±0.0519	-0.0135±0.0049
c* (Log Co)	0.266±0.176	-0.790±0.0859
n <sup>#</sup>	15	6
Kel (hr <sup>-1</sup> )	0.820	0.0311
t <sub>1/2</sub> (hr)	0.845	22.3
Vd (ml)	54.2	616.9
Cl(ml/hr)	44.4	19.2

Notes: \* Slopes and constants are quoted ± Standard Error.

# n= number of points used in each calculation.

The half-life for the alpha phase was very rapid at 50 minutes. The Vd for the alpha phase was smaller than for the other proteins administered. CEA has a molecular weight of 45,000 and its access out of the blood stream appeared to be restricted compared to LA and CA. The elimination half life was very similar to that calculated for LA. CEA had a larger Vd for the tissue compartment than CA and LA. This may be the result of increased cellular uptake. Organ distribution for this protein was not determined however, thus the reason for the larger Vd cannot be established.

Table A3.7.2 lists the urine excretion of  $^{14}\text{C}$  activity following administration of  $^{14}\text{C}$ -CEA. The urine excretion of  $^{14}\text{C}$  activity was extremely low with less than 4% being excreted in 144 hours. This is the reverse of what was expected because of the

rapid loss of activity from plasma. CEA has a molecular weight which is just small enough to be excreted unchanged by the kidney.<sup>(56)</sup> The low excretion of  $^{14}\text{C}$  activity may be because the amino acid that had been labelled with  $^{14}\text{C}$ -methyl in the CEA had been reutilised following the breakdown of the protein.

### 3.4.5 BSA

BSA has a molecular weight of 66296D. Again it was administered to rats as one of the series of proteins with a range of molecular weights, to investigate the effects of molecular weight on pharmacokinetics and rate of transfer from SC and IP sites. In section 3.5, experiments which investigate the possibility of BSA causing an immune response in the rat are described.

$^{125}\text{I}$ -BSA was administered to rats by each of the three routes. The results obtained for the serum concentration of  $^{125}\text{I}$  activity are listed in table A3.8.1 Figure 3.8.1 is a plot of Log % of  $^{125}\text{I}$  dose remaining per ml of serum versus time. Following IV administration the plasma clearance followed a biexponential model. The two phases were explained by distribution and elimination, as for LA. Absorption from the IP injection site occurred more slowly than it did for LA and CA, with peak plasma levels occurring 6 hours after administration. Absorption from the SC injection site was slower, with peak plasma levels occurring between 11 and 22.5 hours after injection. The major factor for the slower rate of absorption of BSA, compared to LA and CA, is probably its relatively large molecular weight. BSA with a molecular weight of 66296 could not be absorbed directly into the blood stream following SC and IP administration. Instead it would have been taken up by the lymph and from there it would have been transferred to the blood stream.

Pharmacokinetic parameters were calculated using the linear section of Figure 3.8.1. In addition parameters were calculated for the alpha phase following IV administration. These parameters are listed in Table 3.8.

Figure 3.8.1:

Serum concentration of  $^{125}\text{I}$  activity following administration of 5mg of  $^{125}\text{I}$ -BSA to rats by IV, IP and SC routes.

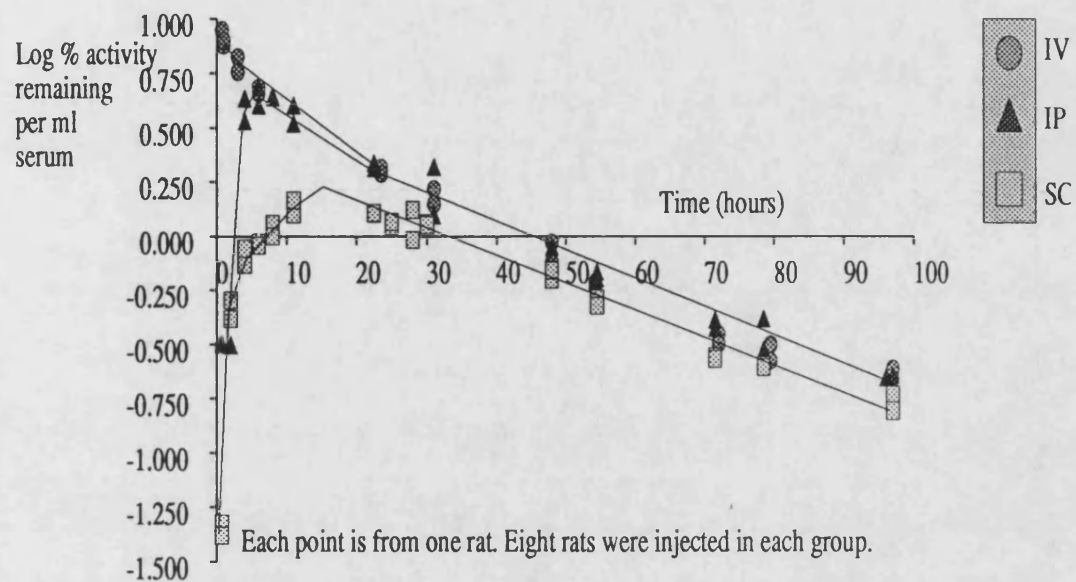
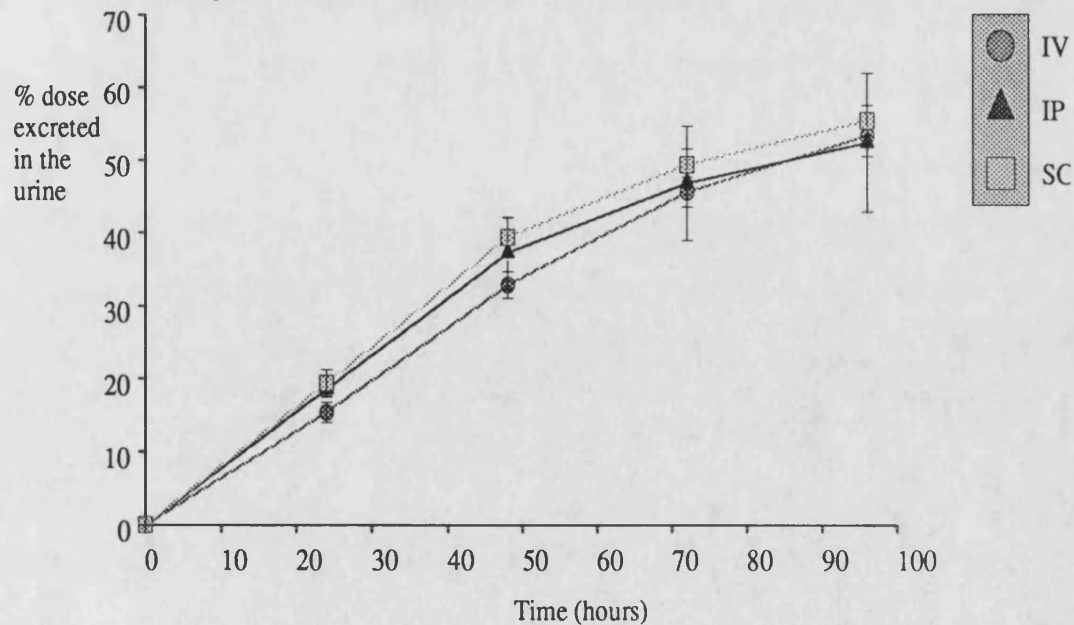


Figure 3.8.2:

Percent of  $^{125}\text{I}$  activity excreted in the urine following administration of 5mg of  $^{125}\text{I}$ -BSA to rats by IV, IP and SC routes.

Each point is mean  $\pm$  S.E.M. (N=3).



**Table 3.8 The Calculated Pharmacokinetic Parameters for <sup>125</sup>I-BSA.**

	IV (alpha)	IV (beta)	IP (beta)	SC (beta)
Time span	0.75-6hr	23.5-97hr	22.5-97hr	22.5-97hr
R <sup>2</sup>	0.9190	0.9621	0.9638	0.9818
m* (hr <sup>-1</sup> )	-0.0894±0.012	-0.0135±0.0008	-0.0137±0.0007	-0.0125±0.0004
c* (Log Co)	0.723±0.043	0.575±0.0488	0.587±0.0481	0.392±0.024
n <sup>#</sup>	7	14	15	18
Kel (hr <sup>-1</sup> )	0.205	0.0311	0.0316	0.0288
t <sup>1/2</sup> (hr)	3.366	22.29	21.96	24.07
Vd (ml)	18.92	26.61	25.88	40.55
Cl (ml/hr)	3.88	0.827	0.817	1.168

Notes: \* Slopes and constants are quoted ± Standard Error.

# n= number of points used in the calculation.

The pharmacokinetic parameters calculated for the elimination phase for each of the routes of administration were very similar. <sup>125</sup>I-BSA had a very small volume of distribution and thus its access into extra-vascular sites appeared to be restricted. The calculated volume of distribution was approximately one tenth of CA and LA. The half-life of elimination correlated with the reported results that 50-60% of endogenous rat albumin is catabolised daily.<sup>(141)</sup> The alpha phase half-life was similar to the one determined by Flessner,<sup>(142)</sup> of 188 minutes, in anaesthetised female Sprague Dawley rats.

Tables A3.8.2 and A3.8.3 list the percentage of radioactivity excreted in the urine and faeces of rats dosed with <sup>125</sup>I-BSA. The percentage excreted in the faeces is roughly equal for each route of administration at approximately 7% of the total dose in 96



hours. Figure 3.8.2 is a plot of %  $^{125}\text{I}$  excreted in the urine versus time. The urine excretion of  $^{125}\text{I}$  activity was between 15 and 19% in 24 hours. The urine excretion for all 3 routes of administration for BSA was compared to the urine excretion of CA (across all routes) at 24 hours and was significant using Student's t-test (probability of between 0.05 and 0.02). Thus there was a significant difference between BSA and CA excretion at 24 hours. This is because CA, with a molecular weight of 29kD, is probably small enough to be excreted unchanged by the kidney.

The organ distribution of  $^{125}\text{I}$  activity was determined at 25 hours and 97 hours for IV and SC dosed rats and at 97 hours for IP dosed rats. Figure 3.8.3 compares the organ distribution determined for IV and SC dosed rats at 25 hours. The results in this figure are expressed as a ratio of activity found in the whole organ divided by activity in 1ml of whole blood.  $^{125}\text{I}$  did not appear to accumulate in any organ apart from the thyroid gland (actual percentage in the thyroid was  $4.95 \pm 1.13\%$  for 4 rats). This indicates that some of the protein had been broken down, with the release of unconjugated  $^{125}\text{I}$ . The levels found in the gut were slightly higher than in the other organs. This was probably due to biliary secretion. These results are similar to the organ distribution described by Takakura et al for iodinated albumin in mice.<sup>(76)</sup> There appeared to be no difference between the distribution in IV and SC dosed rats. At 97 hours the ratios calculated were similar to those of 25 hours.

#### **3.4.6 Human Serum Albumin (HSA).**

$^{125}\text{I}$ -HSA was obtained in a radio-iodinated form from Amersham. It was used, initially, as a check to ensure that the chloramine T method used to iodinate the BSA at Bath, had not led to damage of the protein. If it had, then following administration of the two proteins, different pharmacokinetics would be seen. Also, the pharmacokinetics were compared to the other proteins administered.

The concentration of  $^{125}\text{I}$ -HSA was determined in whole blood for each of the routes of administration. The results obtained are listed in Table A3.9.1. Figure 3.9 is a plot of Log whole blood concentration versus time for each of the routes. The plot is similar to that obtained for BSA. Following IV administration a biexponential clearance was seen.

Figure 3.8.3:  
Organ Distribution of  $^{125}\text{I}$  activity following administration of  
5mg of  $^{125}\text{I}$ -BSA to rats by IV and SC routes. Analysis was determined  
25 hours post injection from 2 rats for each route.

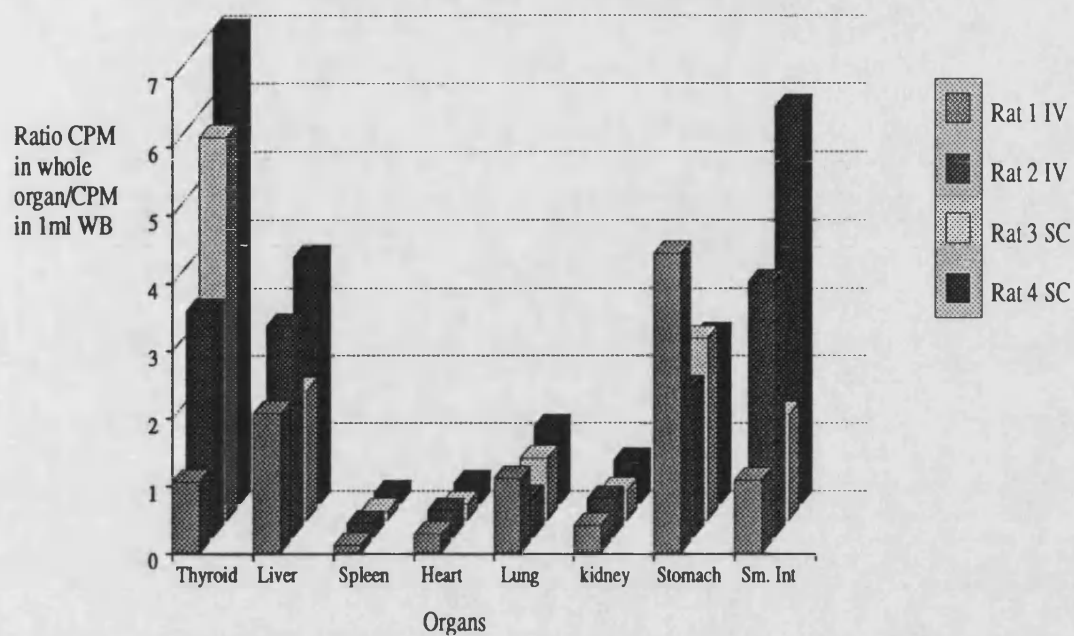
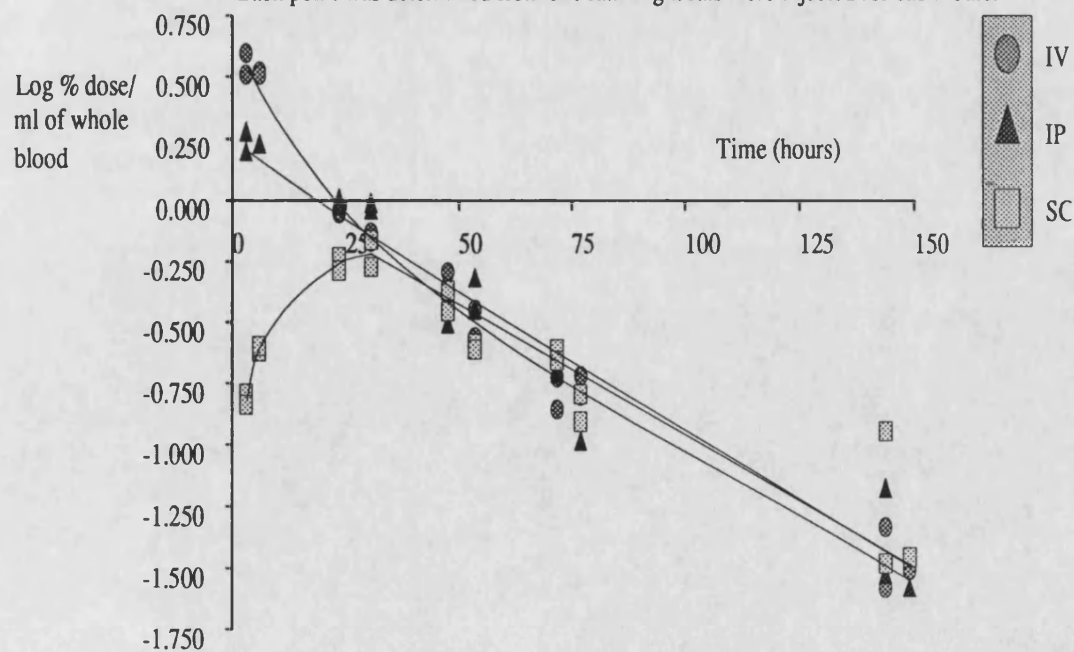


Figure 3.9: Concentration of  $^{125}\text{I}$  activity in whole blood following  
administration of 0.4mg of  $^{125}\text{I}$ -HSA to rats by IV, IP and SC.  
Each point was determined from one rat. Eight rats were injected for each route.



Absorption from IP sites was rapid with peak plasma levels being achieved within 3 hours of administration. Following SC injection peak plasma levels were reached between 23 and 30 hours after administration. Table 3.9 lists the pharmacokinetic parameters calculated for the  $^{125}\text{I}$ -HSA for each of the three routes.

**Table 3.9 Pharmacokinetic Parameters calculated for  $^{125}\text{I}$ -HSA administered to rats by IV, IP and SC injection.**

	IV (alpha)	IV (beta)	IP (beta)	SC (beta)
time span	3-23.5hr	23.5-149	23.5-149hr	30.5-149hr
R <sup>2</sup>	0.9823	0.9682	0.9047	0.9003
m* (hr <sup>-1</sup> )	-0.0659±0.004	-0.0115±0.0006	-0.0118±0.0011	-0.00884±0.00088
c* (Log Co)	0.617±0.062	0.164±0.047	0.178±0.086	-0.038±0.072
n <sup>#</sup>	6	18	18	16
Kel (hr <sup>-1</sup> )	0.152	0.0266	0.0271	0.0204
t <sup>1/2</sup> (hr)	4.57	26.08	25.57	33.97
Vd (ml)	24.15	68.55	66.37	109.2
Cl (ml/hr)	3.67	1.823	1.799	2.228

Notes: \* Slopes and Constants are quoted ± Standard Error.

# n= number of points used in calculation.

The pharmacokinetic parameters calculated for the elimination phase of IV and IP dosed rats were very similar. They were also similar to those calculated for BSA which, assuming that the  $^{125}\text{I}$ -HSA had not been damaged during production at Amersham, suggests that the BSA was not damaged during the chloramine T iodination procedure. The volumes of distribution were larger for the HSA dosed rats than for BSA dosed rats because the parameters had been calculated using whole blood rather than serum data.

### 3.4.7 Rat Serum Albumin (RSA).

RSA was administered, to compare the pharmacokinetics in the rat to those calculated for BSA. Since BSA is a foreign protein in the rat, there is a possibility that it could lead to an immune response following injection. If an immune response was precipitated by BSA then its fate would be different to RSA. In section 3.5 further experiments are described, which would also determine whether BSA was immunogenic in the rat.

RSA was administered to rats at a dose of 5mg by IV, IP and SC routes. In addition it was administered to rats at a dose of 20mg, by IV injection only. Table A3.10.1 lists the serum levels determined for the 5mg dose for each route of administration. Table A3.11.1 lists the serum and whole blood concentrations determined for the 20mg dose of  $^{125}\text{I}$ -RSA. Figure 3.10.1 is a plot of Log  $^{125}\text{I}$  activity remaining in serum versus time for the 5mg dose. The plot is very similar to those obtained for BSA and HSA. Peak serum levels were achieved approximately 4 hours after IP administration and between 7 and 19 hours of SC injection. Following the absorption phase, the serum levels of IP and SC dosed rats closely mirrored the serum levels of IV dosed rats. Pharmacokinetic parameters were calculated for each of the routes of administration for the 5mg dose. They are listed in table 3.10.1.

**Table 3.10.1 The Pharmacokinetic parameters calculated for rats dosed with 5mg of  $^{125}\text{I}$ -RSA by IV, IP and SC injection.**

	IV (alpha)	IV (beta)	IP (beta)	SC (beta)
time span (hr)	0.25-7.25	18.75-97	18.75-97	30-97
R <sup>2</sup>	0.9130	0.9628	0.9297	0.8601
m*	-0.0957±0.0104	-0.0078±0.0004	-0.0074±0.0005	-0.008±0.0009
c*	0.818±0.0401	0.446±0.0223	0.451±0.031	0.437±0.059
n <sup>#</sup>	10	20	19	20
Kel (hr <sup>-1</sup> )	0.220	0.0180	0.0170	0.0186
t <sup>1/2</sup> (hr)	3.144	38.38	40.66	37.26
Vd (ml)	15.20	35.81	35.40	36.56
Cl (ml/hr)	3.34	0.644	0.602	0.680

Notes for table 3.10.1: \* Slopes and Constants are quoted  $\pm$  Standard Error. # n= number of points used in each calculation.

The pharmacokinetic parameters calculated for the elimination phase for each route of administration were very similar. The elimination half-life calculated for RSA was longer than for BSA. These results are consistent with those determined by Matsumura and Maeda.<sup>(143)</sup> They found that mouse serum albumin had a slightly longer half-life than BSA when injected into the mouse but that both proteins had a similar pattern for organ distribution.

Figure 3.10.2 is a plot of Log %  $^{125}\text{I}$  remaining per ml of serum against time for the 5 and 20mg dose of  $^{125}\text{I}$ -RSA administered by IV injection. The % dose remaining/ml for the 5mg dose appeared to be lower than the 20mg dose. The pharmacokinetic parameters were calculated for both whole blood and serum data for the 20mg dose. They are listed in table 3.10.2.

**Table 3.10.2 Pharmacokinetic Parameters for the 20mg dose of  $^{125}\text{I}$ -RSA.**

	Whole Blood		Serum	
	IV (alpha)	IV (beta)	IV (alpha)	IV (beta)
Times span	0.25-6.75	23.5-168	0.25-6.75	23.5-168
R <sup>2</sup>	0.8975	0.9626	0.9303	0.9838
m* (hr <sup>-1</sup> )	-0.066 $\pm$ 0.009	-0.0065 $\pm$ 0.0004	-0.068 $\pm$ 0.0078	-0.0063 $\pm$ 0.0003
c* (Log Co)	0.60990.0367	0.428 $\pm$ 0.0356	0.930 $\pm$ 0.031	0.679 $\pm$ 0.0226
n <sup>#</sup>	8	12	8	12
Kel(hr <sup>-1</sup> )	0.151	0.0149	0.157	0.0145
t <sup>1/2</sup> (hr)	4.587	46.51	4.425	47.69
Vd (ml)	24.60	37.32	8.511	20.94
Cl (ml/hr)	3.715	0.556	1.336	0.304

Notes: \* Slopes and Constants are quoted  $\pm$  Standard Error.# n= number of points used in the calculation.

Figure 3.10.1:

Log %<sup>125</sup>I remaining/ml of serum following administration of 5mg of <sup>125</sup>I-RSA by IV, IP and SC routes.

Each point is from one rat. n=8 for each route.

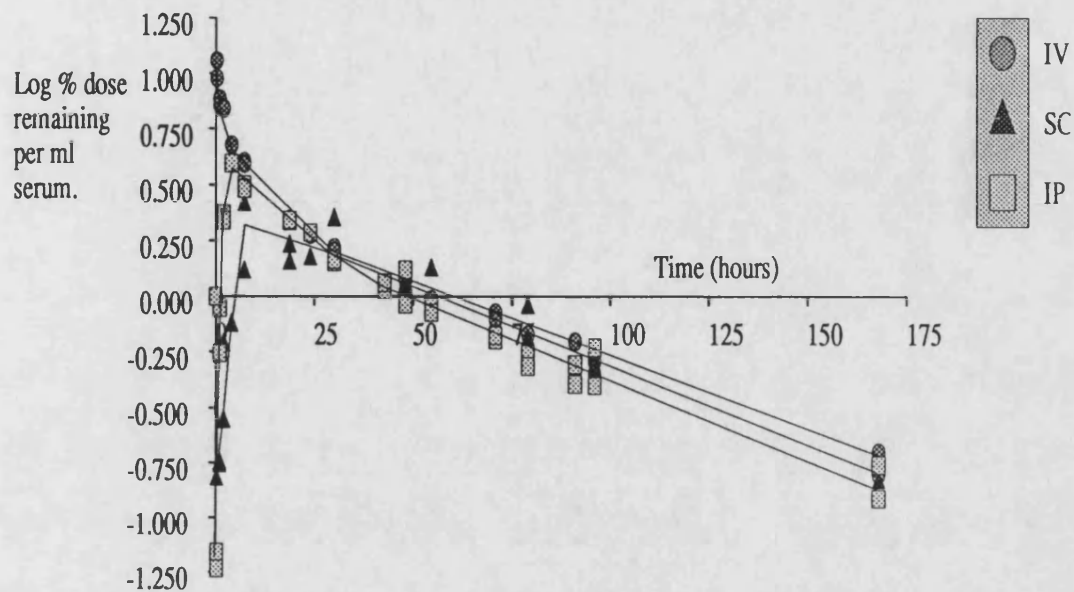
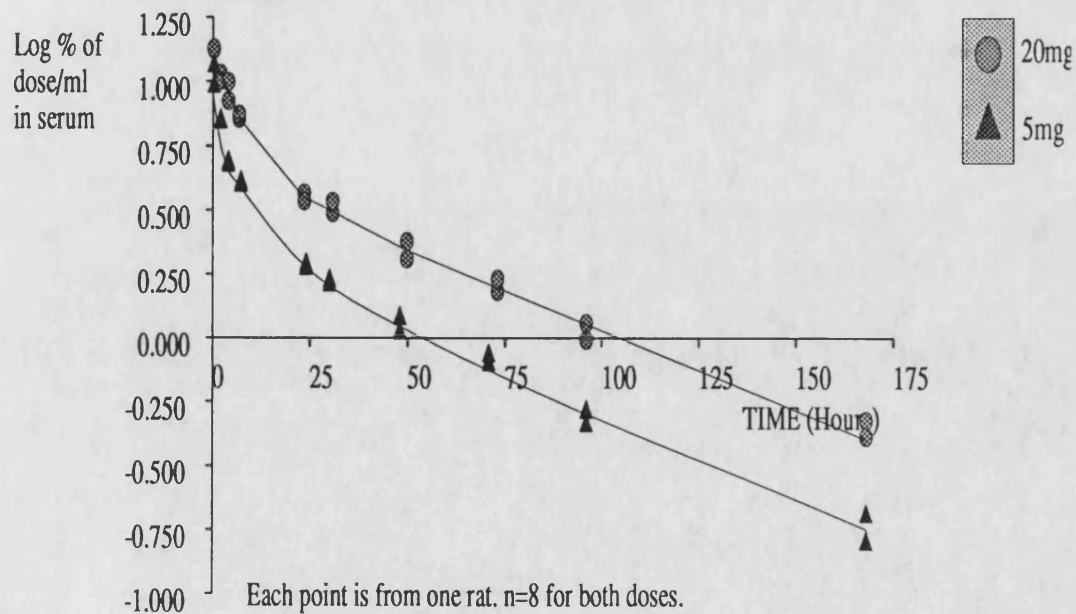


Figure 3.10.2:

The Serum concentrations (Log % of <sup>125</sup>I remaining/ml) following administration of a total dose of 5mg or 20mg of <sup>125</sup>I-RSA by the IV route.



Each point is from one rat. n=8 for both doses.

The pharmacokinetic parameters calculated using whole blood data and serum data were very similar, indicating that the RSA did not accumulate in the cellular component of blood. Volumes of distribution calculated using whole blood data were double those calculated using serum data. This may be attributed to the haematocrit of the rat. The elimination half life calculated for the 5mg dose of RSA (38.4 hours) was shorter than the 20mg dose (47.7 hours) and the volume of distribution was slightly larger for the 5mg dose. This was explained by the lower serum levels seen during the elimination phase. (see figure 3.10.2) The volume of distribution for the alpha phase following administration of 20mg of RSA and using serum data was found to correspond to the serum volume which has been quoted for male wistar rats<sup>(144)</sup>.

The urine excretion of  $^{125}\text{I}$  activity following administration of 5mg of  $^{125}\text{I}$ -RSA is shown in table A3.10.2. Between 31 and 37% of the  $^{125}\text{I}$  dose was excreted over 96 hours. The percentage excreted was lower than for the other proteins administered. Table A3.11.2 shows the percentage  $^{125}\text{I}$  excreted following administration of a 20mg dose of  $^{125}\text{I}$ -RSA. Figure 3.10.3 compares %  $^{125}\text{I}$  excreted in the urine against time for IV administered RSA at doses of 5mg and 20mg. There was no significant difference in the percentage of  $^{125}\text{I}$  excreted between the two doses administered.

Organ distribution of  $^{125}\text{I}$  activity was determined for the 5mg dose of  $^{125}\text{I}$ -RSA at 96 hours after administration. The results are listed in table A3.10.3. Figure 3.10.4 is a histogram showing the whole organ distribution of  $^{125}\text{I}$  activity 96 hours after IV injection. The thyroid appeared to be the only organ investigated that accumulated  $^{125}\text{I}$  activity. The activity in the other organs could be attributed to that present within the blood of the organ. For the other routes of administration a similar distribution of  $^{125}\text{I}$  was seen.

### **3.4.8 Summary for the protein data.**

It was decided to use an  $^{125}\text{I}$ - label for detection of proteins *in vivo*, for a number of reasons. The first reason was the ease of the labelling procedure, with well established methods for the chloramine T labelling protocol. Secondly both  $^{14}\text{C}$  and  $^3\text{H}$  labels were

Figure 3.10.3:  
Percentage  $^{125}\text{I}$  activity excreted following administration of  
5mg or 20mg of  $^{125}\text{I}$ -RSA to rats.  
Each point is a mean  $\pm$  S.E.M. (n=4 for 5mg, n=3 for 20mg)

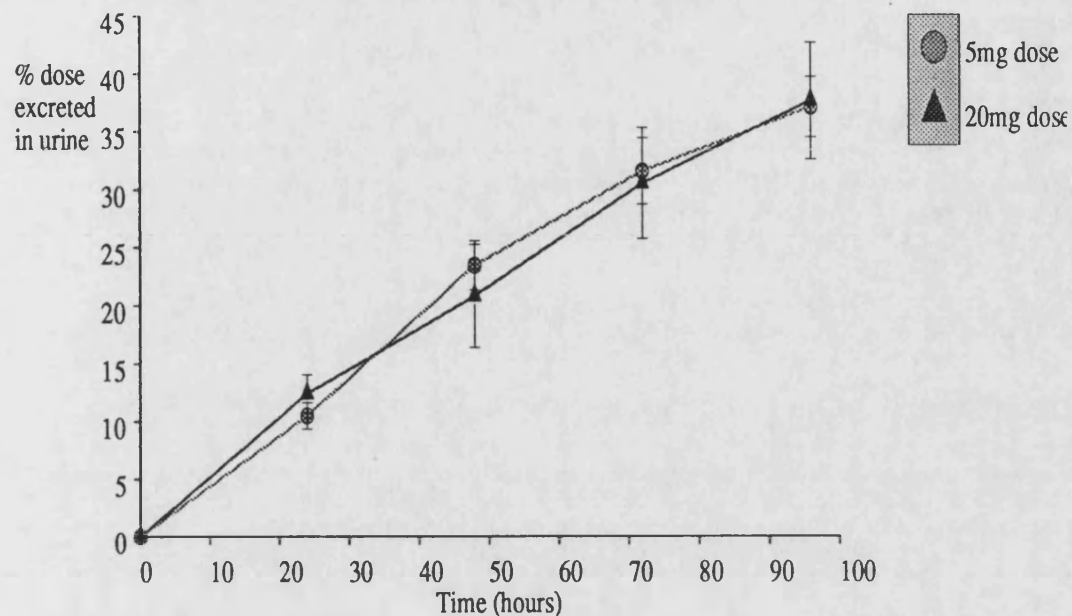
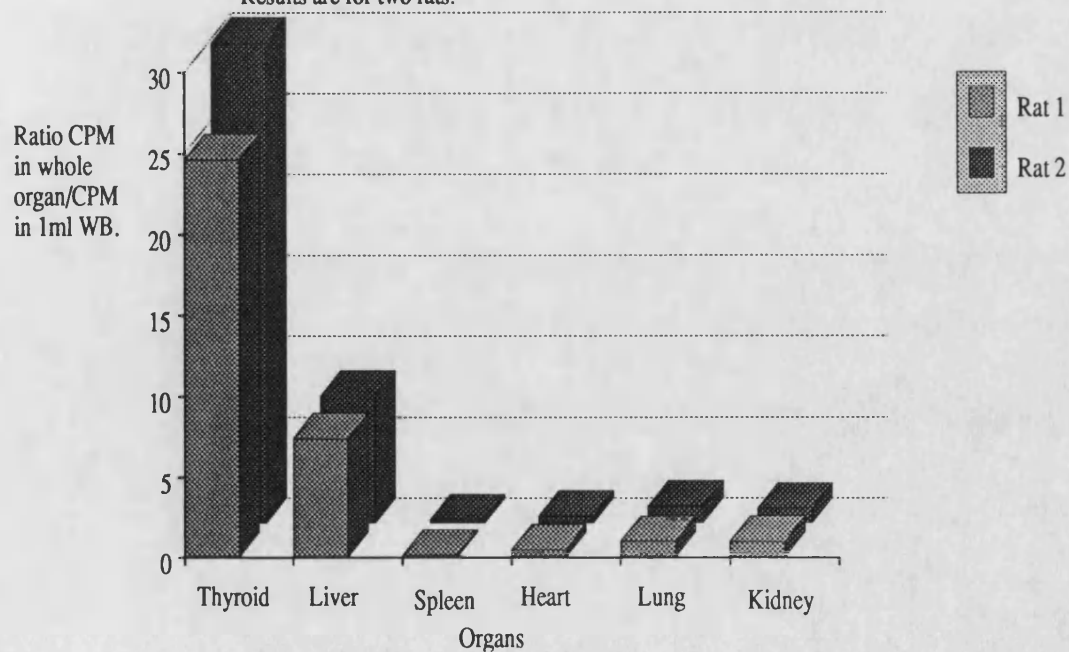


Figure 3.10.4:  
Organ Distribution of  $^{125}\text{I}$  activity 96 hours after administration  
of 5mg of  $^{125}\text{I}$ -RSA by IV injection.  
Results are for two rats.





excreted more slowly by rats than expected for the solute to which they were bound. (see MTX and CEA experiments).

Margen and Tarver<sup>(145)</sup> established guidelines for the ideal tracer molecule. These include, firstly, that the tracer should not alter biological activity of the protein. The tracer should have a high specific activity so that only a small quantity is required. It should be a long-lived isotope so that problems with stability are not encountered. Labelling should be uniform since heavily labelled proteins may behave like a different species. The isotope should not be reincorporated into endogenous proteins after metabolism and it should be rapidly excreted after metabolism.

$^{125}\text{I}$  appeared to fit in with these guidelines. It has a half life of 60 days so no stability problems would be encountered. When it was administered as  $^{125}\text{I}\text{-Na}$ , it was found to have a very rapid initial half-life following IV administration to the rat. During this phase serum levels fell to 0.3% of the injected activity/ml. An organ distribution study showed that the  $^{125}\text{I}$  activity accumulated in the thyroid but not in the liver or kidney. Approximately 46% of the injected dose was excreted in the first 24 hours after injection.

Another advantage of using the  $^{125}\text{I}$  isotope for protein labelling is that organ samples can be analysed directly without any further preparation, whereas both  $^{14}\text{C}$  and  $^3\text{H}$  activities are quenched in biological samples and so a solubilisation and decolourisation step would be required before analysis.

Figure 3.11.1 is a plot of Log serum concentration against time for  $^{125}\text{I}$  labelled RSA, BSA, CA and LA after IV administration. All of these proteins had a biexponential serum clearance. The first phase could be explained by distribution throughout the blood stream and into the rapidly equilibrating (central) compartment. The second phase was explained by distribution into the slowly equilibrating (tissue) compartment and elimination. Table 3.11 summarises the pharmacokinetic data calculated for these proteins after IV injection.

Figure 3.11.1:  
Concentration of  $^{125}\text{I}$  activity in serum following IV administration  
of 5mg of  $^{125}\text{I}$ -labelled protein to rats.  
Each point was obtained from a single rat. (n=8 for each protein).

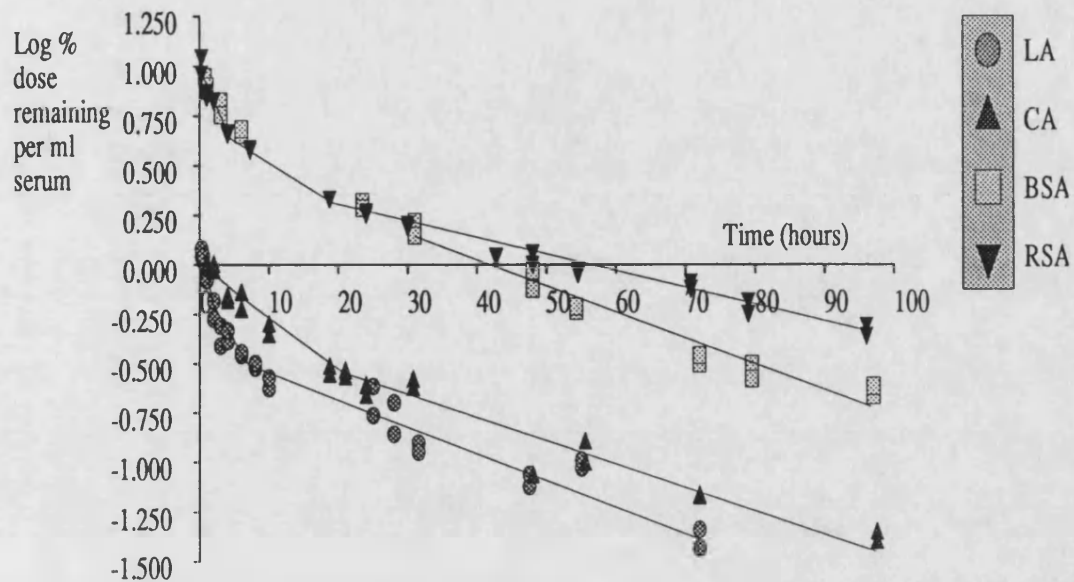
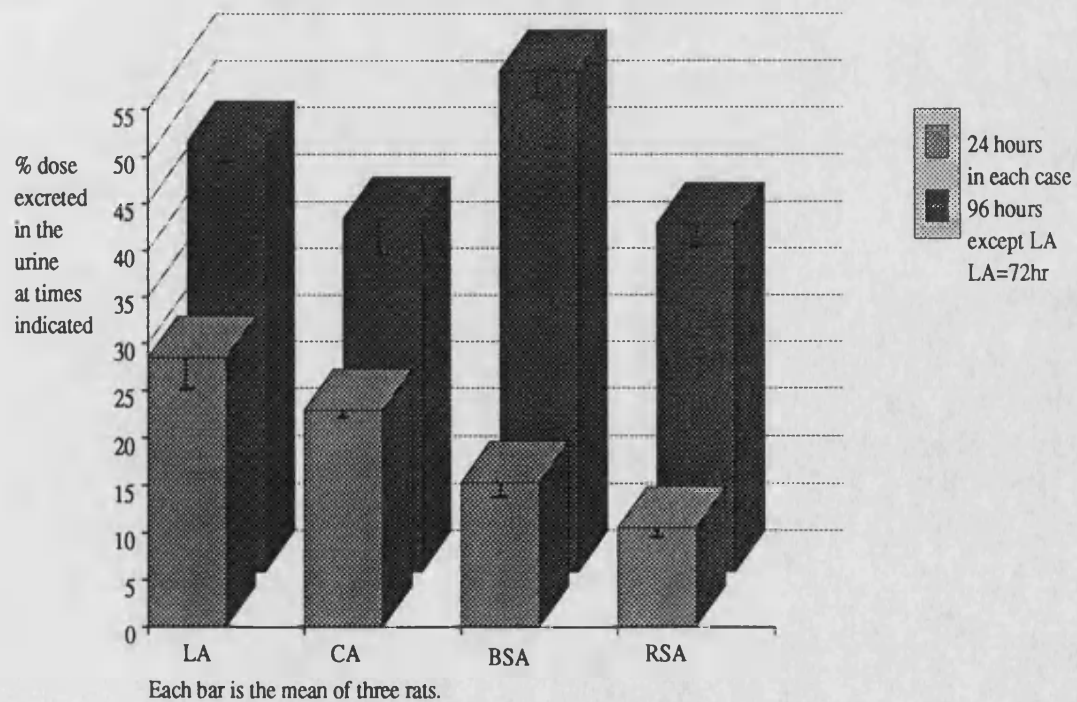


Figure 3.11.2: Percentage of  $^{125}\text{I}$  activity excreted in the urine  
of rats dosed by IV injection with 5mg of  $^{125}\text{I}$  labelled Protein



**Table 3.11 Pharmacokinetic Parameters for 5mg doses of RSA, BSA, CA and LA.**

Protein (mol wt)	(alpha phase)		(beta phase)	
	$t^{1/2}$ (hr)	Vd (ml)	$t^{1/2}$ (hr)	Vd (ml)
RSA (63K)	3.14	15.20	38.38	35.81
BSA (67K)	3.37	18.92	22.29	26.61
CA (29K)	4.03	147.0	27.7	240.0
LA (14K)	0.943	111.0	21.60	236.0

HSA and CEA were not included in this table because they were not administered at a dose of 5mg per rat and thus direct comparison was not valid. RSA and BSA appeared to be very similar over the alpha phase. CA and LA had similar alpha phase Vd (147ml for CA and 111ml for LA) which were approximately five times those of BSA and RSA (15.2 and 18.9 ml respectively). LA had an extremely rapid distribution half-life (56.6 minutes), indicating that it could easily extravasate. Seymour et al<sup>(56)</sup> injected an HPMA co-polymer with a molecular weight of 12000 and found that it had a distribution half-life of only 3 minutes. The copolymer injected with a molecular weight of 40000 had a half life of 72 minutes and this is closer to the value determined for LA. The reason for the rapid clearance of the HPMA copolymer was due to urinary excretion. LA was not excreted to the same extent as the polymer and therefore it is possible that LA was reabsorbed in the kidney tubule.

RSA gave the longest elimination half-life (38.4 hours). The other proteins were of bovine origin and therefore may be metabolised more quickly. (See section 3.5). LA had the shortest elimination half-life (21.6 hours), although this was longer than anticipated because it is small enough to be excreted unchanged by the kidney.

There appeared to be a size selective rate of transfer of proteins from SC and IP sites. For LA and CA peak plasma levels were achieved within 1 hour of administration after both routes of injection (see figures 3.5.1 and 3.6.1) and thus it would appear that these

proteins were absorbed directly into the blood stream from the injection sites. On the other hand, for RSA and BSA, peak plasma levels did not occur until 4 hours after IP administration, and between 10 and 20 hours after SC injection. This would suggest that these proteins are mainly absorbed into the lymph from the injection site and then are transferred into the blood stream. Supersaxo et al<sup>(146)</sup> demonstrated a size selective accumulation of proteins in the lymph of sheep, following SC administration. They believed that proteins of molecular weight above 16kD were absorbed mainly by the lymphatics from this site. In this experiment, it appeared that CA, of molecular weight 29000, was absorbed directly into the blood stream since peak plasma levels were achieved within 1 hour of administration. However the larger proteins did appear to undergo lymphatic absorption from both IP and SC sites. The rapid appearance of CA in the blood stream could also be due to a rapid uptake by the lymphatics, followed by a fast transfer from the lymphatic ducts into the blood vasculature.

Absorption from IP sites occurred more rapidly than SC absorption because there is a larger surface area from which absorption can occur in the peritoneal cavity than at the SC site of injection. The rates of transfer from IP and SC sites are consistent with the results obtained by Seymour et al.<sup>(56)</sup> They found with their HPMA copolymers that peak plasma levels were achieved approximately 4 hours after IP administration and 24 hours after SC injection.

LA and CA had large volumes of distribution for both the alpha (111 and 147 ml) and beta phases (236 and 240 ml) and thus appeared to be widely distributed throughout the body. RSA and BSA had much smaller volumes of distribution during both phases (35.8 and 26.6 ml for the beta phase) suggesting that they are mainly confined to the vasculature, probably due to their higher molecular weight.

Of the proteins investigated, LA showed the greatest rate of excretion in the urine and CA was excreted more rapidly than BSA and RSA. This is because both LA and CA have a molecular weight low enough to be excreted unchanged in the urine. Figure 3.11.2 is a histogram comparing the urine excretion of each of the proteins at 24 hours after injection and at 96 hours after injection.

Organ distribution was determined for each of the proteins. There was no significant accumulation of  $^{125}\text{I}$  activity in any organ investigated (apart from the thyroid) for any of the proteins.

### **3.5 Feasibility of using BSA as a Drug-Carrier in the Rat.**

In Chapter 4 a series of experiments, using BSA as a model carrier for MTX, to evaluate the effects of the protein on the pharmacokinetics of the free drug are described. Before these experiments were performed, it seemed prudent to first investigate the suitability of using BSA as a carrier in the rat. The elimination half-life after IV injection for  $^{125}\text{I}$ -BSA was found to be shorter than that of  $^{125}\text{I}$ -RSA, at 22.3 hours for BSA and 38.4 hours for RSA, although the volumes of distribution were similar. Several factors could contribute to the more rapid plasma clearance of BSA.

1. Injection of a foreign protein into male wistar rats may lead to an inflammatory reaction with increased vascular permeability and excessive leakage of proteins out of the blood compartment into the tissues. Endogenous proteins as well as foreign proteins would be affected by this.
2. It has been documented that injection of extra albumin may lead to an increase in the rate of protein catabolism until the levels return to normal.<sup>(147)</sup>
3. The BSA may have been recognised by the rat as a foreign protein and removed from the bloodstream by normal defence mechanisms without actually causing an inflammatory response. This would not affect endogenous protein levels.

Three experiments were carried out in order to verify whether bovine proteins were suitable candidates as drug carriers in the rat. The first involved the administration of increasing doses of BSA to the rat followed by an analysis of the total protein concentration of rat serum at timed intervals. If injection of BSA had led to an increase in the rate of protein catabolism until protein levels were adjusted to normal then this could be identified using this technique. The maximum dose of BSA that was injected was 80mg and this would represent an increase in serum protein concentration of

approximately 12.5%. In addition, if injection of BSA had led to an increase in vascular permeability resulting in protein leakage, this could also be detected using the above method.

The second experiment involved the administration of Evan's Blue, a dye which is highly plasma protein bound. Under normal circumstances, Evan's Blue is lost only slowly from the vasculature, at the same rate as the leakage of plasma proteins. However, during the inflammatory response, post-capillary venules become leaky,<sup>(19)</sup> allowing the escape of plasma proteins along with any dye which may be bound to them. The plasma elimination half-life of injected Evan's Blue was compared to that of the dye injected with a 20mg dose of BSA. This would determine whether injection of BSA had led to an inflammatory response.

The final experiment determined whether male wistar rats under normal circumstances had an antibody against BSA. This utilised a blot test. BSA was pipetted onto a nitrocellulose sheet, incubated with rat serum, washed, and then incubated with an antibody raised against rat immunoglobulin G (IgG) linked to peroxidase. If there was an anti-BSA IgG present in rat plasma then a dark spot would appear on the nitrocellulose sheet.

### **3.5.1 Administration of BSA.**

Total protein concentration was determined for the three groups of rats at 2, 4 and 7 hours. The results obtained are listed in table A3.12.1. Figure 3.12 is a graph of serum protein concentration against time for the three groups. This plot also shows the normal range of protein concentration determined using 10 control rats. (Normal range was 68mg/ml to 108mg/ml, mean = 87.2mg/ml and standard deviation was 14.58).

A Student's t-test was used to compare the serum protein concentrations for each group of rats at each time point. The t values and probabilities obtained are listed in Table 3.12.

**Table 3.12 The t-values determined by comparing the untreated rat group with the BSA and Saline treated group.**

Time (hr)		BSA vs Untreated	Saline vs Untreated	BSA vs Saline
2	t	0.6	1.47	1.65
	P	0.5632	0.1798	0.1382
4	t	1.43	1.40	0.09
	P	0.1900	0.2003	0.9295
7	t	1.72	1.32	0.44
	P	0.1234	0.2231	0.6685

All t values were non-significant. Thus administration of 20mg of BSA does not alter the total serum protein concentration in male wistar rats. The experiment was repeated using 40 and 80mg doses of BSA with similar results.

### 3.5.2 Evan's Blue.

The serum concentrations determined in rats injected with 1mg of Evan's Blue (group 1) or 1mg of Evan's Blue plus 20mg of BSA (group 2) are shown in table A3.13.1. The serum concentrations versus time are shown in Figure 3.13. The serum concentrations determined for the 2 groups were very similar. The plasma clearance data was biexponential in both cases and pharmacokinetic data were calculated for both phases. These data are listed in Table 3.13.

Figure 3.12: Total Serum Protein Concentration versus time for Control Rats (group 1, untreated), Saline treated rats (group 2) and rats treated with 20mg of BSA (group 3). Each point is a mean ( $n=5$ )  $\pm$  S.E.M.

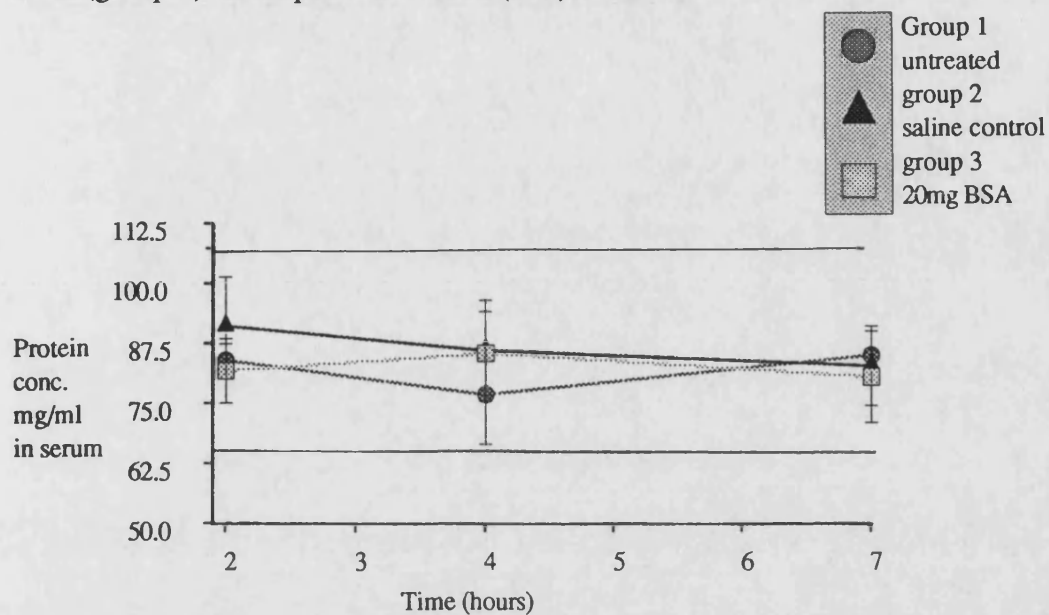
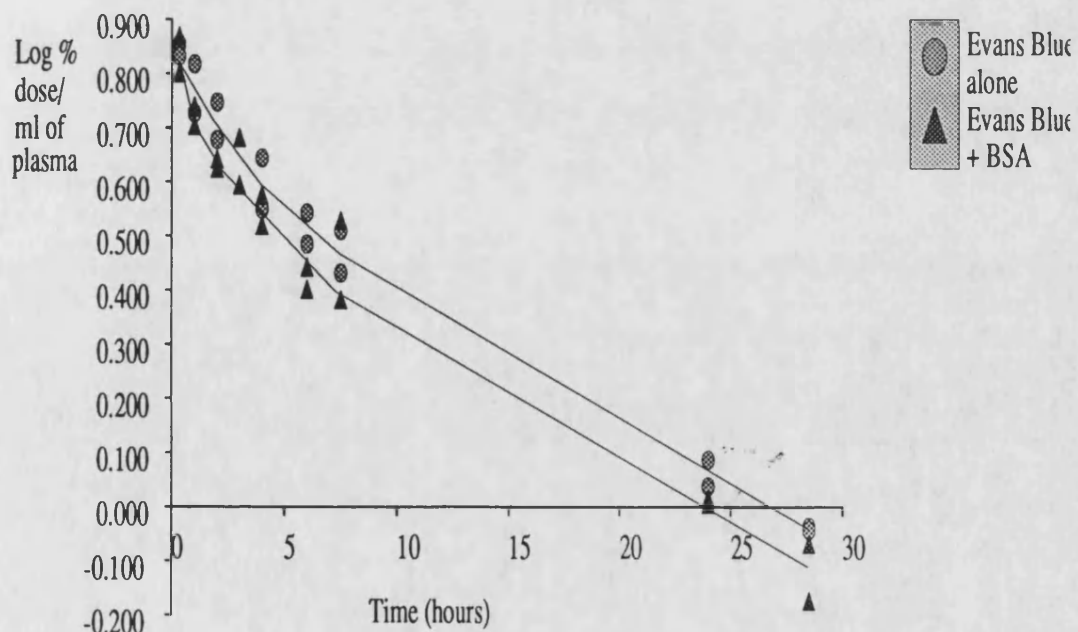


Figure 3.13: Concentration of Evan's Blue in rat plasma following administration of 1mg of dye alone (group 1) or 1mg of dye plus 20mg of BSA (group 2). Each point was determined from one rat.





**Table 3.13: The Pharmacokinetic Parameters Calculated in rats injected with Evans Blue alone and Evans Blue plus 20mg of BSA.**

	EB only	EB + BSA
<u>1. Alpha Phase.</u>		
Time span (hr)	0.33-6	0.33-6
R <sup>2</sup>	0.5727	0.5714
m* (hr <sup>-1</sup> )	-0.137±0.0528	-0.282±0.0924
c*	0.379±0.102	0.281±0.205
n#	10	12
Kel (hr <sup>-1</sup> )	0.316	0.649
t <sup>1/2</sup> (hr)	2.193	1.067
Vd (ml)	41.78	52.36
Cl (ml/hr)	13.20	33.98
<u>2. Beta Phase</u>		
Time span (hr)	7.5-28.5	7.5-28.5
R <sup>2</sup>	0.9854	0.9569
m* (hr <sup>-1</sup> )	-0.0244±0.0015	-0.0273±0.0029
c*	0.653±0.0326	0.654±0.0635
n#	6	6
Kel (hr <sup>-1</sup> )	0.0562	0.0629
t <sup>1/2</sup> (hr)	12.33	11.02
Vd (ml)	22.23	22.18
Cl (ml/hr)	1.249	1.395

Notes: \*Slopes and Constants are quoted ± Standard Error.

# n= number of points used in each calculation.

The parameters calculated for the elimination phase for groups one and two were similar. For the distribution phase the Vd is slightly larger for the Evans Blue plus BSA. This may be due to an error which occurred during the injection of the rats. The injection solution containing BSA was very viscous and some of the solution may have been left in the syringe. In addition, the distribution half life was found to be shorter for the Evans Blue plus BSA group. However, because of the very low regression coefficients for the slopes used in the calculation of the parameters for the distribution phase, a great deal of error has been introduced and so the values calculated could vary within large limits.

To evaluate if injection with BSA increased the plasma clearance of Evan's Blue (this could be the result of an inflammatory response making the vascular bed more permeable to plasma proteins) an analysis of variance comparing the slopes of the Log serum concentration versus time plots for the two groups was performed. A separate analysis of variance was calculated for both the distribution and elimination phases. If the slopes were found to be parallel then this would indicate that the BSA had not increased the loss of Evan's Blue from plasma.

The method used for the analysis of variance, "test for parallelism" was described by Wardlaw. (148) For the distribution phase the log serum concentrations at 20 minutes and 4 hours were used. The method for calculating the F values for this test are described in Appendix 2.2. The F value calculated for parallelism was 1.91 for the distribution phase. The tabulated F value from variance ratio tables is 10.13 for 1 and 3 degrees of freedom at 5% probability. This indicates that there is no deviation from parallelism for the two groups.

For the elimination phase the time points used were 6 hours and 24 hours. The calculated F value for parallelism was 1.29. This again indicates that the two lines were parallel.

For both the distribution and elimination phases the graphs of  $\log_{10}$  serum Evan's Blue concentration versus time for the 2 groups were parallel. Thus a 20mg dose of BSA does not increase the vascular permeability to Evan's Blue.

### **3.4.3 Blot test to determine antigenicity of BSA in rat serum *in vitro*.**

Incubation of BSA with rat serum did not result in a black spot after a further incubation step which included peroxidase linked anti-rat IgG. Thus normal rat serum does not have an antibody to BSA.

The experiments described in this section have established that BSA on a single application does not induce an inflammatory response in the rat. Thus it is a suitable candidate as a soluble macromolecular carrier for anti-cancer drugs.

**CHAPTER 4:**  
**ANALYSIS AND PHARMACOKINETICS OF PROTEIN-MTX CONJUGATES**  
**IN THE RAT.**

In chapter 3 the pharmacokinetics of MTX and the free proteins were determined. In this chapter covalent conjugates between MTX and BSA, RSA or LA were investigated in a similar manner. All calibration curves used in the calculation of values in this chapter are shown in Appendix 1. All tables of data are listed in Appendix 3. These tables have the prefix A. The methods used for calculation of pharmacokinetic data are shown in Appendix 2.

## **4.1 Conjugate Analysis.**

### **4.1.1 FPLC Analysis**

The superose 12 column was calibrated using a series of proteins of known molecular weight immediately prior to analysis of the conjugates (A1.3). Figure 4.1a shows a typical chromatogram obtained for standard BSA (500µg/ml in PBS) on the superose column. BSA had two distinct peaks. The larger peak (93.3% of the total area) with an elution time of 15.5 minutes corresponded to monomeric BSA. The small peak (6.7% of total area) with a retention time of 13.75 minutes was thought to be due to dimers or larger protein aggregates of BSA. Figure 4.1b shows the chromatogram obtained for a typical conjugate. The conjugate chromatogram was very similar to that of 'free' BSA, again there was an initial peak which was thought to be due to protein aggregates. This was slightly larger than for BSA (22.1% of total area). There was also a slight displacement to a quicker elution time indicating that the conjugate had a slightly higher molecular weight. In addition this peak was broader than for BSA. Following injection of the conjugates on to the column, data was captured on an Acorn BBC Master Computer. One thousand points were registered by the computer over a 45 minute period. The computer was programmed to calculate the area occupied by the peaks. The chromatogram was first divided manually into 2 sections, so that the major (monomeric) peak was separated from the preceding peak (see dotted lines on figure 4.1b). A read-out was then obtained for the proportion of conjugate which was present as aggregates and the proportion which was present as single molecules.

Table 4.1. lists the conjugates which were analysed by FPLC. It gives the proportional

Figure 4.1a The Chromatogram obtained for BSA after injection onto the Superose 12 column and detection at 280nm. Flowrate= 0.83ml/minute. Chart Speed= 2mm/minute. Mobile phase = PBS. Concentration = 500 $\mu$ g/ml.

Peak 1 had an elution time of 13 minutes and 45 seconds and peak 2 had an elution time of 15 minutes and 27 seconds.

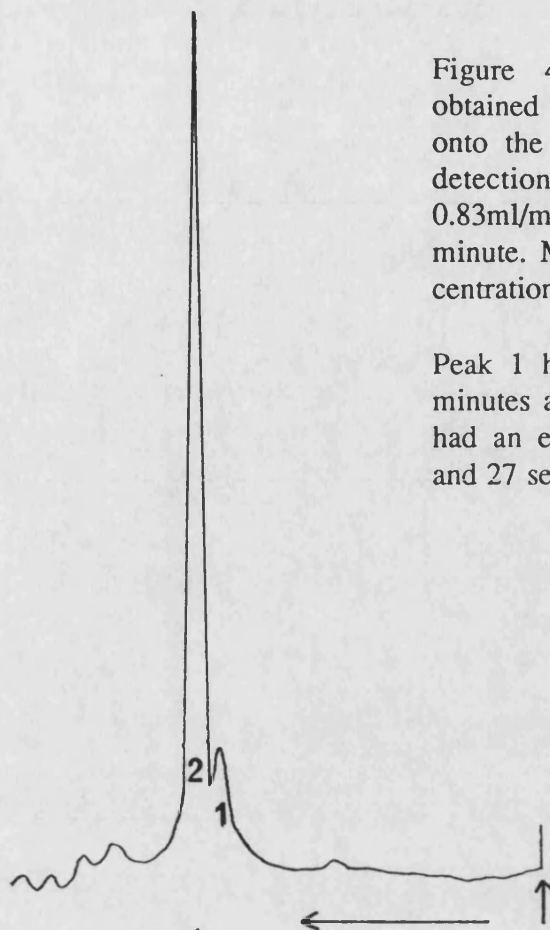
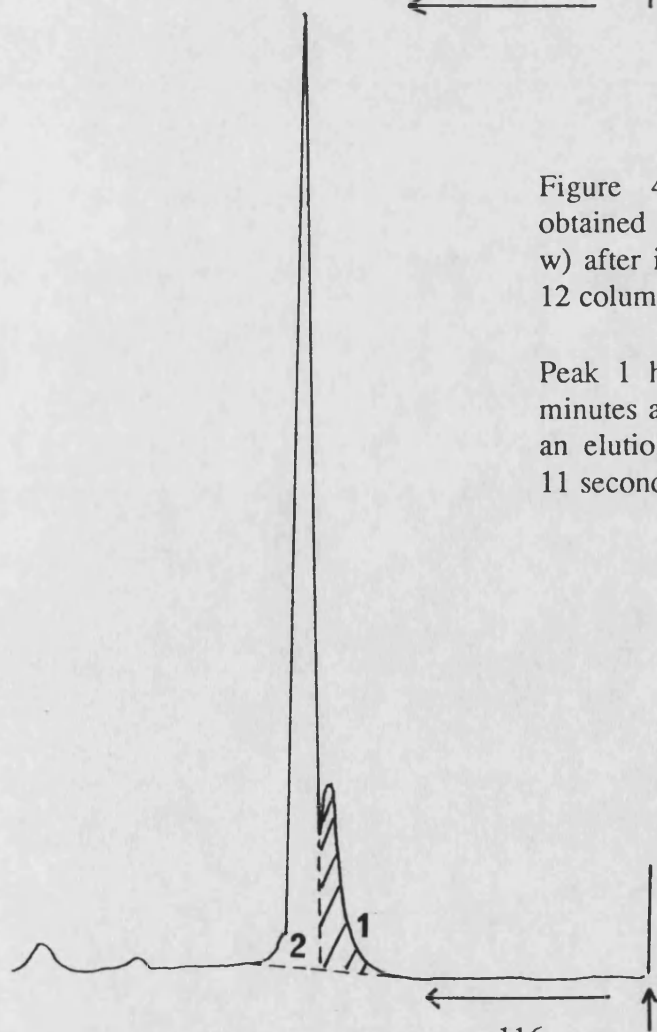


Figure 4.1b The Chromatogram obtained for BSA-MTX (11.76%w/w) after injection onto the Superose 12 column. Conditions as above.

Peak 1 had an elution time of 13 minutes and 34 seconds. Peak 2 had an elution time of 15 minutes and 11 seconds.



area for each of the peaks and the computer calculated weight average molecular weight for each of the fractions.

**Table 4.1. FPLC analysis of the conjugates.**

Conjugate (%w/w)	Peak 1 Area	Wt. Average Mol Wt	Peak 2 Area	Wt.Average Mol Wt.	calculated Mol Wt.
<b>a) BSA and BSA-MTX.</b>					
0 (free BSA)	6.67	140-120K	93.33	67000	66296
4.54	23.09	172K	76.91	71740	69153
9.18	32.32	205K	67.68	72830	72376
11.55	33.03	202K	66.97	74523	74143
11.74	34.65	203K	65.35	74891	74269
11.76	22.08	175K	77.92	73765	74274
13.63	39.04	236K	60.96	76560	75779
13.64	36.36	235K	63.64	77030	75788
<b>b) RSA-MTX.</b>					
6.94	18.40	154K	81.60	67590	67262

The increase in the size of peak 1 (due to aggregated protein) seen in the conjugates could be attributed to the mode of preparation of the conjugate. One of the problems associated with the use of carbodiimide coupling reagents is that they can cause interaction between neighbouring protein molecules, and thus protein aggregates are produced. In every conjugate synthesised there was a peak, determined by FPLC, which could be attributed to protein aggregates. On average it was a protein dimer or trimer that was produced (molecular weight of BSA dimer is 134000D). Although this peak

was also present in 'free' BSA, it represented a much smaller proportion (6.7%) of total protein than it did in the conjugates (18 to 39%). These results are consistent with those reported by Halbert and Florence for their BSA-MTX conjugates.<sup>(149)</sup> They analysed their conjugates, which were prepared by a similar ECDI conjugation procedure, using SDS-PAGE and this technique gave similar profiles for the conjugates as did FPLC. As concentration of MTX in the conjugate was increased there appeared to be an increase in the amount of aggregate present. This was due to the fact that, for the high strength conjugates, there was more ECDI present in the reaction mixture. There is good correlation between the expected molecular weight of each of the conjugates and the computer calculated weight average molecular weight. They were within 3.6% of each other.

After synthesis of the conjugates, free MTX was removed using a gel filtration column which consisted of Sephadex G50. In theory gel filtration could be used to separate the protein aggregates from monomeric conjugates. However Sephadex G50 did not allow separation of the monomeric conjugate molecules from the aggregated protein molecules. They eluted together as one large peak. Although the aggregates could be separated on the Superose 12 column it was not feasible to separate the large quantities of conjugate that were produced in this way. Thus no correction was made for the aggregates in later experiments.

#### **4.1.2 UV scans of the conjugates.**

The UV scans of free MTX, BSA and LA were compared to scans for BSA-MTX and LA-MTX. Figure 4.2a shows the scan obtained for MTX, figure 4.2b shows the scan obtained for LA and figure 4.2c shows the scan obtained for LA-MTX. The scans obtained for BSA and for BSA-MTX were similar to those shown in figures 4.2b and 4.2c respectively. Table 4.2 shows the Lambda max of the MTX, LA, LA-MTX and BSA-MTX.

Figure 4.2a. The UV scan (460nm to 180nm) of MTX (20 $\mu$ g/ml) in 0.1M NaOH.

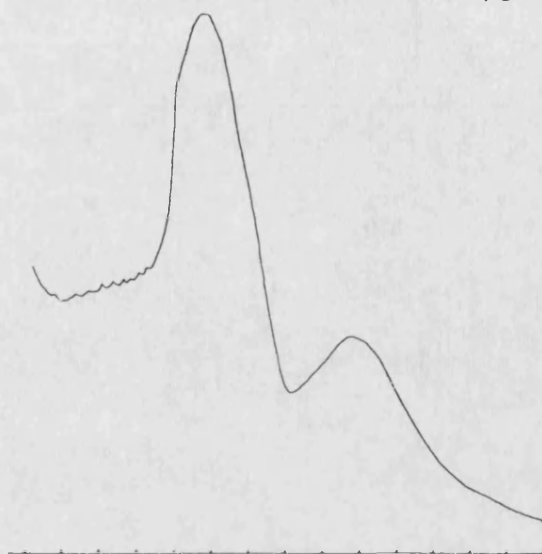


Figure 4.2b. The UV scan (460nm to 180nm) of LA (100 $\mu$ g/ml) in 0.1M NaOH.

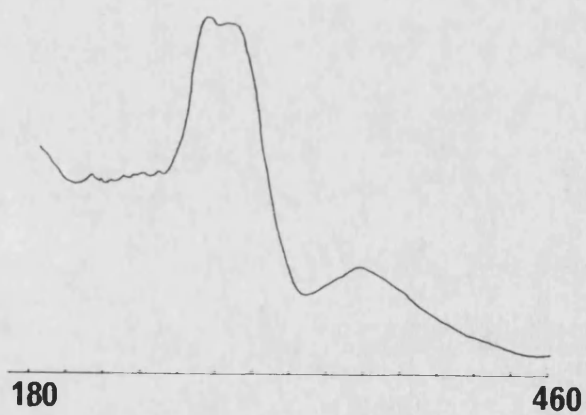
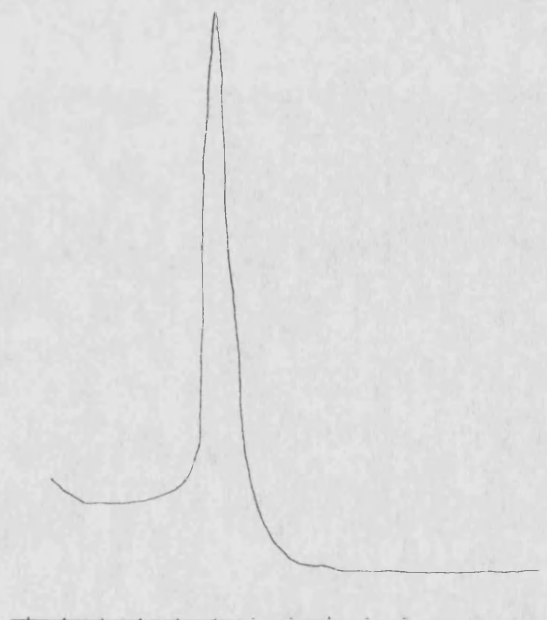


Figure 4.2c The UV scan OF LA-MTX (4.52%w/w) in 0.1M NaOH.





**Table 4.2 The lambda max of MTX, LA, BSA, LA-MTX and BSA-MTX.**

	No of $\lambda_{\max}$	$\lambda_{\max}$ 1	$\lambda_{\max}$ 2	$\lambda_{\max}$ 3
MTX	2	375nm	305nm	-
LA	1	280nm	-	-
BSA	1	280nm	-	-
LA-MTX	3	374nm	300nm	290nm
BSA-MTX	3	373nm	303nm	280nm

The conjugates were dissolved in 0.1M NaOH. Over the absorbance range covered the wavelengths of maximum absorbance for the conjugates were the same or  $\pm 1\text{nm}$  to those of free MTX. In the conjugate there was an additional small peak which corresponded to the protein portion of the conjugate. LA and MTX have peaks at a wavelength of 280nm and 305nm and in the conjugate the peaks at 300nm and 290nm were coincident. The peak at 375nm for MTX was not affected by conjugation with protein. Thus this wavelength was used to calculate the concentration of MTX in the synthesised conjugates (appendix 1.2 shows the calibration curve used to calculate MTX concentrations).

#### **4.2 Pharmacokinetics of BSA-MTX conjugates.**

The pharmacokinetics and organ distribution determined for each conjugate will be discussed individually. Section 4.5 summarises the results for BSA-MTX conjugates.

##### **4.2.1 BSA-MTX (3.4%w/w).**

Table A3.14.1 lists the plasma concentrations determined for  $^{125}\text{I}$  activity following administration of  $^{125}\text{I}$ -BSA-MTX (3.4%w/w) to rats by IV, IP and SC injection. These results are shown graphically in Figure 4.3. A plot of log serum concentration against

Figure 4.3:

Plasma Concentration of  $^{125}\text{I}$  activity following administration of 5mg of  $^{125}\text{I}$ -BSA-MTX (3.4%w/w) to rats by IV, IP and SC routes. Each point was a single determination.

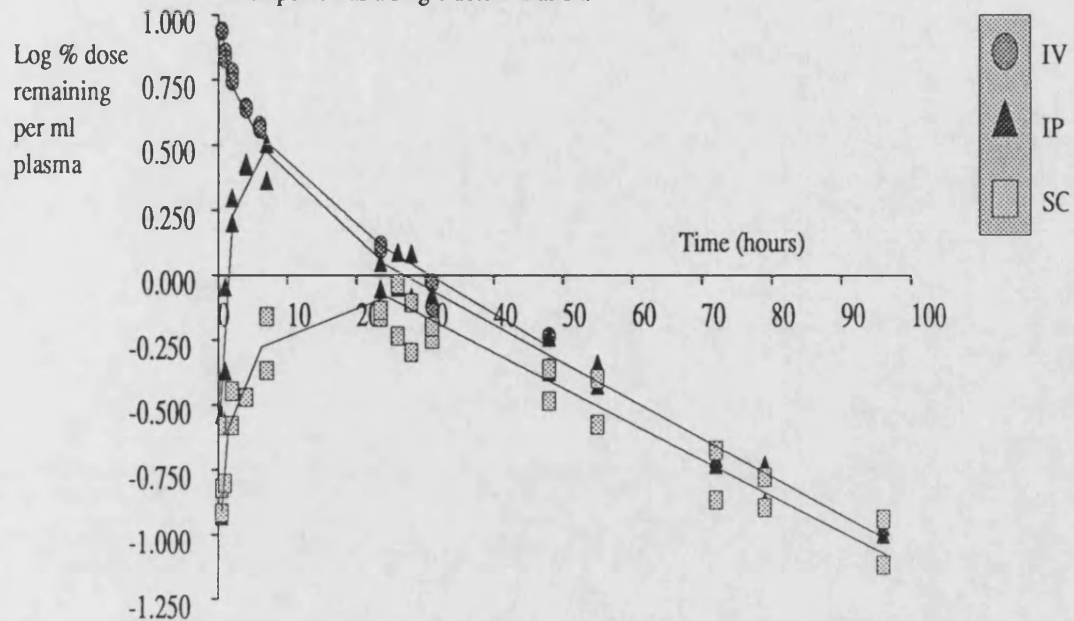
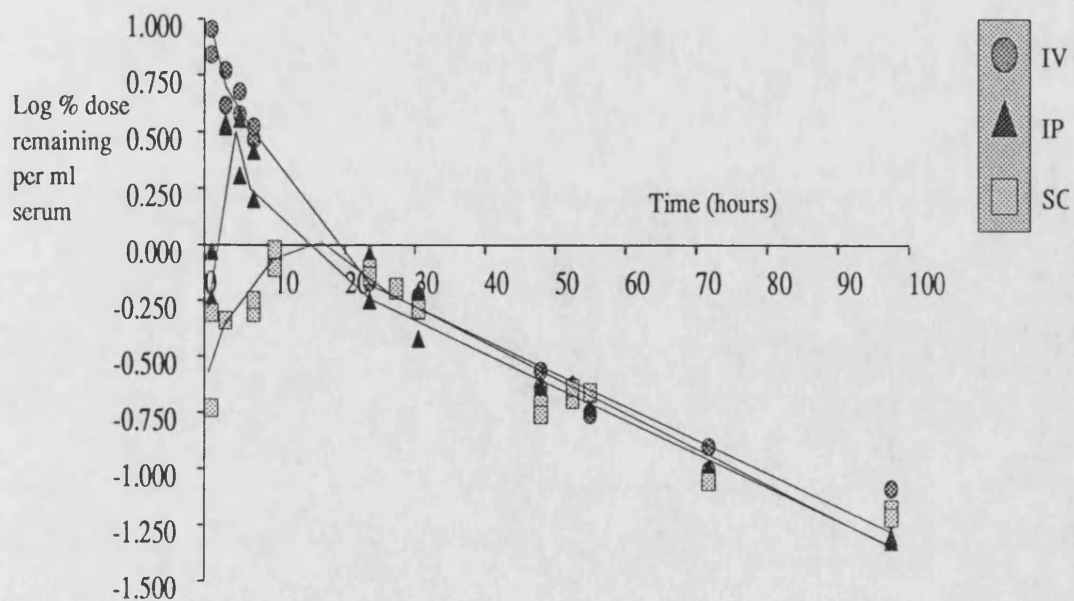


Figure 4.4.1:

Serum Concentration of  $^{125}\text{I}$  activity following administration of 5mg of  $^{125}\text{I}$ -BSA-MTX (5.1%w/w) to rats by IV, IP and SC routes. Each point was determined from one rat. (n=8 for each route).



time for IV dosed rats was biexponential. Absorption following IP injection was faster than for SC injection. Peak plasma levels were achieved within 4 to 7 hours of IP injection and within 23.5 to 26 hours of SC injection. Pharmacokinetic parameters were calculated for each of the routes of administration. These are listed in table 4.3.

**Table 4.3 Pharmacokinetic Parameters Calculated for  $^{125}\text{I}$ -BSA-MTX (3.4 %w/w)**

	IV (alpha)	IV (beta)	IP (beta)	SC (beta)
time span (hr)	0.5-6	23.5-48	23.5-96	23.5-96
R <sup>2</sup>	0.9691	0.9522	0.9635	0.9070
m* (hr <sup>-1</sup> )	-0.105±0.0103	-0.0161±0.0019	-0.0143±0.001	-0.0119±0.001
c* (Log Co)	0.75±0.038	0.457±0.044	0.349±0.0395	0.161±0.054
n <sup>#</sup>	10	6	18	18
Kel (hr <sup>-1</sup> )	0.410	0.0371	0.0329	0.0274
t <sup>1/2</sup> (hr)	1.691	18.70	21.04	25.29
Vd (ml)	17.78	34.87	44.77	68.98
Cl (ml/hr)	7.289	1.29	1.48	1.99

**after IV, IP and SC injection.**

Notes: \* Slopes and constants are quoted ± Standard Error.

# n= number of points used in each calculation.

The parameters calculated for the elimination phase were very similar for each route. Following SC administration the volume of distribution was larger than for the other two routes. This could be explained by incomplete absorption of the conjugate or uptake by cells at the site of administration.

The urine excretion of  $^{125}\text{I}$  activity was determined for all routes and is listed in table A3.14.2. Approximately 60 - 67 % of the  $^{125}\text{I}$  injected was excreted over 96 hours.

#### 4.2.2. BSA-MTX (5.1%w/w).

The serum concentrations of  $^{125}\text{I}$  activity determined for BSA-MTX (5.1%w/w) are listed in Table A3.15.1. Figure 4.4.1 is a plot of log serum  $^{125}\text{I}$  activity/ml against time for each route. Peak plasma levels were achieved between 10 and 23.5 hours after SC injection and between 5 and 7 hours after IP injection. Pharmacokinetic parameters were calculated for the three routes of administration. These are listed in table 4.4.

**Table 4.4: The pharmacokinetic parameters calculated for BSA-MTX (5.1%w/w) administered by IV, IP and SC routes.**

	IV (alpha)	IV (beta)	IP (beta)	SC (beta)
Time span (hr)	1-7	23.5-97.5	23.5-97	23.5-97
R <sup>2</sup>	0.8256	0.9440	0.9619	0.9354
m* (hr <sup>-1</sup> )	-0.0796±0.015	-0.0141±0.001	-0.0156±0.0009	-0.0151±0.001
c* (log Co)	0.867±0.068	0.124±0.058	0.151±0.053	0.155±0.057
n <sup>#</sup>	8	14	14	16
Kel (hr <sup>-1</sup> )	0.183	0.0325	0.0359	0.0348
t <sup>1/2</sup> (hr)	3.780	21.32	19.29	19.93
Vd (ml)	13.58	75.16	70.63	69.98
Cl (ml/hr)	2.487	2.443	2.536	2.435

Notes: \* Slopes and Constants are quoted ± Standard Error.

# n= number of points used in calculation.

The pharmacokinetic parameters calculated for the elimination phases were very similar after each route of administration. The half life for elimination at approximately 20 hours is very similar to that determined for BSA. The calculated volumes of distribution (70 to 75ml) were larger than those calculated for BSA (26ml for the beta phase),

Figure 4.4.2:

Percentage of  $^{125}\text{I}$  activity excreted in the urine following administration of 5mg of  $^{125}\text{I}$ -BSA-MTX (5.1%w/w) to rats by IV, IP and SC routes.

Each point is a mean  $\pm$  S.E.M. (n=3).

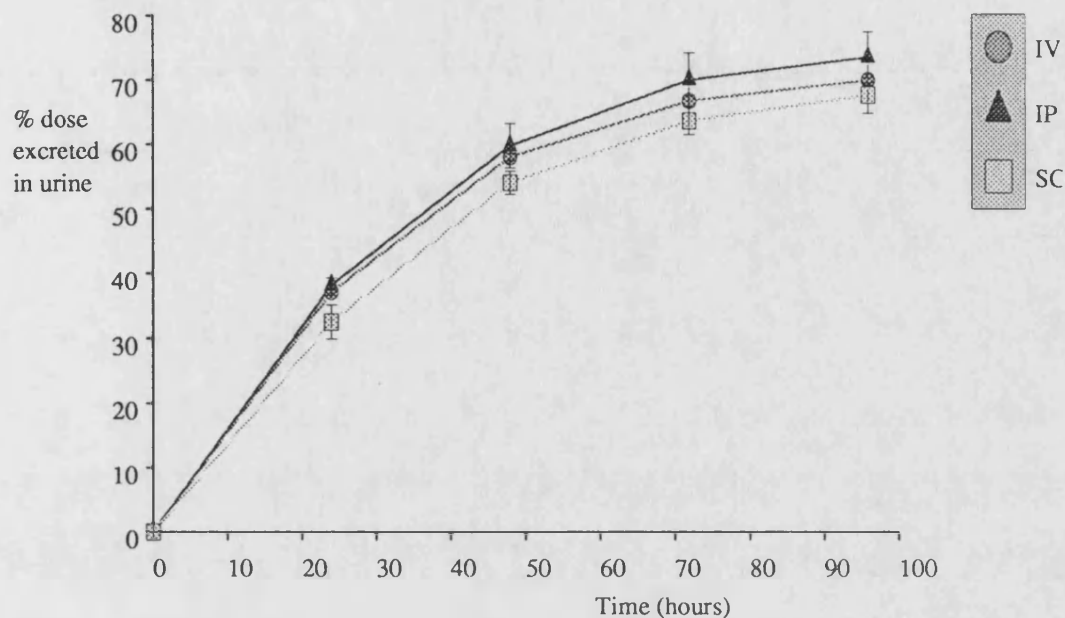
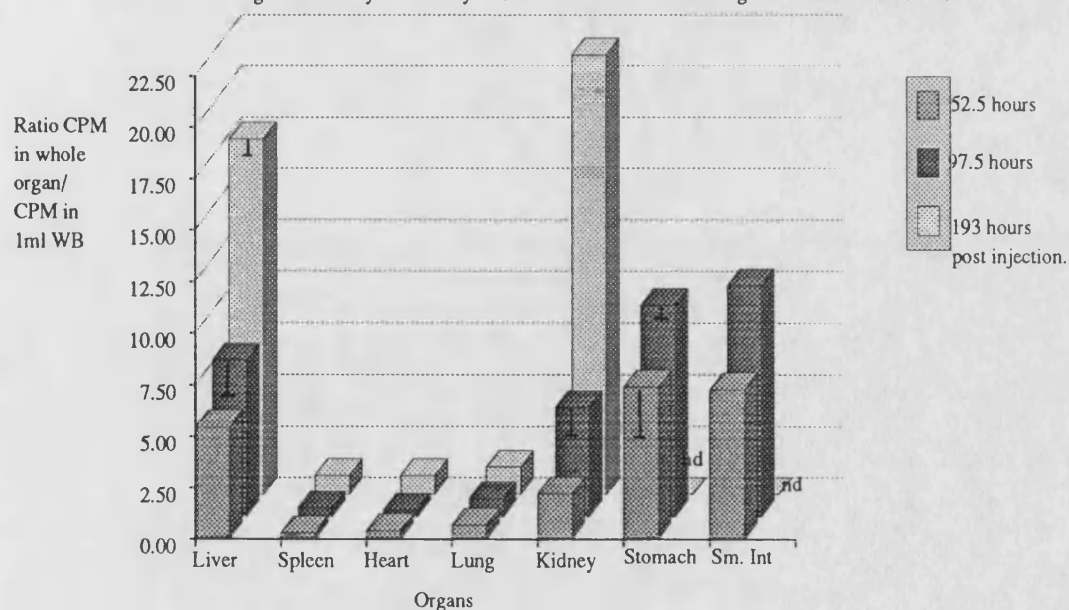


Figure 4.4.3:

Organ Distribution of  $^{125}\text{I}$  activity following administration of 5mg of  $^{125}\text{I}$ -BSA-MTX (5.1%w/w) to rats by the IV route. Results are expressed as a ratio of the activity found in the whole organ divided by the activity in 1ml whole blood. Each histogram is the mean of 2 rats.



indicating that the BSA-MTX (5.1%w/w) could more readily leave the vasculature and enter the tissue compartment.

Urine and faecal excretion of  $^{125}\text{I}$  activity were calculated following administration of  $^{125}\text{I}$ -BSA-MTX (5.1%w/w) to rats by each of the three routes. These results for percent of  $^{125}\text{I}$  dose excreted in urine and faeces are listed in tables A3.15.2 and A3.15.3 respectively. Figure 4.4.2 is a plot of the percentage radioactivity excreted against time. Percentage urine excretion was not significantly different for the three routes of administration. Approximately 70% of the injected dose was excreted in the urine over 96 hours. Faeces excretion accounted for between 7 and 10% of the injected activity over 96 hours.

Organ distribution of  $^{125}\text{I}$  activity was determined 52 hours, 97.5 hours and 193 hours after administration for all 3 routes of injection. Figure 4.4.3 is a histogram showing the ratio of  $^{125}\text{I}$  activity in each tissue investigated divided by the activity in 1ml of whole blood, after IV administration of  $^{125}\text{I}$ -BSA-MTX (5.1%w/w) to rats. Each bar was the mean of the two animals investigated. The range for the rats is shown unless it was below 10%. The organ distribution was very similar at 52.5 hours and 97.5 hours. The  $^{125}\text{I}$  activity did not appear to accumulate in any of the organs investigated apart from the thyroid. However at 193 hours after administration there appeared to be accumulation in the liver and the kidney. Since the whole blood concentration of  $^{125}\text{I}$  at this time point was only 0.008% of the injected activity, this would probably not have any physiological significance. For the other routes of administration the organ distribution was not significantly different from IV.

#### **4.2.3. BSA-MTX (6.2%w/w).**

The plasma concentration determined for  $^{125}\text{I}$  activity following administration of  $^{125}\text{I}$ -BSA-MTX (6.2%w/w) to rats by IV, IP and SC injection are listed in Table A3.16.1 and are represented graphically in Figure 4.5.1. Peak plasma levels were reached within 11 hours of SC administration and within 2 hours of IP administration. Pharmacokinetic parameters were calculated for each route of administration and these

are listed in Table 4.5.

**Table 4.5: The pharmacokinetic parameters calculated for BSA-MTX (6.2%w/w) administered to rats by IV, IP and SC injection.**

	IV (alpha)	IV (beta)	IP (beta)	SC (beta)
time span (hr)	0.5-6.5	22.5-96	22.5-96	22.5-96
R <sup>2</sup>	0.9732	0.9764	0.9211	0.9571
m*	-0.104±0.007	-0.0176±0.0007	-0.0164±0.0013	-0.0152±0.0008
c*	0.729±0.028	-0.0963±0.038	-0.0976±0.068	-0.134±0.0045
n <sup>#</sup>	8	17	16	16
Ke1 (hr <sup>-1</sup> )	0.239	0.0405	0.0378	0.0349
t <sup>1/2</sup> (hr)	2.893	17.12	18.31	19.85
Vd (ml)	18.67	124.8	125.2	136.1
Cl (ml/hr)	4.462	5.055	4.732	4.750

Notes: \* Slopes and constants are quoted ± Standard Error.

# n= number of points used in the calculation.

The parameters calculated for the elimination phase were very similar for each of the routes of injection investigated. The plasma elimination half-lives were slightly shorter than those calculated for BSA-MTX (5.1%w/w). The volume of distribution represented approximately half the body weight of the rat for the 6.2%w/w conjugate.

The urine and faecal excretion of <sup>125</sup>I were determined for each of the routes of administration. These results are listed in tables A3.16.2 and A3.16.3 respectively. There was no significant difference for percent <sup>125</sup>I dose excreted for each of the routes of administration. Approximately 40-48% of the injected <sup>125</sup>I dose was excreted in the urine over 96 hours and approximately 7% of the <sup>125</sup>I dose was excreted in the faeces in 96 hours.

Figure 4.5.1:  
Plasma Concentration of  $^{125}\text{I}$  activity following administration  
of 5mg of  $^{125}\text{I}$ -BSA-MTX (6.2%w/w) to rats by IV, IP and SC routes.  
Each point is from one rat. (n=8 for each route).

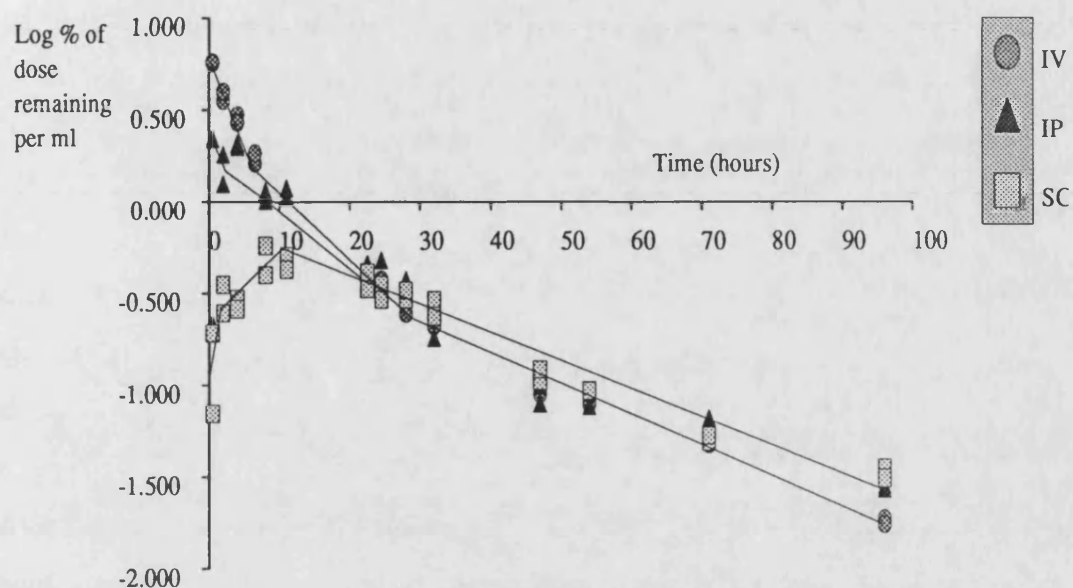
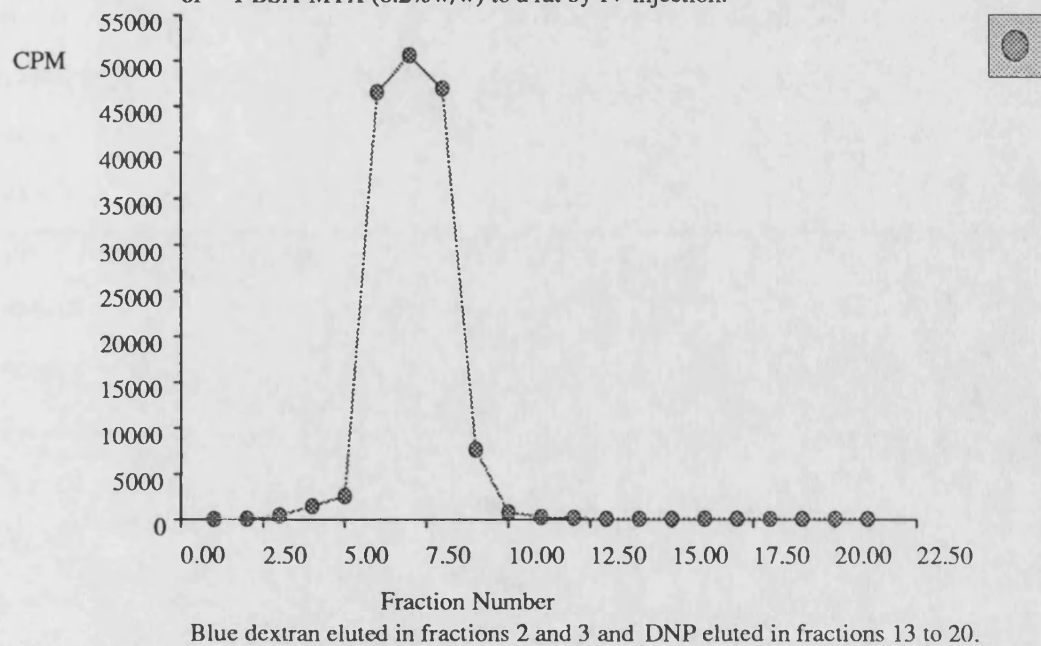


Figure 4.5.2: The  $^{125}\text{I}$  activity of 1ml fractions eluted  
from a Sephadex G25 column to which had been applied a sample of  
urine collected for a period of 24 hours after administration  
of  $^{125}\text{I}$ -BSA-MTX (6.2%w/w) to a rat by IV injection.





### Molecular Weight Determination of the $^{125}\text{I}$ component of Urine.

To samples of 24 hour and 72 hour urine obtained from IV dosed rats, an equal volume of a solution containing blue dextran (relative molecular weight  $2 \times 10^6$ ) and 2,4-dinitrophenylalanine (DNP) was added. This solution was passed down a 10ml gel filtration column consisting of Sephadex G25. The mobile phase was water and elution occurred under gravity. As the blue dextran started to elute, 1ml fractions were collected until all the DNP had eluted. Each fraction was then measured in a gamma counter. Figure 4.5.2 shows the elution profile for a 24 hour sample of urine. The majority of  $^{125}\text{I}$  eluted in fractions 5 to 9. The blue dextran eluted in fractions 2 and 3 and the DNP eluted in fractions 13 to 20. The molecular weight range for resolution for the Sephadex G25 is 5000 to 1000 molecular weight. Since the elution of the  $^{125}\text{I}$  activity occurred before the inclusion volume of the column (fractions 13 to 20) it would appear that it was conjugated to polypeptide fragments (of between 5000 and 1000 molecular weight) of the original BSA-MTX conjugate. The 72 hour urine samples showed a similar profile to the 24 hour samples.

The organ distribution of  $^{125}\text{I}$  activity was determined at 24, 96 and 171 hours after administration of the conjugate. The results are listed in Table A3.16.4. Figure 4.5.3 is a histogram showing the ratio of activity in 1g of organ divided by the activity in 1ml of whole blood for IV dosed rats at each time point. At 24 hours the activity in all organs, apart from the kidney, was low and represented the blood activity in each case. The proximal tubule of the kidney is known to exhibit a high protein uptake and this may explain why the kidney at 24 hours showed accumulation of the  $^{125}\text{I}$  activity. As demonstrated by the urine gel filtration experiment, the  $^{125}\text{I}$  excreted in the urine was conjugated to oligopeptides of molecular weight between 1000 and 5000. These may have been formed by the kidney following uptake of the conjugate. At 96 hours and 171 hours all the organs investigated, and particularly the liver and kidney, showed an elevated ratio compared to 24 hours. It has already been demonstrated that  $^{125}\text{I}$ -Na was not taken up by the liver and kidney and thus it would appear that, following the uptake of the conjugate, the isotope was selectively retained. The activity determined for the

Figure 4.53: Organ Distribution of  $^{125}\text{I}$  activity following administration of 5mg of  $^{125}\text{I}$ -BSA-MTX (6.2%w/w) to rats by the IV route. Each bar is the mean of 2 rats. The range for each ratio is shown. Ratios for 3 time points are shown.

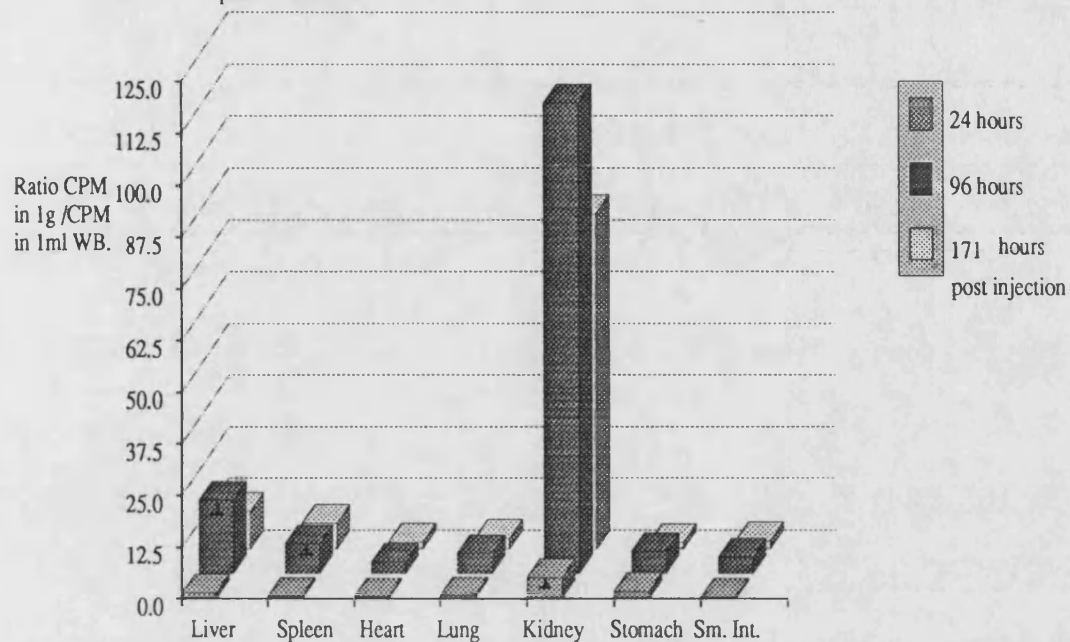
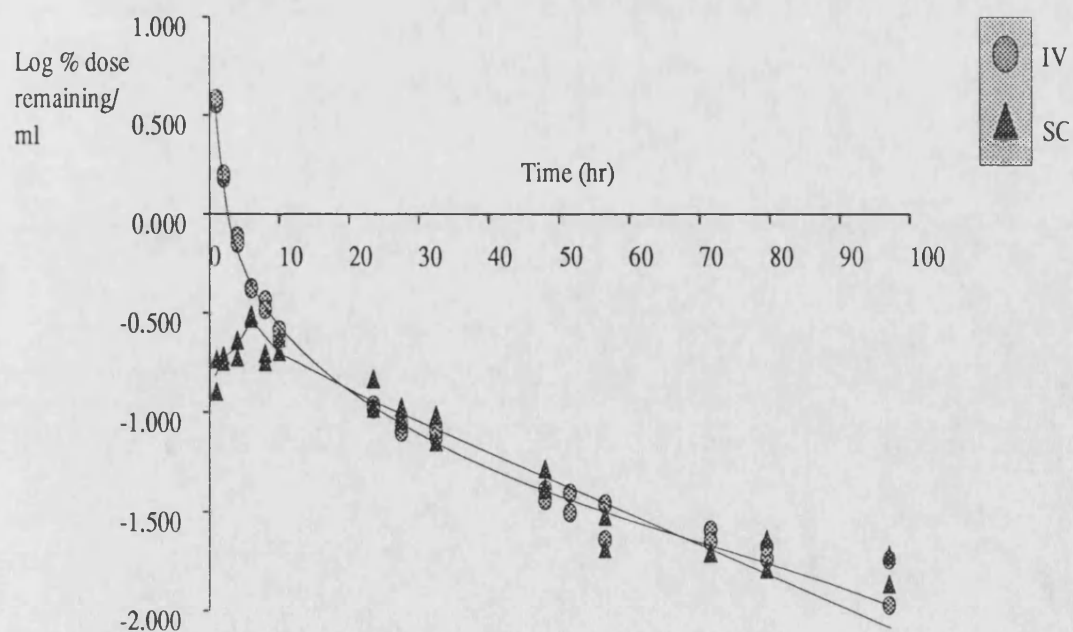


Figure 4.6: Log %  $^{125}\text{I}$  activity remaining per ml of serum following administration of 5mg of  $^{125}\text{I}$ -BSA-MTX (9.18%w/w) to rats by IV and SC routes. Each point was a single determination.



organs after IP and SC injection were similar to IV.

#### 4.2.4. BSA-MTX (9.18%w/w).

Table A3.17.1 lists the serum concentrations of  $^{125}\text{I}$  activity determined following administration of the  $^{125}\text{I}$ -BSA-MTX (9.18%w/w) conjugate to rats by IV and SC routes. Figure 4.6 is a plot of Log serum concentration versus time for both routes. Following IV administration a biexponential serum clearance was seen. Peak serum levels appeared to be achieved within 6 hours of SC administration. Following the absorption phase, serum clearance closely followed that of IV dosed rats. Table 4.6 lists the pharmacokinetic parameters calculated for this conjugate.

**Table 4.6: The Pharmacokinetic Parameters Calculated for the 9.18% w/w conjugate following IV and SC administration in the Rat.**

	IV (alpha)	IV (beta)	SC (beta)
Time span	1-10	23.5-97	23.5-97
R <sup>2</sup>	0.9380	0.9181	0.8815
m*	-0.153±0.0124	-0.0119±0.0009	-0.0128±0.0012
c*	0.511±0.076	-0.772±0.052	-0.712±0.075
n <sup>#</sup>	12	18	16
Kel (hr <sup>-1</sup> )	0.352	0.0272	0.0294
t <sup>1/2</sup> (hr)	1.967	25.46	23.6
Vd (ml)	30.83	594	515
Cl (ml/hr)	10.85	16.16	15.15

Notes: \* Slopes and constants are quoted ± Standard Error.

# n= number of points used in the calculation.

The parameters calculated for IV and SC dosed rats for the elimination phase were very similar. The elimination half-life was longer than that of the other conjugates administered and the volume of distribution was very large, representing twice the body volume of the rat. Thus the BSA-MTX (9.18%w/w) underwent a very wide tissue distribution.

Urine and faecal excretion of  $^{125}\text{I}$  activity was determined for both routes of administration. The results are listed in tables A3.17.2 and A3.17.3 respectively. There was little difference in the total excretion of  $^{125}\text{I}$  for the two routes. Approximately 40-46% of the injected dose was excreted over 96 hours. Faecal excretion accounted for approximately 7% of the injected dose of 96 hours for both routes.

#### **4.2.5 BSA-MTX (11.74%w/w).**

Table A3.18.1 lists the serum concentrations for  $^{125}\text{I}$  activity determined following administration of BSA-MTX (11.74%w/w) to rats by IV, IP and SC routes. These results are shown graphically in Figure 4.7.1. Peak serum levels were achieved within 19 hours of administration by the SC route and approximately 6 hours after IP administration. After the absorption phase for IP and SC dosed rats the serum concentration of  $^{125}\text{I}$  activity closely followed the serum concentrations for IV dosed rats. Pharmacokinetic parameters were calculated for each of the routes of administration. These are listed in Table 4.7 (page 133).

The  $V_d$  for the elimination phase for each route was large, and represents a volume which is greater than the actual rat. Therefore the conjugate had a widespread tissue distribution. Elimination half-lives were longer than for the other conjugates administered. The half-life for the distribution phase following IV administration was very short at 1.6 hours, indicating a rapid initial distribution into the central compartment.

Figure 4.7.1: Concentration of  $^{125}\text{I}$  activity in serum following administration of 5mg of  $^{125}\text{I}$ -BSA-MTX (11.74%w/w) to rats by IV, IP and SC routes. Each point was a single determination.

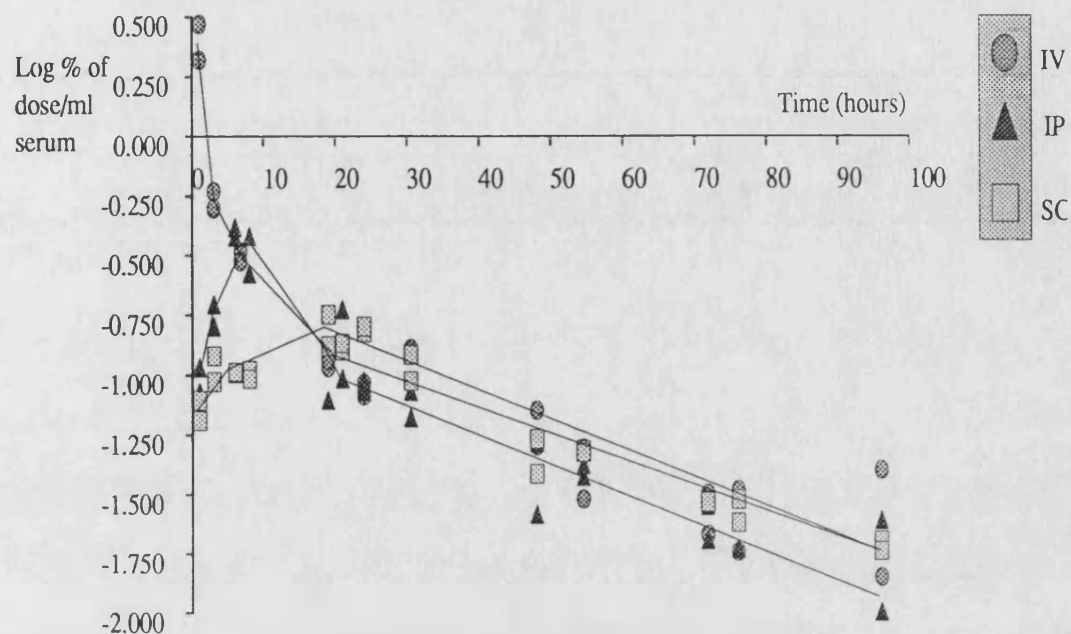
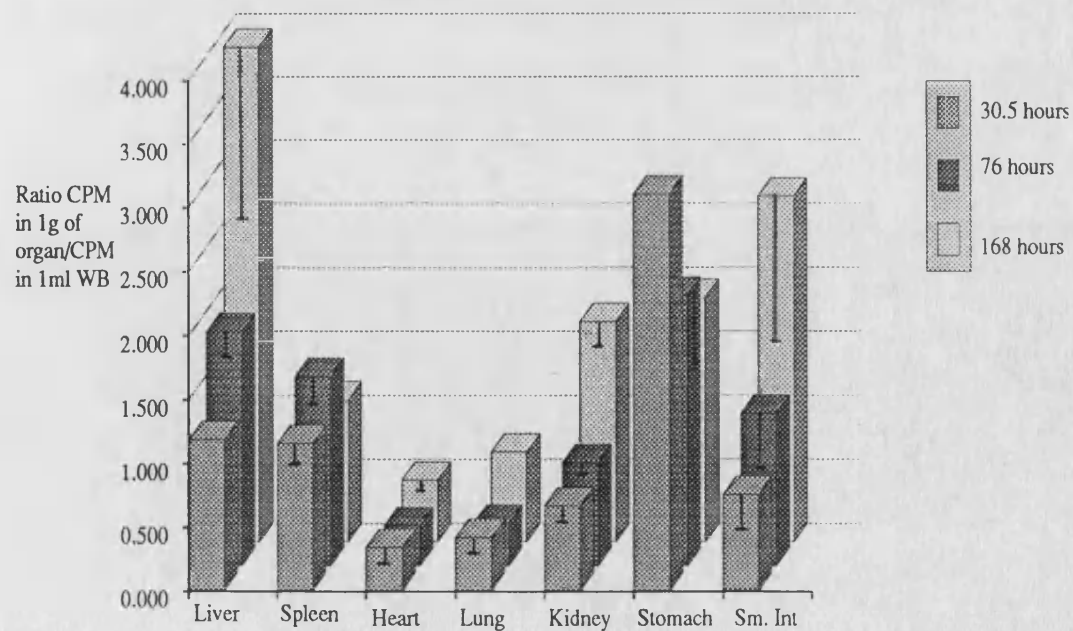


Figure 4.7.2: Organ Distribution of  $^{125}\text{I}$  activity following administration of 5mg of  $^{125}\text{I}$ -BSA-MTX (11.74%w/w) to rats by the IV route. Results are expressed as a ratio of activity in 1g of organ divided by activity in 1ml of blood at 3 time points. Each bar is the mean of 2 animals. The range for the two ratios is shown.



**Table 4.7: Pharmacokinetic Parameters calculated for BSA-MTX (11.74%w/w) administered by IV, IP and SC injection to rats.**

	IV (alpha)	IV (beta)	IP (beta)	SC (beta)
time span (hr)	1-6.75	19-96	19-96	24-96
R <sup>2</sup>	0.8467	0.7776	0.8547	0.9454
m* (hr <sup>-1</sup> )	-0.188±0.04	-0.0104±0.0015	-0.0118±0.0012	-0.0125±0.0007
c* (log Co)	0.387±0.172	-0.751±0.087	-0.767±0.0674	-0.603±0.042
n <sup>#</sup>	6	16	18	18
Kel (hr <sup>-1</sup> )	0.433	0.0240	0.0270	0.0288
t <sup>1/2</sup> (hr)	1.600	29.03	25.5	24.05
Vd (ml)	41.02	564	583	401
Cl (ml/hr)	17.76	13.54	15.74	11.55

Notes: \* Slopes and constants are quoted ± Standard Error. # n= number of points used in the calculation

The urine and faeces excretion for <sup>125</sup>I activity was determined for each of the routes of administration of the BSA-MTX (11.74%w/w) conjugate. These results are listed in Tables A3.18.2 and A3.18.3. There were no significant differences in the percent excreted for each of the routes. Approximately 40-46% of the injected <sup>125</sup>I activity was excreted over 96 hours and approximately 8% of the <sup>125</sup>I activity was excreted in the faeces over 96 hours for each of the routes of administration.

Table A3.18.4 lists the organ distribution of <sup>125</sup>I activity at various time points following administration of <sup>125</sup>I-BSA-MTX (11.74%w/w). A plot summarising these results is shown in Figure 4.7.2. This plot is a histogram for the ratio of <sup>125</sup>I activity found in 1g of organ divided by the activity in 1ml of whole blood after 30.5, 76 and 168 hours post IV administration. There was a significant accumulation of activity in

the liver, spleen (both organs of the RES), stomach and small intestine at 30.5 hours. The ratio was increased in the liver at 76 hours and 168 hours compared to the 24 hour values. Activity probably occurred in the gut after the conjugate had been taken up by the liver and then transferred into the bile. For the other routes of administration the organ distribution was very similar.

#### 4.2.6 BSA-MTX (11.76%w/w).

The serum concentrations determined for  $^{125}\text{I}$  activity following administration of the  $^{125}\text{I}$ -BSA-MTX (11.76%w/w) to rats by IV, IP and SC routes are shown in table A3.19.1 and are represented graphically in Figure 4.8.1. Peak plasma levels were achieved within 6 hours of IP administration and between 8 and 23 hours of SC injection. A biexponential clearance for IV dosed rats was seen. The pharmacokinetic parameters calculated for each route of administration are listed in table 4.8.

**Table 4.8: The Pharmacokinetic Parameters calculated for BSA-MTX (11.76% w/w) following IV, IP and SC administration to rats.**

	IV (alpha)	IV (beta)	IP (beta)	SC (beta)
Time Span (hr)	1-4	24.5-96	24-100	23-96
R <sup>2</sup>	0.9123	0.9652	0.9719	0.9352
m* (hr <sup>-1</sup> )	-0.341±0.053	-0.0102±0.0005	-0.00904±0.0004	-0.0075±0.0005
c* (log Co)	1.091±0.14	-0.205±0.035	-0.339±0.0033	-0.509±0.031
n <sup>#</sup>	6	16	16	16
Kel (hr <sup>-1</sup> )	0.785	0.0236	0.0208	0.0172
t <sup>1/2</sup> (hr)	0.883	29.39	33.29	40.20
Vd (ml)	8.11	160	218	322.5
Cl (ml/hr)	6.37	3.79	4.53	5.48

Notes: \* Slopes and constants are quoted ± Standard Error. # n= number of points used in the calculation.

Figure 4.8.1:

Serum Concentration of  $^{125}\text{I}$  activity following administration of 5mg of  $^{125}\text{I}$ -BSA-MTX (11.76%w/w) to rats by IV, IP and SC routes. Each point is from one rat. n=8 for each route.

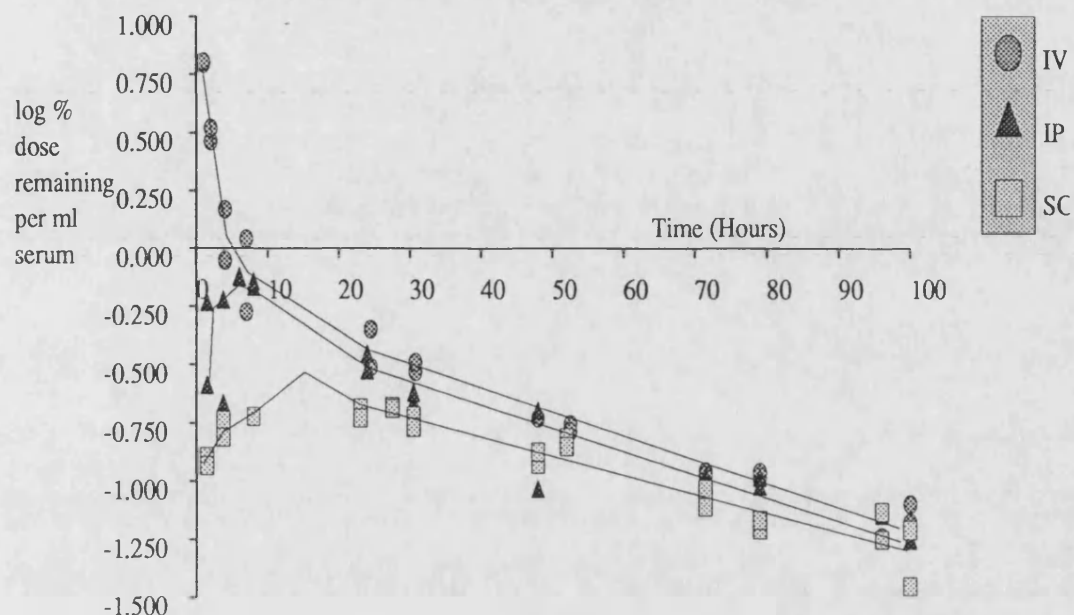
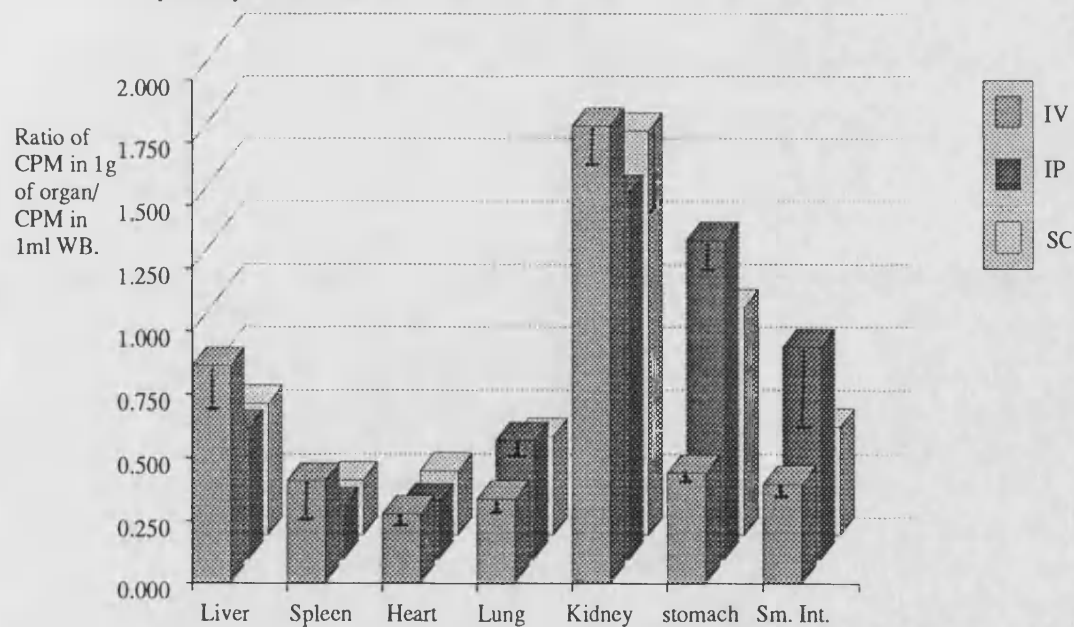


Figure 4.8.2: Organ Distribution of  $^{125}\text{I}$  activity following administration of 5mg of  $^{125}\text{I}$ -BSA-MTX (11.76%w/w) to rats by IV, IP and SC injection. Values were determined at 100 hours post injection, as a ratio of activity in 1g of organ divided by activity in 1ml of blood.



Each bar is the mean of 2 rats and the range is shown unless the difference was less than 10%.



The half-life calculated for the distribution phase for IV dosed rats was only 53 minutes, indicating a rapid distribution into the central compartment. The volume of distribution for the central compartment represented the serum volume of a rat. For the elimination phase the  $V_d$  represented the whole body volume of a rat, thus indicating that the conjugate could readily leave the vasculature. The elimination half life was longest for SC dosed rats. This may indicate that the conjugate was still being absorbed from the injection site during this time. In addition the  $V_d$  was found to be larger for SC dosed rats, and this may be due to incomplete absorption from the injection site or uptake by cells at the site of administration or during its route to the blood stream.

The urine and faeces excretion of  $^{125}\text{I}$  was determined for each route of administration. The results are listed in tables A3.19.2 and A3.19.3. There was no significant difference in the percentage excreted for any route of administration. Approximately 50 to 56 % was excreted in the urine over 96 hours and between 7 and 8 % of the dose was excreted in the faeces over the same period.

Table A3.19.4 and Figure 4.8.2 summarise the organ distribution of  $^{125}\text{I}$  activity after administration of the BSA-MTX (11.76%w/w) conjugate. Organ distribution was determined for each route of administration at 100 hours after administration. There was no significant difference in the ratio (activity in 1g of organ divided by activity in 1ml of blood) for the three routes of administration. The greatest activity was found in liver, kidney, stomach and small intestine. Unexpectedly, the organ distribution of the 11.76%w/w conjugate followed a different pattern to the 11.74%w/w conjugate. Overall levels in the liver and spleen of the 11.76%w/w conjugate were lower than the 11.74%w/w conjugate and levels in the kidney were approximately two times higher than the 11.74%w/w conjugate. On FPLC analysis of these 2 conjugates, the 11.76%w/w conjugate was found to have considerably less protein aggregates than the 11.74%w/w conjugate (22% for 11.76% BSA-MTX and 34.7% for the BSA-MTX (11.74%w/w)). This could account for the different distribution pattern, more of the 11.74%w/w conjugate was taken up by the RES.

#### 4.2.7 BSA-MTX (13.63%w/w)

Table A3.20.1 lists the serum concentrations determined for  $^{125}\text{I}$  activity following administration of  $^{125}\text{I}$ -BSA-MTX (13.63%w/w) to rats by the IV, IP and SC routes. Figure 4.9.1 is a plot of Log percentage of  $^{125}\text{I}$  activity injected per ml of serum versus time for each route of administration. Following IV administration a biexponential clearance from serum was seen. Peak serum levels were achieved between 4.75 and 7.5 hours after IP administration and within 18.5 hours of SC injection. Pharmacokinetic parameters were calculated for each route of administration and they are listed in Table 4.9.

**Table 4.9: Pharmacokinetic parameters calculated for BSA-MTX (13.63%w/w) administered by IV, IP and SC injection to rats.**

	IV (alpha)	IV (beta)	IP (beta)	SC (beta)
Time Span (hr)	0.75-7.5	18.5-94	18.5-94	18.5-94
R <sup>2</sup>	0.9051	0.8767	0.8859	0.9206
m* (hr <sup>-1</sup> )	-0.200±0.0264	-0.00911±0.001	-0.00965±0.001	-0.0092±0.0007
c* (log Co)	1.100±0.124	-0.661±0.0549	-0.561±0.0059	-0.550±0.041
n <sup>#</sup>	8	16	16	17
Kel (hr <sup>-1</sup> )	0.460	0.0210	0.0222	0.0211
t <sup>1/2</sup> (hr)	1.508	33.03	31.20	32.78
Vd (ml)	7.956	458	364	355
Cl (ml/hr)	3.661	9.612	8.089	7.772

Notes: \* Slopes and Constants are quoted ± Standard Error. # n= number of points used in the calculation.

The parameters calculated for the elimination phase for each of the routes of administration were not significantly different. The serum elimination half-life was

Figure 4.9.1 Concentration of  $^{125}\text{I}$  activity in serum following administration of 5mg of  $^{125}\text{I}$ -BSA-MTX (13.63%w/w) to rats by IV, IP and SC routes. Each point was obtained from one rat. (n=8 for each route).

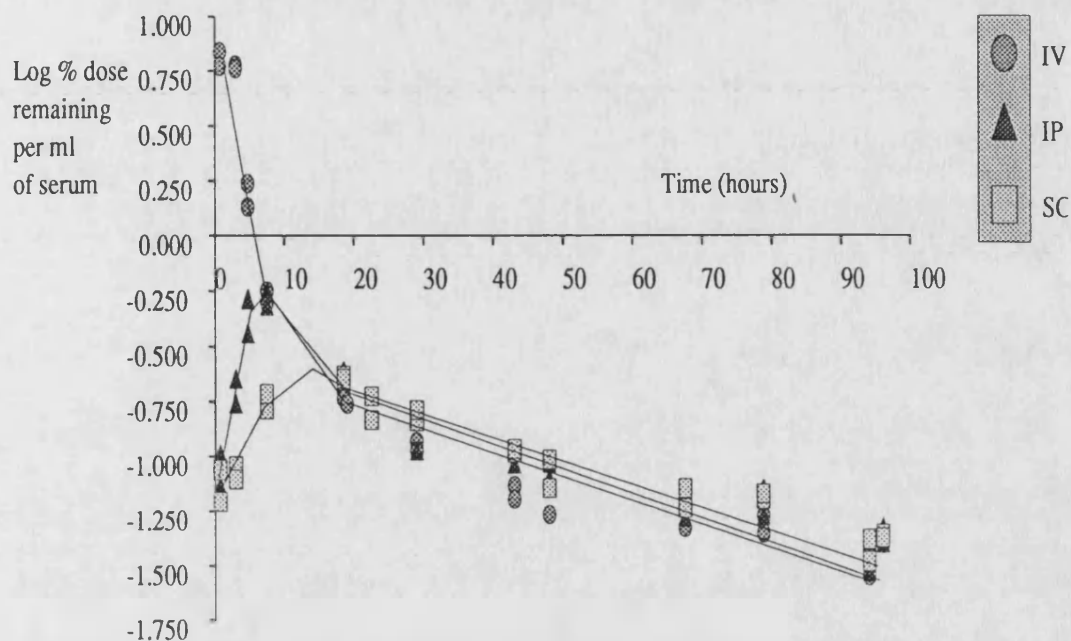
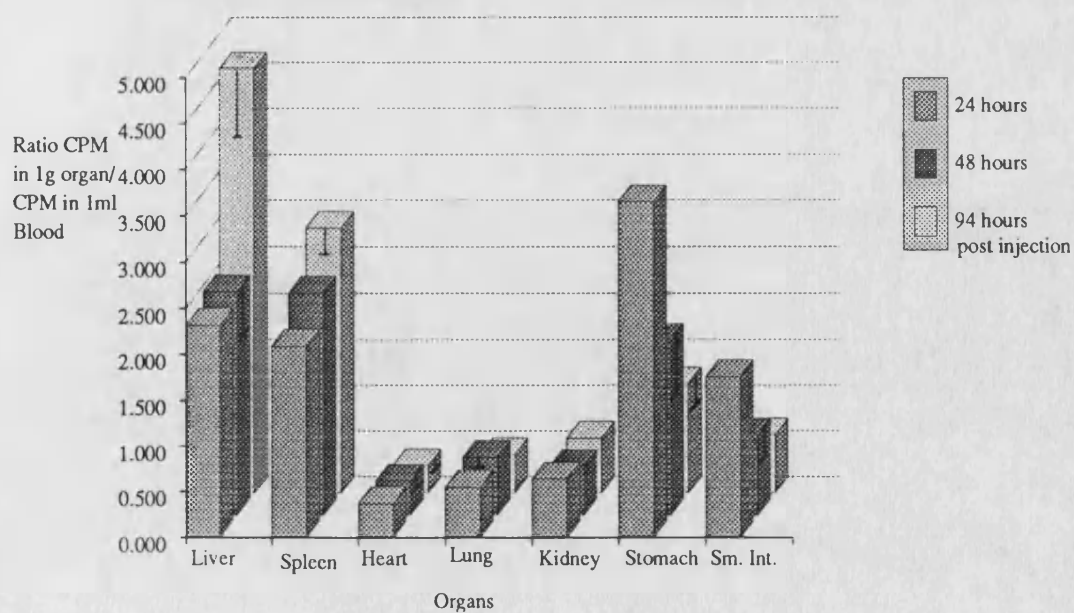


Figure 4.9.2:

Organ Distribution of  $^{125}\text{I}$  activity following administration of 5mg of  $^{125}\text{I}$ -BSA-MTX (13.63%w/w) to rats by the IV route. Values were determined at 3 time points and are a ratio of the activity in 1g of the organ divided by the activity in 1ml of blood. Each bar is the mean from two animals. The range is shown.



longer than for the other conjugates investigated.  $V_d$  was very large and thus it was assumed that the BSA-MTX (13.63%w/w) conjugate could readily leave the vasculature. The  $V_d$  for the distribution phase of IV dosed rats represented the serum volume in a 250g rat. The half-life for the alpha phase was very rapid at 1.5 hours.

Urine and faeces excretion were determined for each route of administration. The results are listed in tables A3.20.2 and A3.20.3. There was no significant difference in the urine excretion between the different routes ( $p>0.05$ ) (determined using Student's t-test at each time point for each route). Between 60 and 65% of the injected radioactive dose was excreted in 96 hours. Excretion in the faeces accounted for approximately 8 to 10% of the injected dose in 96 hours.

Table A3.20.4 summarises the organ distribution determined for the  $^{125}\text{I}$  activity after administration of  $^{125}\text{I}$ -BSA-MTX (13.63%w/w). Organ distribution was determined 24, 48 and 94 hours after administration. Figure 4.9.2 is a histogram for the ratio of  $^{125}\text{I}$  activity in 1g of each organ divided by the activity in 1ml of whole blood, for IV dosed rats at each time point. There was no significant difference for this ratio between organs, at 24 hours and 48 hours.  $^{125}\text{I}$  activity was taken up by liver, spleen, stomach and small intestine. At 94 hours the ratio in the liver was slightly elevated compared to the other time points. There was no difference in the organ distribution of  $^{125}\text{I}$  activity for the other routes of administration.

#### **4.2.8 BSA-MTX (13.64%w/w).**

Table A3.21.1 lists the serum  $^{125}\text{I}$  activity determined following administration of  $^{125}\text{I}$ -BSA-MTX (13.64%w/w) to rats by IV, IP and SC routes. Figure 4.10.1 is a plot of log serum  $^{125}\text{I}$  activity versus time for each of the routes of administration. Following IV administration, two phases for serum clearance were seen. Peak serum levels were achieved approximately 5 hours after administration for IP dosed rats and between 8 and 23 hours after SC administration. Pharmacokinetic parameters were calculated for each route of administration and are listed in table 4.10.

Figure 4.10.1:

Serum Concentration of  $^{125}\text{I}$  activity following administration of 5mg of  $^{125}\text{I}$ -BSA-MTX (13.64%w/w) to rats by IV, IP and SC routes. Each point was determined from one rat. (n=8 for each route.)

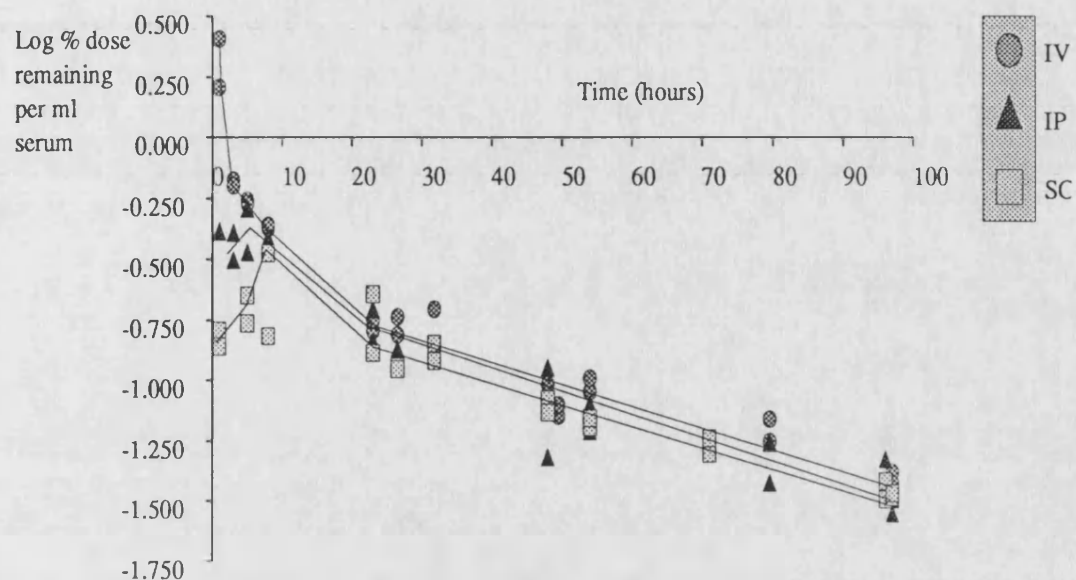
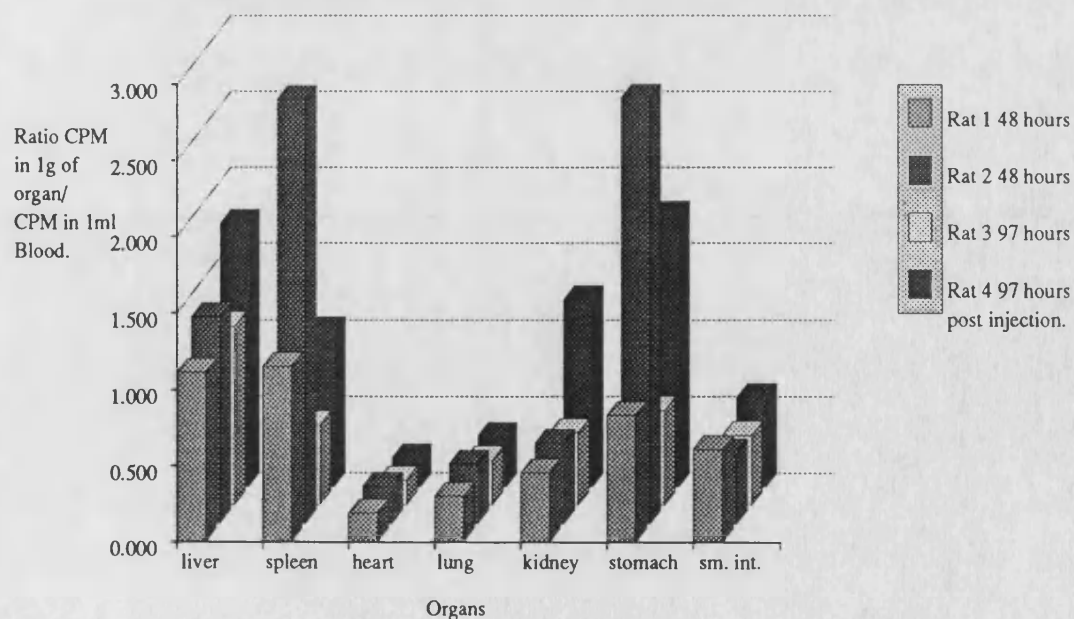


Figure 4.10.2:

Organ Distribution of  $^{125}\text{I}$  activity following IV administration of 5mg of  $^{125}\text{I}$ -BSA-MTX (13.64%w/w) to rats. Values were determined at 2 time points and are a ratio of the activity in 1g of organ divided by the activity in 1ml of blood. Each bar was determined from a single animal.



**Table 4.10: The Pharmacokinetic Parameters calculated for rats dosed with <sup>125</sup>I-BSA-MTX (13.64%w/w) by IV, IP and SC routes.**

	IV (alpha)	IV (beta)	IP (beta)	SC (beta)
Time Span (hr)	1-8	23-96	23-96	23-96
R <sup>2</sup>	0.7816	0.8958	0.8956	0.8969
m* (hr <sup>-1</sup> )	-0.123±0.027	-0.0091±0.0008	-0.0084±0.001	-0.00871±0.0008
c* (log Co)	0.180±0.133	-0.567±0.045	-0.663±0.062	-0.653±0.047
n <sup>#</sup>	8	20	18	16
Kel (hr <sup>-1</sup> )	0.283	0.0210	0.0194	0.0201
t <sup>1/2</sup> (hr)	2.449	32.99	35.70	34.53
Vd (ml)	66.04	369.3	460.9	450.2
Cl (ml/hr)	18.69	7.756	8.941	9.049

Notes \* Slopes and Constants are quoted ± Standard Error. # n= number of points used in the calculation.

The pharmacokinetic parameters calculated for the elimination phase for the three different routes of administration were very similar. The half-lives for the elimination phases were not significantly different from those calculated for the 13.63%w/w conjugate. Volumes of distribution calculated for the 13.64%w/w conjugate were large, indicating that it could readily leave the vasculature.

Urine and faeces excretion was calculated for each of the routes of administration and is listed in tables A3.21.2 and A3.21.3. There was no significant difference for the percentage of activity excreted for any of the routes of administration at 48 to 96 hours after administration. However, at 24 hours the % excreted by the SC dosed rats was found to be significantly lower (p< 0.05 by Student's t-test) from rats dosed IV. This difference could be due to the lower levels of conjugate reaching the kidney over the

first 24 hours (serum levels were lower than IV over this period) during the absorption phase. However, by 48 hours the SC rats had excreted approximately the same amount of activity as the other groups. Between 63 and 72% of the injected radioactivity was excreted in 96 hours. Approximately 10 to 12 % of the radioactive dose was accounted for by faeces excretion in 96 hours.

Organ distribution was determined over 97 hours for each route of administration. The results are listed in table A3.21.4. Figure 4.10.2 (page 140) is a histogram summarising the results for IV dosed rats. The distribution for the other routes of administration was not significantly different from IV. Activity did not accumulate in heart, lung or kidney. There were slightly elevated levels of activity in liver, spleen and gut. The ratios calculated for these organs were not as high as for the BSA-MTX (13.63%w/w) conjugate.

#### **4.3. FPLC determination of Plasma, Urine and Bile samples.**

For rats that had been dosed with an injection of the 7.16%w/w conjugate, the molecular weight of the  $^{125}\text{I}$  fraction present in their serum was determined at time points ranging from 0.5-48 hours. After 48 hours the activity in the serum was too low for accurate measurement of  $^{125}\text{I}$  activity since only 20 $\mu\text{l}$  was applied to the FPLC column. 1ml fractions were collected and the radioactivity determined in each one. Radioactivity was found to occur in 2 peaks. The first had an elution time of approximately 16 minutes and corresponded to intact conjugate. The second had an elution time of 44-45 minutes and corresponded to iodinated tyrosine or  $^{125}\text{I}^-$  (as iodide). (Iodinated tyrosine and sodium iodide both interacted with the column and eluted together). Figure 4.11 shows the elution profile of a 0.5 hour serum sample. Table 4.11 lists the percentage of radioactivity determined for both peaks at each time point investigated.

Figure 4.11: Percentage of  $^{125}\text{I}$  activity in 1ml fractions eluted from the Superose 12 column to which had been applied a sample of serum which had been obtained from a rat, 0.5 hours after it had been injected with  $^{125}\text{I}$ -BSA-MTX (7.16%w/w).

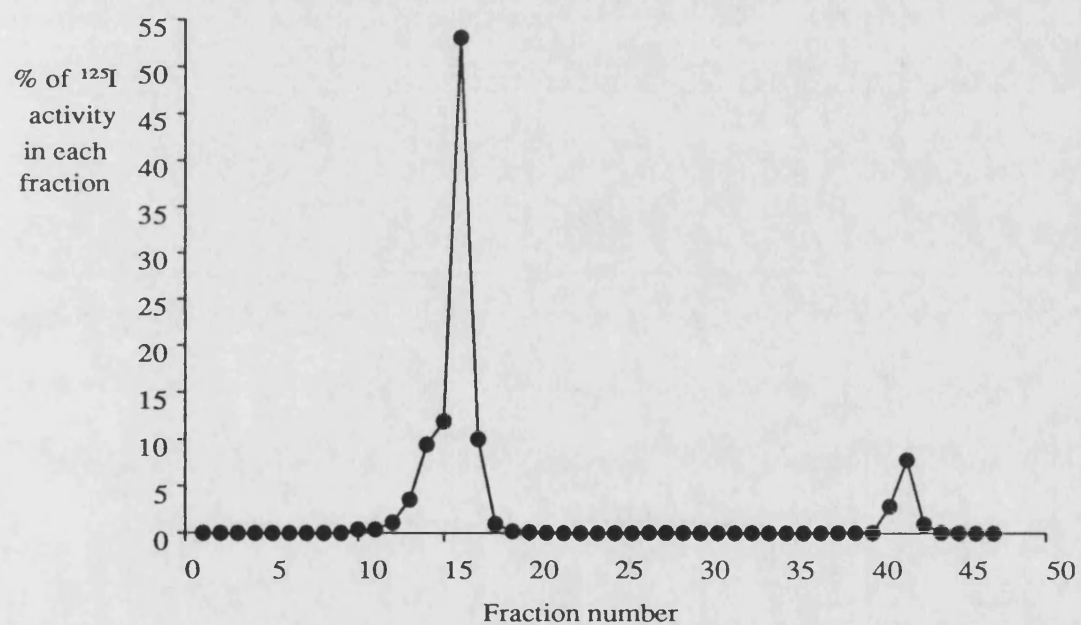




**Table 4.11: Percentage of Radioactivity eluting in Peak 1 (retention time = 16 minutes) and Peak 2 (retention time = 44-45 minutes) after eluting rat plasma samples containing  $^{125}\text{I}$ -BSA-MTX (7.16% w/w) from the Superose 12 column.**

Time of plasma sample (hr)	Peak 1 Kav=0.336	Peak 2 Kav=1.72
0.5	89.66	10.54
0.5	89.33	10.67
1.0	87.33	12.67
4.0	76.59	23.41
6.0	78.31	21.69
6.0	73.21	26.79
24.0	80.66	19.34
24.0	70.24	29.76
48	67.56	32.44
48	87.24	12.76

All the serum samples tested contained at least 67% of intact conjugate. There was a tendency for the percentage of  $^{125}\text{I}$  activity present as iodide or iodinated tyrosine to increase as time after administration increased. No intermediate peaks were seen in the serum samples.

The molecular weight of the  $^{125}\text{I}$  species in urine was also determined in a similar manner to serum. Three urine samples were analysed for each time point (24 hours and 72 hours). The results were similar for both time points. Two peaks of radioactivity were seen. The smaller peak had a retention time of 25 minutes (Kav=0.77) and corresponded to a molecular weight of approximately 1600. The major peak had a retention time of 43 minutes and corresponded to iodinated tyrosine or sodium iodide. For the 24 hour samples the percentage of activity in peak 1 was  $14.6 \pm 1.45$  (S.E.M.) and the radioactivity present in peak 2 was  $85.4 \pm 1.45$ . At 72 hours the percentage of radioactivity present in peak 1 was  $9.34 \pm 0.689$  and the radioactivity present in peak 2 was  $90.66 \pm 0.689$ . Thus the BSA-MTX conjugate was degraded into very small fractions before excretion and the majority of radioactivity excreted was in the form of  $^{125}\text{I}^-$  or

$^{125}\text{I}$ -tyrosine.

Samples of bile which had been obtained from rats that had been given an IV injection of  $^{125}\text{I}$ -BSA-MTX (11.55%w/w) were analysed using the Superose 12 column. Bile was obtained from 2 rats, three hours after the conjugate was administered and bile was collected over a period of 15 minutes. The bile flow rate was approximately 100 $\mu\text{l}$  in 15 minutes. The concentration of the  $^{125}\text{I}$  in bile was found to be 1.323%/ml and 1.247%/ml of the injected dose for the rats. The major peak of radioactivity occurred at the same time point as for the urine samples. 65.15% and 64.12% of the radioactivity was present as either  $^{125}\text{I}$ -tyrosine or  $^{125}\text{I}$ -Na. The remainder of the  $^{125}\text{I}$  was eluted between 24 and 37 minutes after injection onto the column, with 2 peaks at 24 and 27 minutes. These corresponded to molecular weights of 2400 and 712 respectively. The  $^{125}\text{I}$  species present in bile was found to be mainly  $^{125}\text{I}$ -tyrosine or  $^{125}\text{I}$ -Na.

#### **4.4 Administration of $^{125}\text{I}$ -BSA- $^3\text{H}$ -MTX (7.16%w/w).**

The serum levels determined in rats after administration of the  $^{125}\text{I}$ -BSA- $^3\text{H}$ -MTX conjugate for both isotopes are listed in table A3.31.1. Figure 4.12.1 is a plot of log serum isotope concentration versus time for both  $^{125}\text{I}$  and  $^3\text{H}$ . The two isotopes gave very similar values for the % of conjugate remaining per ml of serum. Pharmacokinetic parameters were calculated using both isotopes for the measurement of conjugate in serum. These are shown in table 4.12.

Figure 4.12.1: Serum Clearance of  $^{125}\text{I}$  and  $^3\text{H}$  activity following administration of 0.86mg of  $^{125}\text{I}$ -BSA- $^3\text{H}$ -MTX to rats by the IV route. Each point is a single determinant.

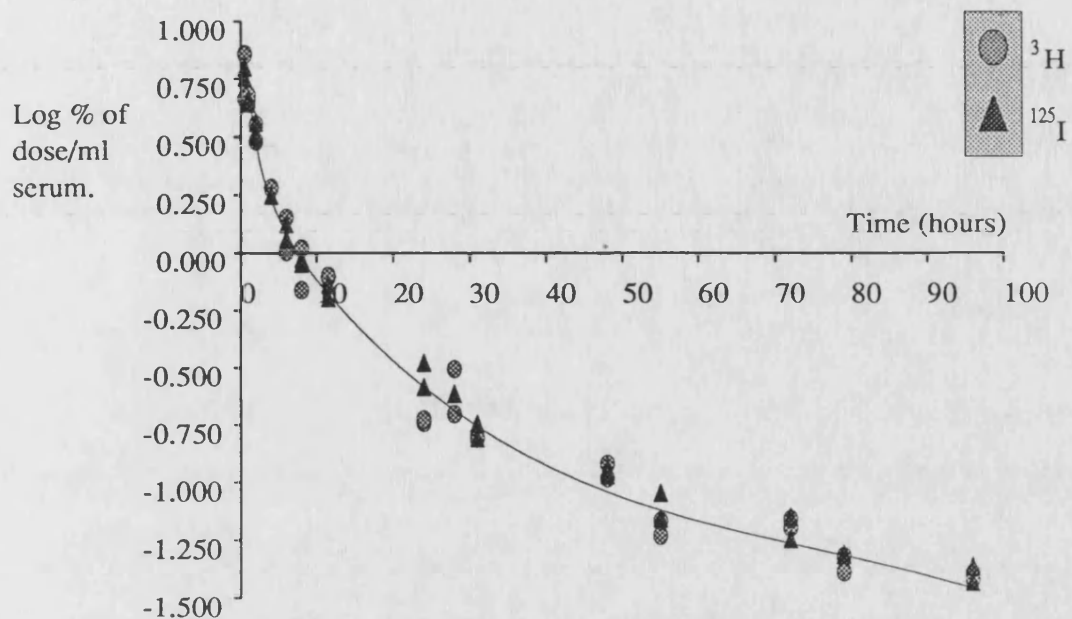
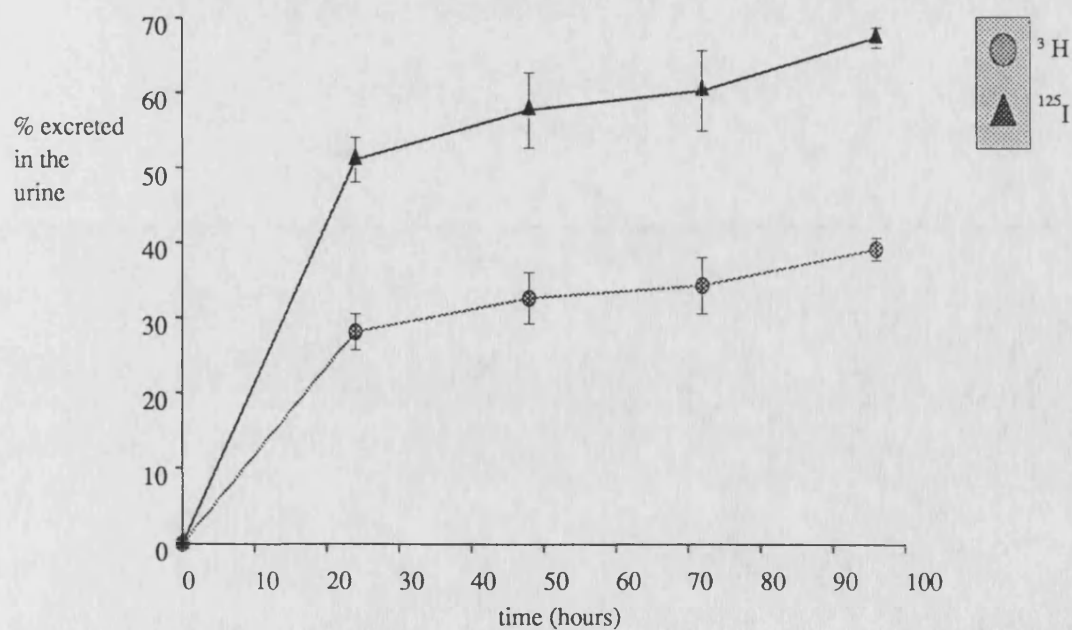


Figure 4.12.2: Excretion of  $^{125}\text{I}$  and  $^3\text{H}$  activity following administration of  $^{125}\text{I}$ -BSA- $^3\text{H}$ -MTX (7.16%w/w) to rats by the IV route. Each point is the mean  $\pm$  S.E.M. (n=3), except 96 hours (n=2).



**Table 4.12: The Pharmacokinetic Parameters Calculated for  $^{125}\text{I}$ -BSA- $^3\text{H}$ -MTX (7.16% w/w) following IV administration to rats.**

	$^{125}\text{I}$	$^3\text{H}$
<b>1. Distribution Phase</b>		
time span (hr)	0.5-11.5	0.5-11.5
$R^2$	0.9574	0.8803
$m^*$ ( $\text{hr}^{-1}$ )	$-0.111 \pm 0.0071$	$-0.0993 \pm 0.011$
$c^*$ (log $C_0$ )	$0.686 \pm 0.0434$	$0.680 \pm 0.0679$
$n^\#$	13	13
$K_{el}$ ( $\text{hr}^{-1}$ )	0.255	0.229
$t^{1/2}$ (hr)	2.712	3.030
$V_d$ (ml)	20.61	20.92
$Cl$ (ml/hr)	5.25	4.79
<b>2. Elimination Phase</b>		
time span (hr)	24-96	24-96
$R^2$	0.9331	0.887
$m^*$ ( $\text{hr}^{-1}$ )	$-0.0119 \pm 0.00085$	$-0.0108 \pm 0.00103$
$c^*$ (log $C_0$ )	$-0.358 \pm 0.0505$	$-0.445 \pm 0.0612$
$n^\#$	16	16
$k_{el}$ ( $\text{hr}^{-1}$ )	0.0274	0.0248
$t^{1/2}$ (hr)	25.29	27.91
$V_d$ (ml)	228	278
$Cl$ (ml/hr)	6.25	6.89

Notes: \* Slopes and Constants are quoted  $\pm$  Standard Error. # n= number of points used in the calculation.

The pharmacokinetic parameters calculated using the two different isotopes were very similar. During the alpha phase the parameters were all within 10% of each other and it can be assumed that both isotopes remained bound to the conjugate during the alpha phase and could both be used accurately to determine the concentration of conjugate within serum.

During the elimination phase, again both isotopes gave similar values for the pharmacokinetic parameters of the conjugate. The elimination half-life, elimination rate constant and clearance were all within 10% of each other. The  $V_d$  calculated for  $^3\text{H}$  isotope was 18% greater than calculated for  $^{125}\text{I}$ . The constants used in the calculation of  $V_d$  from the linear regression (see section A2.1) were both associated with a standard error of 14% and thus the  $V_d$  values calculated for  $^3\text{H}$  could range from 239-316ml and the  $V_d$  for the  $^{125}\text{I}$  isotope could range from 196-260ml. Therefore the pharmacokinetic parameters calculated using both isotopes could be considered to be very similar. Since the levels of the two isotopes remained at the same ratio in the serum samples it can be assumed that both isotopes remained bound to the conjugate and that the conjugate was not broken down in serum with release of either the  $^{125}\text{I}$  or  $^3\text{H}$ , unless of course both were released from the conjugate at the same rate and then had the same fate. In separate experiments the pharmacokinetic parameters were calculated for both  $^3\text{H}$ -MTX and  $^{125}\text{I}$ -Na and they were not the same (Cl from plasma, for alpha phase for MTX was 334 ml/hr and for  $^{125}\text{I}$  was 215ml/hr). Thus it was unlikely that either of the two labels was cleaved from the conjugate during circulation in serum.

The urine excretion of both isotopes was followed over 96 hours after administration of  $^{125}\text{I}$ -BSA- $^3\text{H}$ -MTX. The results are shown in table A3.31.2 and are shown graphically in figure 4.12.2. Considerably less  $^3\text{H}$  activity was excreted in the urine than  $^{125}\text{I}$  activity at 24 hours (51% of the  $^{125}\text{I}$  had been excreted in the urine compared to only 28.5% of the  $^3\text{H}$  activity). Student's t-test was used to compare the % of the two isotopes that was excreted at 24 hours, 48 hours and 72 hours after injection. The % of  $^{125}\text{I}$  excreted was highly significantly greater than that of  $^3\text{H}$  at all time points.  $^{125}\text{I}$  was initially excreted at a faster rate than  $^3\text{H}$ . The rate of excretion of  $^{125}\text{I}$  was 2.13% of the

injected dose per hour over the first 24 hours and for  $^3\text{H}$  was 1.17%/hr. After 24 hours the rates of excretion for both isotopes decreased and were similar to each other. (Rate for  $^{125}\text{I}$  excretion over 24 to 96 hours was 0.225%/hour and for  $^3\text{H}$  was 0.152%/hr).

Table A3.31.3 shows the organ distribution for both isotopes at various time points up to 96 hours after injection of the  $^{125}\text{I}$ -BSA- $^3\text{H}$ -MTX conjugate. Five organs were investigated. These were the liver, spleen, kidney, stomach and small intestine. In addition, the uptake of  $^{125}\text{I}$  by the thyroid was measured. After 24 hours approximately 15% of the  $^{125}\text{I}$  dose was found to be located within the thyroid. The percentage of the activity did not appear to change from the 24 hour value, up to 96 hours after injection. The high concentration of  $^{125}\text{I}$  activity in the thyroid implied that some of the conjugate had been broken down, with the release of  $^{125}\text{I}$  which was in a form which could be utilised by the thyroid gland. (Only 7% of the iodine was present as a TCA soluble fraction in the original injection solution.)

Figures 4.12.3 to 4.12.6 show the  $^{125}\text{I}$  and  $^3\text{H}$  distribution in each of the organs investigated over the 96 hour period. The object of this experiment was to identify the fate of the MTX portion of the conjugate, after it had been taken up by the organs. The conjugate had a dual label. The  $^{125}\text{I}$  was bound to the protein portion of the conjugate and should give an indication of the fate of the BSA after cellular uptake. The  $^3\text{H}$  isotope was part of the MTX molecule and would indicate the distribution of the drug moiety. If the  $^3\text{H}$  activity was distributed in a similar way to the activity of  $^{125}\text{I}$  in the organs, then it could be assumed that the MTX remained bound to the protein fraction of the conjugate after it had been taken up intracellularly.

In the liver, up to 48 hours after administration, the 2 isotopes were present at a similar concentration. However, at 72 hours and 96 hours after administration, the  $^3\text{H}$  levels within the liver were elevated compared to  $^{125}\text{I}$ . At 96 hours, the level of  $^3\text{H}$  in the liver was 1.806% and for  $^{125}\text{I}$  it was 0.437% of the injected dose. (Both are means of the 2 rats investigated). The difference in the concentrations of the 2 isotopes in the liver could be explained by degradation of the conjugate after uptake by the liver. Following breakdown of the conjugate, it would appear that the  $^{125}\text{I}$  degradation products could be

Figure 4.12.3: Accumulation of  $^{125}\text{I}$  and  $^3\text{H}$  isotopes in the liver following administration of  $^{125}\text{I}$ -BSA- $^3\text{H}$ -MTX to rats by the IV route. Each point is the mean of 2 animals. The bars represent the individual ratio for each rat.

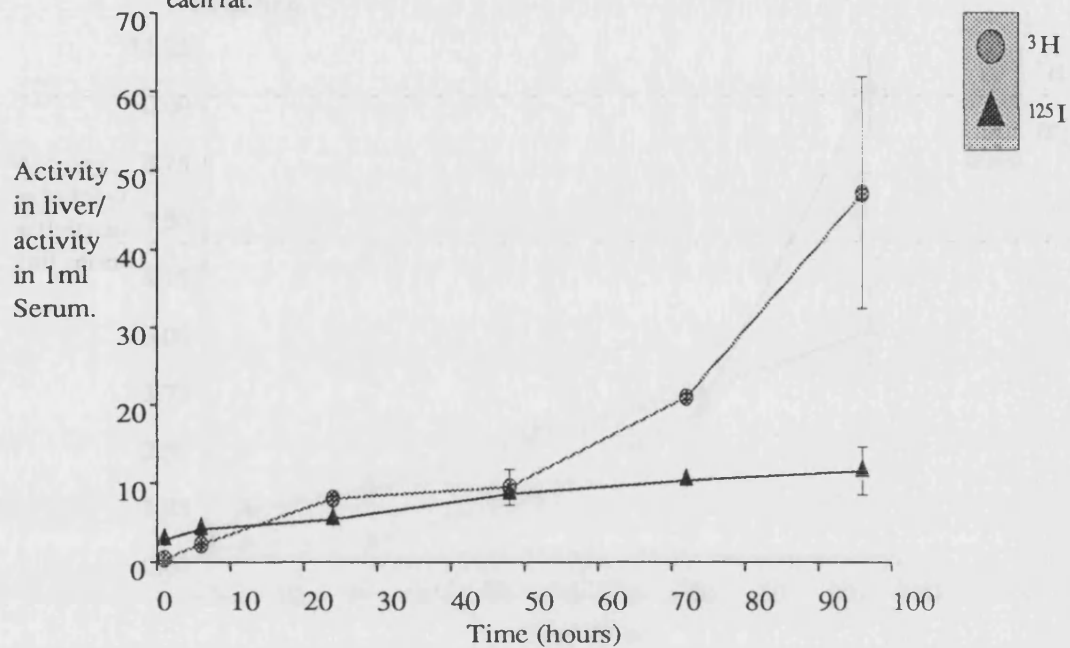


Figure 4.12.4: Accumulation of  $^{125}\text{I}$  and  $^3\text{H}$  activity in the spleen following administration of  $^{125}\text{I}$ -BSA- $^3\text{H}$ -MTX to rats by the IV route. Each point was the mean of 2 rats, the bars represent the value for individual animal.

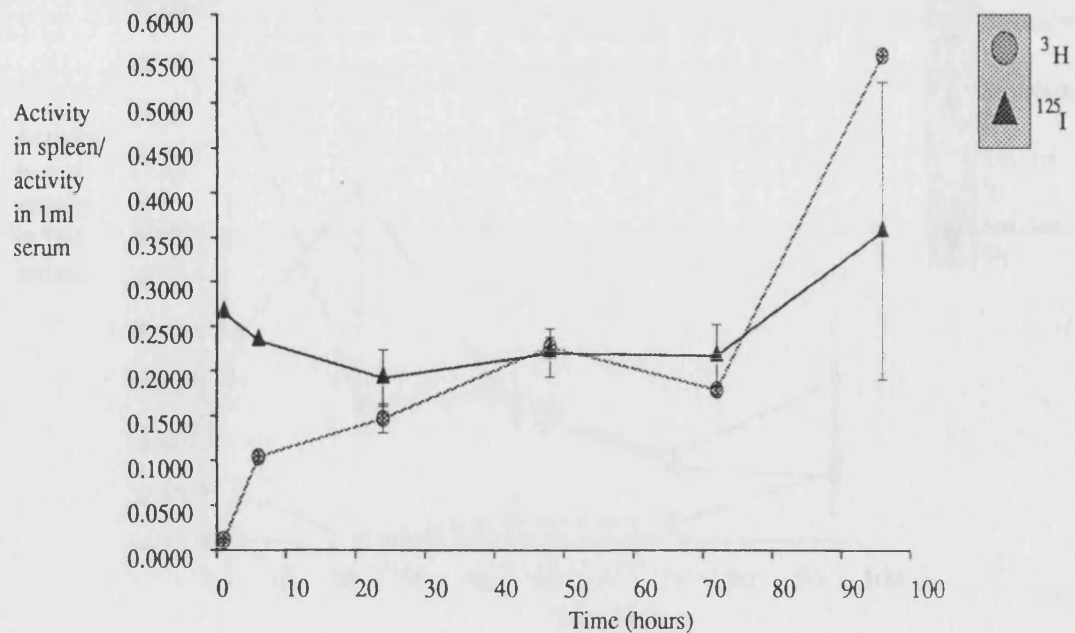


Figure 4.12.5: Accumulation of  $^{125}\text{I}$  and  $^3\text{H}$  activity in the kidney following administration of  $^{125}\text{I}$ -BSA- $^3\text{H}$ -MTX to rats by the IV routes. Each point is a mean of 2 rats. The bars represent individual values for each rat.

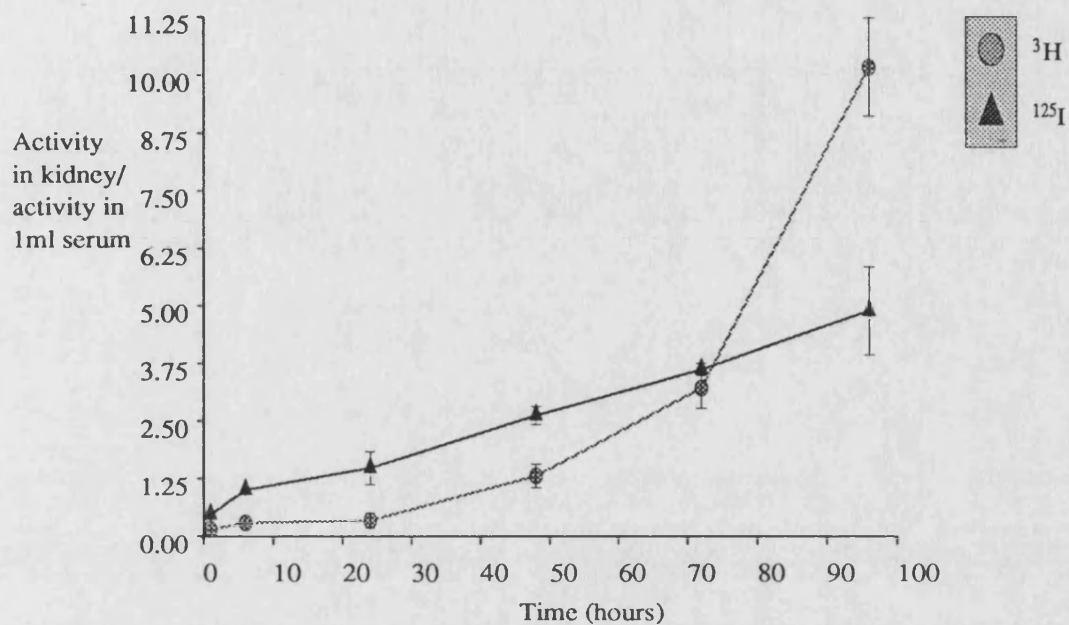
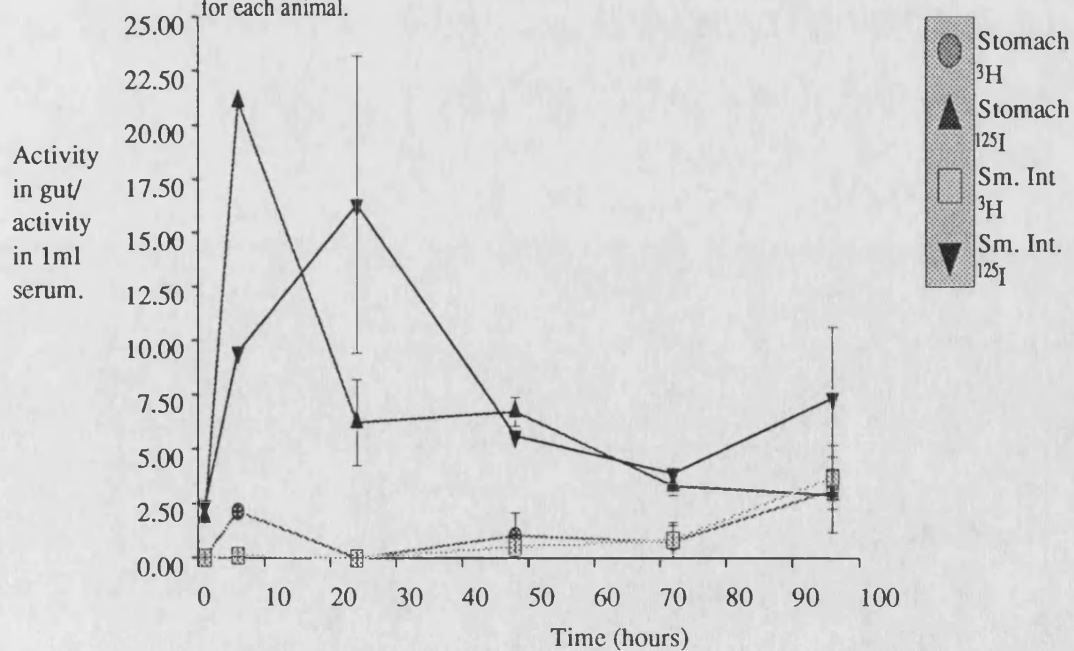


Figure 4.12.6: Accumulation of  $^{125}\text{I}$  and  $^3\text{H}$  in the gut following administration of  $^{125}\text{I}$ -BSA- $^3\text{H}$ -MTX to rats by the IV route. Each point is the mean of 2 rats. Each bar represents the individual reading for each animal.





released whereas the  $^3\text{H}$  moiety was selectively retained by the liver. A similar pattern was seen in the spleen. At 96 hours the level of  $^3\text{H}$  activity was 0.021% and for  $^{125}\text{I}$  it was 0.014%.

In the kidney, up to 72 hours after injection, the  $^3\text{H}$  isotope levels were lower than the  $^{125}\text{I}$  isotope levels. This would explain why the % of  $^3\text{H}$  excreted in the urine was less than that for  $^{125}\text{I}$ . At 96 hours after administration, the  $^3\text{H}$  level in the kidney was considerably higher than the  $^{125}\text{I}$  level (0.399% for  $^3\text{H}$  compared to 0.187% for  $^{125}\text{I}$ ). The increase in  $^3\text{H}$  activity in the kidney was not associated with a corresponding increase in the  $^3\text{H}$  activity excreted in the urine. An explanation for why the  $^3\text{H}$  level was lower than  $^{125}\text{I}$  level in the kidney up to 72 hours after injection, could be that the isotopes only appeared in the kidney after the conjugate had been degraded. It has already been ascertained that the  $^{125}\text{I}$  excreted in the urine was present as low molecular weight species (less than 1600 molecular weight by FPLC). Degradation of the conjugate into low molecular weight polypeptide fragments was expected to occur in the liver. The fate of the two isotopes was different in this organ. After the conjugate had been taken up by the liver, the  $^{125}\text{I}$  could be released (and be distributed to the kidney), whereas the  $^3\text{H}$  activity appeared to accumulate. MTX is known to be polyglutamated within the liver<sup>(112)</sup> and the polyglutamated derivative cannot readily leave the cell. This fact could explain why the  $^3\text{H}$  activity appeared to be retained within the liver and thus could not reach the kidney. The accumulation of  $^3\text{H}$  activity at 96 hours could also be explained by a selective retention in this organ.

Levels of  $^{125}\text{I}$  activity in the stomach and small intestine were elevated compared to  $^3\text{H}$ , up to 72 hours after administration of the conjugate. By 96 hours the levels of  $^3\text{H}$  had begun to rise in the gastro-intestinal tract, and were similar to those of  $^{125}\text{I}$ . An interesting result was seen for the  $^{125}\text{I}$  isotope in the stomach and small intestine. The time when maximum levels were reached in the stomach was six hours, and the time for maximum levels to be reached in the intestine was 24 hours. Organ distribution was determined in different groups of animals for the two time points so this may be due to biological variation. However it may also be because the  $^{125}\text{I}$  that had reached the

stomach due to bile secretion into the intestine and then reflux from the intestine into the stomach, had passed back into the small intestine by 24 hours. The fact that  $^{125}\text{I}$  levels in the gut increased over 1 to 6 hours and  $^3\text{H}$  activity did not, supports the theory that the radioactivity had entered the gut via the bile. If the conjugate had been selectively taken up by the gut then levels of both isotopes would be expected to be similar at initial time points. In fact very little  $^3\text{H}$  activity appeared in the gut until 72 hours after administration of the conjugate. This was because  $^3\text{H}$  appeared to be retained by the liver so less could actually enter the bile.

#### **4.5 Summary of BSA-MTX Conjugates**

Figure 4.13.1 is a plot of Log serum  $^{125}\text{I}$  concentration versus time for  $^{125}\text{I}$ -labelled BSA, BSA-MTX (5.1%w/w) and BSA-MTX (11.76%w/w). The conjugates demonstrated a serum clearance profile that was similar to free BSA. However the plasma levels of free BSA were elevated compared to the conjugates. Table 4.13 summarises the pharmacokinetic data calculated following IV administration of each of the conjugates investigated.

**Table 4.13: Summary of the Pharmacokinetic data calculated after IV administration of each of the BSA-MTX conjugates to male wistar rats.**

Conjugate	(alpha phase)		(beta phase)	
	$t^{1/2}$ (hr)	Vd (ml)	$t^{1/2}$ (hr)	Vd (ml)
Free MTX	0.24	114.7	1.96	1615
Free BSA	3.37	18.9	22.3	26.6
3.4%w/w	1.69	17.8	18.7	34.9
5.1%w/w	3.78	13.6	21.3	75.2
6.2%w/w	2.89	18.7	17.1	124.8
7.16%w/w	2.71	20.6	25.3	228
9.18%w/w	1.97	31.8	25.5	594
11.74%w/w	1.60	41.0	29.0	564
11.76%w/w	0.88	8.11	29.4	160
13.63%w/w	1.51	7.96	33.0	458
13.64%w/w	2.45	66.0	33.0	369

Figure 4.13.1:

Serum Concentration of  $^{125}\text{I}$  activity following IV administration of 5mg of  $^{125}\text{I}$ -BSA,  $^{125}\text{I}$ -BSA-MTX (5.1%w/w) and  $^{125}\text{I}$ -BSA-MTX (11.76%w/w) to rats. Each point was obtained from a single rat. n=8 for each route.

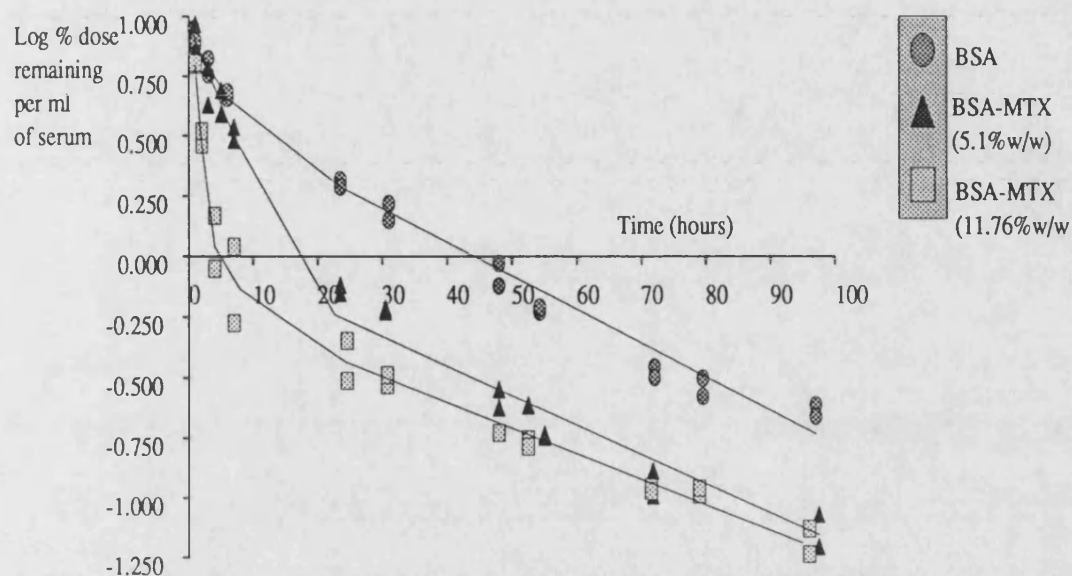
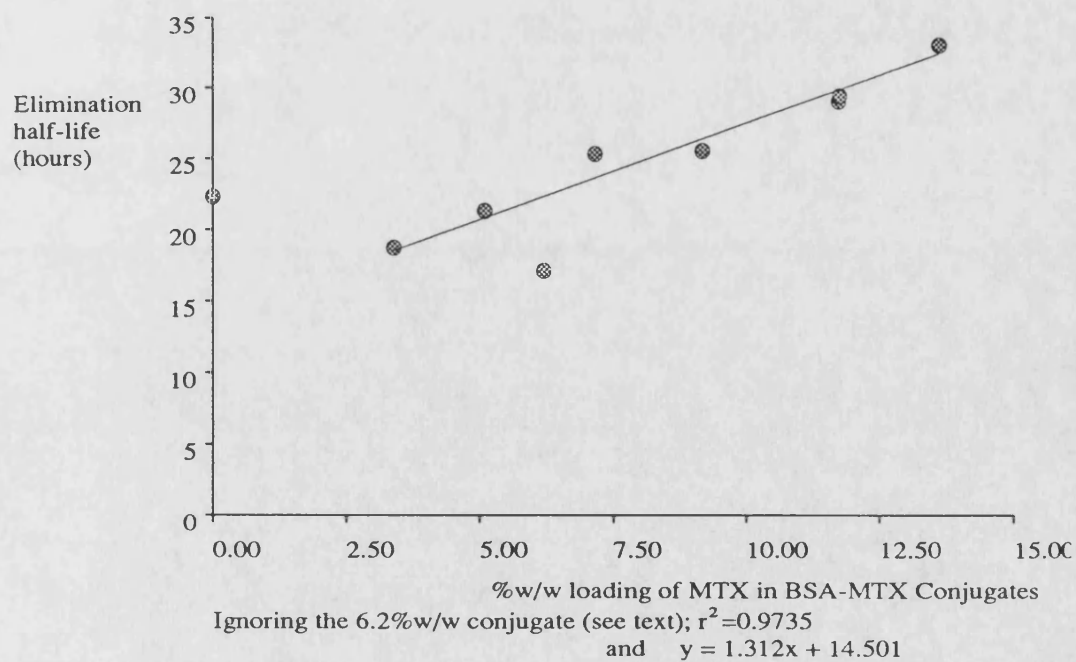


Figure 4.13.2 Serum Elimination Half-life of some BSA-MTX Conjugates versus the concentration of MTX in the conjugate.



There was a tendency during the beta phase for the Vd to increase with increased loading of MTX in the conjugate and every conjugate investigated demonstrated a larger Vd than free BSA.. It would appear that the BSA-MTX conjugates were more able to leave the vasculature. This may be due to a non-specific effect because of the changed character of the protein. The conjugate would be expected to be more hydrophobic than BSA because of the introduction of the large pteridine ring and this could increase its interaction with cell membranes e.g. the endothelial cells and aid its access out of the vasculature.<sup>(150)</sup> The conjugate would be more electro-negative than BSA because MTX was covalently bound to lysine residues in the BSA and in addition because MTX itself has a free carboxylic acid group. Covalent binding of MTX to BSA would be expected to alter the tertiary structure of the protein. All these factors may alter the distribution of BSA in the rat. In addition the Vd may be larger for the conjugates because of the specific effects of MTX. Protein bound MTX may still be able to interact with the folate transporter on cell surfaces. Mell et al <sup>(151)</sup> found that MTX bound to a soluble, large molecular weight carrier using a carbodiimide coupling reaction was still able to bind to DHFR, so this is a realistic possibility.

For the plasma half-lives, there was a tendency for the alpha phase half-life to be decreased compared to free BSA, thus the conjugates more rapidly equilibrated with the central compartment. Trouet et al<sup>(152)</sup> covalently bound daunorubicin to succinylated rabbit albumin using an ECDI reaction. They found that their conjugate, for which no loading of drug in the conjugate was mentioned, had a plasma distribution half-life of 91 minutes in the mouse, and this was very similar to the BSA-MTX conjugates with loadings above 9.2%.

At initial loadings of MTX in the conjugates there was a tendency for the MTX-BSA to have a more rapid elimination half-life than BSA. However, as MTX loading increased in the conjugate, half-life increased. Figure 4.13.2 is a plot of the elimination half-life versus %w/w loading of the conjugate. There appeared to be a linear relationship. One exception to this was the 6.2% w/w conjugate. This was prepared in a slightly different manner from the other conjugates. Instead of the reaction taking place in pH 7.4 buffer,

the reaction was carried out in water. This may have led to a difference in the conjugate produced.

MTX was bound to BSA to evaluate the effects of conjugation to a large molecular weight, soluble carrier, on the pharmacokinetics of the drug. MTX had a very large Vd when injected into rats (for both the alpha and beta phases). Thus, since it can reach many tissues in the body, this may contribute to the side effects of the drug. After conjugation to BSA, the Vd was reduced for every conjugate investigated, thus access into certain sites was limited and this could reduce the toxicity of the drug.

MTX had a very short half-life in the rat and BSA-MTX had a half-life which was at least 10 times that of free drug, and thus the conjugates may be able to act as a slow release formulation of the drug. Halbert et al<sup>(153)</sup> investigated the release of MTX from two BSA-MTX conjugates (3%w/w and 10%w/w). They found that only 10% of the MTX was released in a 72 hour incubation at pH 7.4. Thus the MTX would not be released from the conjugates, to any great extent, during circulation in the plasma. This is advantageous since the target for MTX is intracellular, and therefore in order to be cytotoxic, BSA-MTX would have to be internalised. By conjugating the MTX to BSA, entry of the drug into cells is limited to the process of pinocytosis. Fluid phase pinocytosis is a relatively slow process compared to receptor mediated pinocytosis.<sup>(70)</sup> If a targeting agent was bound to the conjugate, then it would be taken up by receptor mediated pinocytosis, and this may occur before fluid phase pinocytosis could occur in cells without the receptor.

Halbert et al<sup>(153)</sup> also investigated the stability of the conjugates at pH 5, the pH of the lysosome, and found that 16% of the MTX was released in 72 hours. This would not give a sufficient concentration of MTX to kill the cell, since it has been estimated that this requires 10 million molecules per cell.<sup>(154)</sup> However, within the lysosome there are numerous hydrolytic enzymes and these would be expected to break down the BSA-MTX with the liberation of free, active drug. Marriott<sup>(125)</sup> demonstrated the degradation of MTX-HSA when it was incubated with a solution of tritosomes and glutathione at pH 5.6. After 16 hours, 66% of the original conjugate was present as

species of less than 1500 molecular weight. In this chapter proof has been given that the conjugate was actually broken down *in vivo*, since small peptide fragments were found to be excreted in the urine, and also different organ distributions of the two isotopes were found following administration of the  $^{125}\text{I}$ -BSA- $^3\text{H}$ -MTX conjugate.  $^3\text{H}$ -MTX was selectively retained by cells, whereas  $^{125}\text{I}$  fragments were released and appeared in bile and urine.

The BSA-MTX conjugates were administered by three routes of injection i.e. IV, IP and SC. The rationale for employing IP injection was that diseases that are present within the cavity such as ovarian cancer or cancer of the intestine could be “attacked” immediately after injection.<sup>(155)</sup> Sub-cutaneous dosage was applied, because of the inability of the BSA-MTX conjugates to enter the blood stream directly after injection. Flessner et al<sup>(142)</sup> demonstrated, using FITC labelled dextrans and  $^{125}\text{I}$ -BSA, that molecules with a molecular weight above 39,000 were absorbed into the lymphatics and not into the blood stream after IP administration. They were transferred to the blood stream from the lymphatic system at one of the lymphatic ducts. Molecules with a molecular weight below 39,000 were absorbed from the peritoneal cavity partially by the blood stream and also by the lymphatics. Both SC and IP injection routes could be used to get drug into the lymphatic system and to treat metastatic cancer growths which have occurred within the lymphatic vessels. However, it was difficult to keep drug within the peritoneal cavity and lymphatic vessels. Peak plasma levels were achieved within 6 hours of IP administration and within 23 hours of SC administration for all conjugates administered. A targeting agent on the conjugate could influence the distribution, however and may result in the entire dose being taken up by the target organ before it reached the blood stream after SC or IP dosage.

Urine  $^{125}\text{I}$  excretion was determined for each of the  $^{125}\text{I}$  labelled conjugates. There was a tendency for an increase in iodine excretion as conjugate MTX loading was increased. Chu and Whiteley<sup>(99)</sup> measured the excretion of  $^{125}\text{I}$  activity following administration of  $^{125}\text{I}$ -BSA-MTX (8%w/w) in mice. They found that 55-60% of the dose was excreted in 24 hours. This was similar to the excretion determined for the 9.2% conjugate used in

this work, for which 51% was excreted in 24 hours. Chu and Whiteley<sup>(99)</sup> also administered a BSA-<sup>3</sup>H-MTX conjugate. They found a similar rate of excretion for the <sup>3</sup>H isotope as they did for the <sup>125</sup>I isotope. This is contrary to the results for the <sup>125</sup>I-BSA-<sup>3</sup>H-MTX experiment, where 51% of the <sup>125</sup>I was excreted but only 28.5% of the <sup>3</sup>H was excreted and this difference is difficult to explain. Figure 4.13.3 is a histogram showing the urine excretion at 24 hours and a later time point, usually 96 hours for MTX, BSA and the BSA-MTX. All conjugates were excreted more slowly than the MTX. Excretion of the conjugates was actually a measure of the metabolism since MTX-BSA has a molecular weight above the renal threshold. Also FPLC and GPC showed that any <sup>125</sup>I excreted in the urine was present as peptide fragments.

The molecular weight of the <sup>125</sup>I species in urine was determined for the 6.2%w/w conjugate by gel filtration and for the 7.16%w/w conjugate by FPLC. It was found that the molecular weight of the <sup>125</sup>I in urine for the 6.2%w/w conjugate was greater than 1000D. For the 7.16%w/w conjugate the majority of the activity was found to elute at the same time as iodinated tyrosine. Iodinated tyrosine was found to interact with the superose column and eluted at a time similar to potassium iodide. Thus the 7.16% conjugate was probably broken down into amino acid fragments before it was excreted. The 6.2%w/w conjugate was also degraded but the fragments were bigger than single amino acid units. The reason for this could be that the 6.2%w/w conjugate was metabolised in the kidney. (This conjugate was found to accumulate in the kidney after administration and this can be explained since it is known that proximal tubule cells of the kidney demonstrate a high uptake of protein, particularly if it is denatured<sup>(156)</sup>). The 7.16%w/w conjugate could have been metabolised to a greater extent by the liver before being transferred to the blood for excretion by the kidney. <sup>125</sup>I excretion in the urine appeared to increase with increased loading of MTX in the conjugate, indicating that the conjugate was metabolised more rapidly, as MTX loading was increased.

Organ distribution was determined for most of the conjugates administered. Figure 4.13.4 is a histogram comparing the liver uptake for each of the conjugates. There was an increased uptake by the liver compared to free BSA for all of the conjugates

Figure 4.13.3: Percentage of  $^{125}\text{I}$  activity excreted in the urine of rats dosed with an IV injection of  $^{125}\text{I}$ -labelled protein or conjugate or with 2.5mg of MTXNa followed by HPLC detection.

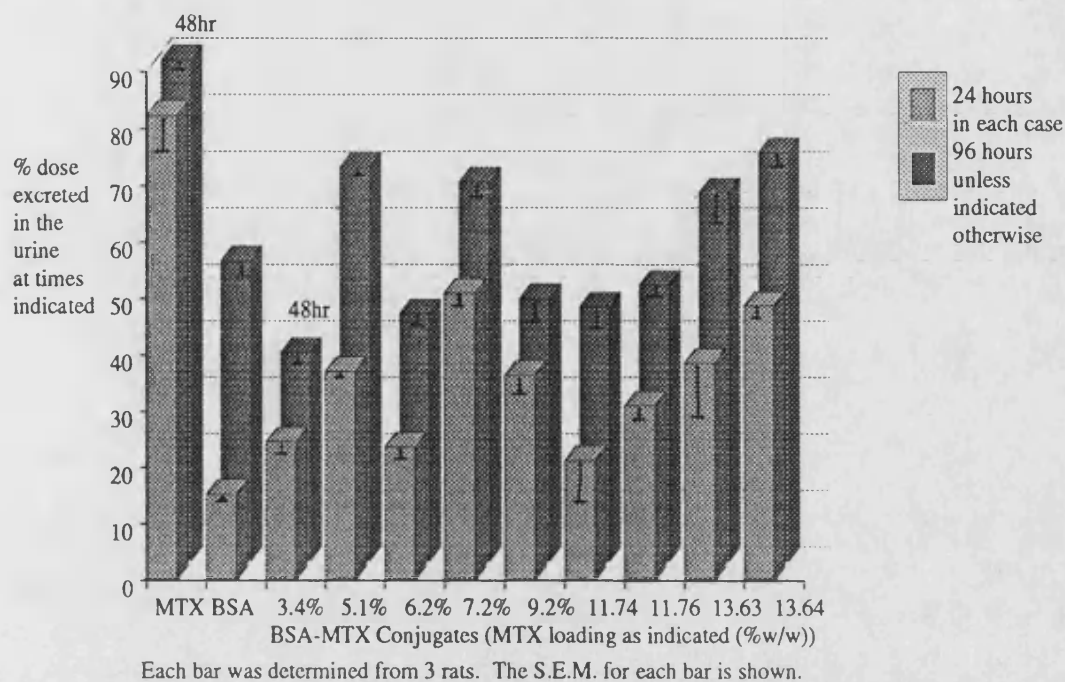
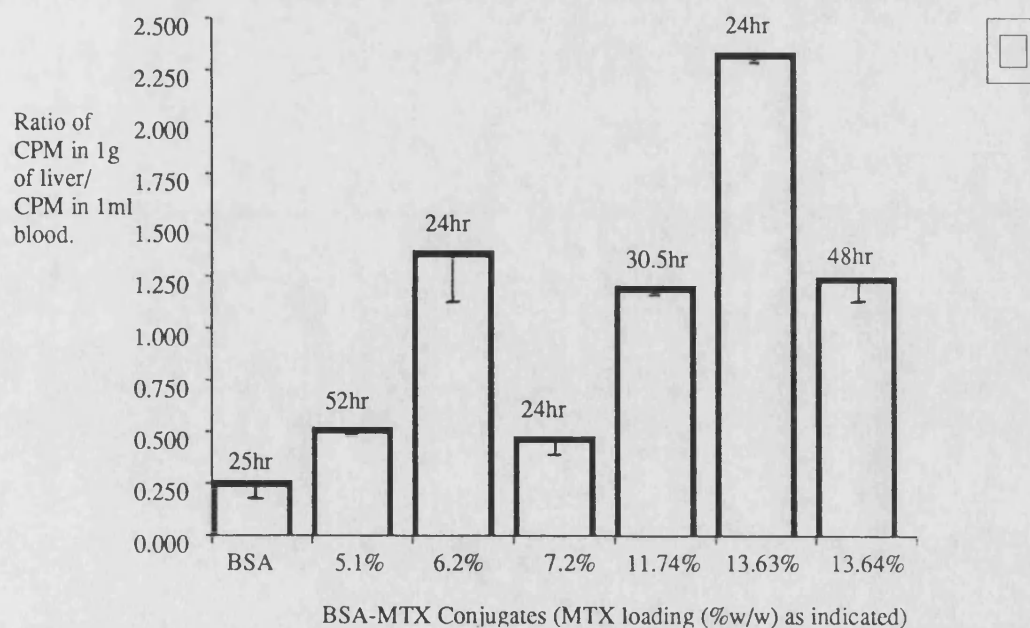


Figure 4.13.4: Accumulation of  $^{125}\text{I}$  activity in 1g of liver following IV administration of 5mg of  $^{125}\text{I}$  labelled BSA or conjugate. Each bar was determined from 2 rats. Analysis was at time point stated. The range for each rat is shown.





investigated. There appeared to be a tendency for the ratio (of activity in the liver divided by the activity in 1ml of blood) to increase as the concentration of MTX in the conjugate increased. In addition the percentage of conjugate present as aggregated protein tended to increase with increased MTX loading and this may explain the increased uptake. Fiume et al<sup>(157)</sup> demonstrated that a phalloidin-Rabbit serum albumin conjugate (with 0.8 to 1.9 phalloidin residues per albumin molecule) and conjugates between cytosine arabinoside or 5-fluorodeoxyuridine (FUDR) and Rabbit SA<sup>(158,159)</sup> were taken up by the liver after administration in mice. The conjugates were found mainly in the non-parenchymal cells and also in other cells of the RES. Fiume's conjugates consisted of nearly entirely aggregated protein and thus would have been recognised as foreign by the RES and this would have resulted in the uptake of the conjugates. The BSA-MTX conjugates used in the present study had less than 35% of the conjugate present as polymers. In a comparative experiment, where Fiume administered a conjugate between FUDR and albumin which had been prepared using the hydroxysuccinimide ester of the albumin, no liver uptake was demonstrated. This conjugate did not contain any aggregated material.<sup>(157)</sup> This suggests that the accumulation of the BSA-MTX in the liver demonstrated in these experiments may not be due to the aggregated protein as first thought, since the BSA-MTX had less aggregated protein than the original conjugates produced by Fiume. Chapter 5 describes an experiment to determine in which liver cell type the BSA-MTX accumulated in (see section 5.2) is described.

In addition to accumulation in the liver, the BSA-MTX conjugates were also taken up by the spleen, the gut and to a lesser extent the kidney. Again, there seems to be relationship between the concentration of MTX in the conjugate and the amount of <sup>125</sup>I taken up. As mentioned previously, the increased uptake could be due to the non-specific effect of changing the characteristics of BSA which had led to uptake by cells of the RES. Another explanation could be that MTX bound to the BSA, helped the conjugate to enter the cells by using the folate transporter system.

Following liver uptake, the <sup>125</sup>I activity would be expected to be transferred into the

bile. Analysis of the bile following administration of  $^{125}\text{I}$ -BSA-MTX (11.55%w/w) showed that quite a high percentage of the injected dose was present in it (1.3%/ml) at 3 hours after injection and this explained why elevated levels of  $^{125}\text{I}$  were found in the gut. FPLC analysis showed that a high proportion of the radioactivity was present either as iodinated tyrosine or  $^{125}\text{I}$  -Na, thus indicating that conjugate taken up by the liver was degraded. There was no relationship between the % of activity excreted in the faeces and the %w/w loading of MTX in the conjugate. Approximately 8-12% of the  $^{125}\text{I}$  dose was excreted in 96 hours. Thus  $^{125}\text{I}$  may be reabsorbed from the gut since conjugates which had been taken up by the liver to a greater extent did not demonstrate greater loss of activity in the faeces.

#### **4.6 Other Protein-MTX Conjugates.**

##### **4.6.1 LA-MTX Conjugates.**

LA, as a lower molecular weight protein, was covalently bound to MTX and administered to the rat, and the effects on distribution of the drug were compared to BSA-MTX. Two LA-MTX conjugates were administered to rats. These had %w/w loadings of MTX of 4.52% and 13.69%. They were prepared by reacting 1 molar equivalent of protein with 10.7 or 20 molar equivalents of MTX respectively. Tables A3.22.1 and A3.23.1 list the serum levels determined for each route of injection for the 4.52%w/w and 13.69%w/w conjugates respectively. Figures 4.14.1 and 4.14.2 are plots of Log serum  $^{125}\text{I}$  concentration versus time for each conjugate, for the three routes of injection. Like 'free' LA itself, peak serum levels were achieved very rapidly after IP and SC injection (within 2 hours). Conjugation of MTX to the LA increased the molecular weight of the protein but only from 14200 to 14774 for LA-MTX (4.52%w/w) and to 16243 for LA-MTX (13.69%w/w) and so it is possible that these conjugates could still enter the blood stream directly from extravascular sites. Following IV injection a biexponential plasma clearance was seen. The pharmacokinetic parameters calculated for each route of administration and both conjugates are shown in table 4.14.1.

Figure 4.14.1

Concentration of  $^{125}\text{I}$  activity in serum following administration of 5mg of  $^{125}\text{I}$ -LA-MTX (4.52%w/w) to rats by IV, IP and SC routes. Each value was determined from one rat. (n=8 for each route.)

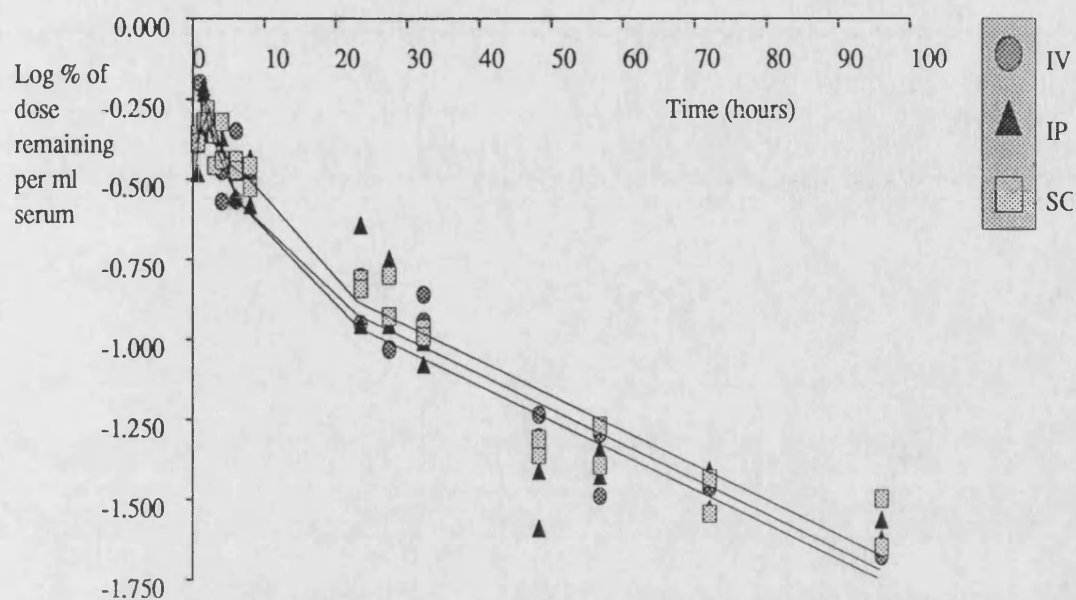
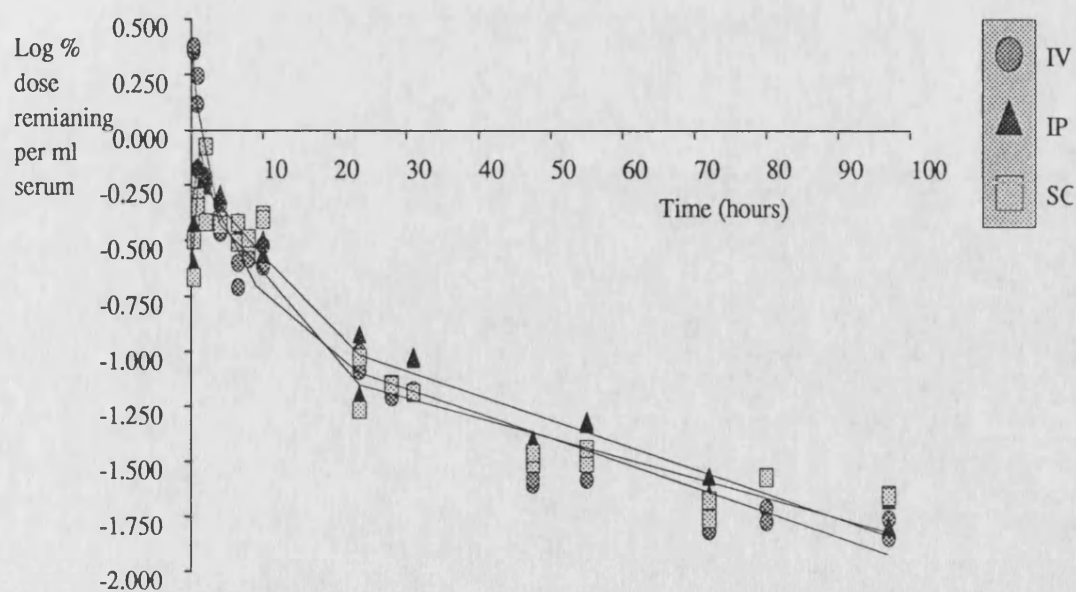


Figure 4.14.2:

Serum Concentration of  $^{125}\text{I}$  activity following administration of 5mg of  $^{125}\text{I}$ -LA-MTX (13.69%w/w) to rats by IV, IP and SC routes. Each point was determined from a single rat. (n=8 for IV and SC, n=6 for IP).



**Table 4.14.1: The Pharmacokinetic parameters for the LA-MTX (4.52%w/w and 13.69%w/w) conjugates following IV, IP and SC administration to rats.**

	IV (alpha)	IV (beta)	IP (beta)	SC (beta)
<u>1. 4.52%w/w</u>				
time span (hr)	1-8	23.5-96	23.5-96	23.5-96
R <sup>2</sup>	0.3339	0.8956	0.7163	0.8621
m* (hr <sup>-1</sup> )	-0.049±0.0199	-0.0109±0.0011	-0.01095±0.0013	-0.0109±0.0013
c* (log Co)	-0.516±0.0868	-0.672±0.0606	-0.687±0.112	-0.644±0.0711
n <sup>#</sup>	14	14	14	14
Kel (hr <sup>-1</sup> )	0.113	0.0251	0.0252	0.0251
t <sup>1/2</sup> (hr)	6.14	27.6	27.5	27.6
Vd (ml)	328	469	486	441
Cl (ml/hr)	37.1	11.8	12.3	11.1
<u>2. 13.69%w/w</u>				
time span (hr)	0.33-6.5	23.5-97	23.5-97	23.5-97
R <sup>2</sup>	0.9176	0.8605	0.8315	0.7961
m* (hr <sup>-1</sup> )	-0.198±0.0209	-0.105±0.0011	-0.00993±0.0014	-0.00785±0.0011
c* (log Co)	0.280±0.0744	-0.916±0.067	-0.840±0.0844	-0.994±0.063
n <sup>#</sup>	11	16	12	16
Kel (hr <sup>-1</sup> )	0.456	0.0242	0.0229	0.0181
t <sup>1/2</sup> (hr)	1.52	28.66	30.30	38.33
Vd (ml)	52.5	824	693	986
Cl (ml/hr)	23.94	19.94	15.86	17.85

Notes: \* Slopes and Constants are quoted ± Standard Error.  
# n = number of points used in the calculation.

The parameters calculated for the elimination phases were similar for the IV and IP routes of administration. Both conjugates demonstrated a large  $V_d$  for this phase which was at least twice the body volume of a rat. Following SC administration the 13.69%w/w conjugate displayed similar pharmacokinetics to free LA administered SC but not to the other routes of administration for the conjugate. The half-life for free LA, following SC administration, was 39.1 hours and the  $V_d$  was 530ml. The reason for the longer half-life seen for SC dosed rats must be that protein and conjugate were still being transferred from the injection site during the elimination phase. However figure 4.14.2 shows that the serum levels determined over the elimination phase were very similar for each route of injection for the 13.69%w/w conjugate, and so the large differences in  $t^{1/2}$  calculated between IV and SC injection may be associated, at least partly, with the errors involved in the calculation.

Tables A3.22.2 and A3.22.3 list the urine and faeces excretion of  $^{125}\text{I}$  following administration of the  $^{125}\text{I}$ -LA-MTX (4.52%w/w), over 96 hours. There was no significant difference in the urine excretion of  $^{125}\text{I}$  activity between any of the routes of administration at any time point. 54-60% of the total dose was excreted in 96 hours. Excretion in the faeces accounted for between 6.6 and 10% of the total activity in 96 hours. The results for urine and faecal excretion of the high strength conjugate are shown in tables A3.23.2 and A3.23.3 respectively. Again there was no significant difference in the amount of  $^{125}\text{I}$  activity excreted for any route of injection. Approximately 7-10% of  $^{125}\text{I}$  injected was excreted in the faeces over 96 hours and between 47 and 54% was excreted in the urine over 96 hours. Figure 4.14.3 is a plot of the %  $^{125}\text{I}$  activity excreted in the urine over 72 hours for  $^{125}\text{I}$ -labelled LA, LA-MTX (4.52%w/w) and LA-MTX (13.69%w/w) following IV injection. At the 24 hour time point there appeared to be a greater % of the  $^{125}\text{I}$  excreted by the groups of conjugate dosed rats than the free LA dosed rats. A Student's t-test was used to compare the excretion of  $^{125}\text{I}$  activity for each group of rats (each group included all routes of injection) at 24 hours and 72 hours after administration. At both time points and for both conjugates and the free LA, the results of the Student's t-test were non-significant ( $p > 0.05$ ).

Figure 4.14.3: Percentage of  $^{125}\text{I}$  activity excreted in the urine following IV administration of  $^{125}\text{I}$ -LA,  $^{125}\text{I}$ -LA-MTX (4.52%w/w) and  $^{125}\text{I}$ -LA-MTX (13.69%w/w) to rats. Each point is a mean  $\pm$  S.E.M. (n=3).

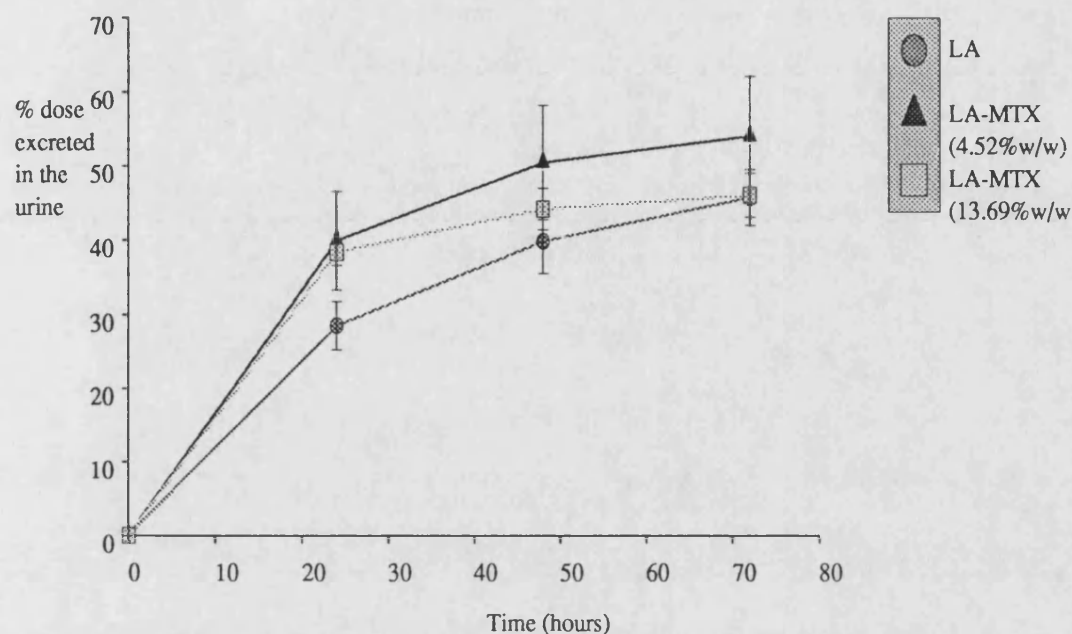


Figure 4.14.4: Concentration of  $^{125}\text{I}$  activity in serum following administration of 5mg of  $^{125}\text{I}$ -LA,  $^{125}\text{I}$ -LA-MTX (4.52%w/w) and  $^{125}\text{I}$ -LA-MTX (13.69%w/w) to rats by IV injection. Points were determined from a single rat.

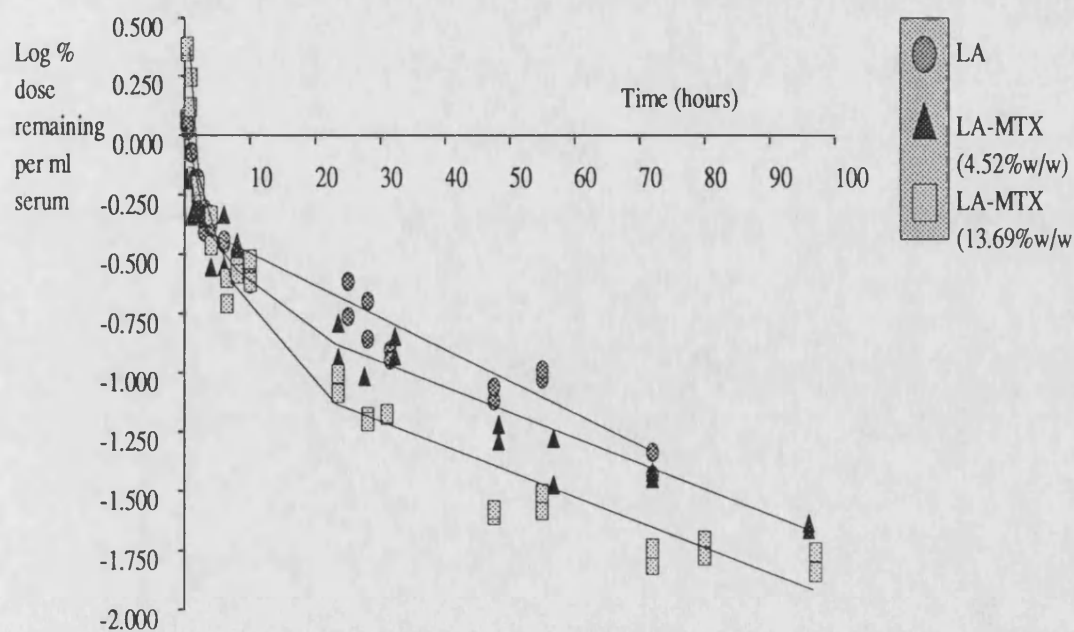


Figure 4.14.4 is a plot comparing the  $^{125}\text{I}$  serum levels determined after IV administration of  $^{125}\text{I}$  labelled LA and both conjugates. The LA showed elevated serum levels compared to the conjugates, indicating that it had a smaller volume of distribution. Table 4.14.2 summarises the pharmacokinetic parameters calculated for IV dosed rats for LA and LA-MTX.

**Table 4.14.2 The Pharmacokinetic parameters calculated for LA, LA-MTX (4.52%w/w) and LA-MTX (13.69%w/w) after IV administration to Rats.**

	Alpha Phase		Beta Phase	
	t <sub>1/2</sub> (hr)	V <sub>d</sub> (ml)	t <sub>1/2</sub> (hr)	V <sub>d</sub> (ml)
LA	0.943	111	21.6	236
LA-MTX (4.52%w/w)	6.14	328	27.6	469
LA-MTX (13.69%)	1.52	52.5	28.7	824

Like conjugates between MTX and BSA, covalent conjugates of LA-MTX demonstrate different pharmacokinetics to the free protein. These differences follow a similar pattern to BSA-MTX. During the elimination phase conjugates were shown to have a longer half-life and a larger V<sub>d</sub> than 'free' protein. There appeared to be a relationship between concentration of MTX in the conjugate and the increase in these parameters, although too few conjugates were administered to make any firm conclusions. During the alpha phase there did not appear to be a relationship between the loading of MTX in the conjugate and the changes in pharmacokinetic parameters compared to free LA. LA-MTX (13.69%w/w) had a similar alpha phase half-life but its V<sub>d</sub> was half that of free LA. The LA-MTX (4.52%w/w) had an alpha phase half life which was 6 times longer than that of free LA, and its V<sub>d</sub> was approximately three times larger. (The regression coefficient for the plot used in the calculation of the parameters for the alpha phase for 4.52%w/w conjugate was only 0.3339 and so the parameters calculated are associated with a large error). Unfortunately organ distribution was not determined for the LA-MTX conjugates so it is not known whether the changes in V<sub>d</sub> were associated

with accumulation in organs of the RES or were due to uptake by the kidney.

In the 13.69%w/w conjugate, 4.5 moles of MTX were associated with 1M of protein. In the 4.52%w/w conjugate only 1.3 moles of MTX were bound to 1 mole of LA. The low strength conjugate would probably demonstrate a difference in tertiary structure compared to free LA but its hydrophobicity and molecular charge would not be expected to be changed to any great extent. It is difficult to predict what effects this would have on the distribution of LA, since it is a milk protein and so which would not normally be found in rat serum anyway. The 13.69%w/w conjugate would be expected to differ from LA in its hydrophobicity and electrical charge, in addition to changes in tertiary structure. These differences probably accounted for the changes in pharmacokinetic parameters calculated for the conjugate. The increased beta phase Vd for the conjugates was possibly due to uptake by the liver, as demonstrated for BSA-MTX conjugates. Free LA, although it was a foreign protein, was not found to be associated with the rat liver at 28 hours after injection.

Both LA-MTX conjugates investigated demonstrated lower Vd, and longer elimination half-lives, than free MTX. However these differences were not as great as those for BSA-MTX. Thus BSA was probably a better choice as a carrier of cytotoxic drugs than LA. The beneficial effect of BSA was possibly due to its greater molecular weight. The aim of a drug-targeting complex is to prevent the premature removal of drug via the kidney and to limit cellular uptake to the process of pinocytosis.<sup>(57)</sup> In practice the ideal conjugate should combine characteristics which would allow it to extravasate at its site of action but also limit its urinary excretion. Although the LA-MTX would be expected to enter cells only by the process of pinocytosis and also it would be able to leave the blood stream (this was demonstrated by the rapid uptake into the vasculature following IP and SC administration), with a molecular weight of approximately 16,000 it would also be expected to be excreted unchanged from the kidney.

#### **4.6.2 RSA-MTX.**

One conjugate was prepared between RSA and MTX. The concentration of MTX in the



reaction was 100 molar equivalents to 1 molar equivalents of protein. This resulted in the preparation of a conjugate of 6.94%w/w MTX. (9.3 molar equivalents of MTX were covalently bound to 1 molar equivalent of RSA). The conjugation efficiency was considerably less than for BSA-MTX. Using the same ratio of reactants a conjugate containing 17.64 molar equivalents of MTX to 1 molar equivalents of BSA was prepared. Unfortunately there is no data available on the structure of RSA but it would be expected to be different from BSA and it may contain less lysine residues than BSA. A conjugate between CA and MTX was attempted using the same reaction conditions as for BSA-MTX. However, although the CA was expected to have a number of lysine residues (human CA contains 18, compared to BSA which has 59 but is twice its size)<sup>(160)</sup>, very little MTX actually reacted with it. It was assumed that the lysine residues in CA were sterically hindered so that they could not react with the large MTX molecule.

The RSA-MTX (6.94%w/w) was analysed by FPLC and found to contain a low percentage of aggregated protein, 18.4% of the total protein being aggregated. The conjugate was radioiodinated and administered to rats by IV injection. The serum levels determined for <sup>125</sup>I activity are shown in Table A3.24.1. Figure 4.15.1 is a plot comparing the serum levels determined following administration of free RSA and RSA-MTX by IV injection. The serum clearance of RSA-MTX followed a biexponential model. The serum levels determined over 96 hours were considerably lower for the conjugate than for the free protein. Table 4.15 lists the pharmacokinetic parameters calculated for the RSA-MTX and RSA.

The pharmacokinetic parameters calculated for the distribution phase were very similar for RSA and the RSA-MTX. RSA-MTX had a slightly faster distribution half-life, but the Vd was not significantly different. During the elimination phase, the half-life for the RSA-MTX was shorter (31.7hr for RSA-MTX compared to 38.4hr for RSA). The Vd for the elimination phase for the conjugate was ten times larger than that calculated for RSA. This significant difference could be due to changes in the protein characteristics or could be due to a specific action of MTX, as already described for BSA-MTX conjugates.

Figure 4.15.1 Serum concentration (log %  $^{125}\text{I}$  activity remaining/ml) after administration of 5mg of  $^{125}\text{I}$ -RSA or 5mg of  $^{125}\text{I}$ -RSA-MTX (6.94%w/w) to male wistar rats.

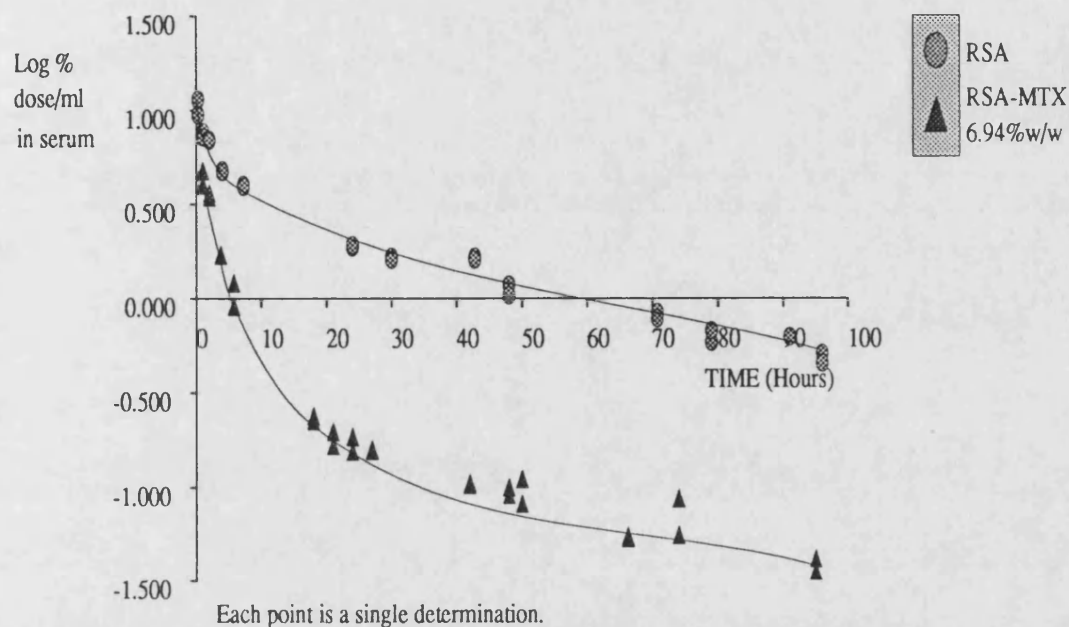
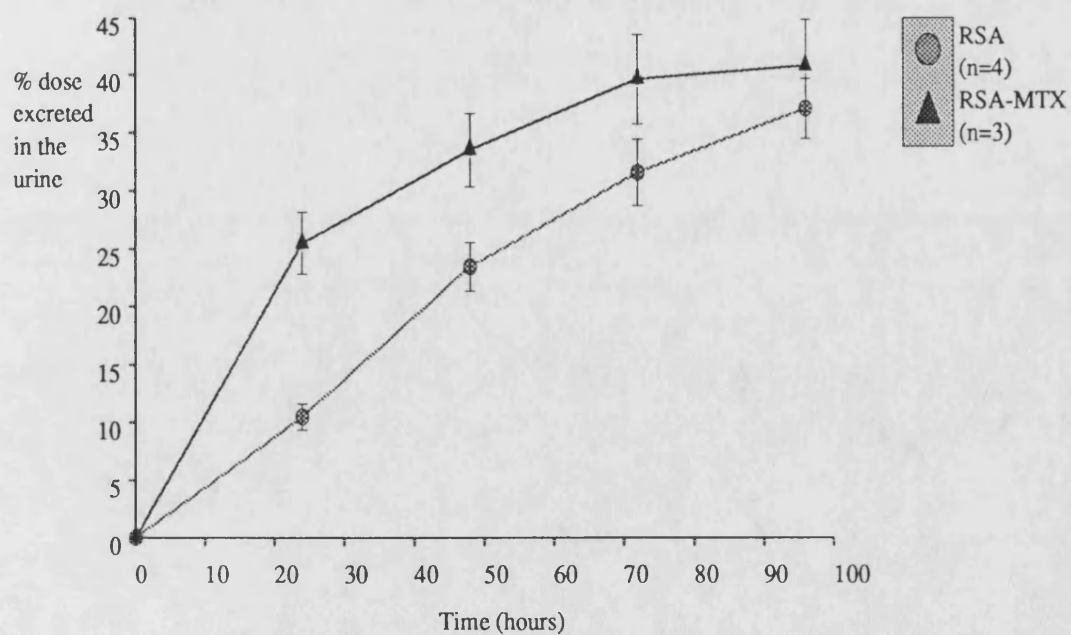


Figure 4.15.2: Percentage of  $^{125}\text{I}$  activity excreted in the urine following IV administration of 5mg of  $^{125}\text{I}$ -RSA or 5mg of  $^{125}\text{I}$ -RSA-MTX (6.94%w/w) to rats. Each point is a mean  $\pm$  S.E.M..



**Table 4.15 The Pharmacokinetic Parameters Calculated for RSA-MTX and RSA following IV administration to Rats.**

	Alpha Phase		Beta Phase	
	RSA	RSA-MTX	RSA	RSA-MTX
time span (hr)	0.25-7.25	1-5.75	18.75-97	18-95
R <sup>2</sup>	0.9130	0.9625	0.9628	0.9230
m*	-0.0957±0.0104	-0.157±0.00122	-0.0078±0.0004	-0.0095±0.00065
c*	0.818±0.0401	0.765±0.0455	0.446±0.0223	-0.557±0.0339
n#	10	8	20	20
Kel (hr <sup>-1</sup> )	0.220	0.362	0.018	0.022
t <sub>1/2</sub> (hr)	3.144	1.917	38.4	31.7
Vd (ml)	15.2	17.15	35.8	360
Cl (ml/hr)	3.34	6.212	0.644	7.885

Notes: \* Slopes and constants are quoted ± Standard Error. # n=number of points used in the calculation.

Tables A3.24.2 and A3.24.3 list the urine and faeces excretion of <sup>125</sup>I activity following administration of radioiodinated conjugate. Approximately 41% of the injected radioactivity was excreted in the urine and 10% was excreted in the faeces over 96 hours. Figure 4.15.2 is a plot of % <sup>125</sup>I excreted in the urine of rats that had been injected with the <sup>125</sup>I labelled conjugate or with RSA. At 24 hours the % excreted by RSA dosed rats was significantly less than RSA-MTX dosed rats (p<0.02). However by the 96 hour time point the difference non-significant.

Organ distribution of <sup>125</sup>I activity was determined for the RSA-MTX conjugate at 24 and 48 hours after administration. The results are listed in table A3.24.4. Figure 4.15.3 is a histogram showing the ratio (activity in 1g of organ divided by activity in 1ml of whole blood) for each of the organs investigated at 24 hours and 48 hours. The ratio in

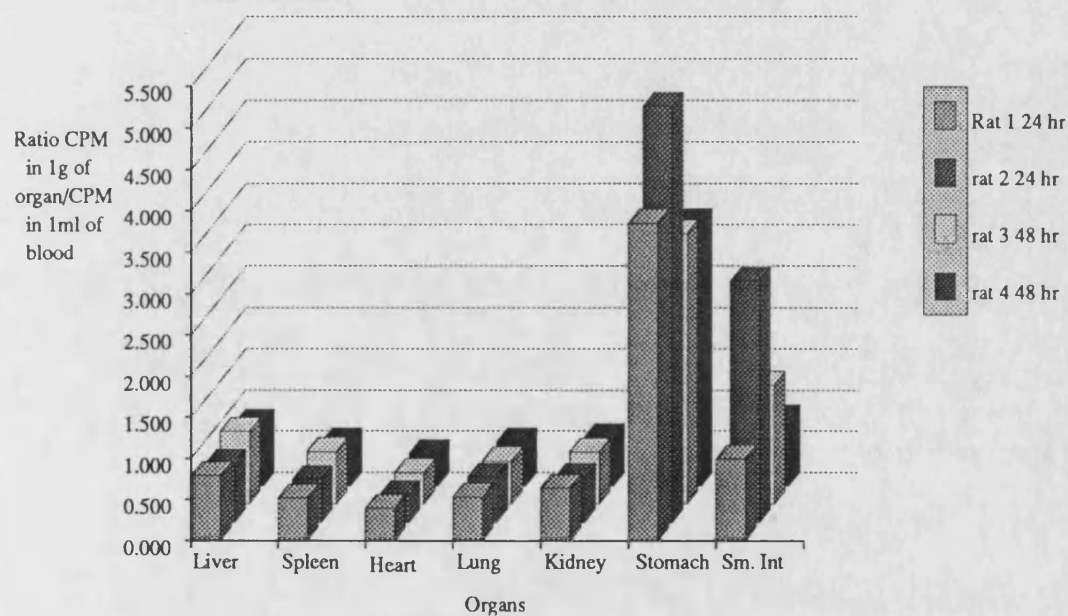
the organs was approximately the same at both time points. The activity in all the organs investigated, apart from the gut, was low and was possibly due to the blood within the organ. The stomach demonstrated higher levels than the small intestine. The ratio in the stomach for the 4 rats investigated was  $3.84 \pm 0.426$  and in the intestine was  $1.55 \pm 0.48$ . This was an unexpected result since activity in the gut was thought to occur due to bile secretion and the bile duct opens out into the intestine. Other workers have also demonstrated high levels in the stomach following administration of  $^{125}\text{I}$ -BSA<sup>(143)</sup>. This effect could be explained by reflux of the intestinal contents into the stomach.

The RSA-MTX did not appear to accumulate in the liver anymore than RSA did itself. The ratio (activity in 1g/activity in 1ml of blood) was similar for both RSA and RSA-MTX. (Ratio for RSA in the liver was 0.616 and 0.710 for the two rats investigated at 96 hours and for RSA-MTX was  $0.79 \pm 0.035$  for 4 rats at 24 and 48 hours). However, direct comparison of RSA and the conjugate at the time points of 24 and 96 hours may not be valid since an increase in accumulation of  $^{125}\text{I}$  activity in liver at 97 hours compared to 24 hours was noted for BSA and may also occur for RSA. Indeed, the ratios in the liver were similar for the RSA-MTX and the BSA-MTX (7.16%w/w) conjugate and so it is possible that the RSA was taken up to a small extent by the liver.

The conjugates prepared from BSA and MTX tended to accumulate in the liver (see Figure 4.13.4, page 159) and this accumulation appeared to be associated with the concentration of MTX in the conjugate. The accumulation of the conjugate in the liver may also have been associated with the percentage of protein aggregates that were present in the conjugate since these also tended to increase with increased loading of MTX in the BSA conjugates. The fact that the RSA-MTX had a low percentage of aggregates and only a low accumulation in the liver was seen supports the latter theory. The RSA-MTX conjugate demonstrated similar pharmacokinetics after IV administration, as did the BSA-MTX conjugates of similar MTX loading. It also tended to accumulate in the gut, as did some of the BSA-MTX conjugates (e.g. BSA-MTX 11.74%w/w and 13.63%w/w). Thus it appeared to be treated in vivo in a similar manner to the BSA conjugates. This may be because, after coating the RSA molecule with MTX, it is indistinguishable from BSA-MTX.

Figure 4.15.3:

Organ distribution of  $^{125}\text{I}$  activity following IV administration of 5mg of  $^{125}\text{I}$ -RSA-MTX (6.94%w/w) to rats. Values were determined at 2 time points and are a ratio of the activity in 1g of organ divided by the activity in 1ml of blood. Each bar was determined from one animal.



## **CHAPTER 5:**

### **VISUALISATION AND BODY DISTRIBUTION OF THE CONJUGATES**

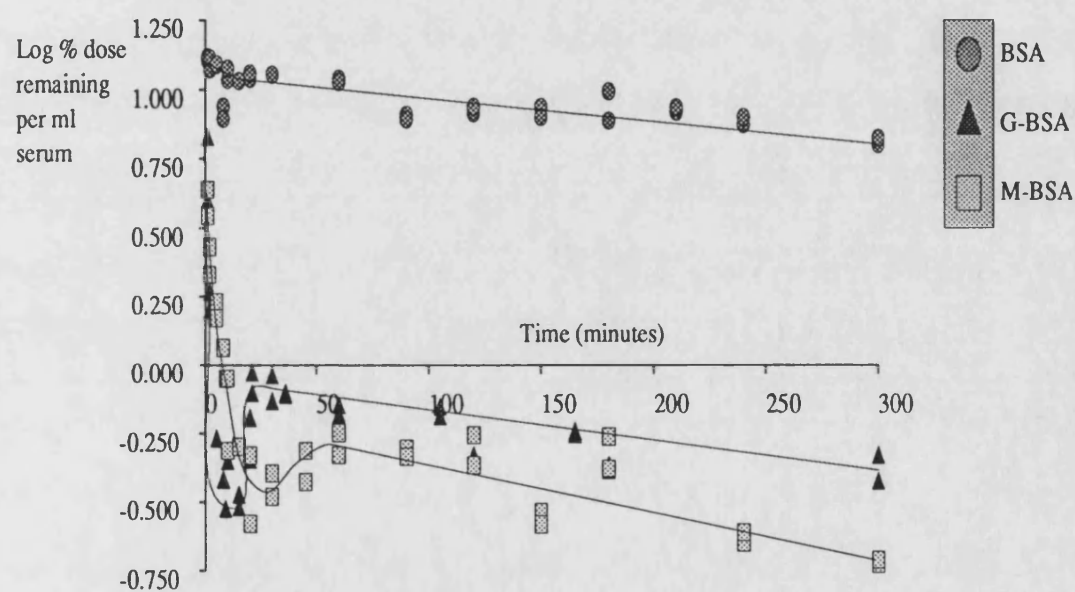
## **5.1 Targeting to the liver**

In the previous chapter the pharmacokinetics of conjugates between MTX and proteins (BSA, LA and RSA) were described. The distribution of the conjugates was determined over a period of 96 hours. The next step seemed to try to target the conjugates and the galactose and mannose receptors found on hepatocytes, and macrophages were chosen as the receptors for targeting. In this chapter the distribution of conjugates between BSA and galactosamine or mannose are described. In addition, the distribution of two BSA-MTX conjugates at time points up to 6 hours after administration is described using both organ distribution and whole body autoradiography.

### **5.1.1 G-BSA and M-BSA.**

G-BSA and M-BSA were obtained from Sigma and contained 26 moles galactosamine or 28 moles mannose per mole of BSA. These were administered to rats as described in section 2.9. Tables A3.28.1 and A3.29.1 show the  $^{125}\text{I}$  serum levels determined following administration of  $^{125}\text{I}$ -labelled G-BSA and M-BSA respectively, over 300 minutes after administration. The serum levels were compared to those of 'free' BSA (table A3.25.1). Figure 5.1.1 is a plot of log serum concentration versus time for the two conjugates and BSA. The concentration of  $^{125}\text{I}$ -BSA in serum only dropped from 13% of the injected dose per ml at 1 minute after injection to 10.8%/ml after 15 minutes, an actual loss of only 17% of the injected dose. For the G-BSA conjugate the levels dropped from 5.23%/ml at 1 minute to 0.3%/ml at 15 minutes. This represented a loss of 94% of the original serum concentration. The serum concentrations for M-BSA over the experimental period were similar to those of G-BSA. At 1 minute after injection the concentration of  $^{125}\text{I}$ -M-BSA was 3.6%/ml and at 15 minutes after injection was 0.5%/ml. This represented a loss of 86% of the dose. Both G-BSA and M-BSA rapidly left the vasculature after IV injection. The loss of serum activity for G-BSA was similar to that shown by Duncan et al<sup>(65,66,161)</sup>, for rats that had been injected with HPMA copolymers to which had been bound galactosamine linked via a diglycyl spacer (4mol% galactosamine per HPMA) and to that described by Stowell and Lee<sup>(162)</sup> for G-BSA and M-BSA (30 moles to 1 mole) in female wistar rats.

Figure 5.1.1:  
Concentration of  $^{125}\text{I}$  activity in serum following administration  
of  $250\mu\text{g}$  of  $^{125}\text{I}$ -BSA,  $^{125}\text{I}$ -M-BSA and  $^{125}\text{I}$ -G-BSA to rats by  
the IV route. Each point was determined from one rat. (n=10 for each protein)





Organ distribution of  $^{125}\text{I}$  activity was determined for BSA, G-BSA and M-BSA at various time points up to 5 hours after injection. The results are listed in tables A3.25.2, A3.28.2 and A3.29.2 respectively. The reason for the rapid loss of  $^{125}\text{I}$  activity from serum for both the G-BSA and M-BSA became evident on examination of the organ distribution results. Figures 5.1.2 and 5.1.3 show the organ distribution of  $^{125}\text{I}$  following administration of G-BSA to rats at 15 minutes after injection and at 5 hours. At 15 minutes the majority of the  $^{125}\text{I}$  dose was found to be located within the liver. For the two rats investigated at this time point, the actual % of the injected dose present within the whole liver were 81.2% and 87.6%. The spleen had taken up approximately 2.5% of the injected dose and when compared weight for weight to the liver, the spleen had taken up approximately half as much as the liver. The percentage of activity present within the heart could be attributed to the blood pool within this organ. For the other organs investigated,  $^{125}\text{I}$  levels within the organ were greater than could be attributed to the contribution of the blood pool. The organ distribution of G-BSA was similar to that described for galactosamine linked to HPMA (G-HPMA) (11 mol%)(<sup>161</sup>) (where 90% of injected dose was found in liver within 10 minutes). At 5 hours after injection, the distribution pattern for the  $^{125}\text{I}$  activity had changed. The percentage within the whole liver had fallen to 2.3% of the injected dose. It is possible that this activity could have been due to the blood within the organ. Indeed for all the organs investigated apart from the gut, the activity present in each organ at 5 hours was probably due to the blood pool within the organ. Duncan et al(<sup>65</sup>) also measured levels of radioactivity at 5 hours after injection for G-HPMA and found a similar redistribution pattern as described here.

In the stomach and small intestine the  $^{125}\text{I}$  levels were elevated compared to the other organs. There was approximately 10% of the injected dose present in both the stomach and small intestine at 5 hours after injection. At 15 minutes after injection the total % of  $^{125}\text{I}$  activity present in the stomach and small intestine ranged from 0.9 to 3 %. This had increased at 30 minutes after injection to between 1.6% and 12% and at 1 hour after injection the activity within the gut appeared to peak (actual concentrations were 11 to 22% of the dose in both the stomach and small intestine). The reason for the progressive accumulation of the  $^{125}\text{I}$  in the gut with time was attributed to bile secretion following

Figure 5.1.2:

Organ Distribution of  $^{125}\text{I}$  activity, 15 minutes after administration of 250 $\mu\text{g}$  of  $^{125}\text{I}$ -G-BSA to rats by the IV route. Each bar was determined from a single rat. Results are expressed as a ratio of activity in 1g of organ divided by activity in 1ml of blood.

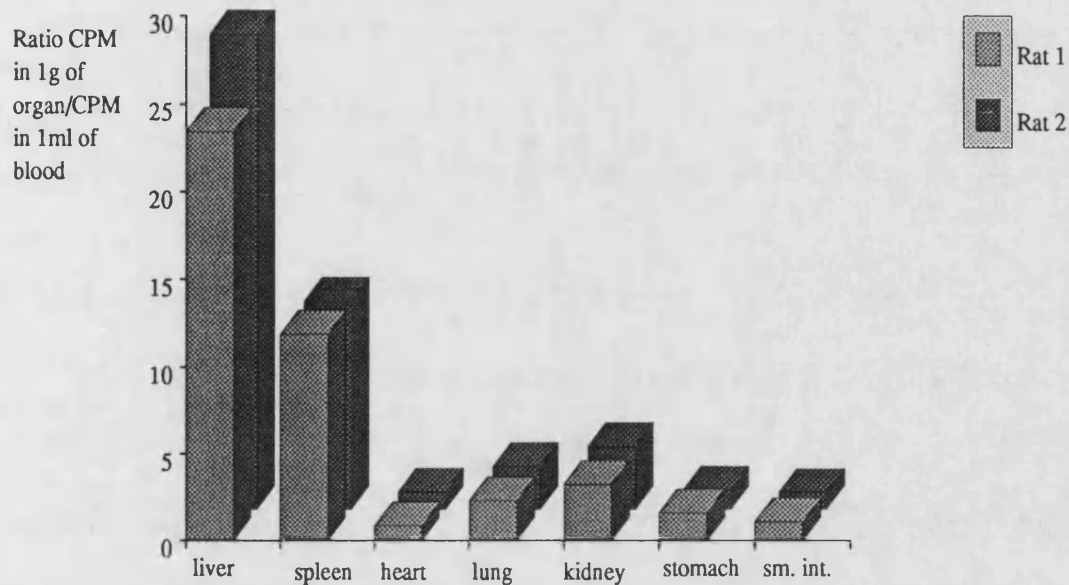
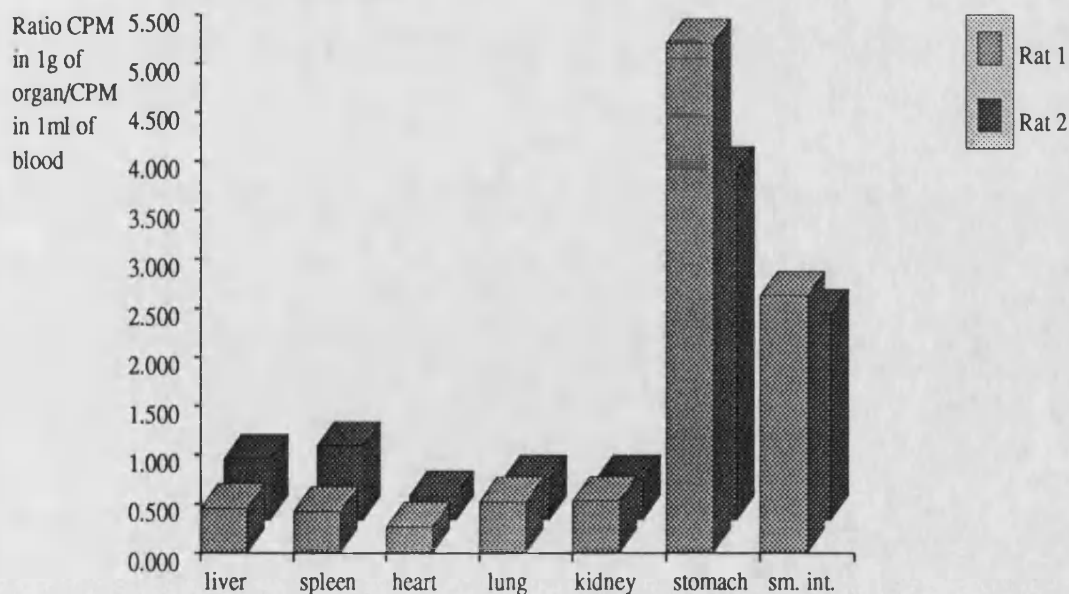


Figure 5.1.3:

Organ Distribution of  $^{125}\text{I}$  activity, 5 hours after IV administration of 250 $\mu\text{g}$  of  $^{125}\text{I}$ -G-BSA to rats. Each bar was determined from a single animal. Results are expressed as a ratio of activity in 1g of organ divided by activity in 1ml of blood.



the rapid uptake of the G-BSA by the liver.

Figures 5.1.4 and 5.1.5 show the organ distribution for M-BSA at 15 minutes and 5 hours after injection. There were subtle differences in the distribution of  $^{125}\text{I}$  after administration of M-BSA compared to G-BSA. At 15 minutes 71.4% and 62.7% of the injected dose for M-BSA had accumulated in the whole liver of the two rats investigated. This is slightly less than for the G-BSA. The difference in activity between G-BSA and M-BSA was found to be present mainly in the spleen but also in the lung and kidney. When compared on a gram for gram basis the percentage accumulated in the spleen was approximately the same as the liver for M-BSA. (An average of 5.3% of the injected dose was present in 1g of liver and 4.2%/g for spleen). But for kidney and lung the levels were at least one third of those in the liver. Duncan et al<sup>(65)</sup> administered an HPMA copolymer which contained 2 mol% mannosamine and found that after 1 hour only 11 % of the injected dose was present in the liver in rats (compared to 69 % of G-HPMA with 2 mol% sugar). This difference could be explained by the receptor which takes up mannose terminating substrates in the liver is less sensitive than the receptor for galactose terminating substrates. In this experiment it was found that the M-BSA and G-BSA were taken up to a similar extent.

The % of  $^{125}\text{I}$  present in the gut of animals dosed with  $^{125}\text{I}$ -M-BSA was less than for animals dosed with G-BSA. The stomach and small intestine of animals dosed with M-BSA both had ratios (activity in 1g of organ divided by activity in 1ml of whole blood) of approximately 0.5 at 15 minutes. (This activity could be attributed to the blood pool within the organ). However the stomach and small intestine of animals dosed with G-BSA had ratios of approximately 1.0, at 15 minutes although the peak of radioactivity in the gut for M-BSA appeared to occur at the same time as for G-BSA at between one and three hours. Like G-BSA, at 5 hours after administration of  $^{125}\text{I}$ -M-BSA the majority of the  $^{125}\text{I}$  activity was found to be present in the stomach (7.2-7.7% of the injected dose) and small intestine (2.6-8%). The activity in the liver had fallen to approximately 3.4% of the total activity injected. At 5 hours the level of  $^{125}\text{I}$  activity present in 1g of spleen was approximately 0.5% and was actually more

Figure 5.1.4

Organ Distribution of  $^{125}\text{I}$  activity 15 minutes after administration of 250  $\mu\text{g}$  of  $^{125}\text{I}$ -M-BSA to rats by the IV route. Each bar was determined from a single rat. Results are expressed as a ratio of the activity in 1g of organ divided by the activity in 1ml blood.

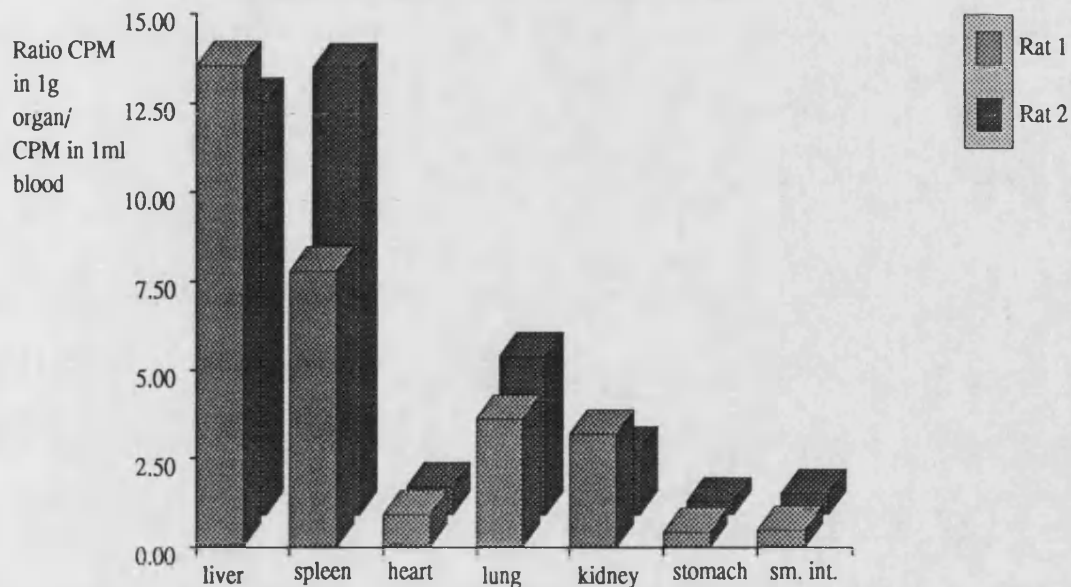
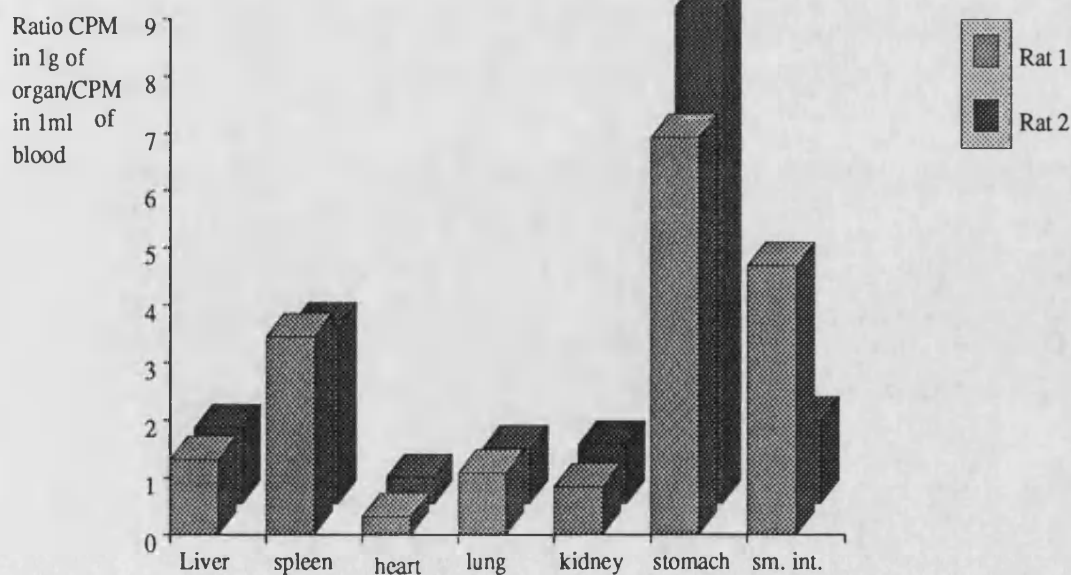


Figure 5.1.5:

Organ Distribution of  $^{125}\text{I}$  activity 5 hours after administration of 250  $\mu\text{g}$  of  $^{125}\text{I}$ -M-BSA to rats by the IV route. Values are expressed as a ratio of activity in 1g of organ divided by activity in 1ml of blood. Each bar was determined from a single rat.



than twice that present in 1g of liver (0.21%). This may be because of the rapid release of  $^{125}\text{I}$  following degradation of the M-BSA by the liver. The liver has two mechanisms for removing break-down products. It is able to secrete substances into the bile, and substances can be removed by the blood stream. The spleen only has one mechanism and would pass its break-down products back into the blood stream. This may be a slower process than the secretion process.

Both G-BSA and M-BSA could be used as targeting agents to selectively deliver substances to the liver. The fact that there are subtle differences in the organ distribution pattern for the conjugates suggests that they have a different fate once they reach the liver. In addition to targeting to the liver, the M-BSA also accumulates in the spleen. The spleen forms part of the RES and is rich in phagocytosing cells. The liver is composed of several cell types.<sup>(163)</sup> The parenchymal cells or hepatocytes are known to have a receptor for galactose on their cell surface.<sup>(6)</sup> The other major cell types in the liver are the Kupffer cells and the sinusoidal endothelial cells. The Kupffer cells are sometimes referred to as liver macrophages and they also form part of the RES. Macrophages are known to have a receptor for mannose terminating glycoproteins<sup>(131)</sup>. In addition, macrophages have a receptor for galactose bearing substrates, particularly if they are particulate in nature<sup>(164,165)</sup>. Since the characteristics of the G-BSA were unknown, with regard to the amount of aggregated protein present, it was possible that the G-BSA could have been taken up by this cell type. However, because of the differences in organ distribution of G-BSA and M-BSA, it was predicted that the G-BSA had targeted to the hepatocytes of the liver and the M-BSA had targeted to the Kupffer cells and so these two BSA conjugates could be used to selectively deliver MTX to different cell types within the liver. In order to verify this prediction, a collagenase perfusion of the liver was carried out following administration of the G-BSA or M-BSA. The perfusion was carried out 15 minutes after injection, because at this time the highest  $^{125}\text{I}$  levels were seen in the liver.

Following the collagenase perfusion, the liver could be separated into 2 fractions. One of these consisted almost entirely of hepatocytes and the other, it was hoped, consisted

of non-parenchymal cells. When the perfusion was carried out initially, it was found that there was no problem in separating the hepatocytes from the other cell types using differential centrifugation techniques. However, after removal of the hepatocytes from the other cells, it was found that the cell suspension was contaminated with a large number of vesicles which formed due to the breakdown of the parenchymal cells. These vesicles sedimented at 500g, the same g force that centrifuged the non-parenchymal cells. Van Berkel<sup>(130)</sup> used protease E to selectively breakdown the hepatocytes and vesicles which contaminated this cell suspension. However when this technique was tried on the cell suspension, it was unsuccessful since it also seemed to remove any non-parenchymal cells that had been in the cell suspension, leaving what could only be described as a gunge when viewed under the microscope. A photograph was taken of the hepatocytes, which had been stained with toluidine blue, and viewed under the light microscope. This is shown in Figure 5.2.

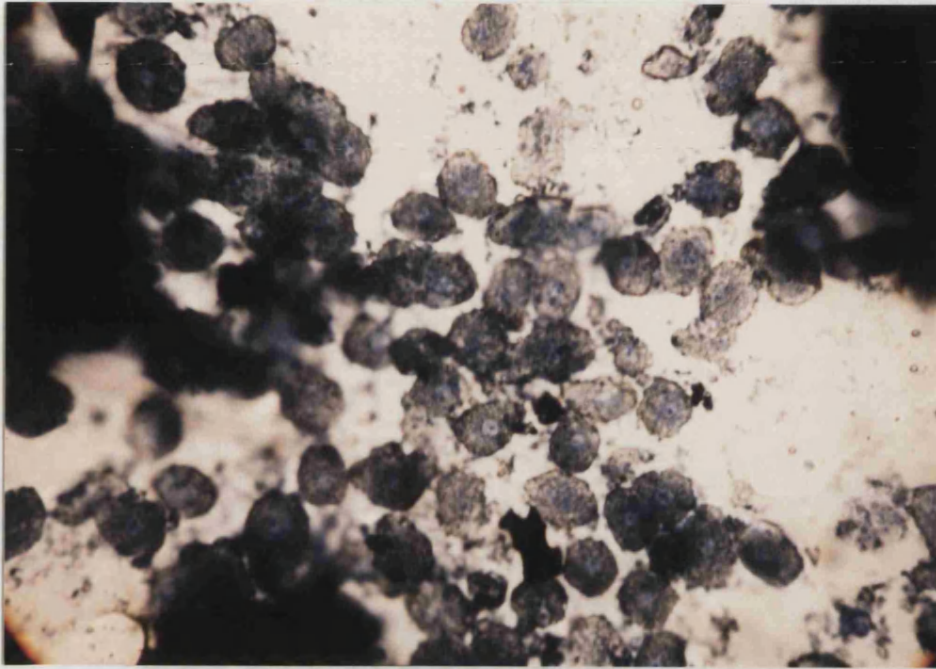
Because of the difficulties in obtaining a suspension which contained non-parenchymal cells, it was hoped that the % of  $^{125}\text{I}$  activity which had been taken up by this cell fraction could be calculated after examination of the parenchymal cell suspension. The number of parenchymal cells present within the rat liver has been calculated at  $128 \pm 7 \times 10^6$  cells per gram<sup>(129)</sup>. After calculation of the activity present within a known number of hepatocytes, the fraction of activity taken up by non-parenchymal cells could be determined from the total activity which had been taken up per gram of liver.

The  $^{125}\text{I}$  activity taken up by the hepatocytes of a rat dosed with  $^{125}\text{I}$ -G-BSA was 3060 CPM/ $10^6$  cells. One gram of liver, determined after the blood pool had been removed from the liver contained 392600 CPM. If it is assumed that the rat, used in this experiment, did have  $128 \times 10^6$  hepatocytes per gram of liver, then the radioactivity present within this cell-type accounted for 99.8% of the dose present in the liver. The G-BSA perfusion was repeated on two other rats. The percentage of the liver uptake which was due to uptake by the hepatocytes was found to be 103.7% and 99.4% for these two rats.  $101 \pm 1.372$  % of the total activity within the liver was taken up by the hepatocytes in the three rats investigated. It could be assumed that very little G-BSA

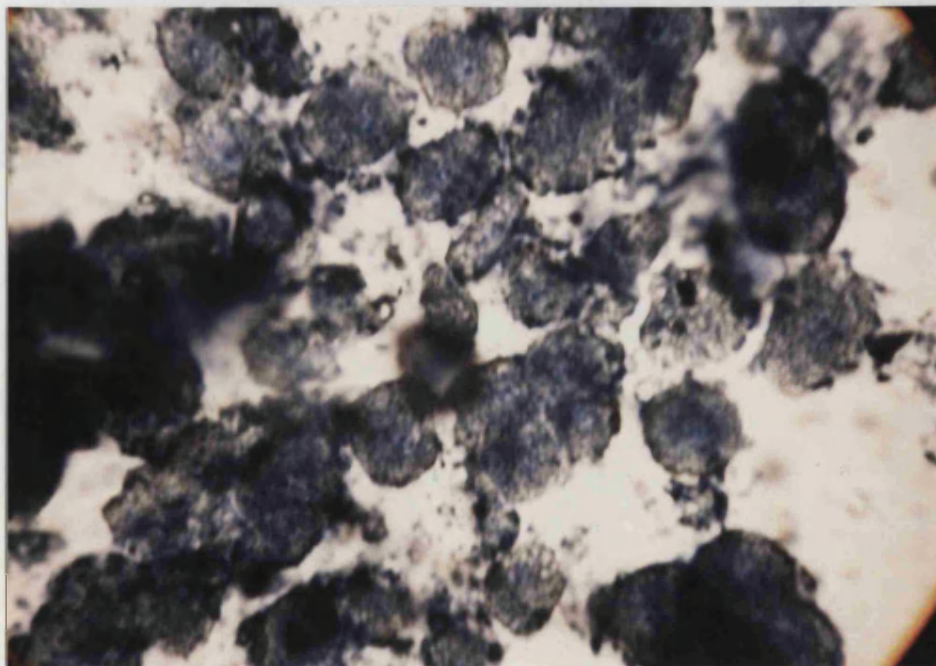


Figure 5.2: Hepatocytes viewed under the light microscope. Cells were stained with toluidine blue and viewed using a Zeiss Ultraphot fitted with a 35mm camera.

a. Magnification 440X



b. Magnification 720X



was taken up by other cells of the liver.

The % of  $^{125}\text{I}$  taken up by hepatocytes following administration of  $^{125}\text{I}$ -M-BSA was  $20.35 \pm 0.664\%$  of the total liver activity. Providing total radioactivity was recovered, this meant that 79.65% of the liver activity had been taken up by non-parenchymal cells. Hepatocytes represent approximately 92% of the volume of the liver<sup>(166)</sup> and so this is an explanation for why these cells took up some of the radioactivity (it could have occurred purely by non-specific pinocytosis). Duncan et al<sup>(66)</sup> investigated the uptake of mannose-HPMA by two fractions of liver cells in a similar manner to described here. They demonstrated that 67% of the total liver radioactivity was present in non-parenchymal cells. The liver perfusion experiment has proved that G-BSA could be used as a selective targeting agent to deliver drugs to the hepatocytes. The majority of M-BSA was assumed to accumulate in the non-parenchymal cells of the liver. In addition, this conjugate was found to accumulate in the spleen. This conjugate could be used to target drugs in the treatment of diseases which affect the RES.

An attempt was made to covalently bind MTX to M-BSA and G-BSA using the carbodiimide reaction described previously. However, in both cases, following addition of the MTX solution to a solution containing the BSA conjugate, and before ECDI had been added, there was extensive precipitation of the protein. Although this precipitation occurred, it may still have been possible to form a conjugate between M-BSA or G-BSA and MTX, so the ECDI was added and incubation was carried out for 24 hours at 4°C. However, separation of the MTX and protein fractions after incubation, on a Biogel P4 column and analysis of each fraction in a UV spectrophotometer at 375nm showed that no reaction between the protein and MTX had occurred. It is difficult to explain why the precipitation of the protein had occurred. The pH of the solution did not alter, when MTX was added. The only explanation could be that the MTX interacted with the protein and led to its aggregation.

In the experiments where BSA-MTX conjugates were administered to rats and serum levels were measured over a period of 96 hours, it was found that a proportion of the radioactivity did accumulate in the liver. Ratios of activity in 1g of liver divided by



activity in 1ml of whole blood ranged from 0.5 to 2, at 24 hours after administration of the conjugates. After performing the experiments with G-BSA and M-BSA it became apparent that they were taken up very rapidly indeed, within 15 minutes of injection. If one of the mechanisms which accounted for the uptake of G-BSA or M-BSA also accounted for the uptake of the MTX-BSA by the liver, then it may be that the accumulation in the liver was in fact more significant than at first realised. The earliest time point where levels of conjugates were measured was at 24 hours. It was shown using the G-BSA and M-BSA that by 5 hours the levels in the liver were significantly less than at 15 minutes. It was decided to carry out a similar experiment using two BSA-MTX conjugates of different MTX loadings and to compare the organ distribution of these to that of free BSA and the G-BSA and M-BSA.

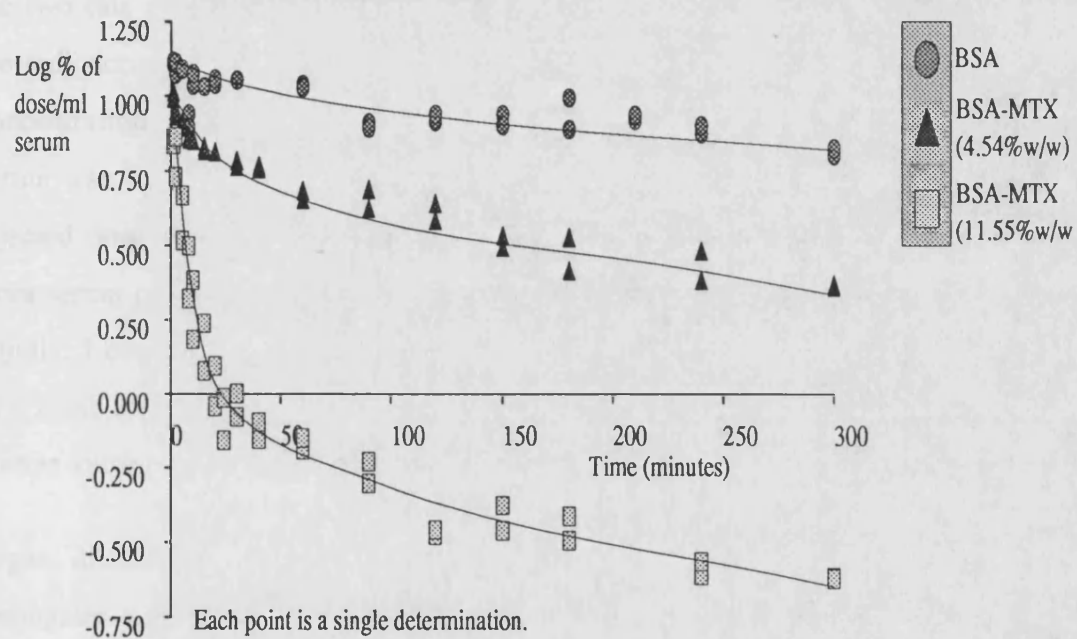
In addition the distribution of LA following IV administration (as described in section 2.9.1) was determined. This protein rapidly left the blood-stream following administration to rats, but excretion in the urine did not account for the clearance. Although levels of LA in serum decreased from 1.15%/ml at 15 minutes to 0.43%/ml at 4.5 hours (the end of the distribution phase), an actual loss from plasma of 63%, only 45-50% of the dose was excreted in 24 hours. In addition a 250g rat has approximately 9.7 ml of serum<sup>(144)</sup>, the serum concentration determined at the 15 minute time point was only 1.15%/ml and this would only account for 11.2% of the dose in the blood stream. The remainder of the dose must have accumulated in a location outside the blood stream. Analysis of the organs at 28 hours did not elucidate where the remainder of the dose had accumulated and so it was decided to analyse organ samples at earlier time points after injection.

## **5.2 Organ Distribution of BSA-MTX Conjugates and LA.**

### **5.2.1 BSA-MTX**

Table A3.25.1 lists the serum concentrations determined over a 5 hour period, for <sup>125</sup>I activity following IV administration of <sup>125</sup>I-BSA to rats. Tables A3.26.1 and A3.27.1 list the serum levels determined for the 4.54%w/w conjugate and the 11.55%w/w

Figure 5.3.1: The Log %<sup>125</sup>I activity/ml of Serum following administration of 200µg of <sup>125</sup>I-BSA, <sup>125</sup>I-BSA-MTX (4.54%w/w) and <sup>125</sup>I-BSA-MTX (11.55%w/w) to male wistar rats by the IV route.



conjugate respectively. Figure 5.3.1 is a plot of log serum  $^{125}\text{I}$  levels versus time for both conjugates and 'free' BSA. Both conjugates demonstrated lower plasma levels than 'free' BSA. There appeared to be a relationship between concentration of MTX in the conjugate and the actual serum levels achieved since the 11.55%w/w conjugate demonstrated lower levels than the 4.54%w/w conjugate.

Clearance of the 11.55%w/w conjugate was associated with a rapid initial loss of radioactivity. At 1 minute, the serum levels were 6.95 and 7.3% of the injected dose for the two rats investigated. By 20 minutes the levels had fallen to 1.24% and 0.91% of the radioactivity. This represented a loss of approximately 85 % of the original plasma concentration in the 19 minute period. For the 4.54%w/w conjugate, the clearance from serum was less rapid. At 1 minute the concentration of  $^{125}\text{I}$  was 9.6% and 10% of the injected dose and this had fallen to  $6.36\% \pm 0.095$  at 20 minutes after injection (a loss from serum of only 34.7% from the one minute value). The BSA was cleared even less rapidly. Levels were 12.7 and 13% of the injected activity at 1 minute and 10.9 and 11.4%/ml at 20 minutes. This represented a loss from serum of only 13% of the 1 minute value.

Organ distribution of  $^{125}\text{I}$  following administration of the  $^{125}\text{I}$  labelled BSA and conjugates was determined, to ascertain where the conjugates had accumulated after leaving the blood stream. Table A3.25.2 lists the organ distribution of BSA and Tables A3.26.2 and A3.27.2 list the organ distribution of the conjugates at various time points, up to 5 hours after administration. Figures 5.3.2 and 5.3.3 are histograms showing the organ distribution of the BSA and conjugates at 15 minutes and 5 hours after administration.

15 minutes after administration of BSA, the activity found in each of the organs, if compared on a gram for gram basis, was very similar and could be attributed to the blood pool within the organ. The actual percentages present in 1g of liver, spleen, heart, lung and kidney ranged from 1 to 2 % of the injected radioactivity. For the G.I.T., the percentages within the organs were slightly lower at between 0.25 and 0.39% per gram of organ.

Figure 5.3.2: Organ Distribution of  $^{125}\text{I}$  activity, 15 minutes post administration of  $^{125}\text{I}$ -Labelled BSA, BSA-MTX (4.54%w/w) and BSA-MTX (11.55%w/w) to rats, b IV injection. Each bar is a single determination.

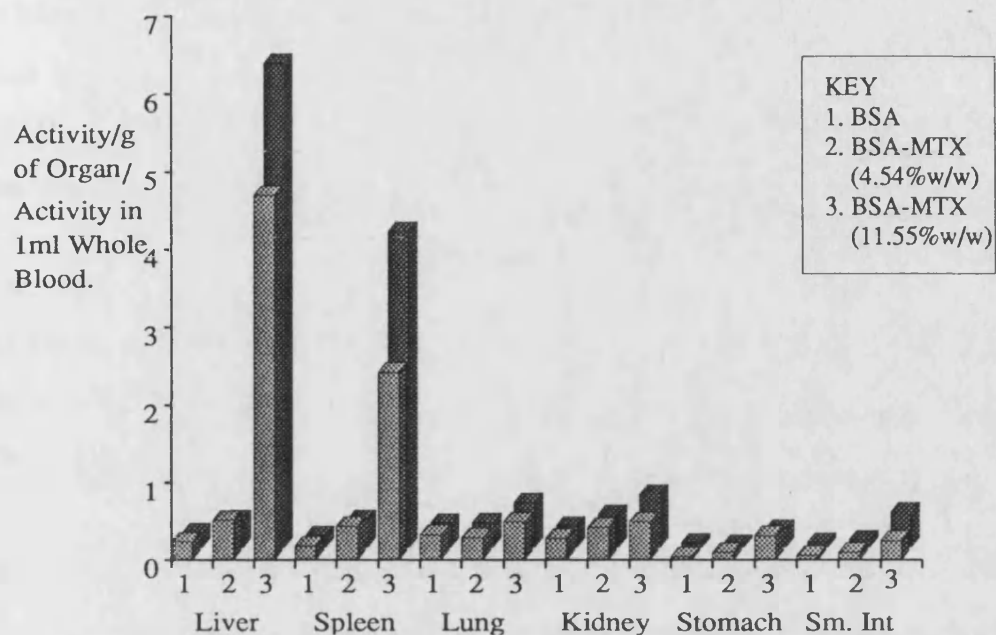
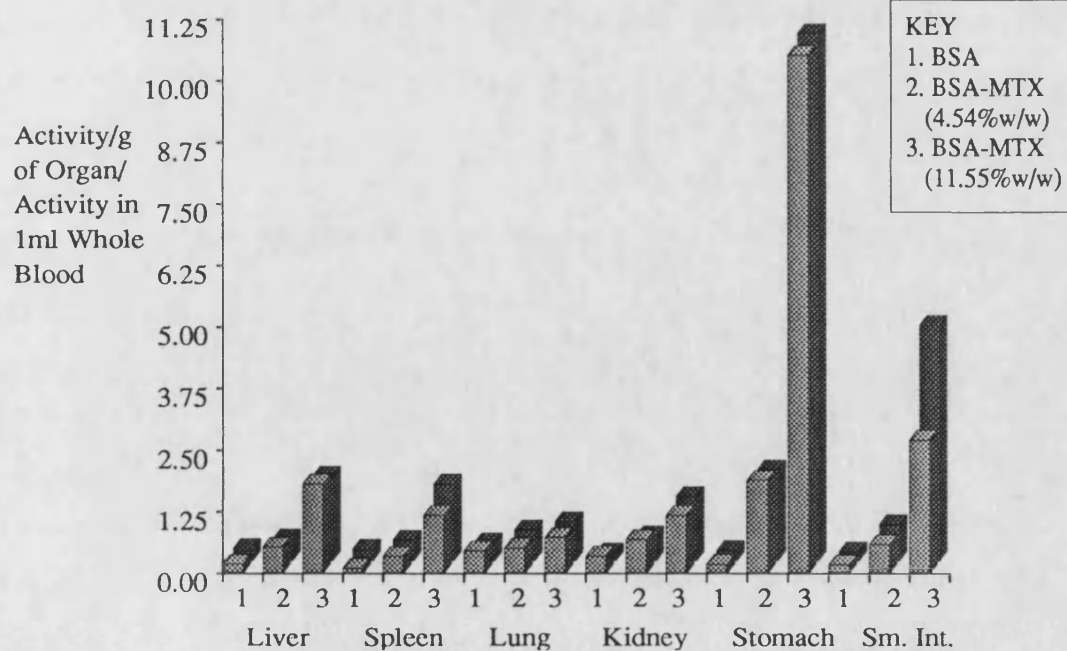


Figure 5.3.3: Organ Distribution of  $^{125}\text{I}$  activity 5 hours post administration of  $^{125}\text{I}$ -Labelled BSA, BSA-MTX (4.54%w/w) and BSA-MTX (11.55%w/w) to rats by IV injection. Each bar is a single determination.



15 minutes after injection, for the 4.54%w/w conjugate, the radioactivity in each of the organs appeared to be elevated when the ratios (activity in 1g of organ/ activity in 1ml of blood) were compared to 'free' BSA, although the actual % of the injected dose in each organ were similar. (Range 0.9 to 1.9% for liver, spleen, heart, lung and kidney and 0.14 to 0.34% for the G.I.T.). No particular organ appeared to selectively take up the  $^{125}\text{I}$ .

For BSA-MTX (11.55%w/w) the majority of radioactivity appeared to have accumulated in the liver and spleen. The actual percentage of the injected dose found in the whole liver, at 15 minutes was 67.15 and 61.43% for the two animals investigated. The spleen had taken up between 3.3 and 3.9% of the injected dose. The other organs all demonstrated a higher ratio (activity in 1g/activity in 1ml blood) than for the BSA and the 4.54%w/w conjugate, but the actual percentages taken up were similar.

By 5 hours after administration, the distribution pattern for the  $^{125}\text{I}$  activity had changed for the 11.55%w/w conjugate. Levels in the liver had fallen to 5.1 and 4.2% of the injected dose for the two animals investigated, and although the ratio was still elevated compared to the other conjugate and free BSA the actual percentage of the dose present was less for the 11.55%w/w conjugate. In the whole spleen the percentage had fallen to 0.2% of the injected dose, again the ratio was elevated compared to BSA and the 4.54%w/w conjugate but the actual percentage of the dose was less. For BSA the percentage in whole liver was 8.2% and 11.9% and for spleen was 0.52% and 0.63% for the two animals investigated. For the BSA-MTX 4.54%w/w conjugate the levels in the whole liver were 7.5% and 7.3% and the spleen were 0.35% and 0.43% of the injected dose for the two animals investigated. Both BSA and BSA-MTX (4.54%w/w) actually exhibited higher serum levels at 5 hours, compared to the 11.55%w/w conjugate, and this could, at least partly, explain why higher % of activity were found in the organs of rats which had been dosed with BSA and the low strength conjugate.

It appeared that most of the activity which had originally been present in the liver following administration of BSA-MTX (11.55%w/w) had been transferred to the G.I.T. At 5 hours after administration, actual percentages were 12.3% and 13% in the stomach and 6.1% and 8.0% in the small intestine. Figure 5.3.4 is a plot showing the  $^{125}\text{I}$  ratio in

Figure 5.3.4: Uptake of  $^{125}\text{I}$  activity by the liver following administration of  $^{125}\text{I}$ -BSA,  $^{125}\text{I}$ -BSA-MTX (4.54%w/w) and  $^{125}\text{I}$ -BSA-MTX (11.55%w/w) to rats by IV injection. In addition the uptake by the gut (stomach + intestine) is shown for BSA-MTX (11.55%w/w). Each point is a single determination.

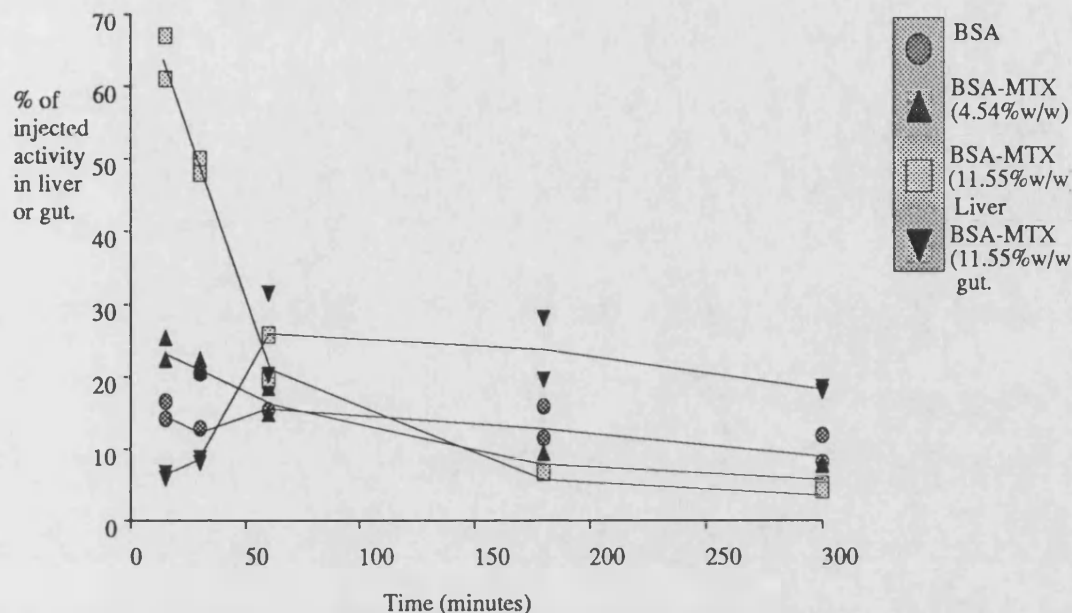
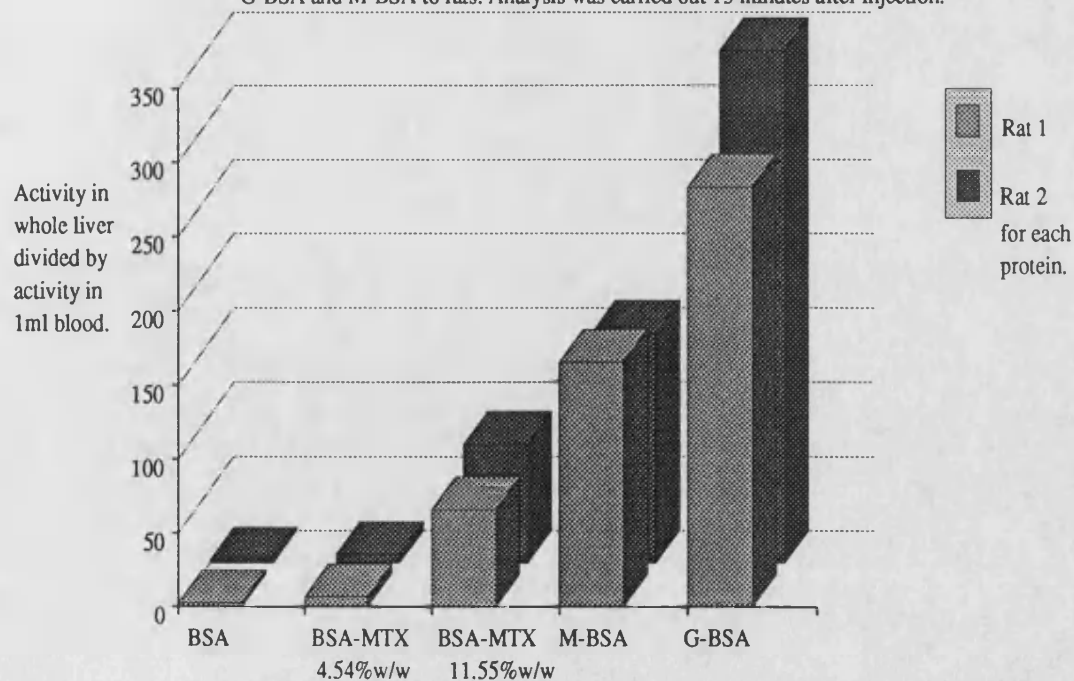


Figure 5.3.5 Ratio of Activity in the Whole Liver divided by activity in 1ml of Blood following Administration of  $^{125}\text{I}$ -labelled BSA, BSA-MTX, G-BSA and M-BSA to rats. Analysis was carried out 15 minutes after injection.



the liver for each of the conjugates and BSA over the 5 hour experimental period. In addition it shows the appearance of activity in the G.I.T., (levels in the stomach and small intestine were added together) for the 11.55%w/w conjugate. Ratios in the other organs investigated were not significantly different at 5 hours to those calculated at the 15 minute time point, for the 11.55%w/w conjugate.

For the 4.54%w/w conjugate, the ratios calculated were slightly elevated compared to BSA at the 5 hour time point. But in all organs apart from the G.I.T they were not significantly different from the 15 minute ratios. Actual percentages present in the stomach were 12.9% and 12% for the two rats investigated and in the small intestine the levels were 5.5% and 8.6% at 5 hours after administration, compared to levels of between 1.7 and 4.7% in the stomach and small intestine at 15 minutes. The accumulation of  $^{125}\text{I}$  in the gut could be attributed to bile secretion, following uptake of the conjugate by the liver. Even free BSA showed elevated levels in the gut 5 hours after administration. Levels had risen from between 1.0% and 3.6% at 15 minutes to between 5.0% and 6.1% of the injected dose at 5 hours for BSA. Thus it could be assumed that even free BSA was taken up to some extent by the liver and then the radioactivity was transferred to the bile, to eventually arrive in the gastro-intestinal tract. Figure 5.3.5 shows the ratio (CPM in whole organ divided by CPM in 1ml of blood) in the liver at 15 minutes after injection for BSA, BSA-MTX, G-BSA and M-BSA. The G-BSA was found to exhibit the highest ratio in the liver and this was followed by M-BSA. Although BSA-MTX (11.55%w/w) was not as good at targeting to the liver as the sugar-BSA conjugates were, a substantial percentage of the radioactivity injected did accumulate in the liver. Analysis of these BSA-MTX conjugates showed that uptake by the liver was associated with the loading of MTX in the conjugate. The 11.55%w/w conjugate was taken up rapidly by the liver. Approximately 65% of the injected dose was located within the liver by 15 minutes after injection. Analysis of the two conjugates investigated by FPLC (see section 4.1) showed that approximately 33% of the protein in the 11.55%w/w conjugate was present in an aggregated form and 23.1% of the protein was aggregated in the 4.54%w/w conjugate. Protein aggregation may contribute to the liver accumulation of the

conjugates<sup>(159)</sup>. Since such a high concentration of the conjugate was found to be located within the liver for the high strength conjugate, it was decided to carry out a collagenase liver perfusion, 15 minutes after administration of the conjugate to rats. The method used was the same as for G-BSA and M-BSA.

Three rats were analysed. The activity present in 1g of perfused liver for rat (1) was 327195 CPM. The activity in the hepatocytes was 981 CPM /  $10^6$  cells. Thus the % of liver radioactivity associated with the hepatocytes (assuming  $128 \times 10^6$  cells per gram) was 38.3%. The % of the liver radioactivity that was found to be present within the hepatocytes for the 3 rats investigated was  $41.43 \pm 3.08\%$ . Thus 58.57% of the liver activity had been taken up by non-parenchymal cells assuming all radioactivity had been collected, and was present within the two cell types. The suspension containing mainly hepatocytes was centrifuged (500g) and supernatant and pellet measured for CPM separately. The activity in the supernatant was negligible. The BSA-MTX (11.55%w/w) had been taken up by both hepatocytes and non-parenchymal cells. Because hepatocytes make up 92% of the volume of the liver, the actual percentage of radioactivity taken up by each non-parenchymal cell was greater than the amount by each hepatocyte. Thus non-parenchymal cells would be exposed to a greater dose of BSA-MTX (11.55%w/w) than the hepatocytes. This could be used as the basis of a passive targeting technique to take MTX to diseased cells within the RES. Certain viruses are known to accumulate in macrophages e.g. pox viruses begin their infectious cycle in this cell type<sup>(157)</sup> and Leishmaniasis is known to proliferate solely in the phagolysosomes of macrophages<sup>(167)</sup>.

The 4.54%w/w conjugate did not appear to accumulate in the liver to a greater extent than it did in any of the other organs investigated. It would appear that conjugates with a lower concentration of MTX may have a more widespread distribution, than either high strength conjugates, which accumulate in the liver or 'free' BSA. (BSA appeared to be retained in the vasculature whereas the 4.54%w/w conjugate had a larger volume of distribution which indicates that it could leave the blood stream and would appear at higher concentration than BSA in the tissue fluid). Co-conjugation of the BSA-MTX



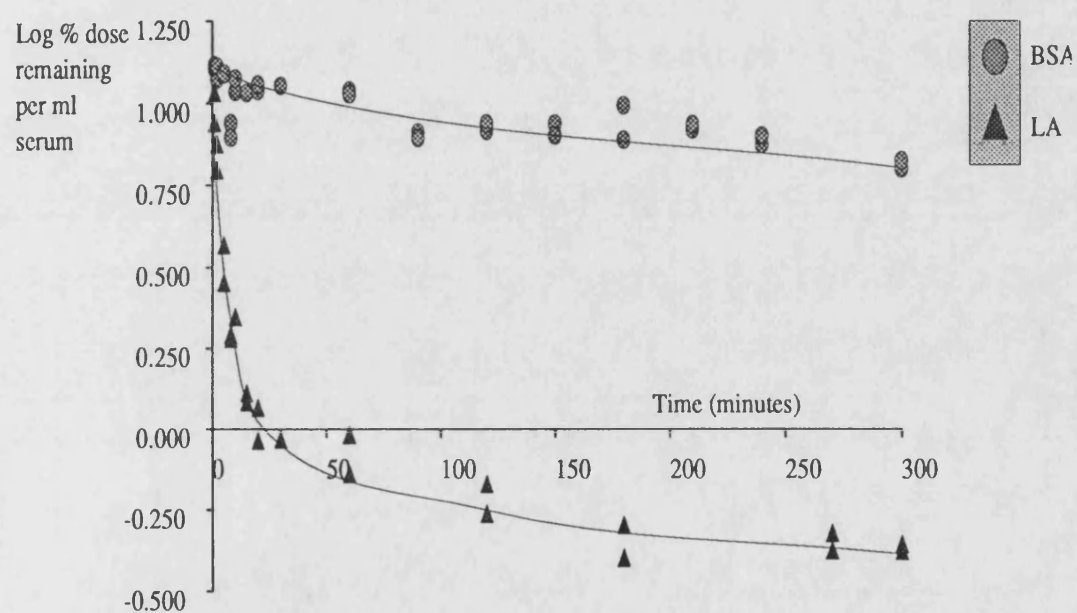
with a selective targeting agent may allow specific uptake of the conjugate by the target cell. Cells which did not exhibit the receptor for the targeting agent may be exposed to extracellular BSA-MTX, but access into the cell would be limited to fluid-phase pinocytosis. Cells with the receptor would take up the conjugate more rapidly.<sup>(70)</sup>

### 5.2.2 LA.

Table A3.30.1 lists the serum concentration of  $^{125}\text{I}$  activity determined following IV administration of  $^{125}\text{I}$ -LA. Figure 5.4.1 is a plot of log % of radioactivity in serum versus time for LA and BSA. LA was cleared more rapidly from serum than BSA. One minute after administration of LA the serum concentrations of  $^{125}\text{I}$  were 8.52% and 10.51%/ml for the two rats investigated. At 20 minutes after injection the serum concentrations of LA were 1.138% and 0.898%/ml for the two rats. The 20 minute concentration represented a loss of serum activity of 89.3% from the one minute value. Over the same period only 13% of the BSA was cleared from serum. Distribution of the  $^{125}\text{I}$  was determined in order to find out where the radioactivity had gone. Table A3.30.2 lists the organ distribution determined for LA at various time points after administration.

Figures 5.4.2 and 5.4.3 show the organ distribution of LA at 15 minutes and 5 hours after administration. At 15 minutes it was shown that the majority of the  $^{125}\text{I}$  was located in the kidney. Actual percentage of  $^{125}\text{I}$  in this organ was 48.5% and 52.1% of the injected dose for the two rats investigated. For the other organs the  $^{125}\text{I}$  activity was low. The % of  $^{125}\text{I}$  activity in 1g of the remaining organs ranged from 0.22% (stomach) to 0.6% (lung). By 30 minutes after injection the concentration of  $^{125}\text{I}$  in the kidney had decreased to 11.5%. The activity in the bladder was measured at this time point and was found to contain approximately 0.3% of the injected dose, so the loss of activity from the kidney was not associated with accumulation in the bladder. Either the  $^{125}\text{I}$  had already been voided from the bladder at this time point, or the  $^{125}\text{I}$ -LA had been reabsorbed from the kidney. Levels found in the gastro-intestinal tract at 30 minutes after injection were quite high at between 17% to 32% of the injected dose (sum of stomach and small intestine activity). At no other time point were the  $^{125}\text{I}$  levels in the

Figure 5.4.1: Serum concentration of  $^{125}\text{I}$  activity following IV administration of 250 $\mu\text{g}$  of  $^{125}\text{I}$ -BSA and  $^{125}\text{I}$ -LA to rats. Each point was determined from a single rat. (n=10 for BSA, n=8 for LA)



gut found to be as high as this. When the total activity found in all the organs investigated was added together, approximately 73% and 78% of the injected radioactivity could be accounted for in the two rats investigated at 30 minutes. The same calculation was carried out for the 15 minute values and approximately 70% and 75% of the injected dose was accounted for at this time point. This calculation would overestimate the  $^{125}\text{I}$  accounted for because the concentration in serum was effectively added to the calculation twice, since no correction for the activity within the blood pool of each organ was made. Since total activity in the body at both time points was very similar, this implies that the LA was reabsorbed from the kidney and not excreted in the urine.

Interestingly, at 1 hour after injection, the measured value for  $^{125}\text{I}$  in the kidney was between 24 and 47% of the injected dose and this was higher than the 30 minute value. There are two explanations for this. Either the differences in kidney uptake at the two time points were due to between-rat biological variation, or the  $^{125}\text{I}$  activity that had been taken up at 15 minutes had been reabsorbed from the tubule by 30 minutes. This had been reintroduced into the circulation and then had accumulated in the kidney again by 1 hour after administration. In order to determine which explanation was correct, the urine that was excreted during the experimental period should have been collected and analysed. Unfortunately, it was not. Total radioactivity, calculated from the organs analysed was 44.1 and 67.2% of the radioactivity for the two rats analysed at 1 hour and so unless the radioactivity had redistributed into some of the organs that were not analysed, it can be assumed that some of the radioactivity had been excreted.

At 5 hours after administration of the LA (see Figure 5.4.3) the percentage of  $^{125}\text{I}$  activity present within the kidney had fallen to approximately 1.3% of the injected dose. Radioactivity appeared to have accumulated in the gastro-intestinal tract since levels in this organ were higher than for the other organs. Between 7.6% and 13% of the injected activity was found in the stomach or intestine of the two rats investigated. Addition of the activities found in the individual organs accounted for 32% and 40% of the injected dose. This implies that some of the radioactivity had been excreted from the body.

Figure 5.4.2: Organ distribution of  $^{125}\text{I}$  activity, 15 minutes after IV administration of  $250\mu\text{g}$  of  $^{125}\text{I}$ -LA to rats. Each bar was determined from one rat. Results are expressed as a ratio of activity in 1g of organ divided by activity in 1ml of blood.

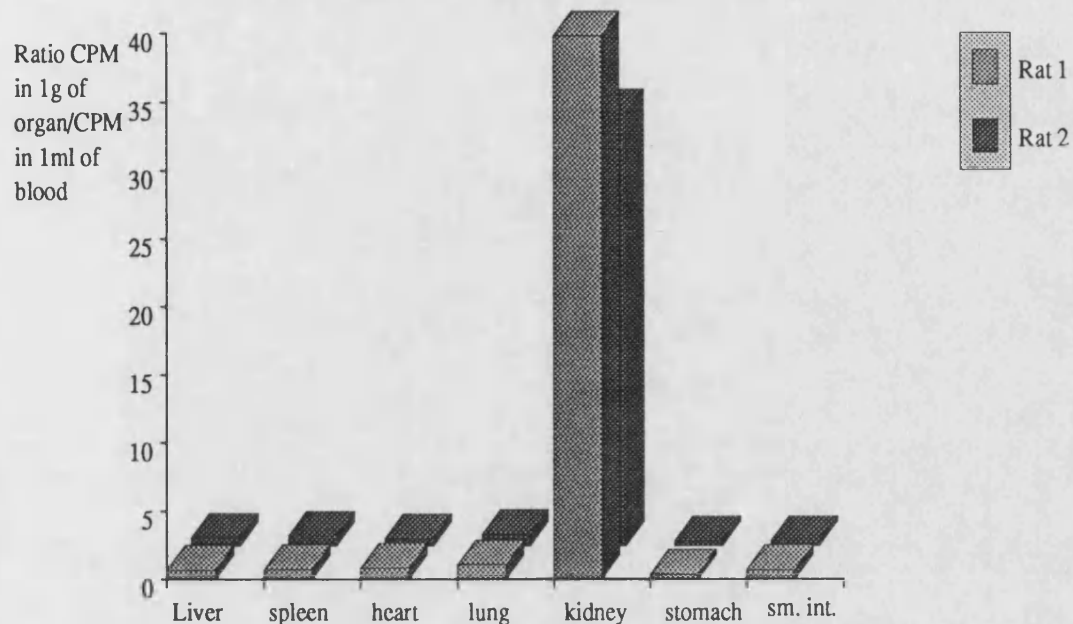
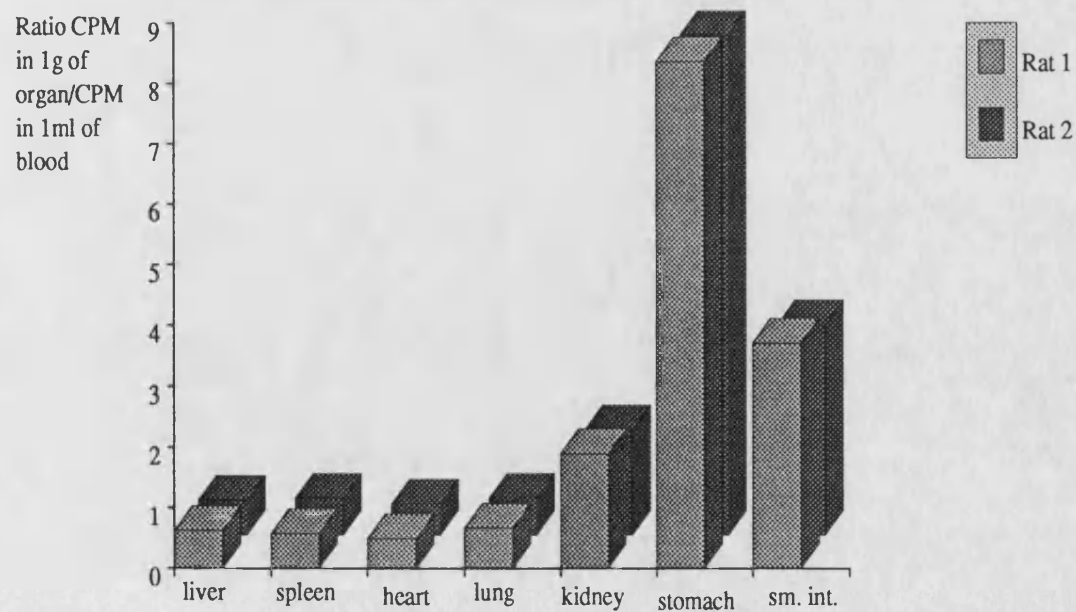


Figure 5.4.3: Organ Distribution of  $^{125}\text{I}$  activity, 5 hours after IV administration of  $250\mu\text{g}$  of  $^{125}\text{I}$ -LA to rats. Each bar was determined from one rat. Results are expressed as a ratio of activity in 1g of organ divided by activity in 1ml of blood.



The seven organs chosen for analysis in the 5 hour organ distribution studies for LA did not account for the entire body dose of the protein. Some radioactivity was located within other organs which were not investigated. Whole body autoradiography was used in order to determine where the remainder of the injected dose was located. It was also carried out for the BSA, G-BSA, M-BSA and BSA-MTX. For BSA and the BSA-MTX conjugates whole body autoradiography was carried out at 15 minutes and 6 hours after administration of the conjugate. For the LA, G-BSA and M-BSA it was carried out at 15 minutes after administration only. The results are shown in Figures 5.5.1 to 5.5.9.

### **5.3 Whole Body Autoradiography for BSA-Conjugates and LA.**

Figure 5.5.1 shows the autoradiogram obtained for BSA, 15 minutes after administration of  $^{125}\text{I}$ -BSA to a 200g rat. The autoradiogram was obtained by exposing longitudinal slices of the rat to film. This figure shows that highest concentrations of BSA were seen in the blood and highly vascularised organs. The heart contents gave an indication of the  $^{125}\text{I}$  content of the blood and the interior of the heart was darker than for any of the organs. An interesting result is seen in the stomach, the lower part of the contents were labelled but the upper part were not. This supports the theory that  $^{125}\text{I}$  activity entered the stomach due to bile secretion into the intestine followed by reflux from the intestine into the stomach. A small amount of radioactivity had localised in the thyroid. A trace of radioactivity was found in all organs apart from the CNS.

Figure 5.5.2 shows the autoradiogram obtained 6 hours following administration of BSA. There was little obvious difference in the distribution of  $^{125}\text{I}$  activity seen at 6 hours compared to that at 15 minutes. The lower stomach contents were labelled but the upper stomach contents were not. The  $^{125}\text{I}$  activity had not reached the faeces at this point. Even 6 hours after injection the blood vessels could be seen to have a greater activity than any of the organs. This is seen most clearly in the liver where the dark blood vessels can be seen on the lighter background of the liver. The activity in the spleen was lower than in the liver and kidney. BSA had not entered the brain and it had not appeared in the eye. The skin appeared to be heavily labelled but this could be attributed to the blood supply running through it. A proportion of the radioactivity had

Figure 5.5.1: Whole Body Autoradiography of a Rat, 15 minutes after administration of 200 $\mu$ g (20 $\mu$ Ci) of  $^{125}$ I-BSA. Each section was exposed to hyperfilm for 2 weeks.

HEAD

TAIL

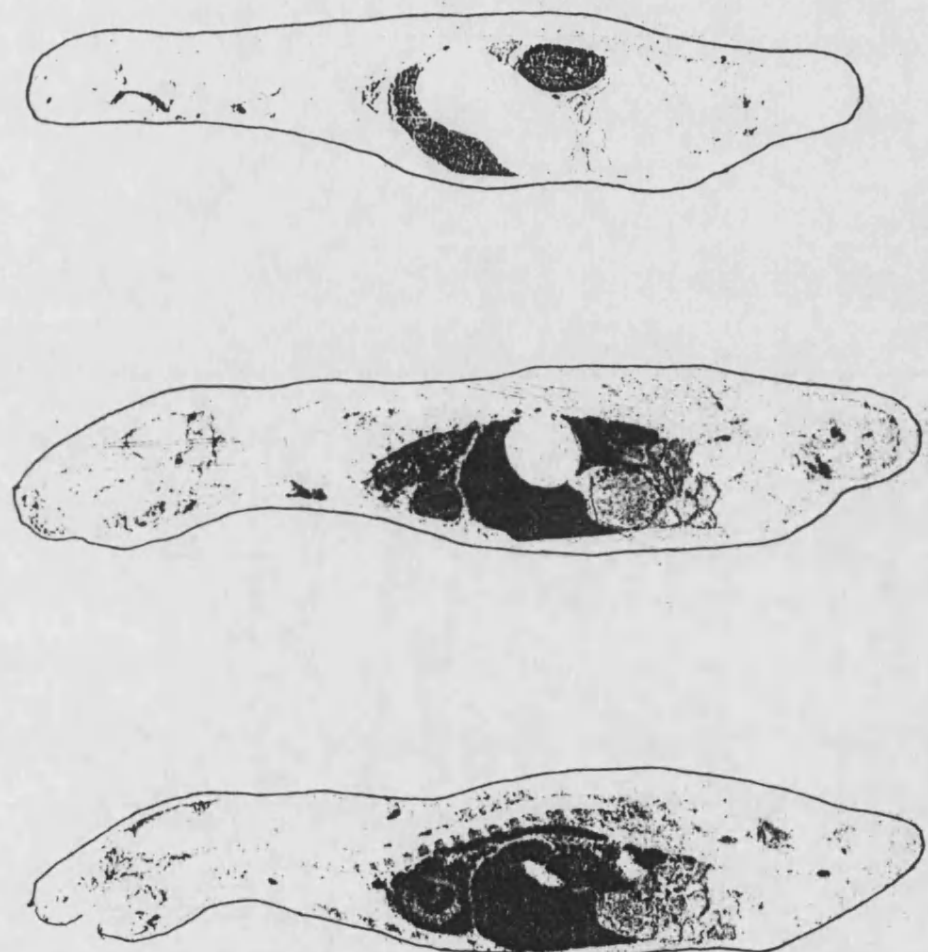


Figure 5.5.2: Whole Body Autoradiography of a Rat, 6 hours after administration of 200 $\mu$ g (20 $\mu$ Ci) of  $^{125}$ I-BSA. Each section was exposed to hyperfilm for 2 weeks.

HEAD

TAIL

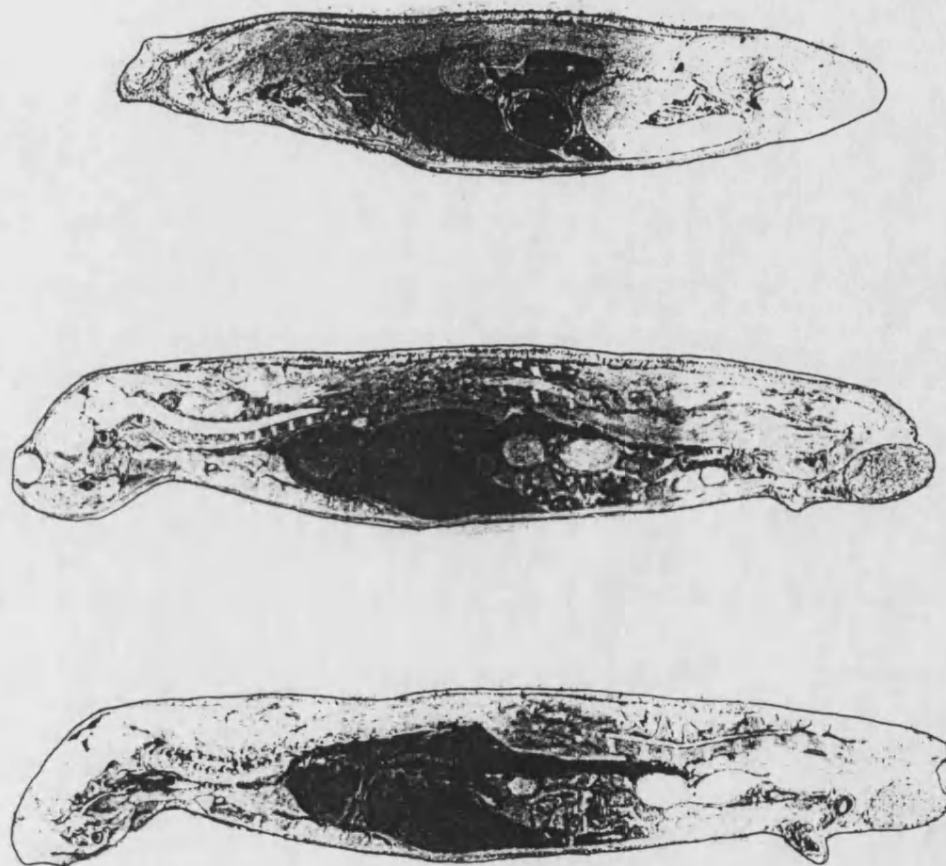


Figure 5.5.3: Whole Body Autoradiography of a Rat, 15 minutes after administration of 200µg (20µCi) of  $^{125}\text{I}$ -BSA-MTX (4.54%w/w). Each section was exposed to hyperfilm for 2 weeks.

HEAD

TAIL

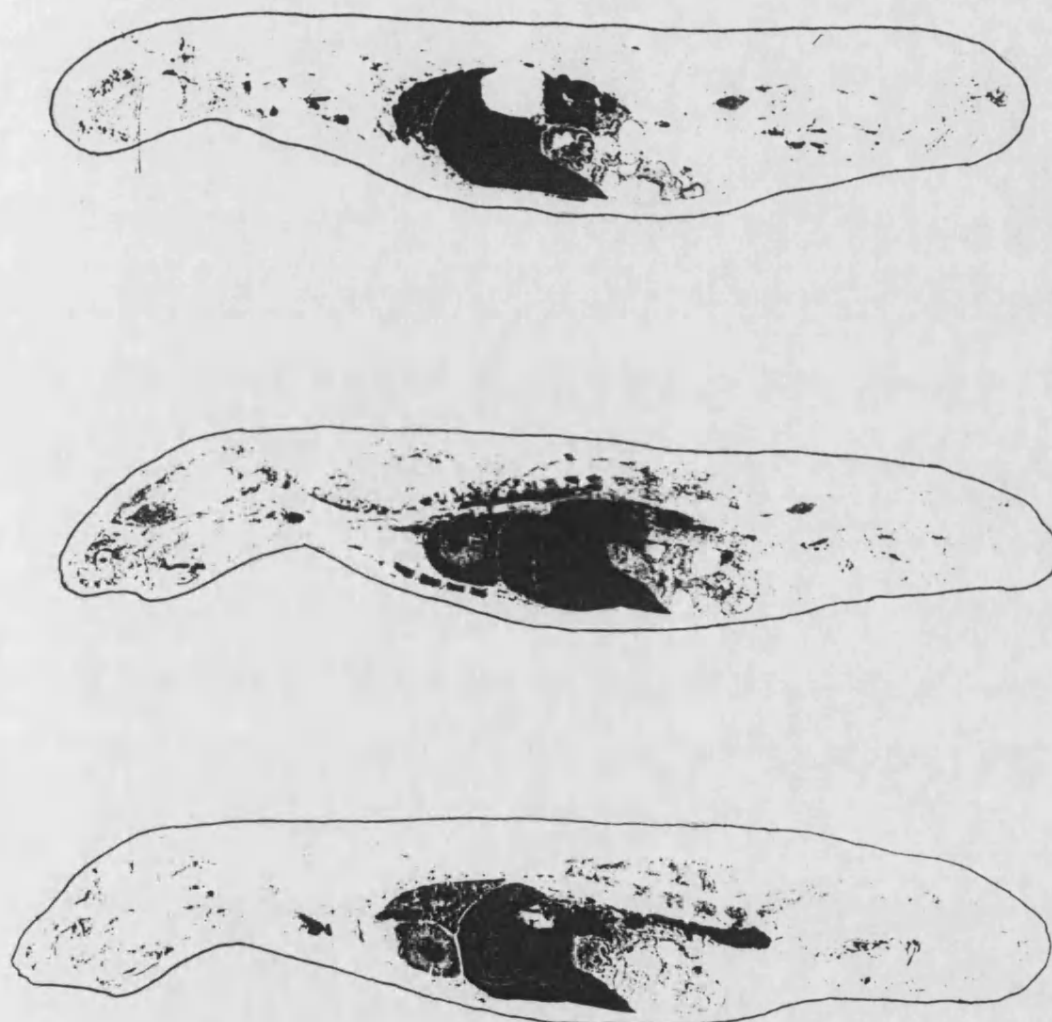




Figure 5.5.4: Whole Body Autoradiography of a Rat, 6 hours after administration of 200 $\mu$ g (20 $\mu$ Ci) of  $^{125}$ I-BSA-MTX (4.54%w/w). Each section was exposed to hyperfilm for 2 weeks.

HEAD

TAIL

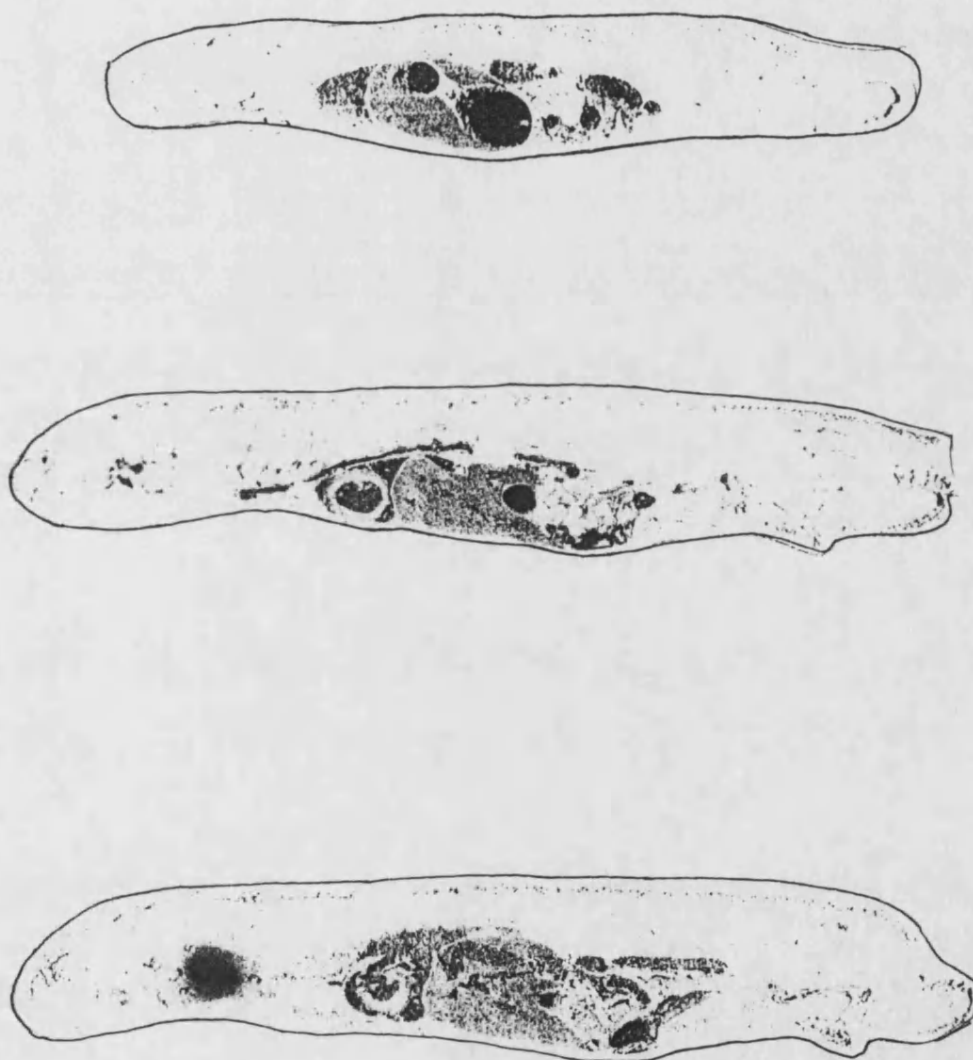


Figure 5.5.5: Whole Body Autoradiography of a Rat, 15 minutes after administration of 200 $\mu$ g (20 $\mu$ Ci) of  $^{125}$ I-BSA-MTX (11.55%w/w). Each section was exposed to hyperfilm for 2 weeks.

HEAD

TAIL

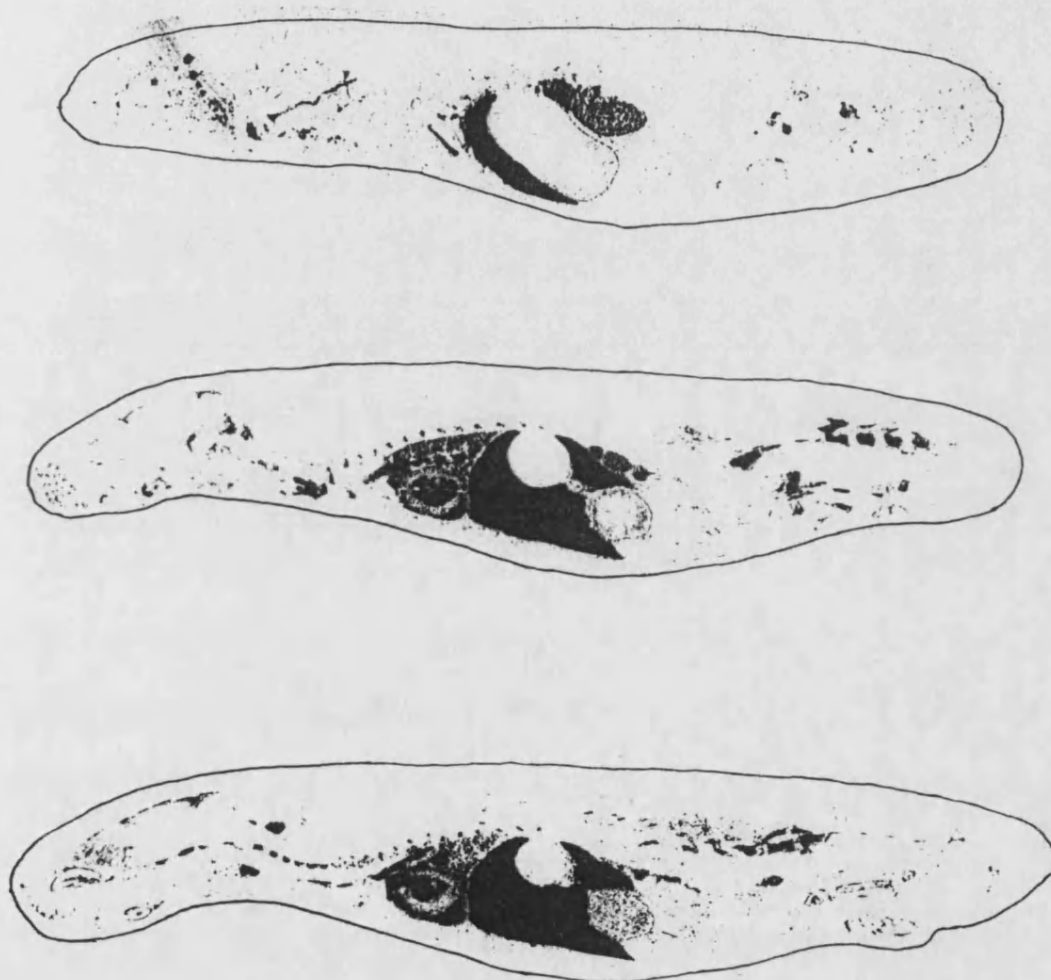


Figure 5.5.6: Whole Body Autoradiography of a Rat, 6 hours after administration of 200 $\mu$ g (20 $\mu$ Ci) of  $^{125}$ I-BSA-MTX (11.55%w/w). Each section was exposed to hyperfilm for 2 weeks.

HEAD

TAIL

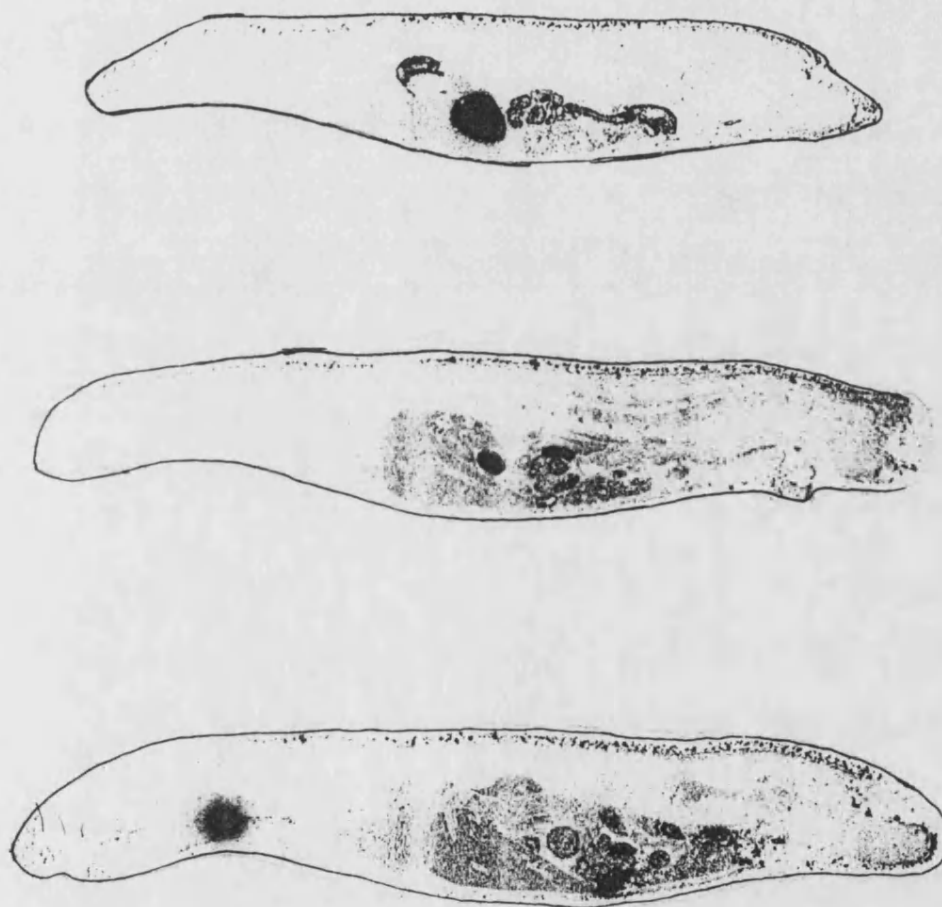


Figure 5.5.7: Whole Body Autoradiography of a Rat, 15 minutes after administration of 200 $\mu$ g (20 $\mu$ Ci) of  $^{125}$ I-G-BSA. Each section was exposed to hyperfilm for 2 weeks.

HEAD

TAIL

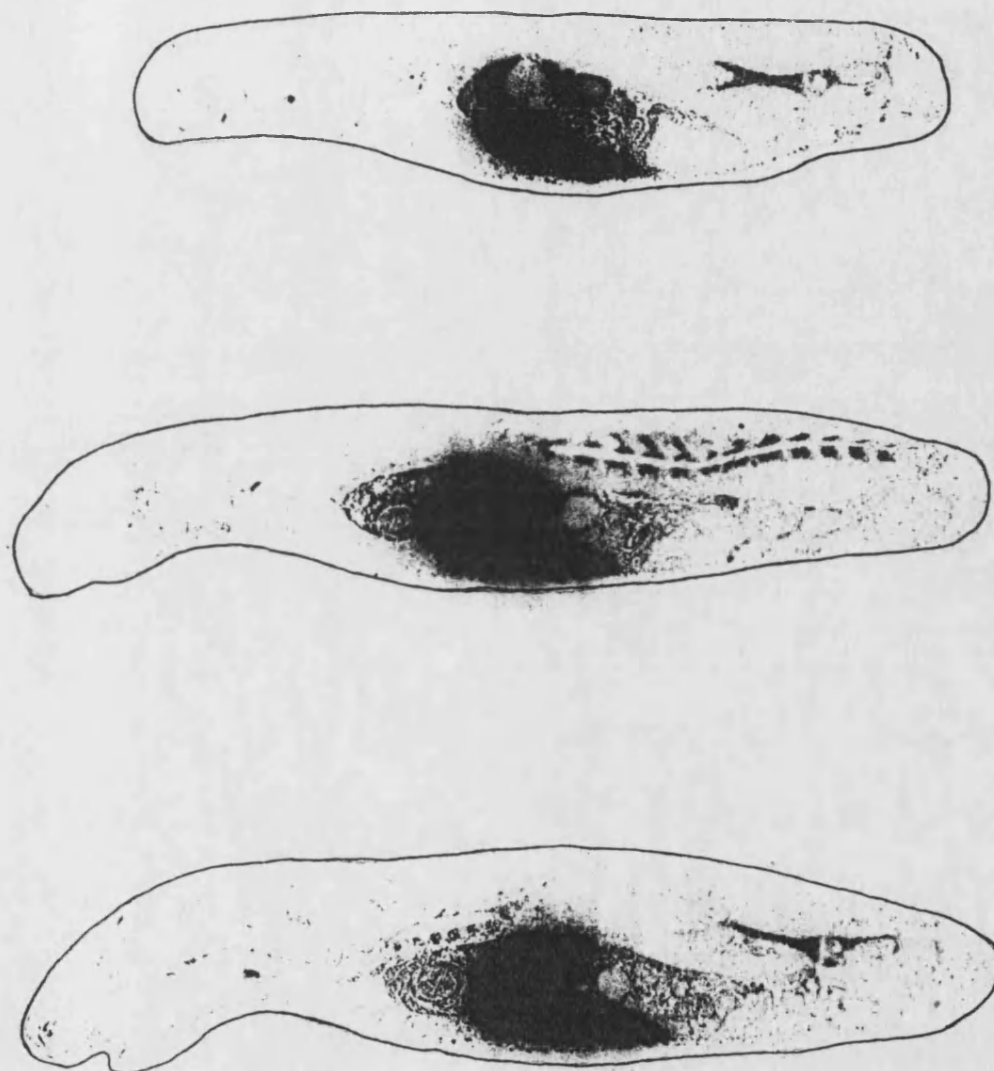


Figure 5.5.8: Whole Body Autoradiography of a Rat, 15 minutes after administration of 200 $\mu$ g (20 $\mu$ Ci) of  $^{125}$ I-M-BSA. Each section was exposed to hyperfilm for 2 weeks.

HEAD

TAIL

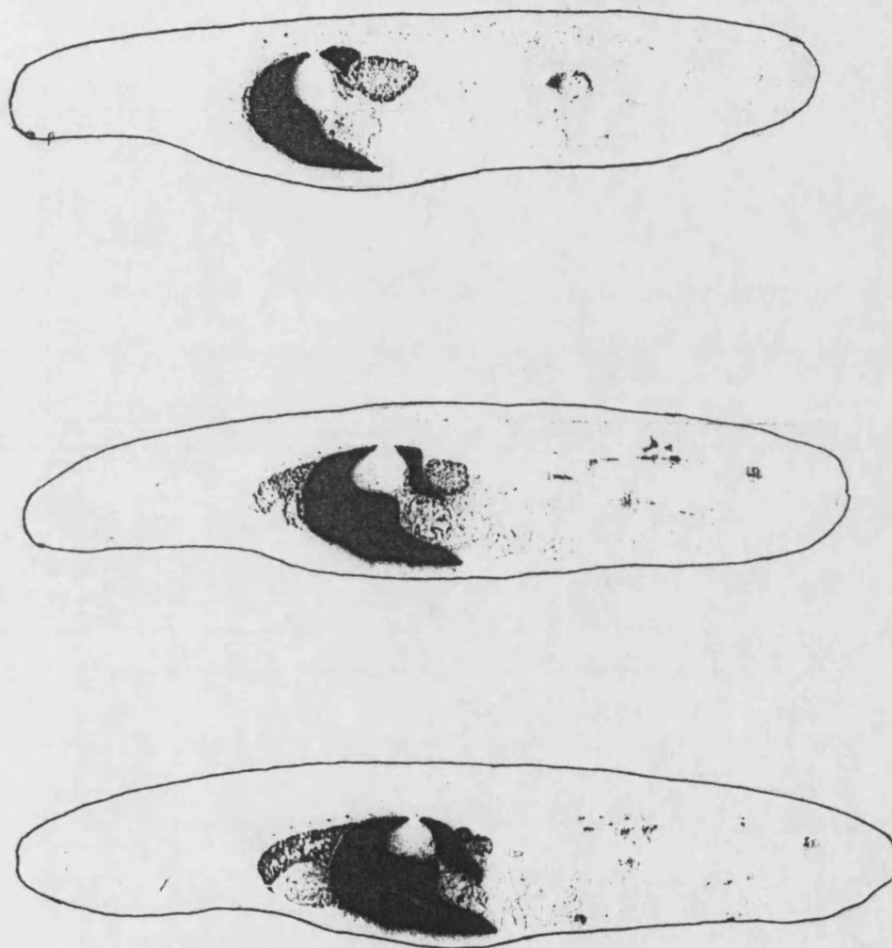
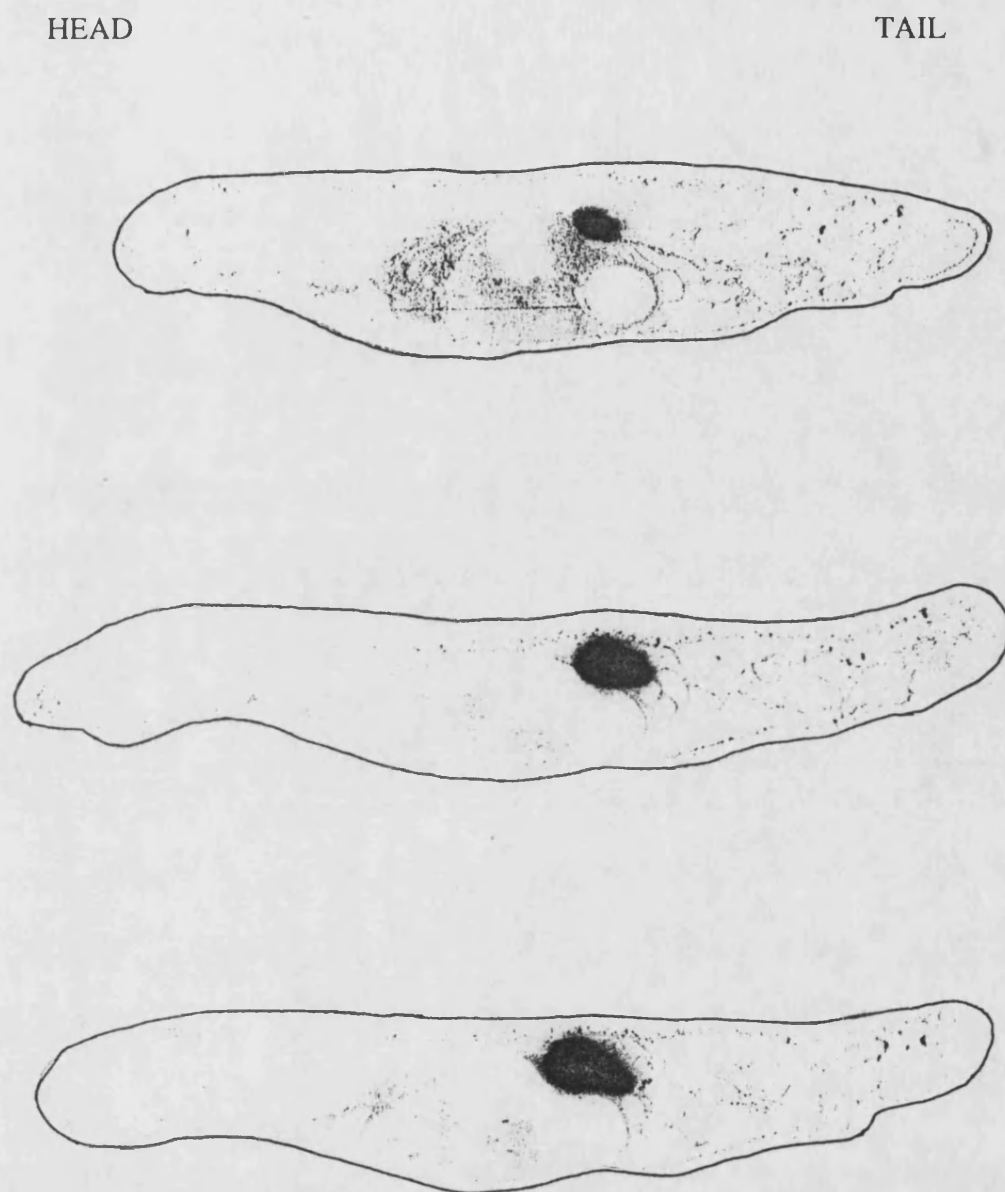


Figure 5.5.9: Whole Body Autoradiography of a Rat, 15 minutes after administration of 200 $\mu$ g (20 $\mu$ Ci) of  $^{125}$ I-LA. Each section was exposed to hyperfilm for 2 weeks.



appeared in the thyroid. This may have been due to some degradation of the  $^{125}\text{I}$ -BSA.

Figure 5.5.3 shows the autoradiogram obtained for the BSA-MTX (4.54%w/w) conjugate, 15 minutes after injection. There did not appear to be an obvious difference in this autoradiogram compared to that obtained for BSA. The majority of the activity was seen in the blood stream and highly vascularised organs such as the liver, lung and kidney. It is impossible to determine whether the activity in these organs had actually extravasated or was still present in the blood stream. Again the activity in the spleen was lower than the liver. The lower stomach contents were labelled but the upper contents were not, as for BSA. Figure 5.5.4 shows the autoradiogram, obtained 6 hours post injection, for a rat dosed with the 4.54%w/w conjugate. Six hours after injection it was seen that a high proportion of the activity was located in the thyroid. This was higher than for the free BSA and may indicate a greater degradation of the conjugate compared to BSA. The stomach contents were also highly labelled, indicating that the  $^{125}\text{I}$  had been transferred from the liver, which would probably have been the site of the degradation. Indeed, the concentration in the liver had decreased compared to the concentration at 15 minutes and also it was less than the concentration within the blood vessels at this time point.

Figure 5.5.5 shows the autoradiogram obtained for the BSA-MTX (11.55%w/w), 15 minutes after administration. This autoradiogram showed that highest levels of radioactivity were present within the liver and spleen. The lower portion of the stomach contents were labelled, indicating that some of the activity had been transferred into the bile from the liver, even at this early time point. Levels which could probably be attributed to the blood pool within the organ were seen in the lung and bone marrow. Low levels were detected in most other organs apart from the brain. Figure 5.5.6 shows the autoradiogram obtained 6 hours after administration of BSA-MTX (11.55%w/w). At this time point levels in the liver and spleen were considerably lower than at 15 minutes. The stomach contents were very highly labelled and the thyroid appeared to have accumulated a considerable amount of the dose. All other organs demonstrated a lower activity than at 15 minutes.

Figure 5.5.7 shows the autoradiogram obtained 15 minutes following administration of G-BSA. Extremely high levels of the conjugate were seen in the liver and spleen. There was very little activity present within the blood stream and other organs, but levels in the lung, bone marrow and kidney were higher than the other organs.

The autoradiogram obtained for M-BSA, 15 minutes after injection is shown in figure 5.5.8. The majority of the activity was detected within the liver and spleen. Very little activity had remained in the blood stream. The autoradiogram is not significantly different from the one obtained for G-BSA.

Figure 5.5.9 shows the autoradiogram obtained 15 minutes after injection of LA. The majority of radioactivity was found to be located within the kidney. The remaining activity appeared to be evenly distributed throughout the body. There was no evidence of uptake by the thyroid. There was a very small amount of activity present within the interior of the lower part of the stomach. There did not appear to be any activity present within the brain.

#### Summary of the Autoradiography results.

The results obtained for the autoradiography experiments were consistent to those obtained for the organ distribution studies in the previous section. G-BSA and M-BSA were selectively taken up by the liver and spleen and it was difficult to distinguish between the two autoradiograms obtained for these conjugates. It was not anticipated that the G-BSA would be taken up by the spleen. However if this conjugate contained any aggregated protein, this would account for its uptake by this organ. Analysis of the G-BSA and M-BSA by FPLC on the Superose 12 column was impossible, since it was found that both conjugates bound very strongly to the Superose.

BSA, 5mg, by IV administration did not seem to selectively accumulate in any organ. It was mainly found in organs with a rich blood supply and it was impossible to tell whether the  $^{125}\text{I}$  activity was present in these organs within the blood stream, or whether it had actually extravasated into the tissue fluid of the organ. A small



proportion of the  $^{125}\text{I}$  dose was found to have accumulated in the thyroid. This could be due to the injection of a small amount of unconjugated iodine present in the original solution, or it could be due to break down of the BSA. Further evidence for the breakdown of BSA was that it appeared in the stomach at quite a high concentration, at 6 hours after injection. The fact that the accumulation in the stomach only occurred in the lower part of it, implied that the  $^{125}\text{I}$  reached the stomach from the intestine and it probably reached the small intestine following secretion from the liver. To enter the bile, the conjugate would have had to be taken up by the cells of the liver.

The low strength conjugate of BSA-MTX (4.54%w/w) did not demonstrate a different distribution pattern from 'free' BSA at 15 minutes after injection. However, 6 hours after injection a greater proportion of the activity was present in the thyroid and this may indicate a greater degradation of the protein. No organ appeared to selectively take up the  $^{125}\text{I}$  following administration of  $^{125}\text{I}$ -BSA-MTX (4.54%w/w).

The BSA-MTX (11.55%w/w) conjugate was found to accumulate in the liver and spleen, 15 minutes after administration and the activity in the other organs was very low. Six hours after administration, the activity had redistributed. A large proportion was found in the gut and thyroid, indicating degradation of the conjugate.

## **CHAPTER 6:**

**Transport Experiments using two cell-lines *in vitro*; Caco-2 and BAE-1 Cells.**

**Uptake of BSA conjugates by Macrophages *in vitro*.**

## 6.1. Caco-2 cells.

Caco-2 cells were used as a model cell-line and the experiments were carried out at the ADDR department at Ciba Geigy. Caco-2 cells were originally obtained from an adult human colon carcinoma. They spontaneously differentiate *in vitro*, to form well polarised monolayers joined by tight junctions, with well developed apical microvilli.<sup>(168,169)</sup> Caco-2 cells express large amounts of disaccharidases and peptidases which are typical of the small intestine.<sup>(170,171)</sup> e.g. they secrete sucrase at a concentration approximately 50% of the small intestine and 50 times that of the colon.<sup>(170)</sup> Cells demonstrate apical microvilli<sup>(172,173)</sup>.

As a model for the intestinal enterocytes, Caco-2 cells are probably the most useful cell-line which have been found to date. However, when using them as a model of the small intestine, care should be taken when interpreting the results. It must not be forgotten that they are malignant cells and as such behave differently to non-neoplastic cells, in their increased requirements for glucose, their production of large quantities of lactic acid and in their accumulation of glycogen.<sup>(174)</sup> Rather than modelling small intestinal cells, there is evidence that they may resemble foetal colonic cells.<sup>(174,175)</sup> e.g. in their similar functional characteristics for Na<sup>+</sup>-sugar co-transport in the brush border membrane<sup>(176)</sup> and in their secretion of newly synthesised lipoproteins.<sup>(177)</sup> Since the Caco-2 cell-line was used purely as a training exercise these factors did not present a problem.

The protocol for filter culture had been established and it was known that a confluent monolayer was formed, 15 days after seeding the cells on to the filters.<sup>(133)</sup> Certain parameters were measured to ensure that the filters used in each of the experiments did actually have a monolayer of cells growing on them. These involved measurement of electrical resistance, the transport of mannitol (a fluid phase marker) across the cell layer and examination of the cell coated filter under the electron microscope. The filters used in these experiments were Millicell HA. These are opaque and therefore cells could not be viewed under the light microscope. The transport of three solutes across

the Caco-2 cell barrier was investigated. These solutes were  $^{14}\text{C}$ -Mannitol,  $^3\text{H}$ -PEG 900 and  $^{14}\text{C}$ -PEG 4000. Mannitol is a fluid phase marker. It is a very hydrophilic molecule and cannot enter cells by diffusion. Therefore, to cross the Caco-2 cell barrier, it must either be transported by transcytosis (through the cell) or cross the monolayer by paracellular passage (between the cells). The two PEG samples would give information about the size selectivity of the monolayer. However PEGs are polydisperse polymers and the degree of polydispersity can vary from batch to batch, so care must be taken in interpreting the results. Two HPLC techniques were used to investigate the polydispersity of the PEGs used.

#### **6.1.1 Investigation of PEGs using HPLC.**

The HPLC assay using reverse phase (Hypersil 5 $\mu$ ) described in section 2.11.3, separated PEG samples below a molecular weight of 1200 into their respective oligomers. Unfortunately the PEG molecular weight standards that were obtained from Polymer Laboratories were found to have a range of molecular weights themselves, and so could not be used to identify the molecular weights of the individual oligomers, as had originally been intended. It was hoped that the standards would give a major peak, which it could be assumed was the average molecule weight stated for the sample. A retention time for the molecular weight could then be determined. Figures 6.1a and b show the chromatograms obtained for the PEG standard (molecular weight 960, polydispersity 1.03) and the sample of  $^3\text{H}$ -PEG 900 from NEN. There did not appear to be a difference between the “standard” PEG and the PEG from NEN. The  $^3\text{H}$ -PEG contained up to 8 different oligomers. It was originally hoped that, after measurement of the transport of  $^3\text{H}$ -PEG 900 into the basolateral fluid, the molecular weight of each of the oligomers could be calculated using the PEG standards which were obtained from Polymer Laboratories but unfortunately this was not possible.

The GPC assay described in section 2.11 separated PEG samples according to molecular weight. It was not sensitive enough to separate out individual oligomers but could detect samples which were more polydisperse because the peak obtained would be broader. Appendix A1.9 shows the retention time for several PEG standards injected

Figure 6.1a: The Chromatogram obtained following injection of the PEG 960 (polydispersity 1.03) (10mg/ml) on to the Hypersil 5 $\mu$  column. Flow rate was 1ml/minute. Chart speed was 1cm/minute.

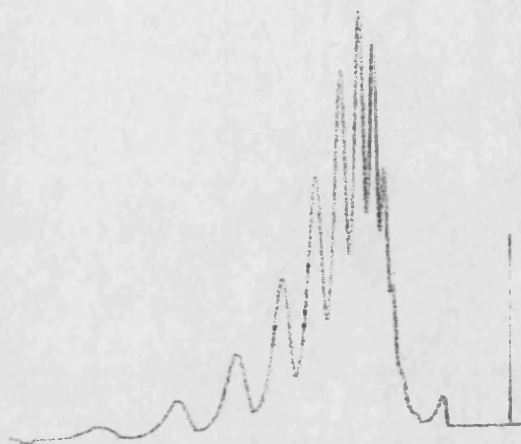
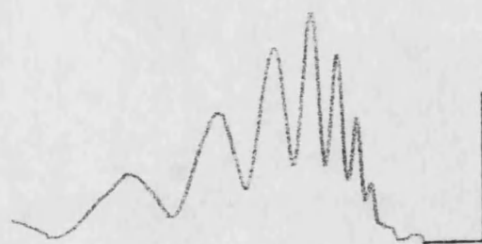


Figure 6.1b: The Chromatogram obtained following injection of  $^3\text{H}$ -PEG 900 onto the column, as above.



onto the column and the calibration curve determined from these samples. The  $^{14}\text{C}$ -PEG-4000 obtained from Amersham was injected onto the column and using refractive index, the retention time was found to be 18.5 minutes. This was the same as for the PEG standard. After collecting 250 $\mu\text{l}$  fractions as they eluted from the refractometer, the retention time was found to be 19.5 minutes. The assay was used to determine the molecular weight of the PEG-4000, that had been transported to the basolateral side of Caco-2 cell monolayers. If the Caco-2 cells acted like a sieve and allowed the passage of oligomers of PEG up to a certain molecular weight then a shift in retention time of the peak would be seen. (see section 6.1.4).

Electrical resistance measurements were obtained for the monolayers used in every experiment after the experiment was complete. Typically the results fell in the range of 400-600 ohms.cm<sup>2</sup> ( $552 \pm 28.9$ ). If a particular filter gave a resistance measurement that fell below 300 ohms.cm<sup>2</sup> then this filter was considered to have a non-confluent monolayer and was not used in the experiment.

### **6.1.2 Mannitol.**

Table 6.1.1 gives the measured % values for the transport of  $^{14}\text{C}$ -Mannitol from the apical to the basolateral side of 15 day old Caco-2 cells grown on filters. The uptake (% of the radioactivity applied to the apical surface of the cells) was also determined for mannitol. An error has been introduced into this calculation since activity was measured for the cells while they were still bound to the filter and no correction for adsorption of the mannitol onto the cellulose filter was made.

**Table 6.1.1 Percentage Transport of  $^{14}\text{C}$ -Mannitol to basolateral compartments by Caco-2 cells and Uptake of mannitol by filter and cells. 9.61nmol of  $^{14}\text{C}$ -Mannitol was applied to the apical surface. Results are means  $\pm$  S.E.M. (n=3).**

Time (hr)	% transported	S.E.M.	% taken up	S.E.M.
1.0	0.1695	0.0375	0.0131	0.0016
3.0	0.474	0.0435	0.0379	0.0074
5.0	0.615	0.0001	0.1076	0.0326
8.0	1.081	0.0030	0.1358	0.0089
15.3	2.009	0.0240	0.2019	0.0203

Figure 6.1.1 is a graph showing the results for % transport of mannitol by the Caco-2 cells and in addition it shows the percentage uptake of the mannitol by the cells and filters. Transport of mannitol was slow, with only 2% of the total activity applied being transferred in 15.3 hours. The Caco-2 cells actually accumulated very little mannitol. After 15.3 hours exposure, the cells had taken up only 0.2% of the radioactivity applied. The low percentage of transport implied that the Caco-2 cells had formed a confluent monolayer. The transport of mannitol by Caco-2 cells appeared to be linear over the 15.3 hours of the experiment. A linear regression analysis was carried out on the plot of transport versus time and it had a regression coefficient of 0.9966. From this plot the rate of transport was calculated to be 0.128% of the  $^{14}\text{C}$  activity per hour. This is lower than the value quoted by Hidalgo,<sup>(177)</sup> who showed that less than 0.2% Mannitol should be transported per hour if the monolayer is to be considered to be confluent.

### 6.1.3 PEG-900.

The percentage of PEG-900 transported to the basolateral side of Caco-2 cells is shown in table 6.1.2. This table also shows the % of  $^3\text{H}$ -PEG-900 taken up by Caco-2 cells. Again no correction was made in the calculation to allow for activity adsorbed to the filter.

Figure 6.1.1 Transport of  $^{14}\text{C}$ -Mannitol by 15 day cultures of Caco-2 cells grown on Millicell HA filters. Media containing 9.61nmol of  $^{14}\text{C}$ -Mannitol was applied to the apical surface of the cells. In addition the uptake of the mannitol was determined by filters and the cell combined. Each point is a mean  $\pm$ S.E.M.(n=3).

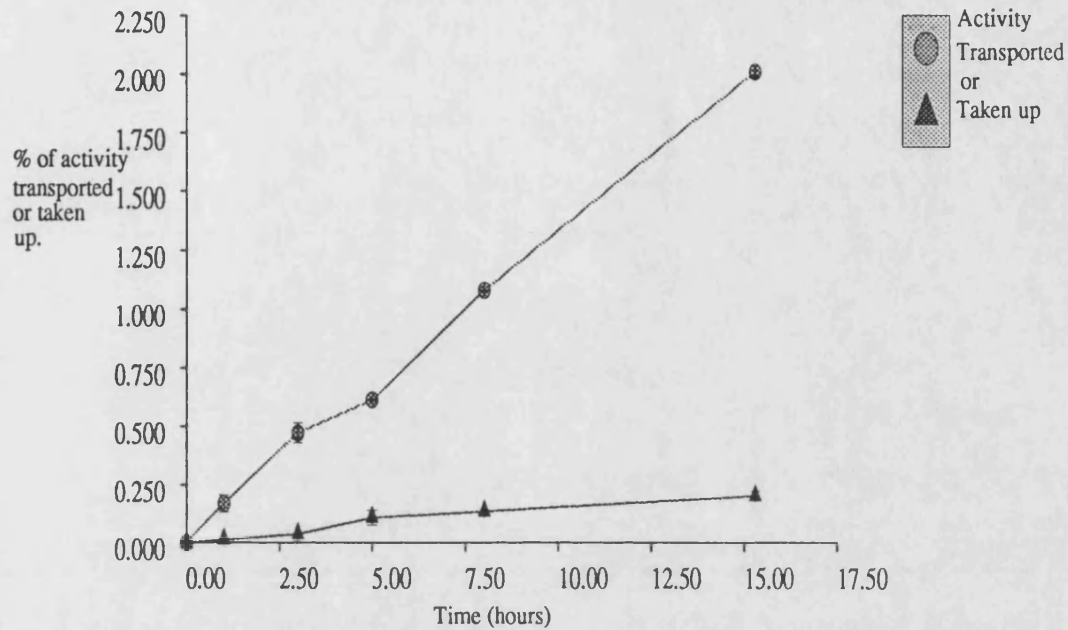
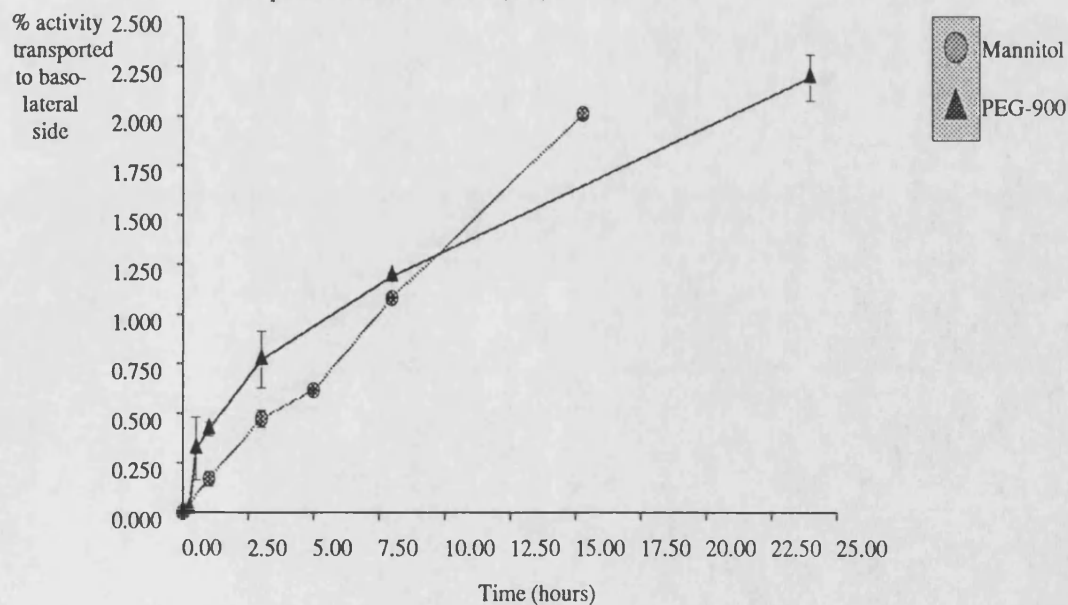


Figure 6.1.2 Transport of  $^{14}\text{C}$ - Mannitol and  $^3\text{H}$ -PEG-900 by 15 day cultures of Caco-2 Cells grown on Millicell HA filters. Media containing 295.9nMol of PEG 900 or 9.61nMol of Mannitol was applied to the apical surface of the cells. Each point is a mean  $\pm$  S.E.M. (n=3).





**Table 6.1.2 Percentage of  $^3\text{H}$ -PEG-900 transported to basolateral side of Caco-2 cells. 295.9nmol of PEG was applied to the apical surface. Percentage taken up by the cells and/or filter is also listed.**

Time (hr)	% Transported	S.E.M.	% taken up	S.E.M.
0.25	0.0166	0.0018	ND	-
0.50	0.3209	0.159	ND	-
1.0	0.4199	0.035	ND	-
3.0	0.7695	0.143	ND	-
8.0	1.1895	0.016	0.321	0.105
24.0	2.1895	0.116	1.025	0.159

Results are expressed as means  $\pm$  S.E.M. (n=3).

Figure 6.1.2 is a graph showing a comparison between the transport of Mannitol and PEG-900. There appeared to be very little difference in the total transport of the two solutes over the experimental period. The percentage transport versus time graph for PEG-900 was not linear. The rate of transport decreased with time. In 1 hour 0.42% of the radioactivity had been transported for PEG-900 and 0.17% of the mannitol radioactivity had been transported. However, after 8 hours exposure, the % of radioactivities transported was more similar for the two solutes at 1.08% for the mannitol and 1.19% for the PEG-900. The reason for the non-linear transport of the PEG-900 could be due to the oligomers within the solution. The lower molecular weight oligomers may be transported more rapidly than those of higher molecular weight and as more of the lower molecular weight material is transported from the apical side, there would be a greater proportion of the radioactivity left, that was high molecular weight oligomers. These would be transported more slowly and would lead to a slowing down of the rate of transport.

Because, during the experimental period, similar amounts of PEG 900 and mannitol

were transported, it can be assumed that PEG 900 could be transported by the paracellular route, since it is known that mannitol can be transported by this route.

#### 6.1.4 PEG 4000.

Table 6.1.3 shows the percentage of  $^{14}\text{C}$ -PEG 4000 transported from apical to basolateral compartments by 15 day cultures of Caco-2 cells.

**Table 6.1.3 Transport of  $^{14}\text{C}$ -PEG 4000 by Caco-2 cells. 8.13nmol of activity was applied to the apical surface of the cells. Appearance of activity in the basolateral fluid was monitored. Results are means for three filters.**

Time (hours)	% Radioactivity transported	S.E.M.
0.5	0.00621	0.00032
1.0	0.0128	0.0010
2.0	0.0247	0.0014
3.0	0.0313	0.0010
6.0	0.0547	0.0055
14.0	0.0819	0.0020
16.0	0.0560	0.00060
20.0	0.0699	0.00495
24.0	0.0799	0.00193
28.0	0.0777	0.00226

The transport of  $^{14}\text{C}$ -PEG 4000 was very low. Only 0.078% of the radioactivity was transported in 28 hours. Figures 6.1.3 and 6.1.4 show the percentage of activity transported by the cells versus time. This plot shows that the transport of PEG-4000 was exponential over the time period investigated.  $^3\text{H}$ -PEG-900 was also shown to be transported at an exponential rate, but 27.5 times more PEG-900 was transported in 24

Figure 6.1.3: Transport of  $^{14}\text{C}$ -PEG 4000 and  $^3\text{H}$ -PEG 900 by 15 day cultures of Caco-2 cells on Millicell HA filters. 8.13nMol of PEG 4000 and 295.9nMol of PEG 900 were applied to the apical cell surface. Results are means for three filters.  $\pm$  S.E.M.

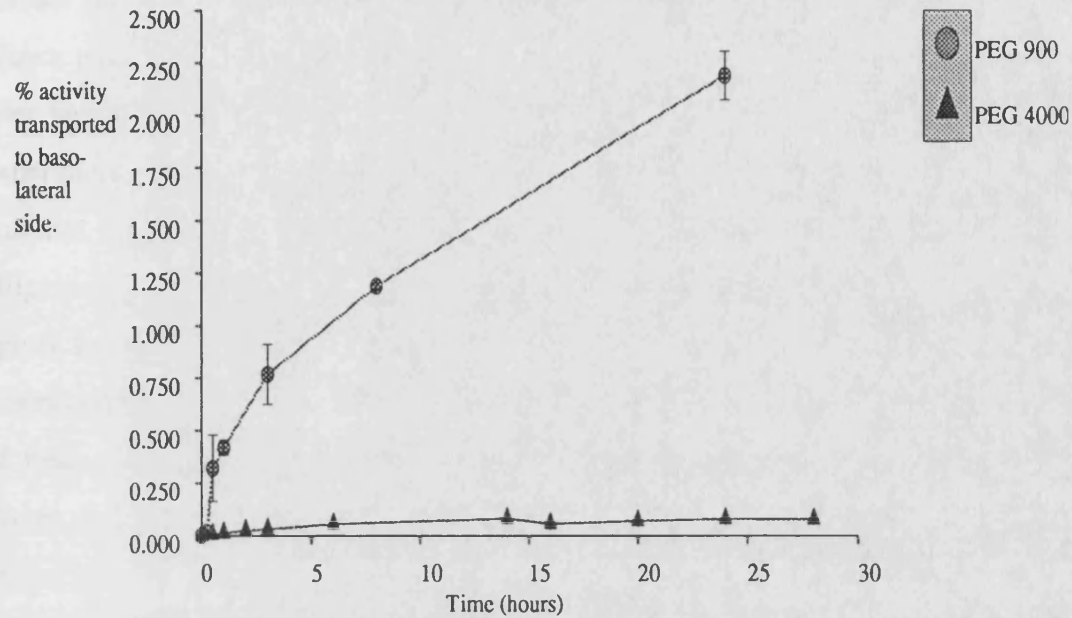
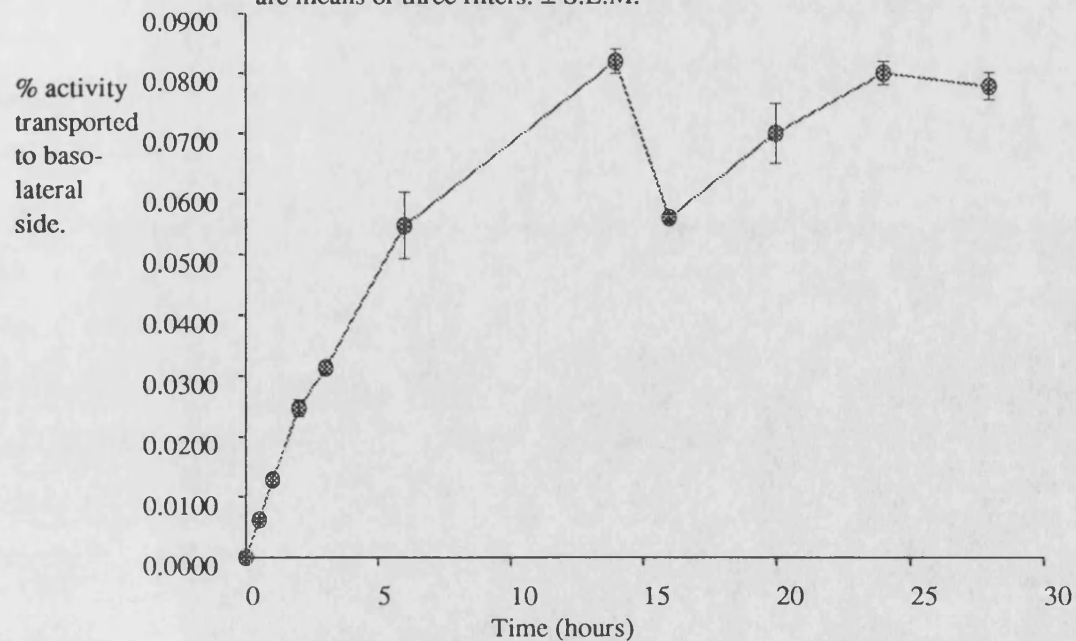


Figure 6.1.4: Transport of PEG 4000 by 15 day cultures of Caco-2 cells grown on Millicell HA filters. 8.13nMol of  $^{14}\text{C}$ -PEG 4000 was applied to the apical cell surface. Points are means of three filters.  $\pm$  S.E.M.



hours than PEG-4000. Hidalgo et al <sup>(172)</sup> applied PEG-4000 to the apical surface of Caco-2 cells grown on collagen coated filters and found that during 90 minutes of contact the rate of transport of PEG-4000 was 0.07%/hour. In this experiment it was shown that only 0.07% of the PEG-4000 was transported in 20 hours. This difference may be due to a greater degree of polydispersity in PEG 4000 used in the Hidalgo experiment. In addition Hidalgo's cultures were 13 days old, compared to the 15 day cultures used in this experiment and this may account for some of the difference. Hilgers et al<sup>(178)</sup> performed a similar experiment, where they applied PEG 4000 to the apical surface of Caco-2 cells grown on collagen coated or non-coated polycarbonate filters and found that during the four hour experimental period that the rate of transport of PEG 4000 was 0.0825%/ hour for coated filters and 0.0625%/ hour for non-coated filters. From these results they concluded that it was not necessary to coat the filters before seeding Caco-2 cells onto them. The rate of transport reported by Hilgers<sup>(178)</sup> was similar to that demonstrated by Hidalgo. Artursson<sup>(179)</sup> also measured the rate of <sup>14</sup>C-PEG-4000 transport by Caco-2 cells. He found that 0.0125% of the <sup>14</sup>C activity was transported in 1 hour. This is similar to the amount found to be transported in this experiment (0.0128%/hr).

The reason for the extremely low transport of PEG-4000 by the Caco-2 cells was probably that the polymer was too big to be transported paracellularly and thus transport to the basolateral side was limited to transcytosis of the polymer. There is a possibility that the <sup>14</sup>C-activity transported was actually bound to PEG oligomers which were smaller than PEG-4000, because of the polydispersity of the sample. To check this, samples of basolateral fluid were injected onto the TSK 3000 column. If the peak was displaced to a later time than the original PEG 4000 solution, then this would imply that the Caco-2 cell monolayer had behaved like a sieve and transported lower molecular weight material, but not PEG 4000 itself. Despite the very low activity in the basolateral fluid, it was possible to discern a peak of activity after elution from the column. The peak was coincident with that of PEG 4000.

The filter culture of Caco-2 cells was used with the intention of setting up a model for the capillary. However, Caco-2 cells in no way mimic endothelial cells. They produce

tight junctions which are impermeable to the transport of PEG-4000 whereas it is known that molecules as big as serum albumin can extravasate from capillaries<sup>(11)</sup>. In addition the apical surface of Caco-2 cells is coated with enzymes and these would break down many of the biological molecules which came into contact with them. Endothelial cells do have a glycocalyx but it is not associated with the same enzymes which coat the Caco-2 cells.

The reason for preparing a model for the capillary was to compare the transport of BSA and the BSA-MTX conjugates to see if an indication could be found to explain why the BSA-MTX conjugates had a larger volume of distribution than BSA itself. It has been demonstrated that the high strength conjugates were rapidly taken up by the liver and this accounts for their increased Vd. However the low strength conjugates were not associated with a specific organ accumulation, though they did appear to be found in most organs at higher levels than free BSA. A possible explanation for the increased general uptake by organs for the low strength conjugates could be that they were more able to leave the vasculature and this could be due to the covalently bound MTX which allowed the conjugate to be transported across the endothelia using the active folate transporter.

## **6.2 BAE-1 Filter Culture.**

The endothelial cell line that was chosen was from bovine aorta endothelia and was known as BAE-1. This cell-line was obtained from ECAC Porton Down. It is known to secrete collagens, but not much is known about the ability of the cell line to form tight junctions in culture. Other workers have used cultures of endothelial cells, obtained from different animals or from different blood vessels,<sup>(180)</sup> and these seem to demonstrate some of the characteristics expected for endothelial cells such as tight junctions.

Electrical resistance was measured as for Caco-2 cells. There was no significant difference in the resistance measured for cells grown on gelatin coated filters and cells grown on uncoated filters. In addition, measurement of cell resistance for cells incubated for 3.75 days, 7 days or 10 days on the filter gave similar values. Values

determined were  $164.98 \pm 17.12$ . This is highly significantly different from the resistance values determined for Caco-2 cells ( $552 \pm 28.9$ ) and this may indicate that Caco-2 cells formed tighter junctions than BAE-1 cells.

### 6.2.1 Transport of $^{125}\text{I}$ -HSA.

The appearance of  $^{125}\text{I}$ -HSA in basolateral fluid was measured over 24 hours for BAE-1 cells which had been grown on gelatin coated filters. Cell cultures were incubated for 3.75 days, 7 days and 10 days before use. The % of intact  $^{125}\text{I}$ -HSA transported over 24 hours for each of the incubation times is shown in Table 6.2.1.

After 24 hours 13.4% of the  $^{125}\text{I}$ -HSA had been transported by cells incubated for 3.75 days, 16.4% by cells incubated for 7 days and 13.4% by cells incubated for 10 days prior to the experiment. t-values calculated at this time point showed that there was no significant difference between the 3.75 days and the 7 days incubation times and the 3.75 days and 10 days incubation times. The t-value for the 7 days versus the 10 days groups was 3.45 ( $p < 0.05$ ), which is a significant difference. A graph showing the  $^{125}\text{I}$ -HSA transport for each of the incubation times is shown in figure 6.2.1. There appeared to be very little difference, overall, in the % transported for each of the three groups.

Siflinger-Birnboim et al<sup>(181)</sup> measured the  $^{125}\text{I}$ -BSA transport by sheep pulmonary artery cells grown on gelatinised polycarbonate filters and they also found, that there was no significant difference in this transport between cells which had been incubated for 3 days and 10 days prior to the experiment. Unfortunately not enough data was given to be able to directly compare the transport of the  $^{125}\text{I}$ -albumin with the results obtained in this experiment.

In addition to examining the BAE-1 transport of  $^{125}\text{I}$ -HSA for cells grown on gelatin coated filters the HSA transport for cells grown on non-coated filters was determined. This experiment was carried out 7 days after cell seeding so that it could be compared directly to the 7 day cultures grown on gelatin coated filters. The appearance of  $^{125}\text{I}$ -HSA in the well chamber of filters (both gelatinised and non-coated) which had not

Table 6.2.1: The transport of  $^{125}\text{I}$ -HSA by BAE-1 cells grown on Gelatin coated Millicell HA filters. 200 $\mu\text{g}$  of  $^{125}\text{I}$ -HSA was applied to the apical surface of the cells and the appearance of intact, TCA insoluble  $^{125}\text{I}$  activity was measured in the basolateral fluid. The transport experiment was carried out at 3 time points after cell seeding. These were 3.75 days, 7 days and 10 days after cell seeding. Each value is a mean  $\pm$  S.E.M.

Time after application	% (of total applied) $^{125}\text{I}$ -HSA measured in basolateral side		
	3.75 days	7 days	10 days
0.5hr	nd	0.261 $\pm$ 0.025	nd
1hr	0.0708 $\pm$ 0.00055	0.268 $\pm$ 0.232	0.159 $\pm$ 0.036
2hr	1.845 $\pm$ 0.0345	0.630 $\pm$ 0.135	0.654 $\pm$ 0.0705
4hr	2.690 $\pm$ 0.0100	3.54 $\pm$ 0.225	0.871 $\pm$ 0.061
6hr	6.531 $\pm$ 0.429	6.285 $\pm$ 0.421	nd
7.5hr	6.841 $\pm$ 0.388	nd	nd
8hr	nd	nd	3.70 $\pm$ 0.333
9hr	nd	6.765 $\pm$ 1.232	nd
12hr	nd	nd	5.97 $\pm$ 0.682
14hr	nd	8.96 $\pm$ 0.327	nd
18hr	7.955 $\pm$ 1.655	10.92 $\pm$ 0.231	nd
24hr	13.39 $\pm$ 2.77	16.43 $\pm$ 0.883	13.37 $\pm$ 0.091

Figure 6.2.1: Percentage of  $^{125}\text{I}$  transported to basolateral side as intact protein following application of  $200\mu\text{g}$  of  $^{125}\text{I}$ -HSA to 3.75 days, 7 days and 10 days cultures of BAE-1 cells grown on gelatin coated, Millicell HA filters. Each point is mean for 3 filters.  $\pm$  S.E.M.

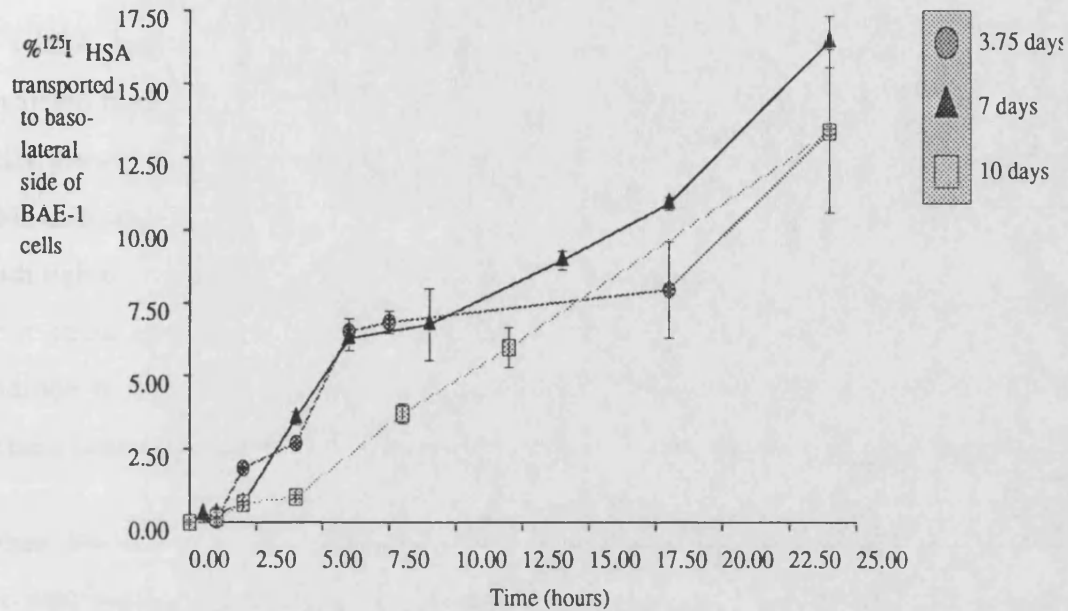
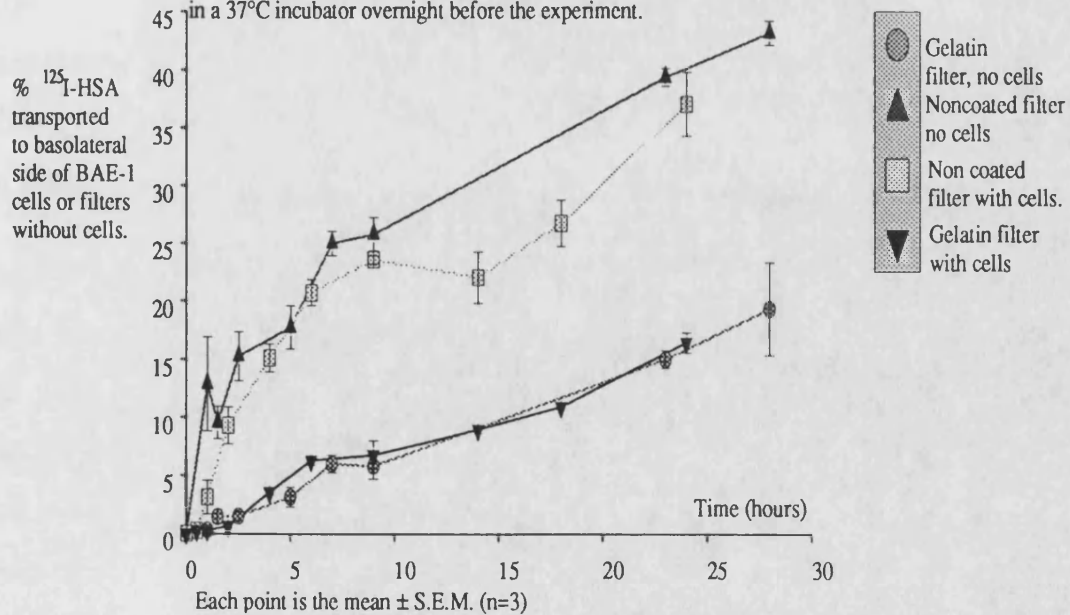


Figure 6.2.2:

The transport of  $^{125}\text{I}$ -HSA by BAE-1 cells grown on gelatin coated or non-gelatin coated filters and the transport of the protein by similar filters which had not been seeded with cells. The BAE-1 cells had been incubated for 7 days before the experiment. The filters without cells had been soaked with media and placed in a  $37^\circ\text{C}$  incubator overnight before the experiment.





been seeded with cells was also determined, in a similar manner to the experiment where cells were seeded on to the filter. The results of these experiments are shown in table 6.2.2 and they are shown graphically in figure 6.2.2. After 24 hours 37% of the  $^{125}\text{I}$ -HSA had appeared in the basolateral compartment of the BAE-1 cells grown on uncoated filters. This was highly significantly greater than the percentage transported by cells grown on gelatin coated filters, where 16.4% of the  $^{125}\text{I}$ -HSA was transported. This difference could be due to the fact that the BAE-1 cells formed better monolayers with tighter cell junctions and well differentiated cells when they were grown on gelatin or it could be because  $^{125}\text{I}$ -HSA not only had to pass through the cell barrier but in addition it had to diffuse through the gelatin layer for coated filters and it may be this gelatin layer that formed the rate limiting step.

When the appearance of HSA in the 'basolateral compartment' (i.e. the well of the six-well plate) was monitored in filters which were not coated with cells, a similar difference in the amount measured, was seen for the coated and non-coated filters. After 28 hours the percentage of  $^{125}\text{I}$ -HSA in the well for coated filters was 19.3% and for the non-coated filters it was 43.2% of the total applied. Using Student's t-test to compare the percentage  $^{125}\text{I}$ -HSA which had diffused through the filter for coated and non-coated filters at the 28 hour time point showed that there was a highly significant difference in the two groups. This implied that the difference in the percentages transported between cells grown on gelatin coated filters and cells grown on uncoated filters was not because the cells formed a better differentiated monolayer when grown on gelatin but because gelatin actually formed a barrier to diffusion.

Student's t-test was used to compare the percentage  $^{125}\text{I}$ -HSA transported by cells grown on uncoated filters and the percentage of  $^{125}\text{I}$ -HSA which had diffused through the filter, for the filters which had not been seeded with cells, at 9 hours after application. The t-value determined was 1.48 ( $p>0.2$ ) and this is a non-significant difference. Thus it would appear that the BAE-1 cells did not present a barrier for the transport of HSA through the filter. A similar comparison for the coated filters at 9 hours, showed that the filters with cells had actually transported more than the filters

Table 6.2.2: The appearance of  $^{125}\text{I}$ -HSA in the basolateral fluid following application of  $200\mu\text{g}$  to the apical surface of 7 day cultures of BAE-1 cells grown on Non-Gelatin coated Millicell HA filters. The transport experiment was also carried out on filters without cells and these were either coated with gelatin or non-coated. The  $^{125}\text{I}$ -HSA concentration in the basolateral fluid was determined after performing a TCA precipitation on it, so that only intact (precipitated)  $^{125}\text{I}$  was measured. Each tabulated value is the mean  $\pm$  S.E.M. (n=3).

Time after application (hours)	% (of total applied) $^{125}\text{I}$ -HSA measured in basolateral side		
	Filter with cells	Gelatin coated filter (no cells)	non-Gelatin filter (no cells)
0.5	0.253 $\pm$ 0.22	nd	nd
1	3.115 $\pm$ 1.424	0.305 $\pm$ 0.115	12.86 $\pm$ 4.064
1.5	nd	1.443 $\pm$ 0.399	9.55 $\pm$ 1.396
2	9.302 $\pm$ 1.594	nd	nd
2.5	nd	1.484 $\pm$ 0.399	15.24 $\pm$ 2.11
4	15.09 $\pm$ 1.207	nd	nd
5	nd	3.128 $\pm$ 0.851	17.71 $\pm$ 1.87
6	20.69 $\pm$ 1.140	nd	nd
7	nd	5.99 $\pm$ 0.785	24.96 $\pm$ 1.07
9	23.55 $\pm$ 0.352	5.82 $\pm$ 1.14	25.76 $\pm$ 1.448
14	22.01 $\pm$ 2.191	nd	nd
18	26.73 $\pm$ 2.026	nd	nd
23	nd	14.98 $\pm$ 0.778	39.34 $\pm$ 0.740
24	37.02 $\pm$ 2.78	nd	nd
28	nd	19.31 $\pm$ 3.97	43.16 $\pm$ 1.029

without cells, though the t-value (0.563) determined was not significant. This suggests that the BAE-1 cells used in these experiments did not form a complete monolayer, since it would not be expected that the  $^{125}\text{I}$ -HSA would pass through a filter which was coated with a monolayer of cells as rapidly as it could pass through the filter without cells.

To determine whether incubation time made a significant difference for cells grown on non-coated filters, the transport of  $^{125}\text{I}$ -BSA was determined on cultures of cells which had been incubated for 3.75 days, 7 days or 10 days prior to the experiment. The results obtained for this experiment are shown in table 6.2.3 and are represented graphically in figure 6.2.3. The plot of %  $^{125}\text{I}$ -BSA transported versus time showed that there was little difference in transport of the  $^{125}\text{I}$ -BSA for any of the incubation times. Student's t-test did not highlight a difference between groups, with between 41 and 43% of the  $^{125}\text{I}$ -BSA, applied to the apical cell surface, being transported in 24 hours. Like HSA, the percentage of BSA transported during the experiment was greater than expected. Transport was roughly linear over the first 12 hours of the experiment. The rates of transport calculated for each of the incubation times were  $2.574 \pm 0.159\%$ /hour for 3.75 days,  $2.389 \pm 0.224\%$ /hour for 7 days and  $2.618 \pm 0.248\%$ /hr for 10 days. There was between 6 and 9 % error involved in the calculation of these rates and because of this they can all be considered to be similar. Since no significant difference could be detected in the transport of BSA by BAE-1 cells, which had been incubated for the 3 different times prior to the experiment, it was decided that a compromise of a 7 day incubation, for the BAE-1 cells would be used in future experiments. If the amount of  $^{125}\text{I}$ -BSA transported to basolateral side was converted to  $\mu\text{l}/\text{minute}$  and a correction was made for the surface area of the filter, the transport rate for BSA by the 3.75 days culture of cells was  $0.189 \mu\text{l}/\text{min}/\text{cm}^2$ . This is similar to the transport rate determined by Del Vecchio et al<sup>(182)</sup> for transport of  $^{125}\text{I}$ -labelled albumin by sheep's aortic cell grown on gelatin coated polycarbonate filters. Their rate was  $0.2 \mu\text{l}/\text{min}/\text{cm}^2$  and is approximately half the rate quoted by Milton and Knutson<sup>(183)</sup> in another cell-line derived from bovine aorta. Milton and Knutson showed in their experiments, a five-fold increase in the percentage of albumin that diffused through a filter without cells compared to transport by the cell monolayer. In this study, the same percentage of

Table 6.2.3: The transport of  $^{125}\text{I}$ -BSA by BAE-1 cells grown on Non-Gelatin coated Millicell HA filters.  $33\mu\text{g}$  of  $^{125}\text{I}$ -BSA was applied to the apical surface of the cells and the appearance of intact, TCA insoluble  $^{125}\text{I}$  activity was measured in the basolateral fluid. The transport experiment was carried out at 3 time points after cell seeding. These were 3.75 days, 7 days and 10 days after cell seeding. Each tabulated value is the mean  $\pm$  S.E.M. (n=3).

Time after application	% (of total applied) $^{125}\text{I}$ -BSA measured in basolateral side		
	3.75 days	7 days	10 days
1hr	1.274 $\pm$ 0.785	0.377 $\pm$ 0.096	1.419 $\pm$ 0.718
2hr	3.199 $\pm$ 1.598	5.417 $\pm$ 1.644	7.324 $\pm$ 1.540
4hr	7.823 $\pm$ 1.626	5.185 $\pm$ 1.903	9.920 $\pm$ 1.247
6hr	14.690 $\pm$ 0.644	13.70 $\pm$ 0.897	14.03 $\pm$ 0.712
8hr	22.51 $\pm$ 0.407	20.11 $\pm$ 2.786	23.84 $\pm$ 0.3813
10hr	23.65 $\pm$ 0.834	24.75 $\pm$ 0.338	29.66 $\pm$ 0.735
13hr	30.99 $\pm$ 0.750	27.63 $\pm$ 1.892	31.50 $\pm$ 1.732
24hr	41.15 $\pm$ 0.451	42.35 $\pm$ 0.987	43.39 $\pm$ 1.451

$^{125}\text{I}$ -BSA was transported by the cell monolayer, as actually diffused through the filter without cells. It may be that the BSA diffused more slowly through the filter without cells than it should have done.

### 6.2.3. Transport of the BSA-MTX conjugates.

Table 6.2.4 lists the results obtained for the transport of BSA and BSA-MTX (4.54%w/w and 11.55%w/w) by monolayers of BAE-1 cells grown on uncoated Millicell HA filters. The results are shown graphically in Figure 6.2.4. Over the first 12 hours of the experiment the rates of transport for BSA and the conjugates were roughly linear. The calculated rates were  $2.652 \pm 0.229$  %/hr for BSA,  $1.696 \pm 0.055$  %/hr for BSA-MTX (4.54%w/w) and  $1.895 \pm 0.118$  %/hr for BSA-MTX (11.55%w/w). BSA-MTX were transported more slowly than BSA itself, but the two conjugates did have very similar transport rates. In 24 hours 30.85% of the BSA-MTX (4.54%w/w) was transported to the basolateral side and 31.3% of the BSA-MTX (11.55%w/w), whereas for BSA itself, 40.8% of the  $^{125}\text{I}$ -BSA was transported. The difference between the transport of BSA and BSA conjugates was highly significant. ( $p < 0.05$  for BSA-MTX (4.54%w/w) and  $p = 0.05$  for BSA-MTX (11.55%w/w)).

The reason for the differences in transport between BSA and BSA-MTX conjugates could be that the conjugates are associated with a percentage of aggregated protein. This aggregated protein would have an overall lower rate of transport than the monomeric conjugate. In addition the BSA-MTX in monomeric form have an elevated molecular weight compared to 'free' BSA anyway. (The molecular weight of BSA is 66296, BSA-MTX (4.54%w/w) is 69153 and BSA-MTX (11.55%w/w) was 74143). However it is unlikely that this small increase in molecular weight would account for the decrease in the rate of transport. Another possible explanation for the increased transport of BSA is that the free protein could occupy the hypothesised 'albumin' receptor, whereas the BSA-MTX conjugates, because their tertiary structure would be expected to be different to BSA, could not occupy the receptor. There is much dispute over whether the albumin receptor actually exists however.<sup>(184,185)</sup> Thus the most likely explanation is that the aggregated protein fraction in the conjugates was transported more slowly.

Table 6.2.4: The transport of  $^{125}\text{I}$ -labelled BSA, BSA-MTX (4.54%w/w) and BSA-MTX (11.55%w/w) by BAE-1 cells grown on Non-Gelatin coated Millicell HA filters. 9.23 $\mu\text{g}$  of  $^{125}\text{I}$ -protein or conjugate was applied to the apical surface of the cells and the appearance of intact, TCA insoluble  $^{125}\text{I}$  activity was measured in the basolateral fluid. The transport experiment was carried out at 7 days after cell seeding. Each tabulated value is the mean  $\pm$  S.E.M. (n=3).

Time after application	% (of total applied) $^{125}\text{I}$ -protein measured in basolateral side		
	'free' BSA	BSA-MTX (4.54%)	BSA-MTX (11.55%)
1hr	1.644 $\pm$ 0.021	2.951 $\pm$ 0.512	2.141 $\pm$ 0.576
2hr	3.711 $\pm$ 1.475	5.401 $\pm$ 0.781	0.814 $\pm$ 0.120
4hr	7.321 $\pm$ 1.082	8.74 $\pm$ 0.401	5.257 $\pm$ 0.405
6hr	13.88 $\pm$ 0.763	12.35 $\pm$ 1.072	10.85 $\pm$ 1.831
8hr	23.42 $\pm$ 0.760	14.31 $\pm$ 0.908	14.01 $\pm$ 1.277
10hr	26.69 $\pm$ 0.289	18.80 $\pm$ 0.137	17.16 $\pm$ 0.800
12hr	27.77 $\pm$ 0.750	22.19 $\pm$ 0.615	21.53 $\pm$ 0.276
24hr	40.81 $\pm$ 2.035	30.85 $\pm$ 1.021	31.32 $\pm$ 2.178

Figure 6.2.3:

The transport of  $^{125}\text{I}$ -BSA by BAE-1 cells grown on Millicell HA filters.  $33\mu\text{g}$  of BSA was applied to the apical side, appearance in the basolateral side was measured, for 3 filters at each time point. BAE-1 cells were incubated on the filters for 3.75, 7 or 10 days before starting the experiment.

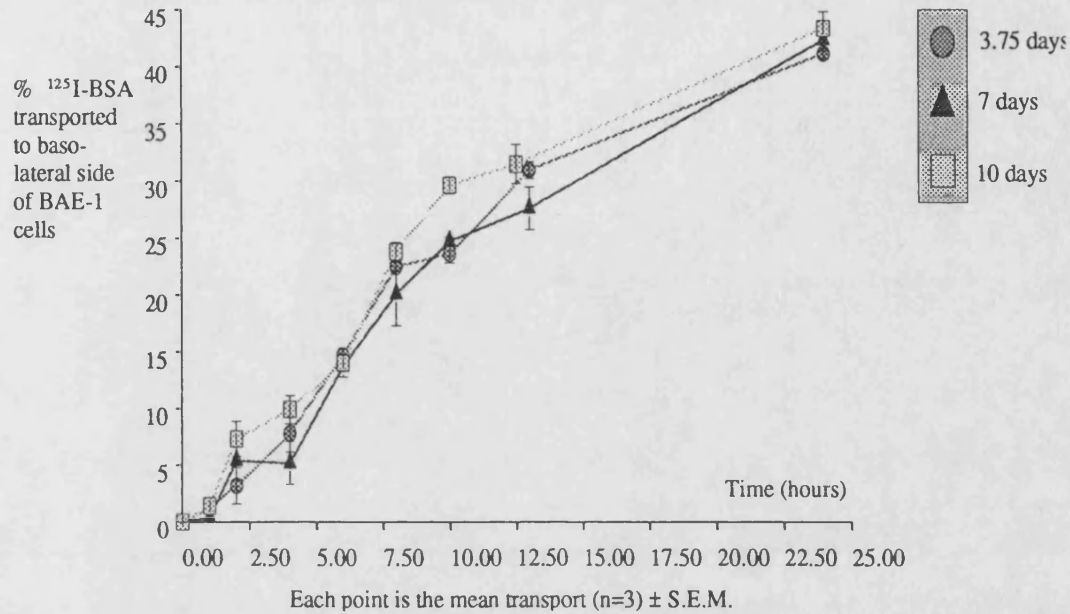
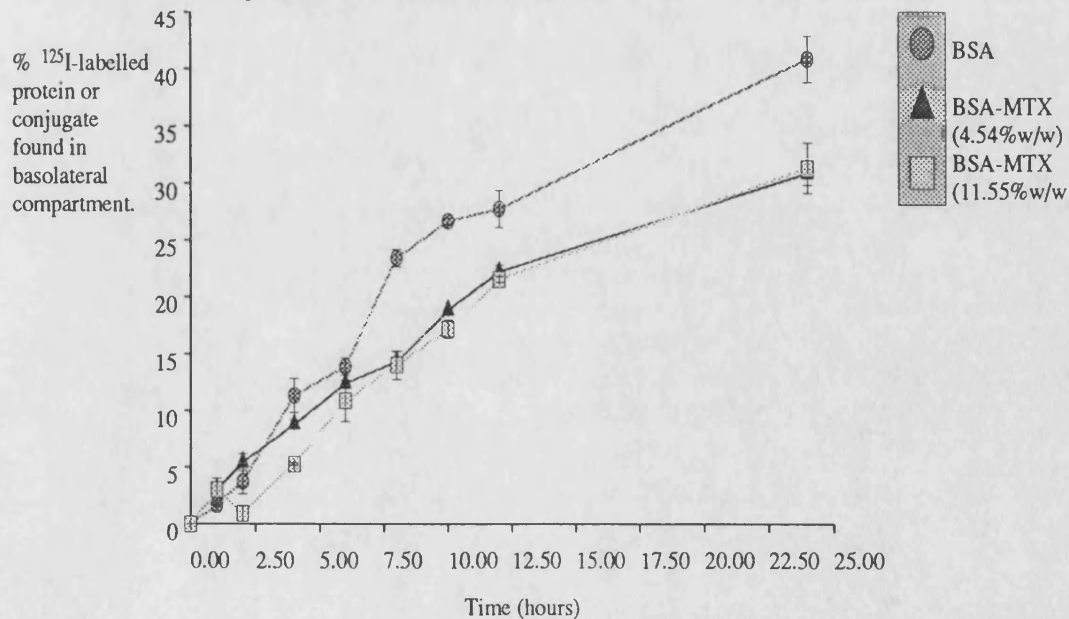


Figure 6.2.4:

The transport of intact protein or conjugate following application of  $9.23\mu\text{g}$  of  $^{125}\text{I}$ -labelled BSA, BSA-MTX (4.54% w/w) and BSA-MTX (11.55% w/w) to the apical surface of 7 day cultures of BAE-1 cells grown on Millicell HA filters. Each point is a mean of three filters.  $\pm$  S.E.M.



The % of  $^{125}\text{I}$  labelled BSA or BSA-MTX taken up by the cells (no correction was made for activity which may have been bound to the filter since the cells were not removed from the filter before analysis) was determined. After 24 hours this was found to be  $0.161 \pm 0.0199\%$  of the total  $^{125}\text{I}$  activity for cells exposed to BSA,  $0.468 \pm 0.0119\%$  for cells exposed to BSA-MTX (4.54%w/w) and  $2.174 \pm 0.073\%$  for cells exposed to BSA-MTX (11.55%w/w). The increased association of the conjugates with the BAE-1 cells was not due to a greater adsorption of the conjugates to the filter. For BSA and BSA-MTX the adsorption to the filter was less than 0.1%. Thus the decreased transport of the conjugates compared to the BSA could be because of the increased retention of the conjugates by the cells.

The % of the activity which was precipitated by a solution of TCA was also determined. This would give an indication as to the degradation of the conjugates and BSA. The % of TCA soluble material in the media of cells exposed to BSA-MTX (11.55%w/w) was greater than in the other groups. At the beginning of the experiment using the 11.55%w/w conjugate the TCA soluble material accounted for 8.61% of the total radioactivity. After 24 hours of incubation with the BAE-1 cells the TCA soluble fraction had increased to  $19.0 \pm 0.321\%$ . This represented an increase of 10.4%. For the 4.54%w/w conjugate, the media at the beginning of the experiment had 7.36% of the total radioactivity present as TCA soluble material. 24 hours after exposure of the BAE-1 cells to this media, the TCA soluble activity represented  $14.43 \pm 0.213$  of the total radioactivity. This represented an increase of 7.07%. Finally for BSA, the TCA soluble  $^{125}\text{I}$  fraction, represented 4.36% of the total activity in the media at the start of the experiment and after 24 hours, the TCA soluble activity had increased to  $8.37 \pm 0.829\%$ . The increase in the degradation of the protein following exposure of the BAE-1 cells to BSA-MTX conjugates rather than 'free' BSA was probably associated with the increase in uptake of the conjugates, and would indicate that not only did the conjugates enter vesicles for transport across the endothelial cells (transcytosis) but also that the conjugates entered coated pits and were transferred to the lysosome for degradation. Only a small proportion of the conjugate actually followed the latter route, however, since it was demonstrated that only a small % of the total  $^{125}\text{I}$ -BSA-MTX was degraded (approximately 10% for BSA-MTX (11.55%w/w). The increased association



of the conjugate with the coated pits may be explained by the increased hydrophobicity of the conjugate compared to free BSA<sup>(150)</sup>.

#### **6.2.4 Transport of Mannitol and LA.**

The transport of <sup>14</sup>C-Mannitol was determined for the 7 day cultures of BAE-1 cells grown on Millicell HA filters. The results for the transport of <sup>125</sup>I-LA and Mannitol are shown in table 6.2.5. Figure 6.2.5 is a plot of % transported versus time by the BAE-1 cells for LA, Mannitol and the transport of mannitol by Caco-2 cells. Mannitol was transported more rapidly by BAE-1 cells than Caco-2 cells. The transport of mannitol by BAE-1 cells was linear up to 8 hours after the start of the experiment. The calculated rate of transport was  $5.851 \pm 0.793$  %/hr. When the rate of mannitol transport for the Caco-2 cells was determined it was only 0.128%/hr. Thus the BAE-1 cells transported the mannitol 46 times more quickly than the Caco-2 cells. The transport rate calculated for LA was  $3.47 \pm 0.132$  %/hr. Thus the monolayer did have a degree of size selectivity for transport. This could be due to the filter itself. The Millicell HA filter is composed of mixed cellulose esters. The pores in this filter are very tortuous and in addition the filter is quite thick compared to the cell monolayer.

Since it was found that solutes were transported more rapidly than anticipated by the BAE-1 cell monolayers and in addition the mannitol was transported more rapidly by BAE-1 compared to Caco-2, it was decided to investigate both cell monolayers using the electron microscope, to see if this could highlight any problems with the BAE-1 cell monolayer. The cells were examined under both the S.E.M. and T.E.M. microscopes. Figure 6.2.6 (page 236) shows an S.E.M. photograph obtained at low magnification for the Caco-2 cell monolayer (magnification was 2000X). This shows that there is great difficulty in demonstrating where one cell finishes and the next cell starts. Thus the junctions between the cells are tight. Figure 6.2.7 is a photograph taken at a similar magnification for the BAE-1 cell monolayer. Examination of this monolayer under the microscope has shown that between some of the cells were gaps which were approximately the size of a cell while other cells were closely packed. Over the whole filter, individual cells could be distinguished quite clearly and thus the cells did not exhibit tight junctions like the Caco-2 cells.

Table 6.2.5: The transport of  $^{125}\text{I}$ -LA, and  $^{14}\text{C}$ -Mannitol by BAE-1 cells grown on Non-Gelatin coated Millicell HA filters. 9.23 $\mu\text{g}$  of  $^{125}\text{I}$ -LA or 10nMol of mannitol was applied to the apical surface of the cells and the appearance of intact, TCA insoluble  $^{125}\text{I}$  activity or  $^{14}\text{C}$  activity was measured in the basolateral fluid. The transport experiment was carried out at 7 days after cell seeding. Each tabulated value is the mean  $\pm$  S.E.M. (n=3). Separate filters were used for each solute.

Time after application	% $^{125}\text{I}$ -LA or $^{14}\text{C}$ -Mannitol found in basolateral side	
	LA	Mannitol
0.5hr	0.305 $\pm$ 0.151	2.218 $\pm$ 0.331
1hr	3.334 $\pm$ 1.164	12.725 $\pm$ 0.995
2hr	9.445 $\pm$ 3.112	14.24 $\pm$ 3.928
3.33hr	11.65 $\pm$ 1.079	30.88 $\pm$ 0.239
5.5hr	20.01 $\pm$ 0.525	39.46 $\pm$ 1.102
8hr	28.59 $\pm$ 1.383	47.5 $\pm$ 0.100
9.5hr	34.38 $\pm$ 1.452	48.9 $\pm$ 0.943
11.5hr	38.59 $\pm$ 0.605	49.07 $\pm$ 0.476
23.33hr	43.36 $\pm$ 0.985	50.52 $\pm$ 0.865

Figure 6.2.5:

The transport of Mannitol and LA from Apical to Basolateral side of 7 day cultures of BAE-1 cells grown on Millicell HA filters and the transport of Mannitol by 15 day cultures of Caco-2 cells grown on similar filters. 9.23 $\mu$ g of LA was applied and 9.61nMol of Mannitol

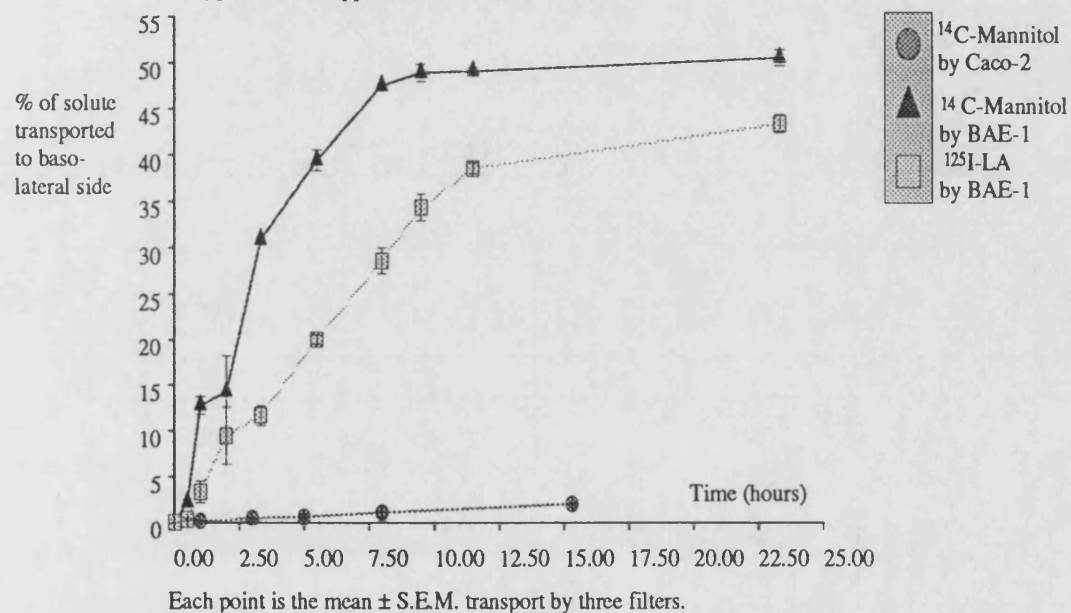


Figure 6.2.8 shows a higher magnification S.E.M. photograph of the Caco-2 cells (7500X). Two different cells can be made out on this photograph, because they have slightly different microvilli, but it is obvious that the cells form very tight junctions indeed. Figure 6.2.9 is an S.E.M. photograph of the BAE-1 cell monolayer at a similar magnification. This photograph shows three cells, which were separated from each other by a distance of approximately 1µm. Many processes had formed which connected the cells. It may be, that if the cells had been incubated for a longer time before taking the picture, the spacers between the cells would have become smaller.

Figure 6.2.10 is a T.E.M. photograph taken of the Caco-2 cells grown on Millicell HA filters. This photograph shows the junction between 2 cells and no gap between them can be seen. Figure 6.2.11 is a T.E.M. photograph at a similar magnification for the BAE-1 cells. Again this photograph shows the junction between 2 cells. A gap can be seen between these cells.

The electron microscope examination of the monolayers has demonstrated that the BAE-1 cells did not form a confluent monolayer within 7 days of cell seeding. This may be because, the incubation time was not long enough to allow differentiation of the cells. Perhaps not enough cells were seeded onto the filter and so they had to undergo cell division before they could differentiate. It may be that the BAE-1 cells require special growth media supplements. Another reason may be the age of the cells. The cells used in these experiments ranged from passage number 25 to 32. It may be that the cells had started to dedifferentiate and no longer resembled endothelial cells.

Shasby and Roberts<sup>(180)</sup> demonstrated tight junctions in 7 day cultures of cells grown on gelatin coated polycarbonate filters, using T.E.M. and this was only with the addition of the equivalent of  $9 \times 10^5$  cells to the filter (in this study  $2 \times 10^6$  cells were added). In cultures of 3-4 days, gap junctions were seen and these were very similar to those seen in the T.E.M. photograph of Figure 6.5b. They used the same growth media as used in these experiments. Shasby and Roberts do not give a passage number for their cell line, however and this may be different for the two cell lines.

Figure 6.2.12 and 6.2.13 show photographs taken from the light microscope for the two cell lines. Again gaps can be seen between the BAE-1 cells quite clearly.

Figure 6.2.6: A photograph of Caco-2 cells taken using a Jeol JSM 35C Scanning Electron Microscope. Cells were incubated for 15 days on Millicell HA filters and then were prepared for microscopy as described in section 2.11.5. (Mag. 2000X)

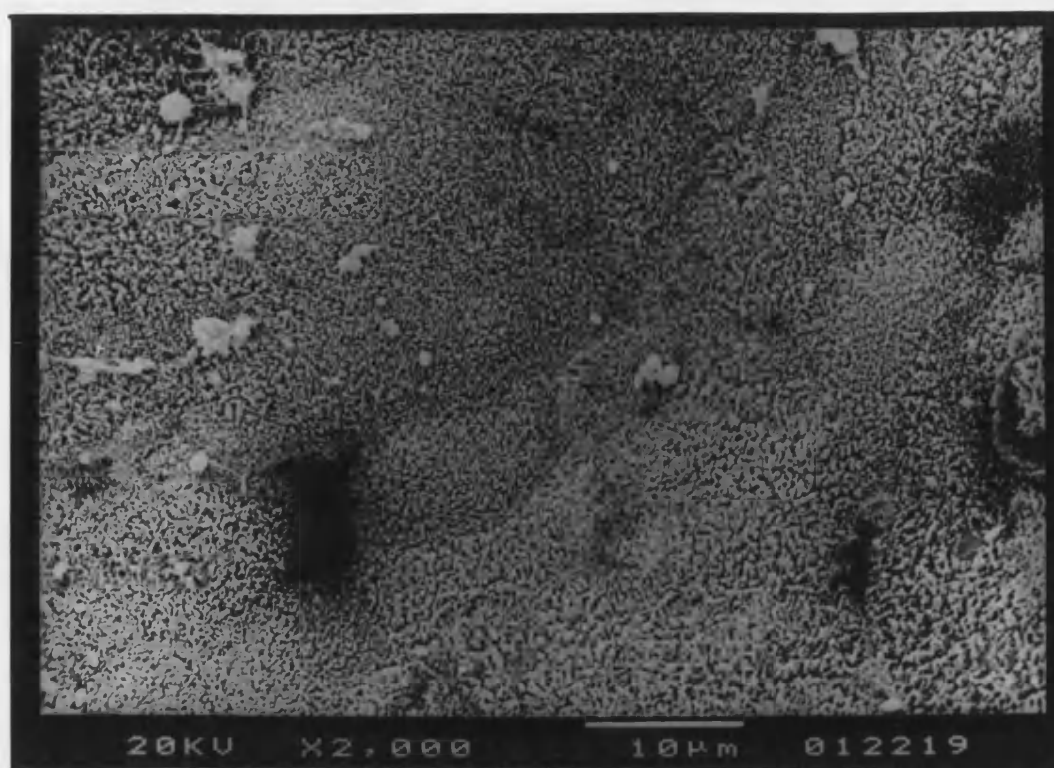


Figure 6.2.7: BAE-1 cells incubated for 7 days prior to preparation as above. (2000X)

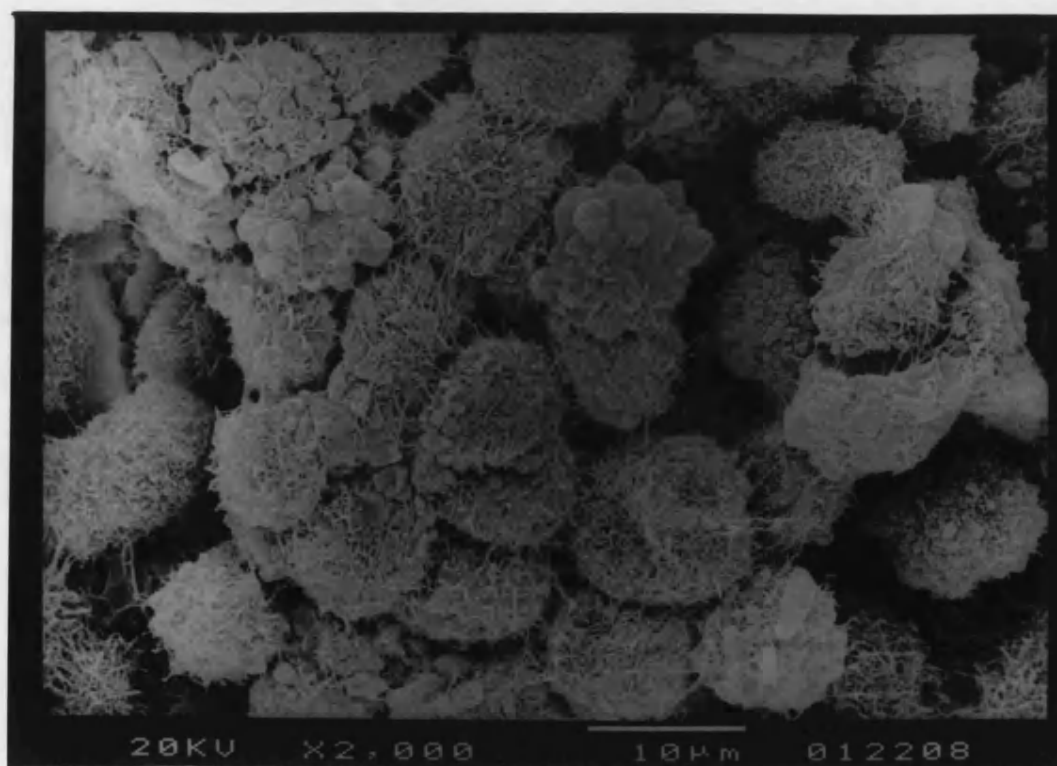


Figure 6.2.8: A photograph of Caco-2 cells taken using a Jeol JSM 35C Scanning Electron Microscope. Cells were incubated for 15 days on Millicell HA filters and then were prepared for microscopy as described in section 2.11.5. (Mag. 7500X)



Figure 6.2.9: BAE-1 cells incubated for 7 days prior to preparation as above. (7500X)

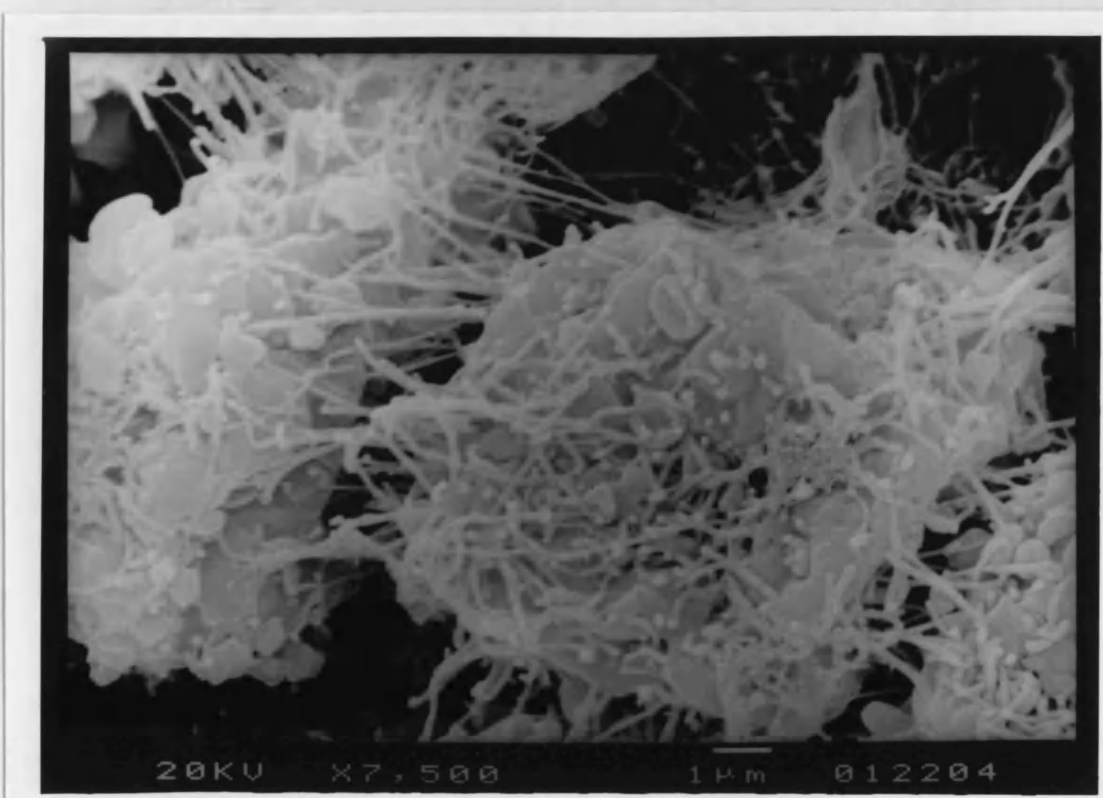


Figure 6.2.10: A photograph of Caco-2 cells taken using a Jeol 1200Ex Transmission Electron Microscope. Cells were incubated for 15 days on Millicell HA filters and then were prepared for microscopy as described in section 2.11.5. (Mag. 5000X)

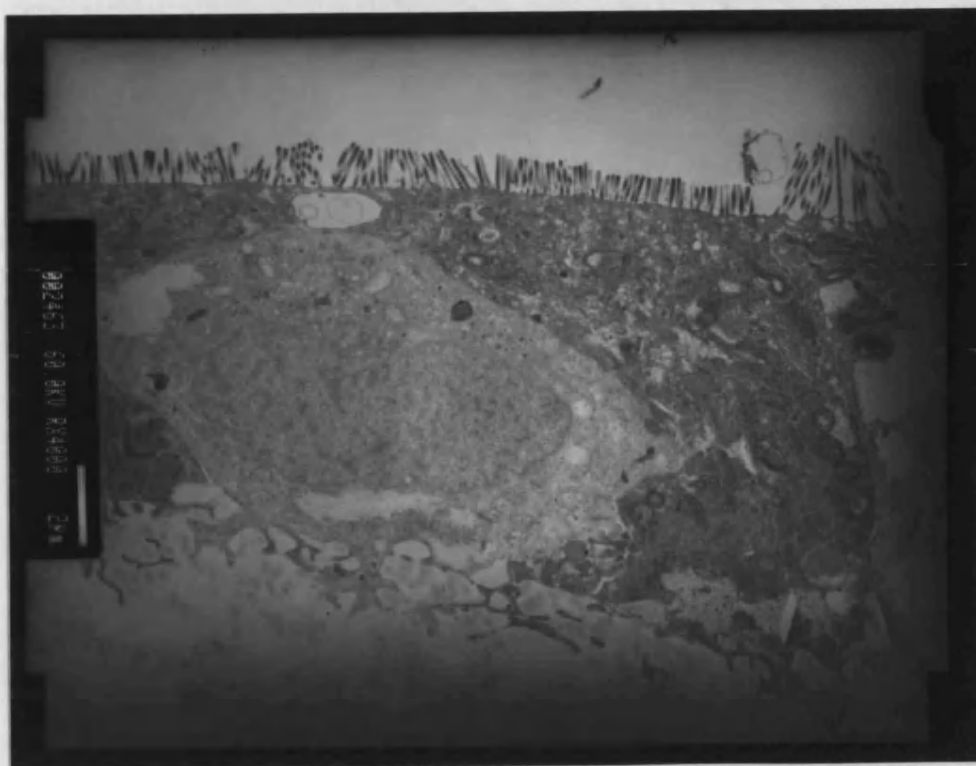


Figure 6.2.11: BAE-1 cells incubated for 7 days prior to preparation as above. (5000X)

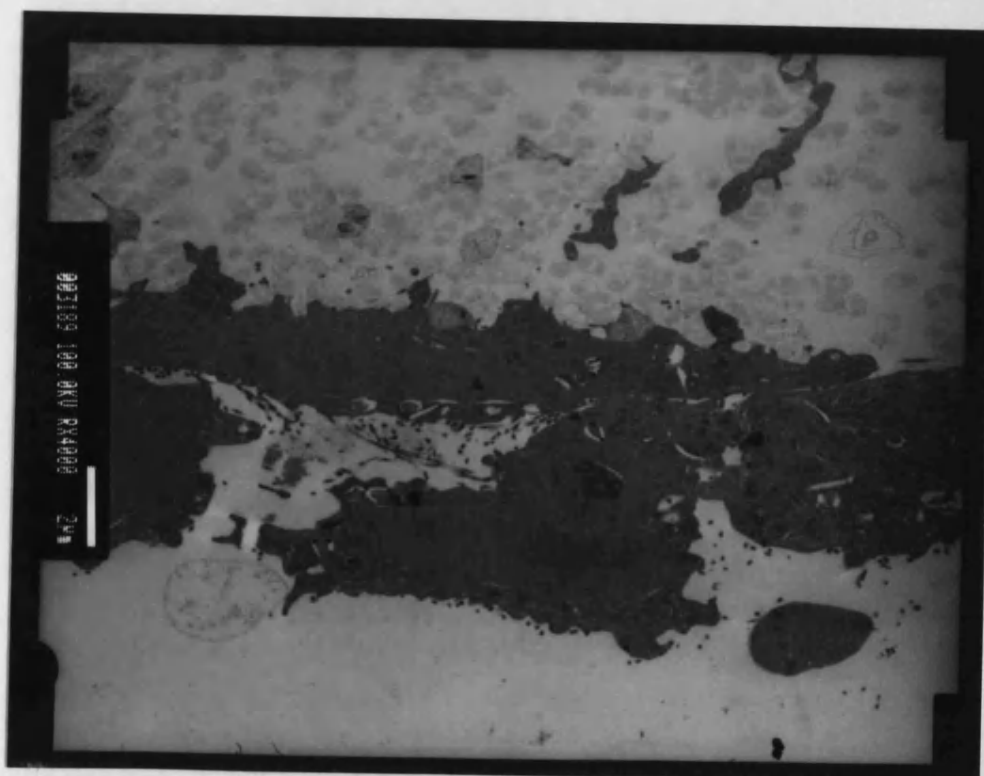




Figure 6.2.12: A photograph of Caco-2 cells taken using Zeiss Ultraphot Microscope fitted with a 35mm camera. Cells were incubated for 15 days on Millicell HA filters and then were prepared for microscopy as described in section 2.11.5. (Mag. 720X)

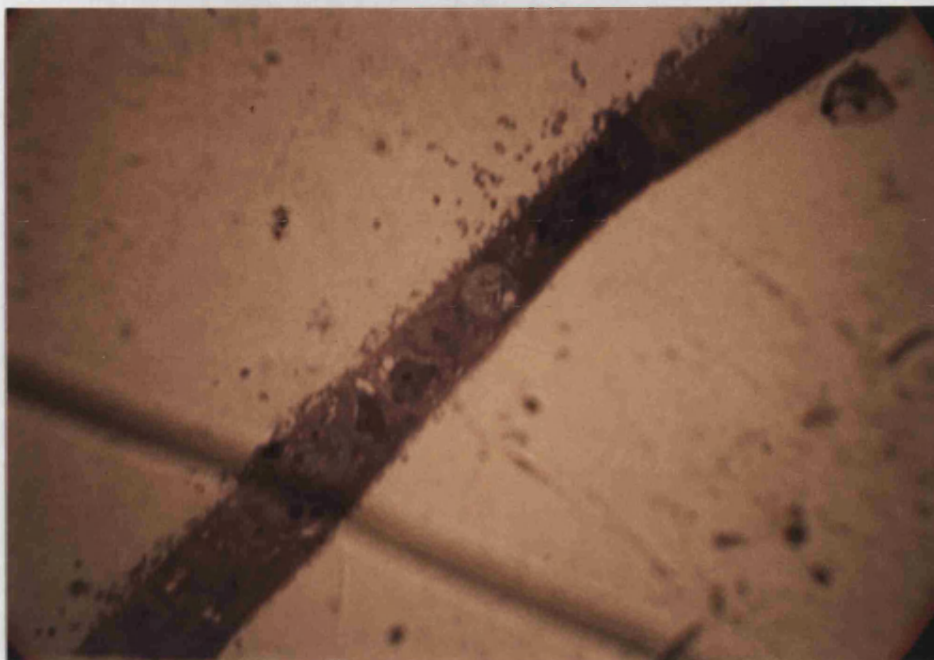


Figure 6.2.13: BAE-1 cells incubated for 7 days prior to preparation as above. (720X)





### 6.3 Uptake of BSA, BSA-MTX, G-BSA and M-BSA by Macrophages *in vitro*.

Since the collagenase liver perfusion experiment (chapter 5) was not successful in separating out a suspension containing mostly non-parenchymal cells, a major cell-type of which would have been the Kupffer cells or liver macrophages, it was decided to determine the uptake of the conjugates and free BSA by peritoneal macrophages *in vitro*. Comparison of the uptake by each conjugate or protein may give an indication of the ability of Kupffer cells *in vivo* to selectively take up the conjugates.

For each radioiodinated conjugate and protein the uptake by macrophages was determined at 4°C and at 37°C, following solubilisation of the cells and measurement in a gamma counter. The rationale for using the two temperatures was that, although the protein could occupy the receptor on the surface of the macrophage at low temperatures, it could not actually be internalised. Proteins that are rapidly internalised at 37°C may also be rapidly degraded intracellularly, and the breakdown products released back into the cell media. Therefore, measurement at 37°C only may lead to a falsely low reading for protein uptake.<sup>(186)</sup> In addition to measuring the actual uptake by the cells, the media was subjected to a TCA precipitation to determine the percentage of <sup>125</sup>I present as TCA soluble, and therefore low molecular weight material. In each of the experiments described in this section the procedure was essentially the same. One million cells were applied to each well, and determinations were carried out, in serum free media, 24 hours later.

Table A3.32.1 (appendix 3) lists the uptake of <sup>125</sup>I-HSA by macrophages at 37° and 4°C over a one hour period. Table A3.32.2 shows the TCA soluble radioactivity present in the media over the same time period. The uptake of the <sup>125</sup>I-HSA at the two temperatures appeared to be very similar and analysis of each time point by a Student's t-test showed that no percentage was significantly different for the two temperatures. Figure 6.3.1 is a graph showing the uptake of <sup>125</sup>I at the two temperatures, following exposure of the cells to 75µg of <sup>125</sup>I-HSA. The percentage uptake at 1 hour was 0.173% ±0.02 for the 37°C temperature and 0.159%±0.0096 at 4°C.

Figure 6.3.1:

Uptake of  $^{125}\text{I}$  activity by rat peritoneal macrophages, exposed to  $75\mu\text{g}$  of  $^{125}\text{I}$ -HSA. each point is a mean uptake for 3 wells  $\pm$  S.E.M.. The experiment was carried out at 2 temperatures;  $4^\circ\text{C}$  and  $37^\circ\text{C}$ .

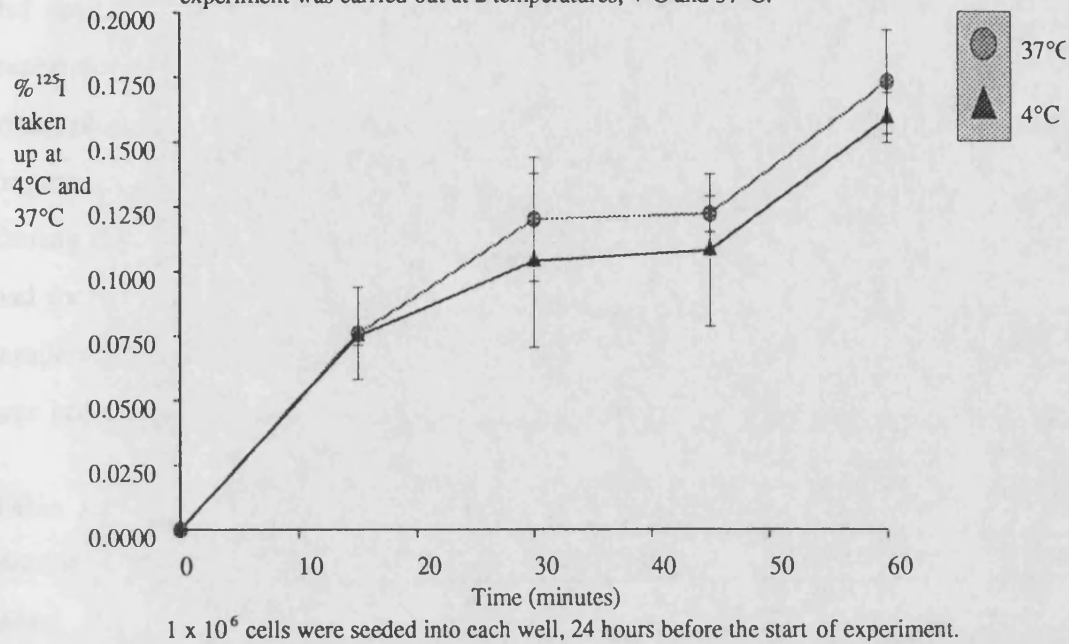


Figure 6.3.2:

Breakdown of  $^{125}\text{I}$ -HSA following exposure of rat peritoneal macrophages, in vitro, to RPMI media, containing  $75\mu\text{g}$  of  $^{125}\text{I}$ -HSA. Each point is a mean  $\pm$  S.E.M. from 3 wells. The experiment was carried out at 2 temperatures;  $4^\circ\text{C}$  and  $37^\circ\text{C}$ .

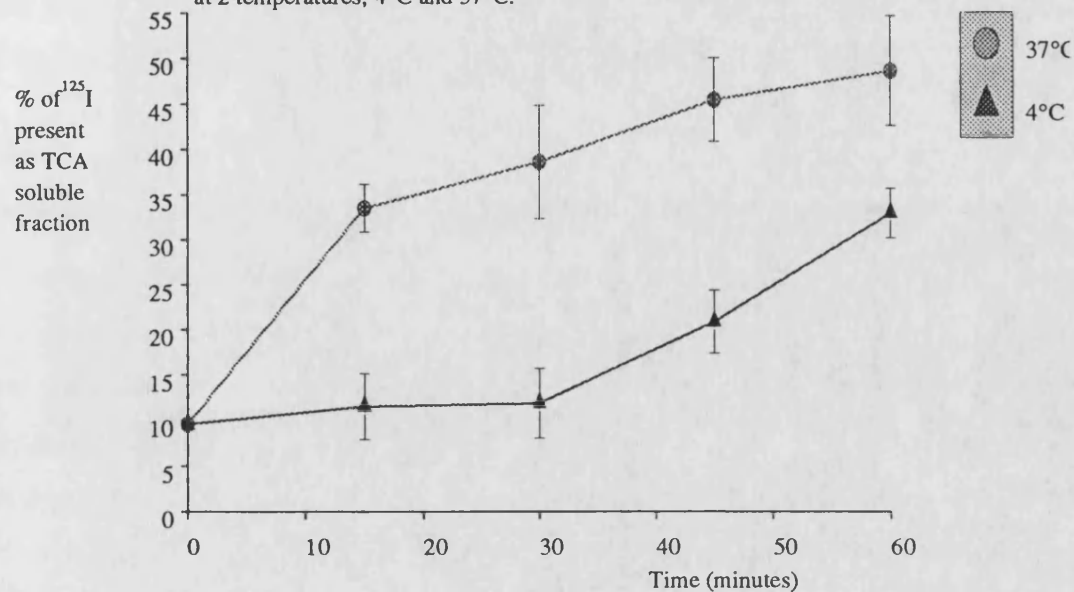


Figure 6.3.2 is a graph showing the break-down of the  $^{125}\text{I}$ -HSA following exposure to macrophages, in RPMI media. The appearance of TCA soluble material containing  $^{125}\text{I}$  did appear to be elevated in the  $37^\circ\text{C}$  experiment. Over the first 30 minutes of the experiment the % of low molecular weight  $^{125}\text{I}$  did not change for the  $4^\circ\text{C}$  macrophages. However for the  $37^\circ\text{C}$  macrophages there was a high proportion of  $^{125}\text{I}$  fragments which were soluble in TCA even 15 minutes after exposure of the cells. During the 15 minute incubation the % of  $^{125}\text{I}$  activity, present as TCA soluble material, had increased from 9.6% to 33.5%. The % of TCA soluble  $^{125}\text{I}$  at 60 minutes, for both temperatures, was compared by means of a Student's t-test. The TCA soluble material was not significantly different ( $p>0.1$ ) for the two temperatures.

Table A3.32.3 lists the  $^{125}\text{I}$ -BSA uptake at  $37^\circ\text{C}$  and  $4^\circ\text{C}$  over a 1 hour period and similar tables for BSA-MTX (4.54%w/w) and BSA-MTX (11.55%w/w) are shown in tables A3.32.5 and A3.32.7 respectively. Figure 6.3.3 is a graph comparing the uptake of the BSA and conjugates by peritoneal macrophages at  $37^\circ\text{C}$ . The concentration of BSA and the conjugates was the same at  $8\mu\text{g}$  per well. At 15 minutes after the start of the experiment the % of BSA taken up was  $0.0377\pm0.0036\%$ . At the same time point for BSA-MTX (11.55%w/w) the % taken up was  $0.161\pm0.0046\%$ . The results at this time point were compared by Student's t-test and were found to be highly significant ( $p<0.01$ ), and for the other time points, all t-values determined were highly significant. Thus the macrophages took up more BSA-MTX (11.55%w/w) conjugate than BSA.

The 4.54%w/w conjugate could only be compared at 30 minutes and 60 minutes (the only corresponding time points). At 30 minutes, the t-value obtained from comparison of BSA and BSA-MTX (4.54%w/w) was 2.71, this value has a probability of 0.0534, which is just non-significant. At 60 minutes the uptake for BSA was not significantly different from BSA-MTX (4.54%w/w) ( $p=0.325$ ). At every time point compared for BSA-MTX (4.54%w/w) and BSA-MTX (11.55%w/w) there was a highly significant difference for the amount of  $^{125}\text{I}$  internalised by the macrophages.

The BSA and BSA-MTX (4.54%w/w) were taken up to a similar extent by rat peritoneal macrophages *in vitro*. The 11.55%w/w conjugate was taken up to a greater

Figure 6.3.3:  
Uptake of  $^{125}\text{I}$ -labelled BSA, BSA-MTX (4.54%w/w) and BSA-MTX (11.55%w/w) by rat peritoneal macrophages in vitro at 37 °C. Each point is the mean determined for three wells.  $\pm$  S.E.M.

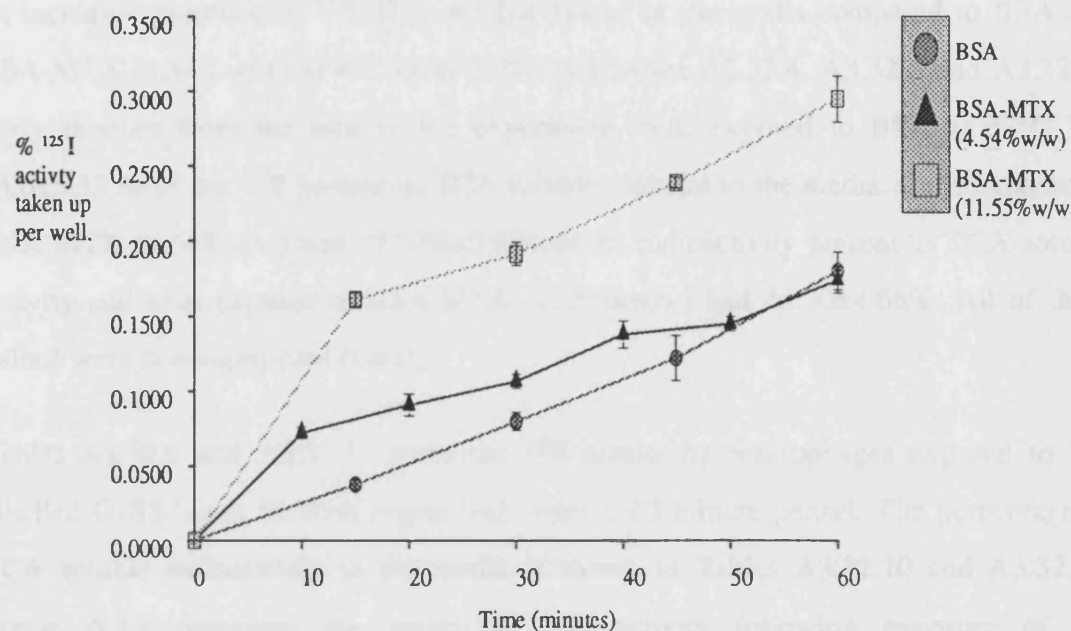
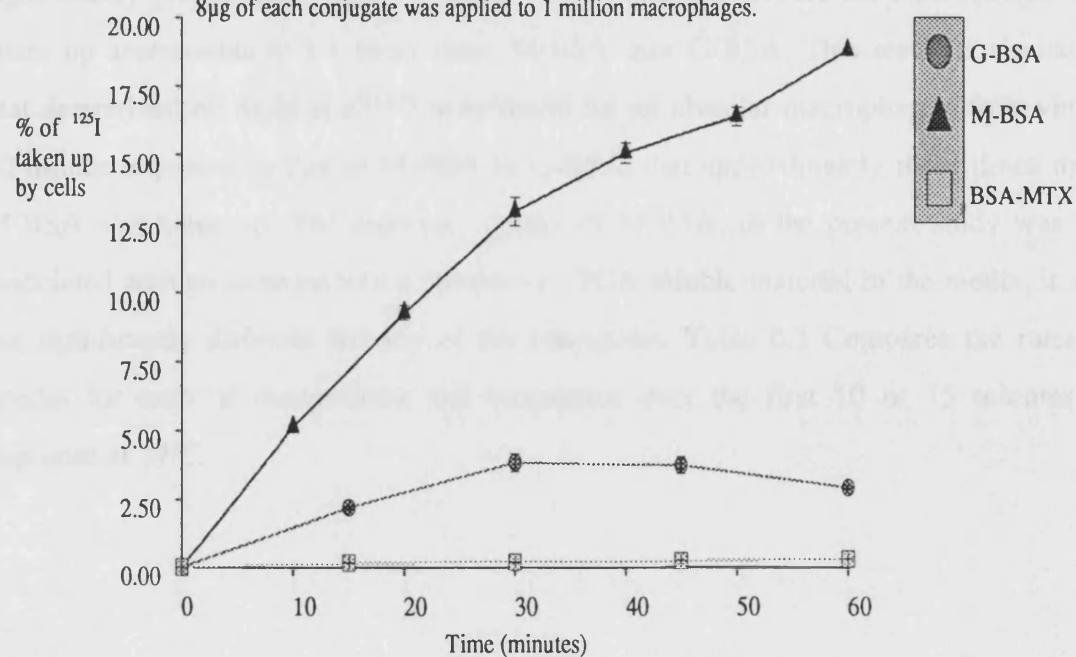


Figure 6.3.4:  
Uptake of  $^{125}\text{I}$ -labelled BSA-MTX (11.55%w/w), G-BSA and M-BSA by rat peritoneal macrophages in vitro at 37°C. Each point is the mean  $\pm$  S.E.M. of 3 wells. 8  $\mu\text{g}$  of each conjugate was applied to 1 million macrophages.



extent than either the low strength conjugate or the 'free' BSA. The increased uptake of the BSA-MTX (11.55%w/w) was also demonstrated at 4°C. It was not associated with an increased presence of  $^{125}\text{I}$  TCA soluble matter in the media compared to BSA and BSA-MTX (4.54%w/w) at 4°C or at 37°C. (see tables A3.32.4, A3.32.6 and A3.32.8). Sixty minutes from the start of the experiment, cells exposed to BSA at 37°C had  $44.0 \pm 5.33$  % of the  $^{125}\text{I}$  present as TCA soluble material in the media. Cells exposed to BSA-MTX (4.54%w/w) had  $47.72\% \pm 3.604$  of the radioactivity present as TCA soluble activity and cells exposed to BSA-MTX (11.55%w/w) had  $45.30 \pm 4.66\%$ . All of these values were non-significant (t-test).

Tables A3.32.9 and A3.32.11 show the  $^{125}\text{I}$  uptake by macrophages exposed to  $^{125}\text{I}$  labelled G-BSA and M-BSA respectively over a 60 minute period. The percentage of TCA soluble radioactivity in the media is shown in Tables A3.32.10 and A3.32.12. Figure 6.3.4 compares the uptake of  $^{125}\text{I}$  activity following exposure of the macrophages to BSA-MTX (11.55%w/w), G-BSA and M-BSA. These experiments were carried out on the same day, using the same batch of macrophages. The uptake of G-BSA by the macrophages was highly significantly different at all time points from the uptake of BSA. In addition the uptake of M-BSA by macrophages was highly significantly greater than for the G-BSA. At 30 minutes exposure the macrophages had taken up approximately 3.4 times more M-BSA than G-BSA. This result is similar to that determined by Stahl et al<sup>(187)</sup>, who found for rat alveolar macrophages, following a 30 minute exposure to 2µg of M-BSA or G-BSA, that approximately three times more M-BSA was taken up. The increased uptake of M-BSA, in the present study was not associated with an increase in the presence of TCA soluble material in the media, it was not significantly different for any of the conjugates. Table 6.3 Compares the rates of uptake for each of the proteins and conjugates over the first 10 or 15 minutes of exposure at 37°C.

**Table 6.3: The Rates of Uptake for BSA, and BSA Conjugates by rat peritoneal macrophages *in vitro* at 37°C.**

Conjugate	Rate of Uptake (% / min)
'free' BSA	$2.51 \times 10^{-3}$
BSA-MTX (4.54%w/w)	$7.22 \times 10^{-3}$ *
BSA-MTX (11.55%w/w)	$1.07 \times 10^{-2}$
G-BSA	0.147
M-BSA	0.513*

\*Uptake rate was calculated over the first 10 minutes of exposure. For the other proteins and conjugates, it was determined over the first 15 minutes of exposure.

It would appear that macrophages have a receptor for mannose-BSA and they selectively ingested this protein. Stahl et al<sup>(188)</sup> demonstrated that  $^{125}\text{I}$ -M-BSA was taken up in rat alveolar macrophages by the process of receptor mediated endocytosis. The endocytosis of  $^{125}\text{I}$ -M-BSA could be inhibited by Fucose-BSA, indicating that fucose enters the cell using the same receptor, but it was not inhibited by galactose-BSA. Tietze <sup>(189)</sup> also demonstrated that the uptake and degradation of M-BSA could be inhibited by Chloroquine and ammonium ions, both of which are inhibitors of lysosomal enzymes.

The rate of uptake for M-BSA, calculated in this experiment, was over 3 times greater than for G-BSA, and 200 times greater than for BSA. The rate of uptake of BSA-MTX was 4 times greater than for free BSA, but when compared to M-BSA it was 50 times less than M-BSA. Thus although the 11.55%w/w conjugate was taken up to a greater extent than the BSA, it would not appear that there was a specific receptor for it. The increased uptake could be due to the presence of aggregated protein in this conjugate. BSA-MTX (4.54%w/w) did not appear to be taken up to a greater extent than free BSA,

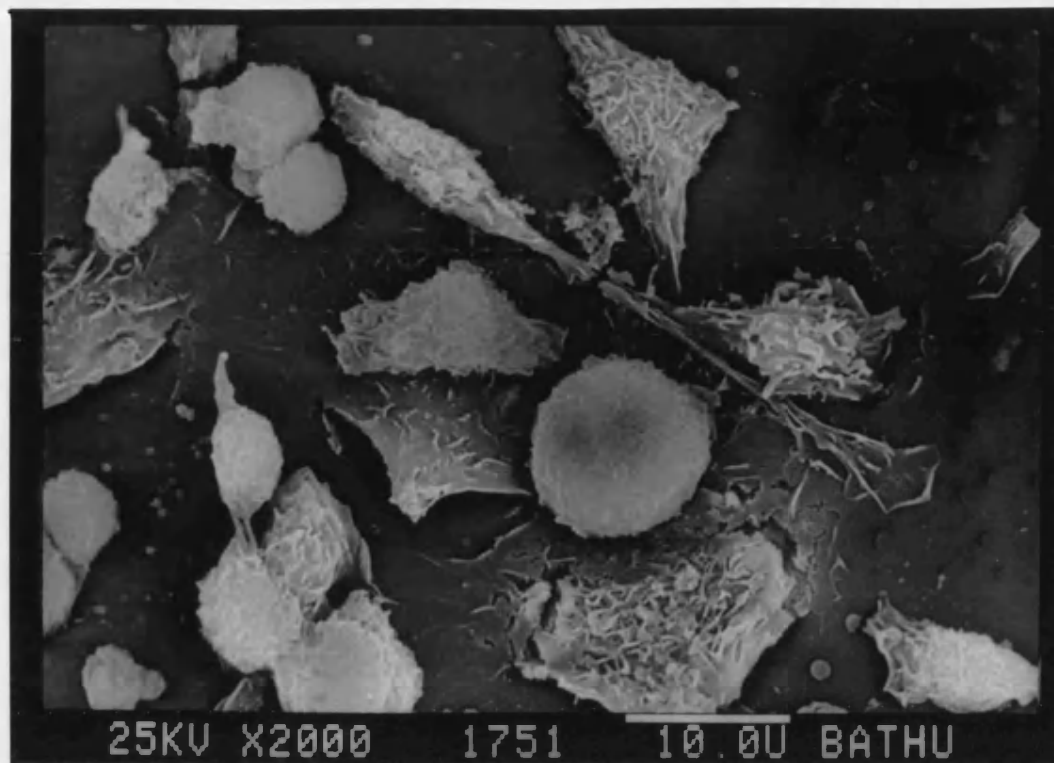
overall, although the initial rate of uptake was over 2 times higher. The increased uptake of the BSA-MTX (11.55%w/w) could also be due to its increased hydrophobicity. Duncan et al<sup>(150)</sup> demonstrated that HPMA polymers with increasing hydrophobicity were taken up to a greater extent by rat visceral yolk sacs. This increased uptake could be inhibited by 2,4 dinitrophenol an inhibitor of pinocytosis.

This work complements the work done on the conjugates *in vivo*, on liver uptake. It was hoped that macrophages *in vitro* may behave in a similar manner to Kupffer cells *in vivo*. Although approximately the same percentage of MTX-BSA (11.55%w/w) was taken up by the liver as M-BSA, the uptake of the conjugates by macrophages was very different. It was shown by the collagenase perfusion of the liver that 40% of the activity within the liver for the BSA-MTX was associated with the hepatocytes, whereas for the M-BSA only 20% of the activity was associated with the hepatocytes. The remaining activity in the liver was assumed to be associated with the non-parenchymal cells. For the BSA-MTX, although the non-parenchymal cells do take up more of the conjugate, than hepatocytes, the rate of uptake by this cell type may be slower than for M-BSA, thus allowing more time for capture by hepatocytes. The rate of uptake by macrophages was shown to be slower for MTX-BSA than for M-BSA.

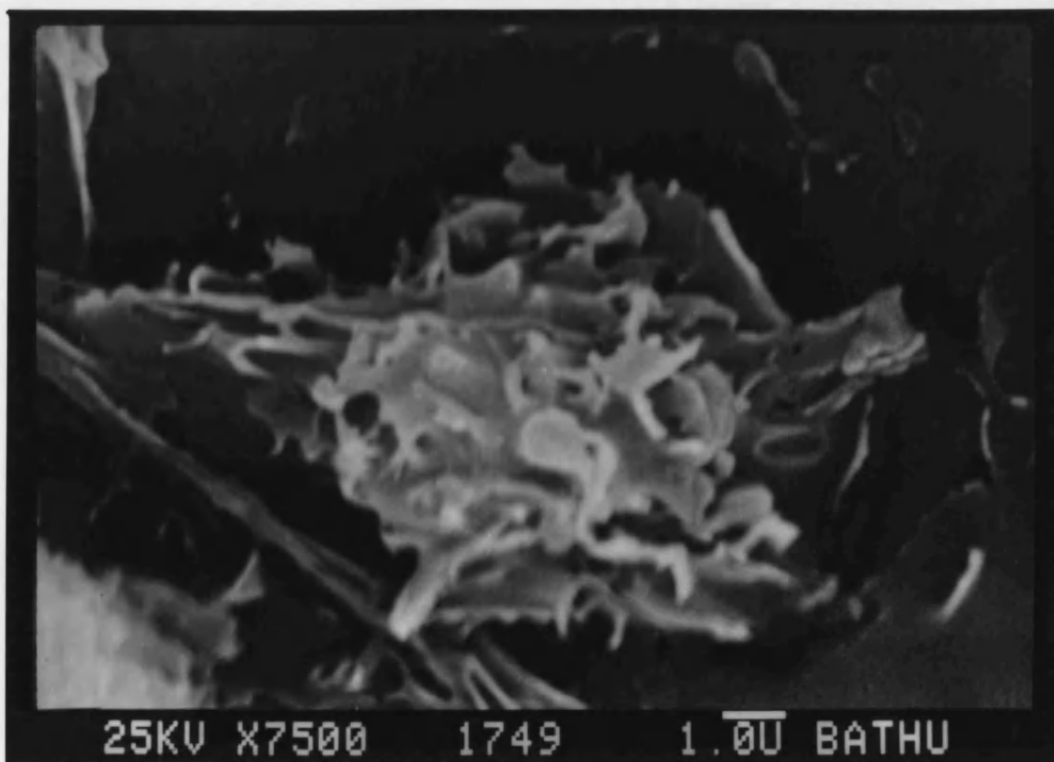
G-BSA was taken up at a faster rate by macrophages *in vitro* than MTX-BSA. From the macrophage results it may have been assumed that Kupffer cells would take up the G-BSA *in vivo*, however, it was shown in the whole liver to be taken up almost entirely by the hepatocytes and so the uptake by peritoneal macrophages *in vitro* alone is not a good model for the uptake by Kupffer cells *in vivo*. This is partly because the liver is a complex organ and consists of several cell types.

Photographs were taken of macrophages that were obtained by peritoneal lavage, as described in section 2.10. These are shown in figure 6.3.5a and b.

Figure 6.3.5a: A photograph of rat peritoneal macrophages taken using the Jeol JSM 35c Scanning Electron Microscope. Cells were prepared for microscopy as described in section 2.10. (Magnification 2000X).



6.3.5b Macrophages photographed as described above (Magnification 7500X).





**CHAPTER 7:**  
**CONCLUSIONS.**

The aim of this thesis was to produce large molecular weight, soluble derivatives of MTX, and to evaluate these derivatives in the rat, for changes in the pharmacokinetic parameters, compared to free MTX. It was hoped that these conjugates would demonstrate certain beneficial properties compared to free MTX such as an increase in circulation half-life giving rise to prolonged levels of the drug in tissue fluid, and limitation of cellular uptake reducing drug side effects. Eventual conjugation of a specific targeting agent to the drug carrier complex would allow entry into cells by the process of receptor mediated pinocytosis which can occur more rapidly than fluid phase pinocytosis.

It was shown that all the BSA-MTX conjugates administered to rats did in fact demonstrate these beneficial changes in pharmacokinetics compared to free MTX. The conjugates had terminal half-lives which were at least ten times those of free drug and Vd were less than a third. They, therefore, have potential as drug-carrier systems.

The actual distribution and pharmacokinetics of the conjugates appeared to be related to the concentration of MTX. At low loadings of MTX in the conjugate the elimination half-life was decreased compared to free BSA, however there was a linear relationship between the terminal half-life for the conjugates and the loading of MTX. BSA-MTX with a loading above 7.16%w/w had a half-life that was greater than that calculated for BSA (see figure 4.13.2). There was a tendency for the volume of distribution to increase with increased concentration of MTX in the conjugate. Whole body autoradiography (figures 5.5.1 to 5.5.9) and organ distribution studies showed the reason for the increased volume of distribution. For low strength conjugates (e.g. 4.54%w/w) there was a generalised increased uptake of the conjugate by most organs investigated compared to free BSA and the higher strength conjugates (e.g. 11.55%w/w) were associated with a rapid uptake by the liver (61-67% in the first 15 minutes).

The reason for the changed distribution pattern compared to free BSA has not been discovered, but may be due to the changed characteristics of the protein. The possible changes include an increased hydrophobicity which could lead to a greater association with cell membranes (this could explain the non-specific accumulation for the low

strength conjugates). The conjugates would be expected to exhibit a greater anionic charge than BSA itself. There is conflicting evidence on whether this would increase or decrease its ability to extravasate. It has been demonstrated that positively charged molecules can enter the urine from the kidney more readily than equally sized negative ones up to a molecular radius of about 4.4nm<sup>(23)</sup>. However, in the lung and intestine, it has been demonstrated that negatively charged molecules are lost from the blood stream more readily than positively charged molecules.<sup>(24,25)</sup> The BSA-MTX conjugates would be expected to have a changed tertiary structure compared to free BSA and this may lead to the conjugates being recognised as foreign and being taken up by the RES (liver, spleen, and bone marrow). Increased uptake by these organs was demonstrated for the 11.55%w/w conjugate. Another change in the conjugates compared to free BSA was the increase in the presence aggregated protein (up to 39% in the 13.6%w/w compared to only 7% in free BSA). This may also cause increased uptake by the RES. The generalised increase in organ uptake for the low strength conjugates may be due to the specific effect of methotrexate itself, which has helped the conjugate to enter the cells using the folate transporter.

BSA and the conjugates were administered with a <sup>125</sup>I label so that they could be detected in serum. There were two problems associated with the use of this label. Firstly, there was the possibility of injecting a small amount of unconjugated <sup>125</sup>I- along with the iodinated conjugate and secondly it was anticipated that the proteins and conjugates would be degraded *in vivo* and this would be followed by the release of <sup>125</sup>I either as iodide or as iodinated tyrosine from the protein. <sup>125</sup>I-Na was administered to rats to investigate, if any unconjugated <sup>125</sup>I would lead to errors in the assay of <sup>125</sup>I-BSA or <sup>125</sup>I-BSA-MTX.

<sup>125</sup>I-Na was shown to have a rapid alpha phase half-life at approximately 50 minutes and a large Vd of 260ml. At 3 hours after injection (the end of the alpha phase) the levels of <sup>125</sup>I in serum had fallen to 0.3%/ml, and this represents only 2.7% of the injected dose in the blood stream. Organ distribution was determined for the liver, kidney and thyroid. <sup>125</sup>I did not accumulate in the liver or kidney but was sequestered

by the thyroid (5-6% of the injected dose in 4 hours), this would be expected to be released at a later stage as  $^{125}\text{I}$ -thyroxine. From these results  $^{125}\text{I}$  (as iodide) present in the original injection solution was not expected to cause a problem at early time points because there was never more than 10% of free iodide in the injection. This iodine would rapidly leave the vasculature and be taken up by the thyroid.

The molecular weight of the serum  $^{125}\text{I}$  was determined following injection of BSA-MTX (7.16%w/w). The majority of radioactivity (more than 67%), measured up to 48 hours after injection was present as conjugate-bound  $^{125}\text{I}$ . The remainder of the radioactivity was present as either iodotyrosine, iodide or possibly  $^{125}\text{I}$ -thyroxine. In addition the longer  $t^{1/2}$  for proteins and conjugates, compared to free  $^{125}\text{I}$ , suggests that it is the actual protein that is being followed and not free tracer.

46% of the injected  $^{125}\text{I}$ -Na was excreted by the kidney in 24 hours. For  $^{125}\text{I}$ -BSA only 15-19% of the radioactivity was excreted in the urine in 24 hours and this again proves that the  $^{125}\text{I}$  was not cleaved from the protein immediately following administration (otherwise the amount excreted would be the same as for unconjugated iodide). For the proteins and conjugates, the excretion by the kidney was actually a measure of their catabolism because they are too large to be excreted unchanged. This explains why more of the conjugate was excreted than BSA (see figure 4.13.3) because the increased uptake by the liver would be expected to result in increased degradation of the protein.

Separate analysis of the protein and drug portions of the conjugate was investigated using a dual label. The BSA was labelled with  $^{125}\text{I}$  as before and the MTX was labelled with  $^3\text{H}$ . The concentration of the two isotopes was measured in serum and the ratios of the two isotopes was found to be similar over the 96 hours of the experiment. This suggests that neither of the labels was cleaved from the conjugate during circulation. The fate of the two isotopes was not the same however, following uptake of the conjugate by the liver and spleen.  $^3\text{H}$  was found to accumulate in the liver and spleen, whereas the  $^{125}\text{I}$  portion of the conjugate was found to be released.  $^{125}\text{I}$  appeared in the G.I.T. rapidly, following administration (within 6 hours) and was identified to be present in bile as iodide or iodotyrosine. The rate of appearance of the  $^3\text{H}$  isotope in the

gut was slower and levels did not begin to rise to similar levels to the  $^{125}\text{I}$  isotope until 72 hours after injection. Likewise the excretion in the urine of the  $^3\text{H}$  isotope occurred more slowly than the  $^{125}\text{I}$  isotope (51% of the  $^{125}\text{I}$  was excreted in the urine whereas only 28.5% of the  $^3\text{H}$  was excreted in 24 hours).

These results suggest that the conjugate was degraded following cellular uptake. The  $^{125}\text{I}$  isotope was released and  $^3\text{H}$  was retained by the cell. It is not known whether the  $^3\text{H}$  retained by the cell was still bound to MTX. Neither is it known whether the whole BSA molecule had been degraded or perhaps just  $^{125}\text{I}$  had been cleaved from it. If the BSA had been degraded it was not known whether the MTX had been cleaved from it and was present intracellularly as active free drug, or was still bound to oligopeptides. The fact that the  $^3\text{H}$  was retained by the cell supports the theory that it was bound to MTX. MTX is known to be sequestered by cells since it becomes polyglutamated and bound to DHFR.

Further experiments utilised RSA and LA as drug carriers for MTX. Only one RSA-MTX was synthesised, so no firm conclusions can be drawn. However, it did appear to show the same distribution characteristics to a BSA-MTX conjugate with a similar loading. Two LA-MTX conjugates were synthesised with loadings of MTX of 4.52%w/w and 13.69%w/w. These were found to have larger  $V_d$  than BSA-MTX and this was probably due to the decreased molecular weight (BSA has a molecular weight of 67kD and LA has a molecular weight of 14kD. The LA-MTX (13.69%w/w) was found to have a larger  $V_d$  than the lower strength conjugate and 'free' LA, this is a similar pattern for that seen for BSA-MTX conjugates and may be the result of increased organ uptake. Unfortunately organ distribution studies were not carried out for LA-MTX and so the reason for the increased  $V_d$  cannot be concluded.

Conjugates between BSA and galactosamine or mannose were administered to rats and the organ distribution determined. It was found that both of these conjugates rapidly targeted to the liver (70 to 80% in 15 minutes). It was hoped that these conjugates could be used to selectively target MTX to 2 cell types; namely the hepatocytes for the G-BSA and the Kupffer cells for the M-BSA. However, a conjugate between MTX and

the G-BSA or M-BSA could not be synthesised using the carbodiimide reaction. The BSA-MTX (11.55%w/w) conjugate was found to accumulate in the liver (60% in 15 minutes). This accumulation was associated with both the hepatocytes (40% of the liver activity) and the non-parenchymal cells (the remainder), thus the non-parenchymal cells were exposed to a greater concentration of the BSA-MTX because they actually represent a smaller proportion of the liver mass, than do the hepatocytes. This liver cell-type selectivity could be used as the basis of passive targeting to diseased cells within the liver such as leishmaniasis infected macrophages.

Some *in vitro* work, which investigated the uptake of BSA, BSA-MTX, G-BSA and M-BSA by rat peritoneal macrophages was carried out. It was hoped that the uptake by the macrophages would mimic the uptake of the conjugates *in vivo* in the liver Kupffer cells. It was found that M-BSA was taken up by the macrophages at a faster rate than any other of the proteins investigated. (It was 3 times greater than G-BSA and over 200 times greater than 'free' BSA.) BSA-MTX (11.55%w/w) was taken up more rapidly than BSA or BSA-MTX (4.54%w/w). The rate of uptake was 5 times faster than 'free' BSA. This increased rate of uptake demonstrated by the macrophages for the 11.55%w/w conjugate was similar to that seen *in vivo* for the liver, where 61 to 67% of the dose accumulated 15 minutes after injection for the BSA-MTX (11.55%w/w) conjugate and only 22 to 25 % of the injected BSA-MTX (4.54%w/w) accumulated.

A second *in vitro* experiment, involved the growth of BAE-1 cells, an endothelial cell-line, on filters and using this system as a model for the capillary. The transport of BSA, BSA-MTX (4.54%w/w) and BSA-MTX (11.55%w/w) was investigated. It was found that 'free' BSA was transported across the cell monolayer at a faster rate than either of the two conjugates. The slower rate for the conjugates could be explained by the larger amount of aggregated protein (BSA only had 7% aggregated protein whereas the conjugates had 23 and 33%). In addition, a greater proportion of the conjugates (0.5 and 2.2%) was found to be associated with the cells themselves compared to BSA (0.16%). It is not known whether the conjugate was adsorbed to the cell surface or was intracellular but this may also account, at least partly, for the decreased transport of the

conjugates compared to BSA. This experiment was carried out to determine whether the generalised uptake by the organs seen for the low strength conjugates could be attributed to an increased ability of the conjugates to extravasate compared to 'free' BSA. It was shown that BSA-MTX conjugates were actually transported more slowly than BSA itself. However there were problems associated with the cell monolayer. Electron microscope analysis of the monolayer showed that there were quite large holes in it.

The BSA-MTX conjugates appear to have achieved, what was initially outlined in the introduction. The lower strength conjugates do increase circulation half-life and decrease Vd and so fulfill the criteria for a successful drug delivery system. Below are some suggestions for future work.

#### **Suggestions for Future Work.**

1. One of the problems associated with synthesis of the BSA-MTX conjugates using the carbodiimide method was the production of protein aggregates. In these experiments the aggregates were not removed and in some cases it is not known whether the distribution could be attributed to the conjugate itself or the aggregated material that it contained. For instance, the increased liver uptake demonstrated for the 11.55%w/w conjugate could be due, at least partly to the aggregated material. 61-67% of the injected dose was taken up by the liver in the first 15 minutes and the conjugate contained approximately 33% of aggregated material. A better fractionation technique could be used to separate the aggregated material from monomeric conjugate or a different method for synthesis of the conjugates could be used. Then conjugates with a low percentage of aggregated material could be administered and compared to the original data.

2. Several possibilities to explain the increased cellular uptake of the BSA-MTX compared to free BSA have been described. One suggestion was, that the increased uptake was due to the MTX actually helping the conjugate into the cell using the folate transporter. Because this is a receptor mediated process, then if cellular uptake was due to this transporter it could be inhibited using high concentrations of unlabelled MTX or

the natural substrate, folate. If extravasation and cellular uptake for the conjugates was inhibited by high concentrations of folate, then this may suggest that cellular uptake did occur by this route.

3. Following uptake of the  $^{125}\text{I}$ -BSA- $^3\text{H}$ -MTX (7.16%w/w) conjugate by the liver it was shown that the  $^{125}\text{I}$  portion was cleaved from the conjugate and released as iodotyrosine or iodide whereas the  $^3\text{H}$  isotope was retained. However, it is not known what form the isotope took. It may have been cleaved from the MTX, it may have been bound to free active drug or it may have been bound to MTX which was still linked to oligopeptides. One way of determining in what form the  $^3\text{H}$  was present would be to homogenise the liver and to analyse the homogenate by HPLC, for free MTX, polyglutamates of MTX and oligopeptides of MTX.

4. There was a significant difference between the amounts of BSA-MTX (4.54%w/w) and BSA-MTX (11.55%w/w) taken up by the liver (20% and 61-67% respectively). Although the increased liver uptake could be used to passively target drug to this organ, the lower strength conjugates did appear to exhibit better overall distribution characteristics. A generalised uptake into most organs was demonstrated. Providing that the cellular uptake was limited to pinocytosis then the conjugates would exhibit decreased toxicity than free drug but they would be present in the tissue fluid for uptake by the target cell. The highest loading of MTX in the conjugate that would achieve this generalised organ uptake rather than liver uptake would probably be the optimal conjugate. Further work needs to be carried out to find out the optimal MTX concentration in the conjugate.

5. Experiments were carried out to try and target the BSA conjugates. Galactose covalently linked to BSA was found to selectively accumulate in the liver hepatocytes. Unfortunately, a conjugate between MTX and G-BSA could not be synthesised using the established ECDI method. Further work needs to be carried out to achieve selective delivery of the BSA-MTX conjugates. This work could utilise the galactose system or a mAb could be used. It was demonstrated that the BSA-MTX conjugates were able to extravasate. However, if an IgG molecule was attached to the conjugate, extravasation



may be inhibited because of the large molecular weight of the complex. Perhaps a better alternative would be to use a Fab fragment of a mAb since these have a lower molecular weight.

6. Although BSA has been shown to demonstrate quite good properties as a drug carrier in this experimental situation, there is the possibility (even when using homologous albumin) that on repeated application an immune response could be precipitated. It is generally considered that synthetic polymers have a lower potential for immunogenicity and so further work could be carried out on synthetic conjugates. There are many examples of synthetic carriers in the literature. The ideal carrier would probably be without molecular charge, since cationic carriers e.g. poly-lysine are actually toxic themselves and should be biodegradable, to avoid long term toxicity problems.

### References.

1. R.L. Juliano, G. Poste and E. Tomlinson, *Advanced Drug Delivery Reviews*, **1/2** (1987).
2. D.R. Friend and S. Pangburn, Site Specific Drug Delivery, *Med Res. Rev.*, **7(1)**, 53-106 (1987).
3. H. Ringsdorf, Structure and Properties of Pharmacologically Active Polymers, *J. Polymer Sci. Symposium*, **51**, 135-153 (1975).
4. K.J. Widder, A.E. Senyei and D.F. Ranney, Magnetically Responsive Microspheres and other Carriers for the Biophysical Targeting of Anti-tumour Agents, *Adv. Pharmacol. Chemother.*, **16**, 213-271 (1979).
5. E. Tomlinson, Passive and Active Vectoring with Microparticles: Localisation and Drug Release, *J. Cont. Rel.*, **2**, 385-391 (1985).
6. G. Ashwell and J. Harford, Carbohydrate Specific Receptors of the Liver, *Ann. Rev. Biochem.* **51**, 531-554 (1982).
7. J.B. Lloyd, Endocytosis and Lysosomes: Recent Progress in Intracellular Traffic in Targeting of Drugs with Synthetic Systems, Ed. G. Gregoriadis, J. Senior and G. Poste, Plenum Press, New York and London (1984).
8. C.R. Hopkins, The Importance of the Endosome in Intracellular Traffic, *Nature*, **304**, 684-685 (1983).
9. N. Simionescu, Cellular Aspects of Transcapillary Exchange, *Phys. Rev.*, **63(4)**, 1536-1579 (1983).
10. J.A.G. Rhodin, Anatomy of Microcirculation, in "Blood Vessels and Lymphatics in Organ Systems", Ed. D.I. Abramson and P.B. Dobbin, Academic Press, New York (1984).
11. A.E. Taylor and D.N. Granger, Exchange of Macromolecules across the Microcirculation, Chapter 11 in *The Handbook of Physiology* Ed. E.M. Renkin and C.C. Michel (1984).
12. M. Bundgaard, Transport Pathways in Capillaries- in Search of Pores, *Ann. Rev. physiol.*, **42**, 325-336 (1980).
13. N. Simionescu, M.A. Simionescu and G.E. Palade, Open Junctions in the Endothelium of Postcapillary Venules of the Diaphragm, *J. Cell Biol.*, **79**, 27-44 (1978).

14. D.G. Garlick and E.M. Renkin, Transport of Large Molecules from Plasma to Interstitial Fluid and Lymph in Dogs, *Am. J. Physiol.*, **219**(6), 1595-1605 (1970).
15. N. Simionescu, M. Simionescu and G.E. Palade, Differentiated Microdomains on the Luminal Surface of the Capillary Endothelium I. Preferential Distribution of Anionic Sites. *J. Cell Biol.*, **90**, 605-613 (1981).
16. N. Simionescu, M. Simionescu, J.E. Silbert and G.E. Palade, Differentiated Microdomains on the Luminal Surface of Capillary Endothelium II. Partial Characteristics of their Anionic Sites, *J. Cell Biol.*, **90**, 614-621 (1981).
17. M. Simionescu, N. Simionescu, G.E. Palade, Differentiated Microdomains on the Luminal Surface of Capillary Endothelium: distribution of Lectin Receptors. *J. Cell Biol.*, **94**, 406-413 (1982).
18. G.L. King and S.M. Johnson, Receptor-mediated Transport of Insulin across Endothelial Cells, *Science*, **227**, 1583-1586 (1985).
19. M. Simionescu, Structural and Functional Differentiation of Microvascular Endothelium, in "Blood Cells and Vessel Walls", *Ciba Foundation Symposium*, **71**, 39-60 (1980).
20. M. Simionescu, N. Simionescu and G.E. Palade, Preferential Distribution of Anionic Sites on the Basal Membrane and the Abluminal Aspect of the Endothelium in Fenestrated Capillaries, *J. Cell Biol.*, **95**, 425-434 (1982).
21. G.E. Palade, M.A. Simionescu and N. Simionescu, Structural Aspects of the Permeability of the Microvascular Endothelium, *Acta Physiol. Scand. Supp.*, **463**, 11-32 (1979).
22. R.L.S. Chang, I.F. Ueki, J.L. Troy, W.M. Deen, C.R. Robertson and B.M. Brenner. Permeability of the Glomerular Capillary Wall to Macromolecules II. Experimental Studies in Rats Using Neutral Dextran, *Biophys. J.*, **15**, 887-906 (1975).
23. M.P. Bohrer, C. Baylis, H.D. Humes, R.J. Glassock, C.R. Robertson and B.M. Brenner, Permeability of the Glomerular Capillary Wall, *J. Clin. Invest.*, **61**, 72-78 (1978).
24. M.A. Perry, J.N. Benoit, P.R. Kvetys and D.N. Granger, Restricted Transport of Cationic Macromolecules across Intestinal Capillaries, *Am. J. Physiol.*, **245**, G568-G572 (1983).
25. J.C. Parker, S. Gilchrist and J.T. Cartledge, Plasma-Lymph Exchange and Interstitial Distribution Volumes of Charged Macromolecules in the Lung, *J. Appl. Physiol.*, **59**(4), 1128-1136 (1985).

26. C.H. Blood and B.R. Zetter, Tumour Interactions with the Vasculature: Angiogenesis and Tumour Metastasis, *Biochim. Biophys. Acta (Reviews on Cancer)*, **1032(1)**, 89-118 (1990).
27. J. Folkman and H.P. Greenspan, Influence of Geometry on Control of Cell Growth, *Biochim. Biophys. Acta*, **417**, 211-236 (1975).
28. I.F. Tannock, The Relationship between Cell Proliferation and The Vascular System in a Transplanted Mouse Mammary Tumour, *Br. J. Cancer*, **22**, 258-273 (1968).
29. B.A. Warren, Tumour Angiogenesis, pp49-76 in "Tumour Blood Circulation: Angiogenesis, Vascular Morphology and Blood Flow of Experimental and Human Tumours", Ed. H.I. Peterson, CRC Press, Florida (1979).
30. D.H. Ausprunk and J. Folkman, Migration and Proliferation of Endothelial Cells in Preformed and Newly Formed Blood Vessels during Tumour Angiogenesis, *Microvasc. Res.*, **14**, 53-65 (1977).
31. J.W. Fett, D.J. Strydom, R.R. Lobb, E.M. Alderman, L.J. Bethune, J.F. Riordan and B.L. Vallee, Isolation and Characterisation of Angiogenin, an Angiogenic Protein from Human Carcinoma Cells, *Biochem.* **24**, 5480-5486 (1985).
32. J.F. Riordan and B.L. Vallee, Human Angiogenin, an Organogenic Protein, *Br. J. Cancer*, **57**, 587-590 (1988).
33. P.A. D'Amore and M. Klagsbrun, Endothelial Cell Mitogens derived from Retina and hypothalamus: Biochemical and Biological similarities. *J. Cell Biol.*, **99**, 1545-1549 (1984).
34. G. Conn and V.B. Hatcher, The Isolation and Purification of 2 Anionic Endothelial Cell Growth Factors from Human Brain, *Biochem. Biophys. Res. Comm.*, **124(1)**, 262-268, (1984).
35. Y. Shing, J. Folkman, R. Sullivan, C. Butterfield, J. Murray and M. Klagsbrun, Heparin Affinity: Purification of a Tumour derived Capillary Endothelial Cell Growth Factor, *Science*, **223**, 1296-1299 (1984).
36. J. Folkman, R. Langer, R.J. Linhardt, C. Haudenschield and S. Taylor, Angiogenesis Inhibition and Tumour Regression caused by Heparin or a Heparin Fragment in the presence of Cortisone, *Science*, **221**, 719-725 (1985).
37. R. Shapiro and B.L. Vallee, Human Placental Ribonuclease Inhibitor Abolishes both Angiogenic and Ribonucleolytic activities of Angiogenin, *Proc. Natl. Acad. Sci. USA*, **84**, 2238-2241 (1987).

38. H. Maeda and Y. Matsumura, Tumoritropic and Lymphotropic Principles of Macromolecular Drugs, *Crit. Rev. Ther. Drug Carrier Systems*, **6**(3), 193-210 (1989).
39. A. Orlidge and P.A. D'Amour, Inhibition of Capillary Endothelial Cell Growth by Pericytes and Smooth Muscle Cells, *J. Cell. Biol.*, **105**, 1455-1462 (1987).
40. R.K. Jain, Transport of Molecules in Tumour Interstitium: A review, *Cancer Res.*, **47**, 3039-3051 (1987).
41. J.C.E. Underwood and I. Carr, The Ultrastructural and Permeability Characteristics of the Blood Vessels of a Transplantable Rat Sarcoma, *J. Pathol.*, **107**, 157-166.
42. H.F. Dvorak, J. Nagy, J.T. Dvorak and A.M. Dvorak, Leaky Vessels and Extravascular Coagulation in Tumours, *FASEB*, **2**, A1410 (1988).
43. S.W. O'Connor and W.F. Bale, Accessibility of Circulating Immunoglobulin G to the Extravascular Compartments of Solid Rat Tumours, *Cancer Res.*, **44**, 3719-3723 (1984).
44. D.T. Connolly, D.M. Heuvalman, R. Nelson, J.V. Olander, B.L. Eppley, J.J. Delfino, N.R. Siegel, R.M. Leimgruber and J. Feder, Tumour Vascular Permeability Factor Stimulates Endothelial Cell Growth and Angiogenesis, *J. Clin. Invest.*, **84**, 1470-1478 (1989).
45. J.A. Nagy, L.F. Brown, D.R. Senger, N. Lanir, L. Van de Water, A.M. Dvorak and H.F. Dvorak, Pathogenesis of Tumour Stroma Generation: A Critical role for Leaky Blood Vessels and Fibrin Deposition, *Biochim. Biophys. Acta*, **948**, 305-326 (1988).
46. D.R. Senger, S.J. Galli, A.M. Dvorak, C.A. Perruzzi, V.S. Harvey and H.F. Dvorak, Tumour Cells Secrete a Vascular Permeability Factor that Promotes Accumulation of Ascites Fluid, *Science*, **219**, 983-985 (1985).
47. Y. Matsumura and N. Maeda, A New Concept for Macromolecular Therapeutics in Cancer Chemotherapy: Mechanism of Tumoritropic Accumulation of Proteins and the Anti-tumour Agent Smancs, *Cancer Res.*, **46**, 6387-6392 (1986).
48. Y. Matsumura, M. Kimura, T. Yamamoto and H. Maeda, Involvement of the Kinin-Generating Cascade in Enhanced Vascular Permeability in Tumour Tissue, *Jpn. J. Cancer Res.*, **79**, 1327-1324 (1988).
49. D.H. Ausprunk, C.L. Boudreau and D.A. Nelson, Proteoglycans in the Microvasculature II. Histochemical Localisation in Proliferating Capillaries of the Rabbit Cornea, *Am. J. Pathology*, **103**, 367-375 (1981).

50. H. Maeda, Y. Matsumura and H. Kato, Purification and Identification of [hydroxypropyl<sup>13</sup>] bradykinin in Ascitic Fluid from a Patient with Gastric Cancer, *J. Biol. Chem.*, **263**(31), 16051-16054 (1988).
51. G.B. Feldman, R.C. Knapp, S.E. Order and S. Hellman, The Role of Lymphatic Obstruction in the Formation of Ascites in Murine Ovarian Carcinoma, *Cancer Res.*, **32**, 1663-1666 (1972).
52. H. Sezaki and M. Hashida, Macromolecular Drug Conjugates in Targeted Cancer Chemotherapy. *Crit. Rev. Therapeut. Drug Carrier Systems*, **1**, 1-38 (1984).
53. V. Subr, J. Kopecek and R. Duncan, Degradation of Oligopeptide Sequences Connecting Poly[N-(2-hydroxypropyl)methacrylamide] Chains by Lysosomal Cysteine Proteinases, *J. Bioactive and Compatible Polymers*, **1**, 133-146 (1986).
54. J. Kopecek, The Potential of Water Soluble Polymeric Carriers in Targeted and Site-Specific Drug Delivery, *J. Cont. Rel.*, **11**, 279-290 (1990).
55. J.B. Lloyd, Targeting with Synthetic Polymers: A Realistic Goal in "Targeting of Drugs with Synthetic Systems", Ed. G. Gregoriadis, J. Senior and G. Poste, Plenum Press, New York, London (1986).
56. L.W. Seymour, R. Duncan, J. Strohalm and J. Kopecek, Effect of Molecular Weight of N-(2-hydroxypropyl)methacrylamide (HPMA) Copolymers on Body Distribution and Rate of Excretion after Subcutaneous, Intraperitoneal and Intravenous Administration to Rats, *J. Biomed. Materials Res.*, **21**, 1341-1358 (1987).
57. R. Duncan and J. Kopecek, Soluble Synthetic Polymers as Potential Drug Carriers, *Adv. Polym. Sci.*, **57**, 51-101 (1984).
58. J.B. Lloyd, R. Duncan and J. Kopecek, Synthetic Polymers as Carriers for Chemotherapeutic Agents, *Biochem. Soc. Trans.*, **14**, 391-392 (1986).
59. R. Duncan, P. Kopeckova-Rejmanova, J. Strohalm, I. Hume, H.C. Cable, J. Pohl, J.B. Lloyd and J. Kopecek, Anticancer Agents Coupled to HPMA copolymers I. Evaluation of Daunomycin and Puromycin Conjugates in vitro, *Br. J. Cancer*, **55**, 165-174 (1987).
60. R. Duncan, P. Kopeckova, J. Strohalm, I. Hume, J.B. Lloyd and J. Kopecek, Anticancer Agents Coupled to HPMA copolymers II. Evaluation of Daunomycin in vivo against L1210 Leukaemia, *Br. J. Cancer*, **57**, 147-156 (1988).

61. B. Rihova, J. Kopecek, P. Kopeckova-Rejmanova, J. Strohalm D. Plocova and H. Semradova, Bioaffinity Therapy with Antibodies and Drugs Bound to Soluble Synthetic Polymers, *J. Chromatogr.*, **376**, 221-233 (1986).
62. R. Duncan, I.C. Hume, P. Kopeckova, K. Ulbrich, J. Strohalm and J. Kopecek, Anticancer Agents Coupled to HPMA copolymers III. Evaluation of Adriamycin Conjugates Against Mouse Leukaemia L1210 in vivo, *J. Cont. Rel.*, **10**, 51-63 (1989).
63. L.W. Seymour, K. Ulbrich, J. Strohalm, J. Kopecek and R. Duncan, The Pharmacokinetics of Polymer Bound Adriamycin, *Biochem. Pharmacol.*, **39**(6), 1125-1131 (1990).
64. B. Rihova, K. Veres, L. Fornusek, K. Ulbrich, J. Strohalm, V. Vetvicka, M. Bilej and J. Kopecek, Action of Polymeric Prodrugs Based on HPMA Copolymers II. Body Distribution and T cell Accumulation of Free and Polymer Bound 125I-Daunomycin, *J. Cont. Rel.*, **10**, 37-49 (1989).
65. R. Duncan, J. Kopecek, P. Rejmanova and J.B. Lloyd, Targeting of HPMA Copolymers to Liver by Incorporation of Galactose Residues, *Biochim. Biophys. Acta*, **755**, 518-521 (1983).
66. R. Duncan, I.C.W. Seymour, L. Scarlett, J.B. Lloyd, P. Rejmanova and J. Kopecek, Fate of HPMA Copolymers with Pendent Galactosamine Residues After Intravenous Administration to Rats, *Biochim. Biophys. Acta.*, **880**, 62-71 (1986).
67. L.J. Arnold, A. Dagan and N.O. Kaplan, Poly(L-lysine) as an Antineoplastic Agent and Tumour-Specific Drug Carrier, pp89-112 in "Targeted Drugs", Ed E.P. Goldberg. John Wiley and Sons (1983).
68. W.C. Shen and H.J.P. Ryser, Poly(L-lysine) and (D-lysine) Conjugates of MTX: Different Inhibitory Effect on Drug Resistant Cells, *Mol. Pharmacol.*, **16**, 614-617 (1979).
69. J.M. Whiteley, Z. Nimec and J. Galivan, Treatment of Reuber H35 Hepatoma Cells with Carrier-Bound MTX, *Mol. Pharmacol.*, **19**, 505-508 (1981).
70. H.J.P. Ryser and W.C. Shen, Drug-Poly(lysine) Conjugates: Their Potential for Chemotherapy and for the Study of Endocytosis, pp103-121 in "Targeting of Drugs with Synthetic Systems", Ed G. Gregoriadis, J.Senior and G. Poste, Plenum Press, New York 1986.
71. J. Pitha, Polymer-Cell Surface Interactions and Drug Targeting, pp113-126 in Targeted Drugs", Ed. E.P Goldberg, John Wiley and Sons (1983).

72. J. Galivan, M. Balinska and J.M. Whiteley; Interactions of MTX(Poly-L-lysine) with Transformed Hepatic Cells in Culture, *Arch. Biochem. Biophys.*, **216**(2), 544-550 (1982).
73. Y. Takakura, S. Matsumoto, M. Hashida and H. Sezaki, Physicochemical Properties and Antitumour Activities of Polymeric Prodrugs of Mitomycin C with different Regeneration Rates, *J. Cont. Rel.*, **10**, 97-105 (1989).
74. T. Fujita, Y. Yasuda, Y. Takakura, M. Hashida and H. Sezaki, Alteration of Biopharmaceutical Properties of Drugs by their Conjugation with water soluble Macromolecules: Uricase-Dextran Conjugate, *J. Cont. Rel.*, **11**, 149-156 (1990).
75. Y. Takakura, M. Kitajima, S. Matsumoto,, M. Hashida and H. Sezaki, Development of a Novel Polymeric Prodrug of Mitomycin C, Mitomycin C-dextran conjugate with Anionic Charge I. Physicochemical Characteristics and in vivo and in vitro Antitumour Activities, *Int. J. Pharmaceutics*, **37**, 135-144 (1987).
76. Y. Takakura, A. Takagi, M. Hashida and H. Sezaki, Disposition and Tumour Localisation of Mitomycin C-Dextran Conjugates in Mice, *Pharm. Res.*, **4**(4), 293-300 (1987).
77. S. Matsumoto, A. Yamamoto, Y. Takakura, M. Hashida, N. Tanigawa and H. Sezaki, Cellular Interaction and in vitro Antitumour Activity of Mitomycin C-Dextran Conjugate, *Cancer Res.*, **46**, 4463-4468 (1986).
78. S. Nakane, S. Matsumoto, Y. Takakura, M. Hashida and H. Sezaki, The Accumulation Mechanism of Cationic Mitomycin C-Dextran Conjugates in the Liver: In vivo Cellular Localisation and in vitro Interaction with Hepatocytes, *J. Pharm. Pharmacol.*, **94**, 401-406 (1988).
79. D. Colcher, J.M. Esteban, J.A. Carrasquillo, P. Sugarbaker, J.C. Reynolds, G. Bryant, S.M. Larson and J. Schlom, Quantitative Analysis of Selective Radiolabelled Monoclonal Antibody Localisation in Metastatic Lesions of Colorectal Cancer Patients, *Cancer Res.*, **47**, 1185-1189 (1987).
80. A.K. Halsall, D.S. Fairweather, A.R. Bradwell, J.C. Blackburn, P.W. Dykes, A. Howell, A. Reeder and K.R. Hine, Localisation of Malignant Germ Cell Tumours by External Scanning after Injection of Radiolabelled Anti-alpha-Fetoprotein, *Br. Med. J.*, **283**, 942-944 (1981).
81. M.V. Pimm, Drug-Monoclonal Antibody Conjugates for Cancer Therapy: Potential and Limitations, *Crit. Rev. in Therapeutic Drug Carrier Systems*, **5**(3), 189-227 (1988).



82. M.J. Embleton, Targeting of Anticancer Therapeutic Agents by Monoclonal Antibodies, *Biochem. Soc. Trans.*, **14**, 393-395 (1986).
83. D.W. Kufe, L. Nadler, L. Sargent, H. Shapiro, P. Hand, F. Austin, D. Colcher and J. Schlom, Biological Behaviour of Human Breast Carcinoma Associated Antigens Expressed during Cellular Proliferation, *Cancer Res.*, **43**, 851-857 (1983).
84. P. Horan Hand, M. Nuti, D. Colcher and J. Schlom, Definition of Antigenic Heterogeneity and Modulation Among Human Mammary Carcinoma Cell Populations using mAb to Tumour Associated Antigens, *Cancer Res.*, **43**, 728-735 (1983).
85. P.E. Thorpe, P.M. Wallace, P.P. Knowles, M.G. Relf, A.N.F. Brown, G.J. Watson, D.C. Blakey and D.R. Newell, Improved Antitumour effects of Immunotoxins Prepared with Deglycosylated Ricin A Chain and Hindered Disulphide Linkages, *Cancer Res.*, **48**, 6396-6403 (1988).
86. U.S. Ryan, D.R. Schultz, P. Delvecchio and J.W. Ryan, Endothelial Cells of Bovine Pulmonary Artery lack Receptors for C3b and for the Fc portion of Immunoglobulin G, *Science*, **208**, 748-749 (1980).
87. M.V. Pimm, J.A. Jones, M.R. Price, J.G. Middle, M.J. Embleton and R.W. Baldwin, Tumour Localisation of mAb against a Rat Mammary Carcinoma and Suppression of Tumour Growth with Adriamycin-Antibody Conjugates, *Cancer Immunol. Immunother.*, **12**, 125 (1982).
88. V. Moshakis, R.A.J. McIlhinney and A.M. Neville, Cellular Distribution of mAb in Human Tumours after Iv Administration, *Br. J. Cancer*, **44**, 663-669 (1981).
89. P.N. Kulkarni, A.H. Blair, T. Ghose and M. Mammen, Conjugation of Methotrexate to IgG antibodies and their F(ab)<sub>2</sub> fragments and the Effect of Conjugated Methotrexate on Tumour Growth in vivo, *Cancer Immunol. Immunother.*, **19**, 211-214 (1985).
90. F. Buchegger, C.M. Haskell, M. Schreyer, B.R. Scazziga, S. Randin, S. Carrel and J.P. Mach, Radiolabelled Fragments of Monoclonal Antibodies against Carcino Embryonic Antigen for Localisation of Human Colon Carcinoma Grafted into Nude Mice, *J. Exp. Med.*, **158**, 413-427 (1983).
91. P.N. Kulkarni, A.H. Blair and T.I. Ghose, Covalent Binding of Methotrexate to Immunoglobulins and the Effect of Antibody-linked Drug on Tumour Growth in vivo, *Cancer Res.*, **41**, 2700-2706 (1981).
92. M.V. Pimm, J.A. Clegg, M.C. Garnett and R.W. Baldwin, Biodistribution and tumour Localisation of a MTX-mAb 791T/36 Conjugate in Nude Mice with Human Tumour Xenografts, *Int. J. Cancer*, **41**, 886-891 (1988).

93. Y. Tsukada, K. Ohkawa and H. Hibi, Therapeutic Effect of Treatment with Polyclonal or Monoclonal Antibodies to alpha-Fetoprotein that have been Conjugated to Daunomycin via a Dextran Bridge: Studies with an alpha-Fetoprotein producing Rat Hepatoma tumor Model, *Cancer Res.*, **47**(16), 4295-4295 (1987).
94. M.C. Garnett, M.J. Embleton, E. Jacobs and R.W. Baldwin. Preparation and Properties of a Drug-Carrier Antibody Conjugate showing Selective Antibody Directed Cytotoxicity in vitro, *Int. J. Cancer*, **31**, 661-670 (1983).
95. M.C. Garnett and R.W. Baldwin, Endocytosis of a mAb Recognising a Cell Surface Glycoprotein Antigen, Visualised using Fluorescent Conjugates, *Eur. J. Cell Biol.*, **41**, 214-221 (1986).
96. D.G. Gilliland, Z. Steplewski, R.J. Collier, K.F. Mitchell, T.H. Chang and H. Koprowski, Antibody Directed Cytotoxic Agents: Use of mAb to direct the Action of Toxin A Chains to Colorectal Carcinoma Cells, *Pro. Natl. Acad. Sci. USA*, **77**, 4539-4543 (1980).
97. P.E. Thorpe, S.I. Detre, D.W. Mason, A.J. Cumber and W.C. Ross, mAb Therapy: Model Experiments with Toxin-Conjugated Antibodies in Mice and Rats, p107 in *Haematology and Blood Transfusion*, vol. 28, Eds. Neth, Gallo, Greaves, Moore and Winkler, Springer Verlag, Berlin-Heidelberg (1983).
98. P.E. Thorpe and W.C.J. Ross, The Preparation and Cytotoxic Properties of Antibody-Toxin Conjugates, *Immunol. Rev.*, **62**, 119-158 (1982).
99. B.C.F. Chu and J.M. Whiteley, High Molecular Weight Derivatives of Methotrexate as Chemotherapeutic Agents, *Mol. Pharmacol.*, **13**, 80-88 (1977).
100. B.C.F. Chu and J.M. Whiteley, Control of Solid Tumour Metastasis with a High Molecular Weight Derivative of MTX, *J. Natl. Cancer Inst.*, **62**, 79-82 (1979).
101. B.C.F. Chu and J.M. Whiteley, The Interaction of Carrier Bound MTX with L1210 Cells, *Mol. Pharmacol.*, **17**, 382-387 (1980).
102. L. Bures, J. Bostik, K. Motycka and L. Rehak, The Use of Protein as a Carrier of MTX for Experimental Cancer Chemotherapy III. Human serum Albumin-MTX Derivative, its Preparation and Basic Testing, *Neoplasma*, **35**, 329-342 (1988).
103. A. Trouet, M. Masquelier, R. Baurain and D. Deprez-de-Campeneere, A Covalent Linkage between Daunorubicin and Proteins that is Stable in Serum and Reversible by Lysosomal Hydrolases, as Required for a Lysosomotropic Drug-Carrier Conjugate: *In Vitro* and *In Vivo* Studies, *Proc. Natl. Acad. Sci. USA*, **79**, 626-629 (1982).

104. J.E Dyr, K. Slavik and Z. Vodrazka, Chemical Binding of Folic Acid and MTX to Bovine Fibrinogen, *Thrombosis Res.*, **31**, 737-746 (1983).
105. J.E Dyr, E. Hermanova, K. Slavik and Z. Vodrazka, The Effect of Fibrinogen-MTX Derivatives on HeLa Cell Growth, *Neoplasma*, **33**, 401-407 (1986).
106. L.K.A. Rahman and S.R. Chhabra, The Chemistry of Methotrexate and its Analogues, *Medicinal Res. Rev.*, **8**(1), 5-156 (1988).
107. J. Jolivet, K.H. Cowan, G.A. Curt, N.J. Glendeninn and B.A. Chabner, The Pharmacology and Clinical use of Methotrexate, *New Eng. J. Med.*, **309**(18), 1094-1103 (1983).
108. B.I. Schweitzer, A.P. Dicker and J.R. Bertino, Dihydrofolate Reductase as a Therapeutic Target, *FASEB J.*, **4**, 2441-2452 (1990).
109. J. Galivan, Evidence for cytotoxic Activity of Polyglutamated derivatives of MTX, *Mol. Pharmacol.*, **17**, 105-110 (1979).
110. W. Werkheiser, The Biochemical, Cellular and Pharmacological Action and Effects of the Folic Acid Antagonists, *Cancer Res.*, **23**, 1277-1285 (1963).
111. G. Fabre, L.H. Matherly, I. Fabre, J.P. Cano and I.D. Goldman, Interactions between 7-Hydroxymethotrexate and Methotrexate at the Cellular Level in the Ehrlich Ascites Tumour in vitro, *Cancer Res.*, **44**, 970-975 (1984).
112. J.J. McGuire and J.K. Coward, Pteroylpolyglutamates: Biosynthesis, Degradation and Function, in "Folates and Pterins (vol I) Chemistry and Biochemistry of Folates", Ed. R.L. Blakley and S.J. Benkovic, John Wiley and Sons, New York.
113. R.G. Matthews and C.M. Baugh, Interactions of Pig Liver Methylene-tetrahydrofolate Reductase with Methylene-tetrahydropteroylpolyglutamate Substrates and with Dihydropteroylpolyglutamate inhibitors, *Biochem.*, **19**, 2040-2045 (1980).
114. C.J. Allegra, B.A. Chabner, J.C. Drake, R. Lutz, D. Rodbard and J. Jolivet, Enhanced Inhibition of Thymidylate Synthase by MTX Polyglutamates, *J. Biol. Chem.*, **260**(17), 9720-9726 (1985).
115. D.S. Rosenblatt, V.M. Whitehead, N. Vera, A. Pottier, M. Dupont and M.-J. Vuchich, Prolonged Inhibition of DNA Synthesis Associated with the Accumulation of Methotrexate Polyglutamates by Cultured Human Cells, *Mol. Pharmacol.*, **14**, 1143-1147 (1978).

116. I. Fabre, G. Fabre and I.D. Goldman, Polyglutamation, an Important element in Methotrexate cytotoxicity and Selectivity in Tumour versus Murine Granulocytic Progenitor Cells in vitro, *Cancer Res.*, **44**, 3190-3195 (1984).
117. J.D. Borsi and P.J. Moe, New Aspects of Clinical and Cellular Pharmacodynamics of Methotrexate, *Acta Paed. Scand., Supp.*, 341 (1987).
118. D.S. Rosenblatt, V.M. Whitehead, M.J. Vuchich, A. Pottier, N.V. Matiaszuk and D. Beaulieu, Inhibition of MTX Polyglutamate Accumulation in Cultured Human Cells, *Mol. Pharmacol.*, **19**, 87-91 (1981).
119. J.P. Perkins and J.R. Berlino, Dihydrofolate Reductase from L1210R Murine Lymphoma, Fluorometric Measurements of the Interaction of the Enzymes, Coenzymes, Substrates and Inhibitors, *Biochem.*, **5**(3), 1005-1012 (1966).
120. B.A. Kamen, W. Whyte-Bauer and J.R. Bertino, A Mechanism of Resistance to Methotrexate, *Biochem. Pharmacol.*, **32**(12), 1837-1841 (1983).
121. P.W. Melera, J.A. Lewis, J.L. Biedler and C. Hession, Antifolate-Resistant Chinese Hamster Cells, *J. Biol. Chem.*, **255**(14), 7024-7028 (1980).
122. G. Milano, A. Thyss, S. Debeauvais, G. Laureys, Y. Benoit and A. Deville, CSF Drug Levels for Children with Acute Lymphoblastic Leukaemia treated by 5g/m<sup>2</sup> Methotrexate, *Eur. J. Cancer*, **26**(4), 492-495 (1990).
123. G. Fabre, I. Fabre, L.H. Mathrely, J.P. Cano and I.D. Goldman, Synthesis and Properties of 7-Hydroxy-Methotrexate Polyglutamyl Derivatives in Ehrlich Ascites Tumour Cells in vitro, *J. Biol. Chem.*, **259**(8), 5066-5072 (1984).
124. P.J. McConahey and F.J. Dixon, Radioiodination of Proteins by the Chloramine T Method, *Methods in Enzymology*, **70**, 210-213 (1980).
125. R.H. Marriott, Synthesis and Characterisation of Macromolecular Carriers of Methotrexate, Ph.D thesis, Bath University (1987).
126. N. So, D.P. Chandra, I.S. Alexander, V.J. Webster and D.W. O'Gorman Hughes, Determination of Serum MTX and 7-OH-MTX Concentration, Method Evaluation showing Advances in HPLC, *J. Chromatogr.*, **337**, 81-90 (1985).
127. Digoxin Injection, *British Pharmacopoeia*, Vol. II, p 784 (1988).
128. O.H. Lowry, N.J. Rosebrough, A. Lewis Farr and R.J. Randall, Protein Measurement with the Folin Phenol Reagent, *J. Biol. Chem.*, **193**, 265-275 (1951).

129. P.O. Seglen, Preparation of Isolated Rat Liver Cells, *Met. Cell Biol.*, **13**, 29-83 (1976).
130. T.J.C. Van Berkel, J. Kar Krujt, M.K. Bijsterbosch, R. de Water and H.J.M. Kempen, Drug Transport and Uptake at sites of Action, Chp 24 in "Novel Drug Delivery and its Therapeutic Application", Ed. L.F. Prescott and W.S. Nimmo, John Wiley (1989).
131. P.Stahl and S. Gordon, Expression of a Mannosyl-Fucosyl Receptor for Endocytosis on Cultured Primary Macrophages and Their Hybrids, *J. Cell Biol.*, **93**, 49-56 (1982).
132. Sj. Van der Wal and L.R. Snyder, Photometric Determination at 185nm For HPLC with either Isocratic or Gradient Elution, *J. Chromatogr.*, **255**, 463-474 (1983).
133. G. Wilson, I.F. Hassan, C.J. Dix, I. Williamson, R. Shah, M. Mackay and P. Artursson, Transport and Permeability Properties of Human Caco-2 Cells: An *in vitro* Model of the Intestinal Epithelial Cell Barrier, *J. Cont. Rel.*, **11**, 25-40 (1990).
134. M.V. Shah, K.L. Audus and R.T. Borchardt, The Application of Bovine Brain Microvessel Endothelial-Cell Monolayers Grown onto Polycarbonate Membranes *in vitro* to Estimate the Potential Permeability of Solutes through the Blood Brain Barrier, *Pharm. Res.*, **6**, 624-627 (1989).
135. A. Siflinger Birnboim, J.A. Cooper, P.J. Del Vecchio, H. Lum and A.B. Malik, Selectivity of the Endothelial Monolayer: Effects of Increased Permeability, *Microvasc. Res.*, **36**, 216-227 (1988).
136. Goodman and Gilman, "Pharmacological Basis of Therapeutics", 7th Ed., Macmillan Press (1985).
137. C.A. Gloff and L.Z. Benet, Pharmacokinetics and Protein Therapeutics, *Adv. Drug Delivery Rev.*, **4**, 359-386 (1990).
138. Martindale Extra Pharmacopoeia, p 1983.
139. Lewis' textbook of Pharmacology, V.Crossland, Ed., Churchill, Livingstone (1980)
140. P. Goddard, L. Hutchinson, J. Brown and L.J. Brookman, Soluble Polymeric Carriers for drug Delivery, Part 2. Preparation and *in vivo* Behavior of N-Acylethylenimine Copolymers, *J. Cont. Rel.*, **10**, 5-16 (1989).
141. A.S. McFarlane, Sites of Protein Catabolism in Physiology and Pathophysiology of Plasma Protein Metabolism, pp87-93, Pergamon Press (1969).

142. M.F. Flessner, R.L. Dedrick and J.S. Schutz, Exchange of Macromolecules Between Peritoneal Cavity and Lymph, *Am. J. Physiol.*, **248**, H15-H25 (1985).
143. Matsumura and Maeda, A New Concept for Macromolecular Therapeutics in Cancer Chemotherapy: Mechanisms of Tumorotropic Accumulation of Proteins and the Antitumour Agent Smancs, *Cancer Res.*, **46**, 6387-6392 (1986).
144. The Laboratory Rat, Vol. I, Biology and Disease, Eds. H.J. Baker, J.R Lindsey and S.H. Weisbroth, Academic Press, 1979.
145. S. Margen and H. Tarver, The Preparation of Labelled Albumin for Turnover Studies, in "Advances in Tracer Methodology", Vol. II, Plenum Press (1965).
146. A. Supersaxo, W. Hein and H. Steffen, Effect of Molecular Weight on the Lymphatic Absorption of Water Soluble Compounds Following Subcutaneous Administration, *Pharm. Res.*, **7**, 167-169 (1990).
147. C.B. Anfinsen, J.B. Edsall and J.M. Richards, Catabolism of Protein, Advances in Protein Chemistry, Vol. 3, Academic Press (1985).
148. A.C. Wardlaw, Practical Statistics for Experimental Biologists, John Wiley and Sons (1987).
149. G.W. Halbert, A.T. Florence, Physicochemical Characterization of Methotrexate-BSA Conjugates, *J. Pharm. Pharmacol.*, **41**, 222-226 (1989).
150. R. Duncan, H.C. Cable, P. Rejmanova, J. Kopecek and J.B. Lloyd, Tyrosinamide Residues Enhance the Pinocytic Capture of HPMA Copolymers, *Biochim Biophys Acta*, **799**, 1-8 (1984).
151. G.P. Mell, J.M. Whitely and F.M. Huennekens, Purification of DHFR via amethopterin-Aminoethyl starch, *J. Biol. Chem.*, **243**, 6074-6075 (1968).
152. A. Trouet, R. Baurain, D. Deprez-de-Campaneere, M. Masquelier and P. Pirson, Targetting of Antitumour and Antiprotozoal Drugs by Covalent Linkage to Protein Carriers, in "Targetting of Drugs", Eds., G. Gregoriadis, J. Senior and A. Trouet, Plenum Press (1982).
153. G.W. Halbert, A.T. Florence and J.F.B. Stuart, Characterisation of in vitro Drug Release and Biological Activity of MTX-BSA Conjugates, *J. Pharm. Pharmacol.*, **39**, 871-876 (1987).
154. C. Pouton, Drug Targeting- Current Aspects and Future Prospects, *J. Clin. Hosp. Pharm.*, **10**, 45-58 (1985).

155. W. Regelson, Advances in Intraperitoneal Administration of Synthetic Polymers for Immunotherapy and Chemotherapy, *J. Bioact. and Comp. Polymers*, **1**, 84-105 (1986).
156. L. Fiume, C. Busi, A. Mattioli and G. Spinosa, Targetting of Antiviral Drugs Bound to Protein Carriers, *Critical Reviews in Therapeutic Drug Carrier Systems*, **4(4)**, 265-284 (1988).
157. L. Fiume, A. Mattioli, P. G. Balboni and G. Barbanti-Brodano, Albumin Conjugates of Fungal Toxins and of Inhibitors of DNA Synthesis, in "Drug Carriers in Biology and Medicine, Ed. G. Gregoriadis, Academic Press (1979).
158. L. Fiume, C. Busi, A. Mattioli, P.G. Balboni, G. Barbanti-Brodano and Th. Wieland, Hepatocyte Targetting of Antiviral Drugs Coupled to Galactosyl-terminating Glycoproteins, in "Targeting of Drugs", Eds. G. Gregoriadis, J. Senior and A. Trouet, Plenum Press (1982).
159. P.G. Balboni, A. Minia, M.P. Grossi, G. Barbanti-Brodano, A. Mattioli and L. Fiume, Activity of Albumin Conjugates of 5-Fluorodeoxyuridine and Cytosine Arabinoside on Pox Viruses as a Lysosomatropic Approach to Antiviral Chemotherapy, *Nature*, **264**, 181-183 (1976).
160. M.O. Dayhoff, Atlas of Protein Sequence and Structure, National Biomedical Research Foundation. Vol 5, suppl. 2 (1976).
161. R. Duncan, A.B. Lloyd, P. Rejmanova and J. Kopecek, Methods of Targeting HPMA Copolymers to Particular Cell Types, *Makromol. Chem. Suppl.*, 3-12 (1985).
162. C.P. Stowell and Y. C. Lee, Neoglycoproteins. The Preparation and Application of Synthetic Glycoproteins, *Adv. Carbohydr. Chem. Biochem.*, **37**, 225-281 (1980).
163. A. Geerts, L. Bouwens, R. de Zanger, H. van Bossuyt, E. Wisse, The Structure of different types of Liver Cells in relation to Uptake and Exchange processes, in "Targeting of Drugs. Anatomical and Physiological Considerations", Eds. G. Gregoriadis and G. Poste, Plenum Press (1988).
164. R. Teradaira, V.K. Bachofen, J. Schlepper-Schafer and H. Kolb, Galactose-particle Receptor on Liver Macrophages. Quantitation of Particle Uptake, *Biochim. Biophys. Acta*, **759**, 306-310 (1983).
165. V.K. Bachofen, The Galactose-particle Receptor on Liver Macrophages: Biological Function and Implications for Clearance of Particulate Material, in "Targeting of Drugs. Anatomical and Physiological Considerations", Eds. G. Gregoriadis and G. Poste, Plenum Press, New York (1988).

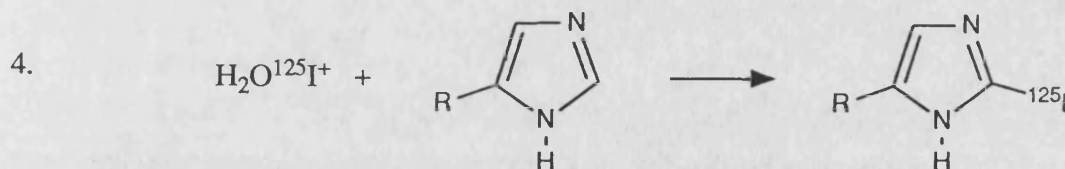
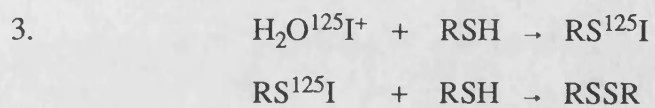
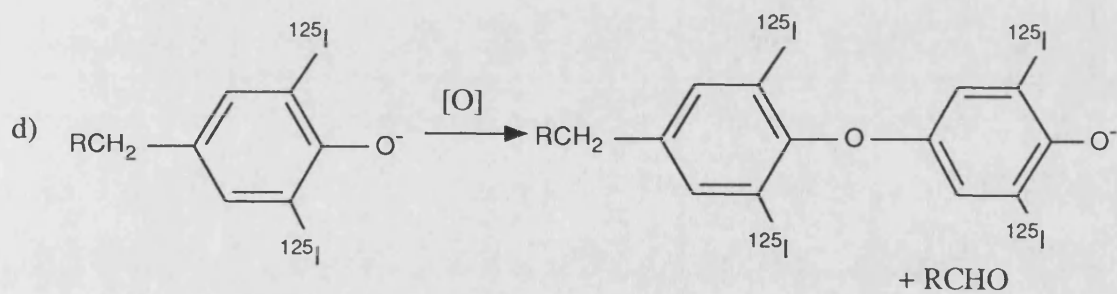
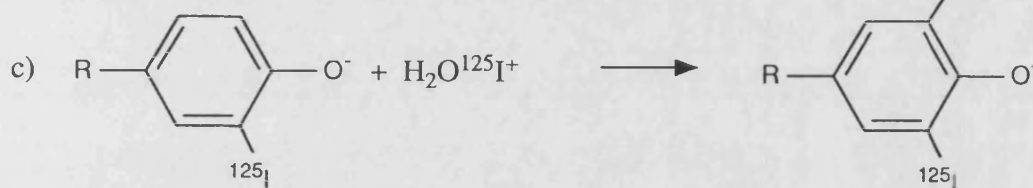
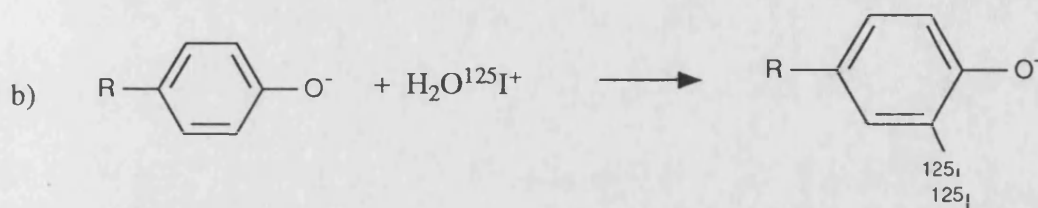
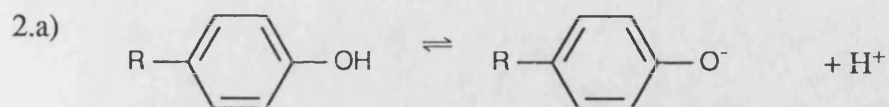
166. J.F. Nagelkerke, K.P. Barto and T.J.C. van Berkel, *In vivo* and *in vitro* Uptake and Degradation of acetylated LDL by Rat Liver Endothelial, Kupffer and Parenchymal Cells. , *J. Biol. Chem.*, **258**, 12221-12227 (1983).
167. G. Chaudhuri, A. Mukhopadhyay and S.K. Basu, Selective Delivery of Drugs to Macrophages through a Highly Specific receptor. An Efficient Chemotherapeutic Approach Against Leishmaniasis, *Biochem. Pharmacol.*, **38(18)**, 2995-3002 (1989).
168. M. Neutra and D. Louvard, Differentiation of Intestinal Cells *in vitro*. in "Functional Epithelial Cells in Culture". A.R. Liss, 1989.
169. E. Grasset, M. Pinto, E. Dussaulx, A. Zweibaum and J.F. Desjuix, Epithelial Properties of a Human Colonic Carcinoma Cell-line Caco-2: Electrical Parameters. *Am. J. Physiol.*, **247**, (*Cell Physiol*, **16**), C260-C267 (1984).
170. M. Pinto, M.D. Appay, P. Simon-Assman, N. Dracopoli, J. Fogh and A. Zweibaum, Enterocyte-Like Differentiation and Polarisation of the Human Colon Carcinoma Cell-line Caco-2 in Culture, *Biol. Cell*, **47**, 323-330 (1983).
171. H. Hauri, Expression and Intracellular transport of Microvillus Membrane Hydrolases in Human Intestinal Epithelial Cells, *J. Cell Biol.*, **101**, 838-851 (1985).
172. I.J. Hidalgo, T.J. Raub and R.T. Borchardt, Characterisation of the Human Colon Carcinoma Cell-line Caco-2 as a Model System for the Intestinal Epithelial Permeability, *Gastroenterology*, **96**, 736-749 (1989).
173. A. Zweibaum, Enterocyte Differentiation of Cultured Human Colon Cancer Cell lines: Negative Modulation by D-Glucose, personal communication.
174. A. Zweibaum, Sucrose-Isomaltose: A Marker of Foetal and Malignant Epithelial Cells of the Human Colon, *Int. J. Cancer*, **32**, 407-412 (1983).
175. A. Blais, P. Bissonnette and A. Berteloot, Common Characteristics for Sodium-dependant Sugar Transport in Caco-2 Cells and Human Foetal Colon, *J. Membrane Biol.*, **99**, 113-125 (1987).
176. M.G. Traber, Polarised Secretion of Newly Synthesised Lipoproteins by the Caco-2 Human Intestinal Cell-line, *J. Lipid Res.*, **28**, 1350-1363 (1987).
177. I.J. Hidalgo, Characterisation of the Aqueous Boundary Layer in Caco-2 Cells using a Novel Diffusion Cell, *Pharm. Res.*, **6**, PD950, 114 (1989).
178. A.R. Hilgers, R.A. Conradi and P.S. Burton, Caco-2 Cell Monolayers as a Model for Drug Transport across Intestinal Mucosa, *Pharm. Res.*, **7**, 902-909 (1990).



179. P.A. Artussen, Epithelial Transport of Drugs in Cell Culture I. A Model for Studying the Passive Diffusion of Drugs over Intestinal Absorptive (Caco-2) Cells, *J. Pharm. Sci.*, **79**(6), 476-482 (1990).
180. D.M. Shasby and R.L. Roberts, Transendothelial transfer of Macromolecules in vitro, *Fed. Proc.*, 2506-2510 (1987).
181. A. Siflinger-Birnboim, P.J. del Vecchio, J.A. Cooper and A.B. Malik, Transendothelial Albumin Flux: Evidence Against Asymmetric Transport, *J. Appl. Physiol.*, **61**(6), 2035-2039 (1986).
182. P.J. del Vecchio, A. Siflinger-birnboim, J.M. Shepard, R. Bizios, J.A. Cooper and A.B. Malik, Endothelial Monolayer Permiability to Macromolecules, *Fed. Proc.*, **46**, 2511-2515 (1987).
183. S.G. Milton and V.P. Knutson, Comparison of the Function of Tight Junctions of Endothelial Cells and Epithelial Cells in Regulating the Movement of Electrolytes and Macromolecules Across the Cell Monolayer, *J. Cell Physiol.*, **144**, 498-504 (1990).
184. A. Siflinger-Birnboim, P.J. del Vecchio, J.A. Cooper and A.B. Malik, Transendothelial Albumin Flux: Evidence Against Active Transport of Albumin, *Fed. Proc.*, **45**, 284 (1986).
- 185 D.M. Shasby and S.S. Shasby, Active Transendothelial Transport of Albumin Interstium to Lumen, *Circulation Res.*, **57**,
186. M.K. Pratten, K.E. Williams and J.B. Lloyd, A Quantitative Study of Pinocytosis and Intracellular Proteolysis in Rat Peritoneal Macrophages, *Biochem. J.*, **168**, 365-372 (1977).
187. P.D. Stahl, J.S. Rodman, M.J. Miller, P.H. Schlesinger, Evidence for Receptor Mediated binding of Glycoproteins, glycoconjugates and Lysosomal glycosidases by alveolar macrophages, *Proc. Natl. Acad. Sci U.S.A.* **75**, 1399-1403 (1978).
188. P.D. Stahl, P.H. Schlesinger, E. Sigardson, J.S. Rodman, Y.C. Lee, Receptor Mediated Pinocytosis of Mannose Glycoconjugates by Macrophages: Characterisation and Evidence for Receptor Recycling, *Cell*, **19**, 207-215 (1980).
189. C. Tietze, P. Schlessinger and P. Stahl, Chloroquine and  $\text{NH}_4^+$  Inhibit Receptor Mediated Endocytosis of Mannose-Glycoconjugates by Macrophages. Apparent Inhibition of Receptor Recyling, *Biochem. Biophys. Res. Comm.*, **93**, 1-8 (1980).

## APPENDIX 1. CALIBRATION CURVES AND REACTION MECHANISMS.

### A1.1 The Reaction Involved in the Iodination of Proteins.



### A1.2 UV Assay of Methotrexate solutions.

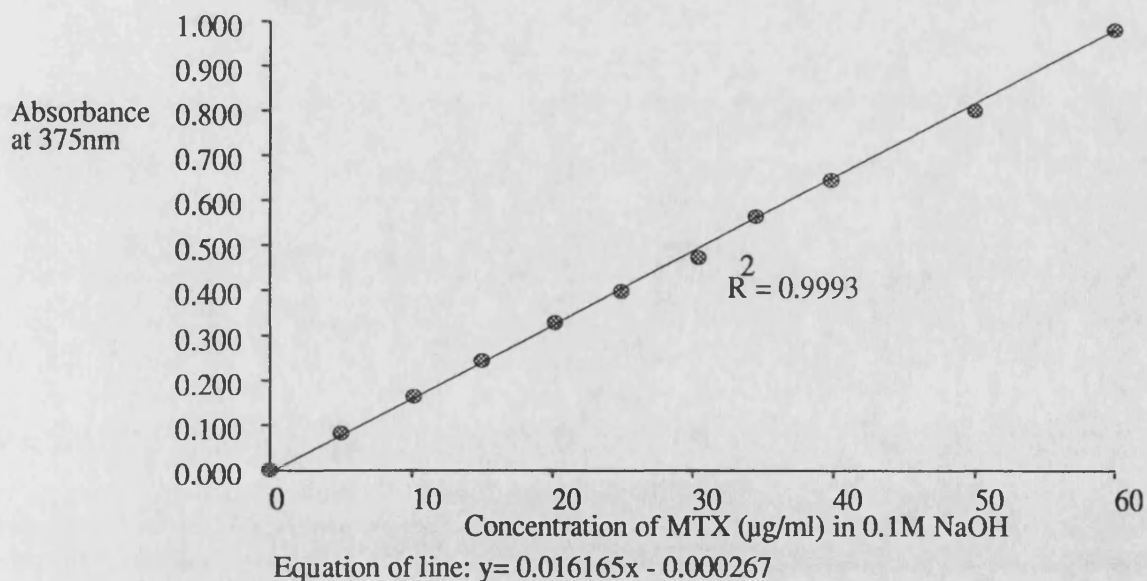
Solutions of Methotrexate were prepared at a range of concentrations (5-60µg/ml) in 0.1M NaOH. Each standard solution was prepared from its own concentrated stock solution. The absorbance of the solutions were determined in a PYE Unicam (PU8610) UV/VIS kinetics spectrophotometer at 375nm against a blank of 0.1M NaOH.

Table A1.1 Absorbance of the standards.

Conc. of Soln. (µg/ml)	Absorbance at 375nm
4.99	0.083
10.12	0.165
14.94	0.245
20.16	0.330
24.9	0.398
30.42	0.473
34.51	0.564
39.84	0.645
50.0	0.800
60.0	0.980

A graph of Absorbance at 375nm against concentration of MTX in the standard solution is shown in Figure A1.2. The plot was used to determine the MTX content of the conjugates.

Figure A1.2 Absorbance of Standard Methotrexate solutions in 0.1M NaOH at 375nm.



### A1.3 Calibration of the Superose 12 Column.

The superose 12 column was calibrated using a series of proteins of known molecular weight. Solutions of 500µg/ml were prepared in PBS. These were injected onto the column via a 20µl loop. The elution time was recorded using a Gilson 113 UV detector set at 280nm attached to a chart recorder. Flow rate was 0.83ml/minute. Total Volume (Vt) of the column was 23.6ml. Kav was calculated for each of the proteins using the formula.

$$K_{av} = \frac{(V_e - V_o)}{(V_t - V_o)}$$

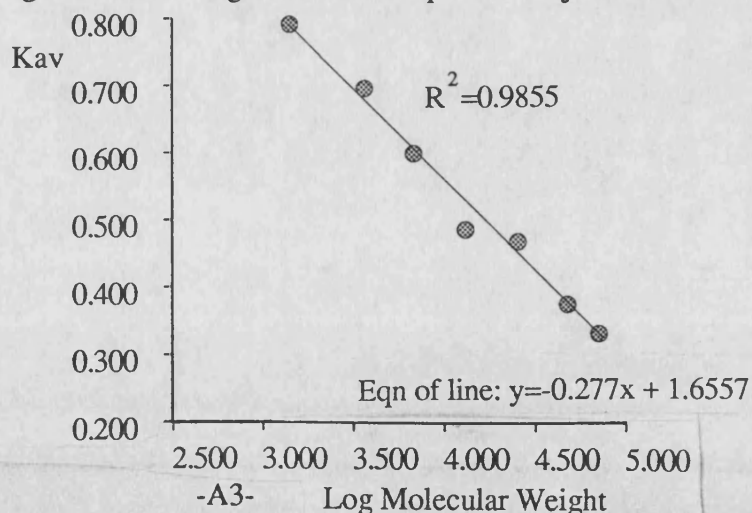
Where Ve is the Elution Volume, calculated by multiplying the elution time by the flow rate. Vo is the void volume which was determined by injecting dextran (molecular weight, 2 000 000). Since the dextran is excluded from the gel bed, it is eluted from the column at the same time as the solvent front. The void volume was calculated by multiplying the elution time of blue dextran by the flow rate. Vt is the total volume of the column. Kav indicates the fraction of stationary phase that is available to the solute.

Table 1.2 Calculated Kav for the injected proteins and for blue dextran.

Standard	Mol Wt.	Log Mol Weight	Elution time (min)	Ve (ml)	Kav
Dextran	2000K	6.301	9.38	7.79	0
BSA	67K	4.826	15.60	12.95	0.326
Ovalbumin	45K	4.653	16.43	13.64	0.370
Trypsinogen	24K	4.380	18.23	15.13	0.464
Cytochrome C	12.4K	4.093	18.57	15.41	0.482
Aprotinin	6.5K	3.813	20.75	17.22	0.596
Insulin Bchain	3496	3.544	22.62	18.77	0.694
Vitamin B <sub>12</sub>	1355.4	3.132	24.45	20.29	0.791

A plot of Kav versus log molecular weight (figure A1.3) was linear over the molecular weight range indicated. This plot could be used to determine molecular weight of the conjugates.

Figure A1.3 Kav versus log molecular weight of standard proteins injected onto the Superose 12 column.



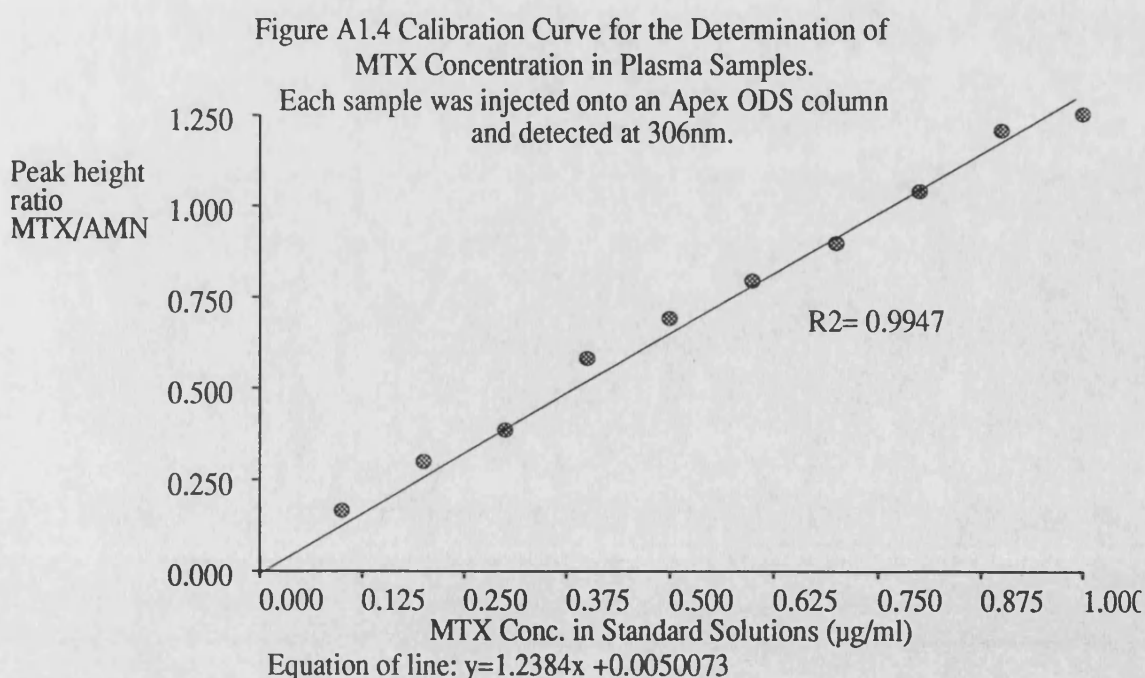
#### A1.4 The Calibration Curve used for Determination of MTX Concentration in Plasma.

The assay used was an HPLC assay as described in the Methods. Standard solutions of MTX were prepared in 'blank' (diluted one in two ) plasma. These were spiked with AMN as internal standard at the concentration described in the methods. The standards were injected onto the column, and the peak heights for MTX and AMN were determined. Peak height ratios (MTX/AMN) were calculated.

Table A1.1 Peak Height and Peak Height Ratio for MTX, AMN and MTX/AMN.

Conc. MTX (µg/ml)	MTX Peak Height (arbitrary values determined by integrator)	AMN Peak Height	Peak height Ratio
0.1	1433	8602	0.1666
0.2	2349	7852	0.2992
0.3	2332	6063	0.3846
0.4	5371	9236	0.5815
0.5	5105	7305	0.6915
0.6	6920	8707	0.7948
0.7	6754	7529	0.8971
0.8	8433	8118	1.0388
0.9	10948	9075	1.2064
1.0	12399	9910	1.2512

The plot of peak height ratio versus concentration of MTX in the standard (figure A1.4) was linear over the range used. The calibration curve was used to determine the concentration of MTX in the plasma of rats which had been injected with 2.5mg of drug.



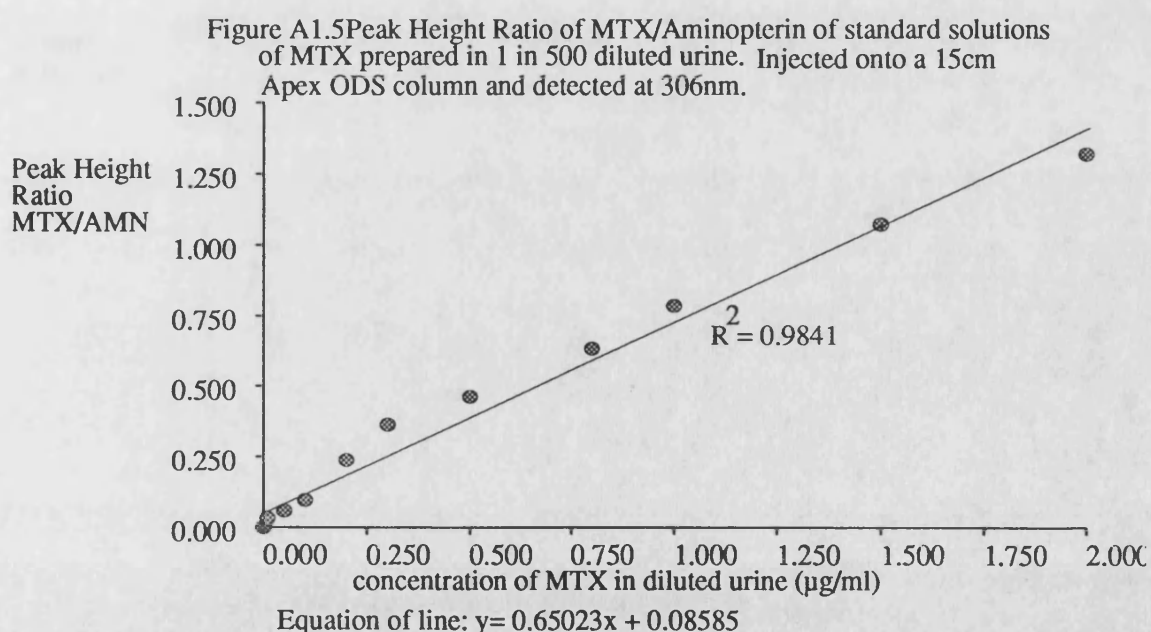
### A1.5 Calibration Curve used to determine the MTX Concentration in Urine.

Methotrexate concentration in urine samples was determined using an HPLC assay. A series of standard solutions (upto 2.0 $\mu$ g/ml) were prepared in 1 in 500 diluted urine. These were spiked with AMN as internal standard as described in the methods and were injected onto the column. Peak height ratios (MTX/AMN) were determined.

Table A1.4 Peak Height Ratios of Standard MTX Solutions.

Conc. of MTX ( $\mu$ g/ml)	Peak Height Ratio MTX/AMN
0.01	0.031
0.05	0.058
0.10	0.096
0.20	0.238
0.30	0.363
0.50	0.462
0.80	0.633
1.0	0.786
1.5	1.073
2.0	1.319

The plot of peak height ratio versus concentration of MTX in the standard (figure A1.5) was linear over the range used. The calibration curve was used to determine MTX concentration in urine samples of rats which had been injected with 2.5mg of MTXNa<sub>2</sub>.





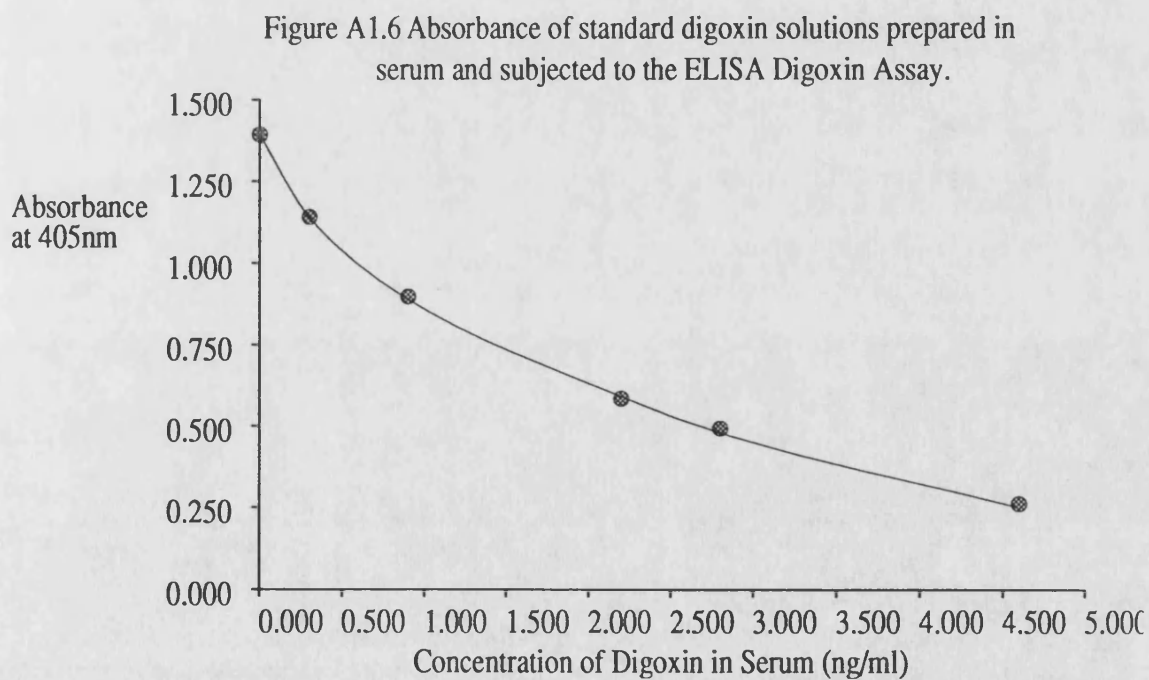
### A1.6 Calibration Curve used to determine Digoxin Concentration in Serum.

Digoxin concentration was determined in serum samples using an ELISA kit obtained from Boehringer Mannheim. The kit instructions have been photocopied and are shown on the next page.

Table A1.5 The UV absorbance of standard Digoxin serum samples.

Conc. of Digoxin (ng/ml)	Absorbance at 405nm
0	1.393
0.3	1.141
0.9	0.898
2.2	0.585
2.8	0.493
4.6	0.261

A plot of Digoxin concentration versus absorbance gave a curve which could be used to determine digoxin concentration of serum samples from rats which had been injected with 250ng of drug.



## A1.6b: The Instructions for Determination of Digoxin in Serum by ELISA (Boehringer Mannheim).

### Procedure

Wavelength: Hg 405 nm (see Note 2)

Spectrophotometer: 420 nm (see Note 2)

Semimicro cuvette: 1 cm light path (see Note 3)

Incubation temperature: +20 to 25°C (see Note 4)

Construct a new calibration curve for each assay series. Duplicate determinations are recommended for both samples and standards.

Reagents and antibody-coated tubes from different kits having the same lot number can be pooled.

It is recommended that the following scheme be adhered to for the pipetting of samples (or standards and control sera) and solution 1a:

Sample 1 + solution 1a; sample 2 + solution 1a; ... sample n + solution 1a. Alternatively, the use of a sample/reagent dispenser is recommended.

Add solution 1a rapidly or mix thoroughly with the sample material. The pipetting and aspiration steps must take place at the same intervals to ensure that all tubes have been incubated for the same length of time.

Tap-water at +20 to 25°C is required to flush out the tubes.

Pipette into tubes: #						
	a	b	Standard c	d	e	Sample/ Control serum
solution 3 a	0.1 ml	–	–	–	–	–
solution 3 b	–	0.1 ml	–	–	–	–
solution 3 c	–	–	0.1 ml	–	–	–
solution 3 d	–	–	–	0.1 ml	–	–
solution 3 e	–	–	–	–	0.1 ml	–
sample	–	–	–	–	–	0.1 ml
solution 1 a	1.0 ml	1.0 ml	1.0 ml	1.0 ml	1.0 ml	1.0 ml
Incubate for 25 min at +20–25°C (see Note 5).						
Aspirate tube contents, discard, and rinse tubes once with tap-water within 5 min. at the latest. The wash water should not stand in the tubes for more than (at most) 20 min. Aspirate carefully and commence the next pipetting within 10 min at the latest. (See Note 6).						
Add solution 4a to each tube in succession, keeping the time interval constant (see Note 7):						
solution 4 a	1.0 ml	1.0 ml	1.0 ml	1.0 ml	1.0 ml	1.0 ml
Do not shake. Avoid exposure to direct sunlight.						
Incubate for 25 min at +20–25°C (see Note 5).						
Mix well prior to measurement.						
Zero the photometer against solution 4 a.						
Transfer tube contents to cuvettes at the same time intervals as solution 4 a was added and read absorbances $A_i$ .						

- 1 **Buffer for incubation**  
(colour code red)  
phosphate buffer 40 mmol/l, pH 6.8
- 2 **Digoxin-POD conjugate**  
(colour code red)  
POD  $\geq 0.6$  U/ml
- 3 **Standards**  
a-e (colour code yellow)  
digoxin in human serum see vial labels  
for concentrations
- 4 **Substrate/Buffer**  
(colour code green)  
phosphate/citrate buffer 100 mmol/l, pH 4.4  
sodium perborate 3.2 mmol/l
- 5 **Chromogen**  
(colour code green)  
ABTS<sup>®</sup> 1.9 mmol/l

### Test principle

This test is based on the competition principle.

In the first incubation step (immunological reaction), serum digoxin and POD-labelled digoxin (digoxin-POD conjugate, soln. 1a) compete for a given limited quantity of digoxin-specific antibodies coated onto the inside wall of the tube. The amount of antibody-digoxin-POD complex formed is a measure of the digoxin content of the sample. The digoxin-POD conjugate not bound by the antibodies is removed along with all other serum constituents in a "bound/free" separation step. In the second incubation step (indicator reaction, soln. 4a), the addition of H<sub>2</sub>O<sub>2</sub> and a chromogen (ABTS<sup>®</sup>) results in formation of a coloured complex whose concentration is proportional to the enzyme activity bound to the tube wall.

The colour intensity that develops within a certain time is measured against the substrate-chromogen solution (4a).

It follows from the competition principle that increasing serum digoxin concentrations will result in less digoxin-POD conjugate-binding by the antibodies and hence in lower enzyme activities.

The results are obtained from a calibration curve that must be set up by investigator using the standards provided in the kit.

### Range of measurement

0–5 ng/ml (0–6.4 nmol/l)



### A1.7: Calibration Curve for Lowry Protein Determination.

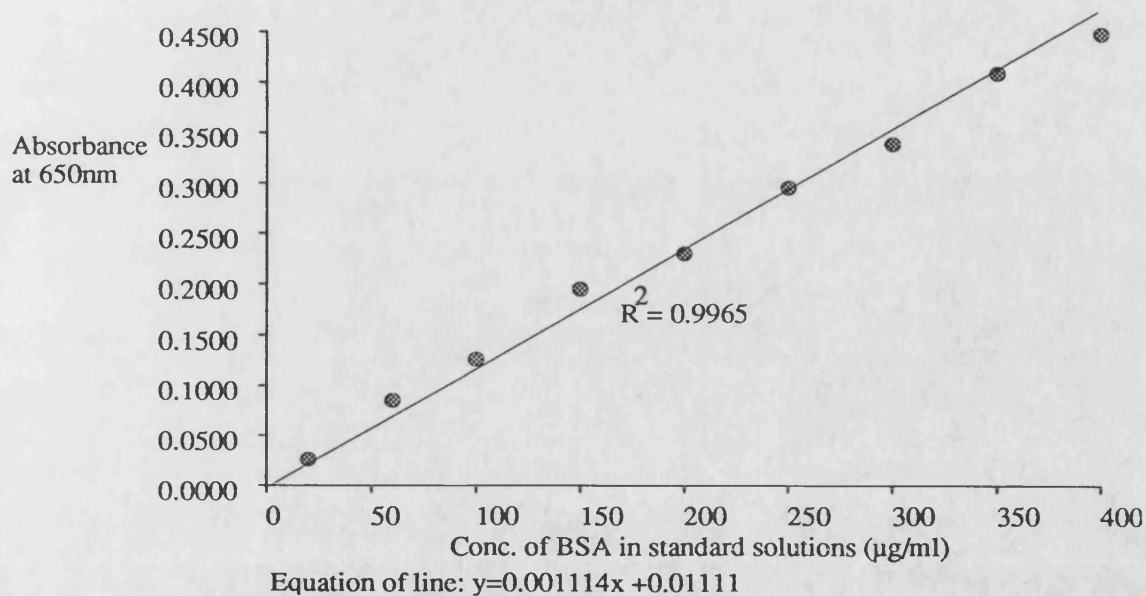
This assay was used to determine the total protein concentration in rat serum. Standard solutions of BSA (20 $\mu$ g-400 $\mu$ g/ml) were prepared in 0.9% NaCl. The standards were incubated as described in the methods (2.7.1a) using the method described by Lowry<sup>(128)</sup> and then the absorbance measured at 650nm against a reagent blank.

Table A1.7: The UV Absorbance of Standard BSA Samples.

Conc. of BSA ( $\mu$ g/ml)	Absorbance at 650nm
20	0.026
60	0.085
100	0.126
150	0.195
200	0.230
250	0.295
300	0.338
350	0.408
400	0.447

A plot of absorbance of BSA standards versus concentration was linear.

Figure A1.7  
Absorbance of standard protein solutions subjected  
to the Lowry Assay for Protein



**A1.8: Calibration curve used to determine the concentration of Evan's Blue in Serum.**

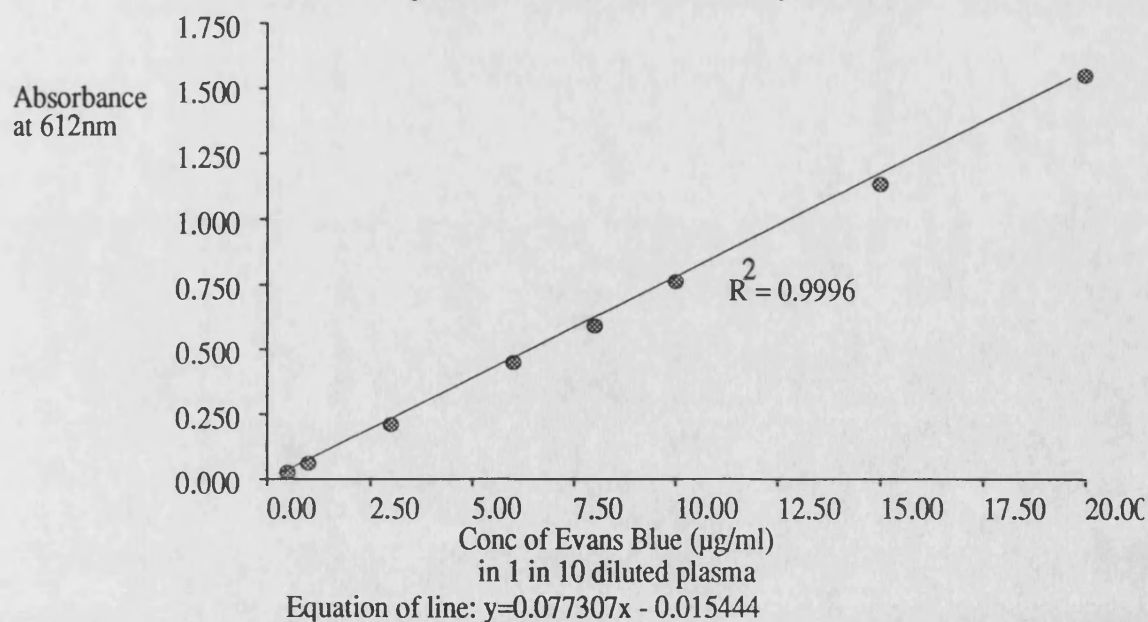
Solutions of Evan's Blue were prepared in one tenth diluted rat serum at a range of 500ng/ml to 20µg/ml. The absorbance was determined at 612nm against a blank of one tenth diluted serum in water.

Table A1.8: Absorbance of Standard Evan's Blue Solutions.

Conc. Evan's Blue (µg/ml)	Absorbance at 612nm
0.5	0.026
1.0	0.060
3.0	0.209
6.0	0.448
8.0	0.589
10.0	0.762
15.0	1.130
20.0	1.546

A plot of absorbance against concentration was linear.

Figure A1.8; Absorbance of Standard Solutions of Evan's Blue in plasma diluted to one tenth strength in water.



### A1.9: Calibration Curve used for molecular weight determination of PEGs on TSK3000.

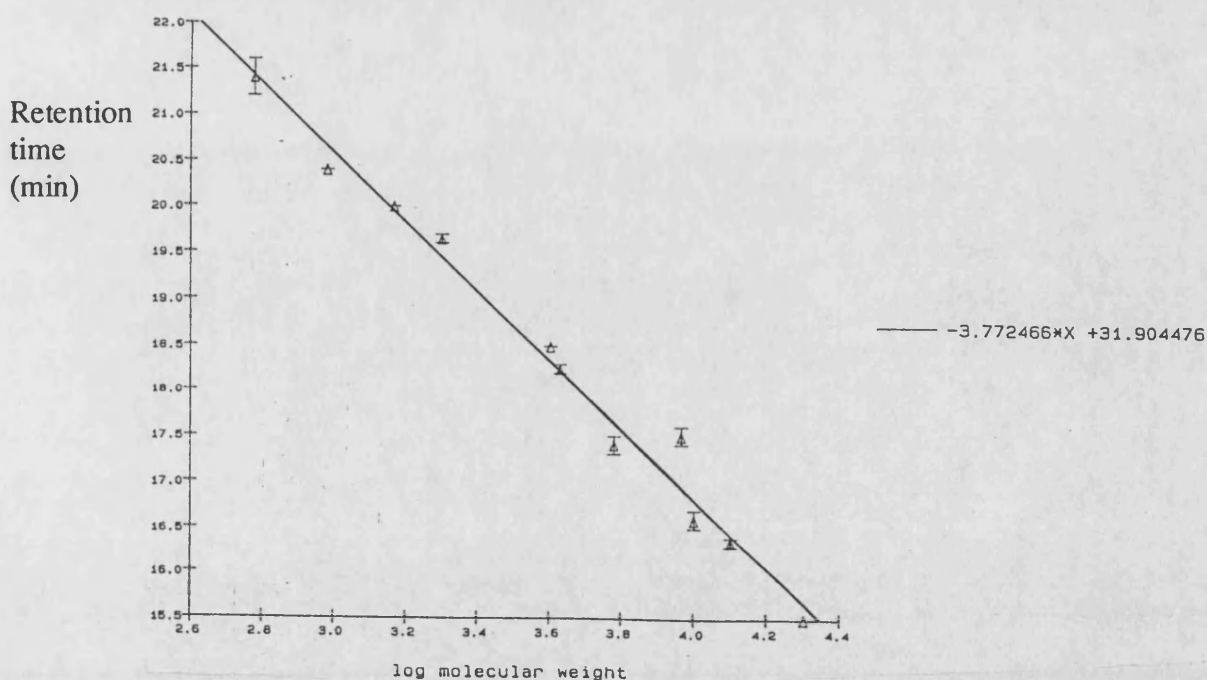
PEGs of molecular weights ranging from 600 to 20,000D (500µg/ml in water) were injected onto the TSK 3000 column and the retention time determined. Detection was by refractive index. Results are means of two injections.

Table A1.9: Retention time of standard molecular weight PEGs on TSK 3000.

Molecular weight	Retention time (minutes)
20,000	15.5
12,600	16.35
10,000	16.6
9,200	17.5
6,000	17.4
4,250	18.3
4,000	18.5
2,000	19.65
1,470	20.0
960	20.4
600	21.4

A graph of Retention time versus log molecular weight of standards is shown in figure A1.9. In the range of molecular weights shown the graph is a straight line and can be used as a calibration curve to determine the molecular weight of unknowns.

Figure A1.9: Retention time of PEG Standards on TSK 3000 Column. ( $R^2=0.9828$ )



## Appendix 2: Formulae and Procedures for calculating Pharmacokinetics and Statistics.

### 2.1 Calculation of Pharmacokinetic Parameters.

When a drug is administered by the IV route, then its pharmacokinetics are due solely to distribution and elimination. For IP and SC administration there is always an absorption step to get drug into the vascular compartment. However this absorption phase may occur very rapidly and may not be detected, if blood samples are not taken early enough.

All the drugs, proteins and conjugates investigated in this work showed a biexponential clearance from serum. i.e. 2 phases were seen. (This was identified on a plot of log serum concentration versus time, where the slope was initially non-linear and then became linear after the first phase was complete). Figure A2.1 is a plot of log serum concentration versus time for RSA, following IV injection. Phase 1 (distribution) and 2 (elimination) are shown. For all substrates investigated the first phase, or alpha phase was thought to be due to distribution in the central compartment (i.e. rapidly equilibrating organs) and the second phase or beta phase was thought to be due to distribution in the tissue compartment and to elimination. Four pharmacokinetic parameters were routinely calculated. These were the Volume of Distribution (Vd), the half-life ( $t^{1/2}$ ), the rate constants for the distribution and elimination phases ( $K_{el}$ ) and the Clearance (Cl).

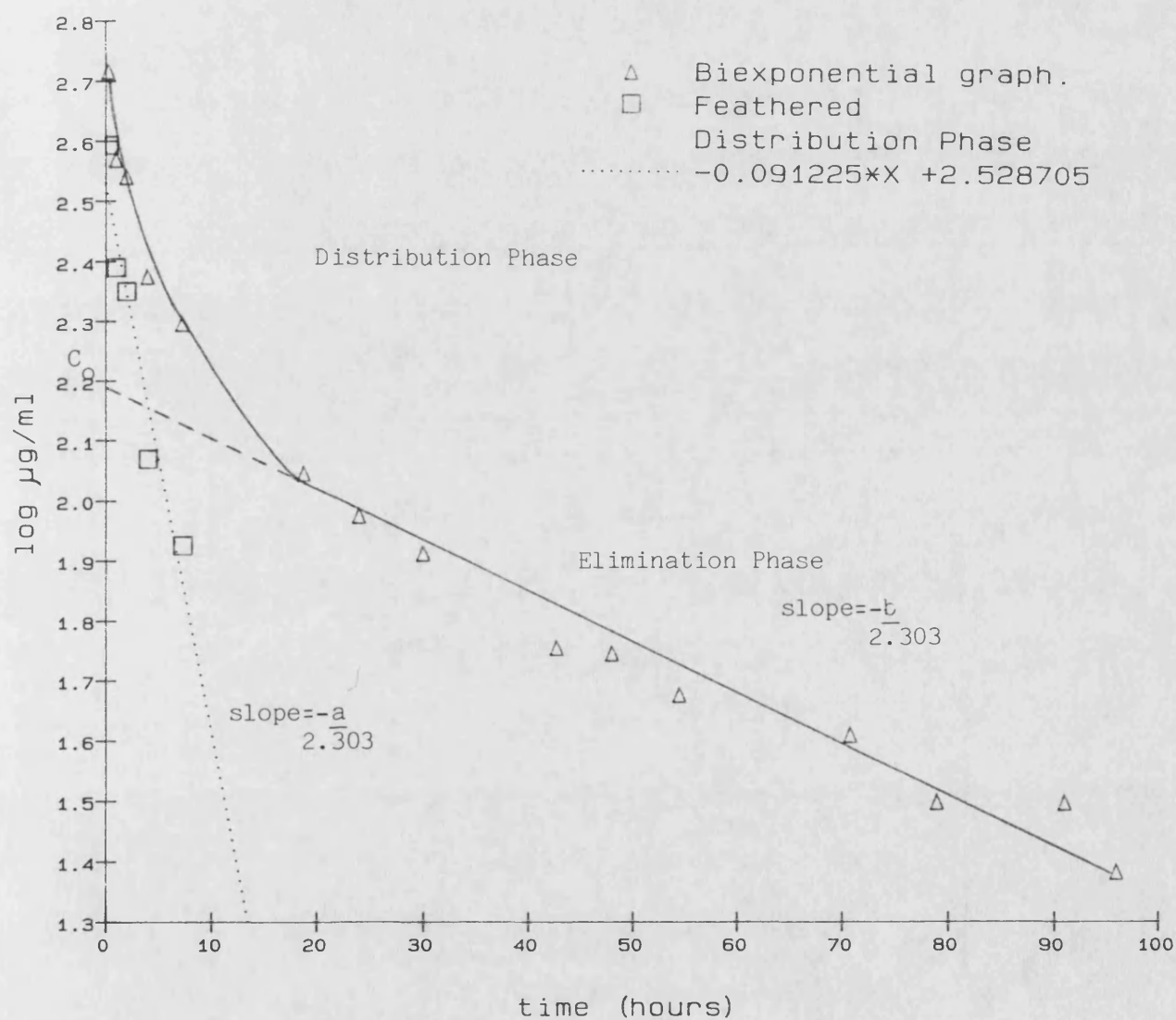
Parameters were calculated using linear regression analysis. For the plot of Log serum concentration versus time (see figure A2.1), the second phase (beta) was shown to be linear and the slope and constants determined from this line were used to calculate the parameters for the beta phase.

#### a) Volume of Distribution (Vd)

At time 0 after injection, the concentration of drug in the body is equivalent to the injected dose. The serum concentration at time 0 ( $C_0$ ) could be determined by extrapolating the linear section of the log serum concentration versus time plot back to the y axis and taking its antilog. Thus the constant for the linear section of the plot could be used to determine Vd.

$$Vd (ml) = \frac{\text{Administered dose}}{C_0}$$

FIGURE A2.1: Serum Clearance of RSA following administration of 5mg of  $^{125}\text{I}$ -RSA to rats by the IV route. This graph shows the feathered plot for the alpha phase.



Values are means  $\pm$  S.E.M. (n=2)

### Elimination Rate Constant (Kel)

The Kel is directly proportional to the slope of the linear section of the log serum versus time plot. It was determined using the equation:

$$kel \text{ (hr}^{-1}\text{)} = 2.303 \times \text{slope}$$

### c) Half-life ( $t^{1/2}$ )

The half-life for the elimination phase can be determined from the Kel.

$$t^{1/2} \text{ (hr)} = \frac{0.693}{Kel}$$

### d) Clearance (Cl)

Clearance is a measure of the body's ability to remove the drug. It represents that volume of plasma cleared of drug in unit time. For most drugs this value is constant.

$$Cl \text{ (ml/hr)} = Kel \times Vd$$

Parameters for the alpha phase involved a more complex calculation. A feathering plot was used to make the alpha phase linear. During the alpha phase, the drug or conjugate was being cleared from plasma or serum by distribution <sup>from</sup> ~~into~~ the central compartment, but in addition the drug was being cleared by the same mechanisms which occur during the beta phase. In order to calculate the alpha phase parameters, the clearance due to the beta phase had to be removed. The hypothetical values for the beta phase at each time point were subtracted from the actual serum concentrations determined during the alpha phase by extrapolating the linear section of the log serum versus time plot back to the y axis.

This feathering of the data for the alpha phase allowed a linear plot for the log serum concentration versus time graph. The parameters were then calculated as described for the beta phase parameters.

For the proteins and conjugates, the alpha phase changed into the beta phase prior to the 24 hour sampling time. Thus beta phase parameters were calculated from time points between 24 hours and usually 96 hours. The alpha phase time points were taken from the remaining sampling times, but care was taken not to include a sampling time which actually fell into the beta phase. It was obvious on carrying out the feathering calculation and plotting the log serum concentration versus time graph, if a point did actually fall into the other phase.

## 2.2 Test for Parallelism.

This test was used to determine whether BSA induced an inflammatory reaction when injected into male wistar rats. Two groups consisting of an equal number of weight matched rats were obtained. To group 1 Evan's Blue was injected and in group 2, dye plus 20mg of BSA was injected. Serum levels of dye were determined for both groups at the same time points. A plot of  $\log_{10}$  serum concentration against time was obtained for both groups. The plot was biexponential and was divided into 2 sections, one for each phase. The slopes for each phase were compared by means of a test for parallelism.

### 1) Alpha Phase.

The test for parallelism was performed between the 20 minute and 4 hour points. A series of factors were calculated in order to perform the analysis of variance. Table A2.1 lists the data required to calculate the F values for the analysis of variance.

**Table A2.1 Sample Results for 4 point Assay of Evans Blue in Plasma.**

Log <sub>10</sub> Evan Blue Concentration (% of dose/ml) (y)					
Observation	E <sub>L</sub>	E <sub>H</sub>	A <sub>L</sub>	A <sub>H</sub>	Q (Totals)
1	0.6445	0.8537	0.5681	0.8615	2.9278
2	0.5495	0.8319	0.5119	0.7939	2.6872
T (totals)	1.1940	1.6856	1.0800	1.6554	5.6150

Where E<sub>L</sub> = Low concentration (4 hour) of Evans Blue only.

E<sub>H</sub> = High concentration (20 minutes) of Evans Blue only.

A<sub>L</sub> = Low concentration (4 hour) of Evans Blue + BSA.

A<sub>H</sub> = High concentration (20 minutes) of Evans Blue + BSA.

$$\begin{aligned}\text{Correction Factor (CF)} &= \frac{(\sum y)^2}{N} \\ &= (5.615)^2/8 \\ &= 3.941\end{aligned}$$

$$E = 1.194 + 1.6856 = 2.8796$$

$$A = 1.08 + 1.6554 = 2.7354$$

$$H = 1.6856 + 1.6554 = 3.341$$

$$L = 1.194 + 1.08 = 2.274$$

There were 8 observations, therefore the total degrees of freedom (d.f.) was 7. This d.f. is subject to 2 independent classifications; between animals (2 animals in each group) which has 1 d.f. and between times ( 4 time points) which has 3 d.f..An interaction (residual or error) d.f. was also required. This was calculated as the product of the 2 sets of d.f. i.e. 3. in addition the 4 time points were subject to 2 independent criteria of classification i.e. one of two injected preparations (1d.f.) and one of two time points (1d.f.).

**Table A2.2 The Analysis of Variance Table.**

Source of variation	d.f.	Sum of Squares (SS)	V (SS/d.f.)	F (V/res error)
Total	7	$\sum y^2 - CF = 0.1544$ (1)	0.0221	-
Between animals	1	$(\sum Q^2/4) - CF = 0.00726$ (2)	0.00726	15.75 (significant)
Between Sampling times	3	$(\sum T^2/2) - CF = 0.0486$ $= 0.146$ (3)	0.0486	-
Slope	1	$((\sum L)^2 + (\sum H)^2/4) - CF = 0.142$ (4)	0.142	309.78 (H. Sig)
Preparations	1	$((\sum E)^2 + (\sum A)^2/4) - CF = 0.00260$ (5)	0.00260	5.658 (non-sig)
Parallelism	1	$(3) - (4) - (5) = 8.778 \times 10^{-4}$	$8.778 \times 10^{-4}$	1.910 (non-sig)
Residual	3	$(1) - (2) - (3) = 1.378 \times 10^{-3}$	$4.594 \times 10^{-4}$	-

The divisor for each of the sum of square terms was the number of observations in the group used to calculate the SS. The F values in the final column were compared to reference values tabulated in Variance Ratio Tables. The test for parallelism over the distribution phase showed that the slopes for group 1 and group 2 were parallel. The highly significant value for the slope F ratio showed that this test was a valid test for the data (the lines must have a slope for the test to be valid). There was no difference in the potency of the preparations used for groups 1 and 2. The significant difference obtained for the between observations was possibly due to differences in the rats used.

The analysis of variance was repeated for the elimination phase. Time points of 6 and 24 hours were used. The slopes for the two groups were parallel. There was a significant difference for the between preparations F value. This could be due to the nature of the injection solution for group 2. Because contained BSA it was more viscous than the injection solution containing Evans Blue only and thus the whole dose may not have been administered to the group 2 rats.



### APPENDIX 3: EXPERIMENTAL DATA FOR CHAPTERS 3 TO 6.

Table A3.1.1: The plasma concentration (% dose remaining/ml) of MTXNa<sub>2</sub> after administration of 2.5mg of drug by IV, IP, SC injection. (n=8 for each route). Each value represents the concentration determined by HPLC for one rat.

IV		IP		SC	
Time (min)	%dose /ml	Time (min)	%dose /ml	Time (min)	%dose /ml
10	0.630	15	0.465	15	0.523
20	0.410	15	0.378	15	0.549
30	0.268	30	0.318	30	0.441
40	0.186	30	0.194	30	0.323
50	0.123	45	0.220	45	0.236
60	0.112	45	0.234	45	0.229
75	0.0877	60	0.184	60	0.156
90	0.0489	60	0.0762	60	0.165
105	0.0292	75	0.0998	75	0.0932
120	0.0242	75	0.0650	75	0.0933
135	0.0255	90	0.0547	90	0.0546
150	0.0309	90	0.0649	90	0.0524
165	0.0220	105	0.0325	105	0.0443
195	0.0189	105	0.0385	105	0.0480
		120	0.0377	120	0.0315
		120	0.0306	120	0.0208
		150	0.0251	165	0.0164
		150	0.0298	165	0.0211
		180	0.0202	180	0.0180
		180	0.0228	180	0.0157

Table A3.1.2: The plasma concentrations (%dose remaining/ml) of <sup>3</sup>H-MTX after administration of a total dose of MTXNa<sub>2</sub> of 2.5mg by IV, IP and SC. (n=8 for each route). Each value represents the results obtained for one rat.

IV		IP		SC	
Time (min)	%dose /ml	Time (min)	%dose /ml	Time (min)	%dose /ml
15	0.400	15	0.271	15	0.331
15	0.421	15	0.246	15	0.480
30	0.195	30	0.174	30	0.273
30	0.186	30	0.192	30	0.235
45	0.157	50	0.136	50	0.162
45	0.143	50	0.159	50	0.0777
60	0.0866	65	0.0874	65	0.0622
60	0.115	65	0.0802	65	0.125
90	0.0488	90	0.0551	90	0.0496
90	0.0518	90	0.0587	90	0.0594
120	0.0551	120	0.0366	120	0.0282
120	0.0447	120	0.0382	120	0.0226
150	0.0379	165	0.0287	165	0.0171
150	0.0302	165	0.0275	165	0.0226
180	0.0225	225	0.0235	225	0.0161
180	0.0458	225	0.0170	225	0.0128
210	0.0267				
210	0.0239				

Table A3.1.3: The plasma levels obtained (% dose remaining/ml) after injecting 0.5mg of <sup>3</sup>H-MTX by IV, IP, SC to male wistar rats. (n=8 for each route).

IV Time (min)	%dose /ml	IP Time (min)	%dose /ml	SC Time (min)	%dose /ml
15	0.425	5	0.239	10	0.347
15	0.521	7	0.362	10	0.407
30	0.295	11	0.479	20	0.312
30	0.205	12	0.324	20	0.357
45	0.143	20	0.354	30	0.229
45	0.154	23	0.400	30	0.196
60	0.0898	29	0.227	40	0.159
60	0.108	30	0.284	40	0.204
80	0.0598	45	0.214	50	0.129
80	0.0511	50	0.198	50	0.174
100	0.0367	60	0.169	60	0.134
100	0.0338	61	0.150	60	0.136
120	0.0348	84	0.126	75	0.117
120	0.0304	85	0.102	75	0.0848
140	0.0246	107	0.0478	85	0.0962
140	0.0247	107	0.0738	90	0.0651
160	0.0242	125	0.0746	105	0.0495
165	0.0213	126	0.0508	105	0.0471
180	0.0460	145	0.0574	120	0.0391
180	0.0227	148	0.0558	120	0.0340
210	0.0401	160	0.0542	150	0.0326
210	0.0180	163	0.0417	160	0.0265
240	0.0146	180	0.0332	180	0.0237
240	0.0162	180	0.0418	180	0.0244
		215	0.0359	210	0.0213
		216	0.0282	210	0.0226
		240	0.0336	240	0.0182
		240	0.0318	240	0.0199

**Table A3.1.4: The Urine Excretion of MTX following Administration of 2.5mg of MTXNa<sub>2</sub> by the IV route and measurement using the HPLC assay for urine samples.**

Results are expressed as mean % dose excreted. (n=4)

Time (hours)	Mean (% of dose excreted)	S.E.M.
6.5	59.5	7.15
24.0	82.3	3.57
48.0	88.7	2.60

**Table A3.1.5: The Urine excretion of <sup>3</sup>H activity (% of total dose administered) following administration of 0.5mg of <sup>3</sup>H-MTX by IV, IP and SC routes.**

Results are expressed as mean % excreted. (n=3 for IP and n=4 for IV and SC).

Time (hr)	IV (%)	S.E.M.	IP (%)	S.E.M.	SC (%)	S.E.M.
7	4.8	2.60	ND		5.4	2.11
24	14.63	2.03	10.48	2.18	14.93	4.11
48	15.7	1.91	12.73	2.33	16.92	3.78
72	16.1	1.94	13.40	2.40	17.33	3.62

**Table A3.1.6: The Urine Excretion of <sup>3</sup>H activity (% of total dose administered) following administration of 2.5mg of <sup>3</sup>H-MTX by IV, IP and SC Injection.**

Results are expressed as mean % excreted. (n=3 for IV and n=4 for IP and SC).

Time (hr)	IV (%)	S.E.M.	IP (%)	S.E.M.	SC (%)	S.E.M.
6	3.8	1.92	7.56	4.23	7.88	3.03
24	14.54	4.70	21.99	4.90	17.04	5.19
48	17.90	5.12	25.01	5.12	18.95	5.84
72	19.55	5.42	25.85	5.12	19.37	5.92

Table A3.2.1: The serum concentration (% dose remaining/ml) of Digoxin after injecting male wistar rats with 250ng of drug by IV, IP or SC routes. Serum levels were determined using an ELISA technique. Each value represents the results obtained for one rat.

	IV	IP	SC
Time (hr)	%dose/ml	%dose/ml	%dose/ml
0.5	1.56	0.702	0.32
0.5	1.70	1.28	0.40
1.0	1.24	0.88	0.22
1.0	1.04	0.66	0.48
1.5	0.90	ND	ND
1.5	0.96	ND	ND
2.0	0.66	0.65	0.80
2.0	0.40	0.52	1.48
2.5	0.44	0.90	0.78
2.5	0.38	0.46	0.64
4.0	0.32	ND	ND
4.0	0.20	ND	ND
4.5	0.22	ND	ND
4.5	0.21	ND	ND
5.0	0.14	0.62	0.36
5.0	0.20	0.33	ND
5.5	0.18	ND	ND
5.5	0.26	ND	ND
6.0	0.24	ND	ND
6.0	0.16	ND	ND
7.0	0.24	0.18	0.12
7.0	0.18	0.22	0.20
17.0	ND	Ndig	0.
17.0	ND	Ndig	0.14

ND= Not determined.

Ndig= Digoxin was not detected.

Table A3.3.1: The plasma concentration of  $^{125}\text{I}$  (%of dose remaining/ml) after administration of 0.654ng of  $^{125}\text{INa}$  to male wistar rats by the IV route. Each value represents the plasma concentration determined for one rat. Eight rats were dosed. Four 0.3ml blood samples were taken from each rat.

Time (hr)	% dose/ml
0.25	0.779
0.25	0.646
0.5	0.490
0.5	0.607
0.75	0.528
0.75	0.366
1.167	0.488
1.167	0.406
1.5	0.449
1.5	0.398
1.833	0.445
1.833	0.442
2.0	0.368
2.0	0.272
2.367	0.338
2.417	0.438
3.0	0.319
3.0	0.238
4.0	0.247
4.0	0.395
5.0	0.266
5.0	0.272
6.0	0.227
6.0	0.179
23.0	0.059
23.0	0.073
27.0	0.069
27.0	0.083
30.75	0.052
30.75	0.073
48.0	0.028

Table A3.3.2: The Urine Excretion of radioactivity following administration of 0.654ng of  $^{125}\text{I}$ -Na to rats by the IV route.

Values are mean % excretion (n=4).

Time (hr)	Mean % excreted	S.E.M.
24	45.54	7.18
48	51.66	7.18
72	56.42	7.74
96	59.35	8.50

Table A3.3.3: The Excretion of radioactivity in the faeces following administration of 0.654ng of  $^{125}\text{I}$ -Na to rats by the IV route.

Values are mean % excretion (n=4).

Time (hr)	Mean % excreted	S.E.M.
24	3.755	1.290
48	5.600	1.489

Table A3.3.4: The Organ Distribution of radioactivity following administration of 0.654ng of <sup>125</sup>I-Na to rats by the IV route.

Results are expressed in 2 forms as a % of the total activity injected in either 1g or the whole tissue and as a ratio of the activity found in 1g (or whole tissue) divided by the activity found in 1ml of whole blood.

Organ	% in 1g	CPM in 1g/ CPM in 1ml WB	% in total	CPM in total/ CPM in 1ml WB
<b>1. Distribution 4 hours post injection.</b>				
Thyroid	ND	ND	5.06	18.88
			6.21	14.14
Whole Blood	ND	ND	0.268%/ml	1
			0.439%/ml	1
Serum	ND	ND	0.247%/ml	0.922
			0.395%/ml	0.900
Liver	0.182	0.679	2.36	8.826
	0.193	0.439	2.17	4.937
Kidney	0.205	0.767	0.404	1.509
	0.199	0.453	0.438	0.997
<b>2. Distribution 27 hours post injection.</b>				
Thyroid	ND	ND	9.40	101.5
			8.52	110.6
Whole Blood	ND	ND	0.0926%/ml	1
			0.0770%/ml	1
Serum	ND	ND	0.083%/ml	0.896
			0.069%/ml	0.896
Liver	0.0471	0.509	0.46	4.966
	0.0453	0.588	0.54	7.000
Kidney	0.0446	0.482	0.094	1.013
	0.0397	0.516	0.083	1.083
<b>3. Distribution 52 hours post injection.</b>				
Thyroid	ND	ND	7.96	169.4
			8.45	325
Whole Blood	ND	ND	0.047%/ml	1
			0.026%/ml	1
Serum	ND	ND	0.042%/ml	0.894
			0.028%/ml	1.077
Liver	0.0221	0.470	0.24	5.100
	0.0153	0.589	0.23	8.930
Kidney	0.0227	0.484	0.055	1.174
	0.0128	0.491	0.027	1.032



**Table A3.4.1: The plasma concentration of  $^{14}\text{C}$ - Inulin (% dose remaining/ml) after administration of 40mg of drug to male wistar rats by SC or IP injection.**

(n=8 for each route), Each value represents the plasma concentration determined for one rat.

Time	SC		IP	
	% dose/ml	S.E.M	% dose/ml	S.E.M.
1	0.0279		0.0382	
1	0.0337		0.0758	
2	0.00541		0.0498	
2	0.00596		0.0314	
3	0.00650		0.0352	
3	0.00866		0.0148	
4	0.00650		0.0265	
4	0.00541		0.0127	
5	0.00571	0.00135 <sup>a</sup>	0.0101	
6	0.00363		0.00463	
6	0.00355			
7.5	0.00571	0.0017 <sup>b</sup>	0.00781	0.00208 <sup>a</sup>
10.66	0.00317		0.00374	0.00131 <sup>a</sup>
10.66	0.00417			

Note where S.E.M. are expressed the values for % dose remaining/ml are expressed as the mean of at least three plasma samples for different rats.

a) n=3

b) n=4

Table A3.5.1: The serum concentrations (% of <sup>125</sup>I activity remaining/ml) determined after administration of 5mg of <sup>125</sup>I-Lactalbumin to male wistar rats by IV, SC or IP routes.

Each value represents the result obtained for one rat. (n=8 for each route).

Time (hour)	IV(%dose/ml)	IP(%dose/ml)	SC(%dose/ml)
0.25	1.0992	ND	ND
0.25	1.205		
0.33	ND	0.286	ND
0.33		0.296	
0.5	1.041	ND	0.173
0.5	1.104		0.274
0.66	ND	0.400	ND
0.66		0.348	
1.0	0.852	0.674	0.446
1.0	0.839	0.593	0.833
2.0	0.659	0.511	0.380
2.0	0.534	0.533	0.481
3.0	0.493	0.463	0.458
3.0	0.391	0.439	0.369
4.0	0.412	0.361	0.350
4.0	0.467	0.386	0.309
6.0	0.350	0.396	0.322
6.0	0.362	0.397	0.238
8.0	0.302	0.258	0.201
8.0	0.319	0.331	0.221
10.0	0.237	0.310	0.152
10.0	0.270	0.309	0.171
25.0	0.243	0.113	0.106
25.0	0.173	0.148	0.111
28.0	0.201	0.161	0.101
28.0	0.139	0.128	0.122
31.5	0.125	0.108	0.115
31.5	0.113	0.126	0.128
47.5	0.076	0.089	0.064
47.5	0.087	0.097	0.080
55.0	0.094	0.096	0.082
55.0	0.103	0.100	0.098
72.0	0.046	0.057	0.039
72.0	0.037	0.050	0.059

**Table A3.5.2: The Urine Excretion of  $^{125}\text{I}$  activity (% of total dose administered) after administration of 5mg of  $^{125}\text{I}$ -Lactalbumin to male wistar rats by IV, IP or SC injection.**

Values expressed are means (n=3)  $\pm$  S.E.M.

Time (hr)	IV (%)	S.E.M.	IP (%)	S.E.M.	SC (%)	S.E.M.
24	28.53	3.267	42.87 <sup>a</sup>	8.510	51.96 <sup>b</sup>	2.549
48	39.84	4.309	55.54	7.773	63.70	2.860
72	45.73	3.788	63.48 <sup>a</sup>	7.500	68.45 <sup>b</sup>	2.517

**Notes**

a= values were non-significantly different from rats dosed IV.(P>0.05)

b= values were highly significantly different from rats dosed IV. (P<0.02)

There was no significant difference in urine excretion for rats dosed IP and SC.

**Table A3.5.3: The excretion of  $^{125}\text{I}$  activity in the faeces (% total dose administered) after administration of 5mg of  $^{125}\text{I}$ -Lactalbumin to male wistar rats by IV, IP or SC routes.**

Values expressed are means (n=3)  $\pm$  S.E.M.

Time (hr)	IV (%)	S.E.M.	IP (%)	S.E.M.	SC (%)	S.E.M.
24	3.32	1.488	3.36	0.460	4.29	0.142
48	4.90	1.708	5.38	0.435	6.97	0.880
72	6.31	1.410	6.70	0.690	8.08	0.907

**Note**

There was no significant difference for the faecal excretion of  $^{125}\text{I}$  for any route of administration.

Table A3.5.4: The organ distribution of  $^{125}\text{I}$  activity after administration of 5mg of  $^{125}\text{I}$ -Lactalbumin to male wistar rats by IV, SC or IP injection.

The results are expressed in 2 forms; as a % of the administered dose in 1g or the whole organ and as a ratio of the activity in the organ / the activity in 1ml of whole blood.

Organ	% of dose /g	<u>CPM in 1g</u> CPM/ml WB	% of dose (total)	<u>CPM(total)</u> CPM/ml WB
<b>1. Distribution 28 hours post IV injection.</b>				
THYROID	ND	ND	6.750	23.85
			4.070	19.66
WHOLE BLOOD	ND	ND	0.283%/ml	1
			0.207%/ml	1
PLASMA	ND	ND	0.201%/ml	0.710
			0.139%/ml	0.671
LIVER	0.114	0.404	0.862	3.046
	0.099	0.478	0.940	4.543
SPLEEN	0.0857	0.303	0.075	0.265
	0.0626	0.302	0.068	0.330
HEART	0.0719	0.254	0.063	0.22
	0.0317	0.153	0.058	0.281
LUNG	0.107	0.378	0.160	0.562
	0.0855	0.412	0.130	0.645
KIDNEY	0.426	1.508	0.865	3.061
	0.460	2.218	0.960	4.637
STOMACH	0.888	3.144	3.24	11.45
	0.348	1.677	1.33	6.417
SM. INTESTINE	0.158	0.559	1.184	4.183
	0.156	0.751	1.22	5.873

Table A3.5.4 Cont. (Organ Distribution following administration of LA).

Organ	%dose /g	CPM/g CPM/ml WB	% dose (total)	CPM (total) CPM/ml WB
<b>2. IV Distribution after 72 hours.</b>				
THYROID	ND	ND	3.81	42.33
			4.25	57.43
WHOLE BLOOD	ND	ND	0.090%/ml	1
			0.074%/ml	1
PLASMA	ND	ND	0.0459%/ml	0.51
			0.0373%/ml	0.504
LIVER	0.0520	0.575	0.528	5.63
	0.0496	0.647	0.530	6.95
SPLEEN	0.0303	0.335	0.023	0.248
	0.0303	0.396	0.029	0.384
HEART	0.0220	0.243	0.022	0.245
	0.0405	0.529	0.034	0.447
LUNG	0.036	0.398	0.0468	0.518
	0.032	0.419	0.051	0.662
KIDNEY	0.314	3.48	0.655	7.24
	0.374	4.88	0.770	10.05
STOMACH	0.0588	0.617	0.260	0.247
	0.0374	0.487	0.220	2.895
SM. INTESTINE	0.0537	0.594	0.509	5.62
	0.0593	0.774	0.540	7.082
<b>3. Distribution 28 hours after SC administration.</b>				
THYROID	ND	ND	5.70	35.63
			8.63	47.94
WHOLE BLOOD	ND	ND	0.16%/ml	1
			0.18%/ml	1
PLASMA	ND	ND	0.101%/ml	0.631
			0.122%/ml	0.678
LIVER	0.052	0.325	0.550	3.442
	0.092	0.500	0.831	4.511
SPLEEN	0.035	0.221	0.045	0.282
	0.051	0.279	0.051	0.276
HEART	0.039	0.244	0.034	0.213
	0.054	0.292	0.047	0.256
LUNG	0.050	0.315	0.068	0.425
	0.067	0.362	0.093	0.508
KIDNEY	0.422	2.367	0.980	6.136
	0.398	2.164	0.939	5.106
STOMACH	0.256	1.601	0.910	5.694
	0.294	1.600	0.884	4.807
SM. INTESTINE	0.078	0.486	0.620	3.862
	0.0819	0.445	0.690	3.781

Table A3.5.4 Cont. (tissue Distribution of LA).

ORGAN	% dose /g	CPM/g/ CPM/ml WB	%dose (total)	CPM (total) CPM/ml WB
<b>4. Distribution 72 hours post SC Administration.</b>				
THYROID	ND	ND	6.98	81.16
			7.42	82.44
WHOLE BLOOD	ND	ND	0.086%/ml	1
			0.090%/ml	1
PLASMA	ND	ND	0.039%/ml	0.455
			0.059%/ml	0.658
LIVER	0.030	0.340	0.320	3.604
	0.086	0.922	0.721	7.653
SPLEEN	0.018	0.199	0.021	0.238
	0.039	0.413	0.038	0.406
HEART	0.026	0.289	0.019	0.217
	0.027	0.286	0.018	0.188
LUNG	0.031	0.346	0.042	0.472
	0.034	0.360	0.041	0.437
KIDNEY	0.305	3.43	0.627	7.049
	0.484	5.18	0.86	9.165
STOMACH	0.033	0.372	0.141	1.582
	0.113	1.208	0.240	2.563
SM. INTESTINE	0.028	0.314	0.228	2.563
	0.045	0.478	0.230	2.476
<b>5. Distribution 28 hours after IP administration.</b>				
THYROID	ND	ND	7.31	33.23
			8.06	44.78
WHOLE BLOOD	ND	ND	0.22%/ml	1
			0.18%/ml	1
PLASMA	ND	ND	0.16%/ml	0.725
			0.13%/ml	0.711
LIVER	0.080	0.361	0.992	4.470
	0.093	0.520	1.25	6.949
SPLEEN	0.056	0.252	0.053	0.239
	0.066	0.366	0.111	0.587
HEART	0.044	0.197	0.042	0.189
	0.056	0.310	0.045	0.255
LUNG	0.0721	0.325	0.099	0.448
	0.082	0.454	0.098	0.543
KIDNEY	0.482	2.172	1.114	5.022
	0.498	2.771	1.167	6.491
STOMACH	0.298	1.345	1.553	6.998
	0.351	1.954	2.53	14.05
SM. INTESTINE	0.303	1.367	3.576	16.11

**Table A3.5.4 cont. (Organ Distribution of LA)**

ORGAN	% dose in 1g	<u>CPM in 1g</u> CPM/ml WB	% dose in total	<u>CPM (total)</u> CPM/ml WB
<b>6. Distribution 72hours after IP administration</b>				
THYROID	ND	ND	5.33	54.39
			7.28	77.45
WHOLE BLOOD	ND	ND	0.098%/ml	1
			0.094%/ml	1
PLASMA	ND	ND	0.056%/ml	0.576
			0.050%/ml	0.529
LIVER	0.050	0.489	0.531	5.178
	0.046	0.475	0.436	4.492
SPLEEN	0.032	0.317	0.023	0.223
	0.025	0.259	0.039	0.397
HEART	0.021	0.205	0.017	0.165
	0.030	0.313	0.022	0.227
LUNG	0.0358	0.351	0.049	0.475
	0.101	1.045	0.121	1.233
KIDNEY	0.375	3.684	0.842	8.253
	0.328	3.379	0.673	6.867
STOMACH	0.123	1.210	0.282	2.797
	0.086	0.881	0.401	4.112
SM. INTESTINE	0.050	0.491	0.432	4.193
	0.038	0.388	0.364	3.750

Table A3.6.1: The Serum concentration (% <sup>125</sup>I activity remaining/ml) determined after administration of 5mg <sup>125</sup>I-Carbonic Anhydrase to rats by IV, IP or SC routes.

Each value represents the result obtained for one rat. (n=8 for each route).

Time (hour)	IV (%dose/ml)	IP (% dose/ml)	SC (% dose/ml)
1.0	0.980	1.084	0.804
1.0	0.948	0.795	0.755
2.0	0.906	0.983	0.755
2.0	0.972	0.955	0.728
4.0	0.640	0.839	0.720
4.0	0.675	0.906	0.712
6.0	0.704	0.710	0.647
6.0	0.578	0.724	0.665
8.0	ND	ND	0.582
8.0	ND	ND	0.616
10.0	0.431	0.657	0.562
10.0	0.488	0.592	0.611
18.75	0.298	0.272	0.272
18.75	0.271	0.356	0.278
21.0	0.263	0.210	0.229
21.0	0.284	0.214	0.253
24.0	0.238	0.247	0.205
24.0	0.211	0.181	0.209
27.0	ND	0.198	0.144
27.0	ND	0.167	0.161
30.75	0.255	0.172	0.130
30.75	0.232	0.177	0.172
48.0	0.0841	0.0830	0.0528
48.0	0.106	0.0732	0.0566
55.5	0.124	0.0564	0.0602
55.5	0.0970	0.0733	0.0542
72.0	0.0653	0.0640	0.0400
72.0	0.0667	0.0558	0.0478
97.5	0.0437	0.0415	0.0383
97.5	0.0392	0.0318	0.0321



**Table A3.6.2: The Urine Excretion of  $^{125}\text{I}$  activity (% of total dose administered) after administration of 5mg  $^{125}\text{I}$ -Carbonic Anhydrase to rats by IV, IP or SC injection.**

Values are means (n=3)  $\pm$  S.E.M.

Time (hr)	IV (%)	S.E.M.	IP(%)	S.E.M.	SC(%)	S.E.M.
24	22.95	1.25	33.31	7.22	20.55	2.38
48	34.22	3.70	41.17	8.24	23.89	2.84
72	36.12	3.83	45.59	7.11	29.47	2.40
96	37.61	4.25	47.15	6.84	30.71	2.44

There was no significant difference for the % of  $^{125}\text{I}$  activity excreted in the urine for each of the routes when analysed using a Students T-test.

**Table A3.6.3: The Excretion of  $^{125}\text{I}$  activity in the faeces (% total dose administered) after administration of 5mg of  $^{125}\text{I}$ -Carbonic Anhydrase to rats dosed IV, IP or SC.**

Values are expressed as means (n=3)  $\pm$  S.E.M.

Time (hr)	IV(%)	S.E.M.	IP(%)	S.E.M.	SC(%)	S.E.M.
24	3.24	0.18	4.05	1.85	6.61	0.44
48	5.07	0.14	4.94	2.03	8.81	0.54
72	5.83	0.34	6.88	2.08	10.29	0.90
96	6.96	0.25	7.61	2.12	11.21	0.99

Analysis of different routes of administration at same time points using a Students T-test showed no significant difference.

Table A3.6.4: The Organ Distribution of <sup>125</sup>I-activity after administration of 5mg of <sup>125</sup>I-Carbonic anhydrase to rats by IV, IP or SC routes.

The results are expressed in 2 forms: as a % of the total dose present in either 1g or the whole organ and as a ratio of the activity in the organ divided by the activity in 1ml of whole blood.

1. Distribution 24 hours post IV injection.

ORGAN	% of dose /g	<u>CPM/g</u> CPM/ml WB	% of dose (total)	<u>CPM (total)</u> CPM/ml WB
THYROID	ND	ND	7.66	26.41
			8.21	30.41
WHOLE BLOOD	ND	ND	0.29%/ml	1
			0.27%/ml	1
SERUM	ND	ND	0.24%/ml	0.821
			0.21%/ml	0.781
LIVER	0.0580	0.198	0.618	2.105
	0.0494	0.183	0.527	1.952
SPLEEN	0.0557	0.189	0.082	0.279
	0.0538	0.198	0.078	0.288
HEART	0.0612	0.208	0.060	0.205
	0.0548	0.203	0.053	0.197
LUNG	0.0886	0.301	0.149	0.508
	0.107	0.397	0.150	0.556
KIDNEY	0.209	0.712	0.436	1.735
	0.223	0.826	0.468	1.735
STOMACH	0.268	0.912	1.144	3.893
	0.499	1.848	1.599	5.922
SM. INTESTINE	0.125	0.424	0.970	3.300
	0.135	0.501	1.042	3.811

Table A3.6.4 Cont. (Organ Distribution of CA).

**2. Distribution 24 hours post SC injection.**

ORGAN	% of dose /g	<u>CPM/g</u> CPM/ml WB	% of dose (total)	<u>CPM(total)</u> CPM/ml WB
THYROID	ND	ND	9.39	64.32
			7.87	63.98
WHOLE BLOOD	ND	ND	0.146%/ml	1
			0.123%/ml	1
SERUM	ND	ND	0.205%/ml	1.404
			0.209%/ml	1.699
LIVER	0.0556	0.382	0.478	3.280
	0.0525	0.425	0.434	3.517
SPLEEN	0.0449	0.308	0.0298	0.204
	0.0478	0.387	0.0375	0.304
HEART	0.0458	0.314	0.0348	0.239
	0.0333	0.270	0.0287	0.233
LUNG	0.0617	0.423	0.0820	0.562
	0.0603	0.488	0.108	0.875
KIDNEY	0.134	0.917	0.270	1.852
	0.174	1.408	0.281	2.276
STOMACH	0.266	1.826	0.729	5.004
	0.536	4.342	1.907	15.443
SM. INTESTINE	0.112	0.768	0.992	6.805
	0.085	0.688	0.577	4.674

Table A3.7.1: The Plasma Concentration (% of  $^{14}\text{C}$  activity remaining/ml) after administration of 0.04mg of  $^{14}\text{C}$ -CEA by the IV route to rats.

Tabulated values are means from 3 different rats. 4 rats were injected.

Time (hr)	Mean %/ml	S.E.M.
0.5	2.377	0.192
1.0	0.896	0.125
2.0	0.330	0.049
4.0	0.213	0.031
6.0	0.151	0.021
24.0	0.087	0.0136

Table A3.7.2: The Urinary Excretion of  $^{14}\text{C}$  activity (% of total dose administered) after administration of  $^{14}\text{C}$ -CEA to rats.

Tabulated values are means (n=3)  $\pm$  S. E.M.

Time (hr)	Mean % excreted	S.E.M.
24	1.44	0.460
48	2.20	0.404
72	2.85	0.375
96	3.30	0.289
120	3.60	0.327
144	3.85	0.202

Table A3.8.1 The Serum Concentration (%  $^{125}\text{I}$  activity remaining/ml) after administration of 5mg of  $^{125}\text{I}$ -BSA to rats by each of the three routes. (n=8) for each route. Each value represents the plasma concentration determined from one rat.

Time (hr)	IV %dose /ml	Time (hr)	IP %dose /ml	Time (hr)	SC %dose /ml
0.75	8.899	0.75	0.306	0.75	0.0476
1.0	7.556	0.75	0.308	0.75	0.0417
1.0	7.925	2.0	0.302	2.0	0.505
3.0	6.685	2.0	0.422	2.0	0.413
3.0	5.702	4.0	3.272	4.0	0.736
6.0	4.548	4.0	4.169	4.0	0.879
6.0	4.841	6.0	4.689	6.0	0.938
23.5	2.077	6.0	3.869	6.0	0.907
23.5	1.935	8.0	4.288	8.0	1.146
31.0	1.652	8.0	4.220	8.0	1.005
31.0	1.409	11.0	3.198	11.0	1.262
48.0	0.755	11.0	3.875	11.0	1.461
48.0	0.935	22.5	2.097	22.5	1.272
54.25	0.589	22.5	1.985	22.5	1.281
54.25	0.617	31.0	2.018	25.0	1.126
72.0	0.351	31.0	1.209	25.0	1.166
72.0	0.317	48.0	0.681	28.0	0.963
79.5	0.265	48.0	0.859	28.0	1.324
79.5	0.315	54.5	0.660	30.0	1.151
97.0	0.244	54.5	0.618	30.0	1.129
97.0	0.219	71.5	0.395	48.0	0.627
		71.5	0.362	48.0	0.693
		78.5	0.401	54.5	0.515
		78.5	0.288	54.5	0.476
		96	0.214	71.5	0.277
		97	0.219	71.5	0.270
		97	0.156	78.5	0.253
				78.5	0.248
				97	0.185
				97	0.156

Table A3.8.2 The Urine Excretion (% of total  $^{125}\text{I}$  dose administered) after administration of 5mg of  $^{125}\text{I}$ -BSA to rats by each of the three routes.

Values are expressed as means (n=3)  $\pm$  S.E.M.

Time (hr)	IV % dose excreted	S.E.M.	IP % dose excreted	S.E.M.	SC % dose excreted	S.E.M.
24	15.33	1.424	18.50	0.929	19.33	1.889
48	32.83	1.822	37.23	4.896	39.40	2.577
72	45.51	2.046	46.73	7.824	49.30	2.150
96	53.27	2.888	52.30	9.515	55.37	2.080

Table A3.8.3 The Faecal Excretion (% of total  $^{125}\text{I}$  activity administered) after administration of 5mg of  $^{125}\text{I}$ -BSA to rats by each of the three routes.

Values are means (n=3)  $\pm$  S.E.M.

Time (hr)	IV % dose excreted	S.E.M.	IP % dose excreted	S.E.M.	SC % dose excreted	S.E.M.
24	0.612	0.298	1.75	0.23	1.24	0.34
48	3.62	0.559	4.39	0.71	3.51	0.077
72	5.54	0.52	6.48	1.15	5.53	0.26
96	6.70	0.51	7.89	1.33	6.65	0.51

Table A3.8.4: The Organ Distribution after administration of 5mg of <sup>125</sup>I-BSA to rats.

Results are expressed in 2 forms; as % of <sup>125</sup>I activity found in 1g or in whole organ and as a ratio of activity in 1g (or whole) of organ divided by the activity in 1ml of whole blood.

Organ	% of dose in 1g	<u>CPM in 1g</u> CPM/ml WB	% of dose in total	<u>CPM in total</u> CPM in 1ml WB
<b>1. Distribution 25 hours post IV administration.</b>				
Thyroid	ND	ND	2.13	1.059
			4.12	3.12
Whole blood	ND	ND	2.0%/ml	1
			1.23%/ml	1
Plasma	ND	ND	2.14%/ml	1.07
			2.02%/ml	1.64
Liver	0.375	0.187	4.16	2.07
	0.383	0.312	3.85	3.13
Spleen	0.258	0.128	0.27	0.13
	0.253	0.205	0.26	0.21
Heart	0.595	0.296	0.59	0.29
	0.520	0.426	0.49	0.40
Lung	1.673	0.832	2.23	1.12
	0.508	0.413	0.72	0.59
Kidney	0.355	0.176	0.85	0.42
	0.375	0.305	0.71	0.57
Stomach	1.600	0.796	8.92	4.44
	0.657	0.535	2.72	2.21
Sm. Intestine	0.202	0.100	2.20	1.09
	0.745	0.606	4.65	3.78

Table A3.8.4 Continued. (Organ Distribution of <sup>125</sup>I-BSA).

Organ	% dose in 1g	CPM in 1g CPM/ml WB	% dose in total	CPM in total CPM/ml WB
<b>2. Distribution 97 hours post IV injection.</b>				
Thyroid	ND	ND	8.91	50.91
			5.29	30.22
Whole Blood	ND	ND	0.175	1
			0.175	1
Plasma	ND	ND	0.219	1.251
			0.244	1.394
Liver	0.058	0.330	0.799	4.555
	0.070	0.398	0.749	4.284
Spleen	0.036	0.206	0.038	0.220
	0.037	0.212	0.040	0.230
Heart	0.052	0.296	0.046	0.261
	0.054	0.374	0.074	0.424
Lung	0.078	0.445	0.112	0.641
	0.095	0.541	0.165	0.943
Kidney	0.062	0.354	0.150	0.856
	0.055	0.313	0.119	0.683
Stomach	0.109	0.623	0.801	4.568
	0.087	0.498	0.521	2.982
Sm. Intestine	0.079	0.452	0.761	4.338
	0.094	0.536	0.896	5.124
<b>3. Distribution 25 hours post SC dosage.</b>				
Thyroid	ND	ND	6.88	5.64
			6.68	6.96
Whole blood	ND	ND	1.22%/ml	1
			0.96%/ml	1
Plasma	ND	ND	1.13%/ml	0.923
			1.17%/ml	1.219
Liver	0.210	0.172	2.340	1.922
	0.282	0.294	3.491	3.639
Spleen	0.167	0.137	0.170	0.138
	0.147	0.153	0.152	0.159
Heart	0.247	0.203	0.291	0.239
	0.278	0.290	0.293	0.305
Lung	0.649	0.533	1.121	0.921
	0.597	0.622	1.090	1.136
Kidney	0.237	0.194	0.552	0.448
	0.281	0.293	0.616	0.643
Stomach	1.528	1.254	3.291	2.697
	0.837	0.872	2.404	2.505
Sm. Intestine	0.245	0.201	1.900	1.562
	0.482	0.503	5.607	5.845



Table A3.8.4 Continued (Organ Distribution of BSA).

Organ	% dose in 1g	<u>CPM in 1g</u> CPM/ml WB	% dose in total	<u>CPM in total</u> CPM/ml WB
<b>4. Distribution 97 hours post SC injection.</b>				
Thyroid	ND	ND	7.61	81.83
			6.05	79.61
Whole Blood	ND	ND	0.093%/ml	1
			0.076%/ml	1
Plasma	ND	ND	0.185%/ml	1.989
			0.156%/ml	2.053
Liver	0.0426	0.458	0.569	6.124
	0.0310	0.409	0.299	3.942
Spleen	0.0194	0.209	0.0185	0.199
	0.0168	0.222	0.0223	0.294
Heart	0.0370	0.398	0.0409	0.441
	0.0277	0.365	0.0234	0.309
Lung	0.0573	0.617	0.109	1.170
	0.0596	0.785	0.102	1.348
Kidney	0.0437	0.470	0.123	1.321
	0.0378	0.498	0.0755	0.994
Stomach	0.0519	0.558	0.397	4.266
	0.103	1.350	0.618	8.140
Sm. Intestine	0.0591	0.636	0.580	6.237
	0.0435	0.572	0.456	6.000
<b>5. Distribution 97 hours post IP dosage.</b>				
Thyroid	ND	ND	8.586	93.73
			5.060	76.67
Whole Blood	ND	ND	0.0916%/ml	1
			0.0660%/ml	1
Plasma	ND	ND	0.219%/ml	2.380
			0.156%/ml	2.360
Liver	0.0353	0.385	0.530	5.787
	0.0417	0.632	0.416	6.307
Spleen	0.0199	0.218	0.0235	0.257
	0.0314	0.477	0.0344	0.522
Heart	0.0371	0.405	0.0410	0.448
	0.0417	0.631	0.0429	0.648
Lung	0.0557	0.608	0.0729	0.796
	0.0774	1.173	0.0904	1.369
Kidney	0.0391	0.427	0.0967	1.056
	0.0493	0.747	0.103	1.557
Stomach	0.0692	0.756	0.584	6.382
	0.150	2.272	0.395	5.981
Sm. Intestine	0.0596	0.651	0.643	7.022
	0.0970	1.470	0.860	13.025

**Table A3.9.1: The Whole Blood Concentration (% <sup>125</sup>I activity remaining/ml) after administration of 0.4mg of <sup>125</sup>I-HSA to rats by each of the three routes.**

Each value represents the result obtained for one rat unless stated otherwise. n=8 for each route.

Time (hr)	IV % dose/ml	IP % dose/ml	SC % dose/ml
3	3.95	1.527	0.161
3	3.231	1.845	0.145
6	3.332	1.641	0.240
6	3.224	1.641	0.253
23.5	0.887	0.984	0.588
23.5	0.903	1.090	0.518
30.5	0.742	0.890	0.691
30.5	0.679	0.944	0.536
47.5	0.510	0.302	0.429
47.5	0.417	0.302	0.350
53.5	0.275	0.343	0.259
53.5	0.358	0.467	0.245
71.75	0.139	0.190	0.246
71.75	0.188	0.196	0.221
77.0	0.191	0.100	0.124
77.0	0.158	0.099	0.161
143.75	0.0264	0.0648	0.114
143.75	0.0468	0.0292	0.0333
149.0 <sup>a</sup>	0.0313±0.0048	0.0257±0.0051	0.0354±0.0044

**Note:**

**a) Value is the mean (n=4) ± S.E.M.**

Table A3.10.1: The whole blood (WB) and serum (S) concentration (% <sup>125</sup>I activity remaining/ml) after administration of 5mg of <sup>125</sup>I-RSA to rats by each of the three routes. Each value represents the concentration determined for one rat (the same rat was used to determine both plasma and whole blood conc. at each time point). n=8 for each route.

	IV		IP		SC	
Time (hr)	WB %/ml	S %/ml	WB %/ml	S %/ml	WB%/ml	S %/ml
0.25	5.285	11.419	0.024	0.0695	0.0430	0.0633
0.25	4.710	9.496	0.045	0.0583	0.106	0.147
1	3.924	7.694	0.306	0.554	0.0989	0.176
1	2.801	7.202	-	0.885	0.102	0.170
2	3.862	6.924	0.112	2.196	0.162	0.272
2	-	7.002	0.166	2.346	0.339	0.600
4	2.661	4.826	1.808	3.940	0.373	0.710
4	2.436	4.698	-	-	0.594	0.759
7.25	2.209	3.916	1.574	3.039	0.571	1.272
7.25	-	4.028	1.579	3.175	-	2.557
18.75	-	2.230	0.904	2.176	0.992	1.396
18.75	-	2.225	0.837	2.203	-	1.664
24	1.056	1.863	1.278	1.932	-	1.449
24	0.987	1.919	-	-	-	1.468
30	0.940	1.665	0.629	1.431	0.679	1.417
30	0.842	1.603	0.470	1.464	1.025	2.191
42.75	0.487	1.145	0.514	1.066	0.688	1.068
42.75	0.666	1.133	0.664	1.151	0.600	1.052
48	0.540	1.039	0.770	0.926	0.606	1.038
48	-	1.188	-	1.319	0.638	1.131
54.5	0.465	0.929	0.275	0.845	0.411	0.881
54.5	0.506	0.972	-	0.895	-	1.306
70.75	-	0.848	-	0.635	-	0.644
70.75	-	0.784	-	0.668	-	0.661
79	0.355	0.586	-	0.549	0.362	0.633
79	0.347	0.677	-	0.485	0.370	0.884
91	-	0.629	-	0.404	-	0.459
91	-	0.625	-	0.495	-	0.446
96	0.315	0.512	0.363	0.589	0.210	0.470
96	0.223	0.454	0.186	0.397	0.299	0.515

Table A3.10.2: The Urine Excretion of  $^{125}\text{I}$  activity (% of total activity injected) after administration of 5mg of  $^{125}\text{I}$ -RSA to rats by each of the three routes.

Values are means (n=4 for IV, n=3 for IP and SC).

Time (hr)	IV % excreted	S.E.M.	IP % excreted	S.E.M.	SC % excreted	S.E.M.
24	10.48	1.128	11.9	0.231	8.54	1.184
48	23.43	2.107	22.66	1.925	22.85	1.555
72	31.55	2.850	27.90	4.213	29.98	1.945
96	37.04	2.611	31.17	6.285	33.85	2.725

Table 3.10.3. The Organ Distribution of  $^{125}\text{I}$  activity after administration of 5mg of  $^{125}\text{I}$ -RSA to rats by each of the three routes. Results are expressed in 2 ways; as a % of the total dose administered in 1g or total organ or as a ratio of the activity in 1g (or whole tissue) divided by the activity in 1ml of whole blood.

Organ	% dose in 1g	<u>CPM in 1g</u> CPM/ml WB	%dose in total	<u>CPM in total</u> CPM/ml WB
<b>1. Distribution 96 hours after IV administration.</b>				
Thyroid	118	374	7.77	24.63
	100	450	6.62	29.73
Whole Blood	ND	ND	0.315%/ml	1
			0.223%/ml	1
Serum	ND	ND	0.512%/ml	1.625
	ND	ND	0.454%/ml	2.036
Liver	0.194	0.616	2.328	7.390
	0.158	0.710	1.758	7.885
Spleen	0.0270	0.0859	0.0395	0.125
	0.0275	0.121	0.0482	0.216
Heart	0.141	0.447	0.148	0.470
	0.101	0.453	0.101	0.452
Lung	0.220	0.699	0.310	0.986
	0.177	0.794	0.239	1.071
Kidney	0.131	0.415	0.294	0.935
	0.095	0.426	0.219	0.984
<b>2. Distribution 168 hours post IV injection.</b>				
Thyroid	ND	ND	5.511	44.09
			5.791	44.21
Whole Blood	ND	ND	0.111%/ml	1
			0.087%/ml	1
Serum	ND	ND	0.201%/ml	1.811
			0.157%/ml	1.804
Liver	0.0432	0.389	0.532	4.793
	0.0459	0.527	0.608	6.990
Spleen	0.0200	0.180	0.0171	0.154
	0.0347	0.399	0.0343	0.394
Heart	0.0407	0.366	0.0611	0.550
	0.0562	0.646	0.145	1.667
Lung	0.0575	0.518	0.0732	0.659
	0.0807	0.928	0.113	1.299
Kidney	0.0292	0.263	0.0672	0.605
	0.0400	0.459	0.088	1.011

Table A3.10.3 Cont. (Organ Distribution of <sup>125</sup>I-RSA).

Organ	%dose in 1g	CPM in 1g CPM in 1ml WB	%dose in total	CPM in total CPM in 1ml WB
<b>3. Distribution 168 hours post SC injection.</b>				
Thyroid	ND	ND	5.1	55.73
			7.4	94.03
Whole Blood	ND	ND	0.0915%/ml	1
			0.0787%/ml	1
Serum	ND	ND	0.167%/ml	1.825
			0.144%/ml	1.830
Liver	0.0538	0.588	0.759	8.297
	0.0345	0.439	0.456	5.793
Spleen	0.0243	0.265	0.0344	0.376
	0.0187	0.238	0.0262	0.333
Heart	0.0619	0.676	0.0804	0.879
	0.0331	0.421	0.0431	0.547
Lung	0.0375	0.410	0.0533	0.583
	0.0489	0.622	0.111	1.410
Kidney	0.0393	0.429	0.0983	1.074
	0.0413	0.525	0.0991	1.259
<b>4. Distribution 168 hours after IP dosage.</b>				
Thyroid	ND	ND	3.9	41.44
			5.2	78.79
Whole Blood	ND	ND	0.0941%/ml	1
			0.066%/ml	1
Serum	ND	ND	0.174%/ml	1.849
			0.122%/ml	1.848
Liver	0.0342	0.364	0.355	3.772
	0.0674	1.021	0.854	12.94
Spleen	0.0248	0.264	0.0292	0.310
	0.0201	0.304	0.0243	0.368
Heart	0.0492	0.523	0.0704	0.748
	0.0940	1.424	0.141	2.136
Lung	0.0203	0.216	0.0473	0.503
	0.158	2.399	0.221	3.351
Kidney	0.0351	0.373	0.0913	0.970
	0.0161	0.244	0.0455	0.689

Table A3.11.1 Whole Blood and Serum Concentrations (%  $^{125}\text{I}$  activity remaining/ml) after administration of 20mg of  $^{125}\text{I}$ -RSA to rats by the IV route.

Each value represents data obtained from one rat. Eight rats were injected.

Time (hr)	Whole Blood %dose/ml	Serum %dose/ml
0.25	7.071	13.29
0.25	6.319	13.44
2.0	5.628	10.73
2.0	5.185	10.06
4.0	5.369	9.973
4.0	4.519	8.417
6.75	3.946	7.181
6.75	3.778	7.463
23.5	1.959	3.683
23.5	1.787	3.429
30.75	1.998	3.422
30.75	1.710	3.082
49.75	1.308	2.041
49.75	1.293	2.393
73.0	1.000	1.527
73.0	0.896	1.711
96.0	0.429	0.982
96.0	0.591	1.147
168.0	0.265	0.478
168.0	0.221	0.412

Table A3.11.2 The % of  $^{125}\text{I}$  activity excreted in the urine following administration of 20 mg of  $^{125}\text{I}$ -RSA to rats by the IV route.

Each value represents the mean % excreted (n=3)  $\pm$  S.E.M.

Time (hours)	Mean % excreted	S.E.M.
24	12.4	1.65
48	20.8	4.44
72	30.5	4.76
96	37.6	5.07

Table A3.12.1 The Measurements for total serum protein concentration, after administration of 0.9% saline (group 2), 20mg BSA in saline (group 3) or for untreated rats (group 1). Each rat had a blood sample taken at the same time and the protein concentration was determined using the Lowry method.

Time (hours)	Concentration of Protein in serum (mg/ml)			
	Control (1)	Saline (2)	20mg BSA (3)	
2	83.19	90.71	87.08	
	81.73	97.34	90.97	
	87.57	82.30	73.53	
	88.54	105.75	83.67	
	80.75	81.42	75.37	
	Mean	84.35	91.50	82.12
	SD	3.500	10.298	6.704
4	85.69	83.40	93.59	
	78.55	96.51	86.91	
	70.46	69.76	78.16	
	62.84	87.07	75.08	
	87.12	93.89	94.10	
	Mean	76.93	86.13	85.57
	SD	10.291	10.539	8.716
7	86.93	96.90	75.69	
	92.05	78.13	84.96	
	87.93	84.18	94.75	
	86.39	77.45	70.03	
	86.38	77.24	75.70	
	Mean	85.03	82.78	80.48
	SD	6.072	8.302	9.594



Table A3.13.1 The Concentration of Evans Blue in serum (% dose remaining/ml) following administration of 1mg of Evans Blue alone or 1mg of dye with 20mg BSA.

Each value represents data from one rat. (n=8 for each route)

Time (hours)	% of EB remaining/ml	
	EB only	EB + BSA
0.33	7.14	7.27
0.33	6.79	6.22
1	5.34	4.98
1	6.57	5.41
2	5.58	4.32
2	4.76	4.15
3	-	4.73
3	-	3.86
4	4.41	3.70
4	3.54	3.25
6	3.05	2.72
6	3.48	2.48
7.5	3.23	3.32
7.5	2.70	2.37
24	1.22	1.02
24	1.09	0.996
28.5	0.918	0.841
28.5	0.905	0.660

Table A3.14.1 Plasma concentration ( % <sup>125</sup>I activity remaining/ml) following administration of 5mg of <sup>125</sup>I-BSA-MTX (3.4%w/w) to male wistar rats by each of the three routes. Each value was measured from 1 rat. (n=8 for each route).

Time	IV %/ml	IP %/ml	SC %/ml
0.5	8.694	0.115	0.151
0.5	8.641	0.281	0.122
1	7.195	0.872	0.174
1	6.785	0.414	0.158
2	6.049	1.539	0.264
2	5.561	1.925	0.357
4	4.433	2.611	0.339
4	4.341	2.539	0.339
6	3.765	-	-
6	3.642	-	-
7	-	3.112	0.429
7	-	2.235	0.694
23.5	1.261	1.084	0.690
23.5	1.311	0.859	0.732
26	-	1.188	0.583
26	-	0.873	0.927
28	-	1.176	0.505
28	-	0.798	0.784
31	0.755	0.816	0.568
31	0.935	0.603	0.636
48	0.442	0.559	0.327
48	0.583	0.412	0.437
55	-	0.444	0.266
55	-	0.365	0.401
72	-	0.181	0.137
72	-	0.192	0.212
79	-	0.130	0.128
79	-	0.181	0.167
96	-	0.098	0.077
96	-	0.105	0.116

Table A3.14.2 The urine excretion (% of total  $^{125}\text{I}$  activity injected) following administration of 5mg of  $^{125}\text{I}$ -BSA-MTX (3.4%w/w) to rats by each of the three routes.

Values are expressed as means of three rats.

Time	IV % excreted	S.E.M	IP % excreted	S.E.M.	SC % excreted	S.E.M.
24	24.55	2.15	29.32	0.64	32.73	3.22
48	37.03	2.16	50.31	1.04	52.39	0.89
72	-	-	57.97	1.47	65.08	1.21
96	-	-	60.02	2.27	67.16	0.36

Table A3.15.1 The Serum Concentrations (% of  $^{125}\text{I}$  activity remaining/ml) after administration of 5mg of  $^{125}\text{I}$ -BSA-MTX (5.1%w/w) to male wistar rats by each of the three routes (n=8 for each route).

Time (hours)	IV %/ml	IP %/ml	SC %/ml
1	6.933	0.556	0.496
1	9.007	0.905	0.424
3	5.899	3.336	0.458
3	4.129	3.220	0.458
5	4.757	1.952	-
5	3.775	3.486	-
7	2.934	2.514	0.497
7	3.335	1.534	0.566
10	-	-	0.953
10	-	-	0.789
23.5	0.678	0.545	0.787
23.5	0.737	0.877	0.727
27.3	-	-	0.625
27.3	-	-	0.647
30.5	0.572	0.599	0.508
30.5	0.590	0.367	0.515
48	0.230	0.206	0.195
48	0.275	0.225	0.175
52.5	0.234	0.233	0.204
52.5	0.236	0.219	0.230
55	0.179	0.210	0.221
55	0.174	0.182	0.221
71.75	0.0989	0.0976	0.0888
71.75	0.126	0.0976	0.0880
97.5	0.0604	0.0464	0.0670
97.5	0.0824	0.0487	0.0617

Table A3.15.2 The Urine Excretion (%<sup>125</sup>I injected) following administration of 5mg of <sup>125</sup>I-BSA-MTX (5.1%w/w).

Values are mean % excreted for 3 rats.

Time	IV % (hours)	S.E.M. excreted	IP %	S.E.M. excreted	SC %	S.E.M. excreted
24	37.13	0.58	38.16	1.17	32.52	2.61
48	57.96	0.59	59.71	3.47	54.0	1.78
72	66.66	0.84	69.90	4.22	63.56	2.19
96	69.84	0.90	73.40	3.90	67.50	2.75

Table A3.15.3 The excretion in the faeces (% <sup>125</sup>I activity injected) following administration of 5mg of <sup>125</sup>I-BSA-MTX (5.1%w/w).

Values are mean % excreted in the faeces for 3 rats.

Time (hours)	IV % excreted	S.E.M.	IP % excreted	S.E.M.	SC % excreted	S.E.M.
24	4.03	1.10	1.37	0.688	2.53	0.75
48	6.57	1.06	4.60	1.44	7.10	0.65
72	8.07	1.02	6.17	1.21	8.63	0.49
96	8.87	1.04	7.23	1.26	9.97	0.27

Table A3.15.4 Organ Distribution of  $^{125}\text{I}$  activity following administration of  $^{125}\text{I}$ -BSA-MTX (5.1%w/w) by the three routes. Results are expressed in 2 forms; as a % of the total radioactivity injected found in 1g of organ or the whole organ and as a ratio of the activity found in 1g (or whole organ) divided by the activity found in 1ml of whole blood.

Organ	% dose in 1g	CPM in 1g CPM in 1ml WB	% dose in total	CPM in total CPM in 1ml WB
<b>1. Distribution 52 hours post IV injection.</b>				
Thyroid	ND	ND	10.00	66.67
			9.47	62.75
Whole Blood	ND	ND	0.15%/ml	1
			0.15%/ml	1
Serum	ND	ND	0.234%/ml	1.563
			0.236%/ml	1.563
Liver	0.0765	0.510	0.759	5.063
	0.0764	0.506	0.880	5.828
Spleen	0.0409	0.273	0.0474	0.316
	0.0786	0.520	0.0464	0.307
Heart	0.0637	0.425	0.0629	0.419
	0.0691	0.461	0.0614	0.407
Lung	0.0780	0.520	0.105	0.699
	0.0891	0.590	0.100	0.665
Kidney	0.151	1.004	0.335	2.236
	0.178	1.183	0.335	2.221
Stomach	0.166	1.109	0.706	4.705
	0.292	1.936	1.525	10.10
Sm. Intestine	0.104	0.693	1.074	7.164
	0.151	1.000	1.117	7.397

Table A3.15.4 Cont. (Organ Distribution of BSA-MTX 5.1%w/w).

Organ	% dose in 1g	<u>CPM in 1g</u> CPM in 1ml WB	% dose in total	<u>CPM in total</u> CPM in 1ml WB
<b>2. Distribution 97.5 hours post IV injection.</b>				
Thyroid	ND	ND	7.201 10.59	186.3 200.9
Whole Blood	ND	ND	0.0386%/ml 0.0527%/ml	1 1
Serum	ND	ND	0.0604%/ml 0.0824%/ml	1.563 1.563
Liver	0.0280 0.0299	0.724 0.567	0.356 0.317	9.210 6.020
Spleen	0.0182 0.0279	0.470 0.529	0.0207 0.0186	0.535 0.354
Heart	0.0157 0.0313	0.406 0.809	0.0179 0.0174	0.340 0.329
Lung	0.0298 0.0226	0.772 0.429	0.0389 0.0409	1.007 0.776
Kidney	0.101 0.133	2.618 2.522	0.233 0.244	6.034 4.635
Stomach	0.0602 0.0620	1.558 1.176	0.351 0.605	9.079 11.478
Sm. Intestine	0.0443 0.0565	1.146 1.071	0.488 0.516	12.639 9.788
<b>3. Distribution 193 hours post IV injection.</b>				
Thyroid	ND	ND	4.186 4.865	528.5 587.8
Whole Blood	ND	ND	0.00792%/ml 0.00828%/ml	1 1
Serum	ND	ND	0.0123%/ml 0.0129%/ml	1.563 1.563
Liver	0.0109 0.0106	1.383 1.343	0.125 0.155	15.81 18.69
Spleen	0.0079 0.0070	1.008 0.845	0.0075 0.0075	0.954 0.912
Heart	0.0063 0.0081	0.793 0.981	0.0060 0.0091	0.756 1.098
Lung	0.0068 0.0083	0.856 1.005	0.0103 0.0114	1.303 1.377
Kidney	0.0767 0.0717	9.680 8.665	0.176 0.169	22.20 20.47

Table A3.15.4 Cont. (Organ Distribution of BSA-MTX 5.1%w/w).

Organ	% dose in 1g	CPM in 1g CPM in 1ml WB	% dose in total	CPM in total CPM in 1ml WB
<b>2. Distribution 52.5 hour post IP injection.</b>				
Thyroid	ND	ND	7.20	48.29
			9.00	64.21
Whole Blood	ND	ND	0.149%/ml	1
			0.140%/ml	1
Serum	ND	ND	0.233%/ml	1.562
			0.219%/ml	1.563
Liver	0.0645	0.433	0.702	4.711
	0.0516	0.346	0.785	5.603
Spleen	0.0588	0.394	0.0501	0.336
	0.0276	0.197	0.0460	0.328
Heart	0.0880	0.590	0.0539	0.362
	0.0472	0.336	0.0559	0.399
Lung	0.111	0.744	0.0911	0.611
	0.0604	0.431	0.101	0.724
Kidney	0.109	0.729	0.225	1.507
	0.0896	0.639	0.214	1.525
Stomach	0.187	1.252	0.871	5.838
	0.209	0.822	0.822	5.865
Sm. Intestine	0.197	1.323	1.853	12.43
	0.154	1.098	1.678	11.97
<b>5. Distribution 97.5 hours post IP injection.</b>				
Thyroid	ND	ND	6.429	205.4
			5.807	176.5
Whole Blood	ND	ND	0.0313%/ml	1
			0.0329%/ml	1
Serum	ND	ND	0.0464%/ml	1.481
			0.0487%/ml	1.480
Liver	0.0214	0.684	0.233	7.452
	0.0235	0.716	0.249	7.578
Spleen	0.0111	0.355	0.0094	0.301
	0.0169	0.516	0.0173	0.527
Heart	0.0119	0.379	0.0099	0.317
	0.0113	0.346	0.0085	0.259
Lung	0.0154	0.493	0.0191	0.612
	0.0160	0.488	0.0274	0.835
Kidney	0.0556	1.779	0.116	3.704
	0.0618	1.882	0.128	3.903
Stomach	0.0715	2.285	0.201	6.426
	0.100	3.056	0.519	15.82
Sm. Intestine	0.0281	0.898	0.271	8.646
	0.0472	1.437	0.491	14.95



Table A3.15.4 Cont. (Organ Distribution of BSA-MTX 5.1%w/w).

Organ	% dose in 1g	CPM in 1g CPM in 1ml WB	% dose in total	CPM in total CPM in 1ml WB
<b>6. Distribution 194 hours post IP injection.</b>				
Thyroid	ND	ND	4.39	654.2
			6.00	688.1
Whole Blood	ND	ND	0.00671%/ml	1
			0.00872%/ml	1
Serum	ND	ND	0.0105%/ml	1.562
			0.0136%/ml	1.562
Liver	0.0064	0.962	0.107	16.01
	0.0077	0.902	0.109	12.60
Spleen	0.0053	0.788	0.0068	1.006
	0.0090	1.033	0.0072	0.827
Heart	0.0044	0.660	0.0066	0.978
	0.0052	0.597	0.0054	0.622
Lung	0.0068	1.018	0.0090	1.347
	0.0083	0.954	0.0083	0.951
Kidney	0.0528	7.871	0.144	21.50
	0.0622	7.133	0.166	19.01
<b>7. Distribution 52.5 hours post SC injection.</b>				
Thyroid	ND	ND	6.429	54.1
			7.827	58.5
Whole Blood	ND	ND	0.119%/ml	1
			0.134%/ml	1
Serum	ND	ND	0.204%/ml	1.718
			0.230%/ml	1.715
Liver	0.0515	0.433	0.639	5.377
	0.0701	0.524	0.666	4.985
Spleen	0.0314	0.264	0.0393	0.331
	0.0498	0.372	0.0473	0.354
Heart	0.0393	0.331	0.0411	0.346
	0.0456	0.341	0.0447	0.334
Lung	0.0639	0.538	0.0774	0.652
	0.0958	0.717	0.119	0.894
Kidney	0.112	0.939	0.258	2.171
	0.186	1.393	0.356	2.666
Stomach	0.248	2.086	1.101	9.263
	0.211	1.576	0.733	5.482
Sm. Intestine	0.109	0.915	1.050	8.837
	0.169	1.268	1.125	9.410

Table A3.15.4 Cont. (Organ Distribution of BSA-MTX 5.1%w/w).

**8. Distribution 97.5 hours post SC injection.**

Organ	% dose in 1g	<u>CPM in 1g</u> CPM in 1ml WB	% dose in total	<u>CPM in total</u> CPM in 1ml WB
Thyroid	ND	ND	8.183 8.182	191.1 207.9
Whole Blood	ND	ND	0.0428%/ml 0.0393%/ml	1 1
Serum	ND	ND	0.0670%/ml 0.0617%/ml	1.566 1.569
Liver	0.0230 0.0267	0.537 0.678	0.278 0.357	6.489 9.089
Spleen	0.0135 0.0204	0.315 0.519	0.0189 0.0152	0.441 0.387
Heart	0.0157 0.0202	0.366 0.513	0.0160 0.0204	0.406 0.519
Lung	0.0180 0.0263	0.421 0.669	0.0296 0.0275	0.692 0.699
Kidney	0.0792 0.0808	1.849 2.053	0.168 0.179	3.935 4.560
Stomach	0.0672 0.117	1.570 2.983	0.354 0.995	8.282 25.30
Sm. Intestine	0.0576 0.0669	1.345 1.700	0.579 0.748	13.53 19.01
<b>9. Distribution 193.5 hours post SC injection.</b>				
Thyroid	ND	ND	4.50 4.39	725 645
Whole Blood	ND	ND	0.0062%/ml 0.0068%/ml	1 1
Serum	ND	ND	0.0097%/ml 0.0106%/ml	1.572 1.569
Liver	0.0054 0.0072	0.874 1.065	0.0715 0.0767	11.49 11.28
Spleen	0.0032 0.0046	0.517 0.677	0.0033 0.0060	0.526 0.877
Heart	0.0043 0.0045	0.690 0.661	0.0041 0.0041	0.658 0.608
Lung	0.0061 0.011	0.976 1.618	0.0088 0.0090	1.413 1.331
Kidney	0.0470 0.0589	7.556 8.668	0.118 0.144	18.93 21.24

Table A3.16.1 The Plasma Concentration (% of  $^{125}\text{I}$  activity remaining/ml) following administration of 5mg of  $^{125}\text{I}$ -BSA-MTX (6.2%w/w) to rats by each of the three routes (n= 8 for each route) .Note a) Value is expressed as mean (n=3)  $\pm$  S.E.M.

Time (hours)	IV %/ml	IP %/ml	SC %/ml
0.5	5.725	0.205	0.0700
0.5	5.787	2.111	0.192
2.0	3.553	1.736	0.354
2.0	3.995	1.199	0.247
4.0	2.978	1.907	0.296
4.0	2.712	1.989	0.260
6.5	1.623	-	-
6.5	1.847	-	-
8	-	0.968	0.399
8	-	1.093	0.575
11	-	1.023	0.506
11	-	1.141	0.427
22.5	0.413	0.433	0.335
22.5	0.375	0.438	0.411
24.5	0.294	0.458	0.352
24.5	0.377	0.315	0.291
28	0.245	0.359	0.294
28	0.245	0.296	0.328
32	0.212	0.173	0.292
32	0.210	0.240	0.239
47	0.0952	0.0762	0.106
47	0.0894	0.0951	0.122
54	0.0791 $\pm$ 0.0014 <sup>a</sup>	0.0868	0.0937
54	-	0.0737	0.0933
71	0.0473	0.0632	0.0490
71	0.0524	0.0519	0.0529
96	0.0188	0.0261	0.0354
96	0.0174	0.0272	0.0311

Table A3.16.2 The Excretion of  $^{125}\text{I}$  activity (% of total injected) in the Urine following administration of 5mg of  $^{125}\text{I}$ -BSA-MTX (6.2%w/w) to rats by each of the three routes.

Values are means (n=3).

Time (hr)	IV % excreted	S.E.M.	IP % excreted	S.E.M.	SC % excreted	S.E.M.
24	23.66	4.05	29.76	1.24	22.56	1.50
48	37.97	3.07	42.41	3.31	32.80	5.08
72	41.90	2.65	45.76	3.74	38.23	6.14
96	43.87	2.48	48.22	3.88	40.6	6.67

Table A3.16.3: The Excretion of  $^{125}\text{I}$  activity (% of dose administered) in the faeces following administration of 5mg of  $^{125}\text{I}$ -BSA-MTX (6.2%w/w) to rats by each of the three routes.

Values are means (n=3).

Time (hr)	IV % excreted	S.E.M.	IP % excreted	S.E.M.	SC % excreted	S.E.M.
24	2.3	0.32	3.3	0.41	1.9	0.50
48	5.1	0.34	4.8	0.40	4.3	0.35
72	6.3	0.49	7.1	0.94	5.2	0.39
96	7.3	0.66	7.9	1.06	5.9	0.49

Table A3.16.4: The Organ Distribution of  $^{125}\text{I}$  activity following administration of 5mg of  $^{125}\text{I}$ -BSA-MTX (6.2%w/w) to male wistar rats by each of the three routes.

Results are expressed in 2 forms; as a % of the total radioactivity injected that was found in 1g or the whole organ and as a ratio of the activity found in 1g of organ (or the whole organ) divided by the activity found in 1ml of whole blood.

Organ	% dose in 1g	<u>CPM in 1g</u> CPM in 1ml WB	% dose in total	<u>CPM in total</u> CPM in 1ml WB
<b>1.Distribution 24 hours post IV injection.</b>				
Thyroid	ND	ND	7.13	34.14
			4.36	17.18
Whole Blood	ND	ND	0.208%/ml	1
			0.241%/ml	1
Serum	ND	ND	0.294%/ml	1.408
			0.377%/ml	1.563
Liver	0.332	1.592	3.887	18.61
	0.273	1.131	3.577	14.81
Spleen	0.152	0.729	0.181	0.867
	0.139	0.575	0.178	0.738
Heart	0.106	0.509	0.125	0.602
	0.101	0.417	0.137	0.568
Lung	0.174	0.831	0.306	1.465
	0.183	0.761	0.265	1.096
Kidney	1.314	6.289	3.787	18.13
	0.995	4.121	3.138	12.99
Stomach	0.677	3.243	1.417	6.786
	0.069	0.288	0.441	1.826
Sm. Intestine	0.089	0.425	0.885	4.239
	0.088	0.365	1.247	5.163

Table A3.16.4 Cont. (Organ Distribution of BSA-MTX 6.2%w/w)

Organ	% dose in 1g	<u>CPM in 1g</u> CPM in 1ml WB	% dose in total	<u>CPM in total</u> CPM in 1ml WB
<b>2. Distribution 96 hours post IV injection.</b>				
Thyroid	ND	ND	4.247 6.522	355.8 575.1
Whole Blood	ND	ND	0.0119%/ml 0.0113%/ml	1 1
Serum	ND	ND	0.0188%/ml 0.0174%/ml	1.577 1.537
Liver	0.189 0.226	15.84 19.96	2.226 2.851	186.5 251.4
Spleen	0.103 0.0678	8.614 5.977	0.125 0.0963	10.48 8.496
Heart	0.0288 0.0365	2.412 3.222	0.0418 0.0695	3.507 6.128
Lung	0.0550 0.0626	4.606 5.521	0.0610 0.0649	5.109 5.720
Kidney	1.234 1.409	103.4 124.2	5.271 3.592	441.7 316.7
Stomach	0.0269 0.0985	2.254 8.684	0.119 0.249	10.47 21.96
Sm. Intestine	0.0538 0.0419	4.505 3.690	0.693 0.479	58.09 42.23
<b>3. Distribution 171 hours post IV injection.</b>				
Thyroid	ND	ND	2.745 2.882	199.5 219.8
Whole Blood	ND	ND	0.0137%/ml 0.0131%/ml	1 1
Serum	ND	ND	0.0226%/ml 0.0199%/ml	1.647 1.521
Liver	0.152 0.0931	11.05 7.094	1.763 1.327	128.3 101.2
Spleen	0.071 0.094	5.168 7.170	0.112 0.108	8.154 8.210
Heart	0.0177 0.0256	1.285 1.948	0.0431 0.0271	3.135 2.067
Lung	0.0379 0.0306	2.760 2.338	0.0529 0.0532	3.851 4.054
Kidney	1.177 1.002	85.66 76.39	2.855 2.799	207.8 213.3
Stomach	0.020 0.0196	1.473 1.494	0.130 0.144	9.497 10.98
Sm. Intestine	0.0244 0.0294	1.777 2.244	0.382 0.494	27.78 37.66

Table A3.16.4 Cont. (organ distribution of BSA-MTX 6.2%w/w)

Organ	% in 1g	CPM in 1g CPM in 1ml WB	% in total	CPM in total CPM/ml WB
<b>4. Distribution 48 hours post IP injection.</b>				
Thyroid	ND	ND	5.982	125.7
			6.311	109.6
Whole Blood	ND	ND	0.0476%/ml	1
			0.0576%/ml	1
Serum	ND	ND	0.0762%/ml	1.600
			0.0949%/ml	1.649
Liver	0.0994	2.088	1.196	25.13
	0.107	1.859	1.262	21.93
Spleen	0.0607	1.276	0.0789	1.658
	0.0551	0.957	0.0628	1.091
Heart	0.0251	0.527	0.0240	0.504
	0.0334	0.580	0.0367	0.638
Lung	0.0453	0.953	0.0697	1.464
	0.0444	0.771	0.0613	1.064
Kidney	0.856	17.98	1.868	39.24
	0.958	16.64	1.935	33.62
Stomach	0.0755	1.587	0.252	5.295
	0.0516	0.896	0.223	3.881
Sm. Intestine	0.0458	0.962	0.534	11.22
	0.0632	1.098	0.619	10.76
<b>5. Distribution 96 hours post IP injection.</b>				
Thyroid	ND	ND	5.846	345.3
			4.844	295.5
Whole Blood	ND	ND	0.0169%/ml	1
			0.0164%/ml	1
Serum	ND	ND	0.0261%/ml	1.546
			0.0272%/ml	1.659
Liver	0.141	8.321	1.376	0.0123
	0.120	7.325	1.329	0.0123
Spleen	0.105	6.189	0.152	8.984
	0.126	7.698	0.119	7.287
Heart	0.023	1.353	0.023	1.413
	0.031	1.893	0.033	2.016
Lung	0.033	1.938	0.033	1.978
	0.029	1.787	0.033	2.043
Kidney	1.330	78.6	2.976	175.9
	0.839	51.3	1.907	116.5
Stomach	0.091	5.411	0.443	26.16
	0.094	5.725	0.299	18.29
Sm. Intestine	0.052	3.104	0.564	33.34
	0.055	3.359	0.658	40.20

Table A3.16.4 Cont. (Organ Distribution of BSA-MTX 6.2%w/w)

Organ	% in 1g	CPM in 1g CPM in 1ml WB	% in total	CPM in total CPM/ml WB
<b>6. Distribution 171 hours post IP injection.</b>				
Thyroid	ND	ND	3.721 3.395	364.8 340.2
Whole Blood	ND	ND	0.0102%/ml 0.00998%/ml	1 1
Serum	ND	ND	0.0154%/ml 0.0152%/ml	1.512 1.522
Liver	0.0661 0.0966	6.481 9.698	0.640 1.414	62.76 141.9
Spleen	0.0315 0.0747	3.086 7.495	0.0569 0.0943	5.577 9.464
Heart	0.0091 0.0296	0.888 2.97	0.0154 0.0334	1.509 3.355
Lung	0.0133 0.0220	1.307 2.205	0.0268 0.0266	2.628 2.671
Kidney	0.485 0.836	47.52 83.85	1.355 2.261	132.8 226.9
Stomach	0.0186 0.0244	1.828 2.445	0.167 0.223	16.4 22.4
Sm. Intestine	0.0160 0.0316	1.572 3.171	0.234 0.364	22.99 36.58
<b>7. Distribution 96 hours post SC injection.</b>				
Thyroid	ND	ND	4.01 6.15	173.6 304.3
Whole Blood	ND	ND	0.0231%/ml 0.0202%/ml	1 1
Serum	ND	ND	0.0353%/ml 0.0311%/ml	1.528 1.540
Liver	0.0433 0.0707	1.882 3.506	0.465 0.691	20.16 34.29
Spleen	0.0171 0.0234	0.743 1.162	0.0338 0.0422	1.464 2.093
Heart	0.0154 0.0168	0.668 0.831	0.0144 0.0174	0.625 0.865
Lung	0.0219 0.0244	0.949 1.209	0.0265 0.0349	1.151 1.730
Kidney	0.761 0.803	33.02 39.82	1.674 1.734	72.59 85.96
Stomach	0.0280 0.0524	1.214 2.270	0.0530 0.234	2.298 11.62
Sm. Intestine	0.0206 0.0372	0.895 1.842	0.221 0.411	9.596 20.40



Table A3.16.4 Cont. (organ distribution of 6.2%w/w conjugate).

Organ	% in 1g	<u>CPM in 1g</u> CPM in 1ml WB	% in total	<u>CPM in total</u> CPM in 1ml WB
<b>8. Distribution 171 hours post SC injection.</b>				
Thyroid	ND	ND	3.779	373
			4.293	421
Whole Blood	ND	ND	0.0101%/ml	1
			0.0102%/ml	1
Serum	ND	ND	0.0146%/ml	1.447
			0.0155%/ml	1.519
Liver	0.0306	3.021	0.355	35
	0.0328	3.221	0.536	52.7
Spleen	0.0209	2.065	0.0184	1.815
	0.0264	2.597	0.0229	2.254
Heart	0.0095	0.943	0.0117	1.150
	0.0208	2.042	0.0255	2.503
Lung	0.0137	1.351	0.0158	1.564
	0.0132	1.296	0.0172	1.688
Kidney	0.542	53.47	1.472	145.3
	0.688	67.58	1.822	179.0
Stomach	0.0091	0.897	0.0669	6.599
	0.0208	2.05	0.153	14.99
Sm. Intestine	0.0121	1.199	0.135	13.38
	0.0137	1.343	0.237	23.27

Table A3.17.1 The Serum Concentration (%  $^{125}\text{I}$  activity remaining/ml) following administration of 5mg of  $^{125}\text{I}$ -BSA-MTX (9.18%w/w) to rats by IV and SC routes. (n=8 for both routes).

Time (hr)	IV %/ml	SC %/ml
1	3.609	0.177
1	3.846	0.122
2	1.515	0.185
2	1.595	0.172
4	0.778	0.181
4	0.712	0.221
6	0.426	0.286
6	0.419	0.298
8	0.370	0.172
8	0.330	0.190
10	0.236	0.194
10	0.261	0.228
23.5	0.109	0.142
23.5	0.104	0.101
27.5	0.0795	0.0879
27.5	0.0873	0.102
32.5	0.0748	0.0928
32.5	0.0815	0.0682
48	0.0363	0.0402
48	0.0411	0.0502
51.5	0.0395	-
51.5	0.0315	-
56.5	0.0349	0.0291
56.5	0.0231	0.0199
71.5	0.0259	0.0191
71.5	0.0227	0.0189
79.5	0.0185	0.0224
79.5	0.0213	0.0158
97	0.0108	0.0187
97	0.0184	0.0133

**Table A3.17.2: The % of  $^{125}\text{I}$  activity excreted in the urine following administration of 5mg of  $^{125}\text{I}$ -BSA-MTX (9.18%w/w) to rats by IV and SC routes. (n=4 for IV and n=3 for SC route).**

Values are mean cumulative % excreted.

Time (hr)	IV		SC	
	% excreted	S.E.M.	% excreted	S.E.M.
24	36.41	4.46	27.5	8.92
48	42.04	4.24	34.9	5.46
72	46.04	4.02	37.47	5.48
96	46.58	4.05	39.76	6.08

**Table A3.17.3: The %  $^{125}\text{I}$  activity excreted in the faeces following administration of 5mg of  $^{125}\text{I}$ -BSA-MTX (9.18%w/w) to rats by IV and SC routes.**

Values are mean cumulative % excreted (n=4 IV, n=3 SC).

Time (hr)	IV		SC	
	% excreted	S.E.M.	% excreted	S.E.M.
24	3.51	0.33	3.82	0.82
48	5.10	0.29	5.78	0.94
72	6.22	0.53	6.41	1.26
96	6.78	0.57	7.43	1.15

Table A3.18.1 The Serum Concentration (% dose <sup>125</sup>I remaining/ml) following administration of 5mg of <sup>125</sup>I-BSA-MTX (11.74%w/w) to male wistar rats by each of the three routes. (n=8 for each route).

Each value was determined from one rat.

Time (hr)	IV %/ml	IP %/ml	SC %/ml
1	2.955	0.0819	0.0782
1	2.089	0.104	0.0645
3	0.584	0.154	0.120
3	0.498	0.190	0.0939
6	-	0.366	0.102
6	-	0.401	0.103
6.75	0.329	-	-
6.75	0.297	-	-
8	-	0.368	0.105
8	-	0.256	0.0964
19	0.116	0.0759	0.179
19	0.108	0.129	0.132
21	-	0.0934	0.127
21	-	0.182	0.136
24	0.0821	0.0829	0.151
24	0.0924	0.0915	0.160
30.5	0.121	0.0642	0.122
30.5	0.129	0.0828	0.0945
48	0.0506	0.0252	0.0541
48	0.0713	0.0504	0.0385
54.5	0.0494	0.0364	0.0487
54.5	0.0303	0.0408	0.0475
71.75	0.0319	0.0197	0.0298
71.75	0.0215	0.0274	0.0294
76	0.0331	0.0181	0.0302
76	0.0182	0.0233	0.0241
96	0.0402	0.00976	0.0201
96	0.0142	0.0238	0.0183

Table A3.18.2 The Urine Excretion of  $^{125}\text{I}$  activity (% of total dose administered) following administration of 5mg of  $^{125}\text{I}$ -BSA-MTX (11.74%w/w) to male wistar rats by each of the three routes.

Results are expressed as mean cumulative % excreted (n=3).

Time (hr)	IV % excreted	S.E.M.	IP % excreted	S.E.M.	SC % excreted	S.E.M.
24	21.33	6.49	20.45	4.44	21.62	5.99
48	34.78	4.77	33.97	7.78	39.12	0.51
72	42.33	4.28	37.91	8.52	44.51	0.80
96	45.07	4.24	39.83	8.98	46.53	1.43

Table A3.18.3 The Excretion of  $^{125}\text{I}$  activity in the faeces following the administration of 5mg of  $^{125}\text{I}$ -BSA-MTX (11.74%w/w) to rats by each of the three routes.

Results are expressed as mean % of dose excreted (n=3).

Time (hr)	IV % excreted	S.E.M	IP % excreted	S.E.M.	SC % excreted	S.E.M.
24	4.45	0.92	3.56	0.98	2.29	0.33
48	6.39	0.83	6.30	0.43	4.42	0.27
72	7.90	0.94	7.30	0.81	5.67	0.18
96	8.48	0.95	8.00	0.81	6.33	0.12

Table A3.18.4 The Organ Distribution following administration of  $^{125}\text{I}$ -BSA-MTX (11.74%w/w) to rats by each of the three routes. Two rats from each group were analysed for each time point. Results were expressed in 2 ways; as a % of the radioactive dose found in 1g or the whole tissue and as a ratio of activity found in 1g (or whole organ) divided by the activity found in 1ml Whole Blood.

Organ	% in 1g	<u>CPM in 1g</u> CPM in 1ml WB	% in total	<u>CPM in total</u> CPM in 1ml WB
<b>1. Distribution 30.5 hours post IV administration.</b>				
Thyroid	ND	ND	9.412	70.77
			8.423	59.32
Whole Blood	ND	ND	0.133%/ml	1
			0.142%/ml	1
Serum	ND	ND	0.121%/ml	0.906
			0.129%/ml	0.906
Liver	0.157	1.179	1.814	13.58
	0.171	1.201	1.925	13.52
Spleen	0.175	1.314	0.169	1.263
	0.144	1.013	0.127	0.889
Heart	0.0632	0.473	0.0583	0.436
	0.0304	0.213	0.0280	0.196
Lung	0.0689	0.516	0.118	0.884
	0.0463	0.325	0.0758	0.532
Kidney	0.104	0.781	0.247	1.850
	0.0799	0.562	0.155	1.087
Stomach	0.427	3.201	1.391	10.42
	0.429	3.011	1.960	13.76
Sm. Intestine	0.137	1.028	1.442	10.80
	0.0699	0.491	0.814	5.72

Table A3.18.4 Cont. (Organ Distribution of BSA-MTX 11.74%w/w)

Organ	% in 1g	CPM in 1g/ CPM in 1ml WB	% in total	CPM in total/ CPM/ml WB
<b>2. Distribution 76 hours post IV injection.</b>				
Thyroid	ND	ND	3.834	119.8
			5.722	154.2
Whole Blood	ND	ND	0.032%/ml	1
			0.037%/ml	1
Serum	ND	ND	0.033%/ml	1.034
			0.018%/ml	0.486
Liver	0.0671	2.082	0.813	25.26
	0.0590	1.591	0.608	16.39
Spleen	0.0392	1.217	0.0610	1.893
	0.0653	1.759	0.0568	1.532
Heart	0.0125	0.388	0.0120	0.372
	0.0095	0.257	0.0097	0.260
Lung	0.0120	0.375	0.0273	0.848
	0.0115	0.309	0.0161	0.433
Kidney	0.0311	0.964	0.0742	2.303
	0.0249	0.670	0.0552	1.487
Stomach	0.0963	2.991	0.442	13.73
	0.0464	1.249	0.414	11.17
Sm. Intestine	0.0660	2.051	0.711	22.08
	0.0130	0.351	0.129	3.479
<b>3. Distribution 168 hours post IV injection.</b>				
Thyroid	ND	ND	3.382	312.4
			3.451	376.7
Whole Blood	ND	ND	0.0108%/ml	1
			0.0092%/ml	1
Serum	ND	ND	0.0104%/ml	0.961
			0.0087%/ml	0.955
Liver	0.0276	2.545	0.347	32.10
	0.0477	5.214	0.473	51.69
Spleen	0.0101	0.931	0.0118	1.093
	0.0118	1.288	0.0205	2.243
Heart	0.0042	0.385	0.0050	0.459
	0.0053	0.585	0.0056	0.608
Lung	0.0069	0.634	0.0950	0.878
	0.0071	0.778	0.0116	1.263
Kidney	0.0160	1.479	0.0374	3.451
	0.0179	1.960	0.0381	4.162
Stomach	0.0197	1.824	0.152	14.00
	0.0182	1.989	0.0413	4.509
Sm. Intestine	0.0435	4.017	0.474	43.79
	0.0127	1.384	0.115	12.60

Table A3.18.4 Cont. (Organ Distribution of BSA-MTX 11.74%w/w)

Organ	% in 1g	CPM in 1g CPM in 1ml WB	% in total	CPM in total CPM/ml WB
<b>4. Distribution 24 hours post IP injection.</b>				
Thyroid	ND	ND	5.58	64.88
			7.80	81.25
Whole Blood	ND	ND	0.086%/ml	1
			0.096%/ml	1
Serum	ND	ND	0.083%/ml	0.965
			0.092%/ml	0.958
Liver	0.127	1.475	1.529	17.79
	0.0604	0.629	0.697	7.273
Spleen	0.0801	0.932	0.106	1.234
	0.0657	0.685	0.0814	0.849
Heart	0.0408	0.475	0.0433	0.504
	0.0314	0.328	0.0283	0.295
Lung	0.0470	0.547	0.0753	0.876
	0.0476	0.497	0.0669	0.698
Kidney	0.0717	0.835	0.186	2.166
	0.0710	0.740	0.156	1.635
Stomach	0.287	3.338	1.036	12.06
	0.270	2.812	1.317	13.73
Sm. Intestine	0.356	4.149	4.344	50.55
	0.139	1.452	1.657	17.28
<b>5 . Distribution 76 hours post IP injection.</b>				
Thyroid	ND	ND	9.12	480
			4.92	189
Whole Blood	ND	ND	0.019%/ml	1
			0.026%/ml	1
Serum	ND	ND	0.018%/ml	0.947
			0.023%/ml	0.896
Liver	0.0288	1.535	0.360	19.17
	0.0290	1.116	0.347	13.36
Spleen	0.0185	0.982	0.0306	1.630
	0.0113	0.435	0.0148	0.568
Heart	0.0088	0.469	0.0090	0.480
	0.0074	0.286	0.0063	0.242
Lung	0.0137	0.729	0.0247	1.314
	0.0116	0.445	0.0185	0.712
Kidney	0.0272	1.451	0.0687	3.659
	0.0233	0.894	0.0587	2.256
Stomach	0.0652	3.473	0.374	19.92
	0.0443	1.701	0.206	7.923
Sm. Intestine	0.0287	1.530	0.321	17.07
	0.0201	0.772	0.224	8.59



Table A3.18.4 Cont. (Organ Distribution of BSA-MTX 11.74%w/w)

Organ	% in 1g	CPM in 1g CPM in 1ml WB	% in total	CPM in total CPM in 1ml WB
<b>6. Distribution 168 hours post IP injection.</b>				
Thyroid	ND	ND	5.07 6.34	520 659
Whole Blood	ND	ND	0.0098%/ml 0.0096%/ml	1 1
Serum	ND	ND	0.0089%/ml 0.0087%/ml	0.912 0.905
Liver	0.008 0.0062	0.902 0.711	0.077 0.089	8.711 9.302
Spleen	0.0039 0.0046	0.399 0.482	0.0045 0.0053	0.465 0.552
Heart	0.0055 0.0045	0.570 0.466	0.0046 0.0052	0.472 0.538
Lung	0.0061 0.0074	0.622 0.772	0.0108 0.0100	1.113 1.044
Kidney	0.0176 0.0155	1.812 1.611	0.0365 0.0375	3.753 3.902
Stomach	0.0165 0.0164	1.70 1.712	0.0914 0.104	9.381 10.855
Sm. Intestine	0.0089 0.0120	0.913 0.808	0.0844 0.148	8.660 15.41
<b>7. Distribution 24 Hours post SC injection.</b>				
Thyroid	ND	ND	4.689 4.041	28.13 23.09
Whole Blood	ND	ND	0.167%/ml 0.175%/ml	1 1
Serum	ND	ND	0.151%/ml 0.160%/ml	0.904 0.914
Liver	0.0685 0.111	0.411 0.633	0.765 1.080	4.590 6.175
Spleen	0.0887 0.112	0.532 0.640	0.107 0.125	0.641 0.713
Heart	0.0668 0.0651	0.401 0.372	0.0692 0.0646	0.415 0.369
Lung	0.0728 0.108	0.436 0.617	0.138 0.204	0.828 1.167
Kidney	0.113 0.149	0.678 0.853	0.265 0.333	1.589 1.905
Stomach	1.132 1.221	6.792 6.980	8.607 5.158	51.62 29.47
Sm. Intestine	0.182 0.353	1.089 2.017	1.972 4.082	11.83 23.33

Table A3.18.4 Cont. (Organ Distribution of BSA-MTX 11.74%w/w).

Organ	% in 1g	CPM in 1g CPM in 1ml WB	% in total	CPM in total CPM in 1ml WB
<b>8. Distribution 76 hours post SC injection.</b>				
Thyroid	ND	ND	8.65	233.8
			8.05	322.1
Whole Blood	ND	ND	0.037%/ml	1
			0.025%/ml	1
Serum	ND	ND	0.0302%/ml	0.816
			0.0241%/ml	0.964
Liver	0.0182	0.491	0.175	4.742
	0.0245	0.993	0.211	8.579
Spleen	0.0121	0.328	0.0075	0.202
	0.0115	0.468	0.0139	0.564
Heart	0.0099	0.269	0.0083	0.225
	0.0133	0.539	0.0131	0.533
Lung	0.0203	0.549	0.0247	0.667
	0.0137	0.556	0.0174	0.706
Kidney	0.0306	0.828	0.0593	1.602
	0.0296	1.202	0.0645	2.615
Stomach	0.0871	2.355	0.246	6.657
	0.0370	1.501	0.0876	3.554
Sm. Intestine	0.0359	0.970	0.330	8.928
	0.0521	2.115	0.432	17.55
<b>9. Distribution 168 hours post SC administration.</b>				
Thyroid	ND	ND	6.29	446
			2.92	278
Whole Blood	ND	ND	0.0141%/ml	1
			0.0105%/ml	1
Serum	ND	ND	0.0127%/ml	0.905
			0.0097%/ml	0.919
Liver	0.0107	0.758	0.157	11.12
	0.0119	1.124	0.173	16.44
Spleen	0.0107	0.758	0.0073	0.520
	0.0059	0.557	0.0075	0.528
Heart	0.0053	0.378	0.0056	0.397
	0.0033	0.313	0.0034	0.317
Lung	0.0081	0.576	0.0109	0.769
	0.0065	0.615	0.0100	0.949
Kidney	0.0185	1.308	0.0434	3.074
	0.0138	1.312	0.0321	3.037
Stomach	0.0179	1.266	0.123	8.687
	0.0144	1.364	0.0532	5.046
Sm. Intestine	0.0158	1.116	0.160	11.34
	0.0088	0.836	0.0908	8.597

Table A3.19.1 The Serum Concentration (%  $^{125}\text{I}$  activity remaining/ml) following administration of 5mg of  $^{125}\text{I}$ -BSA-MTX (11.76%w/w) to rats by IV, IP and SC injection. (n=8 for each route).

Each value was determined from one rat.

Time (hr)	IV %/ml	Time (hr)	IP %/ml	Time (hr)	SC %/ml
1	6.266	1.5	0.250	1.5	0.127
1	6.389	1.5	0.564	1.5	0.117
2	2.906	3.75	0.580	3.75	0.183
2	3.311	3.75	0.210	3.75	0.154
4	1.472	6	0.732	8	0.190
4	0.888	6	0.724	8	0.189
7	0.531	8	0.697	23	0.207
7	1.099	8	0.659	23	0.187
24.5	0.449	24	0.289	27.5	0.210
24.5	0.308	24	0.340	27.5	0.205
30.75	0.295	30.5	0.211	30.5	0.191
30.75	0.324	30.5	0.232	30.5	0.171
48	0.187	48	0.195	48	0.119
48	0.187	48	0.0899	48	0.134
52.5	0.176	52	0.141	52	0.154
52.5	0.164	52	0.151	52	0.142
71.5	0.107	71.5	0.102	71.5	0.0778
71.5	0.111	71.5	0.0927	71.5	0.0927
79	0.103	79	0.101	79	0.0623
79	0.110	79	0.0922	79	0.0683
96	0.0741	96	0.0697	96	0.0564
96	0.0579	96	0.0693	96	0.0742
100	0.0801	100	0.0549	100	0.0619
100	0.0667	100	0.0543	100	0.0354

**Table A3.19.2 The Urine Excretion (% of  $^{125}\text{I}$  administered) following administration of 5mg of  $^{125}\text{I}$ -BSA-MTX (11.76%w/w) to male wistar rats by each of three routes.**

Values are cumulative mean % excreted in the urine (n=3)

Time (hr)	IV % excreted	S.E.M.	IP % excreted	S.E.M.	SC % excreted	S.E.M.
24	30.99	2.06	38.32	2.54	33.10	2.64
48	43.63	2.84	51.05	2.55	46.67	2.62
72	47.31	2.94	54.35	2.42	51.02	2.01
96	49.09	2.56	55.96	2.64	52.40	1.83

**Table A3.19.3 The Excretion of  $^{125}\text{I}$  activity in the faeces (% of radioactivity administered) following administration of 5mg  $^{125}\text{I}$ -BSA-MTX (11.76%w/w) to rats by each of the three routes.**

Values are cumulative mean (n=3) % excreted in the faeces.

Time (hr)	IV % excreted	S.E.M.	IP % excreted	S.E.M	SC % excreted	S.E.M.
24	2.47	0.54	4.70	1.59	3.59	1.39
48	4.85	1.10	6.22	1.81	5.96	1.76
72	5.96	1.17	7.14	1.86	7.20	1.58
96	6.70	1.26	7.91	1.90	8.13	1.31

Table A3.19.4 The Organ Distribution of  $^{125}\text{I}$  activity following administration of 5mg of  $^{125}\text{I}$ -BSA-MTX (11.76%w/w) to male wistar rats by each of the three routes.

Results are expressed in 2 ways; as a % of the total radioactivity found in 1g or total organ and as a ratio of the activity in 1g (or whole organ) divided by activity in 1ml whole blood. Two rats from each group were analysed at each time point.

Organ	% in 1g	<u>CPM in 1g</u> CPM in 1ml WB	% in total	<u>CPM in total</u> CPM in 1ml WB
<b>1. Distribution 100 hours post IV injection.</b>				
Thyroid	ND	ND	6.74	75.73
			7.34	133.45
Whole Blood	ND	ND	0.089%/ml	1
			0.055%/ml	1
Serum	ND	ND	0.081%/ml	0.910
			0.067%/ml	1.213
Liver	0.0945	1.063	0.793	8.922
	0.0362	0.661	0.474	8.635
Spleen	0.0523	0.588	0.0578	0.650
	0.0128	0.233	0.0188	0.342
Heart	0.0275	0.310	0.0281	0.317
	0.0135	0.247	0.0163	0.297
Lung	0.0261	0.294	0.0304	0.343
	0.0211	0.384	0.0288	0.525
Kidney	0.177	1.992	0.328	3.686
	0.0904	1.647	0.267	4.868
Stomach	0.0395	0.444	0.174	1.954
	0.0240	0.438	0.104	1.902
Sm. Intestine	0.0278	0.312	0.191	2.149
	0.0266	0.485	0.227	4.131

Table 3.19.4 Cont. (Organ Distribution of BSA-MTX 11.76%w/w).

Organ	% in 1g	<u>CPM in 1g</u> CPM in 1ml WB	% in total	<u>CPM in total</u> CPM/ml WB
<b>2. Distribution 100 hours post IP injection.</b>				
Thyroid	ND	ND	5.46	218.4
			4.82	109.5
Whole Blood	ND	ND	0.025%/ml	1
			0.044%/ml	1
Serum	ND	ND	0.055%/ml	2.196
			0.054%/ml	1.239
Liver	0.0087	0.355	0.122	4.973
	0.0302	0.690	0.389	8.875
Spleen	0.0026	0.106	0.0021	0.087
	0.0143	0.326	0.0196	0.448
Heart	0.0042	0.170	0.0044	0.178
	0.0128	0.292	0.0143	0.326
Lung	0.0076	0.309	0.0154	0.626
	0.0282	0.644	0.0670	1.528
Kidney	0.0078	0.318	0.0217	0.882
	0.113	2.589	0.306	6.978
Stomach	0.0338	1.373	0.124	5.026
	0.0506	1.155	0.219	4.991
Sm. Intestine	0.0082	0.334	0.0915	3.716
	0.0591	1.348	0.714	16.30
<b>3. Distribution 100 hours post SC injection.</b>				
Thyroid	ND	ND	5.86	90.15
			5.67	163.5
Whole Blood	ND	ND	0.065%/ml	1
			0.035%/ml	1
Serum	ND	ND	0.062%/ml	0.952
			0.035%/ml	1.022
Liver	0.0325	0.502	0.310	4.789
	0.0187	0.538	0.231	6.659
Spleen	0.0148	0.229	0.0162	0.250
	0.0073	0.212	0.0079	0.227
Heart	0.0166	0.256	0.0164	0.253
	0.0088	0.254	0.0113	0.327
Lung	0.0276	0.426	0.0443	0.684
	0.0126	0.363	0.0231	0.666
Kidney	0.0812	1.253	0.229	3.540
	0.0678	1.953	0.215	6.209
Stomach	0.0383	0.592	0.206	3.186
	0.0420	1.211	0.0984	2.837
Sm. Intestine	0.0290	0.448	0.296	4.564
	0.0143	0.412	0.159	4.579

Table A3.20.1 The Serum Concentration (% <sup>125</sup>I activity injected) following administration of 5mg of <sup>125</sup>I-BSA-MTX (13.63%w/w) to male wistar rats by each of the three routes.

Each concentration was determined from one rat. (n=8 for each route).

Time (hr)	IV %/ml	IP %/ml	SC %/ml
0.75	6.921	0.0990	0.0869
0.75	5.919	0.0702	0.0620
3.0	5.998	0.167	0.0908
3.0	5.784	0.217	0.0784
4.75	1.351	0.499	-
4.75	1.730	0.348	-
7.5	0.499	0.467	0.164
7.5	0.562	0.533	0.193
18.5	0.198	0.237	0.234
18.5	0.184	0.231	0.226
19	0.173	-	-
22.5	-	-	0.146
22.5	-	-	0.188
29	0.117	0.102	0.145
29	0.106	0.156	0.163
43	0.0735	0.0883	0.104
43	0.0637	0.103	0.108
48	0.0725	0.0895	0.0965
48	0.0541	0.0760	0.0716
67.5	0.0471	0.0622	0.0716
67.5	0.0625	0.0507	0.0580
78.75	0.0443	0.0513	0.0636
78.75	0.0532	0.0686	0.0675
94	0.0362	0.0395	0.0417
94	0.0283	0.0284	0.0330
96	0.0446	0.0384	0.0440
96	0.0397	0.0455	0.0423

Table A3.20.2 The Urine excretion of  $^{125}\text{I}$  activity (% total dose administered) following administration of 5mg of  $^{125}\text{I}$ -BSA-MTX (13.63%w/w) to rats by each of three routes.

Values are mean % cumulative excretion (n=3).

Time (hr)	IV % excreted	S.E.M.	IP % excreted	S.E.M.	SC % excreted	S.E.M.
24	38.6	9.54	33.9	7.87	24.4	4.02
48	57.1	7.32	48.7	10.33	48.2	2.67
72	63.5	6.45	57.2	9.29	58.2	2.69
96	65.3	6.40	60.2	8.67	61.6	2.78

Table A3.20.3 The excretion of  $^{125}\text{I}$  activity (% of administered dose) in the faeces following administration of  $^{125}\text{I}$ -BSA-MTX (13.63%w/w) to rats by each of the three routes.

Values are mean % cumulative excretion (n=3).

Time (hr)	IV % excreted	S.E.M.	IP % excreted	S.E.M.	SC % excreted	S.E.M.
24	2.17	0.163	4.91	2.35	1.66	0.67
48	5.73	0.76	6.46	2.18	6.80	0.42
72	7.20	0.80	7.74	2.39	9.04	0.45
96	8.03	0.83	8.60	2.41	10.14	0.45



Table A3.20.4 The Organ Distribution of  $^{125}\text{I}$  activity following administration of  $^{125}\text{I}$ -BSA-MTX (13.63%w/w) to rats by each of the three routes.

Results are expressed in 2 ways; as a % of the total radioactivity found in 1g or total organ and as a ratio of the activity in 1g (or whole organ) divided by radioactivity in 1ml whole blood. Two rats were analysed from each group at each time point.

Organ	% in 1g	<u>CPM in 1g</u> CPM in 1ml WB	% in total	<u>CPM in total</u> CPM/ml WB
<b>1. Distribution 24 hours post IV injection.</b>				
Thyroid	ND	ND	7.43	41.05
			6.81	43.10
Whole Blood	ND	ND	0.181%/ml	1
			0.156%/ml	1
Serum	ND	ND	0.173%/ml	0.952
			0.151%/ml	0.968
Liver	0.416	2.298	5.31	29.31
	0.365	2.339	5.29	33.93
Spleen	0.375	2.071	0.61	3.365
	0.331	2.122	0.34	2.207
Heart	0.067	0.370	0.061	0.340
	0.059	0.378	0.058	0.374
Lung	0.099	0.547	0.12	0.641
	0.087	0.557	0.13	0.836
Kidney	0.118	0.655	0.25	1.357
	0.099	0.635	0.20	1.282
Stomach	0.692	3.825	3.39	18.71
	0.541	3.468	2.35	15.05
Sm. Intestine	0.340	1.879	3.87	21.39
	0.256	1.641	2.53	16.25

Table A3.20.4 Cont. (Organ Distribution of 13.63%w/w).

Organ	% in 1g	<u>CPM in 1g</u> CPM in 1ml WB	% in total	<u>CPM in total</u>
<b>2. Distribution 48 hours post IV injection.</b>				
Thyroid	ND	ND	9.28	98.7
			5.91	73.8
Whole Blood	ND	ND	0.094%/ml	1
			0.080%/ml	1
Serum	ND	ND	0.072%/ml	0.805
			0.054%/ml	0.676
Liver	0.235	2.50	2.16	22.95
	0.190	2.38	2.08	26.09
Spleen	0.183	1.947	0.19	1.986
	0.232	2.908	0.29	3.677
Heart	0.026	0.276	0.023	0.243
	0.038	0.483	0.046	0.490
Lung	0.0721	0.766	0.082	0.875
	0.040	0.508	0.050	0.578
Kidney	0.047	0.500	0.098	1.044
	0.046	0.577	0.099	1.546
Stomach	0.243	2.580	0.66	7.063
	0.099	1.248	0.45	5.685
Sm. Intestine	0.058	0.613	0.49	5.199
	0.090	1.135	0.73	9.096
<b>3. Distribution 94 hours post IV injection.</b>				
Thyroid	ND	ND	6.14	122.8
			3.10	62.0
Whole Blood	ND	ND	0.050%/ml	1
			0.050%/ml	1
Serum	ND	ND	0.033%/ml	0.655
			0.039%/ml	0.794
Liver	0.185	3.674	1.374	27.28
	0.276	5.562	2.9	58.64
Spleen	0.170	3.371	0.0894	1.775
	0.119	2.394	0.17	3.385
Heart	0.0178	0.353	0.011	0.221
	0.0125	0.252	0.012	0.243
Lung	0.0227	0.451	0.028	0.570
	0.0196	0.394	0.023	0.470
Kidney	0.0350	0.695	0.065	1.295
	0.0253	0.508	0.060	1.206
Stomach	0.0778	1.546	0.240	4.760
	0.0423	0.851	0.081	1.624
Sm. Intestine	0.0325	0.646	0.231	4.483
	0.0311	0.625	0.307	6.302

Table A3.20.4 Cont. (Organ Distribution of BSA-MTX 13.63%w/w)

Organ	% in 1g	<u>CPM in 1g</u> CPM in 1ml WB	% in total	<u>CPM in total</u> CPM in 1ml WB
<b>4. Distribution 174 hours post IV injection.</b>				
Thyroid	ND	ND	7.83	145
			10.07	197
Whole Blood	ND	ND	0.054%/ml	1
			0.051%/ml	1
Serum	ND	ND	0.031%/ml	0.574
			0.030%/ml	0.588
Liver	0.127	2.338	1.15	21.28
	0.138	2.731	1.26	30.05
Spleen	0.094	1.733	0.068	1.259
	0.146	2.895	0.19	3.743
<b>5. Distribution 48 hours post IP injection.</b>				
Thyroid	ND	ND	5.91	72.07
			8.12	83.71
Whole Blood	ND	ND	0.082%/ml	1
			0.097%/ml	1
Serum	ND	ND	0.0895%/ml	1.092
			0.076%/ml	0.783
Liver	0.0791	0.968	0.87	10.66
	0.144	1.492	1.44	14.95
Spleen	0.0194	0.238	0.017	0.208
	0.0689	0.713	0.083	0.855
Heart	0.0308	0.377	0.033	0.404
	0.0218	0.226	0.025	0.263
Lung	0.0300	0.368	0.030	0.347
	0.0694	0.718	0.13	1.359
Kidney	0.0579	0.709	0.127	1.560
	0.570	0.590	0.160	1.644
Stomach	0.196	2.401	0.73	8.93
	0.354	3.667	1.828	18.92
Sm. Intestine	0.179	2.187	1.86	22.81
	0.138	1.435	1.18	12.21

Table A3.20.4 Cont. (Organ Distribution of BSA-MTX 13.63%w/w Conjugate).

Organ	% in 1g	CPM in 1g CPM in 1ml WB	% in total	CPM in total CPM in 1ml WB
<b>6. Distribution 94 hours post IP injection.</b>				
Thyroid	ND	ND	8.44 2.17	156.3 98.6
Whole Blood	ND	ND	0.054%/ml 0.0225%/ml	1 1
Serum	ND	ND	0.0395%/ml 0.028%/ml	0.731 1.289
Liver	0.0299 0.101	0.558 0.462	0.41 0.11	7.55 4.819
Spleen	0.0156 0.0092	0.291 0.430	0.026 0.011	0.481 0.4545
Heart	0.0123 0.0076	0.228 0.348	0.014 0.0080	0.265 0.368
Lung	0.0188 0.0112	0.351 0.513	0.030 0.011	0.563 0.524
Kidney	0.0353 0.0141	0.658 0.644	0.084 0.029	1.561 1.313
Stomach	0.0660 0.0390	1.227 1.787	0.50 0.27	9.388 12.38
Sm. Intestine	0.0725 0.0279	1.350 1.279	0.79 0.27	14.86 12.38
<b>7. Distribution 174 hours post IP injection.</b>				
Thyroid	ND	ND	8.81 7.04	151.9 167.6
Whole Blood	ND	ND	0.058%/ml 0.042%/ml	1 1
Serum	ND	ND	0.044%/ml 0.037%/ml	0.759 0.881
Liver	0.0435 0.0310	0.749 0.722	0.45 0.39	7.683 9.19
Spleen	0.0214 0.015	0.368 0.366	0.016 0.016	0.280 0.372

Table A3.20.4 Cont. (Organ Distribution of BSA-MTX 13.63%w/w).

Organ	% in 1g	<u>CPM in 1g</u> CPM in 1ml WB	% in total	<u>CPM in total</u> CPM in 1ml WB
<b>8. Distribution 48 hours SC administration.</b>				
Thyroid	ND	ND	8.96	74.67
			9.28	77.33
Whole Blood	ND	ND	0.13%/ml	1
			0.12%/ml	1
Serum	ND	ND	0.0965%/ml	0.743
			0.0716%/ml	0.597
Liver	0.0457	0.344	0.57	4.271
	0.0573	0.463	0.55	4.421
Spleen	0.0433	0.326	0.032	0.242
	0.0768	0.621	0.086	0.698
Heart	0.0317	0.239	0.031	0.230
	0.0269	0.218	0.024	0.195
Lung	0.0556	0.419	0.079	0.593
	0.050	0.404	0.066	0.530
Kidney	0.0705	0.531	0.13	0.998
	0.0557	0.450	0.12	0.999
Stomach	0.311	2.346	1.87	14.12
	0.389	3.138	1.52	12.27
Sm. Intestine	0.406	3.061	3.46	26.09
	0.124	1.000	1.48	11.96
<b>9. Distribution 94 hours post SC injection.</b>				
Thyroid	ND	ND	4.13	60.73
			5.30	84.13
Whole Blood	ND	ND	0.068%/ml	1
			0.063%/ml	1
Serum	ND	ND	0.042%/ml	0.613
			0.033%/ml	0.524
Liver	0.0270	0.398	0.29	4.361
	0.0182	0.287	0.22	3.471
Spleen	0.0147	0.218	0.020	0.295
	0.0106	0.167	0.014	0.224
Heart	0.0157	0.231	0.016	0.232
	0.0137	0.216	0.012	0.183
Lung	0.0306	0.452	0.046	0.674
	0.0237	0.374	0.035	0.550
Kidney	0.0320	0.473	0.077	1.136
	0.0319	0.504	0.065	1.025
Stomach	0.096	1.424	0.40	5.962
	0.108	1.704	0.65	10.24
Sm. Intestine	0.065	0.956	0.66	9.733
	0.119	1.889	1.09	17.24

Table A3.20.4 cont. (Organ Distribution of BSA-MTX 13.63%w/w).

Organ	% in 1g	<u>CPM in 1g</u> CPM in 1ml WB	% in total	<u>CPM in total</u> CPM in 1ml WB
<b>10. Distribution 174 hours post SC injection.</b>				
Thyroid	ND	ND	8.06	158
			3.18	70.7
Whole Blood	ND	ND	0.053%/ml	1
			0.045%/ml	1
Serum	ND	ND	0.021%/ml	0.396
			0.022%/ml	0.489
Liver	0.0106	0.201	0.11	2.147
	0.0096	0.214	0.14	3.083
Spleen	0.0056	0.107	0.008	0.159
	0.0079	0.175	0.012	0.271

Table 3.21.1 Serum Concentration (% <sup>125</sup>I activity remaining/ml) following administration of 5mg of <sup>125</sup>I-BSA-MTX (13.64%w/w) to rats by each of the three routes.

Each value was determined from one rat. There were 8 rats in each group.

Time (hr)	IV %/ml	IP %/ml	SC %/ml
1	2.558	0.399	0.138
1	1.614	0.151	0.161
3	0.668	0.305	-
3	0.634	0.393	-
5	0.552	0.327	0.172
5	0.535	0.493	0.225
8	0.424	0.370	0.334
8	0.436	0.375	0.152
23	0.160	0.141	0.227
23	0.177	0.191	0.130
26.5	0.154	0.131	0.114
26.5	0.183	0.127	0.111
31.75	0.124	0.124	0.120
31.75	0.197	0.127	0.142
48	0.0791	0.109	0.0834
48	0.0959	0.0464	0.0736
49.5	0.0712	-	-
49.5	0.0793	-	-
54	0.0899	0.0595	0.0643
54	0.102	0.0771	0.0697
71	0.0508	0.0512	0.0575
71	0.0564	0.0498	0.0495
79.5	0.0558	0.0363	-
79.5	0.0692	0.0535	-
96	0.0375	0.0456	0.0382
96	0.0353	0.0366	0.0321
97	0.0416	0.0271	0.0328
97	0.0374	0.0311	0.0341

Table A3.21.2 The urine excretion of  $^{125}\text{I}$  activity (% of dose administered) following administration of 5mg of  $^{125}\text{I}$ -BSA-MTX (13.64%w/w) to rats by each of the three routes.

Each value is mean % excreted (n=3).

Time (hr)	IV % excreted	S.E.M.	IP % excreted	S.E.M.	SC % excreted	S.E.M.
24	48.72	1.61	36.47	6.89	31.31 <sup>a</sup>	4.61
48	64.28	1.53	54.81	9.65	54.83	6.98
72	69.69	1.83	60.30	10.48	63.23	7.46
96	72.39	1.99	63.15	10.92	66.45	7.41

Note a) The % excretion for the SC group was compared to the IV group using a T-test at 24 hours and was found to be significant. All other times were non-significant.

Table A3.21.3 The excretion of  $^{125}\text{I}$  activity in the faeces (% of administered dose) following administration of 5mg of  $^{125}\text{I}$ -BSA-MTX (13.64%w/w) to rats by each of the three routes.

Results are expressed as mean % excreted (n=3).

Time (hr)	IV % excreted	S.E.M.	IP % excreted	S.E.M.	SC % excreted	S.E.M.
24	3.35	0.25	2.65	1.77	3.77	0.71
48	6.97	0.39	6.91	1.47	9.10	2.52
72	9.07	0.51	9.08	2.20	11.62	1.74
96	10.41	0.51	10.38	2.11	12.71	1.89



Table A3.21.4 The organ distribution of  $^{125}\text{I}$  activity following administration of 5mg of  $^{125}\text{I}$ -BSA-MTX (13.64%w/w) to rats by each of the three routes.

Results are expressed in 2 ways; as a % of the total radioactivity found in 1g or the whole organ and as a ratio of the activity found in 1g (or whole organ) divided by the activity found in 1ml whole blood. Two rats were analysed for each group for each time point.

Organ	% in 1g	<u>CPM in 1g</u> CPM in 1ml WB	% in total	<u>CPM in total</u> CPM in 1ml WB
<b>1. Distribution 48 hours post IV injection.</b>				
Thyroid	ND	ND	9.26	71.23
			6.65	55.42
Whole Blood	ND	ND	0.13%/ml	1
			0.12%/ml	1
Serum	ND	ND	0.0712%/ml	0.548
			0.0793%/ml	0.649
Liver	0.147	1.113	1.54	11.54
	0.165	1.354	1.37	11.09
Spleen	0.152	1.153	0.14	1.075
	0.340	2.783	0.22	1.781
Heart	0.0249	0.189	0.030	0.222
	0.0303	0.248	0.028	0.228
Lung	0.0401	0.304	0.069	0.516
	0.0479	0.393	0.075	0.609
Kidney	0.0598	0.454	0.15	1.129
	0.0645	0.528	0.13	1.046
Stomach	0.109	0.832	0.47	3.501
	0.341	2.791	0.98	7.917
Sm. Intestine	0.080	0.610	0.60	4.539
	0.057	0.467	0.37	3.007

Table A3.21.4 Cont. (Organ distribution of BSA-MTX 13.64%w/w).

Organ	% in 1g	CPM in 1g CPM in 1ml WB	% in total	CPM in total CPM in 1ml WB
<b>2. Distribution 97 hours post IV administration.</b>				
Thyroid	ND	ND	5.23	58.24
			5.78	63.52
Whole Blood	ND	ND	0.0898%/ml	1
			0.091%/ml	1
Serum	ND	ND	0.0416%/ml	0.463
			0.0374%/ml	0.411
Liver	0.105	1.169	1.10	11.67
	0.149	1.720	1.35	14.78
Spleen	0.0468	0.522	0.076	0.808
	0.0890	1.019	0.101	1.134
Heart	0.0148	0.164	0.015	0.160
	0.0165	0.189	0.021	0.235
Lung	0.0264	0.294	0.043	0.455
	0.0291	0.334	0.061	0.669
Kidney	0.0426	0.475	0.11	1.179
	0.106	1.223	0.26	2.820
Stomach	0.0559	0.623	0.32	3.358
	0.155	1.777	0.42	4.614
Sm. Intestine	0.0410	0.457	0.32	3.362
	0.0511	0.587	0.30	3.322
<b>3. Distribution 31.75 hours post IP injection.</b>				
Thyroid	ND	ND	8.35	52.19
			8.61	54.44
Whole Blood	ND	ND	0.156%/ml	1
			0.158%/ml	1
Serum	ND	ND	0.124%/ml	0.793
			0.127%/ml	0.804
Liver	0.0980	0.626	1.08	6.804
	0.111	0.702	1.365	8.641
Spleen	0.119	0.760	0.21	1.315
	0.133	0.842	0.134	0.850
Heart	0.043	0.275	0.0487	0.309
	0.038	0.241	0.0494	0.313
Lung	0.073	0.468	0.11	0.694
	0.081	0.513	0.122	0.772
Kidney	0.0864	0.552	0.21	1.333
	0.0755	0.478	0.174	1.099
Stomach	1.175	7.50	4.55	29.08
	1.335	8.449	5.74	36.33
Sm. Intestine	0.380	2.425	2.67	17.05
	0.292	1.848	2.89	18.29

Table A3.21.4 Cont. (Organ distribution of BSA-MTX 13.64%w/w).

Organ	% in 1g	CPM in 1g CPM in 1ml WB	% in total	CPM in total CPM in 1ml WB
<b>4. Distribution 97 hours post IP injection.</b>				
Thyroid	ND	ND	2.76	42.46
			5.24	143.2
Whole Blood	ND	ND	0.065%/ml	1
			0.084%/ml	1
Serum	ND	ND	0.0366%/ml	0.563
			0.0456%/ml	0.543
Liver	0.0125	0.201	0.14	2.202
	0.0442	0.553	0.596	7.132
Spleen	0.0096	0.155	0.012	0.187
	0.0238	0.297	0.052	0.624
Heart	0.0099	0.159	0.013	0.203
	0.0124	0.156	0.016	0.193
Lung	0.0234	0.376	0.039	0.598
	0.0255	0.319	0.048	0.571
Kidney	0.0185	0.298	0.054	0.939
	0.0348	0.435	0.097	1.161
Stomach	0.0519	0.836	0.22	3.312
	0.131	1.634	0.961	11.53
Sm. Intestine	0.0144	0.231	0.111	1.757
	0.0298	0.373	0.27	3.284
<b>5. Distribution 97 hours post SC injection.</b>				
Thyroid	ND	ND	4.45	60.96
			7.06	102.3
Whole Blood	ND	ND	0.0727%/ml	1
			0.0692%/ml	1
Serum	ND	ND	0.0328%/ml	0.450
			0.0341%/ml	0.493
Liver	0.0367	0.523	0.59	7.972
	0.0174	0.262	0.21	3.060
Spleen	0.0099	0.141	0.022	0.225
	0.0164	0.247	0.019	0.281
Heart	0.0120	0.171	0.022	0.226
	0.0145	0.218	0.018	0.258
Lung	0.0213	0.304	0.035	0.471
	0.0287	0.432	0.039	0.566
Kidney	0.0356	0.509	0.11	1.543
	0.0382	0.575	0.11	1.530
Stomach	0.108	1.540	0.44	6.055
	0.0373	0.563	0.20	2.886
Sm. Intestine	0.0374	0.532	0.43	5.840
	0.0447	0.673	0.53	7.675

Table A3.22.1 the Serum Concentration of  $^{125}\text{I}$  activity (% of administered dose) following administration of 5mg of  $^{125}\text{I}$ -LA-MTX (4.52%w/w) to male rats by each of the three routes.

Each value was determined from one rat. (n=8 for each route.)

Time (hr)	IV %/ml	IP % /ml	SC %/ml
0.667	-	0.399	0.437
0.667	-	0.322	0.412
1	0.439	-	-
1	0.630	-	-
1.5	0.483	0.597	0.473
1.5	0.453	0.573	0.481
2	0.452	0.486	0.522
2	0.512	0.426	0.481
3	0.433	-	0.438
3	0.454	-	0.348
4	0.269	0.369	0.479
4	0.335	0.417	0.363
6	0.448	0.270	0.363
6	0.271	0.326	0.338
8	0.316	0.256	0.349
8	0.341	0.359	0.298
23.5	0.157	0.108	0.155
23.5	0.112	0.222	0.144
27.5	0.0932	0.108	0.158
27.5	0.0927	0.174	0.118
32.25	0.114	0.0812	0.108
32.25	0.138	0.0960	0.102
48.25	0.0497	0.0379	0.0438
48.25	0.0583	0.0251	0.0490
56.75	0.0324	0.0366	0.0405
56.75	0.0508	0.0443	0.0540
72	0.0345	0.0289	0.0368
72	0.0367	0.0381	0.0286
96	0.0211	0.0233	0.0320
96	0.0224	0.0268	0.0226

Table A3.22.2 the Urine Excretion of  $^{125}\text{I}$  activity (% of total injected dose) following administration of 5mg of  $^{125}\text{I}$ -LA-MTX (4.52%w/w) to rats by each of the three routes.

Values are mean % excreted (n=3).

Time (hr)	IV % excreted	S.E.M.	IP % excreted	S.E.M.	SC % excreted	S.E.M.
24	39.95	6.62	31.16	8.91	38.07	7.73
48	50.45	7.74	45.00	8.85	46.40	5.37
72	54.07	8.06	48.97	7.40	50.80	4.17
96	60.53	9.30	53.97	6.85	56.94	2.74

Table A3.22.3 The excretion of  $^{125}\text{I}$  activity in the faeces (% of total radioactivity injected) following administration of 5mg of  $^{125}\text{I}$ -LA-MTX (4.52%w/w) to rats by each of the 3 routes.

Values are mean % excreted (n=3).

Time (hr)	IV % excreted	S.E.M.	IP % excreted	S.E.M.	SC % excreted	S.E.M.
24	2.93	1.51	3.24	0.77	1.94	1.08
96	6.57	1.84	8.42	0.34	10.20	1.75

Table A3.23.1 Serum Concentration (% <sup>125</sup>I activity remaining/ml) following administration of 5mg of <sup>125</sup>I-LA-MTX (13.69%w/w) to male wistar rats by each of the three routes.

Each concentration was determined from one rat. (n=8 for IV and SC, n=6 for IP).

Time (hr)	IV %/ml	IP %/ml	SC %/ml
0.333	2.259	0.242	0.216
0.333	2.381	0.364	0.318
0.833	1.309	0.658	0.497
0.917	1.753	-	0.447
1	-	0.506	-
2	0.580	0.537	0.383
2	0.613	0.602	0.841
4	0.460	0.484	0.389
4	0.343	0.495	0.372
6.5	0.251	0.338	0.310
6.5	0.196	0.372	0.380
8	0.278	-	0.309
8	0.262	-	0.324
10	0.242	0.266	0.414
10	0.301	0.309	0.394
23.5	0.0818	0.0617	0.0545
23.5	0.0992	0.116	0.0947
28	0.0650	-	0.0714
28	0.0620	-	0.0705
31	0.0661	0.0923	0.0651
31	0.0671	0.0896	0.0654
47.5	0.0250	0.0300	0.0313
47.5	0.0264	0.0387	0.0347
55	0.0263	0.0471	0.0313
55	0.0309	0.0454	0.0363
72	0.0154	0.0263	0.0176
72	0.0182	0.0219	0.0213
80	0.0197	-	0.0271
80	0.0170	-	0.0269
97	0.0145	0.0208	0.0227
97	0.0176	0.0157	0.0223

Table A3.23.2 The Urine excretion of  $^{125}\text{I}$  activity ( % of total dose administered) following administration of 5mg of  $^{125}\text{I}$ -LA-MTX (13.69%w/w) to rats by each of the routes.

Values are mean % excretion (n=3).

Time (hr)	IV % excreted	S.E.M.	IP % excreted	S.E.M.	SC % excreted	S.E.M.
24	38.43	1.84	42.81	3.70	45.47	8.34
48	44.17	2.78	50.00	3.61	51.86	8.60
72	46.05	3.00	52.54	3.48	53.72	8.47
96	46.84	3.07	53.85	2.98	54.51	8.42

Table A3.23.3 The excretion of  $^{125}\text{I}$  activity ( % of dose administered) in the faeces following administration of 5mg of  $^{125}\text{I}$ -LA-MTX (13.69%w/w) to rats by each of the three routes.

Values are mean % excretion (n=3).

Time (hr)	IV % excreted	S.E.M.	IP % excreted	S.E.M.	SC % excreted	S.E.M.
24	4.18	1.48	2.62	0.97	5.47	1.14
48	5.37	1.55	4.75	0.99	8.29	1.90
72	6.11	1.61	6.12	0.63	9.60	1.86
96	6.63	1.65	7.20	0.51	10.21	1.91

Table A3.24.1 The Serum concentration (% radioactivity remaining/ml) following administration of 5mg of  $^{125}\text{I}$ -RSA-MTX (6.94%w/w) to rats by the IV route. (n=8).

Each concentration was determined from one rat.

Time (hr)	% $^{125}\text{I}$ dose/ml
1	3.833
1	4.561
2	3.312
2	3.492
3.75	1.630
3.75	1.628
5.75	1.159
5.75	0.874
18	0.228
18	0.215
21	0.189
21	0.159
24	0.178
24	0.149
27	0.150
27	0.153
42	0.101
42	0.0995
48	0.0962
48	0.0875
50	0.0786
50	0.107
66.25	0.0527
66.25	0.0512
74	0.0535
74	0.0837
95	0.0399
95	0.0343



Table A3.24.2 The Urine Excretion of  $^{125}\text{I}$  (% of total injected) following administration of 5mg of  $^{125}\text{I}$ -RSA-MTX (6.94%w/w) to rats by the IV route.

Each value is mean % excreted (n=3).

Time (hr)	% $^{125}\text{I}$ excreted	S.E.M.
24	25.46	2.69
48	33.49	3.16
72	39.61	3.89
96	40.78	4.05

Table A3.24.3 The excretion of  $^{125}\text{I}$  activity in the faeces (% of radioactivity injected) following administration of 5mg of  $^{125}\text{I}$ -RSA-MTX (6.94%w/w) to rats by the IV route.

Each value is mean % excreted (n=3).

Time (hr)	% $^{125}\text{I}$ excreted	S.E.M.
24	3.27	1.108
48	6.65	0.657
72	8.53	0.709
96	9.54	0.622

Table A3.24.4 The Organ Distribution of radioactivity following administration of 5mg of <sup>125</sup>I-RSA-MTX (6.94%w/w) to rats by the IV route.

Results are expressed in 2 forms; as a % of the radioactivity injected found in 1g or the whole organ and as a ratio of the activity found in 1g (or the whole organ) divided by activity in 1ml whole blood. Two rats were analysed at each time point for each group.

Organ	% in 1g	CPM in 1g CPM in 1ml WB	% in total	% in total CPM in 1ml WB
<b>1. Distribution 24 hours post administration.</b>				
Thyroid	ND	ND	9.761	83.50
			12.81	103.7
Whole Blood	ND	ND	0.117%/ml	1
			0.123%/ml	1
Serum	ND	ND	0.178%/ml	1.521
			0.149%/ml	1.211
Liver	0.0901	0.790	0.939	8.03
	0.0865	0.718	0.980	7.94
Spleen	0.0594	0.521	0.0615	0.526
	0.0635	0.527	0.0542	0.435
Heart	0.0450	0.394	0.0539	0.461
	0.0412	0.342	0.0503	0.407
Lung	0.0608	0.533	0.0674	0.577
	0.0667	0.554	0.0907	0.734
Kidney	0.0736	0.645	0.172	1.468
	0.0670	0.556	0.177	1.435
Stomach	0.439	3.854	1.310	11.209
	0.607	5.042	4.643	37.59
Sm. Intestine	0.113	0.993	1.028	8.798
	0.354	2.935	3.368	27.27
<b>2. Distribution 48 hours post administration.</b>				
Thyroid	ND	ND	13.67	156.6
			12.82	152.6
Whole Blood	ND	ND	0.0873%/ml	1
			0.0840%/ml	1
Serum	ND	ND	0.0962%/ml	1.102
			0.0875%/ml	1.042
Liver	0.0754	0.885	0.765	8.72
	0.0628	0.767	0.627	7.46
Spleen	0.0543	0.638	0.036	0.412
	0.0439	0.536	0.035	0.417
Heart	0.0326	0.382	0.031	0.355
	0.0326	0.398	0.033	0.391
Lung	0.0447	0.525	0.051	0.584
	0.0440	0.538	0.0698	0.831
Kidney	0.0542	0.636	0.128	1.466
	0.0487	0.595	0.101	1.202
Stomach	0.279	3.278	0.597	6.838
	0.262	3.195	0.605	7.202
Sm. Intestine	0.123	1.452	0.778	8.912
	0.0675	0.825	0.417	4.964

Table A3.25.1 The Serum and Whole Blood Concentrations (% radioactivity remaining/ml) following administration of 250µg of <sup>125</sup>I-BSA to male wistar rats by the IV route.

Each value is the serum concentration determined for one rat. Ten rats were injected.

Note: Where Means and S.E.M. are quoted n=4.

Time (minutes)	Whole Blood %/ml	Serum %/ml
1	7.30	12.734
1	6.856	13.08
2	7.552	11.835
2	5.038	12.977
5	7.100	12.284
5	4.736	12.356
8	6.770	8.704
8	4.754	7.862
10	6.668	10.855
10	6.104	11.910
15	6.735±0.175	10.759±0.938
20	6.707	10.942
20	6.165	11.425
30	6.166±0.205	11.314±0.405
60	5.667	10.953
60	5.621	10.681
90	4.639	8.140
90	4.491	7.838
120	4.598	8.247
120	4.496	8.696
150	4.435	8.662
150	4.010	7.982
180	4.075	7.750
180	4.962	9.875
210	4.043	8.323
210	3.851	8.648
240	3.995	7.503
240	3.453	7.975
300	3.688	6.337
300	3.696	6.693

Table A3.25.2 The Organ Distribution following administration of 250µg of <sup>125</sup>I-BSA to rats by the IV route. Two rats were analysed for each time point.

Values are expressed in 2 forms as a % of the total <sup>125</sup>I found in 1g or the whole organ and as a ratio of the activity found in 1g (or the whole tissue) divided by activity found in 1ml whole blood.

Organ	% in 1g	CPM in 1g CPM in 1ml WB	% in total	CPM in total CPM in 1ml WB
<b>1. Distribution 15 minutes post injection.</b>				
Thyroid	ND	ND	0.102 0.108	0.0159 0.0160
Bladder	ND	ND	0.136 0.286	0.0212 0.0424
Whole Blood	ND	ND	6.405%/ml 6.743%/ml	1 1
Serum	ND	ND	8.354%/ml 11.50%/ml	1.304 1.706
Liver	1.487 1.242	0.232 0.184	16.59 14.24	2.590 2.112
Spleen	1.146 1.008	0.179 0.149	0.878 1.390	0.137 0.206
Heart	1.813 1.645	0.283 0.244	2.040 1.809	0.318 0.268
Lung	2.082 2.088	0.325 0.310	2.823 3.094	0.440 0.459
Kidney	1.779 1.838	0.278 0.273	3.684 4.468	0.575 0.663
Stomach	0.243 0.343	0.038 0.0509	0.988 1.210	0.154 0.179
Sm. Intestine	0.340 0.389	0.0531 0.0577	3.101 3.600	0.484 0.534

Table A3.25.2 Cont. (Organ Distribution for BSA)

Organ	% in 1g	CPM in 1g CPM in 1ml WB	% in total	CPM in total CPM in 1ml WB
<b>2. Distribution 30 minutes post injection.</b>				
Thyroid	ND	ND	0.168 0.208	0.0267 0.0195
Bladder	ND	ND	0.116 0.302	0.0184 0.0473
Whole Blood	ND	ND	6.301%/ml 6.391%/ml	1 1
Serum	ND	ND	10.589%/ml 10.644%/ml	1.680 1.665
Liver	1.070 1.703	0.170 0.266	12.898 20.513	2.047 3.210
Spleen	1.023 1.218	0.163 0.190	0.752 0.995	0.119 0.156
Heart	1.356 1.515	0.215 0.237	1.403 1.708	0.223 0.267
Lung	2.202 1.421	0.349 0.222	3.731 1.583	0.592 0.247
Kidney	1.829 1.143	0.290 0.179	3.905 3.448	0.620 0.540
Stomach	0.191 0.349	0.0303 0.0546	1.522 0.872	0.241 0.136
Sm. Intestine	0.336 0.318	0.0534 0.0498	3.081 2.577	0.489 0.403
<b>3. Distribution 1 hour post injection.</b>				
Thyroid	ND	ND	0.454 0.345	0.0801 0.0614
Bladder	ND	ND	0.854 0.199	0.151 0.0354
Whole Blood	ND	ND	5.667%/ml 5.621%/ml	1 1
Serum	ND	ND	10.953%/ml 10.681%/ml	1.933 1.900
Liver	1.364 1.450	0.241 0.258	15.419 18.91	2.721 3.364
Spleen	0.922 0.659	0.163 0.117	0.774 0.683	0.137 0.122
Heart	1.686 2.097	0.298 0.373	1.901 2.622	0.335 0.466
Lung	1.823 1.957	0.322 0.348	3.065 3.128	0.541 0.556
Kidney	1.445 1.485	0.255 0.264	3.232 3.474	0.570 0.618
Stomach	0.455 0.254	0.0802 0.0452	1.746 1.642	0.308 0.292
Sm. Intestine	0.579 0.712	0.102 0.127	5.296 8.478	0.935 1.508

Table A3.25.2 Cont. (Organ Distribution of BSA)

Organ	% in 1g	CPM in 1g CPM in 1ml WB	% in total	CPM in total CPM in 1ml WB
<b>4. Distribution 3 hours post injection</b>				
Thyroid	ND	ND	1.19 1.05	0.292 0.212
Bladder	ND	ND	0.419 0.333	0.103 0.0671
Whole Blood	ND	ND	4.075%/ml 4.962%/ml	1 1
Serum	ND	ND	7.750%/ml 9.875%/ml	1.902 1.990
Liver	1.184 0.893	0.290 0.180	15.866 11.551	3.893 2.328
Spleen	0.638 0.678	0.157 0.137	0.493 0.644	0.121 0.130
Heart	1.448 1.431	0.355 0.288	1.569 1.953	0.385 0.394
Lung	1.695 1.626	0.416 0.328	2.924 2.735	0.718 0.551
Kidney	1.042 1.076	0.256 0.217	2.356 2.541	0.578 0.512
Stomach	0.715 0.846	0.176 0.171	4.229 5.637	1.038 1.136
Sm. Intestine	0.681 0.529	0.167 0.106	7.197 4.696	1.766 0.946
<b>5. Distribution 5 hours post administration.</b>				
Thyroid	ND	ND	1.11 1.36	0.301 0.368
Bladder	ND	ND	0.379 0.195	0.103 0.0527
Whole Blood	ND	ND	3.688%/ml 3.696%/ml	1 1
Serum	ND	ND	6.337%/ml 6.693%/ml	1.718 1.811
Liver	0.732 0.918	0.199 0.248	8.169 11.949	2.215 3.233
Spleen	0.406 0.875	0.110 0.237	0.523 0.628	0.142 0.170
Heart	1.117 1.316	0.303 0.356	1.286 1.392	0.349 0.377
Lung	1.707 1.353	0.463 0.366	2.698 2.194	0.732 0.593
Kidney	1.308 0.600	0.355 0.162	2.717 1.262	0.737 0.341
Stomach	0.712 0.765	0.193 0.207	6.087 5.047	1.650 1.366
Sm. Intestine	0.665 0.511	0.180 0.138	5.846 5.413	1.585 1.464

Table A3.26.1 The Serum and Whole Blood concentrations (% of radioactivity remaining/ml) following administration of 250µg of <sup>125</sup>I-BSA-MTX (4.54%w/w) to rats by the IV route. Ten rats were injected. Each value was determined from one rat.

Note where Mean and S.E.M. are quoted n=4.

Time (minutes)	Whole Blood %/ml	Serum %/ml
1	5.077	10.031
1	5.558	9.597
2	4.563	8.336
2	4.692	8.717
5	4.954	7.997
5	4.195	7.675
8	3.852	7.191
8	3.748	6.996
10	4.063	6.915
10	3.595	6.963
15	3.671	6.592
15	3.731	6.390
20	3.447±0.0817	6.358±0.0947
30	3.553	5.946
30	3.032	5.681
40	2.842	5.575
40	3.020	5.707
60	2.494	4.712
60	2.383	4.411
90	2.379	4.752
90	2.158	4.100
120	2.269	4.262
120	2.094	3.747
150	1.704	3.328
150	1.848	3.041
180	1.418	2.533
180	1.835	3.280
240	1.407	2.356
240	1.624	2.960
300	1.017	2.239
300	1.381	2.279

Table A3.26.2. Organ Distribution following administration of 250µg of <sup>125</sup>I-BSA-MTX (4.54%w/w) to rats by the IV route.

Results are expressed in 2 forms; as a % of the radioactive dose found in 1g or the whole organ and as a ratio of the activity found in 1g (or the whole tissue) divided by the activity in 1ml whole blood. Two rats were analysed at each time point.

Organ	% in 1g	<u>CPM in 1g</u> CPM in 1ml WB	% in total	<u>CPM in total</u> CPM in 1ml WB
<b>1 Distribution 15 minutes following administration.</b>				
Thyroid	ND	ND	0.224 0.415	0.0610 0.111
Bladder	ND	ND	0.284 1.182	0.0774 0.317
Whole Blood	ND	ND	3.671%/ml 3.731%/ml	1 1
Serum	ND	ND	6.592%/ml 6.390%/ml	1.796 1.713
Liver	1.895 1.413	0.516 0.354	25.111 22.304	6.842 5.980
Spleen	1.608 1.320	0.438 0.354	1.289 1.270	0.351 0.340
Heart	0.947 1.261	0.258 0.338	1.599 1.515	0.436 0.406
Lung	1.053 1.175	0.287 0.315	1.260 1.842	0.343 0.494
Kidney	1.547 1.556	0.421 0.424	3.843 3.814	1.047 1.023
Stomach	0.341 0.143	0.0928 0.0382	2.701 1.742	0.736 0.467
Sm. Intestine	0.345 0.346	0.0939 0.0927	4.694 4.196	1.279 1.125



Table A3.26.2 Cont. (Organ Distribution of BSA-MTX (4.54%w/w))

Organ	% in 1g	CPM in 1g CPM in 1ml WB	% in total	CPM in total CPM in 1ml WB
<b>2. Distribution 30 minutes post administration.</b>				
Thyroid	ND	ND	0.366 0.427	0.103 0.141
Bladder	ND	ND	1.580 2.371	0.445 0.782
Whole Blood	ND	ND	3.553%/ml 3.032%/ml	1 1
Serum	ND	ND	5.946%/ml 5.681%/ml	1.673 1.874
Liver	1.684 1.349	0.474 0.445	22.41 20.53	6.307 6.771
Spleen	1.501 1.477	0.424 0.487	1.231 1.925	0.346 0.635
Heart	1.152 0.834	0.324 0.275	1.385 1.243	0.390 0.410
Lung	1.185 1.021	0.334 0.337	1.869 1.811	0.526 0.597
Kidney	1.509 1.070	0.425 0.353	3.408 2.709	0.959 0.893
Stomach	0.530 0.528	0.149 0.174	5.331 5.265	1.500 1.736
Sm. Intestine	0.780 1.216	0.219 0.401	8.423 13.588	2.371 4.482
<b>3. Distribution 1 hour post administration.</b>				
Thyroid	ND	ND	0.700 0.977	0.281 0.410
Bladder	ND	ND	1.780 1.963	0.714 0.824
Whole Blood	ND	ND	2.493%/ml 2.383%/ml	1 1
Serum	ND	ND	4.712%/ml 4.411%/ml	1.890 1.851
Liver	1.319 1.157	0.529 0.485	18.093 14.497	7.254 6.084
Spleen	1.062 1.740	0.426 0.730	1.463 1.087	0.587 0.456
Heart	0.868 0.798	0.348 0.335	1.010 0.804	0.405 0.337
Lung	0.833 0.921	0.334 0.386	1.482 1.448	0.594 0.608
Kidney	1.218 1.148	0.488 0.482	3.353 2.817	1.344 1.182
Stomach	0.483 1.088	0.194 0.456	2.288 4.840	0.917 2.031
Sm. Intestine	0.717 0.652	0.288 0.274	7.506 6.276	3.010 2.634

Table A3.26.2 Cont. (Organ Distribution for BSA-MTX (4.54%w/w))

Organ	% in 1g	CPM in 1g CPM in 1ml WB	% in total	CPM in total CPM in 1ml WB
<b>4. Distribution 3 hours post injection.</b>				
Thyroid	ND	ND	1.672 3.287	1.179 1.791
Bladder	ND	ND	0.891 0.151	0.628 0.0823
Whole Blood	ND	ND	1.418%/ml 1.835%/ml	1 1
Serum	ND	ND	2.533 3.280	1.786 1.787
Liver	0.512 0.629	0.361 0.343	6.274 9.070	4.424 4.948
Spleen	0.446 0.521	0.314 0.284	0.487 0.506	0.343 0.276
Heart	0.636 0.644	0.449 0.351	0.609 0.748	0.430 0.408
Lung	0.628 0.768	0.443 0.419	0.937 1.314	0.661 0.717
Kidney	0.726 1.235	0.512 0.674	1.657 2.931	1.169 1.599
Stomach	1.295 1.817	0.913 0.991	9.261 13.332	6.531 7.274
Sm. Intestine	0.719 1.501	0.507 0.819	6.737 16.933	4.751 9.238
<b>5. Distribution 5 hours post administration.</b>				
Thyroid	ND	ND	3.754 3.753	3.690 2.718
Bladder	ND	ND	0.891 0.151	0.876 0.109
Whole Blood	ND	ND	1.017%/ml 1.381%/ml	1 1
Serum	ND	ND	2.240%/ml 2.279%/ml	2.202 1.650
Liver	0.555 0.612	0.546 0.443	7.526 7.288	7.400 5.279
Spleen	0.357 0.582	0.351 0.422	0.350 0.429	0.344 0.311
Heart	0.429 0.456	0.422 0.330	0.529 0.582	0.520 0.422
Lung	0.531 0.860	0.522 0.623	0.672 1.552	0.660 1.124
Kidney	0.709 0.708	0.698 0.512	1.641 1.679	1.613 1.216
Stomach	1.928 2.551	1.896 1.847	12.864 12.033	12.649 8.715
Sm. Intestine	0.603 1.016	0.592 0.736	5.467 8.565	5.376 6.203

Table A3.27.1 the Serum and Whole Blood Concentration (% of radioactivity remaining/ml) following administration of 250µg of <sup>125</sup>I -BSA-MTX (11.55%w/w) to male wistar rats by IV injection. Each point is a single determination

Time (minutes)	Whole Blood %/ml	Serum %/ml
1	4.508	7.257
1	4.574	6.901
2	3.345	7.312
2	3.192	5.378
5	2.907	4.655
5	1.900	3.288
8	1.953	3.152
8	1.394	2.101
10	1.430	1.527
10	0.989	2.419
15	1.021	1.733
15	0.764	1.197
20	0.753	1.243
20	0.602	0.9088
24	0.571	0.697
24	0.645	0.973
30	0.724	1.006
30	0.640	0.838
40	0.522	0.704
40	0.599	0.806
60	0.505	0.647
60	0.500	0.710
90	0.347	0.499
90	0.488	0.590
120	0.320	0.334
120	0.254	0.348
150	0.311	0.346
150	0.387	0.421
180	0.245	0.320
180	0.303	0.387
240	0.231	0.245
240	0.220	0.272
300	0.202	0.241
300	0.170	0.239

Table A3.27.2 The Organ distribution following administration of 250mg of <sup>125</sup>I-BSA-MTX (11.55%w/w) to rats by the IV route.

Values are expressed in 2 forms; as a % of the the totalradioactive dose found in 1g or the whole organ and as a ratio of the activity in 1g (or whole organ) divided by the activity in 1ml whole blood.

Organ	% in total	<u>CPM in 1g</u> CPM in 1ml WB	% in total	<u>CPM in total</u> CPM/ml WB
<b>1. Distribution 15 minutes post injection.</b>				
Thyroid	ND	ND	0.204 0.137	0.200 0.179
Bladder	ND	ND	0.720 0.141	0.705 0.184
Whole Blood	ND	ND	1.021%/ml 0.764%/ml	1 1
Serum	ND	ND	1.733%/ml 1.197%/ml	1.698 1.567
Liver	4.797 4.763	4.699 6.234	67.15 61.43	65.77 80.40
Spleen	2.472 3.113	2.421 4.074	3.27 3.91	3.203 5.118
Heart	0.287 0.284	0.281 0.371	0.366 0.351	0.358 0.459
Lung	0.503 0.441	0.493 0.577	0.763 0.789	0.747 1.033
Kidney	0.503 0.521	0.493 0.682	1.185 1.310	1.161 1.715
Stomach	0.318 0.174	0.311 0.228	3.706 1.750	3.630 2.304
Sm. Intestine	0.251 0.350	0.246 0.458	2.633 5.450	2.579 7.133

Table A3.27.2 Cont. (Organ Distribution of MTX-BSA (11.55%w/w))

Organ	% in 1g	CPM in 1g CPM in 1ml WB	% in total	CPM in total CPM in 1ml WB
<b>2. Distribution 30 minutes post injection.</b>				
Thyroid	ND	ND	0.36 0.45	0.497 0.703
Bladder	ND	ND	0.928 0.921	1.282 1.439
Whole Blood	ND	ND	0.724%/ml 0.640%/ml	1 1
Serum	ND	ND	1.006%/ml 0.838%/ml	1.389 1.309
Liver	4.337 3.390	5.994 5.169	49.776 47.676	68.80 74.44
Spleen	2.418 3.311	3.341 5.169	3.350 3.485	4.630 5.441
Heart	0.286 0.305	0.395 0.476	0.324 0.393	0.448 0.614
Lung	0.479 0.381	0.662 0.595	0.802 0.688	1.109 1.075
Kidney	0.642 0.627	0.887 0.979	1.533 1.880	2.119 2.935
Stomach	0.419 0.307	0.579 0.480	3.763 3.282	5.201 5.124
Sm. Intestine	0.481 0.479	0.665 0.749	5.470 5.317	7.560 8.302
<b>3. Distribution 1 hour post administration.</b>				
Thyroid	ND	ND	0.715 0.837	1.416 1.674
Bladder	ND	ND	4.354 0.652	8.622 1.304
Whole Blood	ND	ND	0.505%/ml 0.500%/ml	1 1
Serum	ND	ND	0.647%/ml 0.710%/ml	1.281 1.42
Liver	1.619 1.970	3.207 3.937	19.749 25.802	39.11 51.55
Spleen	2.192 4.031	4.340 8.055	1.606 2.058	3.180 4.111
Heart	0.267 0.339	0.529 0.678	0.267 0.257	0.529 0.514
Lung	0.351 0.444	0.696 0.888	0.582 0.665	1.153 1.329
Kidney	0.826 0.939	1.635 1.875	1.774 2.062	3.514 4.121
Stomach	1.259 2.039	2.492 4.075	10.080 21.305	19.961 42.567
Sm. Intestine	1.010 0.848	2.001 1.694	10.709 10.672	21.21 21.32

**Table A3.27.2 Cont. (Organ Distribution of BSA-MTX (11.55%w/w))**

Organ	% in 1g	CPM in 1g/ CPM in 1ml WB	% in total	CPM in total CPM in 1ml WB.
<b>4. Distribution 3 hours post injection.</b>				
Thyroid	ND	ND	3.50 4.04	14.29 13.33
Bladder	ND	ND	0.516 0.141	2.106 0.465
Whole Blood	ND	ND	0.245%/ml 0.303%/ml	1 1
Serum	ND	ND	0.320%/ml 0.387%/ml	1.307 1.277
Liver	0.567 0.504	2.316 1.665	6.643 6.718	27.13 22.19
Spleen	0.509 0.837	2.078 2.763	0.342 0.660	1.397 2.180
Heart	0.119 1.667	0.485 0.550	0.136 0.208	0.556 0.687
Lung	0.223 0.226	0.910 0.748	0.332 0.319	1.355 1.053
Kidney	0.374 0.423	1.526 1.398	0.843 1.028	3.442 3.394
Stomach	3.949 2.858	16.126 9.440	21.488 12.561	87.74 41.49
Sm. Intestine	0.953 0.840	3.893 2.776	6.956 7.545	28.40 24.92
<b>5. Distribution 5 hours post administration.</b>				
Thyroid	ND	ND	6.999 5.960	34.65 35.06
Bladder	ND	ND	0.198 1.010	0.980 5.941
Whole Blood	ND	ND	0.202%/ml 0.170%/ml	1 1
Serum	ND	ND	0.241%/ml 0.239%/ml	1.193 1.406
Liver	0.368 0.291	1.821 1.712	5.133 4.217	25.39 24.76
Spleen	0.240 0.265	1.185 1.555	0.206 0.199	1.018 1.170
Heart	0.0857 0.0850	0.424 0.499	0.112 0.101	0.557 0.594
Lung	0.149 0.135	0.736 0.794	0.271 0.246	1.342 1.443
Kidney	0.239 0.223	1.182 1.307	0.658 0.590	3.253 3.466
Stomach	2.124 1.821	10.507 10.693	12.349 13.002	61.08 76.35
Sm. Intestine	0.548 0.813	2.709 4.772	6.144 8.019	30.39 47.09

Table A3.28.1 The Serum and Whole Blood concentrations (% of radioactivity remaining/ml) following administration of 250µg of <sup>125</sup>I-G-BSA to rats by the IV route.

Where mean and S.E.M are quoted, 3 animals were sampled at the same time point. 10 rats were dosed altogether.

Time (minutes)	Whole Blood %/ml	Serum %/ml
1	2.406	3.885
1	4.270	6.577
2	1.059	1.550
2	1.113	1.795
5	0.365	0.525
5	0.360	0.525
8	0.278	0.372
8	0.271	0.371
9	0.232	0.290
10	0.342±0.104	0.435±0.124
15	0.287	0.327
15	0.253	0.294
20	0.360	0.440
20	0.482	0.624
21	0.565	0.767
21	0.761	0.912
30	0.604	0.717
30	0.729	0.892
36	0.577	0.755
36	0.602	0.769
60	0.530	0.695
60	0.552	0.642
105	0.489	0.633
105	0.507	0.685
120	0.485	0.444
120	0.491	0.457
165	0.561	0.558
165	0.534	0.544
180	0.356	0.420
180	0.391	0.402
300	0.471	0.367
300	0.330	0.457

Table A3.28.2 The Organ Distribution following administration of 250µg of <sup>125</sup>I-G-BSA to rats by the IV route. 10 rats were dosed. Two animals were sampled at each time point.

Results are tabulated in 2 forms; as a % of the total radioactivity found in a particular organ and as a ratio of the activity found in 1g (or the whole organ) divided by the activity in 1ml whole blood.

Organ	% in 1g	CPM in 1g CPM in 1ml WB	% in total	CPM in total CPM in 1ml WB
<b>1. Distribution 15 minutes post injection.</b>				
Thyroid	ND	ND	0.187 0.128	0.652 0.508
Bladder	ND	ND	0.017 0.018	0.0592 0.0714
Whole Blood	ND	ND	0.287%/ml 0.252%/ml	1 1
Serum	ND	ND	0.327%/ml 0.294%/ml	1.139 1.167
Liver	6.721 6.867	23.417 27.143	81.21 87.59	283.0 346.2
Spleen	3.407 3.016	11.873 11.923	2.402 2.636	8.370 10.42
Heart	0.245 0.252	0.854 0.996	0.255 0.278	0.890 1.099
Lung	0.658 0.621	2.294 2.453	0.904 0.781	3.150 3.088
Kidney	0.933 0.908	3.251 3.591	2.322 2.149	8.090 8.493
Stomach	0.457 0.273	1.594 1.078	1.345 0.863	4.687 3.412
Sm. Intestine	0.310 0.243	1.082 0.961	3.119 2.314	10.87 9.146



Table A3.28.2 Cont. (Organ distribution of G-BSA).

Organ	% in 1g	CPM in 1g CPM in 1ml WB	% in total	CPM in total CPM in 1ml WB
<b>2. Distribution 30 minutes post injection</b>				
Thyroid	ND	ND	0.742 0.386	1.228 0.529
Bladder	ND	ND	0.136 0.073	0.225 0.0818
Whole Blood	ND	ND	0.604%/ml 0.729%/ml	1 1
Serum	ND	ND	0.717%/ml 0.892%/ml	1.187 1.224
Liver	4.304 4.254	7.126 5.835	42.02 54.96	69.57 75.39
Spleen	3.168 2.835	5.245 3.889	1.903 2.003	3.151 2.748
Heart	0.581 0.445	0.962 0.610	0.620 0.531	1.027 0.728
Lung	1.072 0.841	1.775 1.153	1.477 0.956	2.445 1.312
Kidney	1.044 0.818	1.729 1.123	2.366 2.061	3.917 2.827
Stomach	0.702 0.486	1.162 0.666	1.672 2.311	2.768 3.170
Sm. Intestine	0.796 1.278	1.318 1.753	5.764 12.33	9.543 16.91
<b>3. Distribution 1 hour post administration.</b>				
Thyroid	ND	ND	1.89 1.962	3.565 3.554
Bladder	ND	ND	1.486 0.420	2.804 0.761
Whole Blood	ND	ND	0.530%/ml 0.552%/ml	1 1
Serum	ND	ND	0.695%/ml 0.642%/ml	1.311 1.163
Liver	0.603 0.674	1.138 1.222	8.607 8.594	16.24 15.57
Spleen	0.821 0.955	1.549 1.731	0.541 0.683	1.020 1.238
Heart	0.224 0.220	0.422 0.398	0.230 0.248	0.434 0.450
Lung	0.452 0.425	0.853 0.770	0.670 0.540	1.264 0.978
Kidney	0.561 0.478	1.059 0.866	1.418 1.297	2.675 2.350
Stomach	2.442 2.576	4.607 4.666	12.858 22.48	24.26 40.72
Sm. Intestine	1.090 2.090	2.057 3.786	11.131 22.35	21.00 40.48

Table A3.28.2 Cont. (organ distribution of G-BSA)

Organ	% in 1g	CPM in 1g CPM in 1ml WB	% in total	CPM in total CPM in 1ml WB
<b>4. Distribution 3 hours post injection.</b>				
Thyroid	ND	ND	8.320 7.975	23.44 20.40
Bladder	ND	ND	0.615 0.0636	1.733 0.162
Whole Blood	ND	ND	0.356%/ml 0.391%/ml	1 1
Serum	ND	ND	0.420%/ml 0.402%/ml	1.180 1.028
Liver	0.262 0.276	0.738 0.705	3.403 4.008	9.567 10.239
Spleen	0.258 0.404	0.726 1.031	0.221 0.190	0.622 0.486
Heart	0.132 0.161	0.371 0.412	0.136 0.165	0.383 0.421
Lung	0.270 0.267	0.759 0.683	0.561 0.457	1.576 1.167
Kidney	0.308 0.289	0.866 0.739	0.738 0.755	2.074 1.928
Stomach	1.218 3.076	3.425 7.859	10.341 19.74	29.07 50.43
Sm. Intestine	1.224 1.157	3.442 2.955	10.667 11.815	29.99 30.19
<b>5. Distribution 5 hours post administration.</b>				
Thyroid	ND	ND	11.13 11.12	23.64 33.69
Bladder	ND	ND	0.469 0.117	0.997 0.356
Whole Blood	ND	ND	0.471%/ml 0.659%/ml	1 1
Serum	ND	ND	0.367%/ml 0.456%/ml	0.779 0.692
Liver	0.214 0.206	0.455 0.623	2.349 2.339	4.987 3.549
Spleen	0.198 0.250	0.421 0.758	0.136 0.130	0.289 0.198
Heart	0.125 0.164	0.265 0.249	0.122 0.195	0.259 0.296
Lung	0.244 0.272	0.518 0.412	0.351 0.319	0.745 0.485
Kidney	0.248 0.274	0.528 0.416	0.515 0.675	1.093 1.024
Stomach	2.451 2.350	5.204 3.565	10.334 9.375	21.94 14.23
Sm. Intestine	1.240 1.394	2.632 2.115	10.640 10.859	22.59 16.48

Table A3.29.1 The Serum and Whole Blood Concentration (% of  $^{125}\text{I}$  dose remaining/ml) following administration of 250 $\mu\text{g}$  of  $^{125}\text{I}$ -M-BSA to rats by the IV route.

Where mean and S.E.M. are quoted four animals were sampled at the same time point Ten rats were dosed altogether. Whole Blood and serum concentrations were determined from the same animals at each time point.

Time (minutes)	Whole Blood %/ml	Serum%/ml
1	2.581	4.358
1	2.377	3.504
2	1.739	2.702
2	1.447	2.145
5	1.108	1.702
5	1.157	1.482
8	0.884	1.156
9	0.681	0.890
10	0.558	0.894
10	0.328	0.487
15	0.321 $\pm$ 0.0579	0.505 $\pm$ 0.0968
20	0.318	0.469
20	0.181	0.263
30	0.315	0.403
30	0.285	0.331
45	0.365	0.375
45	0.457	0.487
60	0.362	0.470
60	0.436	0.565
90	0.514	0.496
90	0.363	0.464
120	0.435	0.556
120	0.337	0.431
150	0.221	0.291
150	0.205	0.262
180	0.448	0.420
180	0.304	0.548
240	0.151	0.225
240	0.154	0.245
300	0.160	0.188
300	0.164	0.195

Table A3.29.2 The Organ Distribution following administration of 250µg of <sup>125</sup>I-M-BSA to rats by the IV route.

Ten rats were dosed. Results are expressed in 2 forms; as a % of the radioactivity injected found in 1g or the whole organ and as a ratio of the activity found in 1g (or the whole tissue) divided by the activity found in 1ml of whole blood.

Organ	% in 1g	CPM in 1g CPM in 1ml WB	% in total	CPM in total CPM in 1ml WB
<b>1. Distribution 15 minutes post administration</b>				
Thyroid	ND	ND	0.086 0.107	0.199 0.265
Bladder	ND	ND	0.0614 0.113	0.142 0.280
Whole Blood	ND	ND	0.431%/ml 0.404%/ml	1 1
Serum	ND	ND	0.744%/ml 0.581	1.726 1.438
Liver	5.825 4.693	13.516 11.617	71.40 62.71	165.65 155.21
Spleen	3.353 5.090	7.779 12.600	2.851 4.148	6.615 10.27
Heart	0.398 0.324	0.923 0.803	0.357 0.344	0.827 0.852
Lung	1.564 1.818	3.628 4.499	2.560 2.777	5.940 6.873
Kidney	1.377 0.731	3.195 1.810	3.556 1.936	8.251 4.791
Stomach	0.184 0.157	0.426 0.390	2.252 2.093	5.225 5.182
Sm. Intestine	0.207 0.249	0.481 0.617	2.184 3.033	5.067 7.508

Table A3.29.2 Cont. (Organ Distribution of M-BSA)

Organ	% in 1g	CPM in 1g/ CPM in 1ml WB	% in total	CPM in total/ CPM in 1ml WB
<b>2. Distribuion 30 minutes post administration.</b>				
Thyroid	ND	ND	0.441 0.289	1.4 1.014
Bladder	ND	ND	0.209 0.232	0.663 0.814
Whole Blood	ND	ND	0.315%/ml 0.285%/ml	1 1
Serum	ND	ND	0.403%/ml 0.331%/ml	1.279 1.161
Liver	3.742 2.690	11.879 9.440	50.09 43.83	159.03 153.78
Spleen	7.611 8.688	24.16 30.48	5.357 8.394	17.01 29.45
Heart	0.313 0.312	0.994 1.095	0.396 0.465	1.257 1.633
Lung	1.587 1.180	5.037 4.140	2.234 1.899	7.092 6.664
Kidney	0.720 0.571	2.285 2.004	1.784 1.475	5.664 5.177
Stomach	0.329 0.358	1.045 1.257	4.799 2.601	15.23 9.125
Sm. Intestine	0.479 0.454	1.520 1.595	4.915 5.535	15.61 19.42
<b>3. Distribution 1 hour post administration.</b>				
Thyroid	ND	ND	1.678 1.780	4.635 4.083
Bladder	ND	ND	0.765 0.894	2.113 2.050
Whole Blood	ND	ND	0.362%/ml 0.436%/ml	1 1
Serum	ND	ND	0.470%/ml 0.565%/ml	1.298 1.296
Liver	1.603 1.818	4.427 4.179	22.435 23.475	61.975 54.587
Spleen	3.572 4.597	9.868 10.568	2.524 2.559	6.974 5.883
Heart	0.358 0.329	0.989 0.757	0.486 0.342	1.343 0.786
Lung	1.072 1.071	2.960 2.3910	1.734 1.346	4.791 3.095
Kidney	0.704 0.371	1.945 0.852	1.976 0.952	5.459 2.190
Stomach	1.686 0.360	4.658 0.828	14.178 3.568	39.17 8.202
Sm. Intestine	0.857 2.099	2.369 4.826	9.741 20.37	26.91 46.83

Table A3.29.1 Cont. (Organ Distribution of M-BSA)

Organ	% in 1g	CPM in 1g CPM in 1ml WB	% in total	CPM in total CPM in 1ml WB
<b>4. Distribution 3 hours post administration.</b>				
Thyroid	ND	ND	9.906 6.230	22.11 20.49
Bladder	ND	ND	0.762 0.177	1.700 0.582
Whole Blood	ND	ND	0.448%/ml 0.304%/ml	1 1
Serum	ND	ND	0.548%/ml 0.420%/ml	1.223 1.382
Liver	0.501 0.485	1.119 1.596	5.276 5.423	11.777 17.858
Spleen	1.345 0.943	3.002 3.101	0.775 0.968	1.729 3.186
Heart	0.226 0.203	0.505 0.667	0.238 0.228	0.530 0.749
Lung	0.322 0.433	0.718 1.426	0.419 0.752	0.934 2.474
Kidney	0.539 0.457	1.203 1.503	1.246 1.172	2.780 3.855
Stomach	2.767 6.316	6.177 20.776	10.334 24.678	23.066 81.179
Sm. Intestine	1.319 1.127	2.944 3.707	9.048 9.408	20.197 30.947
<b>5. Distribution 5 hours post administration.</b>				
Thyroid	ND	ND	9.210 12.555	57.56 76.52
Bladder	ND	ND	0.518 0.137	3.238 0.835
Whole Blood	ND	ND	0.160%/ml 0.164%/ml	1 1
Serum	ND	ND	0.188%/ml 0.195%/ml	1.175 1.189
Liver	0.211 0.217	1.319 1.321	3.271 3.567	20.445 21.751
Spleen	0.552 0.506	3.452 3.089	0.405 0.401	2.534 2.443
Heart	0.0524 0.0764	0.327 0.466	0.0797 0.118	0.499 0.717
Lung	0.174 0.158	1.087 0.964	0.314 0.292	1.963 1.782
Kidney	0.136 0.169	0.847 1.033	0.445 0.533	2.780 3.248
Stomach	1.109 1.422	6.931 8.669	7.220 7.713	45.13 47.03
Sm. Intestine	0.749 0.239	4.684 1.454	7.970 2.581	49.81 15.74

Table A3.30.1 The Whole Blood and Serum Concentration (% of radioactivity/ml) following administration of 250µg of <sup>125</sup>I-LA to rats by the IV route. Eight rats were injected. Each value was determined from one rat. (Except see note a below).

Time (min)	Whole Blood %/ml	Serum %/ml
1	3.620	8.52
1	4.505	10.51
2	2.837	6.118
2	2.800	7.338
5	1.801	2.771
5	2.195	3.618
8	1.339	1.915
8	1.185	1.857
10	0.991	2.167
15	0.619	1.261
15	0.688	1.182
20	0.541	1.138
20	0.553	0.898
30	0.484±0.031 <sup>a</sup>	0.908±0.0666 <sup>a</sup>
60	0.485	0.936
60	0.367	0.708
120	-	0.659
120	-	0.534
180	-	0.493
180	-	0.391
270	-	0.412
270	-	0.467
300	0.335	0.410
300	0.345	0.431

Note

a) Value is mean ± S.E.M. (n= 3)

Table A3.30.2 The Organ Distribution following administration of 250µg of <sup>125</sup>I-LA to rats by the IV route.

Eight rats were dosed. Two animals were used for each time point. Results are expressed in 2 forms; as a % of the total radioactivity found in 1g or the whole tissue and as a ratio of the activity in 1g (or the whole organ) divided by the activity found in 1ml of whole blood.

Organ	% in 1g	<u>CPM in 1g</u> CPM in 1ml WB	% in total	<u>CPM in total</u> CPM in 1ml WB
<b>1. Distribution 15 minutes post administration.</b>				
Thyroid	ND	ND	0.136 0.137	0.220 0.199
Bladder	ND	ND	0.301 0.301	0.486 0.438
Whole Blood	ND	ND	0.619%/ml 0.688%/ml	1 1
Serum	ND	ND	1.261%/ml 1.182%/ml	2.037 1.718
Liver	0.424 0.426	0.684 0.619	4.421 5.150	7.142 7.485
Spleen	0.443 0.518	0.715 0.753	0.256 0.356	0.419 0.517
Heart	0.504 0.386	0.813 0.561	0.500 0.417	0.808 0.606
Lung	0.659 0.596	1.065 0.869	0.853 0.860	1.378 1.250
Kidney	24.644 21.809	39.81 31.70	48.46 52.14	78.32 75.78
Stomach	0.218 0.227	0.352 0.367	1.271 1.338	2.053 1.930
Sm. Intestine	0.425 0.270	0.687 0.392	3.455 2.289	5.591 3.327



**Table A.3.30.2 Cont. (organ distribution of LA).**

Organ	% in 1g	CPM in 1g CPM in 1ml WB	% in total	CPM in total CPM/1ml WB
<b>2. Distribution 30 mnutes following administration.</b>				
Thyroid	ND	ND	0.055 0.150	0.117 0.342
Bladder	ND	ND	0.269 0.312	0.571 0.712
Whole Blood	ND	ND	0.471%/ml 0.438%/ml	1 1
Serum	ND	ND	0.982%/ml 0.967%/ml	2.085 2.208
Liver	0.340 0.516	0.722 1.178	4.412 4.257	9.367 9.719
Spleen	0.576 0.288	1.223 0.657	0.261 0.270	0.554 0.616
Heart	0.387 0.385	0.822 0.879	0.332 0.274	0.705 0.626
Lung	1.128 0.556	2.395 1.269	1.562 0.718	3.316 1.639
Kidney	5.089 6.463	10.80 14.76	11.53 11.27	24.48 25.73
Stomach	3.454 4.388	7.333 10.02	16.92 21.22	35.92 48.45
Sm. Intestine	4.035 3.638	8.567 8.306	32.27 24.88	68.51 56.80
<b>3. Distribution 1 hour post administration.</b>				
Thyroid	ND	ND	1.353 1.609	2.789 4.384
Bladder	ND	ND	1.493 3.299	3.078 8.990
Whole Blood	ND	ND	0.485%/ml 0.367%/ml	1 1
Serum	ND	ND	0.936%/ml 0.708%/ml	1.930 1.929
Liver	0.610 0.278	1.258 0.757	4.543 3.095	9.367 8.435
Spleen	0.966 0.887	1.992 2.418	0.416 0.531	0.859 1.448
Heart	0.488 0.493	1.007 1.342	0.456 0.303	0.941 0.825
Lung	0.518 0.651	1.069 1.774	0.475 0.734	0.980 2.000
Kidney	13.996 21.80	28.86 59.39	23.98 46.81	49.44 127.5
Stomach	0.145 0.288	0.300 0.784	0.426 1.141	0.879 3.108
Sm. Intestine	0.256 0.283	0.528 0.771	1.858 2.762	3.830 7.525

Table A3.30.2 Cont. (organ distribution of LA).

Organ	% in 1g	CPM in 1g CPM in 1ml WB	% in total	CPM in total CPM in 1ml WB
<b>4. Distribution 5 hours post administration.</b>				
Thyroid	ND	ND	6.886 7.321	20.55 21.21
Bladder	ND	ND	0.128 0.154	0.83 0.446
Whole Blood	ND	ND	0.335%/ml 0.345%/ml	1 1
Serum	ND	ND	0.410%/ml 0.431%/ml	1.224 1.249
Liver	0.208 0.199	0.620 0.577	2.217 2.306	6.619 6.685
Spleen	0.193 0.209	0.575 0.606	0.144 0.211	0.430 0.612
Heart	0.163 0.177	0.487 0.513	0.103 0.139	0.307 0.404
Lung	0.222 0.208	0.663 0.603	0.277 0.293	0.827 0.850
Kidney	0.633 0.599	1.890 1.736	1.193 1.369	3.560 3.969
Stomach	2.799 2.845	8.355 8.246	7.578 13.09	22.62 37.93
Sm. Intestine	1.240 1.332	3.702 3.450	9.100 11.32	27.17 32.82

Table A3.31.1: The Serum Concentrations determined following administration of  $^{125}\text{I}$ -BSA- $^3\text{H}$ -MTX (7.16%w/w) to rats by the IV route. The concentration for both isotopes was determined and compared. Ten rats were injected with the conjugate. Two rats were sampled at each time point.

Time (hours)	$^3\text{H}$ activity %/ml	$^{125}\text{I}$ activity %/ml
0.5	4.618	5.496
0.5	7.204	6.097
1.0	4.477	4.449
1.0	4.780	4.270
2.0	3.034	3.100
2.0	3.575	3.530
4.0	1.916	1.714
6.0	1.426	1.293
6.0	1.013	1.117
8.0	1.048	0.911
8.0	0.690	0.870
11.5	0.785	0.705
11.5	0.796	0.613
24	0.182	0.321
24	0.188	0.251
28	0.198	0.235
28	0.312	0.235
31	0.157	0.150
31	0.155	0.174
48	0.120	0.111
48	0.104	0.104
55	0.0587	0.0869
55	0.0682	0.0675
72	0.0637	0.0686
72	0.0695	0.0547
79	0.0479	0.0472
79	0.0409	0.0469
96	0.0404	0.0420
96	0.0379	0.0357

Table A3.31.2 The Urine Excretion of radioactivity following administration of  $^{125}\text{I}$ -BSA- $^3\text{H}$ -MTX (7.16%w/w) to rats by the IV route. The percentage of isotope excreted by each rat is listed as well as the mean isotope excretion at each time point.

Time (hours)	$^3\text{H}$ % activity excreted	$^{125}\text{I}$ % activity excreted
24	23.47	45.50
	31.50	55.44
	29.49	52.20
Mean	28.15	51.05 <sup>a</sup>
S.E.M.	2.412	2.927
48	25.84	47.59
	35.24	62.52
	36.64	62.66
Mean	32.57	57.59
S.E.M.	3.391	5.000 <sup>b</sup>
72	26.97	49.52
	36.35	64.71
	39.52	66.34
Mean	34.28	60.19
S.E.M.	3.768	5.356 <sup>c</sup>
96	37.61	65.90
	40.58	68.57
Mean	39.10	67.23

Notes

a) t value for  $^3\text{H}$  versus  $^{125}\text{I}$  excreted at 24 hours is 6.04. Probability <0.1%, highly significant.

b) t value for  $^3\text{H}$  versus  $^{125}\text{I}$  at 48 hours is 4.19. Probability <1%, highly significant.

c) t value for  $^3\text{H}$  versus  $^{125}\text{I}$  at 72 hours is 3.955. Probability <1%, highly significant.

Table A3.31.3 The Organ Distribution following administration of  $^{125}\text{I}$ -BSA- $^3\text{H}$ -MTX (7.16%w/w) to rats by the IV route. Results are expressed in 2 forms; as a % of the total radioactivity found in 1g or the whole organ and as a ratio of the activity found in 1g (or the whole organ) divided by the activity in 1ml of Serum (S). One rat was analysed at one hour and six hours. Two rats were analysed at 24, 48, 72 and 96 hours.

Organ	% $^3\text{H}$ in 1g	% $^{125}\text{I}$ in 1g	$\frac{^3\text{H CPM in 1g}}{\text{CPM in 1ml S}}$	$\frac{^{125}\text{I CPM in 1g}}{\text{CPM in 1ml S}}$	% $^3\text{H}$ in total	% $^{125}\text{I}$ in total	$\frac{^3\text{H CPM in total}}{\text{CPM in 1ml S}}$	$\frac{^{125}\text{I CPM in total}}{\text{CPM in 1ml S}}$
<b>1. Distribution 1 hour post administration.</b>								
Thyroid	-	-	-	-	-	1.788	-	0.402
Bladder	-	-	-	-	-	0.100	-	0.0225
Serum	-	-	-	-	4.477%/ml	4.449%/ml	1	1
Liver	0.169	1.150	0.038	0.258	1.850	12.53	0.413	2.82
Spleen	0.432	1.955	0.096	0.439	0.261	1.181	0.0117	0.265
Kidney	0.317	0.969	0.071	0.32	0.694	2.118	0.155	0.476
Stomach	0	0.901	0	0.203	0	8.35	0	1.869
Sm. Intestine	0	0.915	0	0.206	0	10.66	0	2.390
<b>2. Distribution 6 hours post administration.</b>								
Thyroid	-	-	-	-	-	5.667	-	4.383
Bladder	-	-	-	-	-	0.218	-	0.169
Serum	-	-	-	-	1.426%/ml	1.117%/ml	1	1
Liver	0.341	0.495	0.238	0.443	3.193	4.638	2.239	4.152
Spleen	0.255	0.447	0.179	0.400	0.149	0.261	0.104	0.234
Kidney	0.206	0.548	0.145	0.491	0.423	1.124	0.297	1.006
Stomach	0.396	3.06	0.278	2.74	3.05	23.57	2.14	21.10
Sm. Intestine	0.0243	1.795	0.017	1.607	0.143	10.58	0.100	9.47

Table A3.31. 3 Cont. (Organ distribution of  $^{125}\text{I}$ -BSA- $^3\text{H}$ -MTX)

Organ	% $^3\text{H}$ in 1g	% $^{125}\text{I}$ in 1g	$\frac{^3\text{H CPM in 1g}}{\text{CPM in 1ml S}}$	$\frac{^{125}\text{I CPM in 1g}}{\text{CPM in 1ml S}}$	% $^3\text{H}$ in total	% $^{125}\text{I}$ in total	$\frac{^3\text{H CPM in total}}{\text{CPM in 1ml S}}$	$\frac{^{125}\text{I CPM in total}}{\text{CPM in 1ml S}}$
<b>3. Distribution 24 hours post administration.</b>								
Thyroid	-	-	-	-	-	14.55 15.46	- -	45.33 61.59
Bladder	-	-	-	-	-	0.145 0.117	- -	0.452 0.466
Serum	-	-	-	-	0.182%/ml 0.188%/ml	0.321%/ml 0.251%/ml	1 1	1 1
Liver	0.131 0.124	0.140 0.124	0.722 0.661	0.436 0.494	1.517 1.455	1.616 1.452	8.34 7.739	5.03 5.784
Spleen	0.048 0.0557	0.104 0.102	0.265 0.296	0.325 0.406	0.0237 0.0307	0.0514 0.0561	0.130 0.163	0.160 0.223
Kidney	0.053 0.0149	0.204 0.206	0.290 0.0797	0.637 0.820	0.0927 0.0337	0.359 0.463	0.509 0.179	1.118 1.845
Stomach	0 0	0.788 0.294	0 0	0.245 1.172	0 0	2.632 1.063	0 0	8.199 4.235
Sm. Intestine	0 0	0.324 0.689	0 0	1.011 3.668	0 0	3.024 5.82	0 0	9.42 23.18

Table A3.31.3 Cont. (Organ Distribution of  $^{125}\text{I}$ -BSA- $^3\text{H}$ -MTX)

Organ	% $^3\text{H}$ in 1g	% $^{125}\text{I}$ in 1g	$\frac{^3\text{H CPM in 1g}}{\text{CPM in 1ml S}}$	$\frac{^{125}\text{I CPM in 1g}}{\text{CPM in 1ml S}}$	% $^3\text{H}$ in total	% $^{125}\text{I}$ in total	$\frac{^3\text{H CPM in total}}{\text{CPM in 1ml S}}$	$\frac{^{125}\text{I CPM in total}}{\text{CPM in 1ml S}}$
<b>4. Distribution 48 hours post administration.</b>								
Thyroid	-	-	-	-	-	16.18 11.56	-	145.8 111.1
Bladder	-	-	-	-	-	0.219 0.207	-	1.973 1.990
Serum	-	-	-	-	0.120%/ml 0.104%/ml	0.111%/ml 0.104%/ml	1 1	1 1
Liver	0.0726 0.082	0.0749 0.064	0.607 0.785	0.673 0.612	0.864 1.226	0.891 0.957	7.218 11.79	8.005 9.202
Spleen	0.0438 0.0188	0.0465 0.0323	0.366 0.181	0.418 0.311	0.0259 0.0117	0.0275 0.0201	0.216 0.238	0.247 0.193
Kidney	0.062 0.064	0.133 0.116	0.519 0.618	1.197 1.113	0.126 0.163	0.270 0.294	1.053 1.567	2.426 2.822
Stomach	0 0.0214	0.0986 0.0760	0 0.206	0.886 0.731	0 0.216	0.674 0.768	0 2.077	6.056 7.385
Sm. Intestine	0 0.0108	0.0803 0.0562	0 0.104	0.721 0.540	0 0.110	0.641 0.570	0 1.058	5.760 5.480

Table A3.31.3 Cont (Organ Distribution of <sup>125</sup>I-BSA-<sup>3</sup>H-MTX)

Organ	% <sup>3</sup> H in 1g	% <sup>125</sup> I in 1g	<sup>3</sup> H CPM in 1g CPM in 1ml S	<sup>125</sup> I CPM in 1g CPM in 1ml S	% <sup>3</sup> H in total	% <sup>125</sup> I in total	<sup>3</sup> H CPM in total CPM in 1ml S	<sup>125</sup> I CPM in total CPM in 1ml S
<b>5 Distribution 72 hours post administration.</b>								
Thyroid	-	-	-	-	-	16.38 17.78	-	238.8 326.0
Bladder	-	-	-	-	-	0.0249 0.0558	-	0.363 1.020
Serum	-	-	-	-	0.0637%/ml 0.0695%/ml	0.0686%/ml 0.0547%/ml	1 1	1 1
Liver	0.101 0.106	0.0548 0.0402	1.590 1.525	0.799 0.739	1.307 1.484	0.707 0.562	20.52 21.35	10.31 10.33
Spleen	0.0225 0.0263	0.0240 0.0298	0.353 0.378	0.350 0.547	0.0117 0.0121	0.0125 0.0137	0.184 0.174	0.182 0.252
Kidney	0.102 0.0802	0.104 0.0848	1.601 1.154	1.516 1.559	0.233 0.193	0.239 0.204	3.658 2.777	3.484 3.751
Stomach	0 0.0136	0.062 0.0268	0 0.196	0.904 0.493	0 0.104	0.197 0.205	0 1.496	2.872 3.770
Sm. Intestine	0 0.0144	0.0366 0.0258	0 0.207	0.488 0.474	0 0.115	0.301 0.206	0 1.655	4.008 3.787



Table A3.31.3 Cont. (Organ Distribution of  $^{125}\text{I}$ -BSA- $^3\text{H}$ -MTX)

Organ	% $^3\text{H}$ in 1g	% $^{125}\text{I}$ in 1g	$^3\text{H}$ CPM in 1g CPM in 1ml S	$^{125}\text{I}$ CPM in 1g CPM in 1ml S	% $^3\text{H}$ in total	% $^{125}\text{I}$ in total	$^3\text{H}$ CPM in total CPM in 1ml S	$^{125}\text{I}$ CPM in total CPM in 1ml S
<b>6. Distribution 96 hours post administration.</b>								
Thyroid	-	-	-	-	-	11.8 15.1	-	280.9 421.8
Bladder	-	-	-	-	-	0.387 0.334	-	9.214 9.356
Serum	-	-	-	-	0.0404%/ml 0.0379%/ml	0.0420%/ml 0.0357%/ml	1 1	1 1
Liver	0.111 0.247	0.0302 0.0549	2.75 6.528	0.718 1.537	1.309 2.340	0.356 0.519	32.4 61.74	8.476 14.54
Spleen	0.0388 0.0429	0.0176 0.0315	0.96 1.134	0.42 0.883	0.0176 0.0255	0.0080 0.0187	0.436 0.673	0.190 0.524
Kidney	0.193 0.164	0.070 0.0991	4.78 4.316	1.675 2.776	0.453 0.345	0.165 0.209	11.21 9.103	3.928 5.850
Stomach	0.0189 0.071	0.008 0.091	0.469 1.86	0.191 2.55	0.116 0.129	0.0492 0.166	2.87 3.40	1.17 4.65
Sm. Intestine	0.0098 0.0302	0.0184 0.058	0.244 0.796	0.438 1.626	0.091 0.197	0.170 0.379	2.252 5.198	4.048 10.62

Table A3.32.1 The Uptake of  $^{125}\text{I}$  following exposure of rat peritoneal macrophages, *in vitro*, to 75 $\mu\text{g}$  of  $^{125}\text{I}$ -HSA in RPMI media without serum. The uptake was determined at 37°C and 4°C. Results are means for 3 wells at each time point  $\pm$  S.E.M..

Time (min)	Uptake at 37°C % $^{125}\text{I}$ applied	Uptake at 4°C % $^{125}\text{I}$ applied
15	0.076 $\pm$ 0.018	0.075 $\pm$ 0.0036
30	0.120 $\pm$ 0.024	0.104 $\pm$ 0.034
45	0.122 $\pm$ 0.007	0.108 $\pm$ 0.029
60	0.173 $\pm$ 0.020	0.159 $\pm$ 0.009

Table A3.32.2: The Degradation of  $^{125}\text{I}$ -HSA by rat peritoneal macrophages *in vitro*. Macrophages were exposed to RPMI media which contained 75 $\mu\text{g}$  of  $^{125}\text{I}$ -HSA for a 1 hour period. Measurement of TCA soluble  $^{125}\text{I}$  was carried out at various time points on 3 wells. Results are expressed as mean  $\pm$  S.E.M.

Time (min)	% $^{125}\text{I}$ present as TCA Soluble (37°C)	% $^{125}\text{I}$ present as TCA Soluble (4°C)
0	9.58	9.58
15	33.5 $\pm$ 2.69	11.52 $\pm$ 3.58
30	38.6 $\pm$ 6.26	11.86 $\pm$ 3.83
45	45.4 $\pm$ 4.58	20.83 $\pm$ 3.49
60	48.6 $\pm$ 6.00	32.93 $\pm$ 2.77

Table A3.32.3: The Uptake of  $^{125}\text{I}$  following exposure of rat peritoneal macrophages, *in vitro*, to  $8\mu\text{g}$  of  $^{125}\text{I}$ -BSA in RPMI media without serum. The uptake was determined at  $37^\circ\text{C}$  and  $4^\circ\text{C}$ . Results are means for 3 wells at each time point  $\pm$  S.E.M..

Time (min)	Uptake at $37^\circ\text{C}$ % $^{125}\text{I}$ applied	Uptake at $4^\circ\text{C}$ % $^{125}\text{I}$ applied
15	$0.038 \pm 0.0036$	$0.072 \pm 0.0016$
30	$0.080 \pm 0.00608$	$0.110 \pm 0.024$
45	$0.122 \pm 0.0152$	$0.108 \pm 0.031$
60	$0.180 \pm 0.0127$	$0.175 \pm 0.010$

Table A3.32.4: The Degradation of  $^{125}\text{I}$ -BSA by rat peritoneal macrophages *in vitro*. Macrophages were exposed to RPMI media which contained  $8\mu\text{g}$  of  $^{125}\text{I}$ -BSA for a 1 hour period. Measurement of TCA soluble  $^{125}\text{I}$  was carried out at various time points on 3 wells. Results are means  $\pm$  S.E.M.

Time (min)	% $^{125}\text{I}$ present as TCA Soluble ( $37^\circ\text{C}$ )	% $^{125}\text{I}$ present as TCA Soluble ( $4^\circ\text{C}$ )
0	5.3	5.3
15	$30.6 \pm 1.73$	$8.56 \pm 2.58$
30	$33.2 \pm 2.65$	$11.93 \pm 1.83$
45	$39.3 \pm 4.33$	$19.23 \pm 1.49$
60	$44.0 \pm 5.37$	$29.92 \pm 2.97$

Table A3.32.5: The Uptake of  $^{125}\text{I}$  following exposure of rat peritoneal macrophages, *in vitro*, to 8 $\mu\text{g}$  of  $^{125}\text{I}$ -BSA-MTX (4.54%w/w) in RPMI media without serum. The uptake was determined at 37°C and 4°C. Results are means for 3 wells at each time point  $\pm$  S.E.M..

Time (min)	Uptake at 37°C % $^{125}\text{I}$ applied	Uptake at 4°C % $^{125}\text{I}$ applied
10	0.0722 $\pm$ 0.00386	0.0905 $\pm$ 0.0114
20	0.0908 $\pm$ 0.0075	0.0937 $\pm$ 0.0018
30	0.107 $\pm$ 0.00465	0.132 $\pm$ 0.0193
40	0.131 $\pm$ 0.00902	0.140 $\pm$ 0.0079
50	0.145 $\pm$ 0.005	0.158 $\pm$ 0.0102
60	0.174 $\pm$ 0.0086	0.168 $\pm$ 0.0265

Table A3.32.6: The Degradation of  $^{125}\text{I}$ -BSA-MTX (4.54%w/w) by rat peritoneal macrophages *in vitro*. Macrophages were exposed to RPMI media which contained 8 $\mu\text{g}$  of  $^{125}\text{I}$ -BSA-MTX (4.54%w/w) for a 1 hour period. Measurement of TCA soluble  $^{125}\text{I}$  was carried out at various time points on 3 wells. Results are means  $\pm$  S.E.M.

Time (min)	% $^{125}\text{I}$ present as TCA Soluble (37°C)	% $^{125}\text{I}$ present as TCA Soluble (4°C)
0	7.4	7.4
10	26.31 $\pm$ 1.19	7.33 $\pm$ 2.58
20	32.85 $\pm$ 4.27	10.85 $\pm$ 1.83
30	38.53 $\pm$ 0.729	15.23 $\pm$ 1.67
40	40.61 $\pm$ 1.513	25.92 $\pm$ 2.97
50	42.15 $\pm$ 2.11	25.39 $\pm$ 1.92
60	47.72 $\pm$ 3.60	30.11 $\pm$ 3.33

Table A3.32.7: The Uptake of  $^{125}\text{I}$  following exposure of rat peritoneal macrophages, *in vitro*, to  $8\mu\text{g}$  of  $^{125}\text{I}$ -BSA-MTX (11.55%w/w) in RPMI media without serum. The uptake was determined at  $37^\circ\text{C}$  and  $4^\circ\text{C}$ . Results are means for 3 wells at each time point.  $\pm$  S.E.M..

Time (min)	Uptake at $37^\circ\text{C}$ % $^{125}\text{I}$ applied	Uptake at $4^\circ\text{C}$ % $^{125}\text{I}$ applied
15	$0.161 \pm 0.00463$	$0.124 \pm 0.0113$
30	$0.192 \pm 0.0077$	$0.209 \pm 0.0246$
45	$0.239 \pm 0.0034$	$0.211 \pm 0.0221$
60	$0.295 \pm 0.0154$	$0.254 \pm 0.019$

Table A3.32.8: The Degradation of  $^{125}\text{I}$ -BSA-MTX (11.55%w/w) by rat peritoneal macrophages *in vitro*. Macrophages were exposed to RPMI media which contained  $8\mu\text{g}$  of  $^{125}\text{I}$ -BSA-MTX (11.55%w/w) for a 1 hour period. Measurement of TCA soluble  $^{125}\text{I}$  was carried out at various time points on 3 wells. Results are means  $\pm$  S.E.M.

Time (min)	% $^{125}\text{I}$ present as TCA Soluble ( $37^\circ\text{C}$ )	% $^{125}\text{I}$ present as TCA Soluble ( $4^\circ\text{C}$ )
0	8.54	8.54
15	$31.3 \pm 2.25$	$9.56 \pm 1.42$
30	$35.67 \pm 6.63$	$19.73 \pm 2.83$
45	$40.26 \pm 3.33$	$18.73 \pm 1.67$
60	$45.30 \pm 4.66$	$25.42 \pm 3.07$

Table A3.32.9: The Uptake of  $^{125}\text{I}$  following exposure of rat peritoneal macrophages, *in vitro*, to  $8\mu\text{g}$  of  $^{125}\text{I}$ -G-BSA in RPMI media without serum. The uptake was determined at  $37^\circ\text{C}$  and  $4^\circ\text{C}$ . Results are means for 3 wells at each time point  $\pm$  S.E.M..

Time (min)	Uptake at $37^\circ\text{C}$ % $^{125}\text{I}$ applied	Uptake at $4^\circ\text{C}$ % $^{125}\text{I}$ applied
15	$2.204 \pm 0.0483$	$1.468 \pm 0.0105$
30	$3.844 \pm 0.331$	$1.544 \pm 0.0321$
45	$3.742 \pm 0.318$	$1.512 \pm 0.0263$
60	$2.932 \pm 0.0588$	$1.864 \pm 0.055$

Table A3.32.10: The Degradation of  $^{125}\text{I}$ -G-BSA by rat peritoneal macrophages *in vitro*. Macrophages were exposed to RPMI media which contained  $8\mu\text{g}$  of  $^{125}\text{I}$ -G-BSA for a 1 hour period. Measurement of TCA soluble  $^{125}\text{I}$  was carried out at various time points on 3 wells. Results are means  $\pm$  S.E.M.

Time (min)	% $^{125}\text{I}$ present as TCA Soluble ( $37^\circ\text{C}$ )	% $^{125}\text{I}$ present as TCA Soluble ( $4^\circ\text{C}$ )
0	10.12	10.12
15	$46.63 \pm 2.512$	$43.9 \pm 2.176$
30	$51.36 \pm 6.387$	$41.21 \pm 7.23$
45	$49.99 \pm 1.238$	$40.87 \pm 1.226$
60	$51.11 \pm 1.284$	$42.8 \pm 1.462$

Table A3.32.11: The Uptake of  $^{125}\text{I}$  following exposure of rat peritoneal macrophages, *in vitro*, to 8 $\mu\text{g}$  of  $^{125}\text{I}$ -M-BSA in RPMI media without serum. The uptake was determined at 37°C and 4°C. Results are means for 3 wells at each time point  $\pm$  S.E.M..

Time (min)	Uptake at 37°C % $^{125}\text{I}$ applied	Uptake at 4°C % $^{125}\text{I}$ applied
10	5.13 $\pm$ 0.0921	3.94 $\pm$ 0.11
20	9.27 $\pm$ 0.264	6.21 $\pm$ 0.386
30	12.92 $\pm$ 0.514	7.37 $\pm$ 0.49
40	15.04 $\pm$ 0.369	8.30 $\pm$ 0.069
50	16.39 $\pm$ 0.345	7.09 $\pm$ 0.202
60	18.80 $\pm$ 0.0463	6.90 $\pm$ 0.152

Table A3.32.12: The Degradation of  $^{125}\text{I}$ -M-BSA by rat peritoneal macrophages *in vitro*. Macrophages were exposed to RPMI media which contained 8 $\mu\text{g}$  of  $^{125}\text{I}$ -M-BSA for a 1 hour period. Measurement of TCA soluble  $^{125}\text{I}$  was carried out at various time points on 3 wells. Results are means  $\pm$  S.E.M.

Time (min)	% $^{125}\text{I}$ present as TCA Soluble (37°C)	% $^{125}\text{I}$ present as TCA Soluble (4°C)
0	11.12	11.12
10	31.4 $\pm$ 3.67	30.84 $\pm$ 1.731
20	30.50 $\pm$ 3.17	42.51 $\pm$ 1.075
30	36.00 $\pm$ 1.83	47.70 $\pm$ 1.34
40	40.53 $\pm$ 1.51	51.59 $\pm$ 3.35
50	40.37 $\pm$ 2.05	47.30 $\pm$ 0.682
60	45.12 $\pm$ 0.464	46.8 $\pm$ 2.32